

THE JOURNAL OF PHYSICAL CHEMISTRY

Volume 74, Number 21 October 15, 1970

Symposium on Structures of Water and Aqueous Solutions,

Held in Honor of Thomas Fraser Young at the University of Chicago, Chicago, Ill., June 1969

- Effective Pair Interactions in Liquids. Water **F. H. Stillinger, Jr.** 3677
- Approximate Methods for Determining the Structure of H₂O and HOD Using Near-Infrared Spectroscopy
. **W. A. P. Luck and W. Ditter** 3687
- A Neutron Inelastic Scattering Investigation of the Concentration and Anion Dependence of Low Frequency
Motions of H₂O Molecules in Ionic Solutions **P. S. Leung and G. J. Safford** 3696
- A Neutron Inelastic Scattering Investigation of the H₂O Molecules in Aqueous Solutions and Solid Glasses of
Lanthanum Nitrate and Chromic Chloride **P. S. Leung, S. M. Sanborn, and G. J. Safford** 3710
- Permittivity and Dielectric and Proton Magnetic Relaxation of Aqueous Solutions of the Alkali Halides
. **K. Giese, U. Kaatze, and R. Pottel** 3718
- Direct Proton Magnetic Resonance Cation Hydration Study of Uranyl Perchlorate, Nitrate, Chloride, and
Bromide in Water-Acetone Mixtures
. **Anthony Fratiello, Vicki Kubo, Robert E. Lee, and Ronald E. Schuster** 3726
- A Hydrogen-1 and Tin-119 Nuclear Magnetic Resonance Cation Hydration Study of Aqueous Acetone Solutions
of Stannic Chloride and Stannic Bromide
. **Anthony Fratiello, Shirley Peak, Ronald E. Schuster, and Don D. Davis** 3730
- Molecular Motion and Structure of Aqueous Mixtures with Nonelectrolytes as Studied by Nuclear Magnetic
Relaxation Methods **E. v. Goldammer and H. G. Hertz** 3734
- Theory of Mixed Electrolyte Solutions and Application to a Model for Aqueous Lithium Chloride-Cesium Chloride
. **Harold L. Friedman and P. S. Ramanathan** 3756
- Ultrasonic Relaxation in Manganese Sulfate Solutions **LeRoy G. Jackopin and Ernest Yeager** 3766
- Ionization of Moderately Strong Acids in Aqueous Solution. I. Trifluoro- and Trichloroacetic Acids
. **A. K. Covington, J. G. Freeman, and T. H. Lilley** 3773
- Young's Mixture Rule and Its Significance **Yung-Chi Wu** 3781
- Osmotic and Activity Coefficients for Binary Mixtures of Sodium Chloride, Sodium Sulfate, Magnesium Sulfate, and
Magnesium Chloride in Water at 25°. III. Treatment with the Ions as Components
. **G. Scatchard, R. M. Rush, and J. S. Johnson** 3786
- Equilibria and Proton Transfer in the Bisulfate-Sulfate System **D. E. Irish and H. Chen** 3796
- Solvent Structure in Aqueous Mixtures. II. Ionic Mobilities in *tert*-Butyl Alcohol-Water Mixtures at 25°
. **T. L. Broadwater and Robert L. Kay** 3802
- Transport Processes in Hydrogen-Bonding Solvents. IV. Conductance of Electrolytes in Formamide at 25 and 10°
. **John Thomas and D. Fennell Evans** 3812
- Raman Spectra of Silver Nitrate in Water-Acetonitrile Mixtures **B. G. Oliver and G. J. Janz** 3819

NOTES

Salt Effects on the Critical Micelle Concentrations of Nonionic Amphiphiles	John E. Gordon	3823
Salt Effects on the Critical Micelle Concentrations of Nonionic Surfactants	Pasupati Mukerjee	3824
Evaluation of the Basicity of Methyl Substituted Nitroguanidines by Ultraviolet and Nuclear Magnetic Resonance Spectroscopy	E. Price, L. S. Person, Y. D. Teklu, and A. S. Tompa	3826
Miscibility of Liquid Metals with Salts. IX. The Pseudobinary Alkali Metal-Metal Halide Systems: Cesium Iodide-Sodium, Cesium Iodide-Lithium, and Lithium Fluoride-Potassium	A. S. Dworkin and M. A. Bredig	3828
Reactivity of the Cyclohexane Ion	L. W. Sieck, S. K. Searles, R. E. Rebbert, and P. Ausloos	3829
Mechanism of Ethylene Hydrogenation on Tungsten Trioxide	S. J. Tauster and J. H. Sinfelt	3831
Time-Dependent Adsorption of Water Vapor on Pristine Vycor Fiber	Victor R. Deitz and Noel H. Turner	3832

COMMUNICATIONS TO THE EDITOR

Electron Spin Resonance Spectra of Radicals Formed from Nitrogen Dioxide and Olefins	M. C. R. Symons	3834
Kinetic Evidence that G_{OH} in the Radiolysis of Aqueous Sulfuric and Nitric Acid Solutions Is Proportional to Electron Fraction Water	R. W. Matthews, H. A. Mahlman, and T. J. Sworski	3835

AUTHOR INDEX

Ausloos, P., 3829	Freeman, J. G., 3773	Kay, R. L., 3802	Pottel, R., 3718	Sinfelt, J. H., 3831
Bredig, M. A., 3828	Friedman, H. L., 3756	Kubo, V., 3726	Price, E., 3826	Stillinger, F. H., Jr., 3677
Broadwater, T. L., 3802	Giese, K., 3718	Lee, R. E., 3726	Ramanathan, P. S., 3756	Sworski, T. J., 3835
Chen, H., 3796	Goldammer, E. v., 3734	Leung, P. S., 3696, 3710	Rebbert, R. E., 3829	Symons, M. C. R., 3834
Covington, A. K., 3773	Gordon, J. E., 3823	Lilley, T. H., 3773	Rush, R. M., 3786	
	Hertz, H. G., 3734	Luck, W. A. P., 3687		Tauster, S. J., 3831
Davis, D. D., 3730		Mahlman, H. A., 3835	Safford, G. J., 3696, 3710	Teklu, Y. D., 3826
Deitz, V. R., 3832	Irish, D. E., 3796	Matthews, R. W., 3835	Sanborn, S. M., 3710	Thomas, J., 3812
Ditter, W., 3687		Mukerjee, P., 3824	Scatchard, G., 3786	Tompa, A. S., 3826
Dworkin, A. S., 3828	Jackopin, L. G., 3766	Oliver, B. G., 3819	Schuster, R. E., 3726, 3730	Turner, N. H., 3832
Evans, D. F., 3812	Janz, G. J., 3819	Peak, S., 3730	Searles, S. K., 3829	Wu, Y.-C., 3781
	Johnson, J. S., 3786	Person, L. S., 3826	Sieck, L. W., 3829	Yeager, E., 3766
Fратиello, A., 3726, 3730	Kaatze, U., 3718			

THOMAS FRASER YOUNG

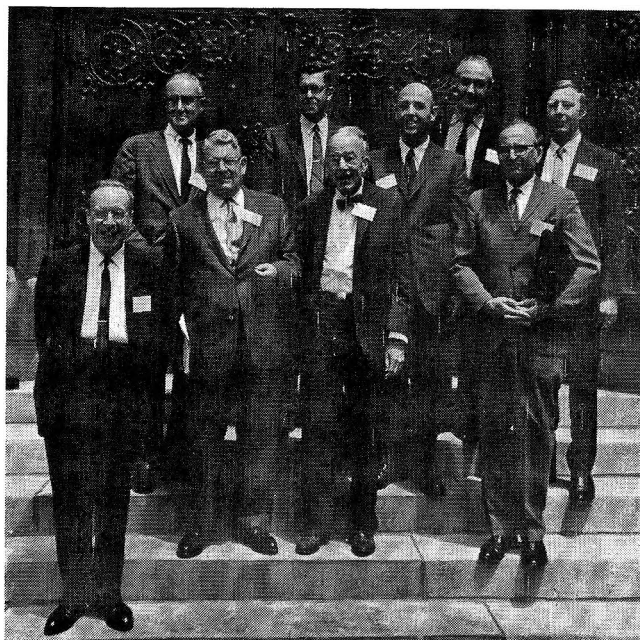
by George E. Walrafen

*Bell Telephone Laboratories, Incorporated,
Murray Hill, New Jersey 07974*

Thomas Fraser Young was born in Sumter, S. C., on September 28, 1897. His family moved to Stockton, Calif. in 1901 where his father became a judge of the superior court. In 1916 he went to Berkeley to work for the B.A. degree at the University of California. Then in 1918 he volunteered for duty with the U. S. Army, but he was released in 3 months with the end of hostilities. He returned to Berkeley, where he finished the B.A. in 1920, and continued for the Ph.D. degree in chemistry. During his Ph.D. work he was associated with Professors E. D. Eastman and G. N. Lewis; his thesis advisor was Professor A. R. Olson. He also ably assisted G. N. Lewis with the classic text, "Thermodynamics and the Free Energy of Chemical Substances," and received his doctorate in 1923.

Dr. Young joined the faculty of The University of Chicago as an instructor shortly after obtaining his degree. He rose to assistant professor in 1927, to associate professor in 1931, and to professor in 1943. In his early work at the university he was closely associated with Professor W. D. Harkins, and that association resulted in important contributions to the "International Critical Tables" ("Surface Tension," Vol. IV, p 434). He also assumed the teaching of chemical thermodynamics at the university, and he continued to teach that subject for nearly 40 years. One of his early students was Mary Allen Walker. They were married in 1931 and have two sons, Thomas Fraser Young, Jr., and Richard McLeod Young.

The subject of chemical thermodynamics unquestionably constituted the central theme of Professor Young's career, despite the fact that his publications range from such diverse subjects as electrostatic charges on insulated surfaces to Raman spectra of fused salts. His approach to chemical problems was primarily thermodynamic in nature, many of his research ideas arose from unanswered thermodynamic questions, and his rigorous teaching of that subject unquestionably inspired his students, as evidenced by the book written by Irving M. Klotz, "Chemical Thermodynamics, Basic Theory and Methods." It is hardly surprising, therefore, that Professor Young's greatest contribution to physical chemistry involves the thermodynamics of mixing, now generally known as Young's rules of mixing.



Among those present at the Symposium on Structures of Water and Aqueous Solutions, held in honor of Dr. T. F. Young (left to right): H. S. Frank, R. A. Robinson, T. F. Young, D. E. Irish, G. Scatchard, G. E. Walrafen, L. A. Blatz, I. M. Klotz, and F. H. Stillinger, Jr.

My association with Professor Young came late in his career and did not directly involve his thermodynamic interests. In the late 1940's Professor Young became interested in using Raman spectroscopy to study solutions, and in particular to determine the concentrations of species present in very concentrated aqueous solutions. His friend Professor Otto Redlich had done some pioneering work in this area, and he inspired Dr. Young to construct a photoelectric recording Raman spectrometer, and he sent his students Frank Maranville and Harlan Smith to help with the construction. The construction was soon completed, and the instrument was later improved by Drs. L. A. Blatz and A. C. Jones. Professor Young and his students then employed the Raman instrument to solve a number of interesting problems involving the dissociation of strong acids and the constitution of complex ions and of molten salts. When I first began research

work under Dr. Young in 1957, I was simply presented with a sophisticated, fully operative photoelectric Raman instrument. I had not been privileged to develop it, but that it was a privilege to work with the man who did soon became apparent, and it also became apparent that Raman spectroscopy of solutions was only an extension of his thermodynamic interests. Some important characteristics of Dr. Young as a scientist and particularly as a teacher also quickly became evident.

Any of Dr. Young's students, or anyone who has been associated with him scientifically, knows him to be a devoted scientist of unassailable intellectual honesty. His approach to research involves a high order of rigor and meticulous attention to details of all kinds. However, one of his greatest assets was his willingness to teach and to help his students, and this probably made him more successful with them than anything else. Dr. Young always gave his graduate students a great deal of individual attention, and he tried to have no more than one finishing Ph.D. student per year. Further, during the writing of the thesis he would nearly always invite the student to his summer home for a week or more and in that time he would examine every sentence and every calcula-

tion in detail. However, he would also manage to interperse the thesis work with boating, swimming, dinners, and other activities, and after graduation he always followed the student's career closely, in most cases over a period of years.

Dr. Young retired from The University of Chicago in 1962. Since then he has been at the Argonne National Laboratory. As expected, he took his last student, Earl Gasner, with him; Dr. Gasner finished his Ph.D. work at the Argonne National Laboratory in the area of laser-Raman spectroscopy.

During June 16, 17, and 18 of 1969 a symposium, arranged by Dr. Young's students, was held in his honor at the Chemistry Department of The University of Chicago. The symposium was titled "Structures of Water and Aqueous Solutions." A special session of the symposium was devoted to Young's mixture rules, and an important paper in that symposium was given by one of Dr. Young's oldest friends, Professor George Scatchard of the Massachusetts Institute of Technology. Twenty-eight talks were given at the symposium, beginning with the keynote talk given by Professor H. S. Frank. The articles that follow in this special issue of *The Journal of Physical Chemistry* constitute some of the talks given at the symposium in honor of T. F. Young.

THE JOURNAL OF PHYSICAL CHEMISTRY

Registered in U. S. Patent Office © Copyright, 1970, by the American Chemical Society

VOLUME 74, NUMBER 21 OCTOBER 15, 1970

Effective Pair Interactions in Liquids. Water

by F. H. Stillinger, Jr.

Bell Telephone Laboratories, Incorporated, Murray Hill, New Jersey 07974 (Received March 2, 1970)

A variational principle is proposed to determine an optimal "effective pair potential" v in liquids whose molecules actually experience nonadditive interactions. A formal perturbation method is outlined which in principle determines v iteratively. On account of the temperature and density dependence of v , and because this function contains a weak "tail" of macroscopic range, the usual statistical-mechanical expressions for energy, pressure, and isothermal compressibility suffer fundamental changes. The theory is applied to water, and tentative conclusions are offered about the way that the bare two-molecule potential differs from the liquid phase v for this substance.

I. Introduction

It is conventional to use pairwise-additive potentials in developing the formal theory of the liquid state.¹ This tactic apparently preserves most qualitative features of the observed properties of real liquids. It is also justified by the remarkable simplicity of expressions for thermodynamic energy and pressure that result from the pair potential assumption. Nowadays, electronic computer simulation of liquids^{2,3} has become routine, and in that context pairwise-additive potentials again prove convenient.

Unfortunately, there is evidence that the pairwise-additivity assumption commits significant quantitative errors even for nonpolar substances.⁴ Surely the situation is even worse for polar materials and ionic fluids in which large fluctuating electric fields exist. It is therefore clear in the strict sense that precise statistical-mechanical theory of real liquids requires inclusion of many-body forces.

We shall demonstrate nevertheless that a rational procedure exists for selection of a "best" approximate pair potential which incorporates the average effects of nonadditive potentials. This "effective pair potential" satisfies a variational principle that has been selected by the requirement that the sum of effective pair interactions preserves all local order as well as possible. Our

effective pair potential therefore differs in a fundamental way from the one advocated by Sinanoğlu,⁵⁻⁷ which was designed previously to reproduce the thermodynamic energy.

The next section, II, introduces the fundamental variational principle, and displays a few general results that may be derived therefrom. Section III provides details of a formal perturbative method of constructing the effective pair potential. The modifications of standard statistical-mechanical formulas for energy, pressure, and compressibility that result from temperature and density dependence of the effective pair potential are listed in section IV.

On account of its fundamental importance in the physical and biological sciences, water has been selected here to illustrate the application of the effective potential concept. Section V is devoted to this one liquid, and conclusions are offered there about the way that the

(1) S. A. Rice and P. Gray, "The Statistical Mechanics of Simple Liquids," Interscience, New York, N. Y., 1965.

(2) W. W. Wood, *J. Chem. Phys.*, **48**, 415 (1968).

(3) B. J. Alder and T. E. Wainwright, *ibid.*, **33**, 1439 (1960).

(4) N. R. Kestner and O. Sinanoğlu, *ibid.*, **38**, 1730 (1963).

(5) O. Sinanoğlu, *Chem. Phys. Lett.*, **1**, 340 (1967).

(6) O. Sinanoğlu, *Advan. Chem. Phys.*, **12**, 283 (1967).

(7) T. Halcioglu and O. Sinanoğlu, *J. Chem. Phys.*, **49**, 996 (1968).

effective interaction differs at both large and small distances from the "bare" pair potential for two molecules *in vacuo*.

The final discussion in section VI outlines other important substances to which the present concepts could fruitfully be applied. Also we mention there possible conditions under which the effective pair potential method would have substantial shortcomings.

II. General Relations

Although the quantum-mechanical generalization is straightforward, we shall use classical statistics throughout the following analysis.

For any liquid of interest, we suppose that N molecules are confined to the interior of a large, but finite, vessel with volume \mathcal{V} . The configuration of each molecule will be described by a vector \mathbf{x} whose components comprise coordinates of the molecular center, and a set of angles to fix the molecular orientation. The free energy F for the liquid may in principle be obtained from the canonical partition function

$$\exp(-\beta F) = \frac{1}{N!} \left(\frac{\mathcal{V} Q_{\text{int}}(\beta)}{\Omega} \right)^N Z_N(\beta)$$

$$\beta = 1/kT; \quad \Omega = \int d\mathbf{x} \quad (2.1)$$

Here, Q_{int} is essentially the rotational-vibrational partition function for an isolated molecule, and Z_N is the N -molecule configuration integral.

We shall let $V_N(\mathbf{x}_1 \dots \mathbf{x}_N)$ stand for the total potential of interaction among the N molecules in the specified configuration $\mathbf{x}_1 \dots \mathbf{x}_N$. The classical configuration integral Z_N appearing in eq 2.1 hence may be written

$$Z_N(\beta) = \int d\mathbf{x}_1 \dots \int d\mathbf{x}_N \exp[-\beta V_N(\mathbf{x}_1 \dots \mathbf{x}_N)] \quad (2.2)$$

Although we do not explicitly indicate them, the integration limits on the \mathbf{x}_j are all finite, and depend upon the volume \mathcal{V} for molecular center positions, and upon the specific choice of orientation angles. It is convenient to introduce now an inner product of two functions, $f(\mathbf{x}_1 \dots \mathbf{x}_N)$ and $h(\mathbf{x}_1 \dots \mathbf{x}_N)$, as the integral of their product with the same finite limits as used in eq 2.2.

$$\{f, h\} = \int d\mathbf{x}_1 \dots \int d\mathbf{x}_N f(\mathbf{x}_1 \dots \mathbf{x}_N) h(\mathbf{x}_1 \dots \mathbf{x}_N) \quad (2.3)$$

In concordance with this definition, we can express Z_N as the inner product of a function with itself

$$Z_N(\beta) = \left\{ \exp(-1/2\beta V_N), \exp(-1/2\beta V_N) \right\} \quad (2.4)$$

The generic functions and their inner product in eq 2.3 are quite analogous to ordinary vectors and the scalar product for pairs of such vectors. Indeed it is valid to regard functions f and h as infinite-dimensional vectors whose scalar product is given in eq 2.3. By the same token, eq 2.4 exhibits Z_N as the square of an infinite-dimensional vector. The square of the dis-

tance between two vectors (functions) f and h may also be expressed as an inner product

$$D^2(f, h) = \{f - h, f - h\} = \int d\mathbf{x}_1 \dots \int d\mathbf{x}_N [f(\mathbf{x}_1 \dots \mathbf{x}_N) - h(\mathbf{x}_1 \dots \mathbf{x}_N)]^2 \quad (2.5)$$

in complete analogy with ordinary vectors.

Our central problem in this paper consists in finding an optimal effective pair interaction $v(\mathbf{x}_i, \mathbf{x}_j)$ to represent the liquid which is actually subject to the very complicated nonadditive potential V_N . In the convention of eq 2.4, we seek to approximate Z_N by an inner product of the form

$$\left\{ \exp\left[-\frac{1}{2}\beta \sum_{i < j=1}^N v(ij)\right], \exp\left[-\frac{1}{2}\beta \sum_{i < j=1}^N v(ij)\right] \right\} \quad (2.6)$$

The effective pair potential v clearly should be chosen to minimize the distance between the function-space vectors appearing in eq 2.4 and 2.6

$$D^2\left\{ \exp[-1/2\beta V_N], \exp[-1/2\beta \sum v(ij)] \right\} = \text{minimum} \quad (2.7)$$

or

$$\min = \int d\mathbf{x}_1 \dots \int d\mathbf{x}_N \left\{ \exp\left[-\frac{\beta}{2} V_N(1 \dots N)\right] - \exp\left[-\frac{1}{2}\beta \sum v(ij)\right] \right\}^2 \quad (2.8)$$

This constitutes the basic variational principle of our effective potential theory.

If it were to happen that

$$V_N(\mathbf{x}_1 \dots \mathbf{x}_N) = \sum_{i < j=1}^N V_2(\mathbf{x}_i, \mathbf{x}_j) \quad (2.9)$$

in other words that the exact N -molecule potential were a pairwise sum of exact 2-molecule potentials, then certainly the variational principle (2.8) would force v to equal V_2 identically, and the distance D would be reduced to zero. However under the more realistic circumstance that V_N contains three-body, four-body, ... contributions, the minimum attainable D in eq 2.7 presumably is still greater than zero. We must bear in mind that the effective pair potential v which produces that minimum D can be both temperature and density dependent.

The functional equation which determines v may be obtained by setting equal to zero the first functional derivative of the right member of (2.8) with respect to $v(\mathbf{x}_i, \mathbf{x}_j)$. One finds

$$\int d\mathbf{x}_3 \dots \int d\mathbf{x}_N \exp\{-1/2\beta [V_N + \sum v(ij)]\} = \int d\mathbf{x}_3 \dots \int d\mathbf{x}_N \exp\{-\beta \sum v(ij)\} \quad (2.10)$$

which must be obeyed for all $\mathbf{x}_1, \mathbf{x}_2$. We will suppose for convenience that periodic boundary conditions apply to \mathcal{V} ; since V_N then possesses full translation in-

variance, so too will v . If \mathcal{U} is macroscopically large and the system is in a fluid phase exclusively, then v will also possess the rotational invariance expected of a pair of rigid bodies in space.

In view of the multidimensional integrals it contains, nonlinear integral eq 2.10 is not trivial to solve for v (though we outline an iterative method in the next section). Nevertheless, some general characteristics of v may be deduced directly from eq 2.10. If both sides of that equation are integrated with respect to \mathbf{x}_1 and \mathbf{x}_2 , one finds

$$Z_N \{ \sum v(ij) \} = Z_N \{ {}^{1/2}V_N + {}^{1/2} \sum v(ij) \} \quad (2.11)$$

in other words the configuration integrals are equal for two hypothetical assemblies of N molecules, the first of which interacts with the additive effective potential, and the second of which interacts with the *average* of V_N and the additive effective potential. Of course neither of the two Z_N in eq 2.11 necessarily equals the liquid's correct configuration integral, $Z_N \{ V_N \}$, but still we can use the Schwartz inequality⁸ to establish

$$Z_N \{ V_N \} Z_N \{ \sum v(ij) \} \geq Z_N^2 \{ {}^{1/2}V_N + {}^{1/2} \sum v(ij) \} \quad (2.12)$$

By referring to eq 2.11, we conclude that

$$Z_N \{ V_N \} \geq Z_N \{ \sum v(ij) \} \quad (2.13)$$

In view of eq 2.1 therefore, it is clear that replacement of an actual V_N by its optimal effective pairwise potential approximation never lowers the free energy

$$F \{ V_N \} \leq F \{ \sum v(ij) \} \quad (2.14)$$

A somewhat more general result follows from Hölder's inequality,⁸ namely

$$Z_N^{1/p} \{ {}^{1/2p}V_N \} Z_N^{1/q} \{ {}^{1/2q} \sum v(ij) \} \geq Z_N \{ {}^{1/2}V_N + {}^{1/2} \sum v(ij) \} \\ p, q > 1; \quad (1/p) + (1/q) = 1 \quad (2.15)$$

The previous eq 2.12 corresponds to $p = q = 2$. In terms of free energies all computed at the same temperature and density

$$\frac{1}{p} F \left\{ \frac{p}{2} V_N \right\} + \frac{1}{q} F \left\{ \frac{q}{2} \sum v(ij) \right\} \leq F \left\{ \frac{1}{2} V_N + \frac{1}{2} \sum v(ij) \right\} \quad (2.16)$$

The set of n -molecule correlation functions for the liquid is defined as

$$g^{(n)}(\mathbf{x}_1 \dots \mathbf{x}_n) = \frac{\int \Omega^n \int d\mathbf{x}_{n+1} \dots \int d\mathbf{x}_N \exp[-\beta V_N(\mathbf{x}_1 \dots \mathbf{x}_N)]}{\int d\mathbf{x}_1 \dots \int d\mathbf{x}_N \exp[-\beta V_N(\mathbf{x}_1 \dots \mathbf{x}_N)]} \quad (2.17)$$

In the large \mathcal{U} limit, and as the n molecules mutually separate from one another, $g^{(n)}$ approaches unity. With

obvious modifications, definition 2.17 applies equally for other intermolecular potentials besides V_N . Equations 2.10 and 2.11 allow us to conclude

$$g^{(2)}(\mathbf{x}_1, \mathbf{x}_2 | \sum v(ij)) = g^{(2)}(\mathbf{x}_1, \mathbf{x}_2 | {}^{1/2}V_N + {}^{1/2} \sum v(ij)) \quad (2.18)$$

so that like Z_N , the pair correlation function is identically the same for the additive effect potential, and for the average of V_N with this additive effective potential. Unfortunately it is not possible to obtain $g^{(2)}$ inequalities analogous to eq 2.12–2.16.

III. Perturbation Expansion

It is always possible to separate V_N into a part attributable strictly to bare pair interactions V_2 and a remainder V^\dagger comprising all many-body effects

$$V_N(\mathbf{x}_1 \dots \mathbf{x}_N) = \sum_{i < j = 1}^N V_2(\mathbf{x}_i, \mathbf{x}_j) + \lambda V^\dagger(\mathbf{x}_1 \dots \mathbf{x}_N) \quad (3.1)$$

The "coupling constant" λ introduced here has no fundamental significance, and will be used only to generate an iterative construction for v . At the end of that construction, we will set $\lambda = 1$. Corresponding to 3.1, there will be a formal λ series for v

$$v(\mathbf{x}_i, \mathbf{x}_j) = \sum_{n=0}^{\infty} \lambda^n v_n(\mathbf{x}_i, \mathbf{x}_j) \quad (3.2)$$

where of course

$$v_0(\mathbf{x}_i, \mathbf{x}_j) \equiv V_2(\mathbf{x}_i, \mathbf{x}_j) \quad (3.3)$$

Insert expressions 3.1 and 3.2 into the basic v eq 2.10, and expand the exponential functions into λ power series. The result appears as

$$0 = \int d\mathbf{x}_3 \dots \int d\mathbf{x}_N \exp \left[-\beta \sum_{i < j = 1}^N V_2(ij) \right] \times \\ \left\{ \lambda \left[\sum_{i < j = 1}^N v_1(ij) - V^\dagger(1 \dots N) \right] + \right. \\ \lambda^2 \left[\sum_{i < j = 1}^N v_2(ij) + \frac{\beta}{4} \left(V^\dagger + \sum_{i < j = 1}^N v_1(ij) \right)^2 - \right. \\ \left. \beta \left(\sum_{i < j = 1}^N v_1(ij) \right)^2 \right] + \lambda^3 \left[\sum_{i < j = 1}^N v_3(ij) + \right. \\ \left. \beta \left(V^\dagger - 3 \sum_{i < j = 1}^N v_1(ij) \right) \sum_{k < l = 1}^N v_2(kl) - \frac{\beta^2}{24} \times \right. \\ \left. \left(V^\dagger + \sum_{i < j = 1}^N v_1(ij) \right)^3 + \frac{\beta^2}{3} \left(\sum_{i < j = 1}^N v_1(ij) \right)^3 \right] + 0(\lambda^4) \left. \right\} \quad (3.4)$$

Since λ may be regarded at this stage as an arbitrary parameter, the terms of different order in λ in eq 3.4 must separately vanish. The first-order equation

(8) F. Riesz and B. Sz.-Nagy, "Functional Analysis," Frederick Ungar Publishing Co., New York, N. Y., 1955, pp 40–43.

$$0 = \int d\mathbf{x}_3 \dots \int d\mathbf{x}_N \exp \left[-\beta \sum_{i < j=1}^N V_2(ij) \right] \times \left[\sum_{i < j=1}^N v_1(ij) - V^\dagger(1 \dots N) \right] \quad (3.5)$$

is a linear integral equation for determining v_1 in terms of V^\dagger . Once v_1 has been obtained, the second-order equation

$$0 = \int d\mathbf{x}_3 \dots \int d\mathbf{x}_N \exp \left[-\beta \sum_{i < j=1}^N V_2(ij) \right] \times \left[\sum_{i < j=1}^N v_2(ij) + \frac{\beta}{4} \left(V^\dagger(1 \dots N) + \sum_{i < j=1}^N v_1(ij) \right)^2 - \beta \left(\sum_{i < j=1}^N v_1(ij) \right)^2 \right] \quad (3.6)$$

similarly determines v_2 , once V^\dagger and the previously calculated v_1 are inserted. This trend persists to all succeeding orders; the λ^n -order linear integral equation requires knowledge of V^\dagger and each of the previously determined $v_1 \dots v_{n-1}$. Hence one has in principle an iterative technique for constructing the effective pair interaction v .

We now examine the first-order integral eq 3.5 in depth. The average value of V^\dagger in the assembly of N molecules interacting only *via* direct pair potentials V_2 may be written thus

$$N\epsilon_1^\dagger = [Z_N \{ \sum V_2(ij) \}]^{-1} \times \int d\mathbf{x}_1 \dots \int d\mathbf{x}_N V^\dagger(1 \dots N) \exp \left[-\beta \sum_{i < j=1}^N V_2(ij) \right] \quad (3.7)$$

where the average value per molecule, ϵ_1^\dagger , clearly depends on both temperature and density. The analogous average of V^\dagger when molecules 1 and 2 are constrained to preassigned configurations \mathbf{x}_1 and \mathbf{x}_2 may next be expressed as

$$[N\epsilon_1^\dagger + f_1^\dagger(\mathbf{x}_1, \mathbf{x}_2)] g^{(2,0)}(\mathbf{x}_1, \mathbf{x}_2) = \frac{\Omega^2}{Z_N \{ \sum V_2(ij) \}} \int d\mathbf{x}_3 \dots \int d\mathbf{x}_N V^\dagger(1 \dots N) \times \exp \left[-\beta \sum_{i < j=1}^N V_2(ij) \right] \quad (3.8)$$

Here and in the following, the $g^{(n,0)}$ stand for correlation functions

$$g^{(n,0)} \equiv g^{(n)} \left(\mathbf{x}_1 \dots \mathbf{x}_n \left| \sum_{i < j=1}^N V_2(ij) \right. \right) \quad (3.9)$$

for molecules interacting only through the V_2 sum. The quantity f_1^\dagger in eq 3.8 represents the variation in the V^\dagger average at small distances between 1 and 2 due to local order in the liquid. We expect f_1^\dagger to decay rapidly to zero with increasing separation.

If eq 3.5 is multiplied throughout by $\Omega^2/Z_N \{ \sum V_2 \}$, the result may be transformed to yield

$$N\epsilon_1^\dagger + f_1^\dagger(12) = v_1(12) + \frac{N-2}{\Omega} \int d\mathbf{x}_3 [v_1(13) + v_1(23)] \frac{g^{(3,0)}(123)}{g^{(2,0)}(12)} + \frac{(N-2)(N-3)}{2\Omega^2} \int d\mathbf{x}_3 \int d\mathbf{x}_4 v_1(34) \frac{g^{(4,0)}(1234)}{g^{(2,0)}(12)} \quad (3.10)$$

Set

$$v_1(\mathbf{x}_1, \mathbf{x}_2) = \frac{2\epsilon_1^\dagger}{N-1} + \hat{v}_1(\mathbf{x}_1, \mathbf{x}_2) \quad (3.11)$$

when this expression is inserted in eq 3.10, the quantity ϵ_1^\dagger drops out entirely to leave a linear integral equation for \hat{v}_1

$$f_1^\dagger(12) = \hat{v}_1(12) + \frac{N-2}{\Omega} \int d\mathbf{x}_3 [\hat{v}_1(13) + \hat{v}_1(23)] \frac{g^{(3,0)}(123)}{g^{(2,0)}(12)} + \frac{(N-2)(N-3)}{2\Omega^2} \times \int d\mathbf{x}_3 \int d\mathbf{x}_4 \hat{v}_1(34) \frac{g^{(4,0)}(1234)}{g^{(2,0)}(12)} \quad (3.12)$$

Had the many-body potential V^\dagger been at the outset a constant independent of molecular configurations, then f_1^\dagger would have vanished identically and the implied v_1 would have been equal precisely to $2\epsilon_1^\dagger/(N-1)$ for all pairs. Evidently \hat{v}_1 for more general V^\dagger will be confined primarily to small pair distances, as dictated by the nonvanishing of f_1^\dagger there.

Although one normally is concerned with very large systems and hence large N , it is extremely important not to drop the very small constant term proportional to $(N-1)^{-1}$ in the right member of eq 3.11. After all, this is a very long-ranged contribution to the effective potential, and acts on all $N(N-1)/2$ molecular pairs at once. The totality of these long-range effective interactions consequently is proportional to N , and therefore provides a nonvanishing effect on the free energy in the conventional large-system limit.

A comparison of eq 3.7 and 3.8 allows one to conclude

$$0 = \frac{1}{\Omega} \int d\mathbf{x}_1 \int d\mathbf{x}_2 f_1^\dagger(\mathbf{x}_1, \mathbf{x}_2) g^{(2,0)}(\mathbf{x}_1, \mathbf{x}_2) \quad (3.13)$$

Next multiply both sides of eq 3.12 by $\Omega^{-1}g^{(2,0)}(12)$ and integrate with respect to \mathbf{x}_1 and \mathbf{x}_2 to obtain (for the finite system function \hat{v}_1)

$$0 = \frac{1}{\Omega} \int d\mathbf{x}_1 \int d\mathbf{x}_2 \hat{v}_1(\mathbf{x}_1, \mathbf{x}_2) g^{(2,0)}(\mathbf{x}_1, \mathbf{x}_2) \quad (3.14)$$

This last relation allows us to put integral eq 3.12 into a form most suitable for passage to the conventional large-system limit

$$f_1^\dagger(12) = \vartheta_1(12) + \frac{N-2}{\Omega} \int d\mathbf{x}_3 [\vartheta_1(13) + \vartheta_1(23)] \frac{g^{(3,0)}(123)}{g^{(2,0)}(12)} + \frac{(N-2)(N-3)}{2\Omega^2} \int d\mathbf{x}_3 \int d\mathbf{x}_4 \vartheta_1(34) \times \left[\frac{g^{(4,0)}(1234)}{g^{(2,0)}(12)} - g^{(2,0)}(34) \right] \quad (3.15)$$

Now the integrals will become strictly confined to regions of molecular size. Of course

$$\frac{N-2}{\Omega} \rightarrow \rho^{(i)}, \quad \frac{(N-2)(N-3)}{2\Omega} \rightarrow \frac{(\rho^{(i)})^2}{2} \quad (3.16)$$

in that large-system limit, where $\rho^{(i)}$ is the fixed singlet density N/Ω .

Equation 3.15 is the basic first-order equation that must in principle be solved for ϑ_1 . In a practical sense that would be very difficult, though nowadays evaluation of integrals of the type it contains is becoming increasingly more feasible with rapid electronic computers. As section V below will illustrate, however, that equation may be used (without being fully solved) to infer important features of the effective potential for specific substances.

There may well exist applications in which the many-body potential V^\dagger has significant magnitude, but for which the error incurred in the first-order estimate $v(ij) \cong V_2 + v_1(ij)$ is quite small. In this connection it should be realized that the free energy F is unchanged to linear order in λ by replacement of V^\dagger by the effective pair-potential sum, due to the extremum character of our variational principle. Likewise, the pair correlation function will be unchanged through first order in λ upon making that potential replacement.

The concepts involved in the first-order equation which generates v_1 (i.e., ϵ_1^\dagger and ϑ_1) from a given V^\dagger may readily be applied in succeeding orders. To do so, it is useful to recognize that the first-order calculation amounts to a linear projection operation \mathbf{P}

$$\mathbf{P}V^\dagger(1\dots N) = \sum_{i<j=1}^N v_1(ij) \quad (3.17)$$

$$\mathbf{P}^2 = \mathbf{P} \quad (3.18)$$

The second of these relations is required for all projections, and states in the present case that any potential V^\dagger already in pairwise additive form is carried identically into the effective potential.

By comparing the second-order eq 3.6 with the first-order eq 3.5 we see that

$$\mathbf{P} \left\{ \beta \left[\sum_{i<j=1}^N v_1(ij) \right]^2 - \frac{\beta}{4} \left[V^\dagger(1\dots N) + \sum_{i<j=1}^N v_1(ij) \right]^2 \right\} = \sum_{i<j=1}^N v_2(ij) \quad (3.19)$$

in other words, the second-order effective pair potential

v_2 is projected out of a combination of V^\dagger and v_1 just as v_1 before was projected out of V^\dagger . Equation 3.19 may be rewritten thus

$$\mathbf{P}V_2^\dagger(1\dots N) = \sum_{i<j=1}^N v_2(ij)$$

$$V_2^\dagger(1\dots N) = \frac{\beta}{4} \left[3 \sum_{i<j=1}^N v_1(ij) + V^\dagger(1\dots N) \right] \times \left[\sum_{k<l=1}^N v_1(kl) - V^\dagger(1\dots N) \right] \quad (3.20)$$

which shows directly that if V^\dagger is a pairwise additive function (which becomes identified in first order as $\sum v_1(ij)$), then v_2 vanishes identically. One incidentally sees here from the factor β in V_2^\dagger that v_2 will tend toward zero as the temperature is raised at fixed density.

The detailed procedure of carrying out the projection in second order is entirely the same as before. The new "many-body potential" V_2^\dagger takes the place of V^\dagger , and by the same strategy as shown by eq 3.7 and 3.8 with V_2^\dagger inserted for V^\dagger , one first computes ϵ_2^\dagger and $f_2^\dagger(\mathbf{x}_1, \mathbf{x}_2)$. Then after writing

$$v_2(\mathbf{x}_1, \mathbf{x}_2) = \frac{2\epsilon_2^\dagger}{N-1} + \vartheta_2(\mathbf{x}_1, \mathbf{x}_2) \quad (3.21)$$

in direct correspondence with eq 3.11 for v_1 , we will have a linear integral equation for determination of the short-range second-order function ϑ_2 which is isomorphous with eq 3.12 above. Second-order analogs of integral conditions 3.13 and 3.14 are also available, and they lead finally to the second-order version of eq 3.15

$$f_2^\dagger(2) = \vartheta_2(12) + \frac{N-2}{\Omega} \int d\mathbf{x}_3 \times [\vartheta_2(13) + \vartheta_2(23)] \frac{g^{(3,0)}(123)}{g^{(2,0)}(12)} + \frac{(N-2)(N-3)}{2\Omega^2} \int d\mathbf{x}_3 \int d\mathbf{x}_4 \vartheta_2(34) \left[\frac{g^{(4,0)}(1234)}{g^{(2,0)}(12)} - g^{(2,0)}(34) \right] \quad (3.22)$$

In the projection-operator terminology, the third-order equation is

$$\mathbf{P} \left\{ \frac{\beta^2}{24} [V^\dagger - \sum v_1(ij)] [(V^\dagger)^2 + 4V^\dagger \sum v_1(ij) + 7(\sum v_1(ij))^2] - \beta [V^\dagger - 3 \sum v_1(ij)] \sum v_2(ij) \right\} = \sum v_3(ij) \quad (3.23)$$

If V^\dagger is pairwise additive, this relation shows that v_3 would vanish as v_2 would. In the high temperature regime, v_3 will be proportional to β^2 .

By continuation of the procedure we have outlined,

we would eventually obtain (appropriate to the large-system limit functions $\hat{\nu}_n$ and $g^{(n,0)}$)

$$\epsilon = \sum_{n=1}^{\infty} \left[\epsilon_n^\dagger - \frac{\rho^{(1)}}{2} \int d\mathbf{x}_2 \hat{\nu}_n(\mathbf{x}_1, \mathbf{x}_2) g^{(2,0)}(\mathbf{x}_1, \mathbf{x}_2) \right]$$

$$\hat{\nu}(\mathbf{x}_1, \mathbf{x}_2) = V_2(\mathbf{x}_1, \mathbf{x}_2) + \sum_{n=1}^{\infty} \hat{\nu}_n(\mathbf{x}_1, \mathbf{x}_2) \quad (3.24)$$

after having set λ equal to unity. The corresponding effective pair potential approximation to the partition function thereupon becomes

$$\exp(-\beta F) \cong \frac{1}{N!} \left(\frac{\mathcal{U} Q_{\text{int}}(\beta)}{\Omega} \right)^N \exp(-N\beta\epsilon) \times$$

$$\int d\mathbf{x}_1 \dots \int d\mathbf{x}_N \exp \left[-\beta \sum_{i < j=1}^N \hat{\nu}(\mathbf{x}_i, \mathbf{x}_j) \right] \quad (3.25)$$

IV. Effective Pair Potential Formulas

A criterion has now been advanced for representing a given substance by a "model substance," whose hypothetical molecules interact by the effective pairwise-additive potential which optimally preserves the original local order. The next step must be deduction of the thermodynamic properties of this model substance, and to that end we shall now derive statistical-mechanical expressions for mean energy, pressure, and compressibility. This task is rendered nontrivial by the density and temperature dependence of the effective pair potential. In this section we shall denote correlation functions in the model system by an extra superscript "m"

$$g^{(n,m)}(1 \dots n) \equiv g^{(n)}(1 \dots n | \sum v(ij)) \quad (4.1)$$

and $\hat{\nu}$ will be strictly the infinite-system limit function.

The thermodynamic energy E may be obtained from the Helmholtz free energy F by means of the thermodynamic relation

$$E = \left(\frac{\partial \beta F}{\partial \beta} \right)_{N, \mathcal{U}} \quad (4.2)$$

By applying this operation to the logarithm of the model partition function (3.25), one finds the energy per particle to be

$$\frac{E}{N} = \frac{E_0}{N} + \left(\frac{\partial \beta \epsilon}{\partial \beta} \right)_{N, \mathcal{U}} + \frac{N-1}{2\Omega^2} \times$$

$$\int d\mathbf{x}_1 \int d\mathbf{x}_2 \left(\frac{\partial \beta \hat{\nu}(12)}{\partial \beta} \right)_{N, \mathcal{U}} g^{(2,m)}(12) \quad (4.3)$$

where E_0 is the zero-density energy for N widely separated molecules. This general result is equally applicable to all phases, fluid or crystalline. If the model system is in the liquid state and is macroscopically large, then both $\hat{\nu}$ and $g^{(2,m)}$ depend only on relative configuration coordinates so that eq 4.3 may be simplified somewhat to

$$\frac{E}{N} = \frac{E_0}{N} + \left(\frac{\partial \beta \epsilon}{\partial \beta} \right)_{N, \mathcal{U}} + \frac{\rho^{(1)}}{2} \int d\mathbf{x}_2 \left(\frac{\partial \beta \hat{\nu}(12)}{\partial \beta} \right)_{N, \mathcal{U}} g^{(2,m)}(12)$$

$$\rho^{(1)} = \frac{N}{\Omega} \quad (4.4)$$

The pressure in the model system may be computed from

$$p = - \left(\frac{\partial F}{\partial \mathcal{U}} \right)_{N, \beta} \quad (4.5)$$

If once again we utilize eq 3.25 for F , the result may be expressed in terms of a $g^{(2,m)}$ integral by using Green's technique for volume differentiation of configuration integrals.⁹ One finds for the fluid phases

$$\frac{\beta p}{\rho} = 1 + \beta \rho \left(\frac{\partial \epsilon}{\partial \rho} \right)_\beta - \frac{\beta \mathcal{U} \rho}{2\Omega} \int d\mathbf{x}_2 \left\{ \frac{1}{3} \mathbf{r}_{12} \cdot \nabla_{\mathbf{r}_{12}} \hat{\nu}(12) - \right.$$

$$\left. \rho \left(\frac{\partial \hat{\nu}(12)}{\partial \rho} \right)_\beta \right\} g^{(2,m)}(12), \quad \rho = \frac{N}{\mathcal{U}} = \frac{\Omega \rho^{(1)}}{\mathcal{U}} \quad (4.6)$$

The vector \mathbf{r}_{12} is the spatial separation between the centers of molecules 1 and 2, and the gradient operator following it in eq 4.6 acts only on those position coordinates.

The isothermal compressibility κ_T is defined as

$$\kappa_T = \frac{1}{\rho} \left(\frac{\partial \rho}{\partial p} \right)_\beta \quad (4.7)$$

or equivalently

$$\left(\frac{\partial \beta p}{\partial \rho} \right)_\beta = \frac{\beta}{\rho \kappa_T} \quad (4.8)$$

Now set

$$\frac{\beta}{\rho \kappa_T} = 1 - \frac{\beta \mathcal{U} \rho}{6\Omega} \int d\mathbf{x}_2 \mathbf{r}_{12} \cdot \nabla_{\mathbf{r}_{12}} \hat{\nu}(12) \times$$

$$\left[2g^{(2,m)}(12) + \rho \left(\frac{\partial g^{(2,m)}(12)}{\partial \rho} \right)_{\beta, \hat{\nu}} \right] \quad (4.9)$$

by indicating that $\hat{\nu}$ is held fixed in the partial derivative of $g^{(2,m)}$, we mean to include *only* the contribution due to the explicit variation in density, and not the implicit variation occurring through variation of the effective potential. We can verify from eq 4.6 and 4.8 that κ_T is the isothermal compressibility for a system of molecules that interact at *all* temperatures and densities with a short-range potential that coincidentally equals $\hat{\nu}$ when the latter is evaluated at the actual temperature and density of interest. The general fluctuation-compressibility theorem¹⁰ applies in the case of such temperature and density independent interactions of short range, and allows us to write

(9) H. S. Green, "The Molecular Theory of Fluids," North-Holland Publishing Co., Amsterdam, 1952, p 51.

(10) T. L. Hill, "Statistical Mechanics," McGraw-Hill, New York, N. Y., 1956, p 236.

$$\frac{\rho \kappa_T}{\beta} = 1 + \frac{\mathcal{U}}{\Omega} \int d\mathbf{x}_2 [g^{(2,m)}(12) - 1] \quad (4.10)$$

The pair correlation function occurring here must strictly be taken as the infinite-system limit function, before the integration is carried out.

After eq 4.6 is multiplied throughout by ρ , the application of an isothermal density derivative leads to the following compressibility formula

$$\begin{aligned} \frac{\beta}{\rho \kappa_T} &= \frac{\beta}{\rho \kappa_T} + \beta \frac{\partial}{\partial \rho} \rho^2 \left(\frac{\partial \epsilon}{\partial \rho} \right)_\beta + \\ &\frac{\beta \mathcal{U} \rho^2}{2\Omega} \int d\mathbf{x}_2 \left(\frac{\partial \hat{\phi}(12)}{\partial \rho} \right)_\beta \left(\frac{\partial g^{(2,m)}(12)}{\partial \rho} \right)_{\beta, \hat{v}} - \\ &\frac{\beta \mathcal{U} \rho^2}{2\Omega} \int d\mathbf{x}_2 \left\{ \frac{1}{3} \mathbf{r}_{12} \cdot \nabla_{12} \left(\frac{\partial \hat{\phi}(12)}{\partial \rho} \right)_\beta - 3 \left(\frac{\partial \hat{\phi}(12)}{\partial \rho} \right)_\beta - \right. \\ &\left. \rho \left(\frac{\partial^2 \hat{\phi}(12)}{\partial \rho^2} \right)_\beta \right\} g^{(2,m)}(12) - \frac{\beta \mathcal{U} \rho^2}{2\Omega} \times \\ &\int d\mathbf{x}_2 \int d\mathbf{x}_3 \int d\mathbf{x}_4 \left\{ \frac{1}{3} \mathbf{r}_{12} \cdot \nabla_{12} \hat{\phi}(12) - \rho \left(\frac{\partial \hat{\phi}(12)}{\partial \rho} \right)_\beta \right\} \times \\ &\frac{\delta g^{(2,m)}(12)}{\delta \hat{\phi}(34)} \left(\frac{\partial \hat{\phi}(34)}{\partial \rho} \right)_\beta \quad (4.11) \end{aligned}$$

The implicit density variation of $g^{(2,m)}$ through $\hat{\phi}$ enters this last expression *via* the functional derivative

$$\begin{aligned} \frac{\delta g^{(2,m)}(12)}{\delta \hat{\phi}(34)} &= -\frac{1}{2} \beta (\rho^{(1)})^2 [g^{(4,m)}(1234) - \\ &g^{(2,m)}(12)g^{(2,m)}(34)] - \beta \rho^{(1)} [g^{(3,m)}(124) \times \\ &\delta(\mathbf{x}_1 - \mathbf{x}_3) + g^{(3,m)}(123)\delta(\mathbf{x}_2 - \mathbf{x}_4)] - \\ &\beta g^{(2,m)}(12)\delta(\mathbf{x}_1 - \mathbf{x}_3)\delta(\mathbf{x}_2 - \mathbf{x}_4) \quad (4.12) \end{aligned}$$

Under conventional circumstances one expects an expression of type 4.10 to yield the isothermal compressibility of a fluid system. Indeed that is invariably true with interactions of limited range, whether those interactions are pairwise additive or not. However the model system effective pair potential has essentially infinite range. This infinite range is clear enough in the constant "tail" $2\epsilon/(N-1)$ of $\hat{v}(\mathbf{x}_1, \mathbf{x}_2)$, but it is also manifest in the density dependence of $v(\mathbf{x}_1, \mathbf{x}_2)$ as extra particles are placed into the volume \mathcal{U} macroscopically far from molecules 1 and 2. The terms in κ_T expression 4.11 following the one containing κ_T are the direct result of these long-ranged contributions.

The compressibility κ_T measures the local (but large-dimension) density fluctuations in the effective potential model system. It is this local compressibility which determines the intensity of X-ray scattering extrapolated to zero scattering angle. Conventionally this would be identical with the thermodynamic compressibility for an overall compression of the entire system, but the long-range interactions induce a difference. The magnitude of $\kappa_T - \kappa_T$ hence measures the

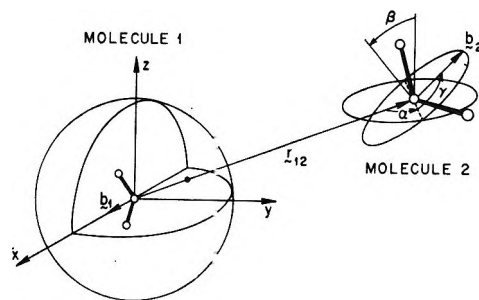


Figure 1. Relative configuration variables for a pair of water molecules. r_{12} is the separation between the oxygen nuclei, and b_1 and b_2 are unit vectors along the molecular symmetry axes. Euler angles α, β, γ are an ordered set of rotations which carry the orientation of molecule 1 into that of molecule 2. Configurations for which r_{12} does not pierce the sphere quadrant as shown may be generated by reflection in symmetry planes xy or xz or both.

inability of the model system to mimic the local density fluctuations of the initial real liquid. If the effective potential approximation has validity, this difference should be small.

V. Application to Water

The water molecule possesses C_{2v} symmetry. Measurements indicate¹¹ that an isolated molecule incorporates O-H bonds of length 0.957 Å, and an angle between these bonds at the oxygen nucleus of 104.5°. Consequently we treat each molecule in the liquid as a rigid asymmetric rotor with the same symmetry. Each configuration vector \mathbf{x}_i will involve six components: three to specify the Cartesian coordinates of the oxygen nucleus, plus three Euler angles to fix the molecule's orientation in space.

The three normal modes of vibration, ν_1, ν_2 , and ν_3 , for the water molecule occur at 3656.65, 1594.59, and 3755.79 cm^{-1} .¹² At room temperature these vibrations are virtually all unexcited, so the partition function for internal degrees of freedom will contain the factor

$$\exp[-1/2\beta h(\nu_1 + \nu_2 + \nu_3)] \quad (5.1)$$

The potential energy V_2 for an isolated pair of water molecules depends irreducibly upon six relative configuration variables. Figure 1 shows that these variables may be taken to be the polar coordinates of the second oxygen nucleus relative to the first, and Euler angles for the rotation which would carry the first molecule into the orientation of the second. Figure 1 also demonstrates that the O-O polar coordinates need only be considered in one quadrant, since the other configurations differ only by symmetry operations permitted by the molecular C_{2v} symmetry. For fluid phases, the functions $\hat{\phi}$ and $g^{(2,m)}$ depend on the same

(11) D. Eisenberg and W. Kauzmann, "The Structure and Properties of Water," Oxford University Press, New York, N. Y., 1969, p. 4.

(12) Reference 11, p. 7.

relative configuration variables as V_2 , and exhibit the same symmetry properties.

The many-body potential $V^\dagger(1 \dots N)$ is surely significant in liquid water. Since the isolated molecules have a large permanent dipole moment (1.84 D), there must be large local fluctuating electric fields in the liquid. These fields polarize the molecules, and the correspondingly modified molecular moments in turn affect the fluctuating fields.

At small distances, hydrogen bonding is the most important aspect of water molecule interactions. This type of interaction is already manifest in V_2 , which would plunge to about -5 kcal/mol for a fully formed, essentially linear, hydrogen bond.¹³ However it has been suggested^{14,15} that the energy of hydrogen bonding is not additive, and detailed quantum-mechanical calculations support this hypothesis. Although energy nonadditivity is found to be nonuniform in sign,¹⁶ the predominant influence of sequential sets of hydrogen bonds in any condensed phase appears to amount to an effective strengthening of each hydrogen bond.^{16,17}

Thus it appears that V^\dagger is negative for most configurations of interest in liquid water. The quantity $\epsilon(\beta, \rho)$ is most likely dominated by $\epsilon_1^\dagger(\beta, \rho)$, and since eq 3.7 shows this latter to be a canonical average of V^\dagger , we tentatively conclude that

$$\epsilon(\beta, \rho) \leq 0 \quad (5.2)$$

for liquid water. Although ϵ provides an important contribution to the water model-system chemical potential (and therefore affects that model system's phase changes), it has the same numerical value for all molecular configurations. Consequently it has no effect whatever upon the local order established by the molecules in the model system.

On the other hand it is clear that the difference between the bare two-molecule potential V_2 and the short-range effective pair potential \hat{v} is directly reflected in the local molecular arrangements. Without having to solve the sequence of linear \hat{v}_n integral equations derived in the previous section, we can with some confidence infer the major features of the difference between V_2 and \hat{v} , by keeping in mind that this difference must be selected to produce substantially the same structural shifts as V^\dagger .

The best currently available *ab initio* Hartree-Fock calculations of V_2 indicate that the lowest energy for a pair of water molecules is achieved in the configuration shown in Figure 2. The O-O distance is 3.00 \AA , and the energy of the hydrogen bond at that nuclear configuration is -4.72 kcal/mol.¹⁶

Within the regular hexagonal ice lattice one can identify sequences of hydrogen bonds of any length passing from oxygen to oxygen. As already pointed out, these sequential groupings (the most common type for a given large number of molecules) produce extra energy stabilization beyond that for just V_2 interac-

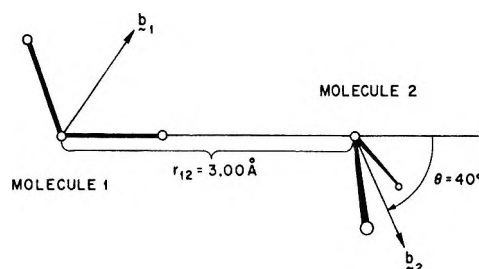


Figure 2. Stable water-molecule pair configuration according to Hartree-Fock calculations (ref 16). Molecules 1 and 2 lie in perpendicular planes.

tions. It has also been established (at least for sequential triplets) that this hydrogen-bond nonadditivity contribution to V^\dagger acts to compress distances in the crystal.

The melting of ice to produce liquid water obviously adds configurational disorder: the new phase lacks long-range periodicity and exhibits fluidity. Still, the melting energy only amounts to about one-eighth of the crystal's sublimation energy, so the liquid presumably consists of a random space-filling network of strained hydrogen bonds, incorporating occasional broken bonds and interstitials. Indeed the X-ray scattering from water¹⁸ shows that this network is spatially quite homogeneous (not broken up into disconnected "clusters"), and retains the local propensity for tetrahedral coordination that always appears in the ices and clathrates.¹⁹

Although hydrogen-bond sequences may be somewhat fewer in number and shorter in average length in the liquid compared to ice, they should still exert the same stabilizing and compressing effects. The short-range effective potential \hat{v} can produce the same result by exhibiting a deeper hydrogen-bond energy minimum than V_2 , at a somewhat smaller O-O distance. Figure 3 illustrates this presumption by comparing schematic V_2 and \hat{v} curves for r_{12} variation in the configuration shown in Figure 2. One must keep in mind here that a deepening of the hydrogen-bond part of the pair potential must be compensated by a rise for some other configurations, since eq 3.14 and its analogs for $\hat{v}_2, \hat{v}_3, \dots$ imply for liquid water that in a finite system

$$0 = \int d\mathbf{x}_2 [V_2(\mathbf{x}_1, \mathbf{x}_2) - \hat{v}(\mathbf{x}_1, \mathbf{x}_2)] g^{(2,0)}(\mathbf{x}_1, \mathbf{x}_2) \quad (5.3)$$

But in any event the primary structural effect here is a strengthening of the hydrogen bonds in the random

(13) P. A. Kollman and L. C. Allen, *J. Chem. Phys.*, **51**, 3286 (1969).

(14) H. S. Frank and W. Y. Wen, *Disc. Faraday Soc.*, **24**, 133 (1957).

(15) H. S. Frank, *Proc. Roy. Soc.*, **A247**, 481 (1958).

(16) D. Hankins, J. W. Moskowitz, and F. H. Stillinger, *Chem. Phys. Lett.*, **4**, 527 (1970).

(17) J. DelBene and J. A. Pople, *ibid.*, **4**, 426 (1969).

(18) A. H. Narten and H. A. Levy, *Science*, **165**, 447 (1969).

(19) G. A. Jeffrey and R. K. McMullan, *Progr. Inorg. Chem.*, **8**, 43 (1967).

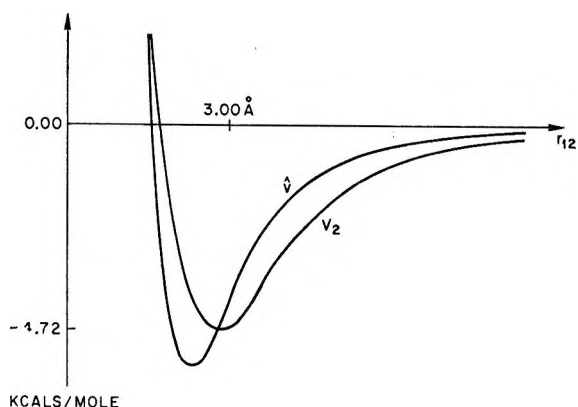


Figure 3. Qualitative shift expected between V_2 and $\hat{\phi}$. The hydrogen-bond nonadditivity effect of sequential groupings of molecules in the liquid deepen the minimum and move it to shorter O-O distance. The pair geometry is the one shown in Figure 2, except for the r_{12} variation. The V_2 minimum parameters shown are taken from ref 16.

liquid network, so at a given temperature $\hat{\phi}$ produces more hydrogen bonds on the average than V_2 alone would produce.

The quantity V^\dagger very likely also affects the directionality of hydrogen bonding in liquid water. Hartree-Fock calculations^{13,16,20} agree that the θ variation of V_2 in the pair arrangement shown in Figure 2 (with fixed r_{12} and maintaining the symmetry plane) gives a broad and flat featureless minimum. Consequently the lone pairs of electrons in the valence shell of the proton acceptor molecule must be quite delocalized. In particular this θ variation of V_2 fails to display relative minima localized about $\theta = +54^\circ 44'$ and $\theta = -54^\circ 44'$, the characteristic angles for perfect tetrahedral coordination about the acceptor molecule oxygen nucleus.

According to Coulson²¹ the observed bond angle in water implies substantial hybridization of the oxygen 2s and 2p orbitals involved in the bonding. The lone pairs of electrons on the oxygen are therefore also partially hybridized. However it is clear that the hybridization is not of the full sp^3 type that obtains in methane,²² so indeed the full set of tetrahedral coordination directions is not inherent in the electronic structure of an isolated water molecule.

Tetrahedral coordination however appears to occur with high probability in the liquid. Consistent with this presumption, consider a pair of water molecules in the configuration shown in Figure 2, but with θ equal to $\pm 54^\circ 44'$. The resulting hydrogen bond along one of these ideal tetrahedral directions surely will increase the degree of hybridization of the acceptor oxygen toward pure sp^3 , and the lone pair of electrons not involved in that hydrogen bond will then be more localized along the remaining tetrahedral direction. Consequently the formation of a second hydrogen bond to the acceptor oxygen (right-hand molecule in Figure 2) will be confined to that remaining tetrahedral direction. This

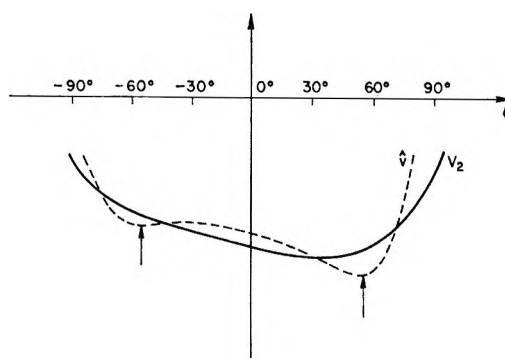


Figure 4. Angular variation of V_2 and $\hat{\phi}$. Figure 2 gives the relevant configurations, with only θ varying. As a result of enhanced hybridization of oxygen orbitals in the liquid, one expects $\hat{\phi}$ to be depressed relative to V_2 at the ideal tetrahedral angles indicated by arrows.

argues in favor of a cooperativity to tetrahedral geometry in that initial formation of tetrahedral hydrogen bonding facilitates extension of that local geometry in further hydrogen bonding. As advocated, this amounts to a three-molecule effect.

The effective pair potential $\hat{\phi}$ consequently should manifest those tetrahedral angles more obviously than V_2 . As Figure 4 indicates, we surmise that $\hat{\phi}$ should be depressed relative to V_2 at the ideal tetrahedral angles. The model system would then exhibit the enhanced extent of local tetrahedral order that is possible in real water as a result of nonadditive contributions to the potential energy in the latter.

As a final aspect of the qualitative behavior of $\hat{\phi}$ for water, we inquire about the large r_{12} regime. For these large distances it is known²³ that the pair correlation function behaves thus

$$g^{(2)}(\mathbf{x}_1, \mathbf{x}_2) - 1 \sim -\frac{9g_K(D-1)}{4\pi\rho(2D+1)} \mathbf{b}_1 \cdot \mathbf{T}_{12} \cdot \mathbf{b}_2$$

$$\mathbf{T}_{12} = \frac{1}{r_{12}^3} \left[1 - \frac{3\mathbf{r}_{12}\mathbf{r}_{12}}{r_{12}^2} \right] \quad (5.4)$$

In this expression, the \mathbf{b} 's are unit vectors along the molecular symmetry axes, D is the static dielectric constant, and g_K is the Kirkwood²⁴ orientational correlation function

$$g_K = 1 + \frac{\rho}{8\pi^2} \int d\mathbf{x}_2 (\mathbf{b}_1 \cdot \mathbf{b}_2) g^{(2)}(\mathbf{x}_1, \mathbf{x}_2) \quad (5.5)$$

(20) K. Morokuma and L. Pedersen, *J. Chem. Phys.*, **48**, 3275 (1968).

(21) C. A. Coulson, "Valence," Oxford University Press, New York, N. Y., 1961, p 221.

(22) R. F. W. Bader, *J. Amer. Chem. Soc.*, **86**, 5070 (1964).

(23) A. Ben-Naim and F. H. Stillinger, "Aspects of the Statistical Mechanical Theory of Water" in "Structure and Transport Processes in Water and Aqueous Solutions," R. A. Horne, Ed., Wiley, New York, N. Y., in press.

(24) J. G. Kirkwood, *J. Chem. Phys.*, **7**, 911 (1939).

We shall assume that the first-order perturbation estimate of \hat{v} as outlined in section III above predicts the correct qualitative trend at large r_{12} . In this order of approximation we know that $g^{(2)}$ and $g^{(2,m)}$ agree, so in fact g_K will be the same in the model system subject to \hat{v} as in the real liquid. Equation 5.4 then shows that the static dielectric constant D will also be the same in first order.

The true molecular pair interaction V_2 at large separation possesses dipole-dipole behavior

$$V_2(\mathbf{x}_1, \mathbf{x}_2) \sim \mu_v^2 \mathbf{b}_1 \cdot \mathbf{T}_{12} \cdot \mathbf{b}_2 \quad (5.6)$$

appropriate for the dipole moment $\mu_v = 1.84$ D of an isolated molecule under vacuum. Two principal modifications of this form will be produced by many-body interactions in the liquid. (a) There will be an enhancement of the dipole moment μ_v to a larger average value μ_l due to charge transfer and polarization in hydrogen bonding with the molecule's immediate neighbors. (b) A form of dielectric shielding of $V_2(12)$ by intervening molecules will take place, even if these molecules are not permitted to reorient in the electric field of molecules 1 and 2. This polarization is partly electronic, but also involves nuclear displacement in the three normal vibrational modes at fixed molecular orientation. The appropriate dielectric constant D_{ir} refers experimentally to a wavelength range around 0.1–1.0 mm.

The first-order perturbation eq 3.15 is designed to assure that the mean value of the many-body interactions V^\dagger as a function of $\mathbf{x}_1, \mathbf{x}_2$ is the same as the mean of $N\epsilon_1 + \sum v_1(ij)$. In particular the right side of that equation has terms giving: (1) the effective interaction acting directly between molecules 1 and 2; (2) the effective interaction of 1 with 2's "correlation cloud" and of 2 with 1's correlation cloud; and (3) the effective potential between the two correlation clouds. Effects a and b above suggest that $\hat{v} (\cong V_2 + \hat{v}_1)$ at large r_{12} acts as the interaction of two point dipoles μ_l embedded in a dielectric medium with constant D_{ir} , and each (for computational simplicity) located centrally in an otherwise empty spherical cavity. An elementary computation then yields

$$\begin{aligned} \hat{v}(\mathbf{x}_1, \mathbf{x}_2) &\cong V_2(\mathbf{x}_1, \mathbf{x}_2) + \hat{v}_1(\mathbf{x}_1, \mathbf{x}_2) \\ &\sim \frac{9D_{ir}}{(2D_{ir} + 1)^2} \left(\frac{\mu_l}{\mu_v}\right)^2 V_2(\mathbf{x}_1, \mathbf{x}_2) \end{aligned} \quad (5.7)$$

When the liquid is at or near its melting point, μ_l is probably close to the molecular dipole moment in ice. This latter has been estimated²⁵ to be 2.95 D. Furthermore, the high-frequency dielectric constant has been reported to be 4.5.²⁶ Using these numbers we find

$$\frac{9D_{ir}}{(2D_{ir} + 1)^2} \left(\frac{\mu_l}{\mu_v}\right)^2 = 1.03 \quad (5.8)$$

Considering the uncertainty of μ_l and D_{ir} , this factor

should be regarded as currently indistinguishable from unity. It is curious that in the large r_{12} regime apparently little modification of V_2 is required; effects a and b above essentially cancel each other.

VI. Discussion

(1) The N -molecule potential $V_N(\mathbf{x}_1 \dots \mathbf{x}_N)$ was regarded above as temperature independent. In most applications (including water at ordinary temperatures) this assumption is correct. But neighboring molecules in interaction with each other tend to perturb their vibrational frequencies. If these internal vibrations are thermally excited under the ambient conditions, then the appropriate potential function, which includes a shift in vibrational free energy, becomes a function of temperature: $V_N(\mathbf{x}_1 \dots \mathbf{x}_N; \beta)$. However this elaboration in no way changes the effective potential formalism presented above.

(2) Besides water, liquid metals provide an interesting class of fluids for application of the effective pair potential technique. The ions in a liquid metal move about under the influence of some potential function $V_N(\mathbf{r}_1 \dots \mathbf{r}_N; \beta)$ that is strongly influenced by the presence of degenerate conduction electrons. Certainly this many-ion potential is not precisely resolvable into pair contributions, but for certain purposes it would be convenient to know the optimal effective pair potential approximation.^{27,28} For these substances in particular it should be possible experimentally to detect a difference between the two isothermal compressibilities κ_T and κ_T' .

(3) No barrier exists in principle to the extension of the effective potential method to liquid mixtures. Of course a distinct temperature and composition dependent effective potential $v_{ab}(\mathbf{x}_a, \mathbf{x}_b)$ would have to be introduced for each different pair of molecular species. The multicomponent version of variational principle (2.8) then would require minimization over variation of all these v_{ab} . A particularly interesting application would be fused salts, where one would look for the dielectric shielding of the Coulomb interaction at large ion pair separation, and for the extent to which the ϵ_a for different ions could be identified as Born cavity energies.²⁹

(4) The critical region for a fluid very likely will be more poorly described by the effective pair potential model than the liquid near the triple point. This does

(25) L. Onsager and M. Dupuis, "The Electrical Properties of Ice" in "Electrolytes," B. Pesce, Ed., Pergamon Press, New York, N. Y., 1962, p 27.

(26) E. H. Grant, T. J. Buchanan, and H. F. Cook, *J. Chem. Phys.*, **26**, 156 (1957).

(27) M. D. Johnson, P. Hutchinson, and N. H. March, *Proc. Roy. Soc.*, **A282**, 283 (1964).

(28) P. Ascarelli and R. J. Harrison, *Phys. Rev. Lett.*, **22**, 385 (1969).

(29) F. H. Stillinger, "Equilibrium Theory of Pure Fused Salts" in "Molten Salt Chemistry," M. Blander, Ed., Interscience, New York, N. Y., 1964.

not mean to say that the model fluid will necessarily fail to exhibit nonclassical critical exponents.³⁰ However, a fluid in the critical state has density fluctuations of large spatial extent and magnitude. The definition of $v(\mathbf{x}_1, \mathbf{x}_2; \beta, \rho)$ does not permit this function to adjust its density dependence to the local value of the density (which may be sensibly constant over many molecular diameters). Instead, only the overall density is recognized, and the average many-body structural effects built into v may be a significant misrepresentation. One possible outcome is a substantial displacement of the model system critical point from that of the real substance it attempts to imitate.

(5) In order to quantify our qualitative analysis of \hat{v} for water, an iterated series of quantum-mechanical and statistical-mechanical calculations should be carried out. One might start by guessing a reasonable approximation to \hat{v} , consistent with the few currently known facts about V_2 and the qualitative changes

taking V_2 to \hat{v} .³¹ By then using high-speed electronic computers to simulate the corresponding model liquid (via either a Monte Carlo or molecular dynamics technique), it would be possible to observe which local arrangements of molecules predominate in the liquid (at least as predicted by that approximate \hat{v}). These local arrangements of small groupings of, say, two to five molecules thereupon should be the ones examined by extensive and accurate quantum-mechanical calculations of V_2 and nonadditivity energies. With better estimates of the V_N , the computer liquid simulation could be used to refine \hat{v} (and estimate ϵ), and finally the entire procedure would be recycled until convergence obtained.

(30) M. E. Fisher, "Lectures in Theoretical Physics VII C," University of Colorado Press, Boulder, Colo., 1965, pp 1-159.

(31) One such choice for an analytic fit to \hat{v} for water is suggested in ref 23.

Approximate Methods for Determining the Structure of H₂O and HOD Using Near-Infrared Spectroscopy

by W. A. P. Luck* and W. Ditter

Hauptlaboratorium der Badischen Anilin- & Soda-Fabrik AG, Ludwigshafen/Rh., Germany (Received March 2, 1970)

Approximate methods are described for determining the H-bonded state of liquid water to the critical region. It is shown that differences between spectra of solutions, and liquids in the bulk, indicate H bonds having different angles and distances. Spectra from water in solution in HF and NH₃ and in the gas-hydrate state are also presented.

Various theories of liquids have been advanced that assume lattice-like structures having cavity defects. A simple application of such liquid models can be demonstrated for densities under saturation conditions (Figure 1). The upper parts of the curves show the densities of different liquids. At low temperatures the densities of normal liquids decrease with increasing temperature in a linear fashion. (Increasing amplitudes of thermal motions.) The straight lines at high temperatures are the geometrical locus of the sum of densities of liquid and vapor in the saturated state. (One consequence of this is known as the rule of Cailletet and Mathias.) In a simple model the straight line gives the density of an ideal liquid. (Density decreases only as a result of thermal motions.) In addition the model assumes that the density of a real liquid depends upon the num-

ber of cavity defects. The number of these defects in our model is exactly equal to the number of molecules in the vapor state. In liquids with hydrogen bonds (H bonds) we must also take orientation defects into account, because the H bonds are dependent upon the angle between the proton axis and the axis of the free electron pair of the H-bond acceptor.¹ Therefore, a lattice-like model of liquids having H bonds must also involve the orientational defects of open H bonds. These orientational defects are especially important for water. The goal of our experiments has thus been to obtain information about the concentration of these orientational defects in water, CH₃OH, and C₂H₅OH.

* To whom correspondence should be addressed.

(1) W. Luck, *Naturwissenschaften*, **52**, 25, 49 (1965); **54**, 601 (1967).

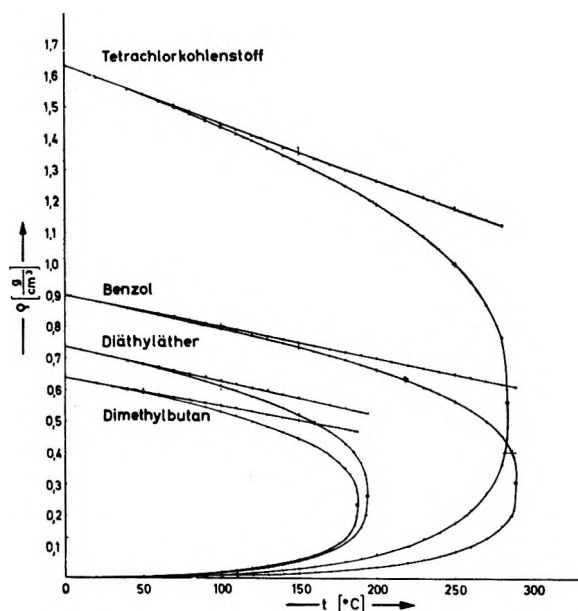


Figure 1. Curves, saturation density in liquid ρ_l and vapor state ρ_v ; straight line, extrapolated liquid density at low temperatures or $\rho_l + \rho_v$. (Tetrachlorkohlenstoff = CCl_4 , benzol = benzene, diäthyläther = diethyl ether, dimethylbutan = 2-methylbutane).

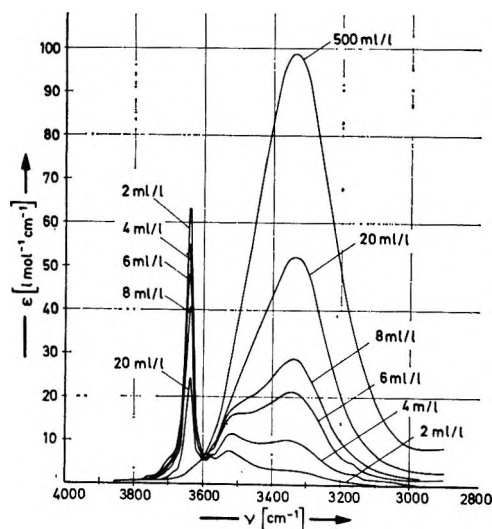


Figure 2. Fundamental OH vibration of CD_3OH in CCl_4 at room temperature: sharp free OH band, 3640 cm^{-1} ; H-bond band, 3340 cm^{-1} ; H-bond band of cyclic dimers, 3640 cm^{-1} .

One useful method for determining the number of closed H bonds is to determine the concentration dependence of the OH- or NH- vibrations from ir. Figure 2 shows extinction coefficients of solutions of CD_3OH in CCl_4 in the wavelength region of the fundamental OH stretching vibration. With increasing concentration the sharp OH band at 3640 cm^{-1} decreases in extinction. It can be related to the non-H-bonded OH groups (free OH groups). In the medium-concentration range a broader band appears at 3520 cm^{-1} . In the same concentration range a minimum is observed in

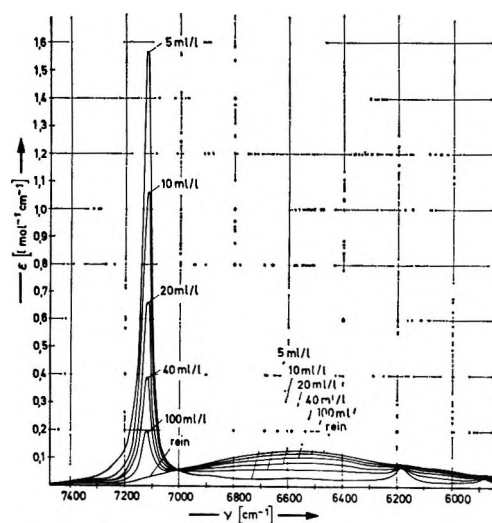


Figure 3. First overtone vibration of CD_3OH in CCl_4 at 20°C : sharp free OH band, 7120 cm^{-1} ; H-bond band, maximum 6550 cm^{-1} .

the dipole moment.^{2,3} This broader band can be related to energetically unfavored H bonds. The dipole moment minimum indicates the presence of cyclic dimers or higher aggregates in cyclic forms. At higher concentrations a broad and intense H-bond band appears at 3340 cm^{-1} . It is shifted down by 300 cm^{-1} from the free OH band. The first overtone spectra (Figure 3) show similar effects. But contrary to the fundamental band the intensity of the first overtone H-bond band is less and its frequency shift is about double. This makes it advantageous to employ overtone spectra in the study of broad liquid spectra because the overlapping between free and H-bond bands is less in the overtone region. In addition the photometric accuracy is much higher in the overtone region and the accuracy in the thicknesses of the absorption cells is also much higher. (Our experiments were conducted with the Cary Model 14 instrument.)

Investigations of the concentration dependences of the ir spectra make it possible to examine equilibria related to H-bond association. This method cannot be readily applied to water, however, because there are no solvents that dissolve water in sufficiently high concentrations without forming H bonds. We thus have two possibilities for study in this case.

1. Complexes of Water

We shall first examine complexes of water with organic molecules. (See ref 4.) The dashed curve (---) in Figure 4 shows a combination band of 5 g of water/l. of dioxane. (The spectrum of dioxane is subtracted by compensation in the reference beam.) The band that is

(2) R. Mecke and A. Reuter, *Z. Naturforsch. A*, **4**, 368 (1949).

(3) D. A. Ibbitson and L. F. Moore, *J. Chem. Soc. B*, 76 (1967).

(4) S. C. Mohr, W. D. Wilk, and G. M. Barrow, *J. Amer. Chem. Soc.*, **87**, 3048 (1965).

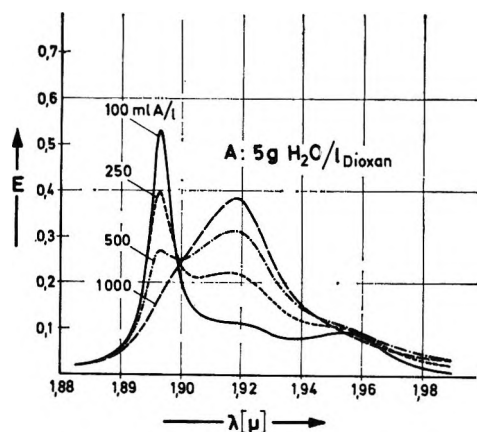


Figure 4. Combination band of H_2O diluted in dioxane: A = 5 g of H_2O /l. of dioxane, 20° , upper curves mixtures of A in CCl_4 , dioxane spectra compensated.

maximal at 1.92μ refers to the OH-combination band of water in the H-bonded state, water-dioxane. The other curves of Figure 4 are water spectra obtained by dilution of the mixture A = 5 g of H_2O /l. of dioxane with CCl_4 . (All spectra were obtained with a constant number of water molecules by keeping the product $C_{\text{H}_2\text{O}}d = 2.5$ ($\text{g l}^{-1} \text{cm}$), where d = cell thickness, constant.)

The new band of the dilute systems is in the wavelength range corresponding to the free-OH vibration. The appearance of two bands with a reasonably good isosbestic point indicates that the band with a maximum at 1.92μ belongs to water molecules with both OH groups H bonded to dioxane—the band in the short wavelength range belongs to free OH groups of water molecules whose second OH group is H bonded to dioxane. The free OH bond cannot belong to free water molecules without H bonds to dioxane because the solubility of water in CCl_4 is so small that nearly all water molecules must be in a complex-bonded form with dioxane.

The following experiments indicate that the change in the position of free OH bands of water is only small if the second OH group engages in H bond interactions with another molecule.

(a) van Thiel, Becker, and Pimentel⁵ employed the matrix technique (H_2O in solid N_2) at medium concentration and they observed a splitting of the free-OH vibration into two bands with a frequency difference of 25 cm^{-1} .

(b) Mohr, Wilk, and Barrow⁴ studied a series of mixtures, water-solvent, in the fundamental vibrational region in a manner similar to that used for Figure 4. If we plot their frequencies corresponding to the maximum of the free-OH water band against the frequency of the H-bond band, water-solvent (Figure 5),⁴ we obtain a straight line with a slope of about 10 cm^{-1} change in the band maximum of the free OH band per 115 cm^{-1} difference of the maximum of the H-bond band, water-solvent, to the maximum of the free-water

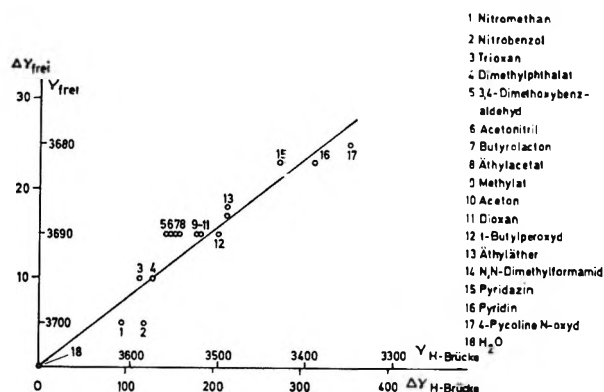


Figure 5. Frequency of the free OH fundamental vibration of H_2O as a function of the frequency of the band of H bonds: H_2O -different acceptors 1 to 17; diluted solutions in CCl_4 .⁴

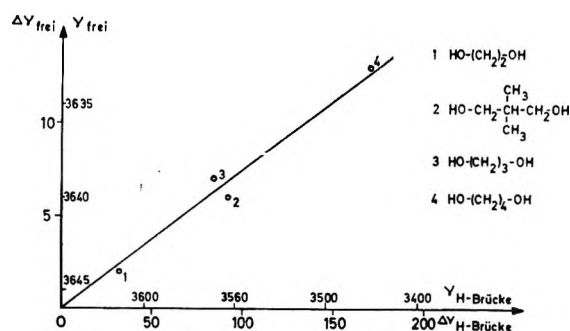


Figure 6. Frequency of the free OH fundamental vibration of dialcohols as a function of the frequency of the intramolecular H-bond band; diluted solutions in CCl_4 .

band, water in CCl_4 . From the point of view of the Badger-Baur rule the frequency shift of the abscissa is proportional to the H-bond interaction energy. Figure 5 allows us to make the statement that the frequency of the free-OH group in water shifts proportionately to the H-bond interaction energy of the second OH group.

(c) Dialcohols very dilute in CCl_4 show intramolecular H bonds.^{1,6} The spectra show a band of the intramolecular H-bonded OH group and a band of the second OH group that is not H bonded. With increasing number of CH_2 groups of aliphatic dialcohols the bond angle of the intramolecular H bond is favored.¹ Therefore, the H-bond interaction energy and the frequency shift of the H-bond band is favored. Figure 6 shows the relation between the frequency of the free-OH band and the band of the H-bonded OH group. Again we find a similar slope of 10 cm^{-1} change of the free OH band with a frequency shift of 130 cm^{-1} between the intramolecular H-bond band and the free-OH band.

(d) Results similar to those of Figure 4 were obtained with water- CH_3OH mixtures (Figure 7).

(5) M. van Thiel, E. D. Becker, and G. C. Pimentel, *J. Chem. Phys.*, **27**, 95, 243, 486 (1957).

(6) L. P. Kuhn, *J. Amer. Chem. Soc.*, **74**, 2492 (1952); **76**, 9323 (1954); **80**, 5950 (1958); **86**, 650 (1964); *J. Org. Chem.*, **28**, 721 (1963).

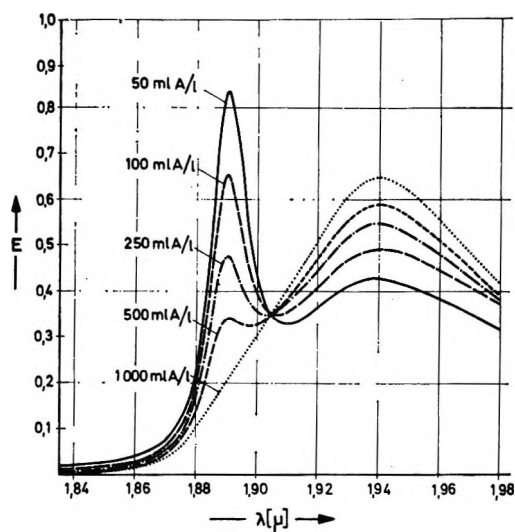


Figure 7. Dotted curve combination band of H₂O (diluted solution in CH₃OH) at 20°C: A = 20 g of H₂O/l. of CH₃OH; CH₃OH spectrum compensated, $d = 10$ cm; upper curves mixtures of A with CCl₄.

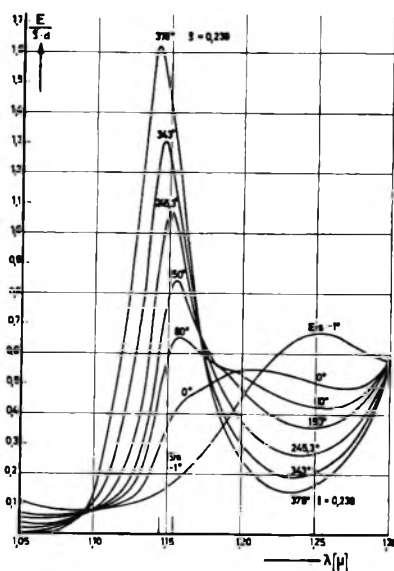


Figure 8. Combination band of liquid water under saturation conditions.

Compared to Figure 4 the H-bond band absorbs at a longer wavelength because of the stronger H-bond interaction. The spectra ($A = 5$ cm³ of H₂O/l. of dimethyl sulfoxide) are very similar to the spectra of Figure 7. The maximum of the H₂O-DMSO H-bond band occurs at 1.94 μ .

A comparison of Figure 7 and of the DMSO results with Figure 4 shows that the concentration of free OH in dioxane is larger in agreement with the smaller frequency shift (H-bond energy).

2. Temperature Dependence of Liquid Spectra

Examination of the temperature dependence of spectra from liquids presents the possibility of obtaining


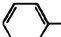
information about the H-bond state of liquids. This is accomplished with high-pressure cells.⁷ Figure 8 provides an example of one overtone band from liquid water under saturation conditions. With higher temperatures a band appears having its maximum in the region of free OH. The ice band gives information about the absorption due to ideal linear H bonds of water. Between the maxima of the ice band and the free-OH band at higher temperatures the intensity is higher than in the solution experiments. We have found the same situation by studying the temperature dependence of spectra from alcohols in bulk in comparison with the solution spectra.⁸

In the following section we shall give some indications of how higher intensities between the two bands that appear in the complex spectra (Figures 4 and 7) can be understood.

(a) Let us first consider the fact that the H-bond interaction depends upon the distance between the proton donor and proton acceptor.⁹ This can be demonstrated from the temperature dependence of the ice spectra (Figure 9). With lower temperatures the distances decrease and the H-bond interaction should increase. In agreement with this we find an increase of frequency shift of the ice band with decreasing temperature.

(b) The H-bond interaction depends upon the orientation of the H-bond systems.¹⁰ This can be

Table I: X-(CH₂)_n-OH, ^a $\Delta\nu$ (cm⁻¹)

X	n				
	1	2	3	4	5
Fundamental Stretching Vibration					
OH		30	78	156	153
OCH ₃		30	86	180	
CH ₂ =CH—	18	40			
	18	28	40		
HC≡C—		42	50		
First Overtone					
OH		58	150		
OCH ₃		70	(200)		
CH ₂ =CH—	32	79			
	40	67			

^a The angle between the proton axis of the OH group and the axis of the free electron pair orbital of the acceptor decreases with increasing n . For $n = 4$ this angle is zero and has a maximum.

(7) W. Luck, *Ber. Bunsenges. Phys. Chem.*, **69**, 626 (1965); *Z. Naturforsch. B*, **24**, 482 (1969).

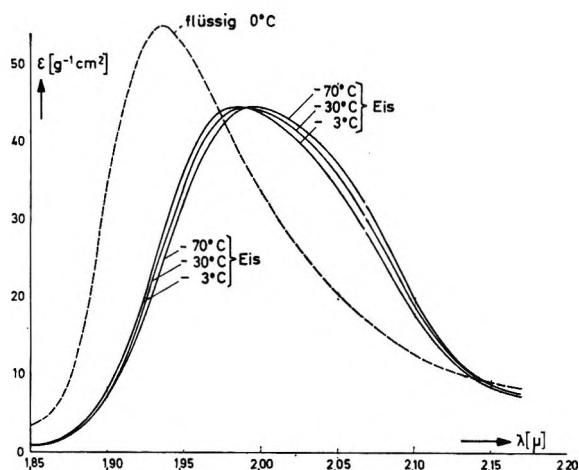
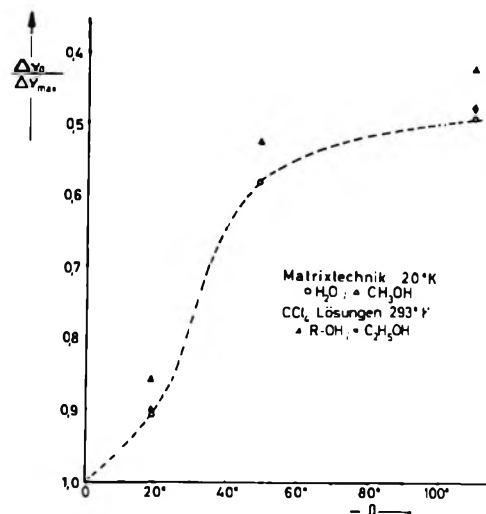
(8) W. A. P. Luck and W. Ditter, *Ber. Bunsenges. Phys. Chem.*, **72**, 365 (1968).

(9) T. T. Wall and D. F. Hornig, *J. Chem. Phys.*, **43**, 2079 (1965); W. A. P. Luck and W. Ditter, *J. Mol. Struct.*, **1**, 261 (1967-1968).

(10) W. G. Schneider, *J. Chem. Phys.*, **23**, 26 (1955); H. A. Staab, "Einführung in die Theoretische Organische Chemie," Verlag Chemie, Weinheim, 1959.

Table II

	H ₂ O						CH ₃ OH		
	ν	$\Delta\nu$	$\Delta\nu/\Delta\nu_{\max}$	ν	$\Delta\nu$	$\Delta\nu/\Delta\nu_{\max}$	ν	$\Delta\nu$	$\Delta\nu/\Delta\nu_{\max}$
Free OH in a free molecule	3725			3640			3660		
Free OH in a molecule whose second OH is H bonded	3700	25	0.06	3620	20	0.05			
H-bond band of a dimer	3545	180	0.46	3435	205	0.49	3490	170	0.42
H-bond band of a trimer	3510	215	0.55				3445	215	0.52
H-bond band of a tetramer	3390	335	0.86	3260	380	0.9	3290	370	0.9
Ideal H-bond band of a polymer	3335	390	1	3220	420	1	3250	410	1

Figure 9. Temperature dependence of the 2- μ combination band of ice.Figure 10. Angle dependence of the frequency shift $\Delta\nu_{\beta}$ between the free OH fundamental vibration and the H-bond band, standardized by division by the frequency shift $\Delta\nu_{\max}$ of the band of ideal H bonds (angle zero).

demonstrated by spectroscopic methods.¹ Studies of intramolecular H bonds of aliphatic molecules with proton donors and proton acceptors on the ends give the frequency shifts in Table I.¹¹

(c) The matrix studies with water⁵ give further indications of this angle effect of H bonds. The different bands found in the matrix technique can easily be analyzed as in Table II. If we assume that the aggregates are cyclic we can determine the angle between the proton axis and the axis of the free electron pair orbital or the H-bond acceptor. We thus obtain a relation between the H-bond band frequency shift, $\Delta\nu$, and the H-bond angles¹ (Figure 10). The data from the dimer agree with the frequency of the 3520-cm⁻¹ band observed in CCl₄ solutions (Figure 2). From the Badger-Baur rule, $\Delta\nu$ is proportional to the interaction energy. Figure 10 therefore provides approximate information about the effect of angle on the H-bond energy.

(d) Similar information about the effect of angle on the H bonds was obtained from the intramolecular H-bond data from oximes¹ and from the intramolecular H-bond data from dialcohols.¹

In bulk solvents we expect the intramolecular H bonds to have a distribution of H-bond angles and

distances. The X-ray scattering data show that the distance distribution function is not a continuum distribution function without accumulation at certain distances. Similar behavior is expected from the orientational distribution. Accumulation at angles is expected for values of $\beta = 0$ and at the angles of different cyclic aggregates. (In a cyclic dimer the total interaction energy is twice the interaction energy corresponding to $\beta = 109^\circ$; equal to about the energy of one H bond with $\beta = 0$, etc.) In addition from the point of view of Figure 10 we must expect an accumulation of $\Delta\nu$ values near $\Delta\nu = \Delta\nu_{\max}$ and $\Delta\nu \approx 0.5\Delta\nu_{\max}$.

The extinction coefficients of the maxima of the H-bond bands decrease with $\Delta\nu$ because of the increased broadening effect with $\Delta\nu$. This presents the spectroscopic possibility of recognizing the free-OH band, with $\beta \approx 180^\circ$. Such statements present a point of view between the continuum model of liquids^{12,13} and the

(11) W. A. P. Luck and W. Ditter, *Ber. Bunsenges. Phys. Chem.*, in press.

(12) M. Falk and T. A. Ford, *Can. J. Chem.*, **44**, 1699 (1966).

(13) V. Vand and W. A. Senior, *J. Chem. Phys.*, **43**, 1896 (1965).

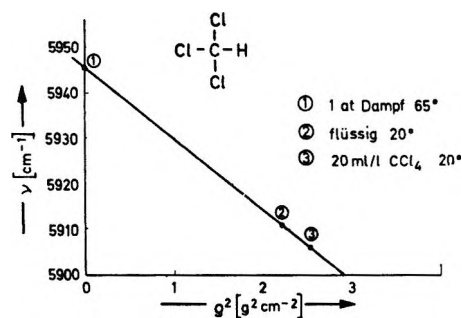


Figure 11. The density (ρ) dependence of a CH overtone band of chloroform.

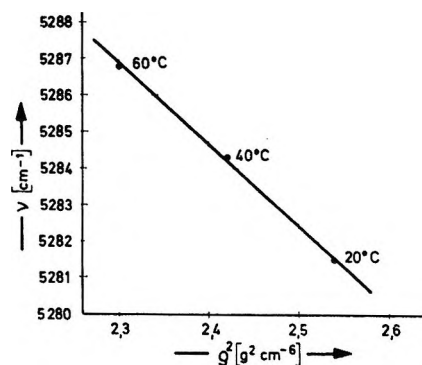


Figure 12. The density dependence of the maximum of a combination band of H₂O, diluted solutions in CCl₄ at different temperatures.

mixture model. However, the experiments with water-solvent complexes presented before indicate that this accumulation effect for certain angles cannot be neglected.

The complete analysis of different H bonds is not possible by ir methods because the effects of band overlap are severe. In addition Fermi resonance may occur between H-bond bands and some other weak bands. Therefore, we prefer to analyze the intensity of the free-OH vibration bands. The overlapping effects are small with H-bond bands in the region of the sharper free-OH bands. Effects of Fermi resonance with other weak bands can be cancelled by analysis of different overtone bands. Therefore, we have studied four H₂O overtone bands, two D₂O overtone bands, and one HOD overtone band.^{7,14,15} The determinations of free OH from these bands gave similar results. We thus conclude that Fermi-resonance effects cannot be very important in our method. Nevertheless, our method is only approximate. There are some weak overlapping effects involving H-bond bands. In addition the frequency of the free-OH band depends upon the density ρ of the environment. But this is a second-order effect. Empirically we found that the effect of environment is proportional to ρ^2 (Figures 11–13) for all systems that we studied. The environmental effects are listed as follows. The “jump” at the critical point in Figure 13

CCl ₃	$d(\Delta\nu)/d(\rho^2) \approx 15 \text{ cm}^{-1} \text{ g}^{-2} \text{ cm}^6$
H ₂ O in CCl ₄	$d(\Delta\nu)/d(\rho^2) \approx 20 \text{ cm}^{-1} \text{ g}^{-2} \text{ cm}^6$
Liquid HOD	$d(\Delta\nu)/d(\rho^2) \approx 60 \text{ cm}^{-1} \text{ g}^{-2} \text{ cm}^6$

may arise from the effect of the free-OH change in a molecule whose second OH is bonded to a free molecule with two free OH's (see section 1).

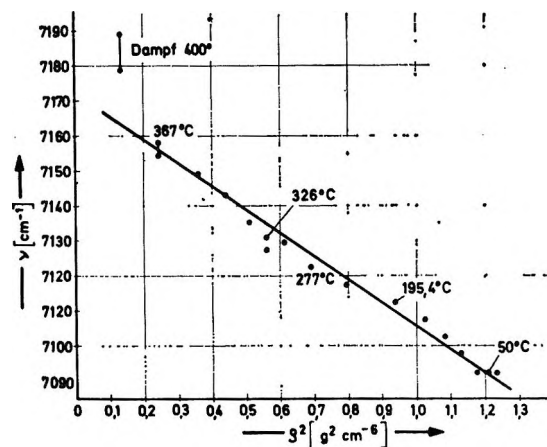


Figure 13. The density dependence of the first free-OH overtone band of HOD, liquid state under saturation conditions.

3. Analysis of the HOD Overtone Spectra

We shall demonstrate a method for determining the percentage of free OH's from the first overtone spectral band from HOD (Figure 14). With HOD the effects of overlapping between different bands are smaller—therefore the spectra are more useful. The second overtone of the OH stretch absorbs at 1.392 μ for $T > T_K$ (free OH) and at 1.562 μ in ice (ideal H bond). The 1.59 μ (free band) and the 1.718 μ (ice band) belong to a combination band. The combination band 1.59 to 1.718 μ has a frequency shift and an intensity quotient that are similar to the corresponding quantities for fundamental free and H-bond bands.^{12,16} Therefore this band is not useful for distinguishing between different bands (free, H-bond bands, etc). It is known¹⁵ that the possibility of observing peaks or shoulders from two overlapping bands depends upon the ratio of frequency shift $\Delta\nu$ to the half-width $\Delta\nu_{1/2}$ of the two bands. For two bands with the same intensity I and the same $\Delta\nu_{1/2}$, peaks or shoulders can only be observed if¹⁵

$$\Delta\nu > 0.85\Delta\nu_{1/2}$$

(14) W. Luck, *Fortschr. Chem. Forsch.*, **4**, 653 (1964); “Physico-Chemical Processes in Mixed Aqueous Solvents,” Heinemann, London, 1967, p 11; *Ber. Bunsenges. Phys. Chem.*, **67**, 186 (1963); W. Luck and W. Ditter, *ibid.*, **70**, 1113 (1966); W. Luck, G. Böttger, and H. Harders, *J. Phys. Chem.*, **71**, 459 (1967).

(15) W. Luck and W. Ditter, *J. Mol. Struct.*, **1**, 339 (1967–1968).

(16) E. U. Franck and K. Roth, *Discuss. Faraday Soc.*, **43**, 108 (1967).

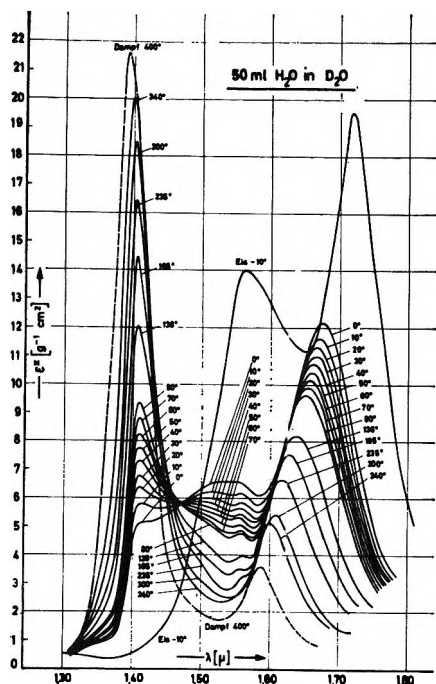


Figure 14. First overtone band (1.4–1.56 μ) and combination band (1.58–1.72 μ) of HOD (20 ml of H_2O /l. of D_2O) under saturation conditions.

If two bands overlap with different intensity or different $\Delta\nu_{1/2}$ the chance of observing peaks or shoulders is less.¹⁵

For HOD we obtain the data in Table III. Theoretical calculations involving the overlapping of two bands in conjunction with the data of Table III have shown¹⁵ that we cannot expect distinct indications of overlapping from bands of different species in the

Table III

	μ	$\Delta\nu/\Delta\nu_{1/2}$	$I(\text{free})/$ $I(\text{ice})$
Fundamental ¹⁶	4	~ 1.3	~ 0.2
Combination	1.59–1.718	1.15	0.18
First overtone	1.392–1.562	2.5	1.55

case of the HOD fundamental and combination band, but we must expect such indications for the overtone band. This provides a useful means of understanding statements in various articles dealing with spectra from water. The overtone spectra do not show isosbestic points for large temperature regions, but they give indications of isosbestic points for small temperature regions (Figure 8). In small temperature regions we can assume that water structure changes only by the change in the concentrations of two different species. But for the entire temperature region we should assume changes arising from more than two species. These may be open OH groups, and different types of H bonds.

As a first approximation we shall attempt to deter-

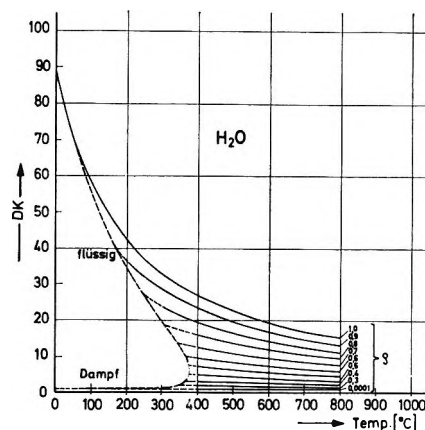


Figure 15. Dielectric constants of H_2O as functions of temperature and density (measurements see ref 17).

mine the percentage of free-OH groups that have no H-bond interactions by determining the optical density at the wavelength of the maxima for $T > T_K$. We shall assume that all H bonds are closed in ice, but that for $T > T_K$ all H bonds are open. The assumption for $T > T_K$ is only approximate. We arrive at this from the observation that for $\rho = \rho_K$ and $T > T_K$, the optical density of water is constant. This is not true for CH_3OH and $\text{C}_2\text{H}_5\text{OH}$, but for both of the alcohols it is true for $T > T_K$ (H_2O).⁸ This may mean that T_K for these alcohols depends upon the dispersion interaction of the CH groups and the H bond of the OH groups. But in the case of water the H bond dominates. The H-bond interaction of one OH group in water is similar in magnitude to that in alcohols. This follows from the $\Delta\nu$ of the H-bond bands.

In the case of water there may be a small amount of H-bond-like interactions above T_K , but examination of the dielectric constant data¹⁷ (Figure 15) shows that the remainder cannot be large. Figure 16 shows the percentage P of non-H-bonded OH groups of water under saturation conditions as a function of T . The approximate analysis of three different bands gives similar results.

Our approximation method neglects changes of extinction coefficients with T . Therefore, it may be preferable to determine P from the areas of bands. It may be shown that the area of the free-OH band in the case of a strong change in environment does not change during the temperature rise for saturated alcohol vapor.⁸ To minimize overlap effects we have taken only the area of the free-OH bands from short wavelength up to the maximum. Figure 17 gives the results for five different bands. The three bands involving the best experimental conditions agree very well with Figure 16. Therefore our approximate method for determining P can be examined, and it yields the experimental possibil-

(17) A. S. Quist and W. L. Marshall, *J. Phys. Chem.*, **69**, 3165 (1965).

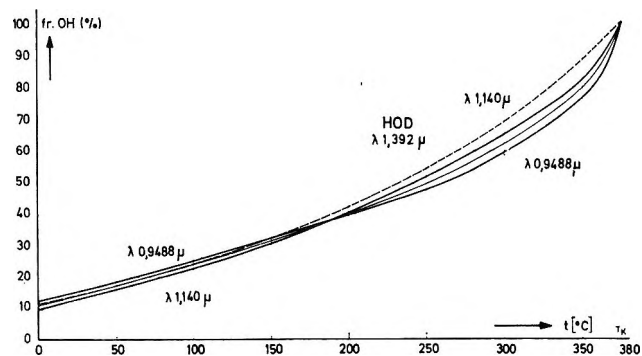


Figure 16. Percentage of free OH in liquid water under saturation conditions, determined by the optical density of different free OH bands of H_2O and one of HOD (values of first approximation).

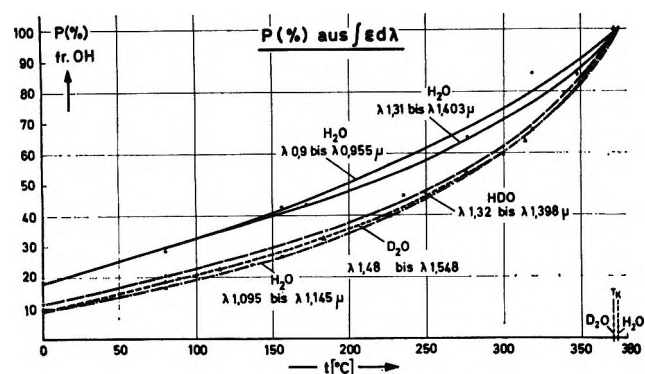


Figure 17. Percentage P of free OH in water, determined by the areas of different free-OH bands of H_2O , D_2O , and HOD (second approximation).

ity of obtaining information on the structure of various H-bonded liquids. For example Walrafen's Raman data from water¹⁸ agree very well with our ir data, and it is possible to show that with our experimental P values (Figure 17) one can calculate thermodynamic quantities for water and alcohols.¹⁹ This is possible only with the two-state approximation—free OH and H-bonded OH. This very simple model may mean that the second state is an average of H-bonded states. In addition we can show that not only the behavior of water, but also the profiles of all bands even to the fine details can be obtained by use of the Du Pont curve analyzer with three band systems: ice-like, free, and a broad band of energetically unfavored H bonds between the other two band systems.²⁰

Solution Spectra

The spectra of an aqueous electrolyte solution at a given temperature are similar to the spectra of pure water at some other temperature. If we classify ions in a series according to their influence on water spectra we obtain the lyotropic ion series identified by effects on water structure as follows.²¹ Some ions produce an increase in intensity in the wavelength region of free

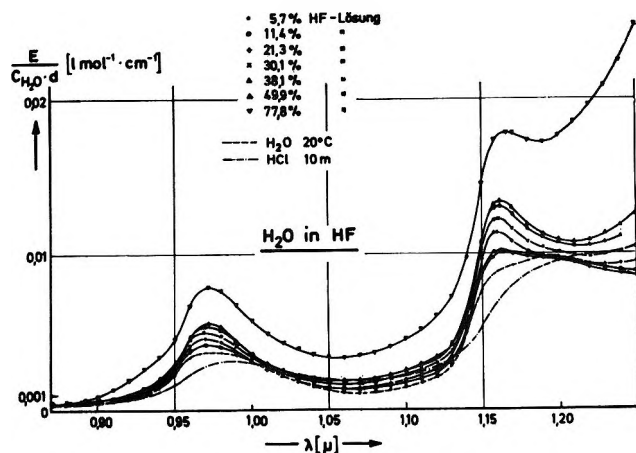


Figure 18. Extinction coefficients of water in H_2O -HF solutions. The intensity in the region of the free OH absorption increases with increasing concentration of HF.

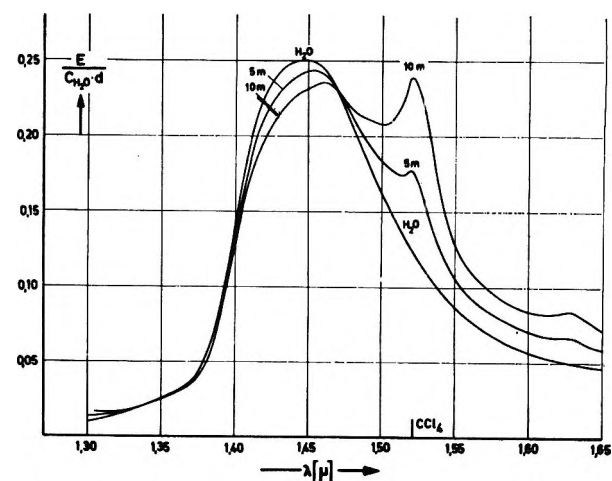


Figure 19. Optical density over water concentration of the first overtone band, solutions of NH_3 in water.

OH (structure breakers). As an example consider Figure 18 showing spectra from HF- H_2O mixtures. The strong association of HF seems to disturb the water structure, and in agreement with the spectroscopic results such mixtures yield a large density maximum as a function of composition.

Some ions produce a decrease of intensity in the region of the free-OH vibration (structure makers). As an example Figure 19 shows spectra from aqueous solutions of NH_3 —a decrease of intensity in the region of 1.4 to 1.45 μ is apparent in the figure. In addition these spectra give evidence of the NH vibration at 1.52 μ . The band maxima of NH_3 in CCl_4 are included in Figure

(18) G. E. Walrafen in "Hydrogen Bonded Solvent Systems," A. K. Covington and P. Jones, Ed., Taylor and Francis London, 1968.

(19) W. Luck, *Discuss. Faraday Soc.*, **43**, 115 (1967).

(20) W. Luck and W. Ditter, *Z. Naturforsch. B*, **24**, 482 (1969).

(21) W. Luck, *Ber. Bunsenges. Phys. Chem.*, **69**, 69 (1965).

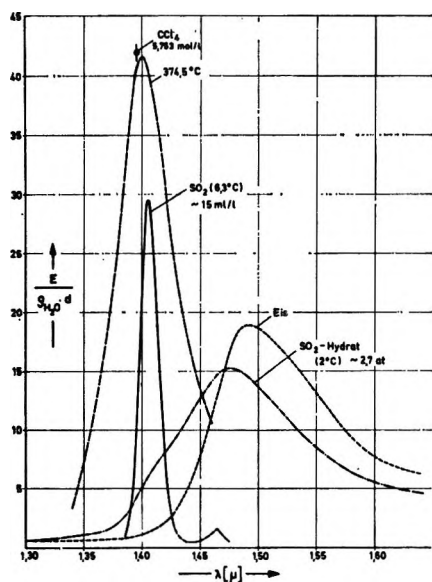


Figure 20. Extinction coefficients of the first overtone band of water at T_K , in different solutions, in ice, and of the gas hydrate in SO_2 . (Substitute 5.75 mmol/l. instead of 5.75 mol/l.)

19. The frequency of the NH band is not changed in the aqueous solution. This result could mean that NH_3 acts as an acceptor for free OH groups of water. The separation between ions having spectra that look like spectra of pure water at temperatures higher than the solution temperature (structure breakers) and ions having spectra that look like water at (relatively) lower temperatures (structure makers) depends upon the solution temperature.²¹ At higher temperatures the number of structure "breakers" decreases. The position of a given salt ion in this series depends mainly upon the anions; the role of the anions depends upon e^2/r .

Pauling has assumed in one article that liquid water has a gas-hydrate structure.²² A study of gas hydrates, therefore, is of interest. Figure 20 shows SO_2 gas-hydrate spectra in the solid state. In this system we found a broad ice-like band. The maximum is shifted to shorter wavelengths. We expected this because the

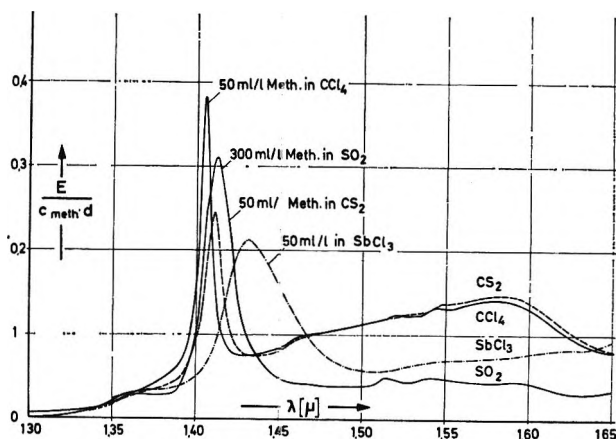


Figure 21. Extinction coefficients of the first CH_3OH overtone band, CH_3OH in different solutions at 20° . The spectrum of the SO_2 solutions indicates a small interaction of the OH protons with SO_2 , a small concentration of CH_3OH H-bond aggregates, and therefore a strong $\text{CH}_3\text{OH}-\text{SO}_2$ interaction.

water molecules in the gas-hydrate structure are primarily in five-membered rings with $\beta \approx 10^\circ$. The difference between the value of β and zero induces an unfavored H bond with a smaller $\Delta\nu$, compared to ice. The spectra of water diluted in SO_2 give only a small $\Delta\nu$ in comparison to water diluted in CCl_4 . This implies a small interaction between water protons and SO_2 .

It may be that special interactions exist between the O atoms of the OH groups and SO_2 . This is demonstrated by Figure 21. The figure indicates a small wavelength shift for the free OH vibration of methanol in liquid SO_2 . A comparison of this spectrum with spectra in different solvents shows a smaller intensity of the H-bond band (1.45 to 1.6 μ) for SO_2 as solvent. This agrees with the observation of complexes between SO_2 and ketones.²³

(22) L. Pauling in D. Hačzi, "Hydrogen Bonding," Pergamon Press, London, 1959, p 1.

(23) H. Winde, *Z. Phys. Chem. (Leipzig)*, 234, 225 (1967); "Gmelin's Handbuch der Anorganischen Chemie," 8 Aufl., Verlag Chemie, Weinheim, 1960, 9S [B] 1125.

A Neutron Inelastic Scattering Investigation of the Concentration and Anion Dependence of Low Frequency Motions of H₂O Molecules in Ionic Solutions¹

by P. S. Leung and G. J. Safford*

Union Carbide Corporation, Sterling Forest Research Center, Tuxedo, New York 10987 (Received March 2, 1970)

The dependences of intermolecular frequencies and of diffusive kinetics on concentration, on cation, and on anion have been investigated using neutron inelastic scattering for H₂O molecules in aqueous solutions. In CsCl, NaCl, and MgCl₂ solutions, water frequencies are observed up to concentrations of about 0.5 *m*. In contrast, characteristic frequencies of water persist to concentrations above 4.6 *m* for KCl, but for LiCl any correspondence with water frequencies is lost above 0.02 *m*. With further increases in concentration, intermolecular frequencies characteristic of primary ion-water hydration complexes appear and intensify. Below 25°, the diffusive kinetics were in accord with a delayed-diffusion mechanism. For dilute solutions (especially <0.5 *m*), the values of the self-diffusion coefficients (*D*) and residence times (τ_0) were nearly identical with those for water. At 1°, with increasing concentration, the *D*'s decrease and the τ_0 's increase relative to water for KF, NaCl, LiCl, MgCl₂, MgSO₄, and CrCl₃ ("positive hydration"), while the reverse is true for CsCl, CsBr, KSCN, KI, KBr, and KCl ("negative hydration"). However, for concentrated solutions of certain strongly hydrating cations (*e.g.*, Cr³⁺ and Li⁺), jump reorientations of individual waters in the primary layers are sufficiently restricted, so that diffusion of entire cation-water complexes is observed. For CsCl and CsBr, the *D*'s increase and the τ_0 's decrease initially with increasing concentration, but become nearly constant, due to increased ion pairing. For KSCN solutions, with increasing concentration *D* increases and τ_0 decreases initially relative to water. They then go through a maximum and minimum, respectively, and approach the values for water corresponding to a decrease in "negative hydration." Thus, while SCN⁻ ions increase the diffusive mobility in the solvent, reorientations of waters in primary hydration coordinations are at least as restricted as those in water. In concentrated solutions of small and/or highly charged cations (*i.e.*, Li⁺, Mg²⁺, La³⁺), the frequencies and diffusive characteristic parameters are primarily determined by the cation, and only secondarily by 1- anions. The replacement of Cl⁻ anions by NO₃⁻ anions primarily causes small broadenings and loss of resolution of the intermolecular frequencies together with a slight increase in *D* and a decrease in τ_0 . Relative to MgCl₂, in MgSO₄ solution, the SO₄²⁻ ion decreases slightly the anharmonicity of the vibrations of waters coordinated to the cations, but mainly restricts the diffusive mobility of water molecules beyond the primary layers. In contrast, for solutions of larger, singly charged cations, the intermolecular frequencies and the diffusive kinetics show a strong dependence on anion. Thus, in potassium halide solutions, the "structure-breaking" influence of the anions increases as Cl⁻ < Br⁻ < I⁻, and F⁻ acts as a "structure maker." Experimental evidence and a tentative explanation are given for abrupt variations with temperature in intermolecular frequencies and in the diffusive kinetics of a 4.6 *m* KCl solution near 25°.

Introduction

Neutron inelastic scattering (nis)²⁻⁴ has been used previously to study the motions of H₂O molecules in solids, in liquids, and in concentrated ionic solutions. Due to the large scattering cross section of hydrogen relative to other elements, the nis spectra correspond primarily to vibrational and diffusive motions of H₂O molecules. As the spectra are not subject to optical selection rules, all intermolecular modes below 900 cm⁻¹ as well as diffusive motions of H₂O molecules which occur within the interaction time,⁵ in principle, are observed. Previous nis measurements¹² on ionic solutions, which were primarily restricted to higher concentrations (typically 4.6 *m*), have shown the following.

(a) The spectra of solutions with strongly hydrating, small and/or highly charged ions (*e.g.*, La³⁺, Mg²⁺, Li⁺, and F⁻), showed the rocking, twisting, and

wagging librational modes and fundamental metal-oxygen stretching and bending modes of ion-water hydration complexes at frequencies similar to those observed in nis spectra of the corresponding solid salt

* To whom correspondence should be addressed.

(1) This work was supported by the Office of Saline Water of the Department of the Interior.

(2) G. J. Safford, P. S. Leung, A. W. Naumann, and P. C. Schaffer, *J. Chem. Phys.*, **50**, 4444 (1969).

(3) (a) K. E. Larsson and U. Dahlborg, *J. Nucl. Energy Parts A/B*, **16**, 81 (1962); (b) K. E. Larsson in "Thermal Neutron Scattering," P. A. Egelstaff, Ed., Academic Press, New York, N. Y., 1965, p 347.

(4) T. Springer, *Nukleonik*, **3**, 110 (1961). This paper constitutes one of the most complete reviews of the application of neutron scattering to the studies of vibrations and of diffusive motions of H₂O molecules in water and ice to be found in the literature. Pertinent theories and infrared and Raman measurements are also reviewed.

(5) K. E. Larsson, *Inelastic Scattering Neutrons, Proc. Symp.*, **1964**, **2**, 3 (1965).

hydrates. Further, the spectra⁶ for concentrated supercooled solutions of $\text{La}(\text{NO}_3)_3$ and CrCl_3 above and below their glass transitions have been compared. In the glasses, any coupling of the hydrated ions to the lattice, which is characteristic of the crystalline hydrates, is absent. Below 900 cm^{-1} , an even more pronounced degree of correspondence is observed between intermolecular frequencies of the supercooled solutions and of the solid glasses. Such similarities in frequency indicate that the local orderings of H_2O molecules in primary hydration layers of such ions are similar in solution to those in their glasses and solid hydrates. The strong primary ion-water interactions disrupt the initial solvent structure to form specific ion-water hydration coordinations. Similar results for aqueous solutions have also been obtained from Raman and infrared studies⁷⁻¹² of the low frequency lines and their intensity variations. These optical measurements have provided important information on the symmetries and bond strengths of hydration complexes. Raman results have suggested that a degree of electron sharing in metal ion primary H_2O bonds is common. Thus, the finite intensities of metal-water lines have been taken as evidence of covalent bonds in $\text{Mg}(\text{H}_2\text{O})_6^{2+}$ and $\text{Zn}(\text{H}_2\text{O})_6^{2+}$. The nls results² indicated that increasing temperature partially disorders these coordinations, increases the anharmonicity and multiphonon contributions, and causes the corresponding frequencies to broaden and become less resolved.

(b) The spectra for solutions of the larger, singly charged cations (*e.g.*, Cs^+ , K^+ , and Na^+) also showed frequencies characteristic of primary ion-water complexes which were specific to a given salt. Such primary ion-water coordinations, while weaker than those involving small or highly charged cations, were still stronger than the average H_2O - H_2O bonds in the solvent. Thus, with increasing temperature, H_2O - H_2O coordinations were rapidly disrupted, and the number of primary hydration waters increased, so that their corresponding intermolecular frequencies became sharper and better defined.

(c) Analyses of the angular and temperature dependences of the width of the diffusively broadened incident energy distributions (the "quasi-elastic component") for concentrated solutions (typically 4.6 *m* or 12 waters per ion pair) show that, below 25° , a delayed-diffusion model¹³ adequately approximated the diffusive kinetics. Values of self-diffusion coefficients (*D*) and of residence times (τ_0) were obtained, which were in agreement with those from other techniques, within experimental uncertainty.^{2,14-18} For solutions containing small and/or highly charged ions, at all temperatures, the *D*'s were decreased and the τ_0 's were increased relative to water, and such ions acted as "positive hydrators" in the terminology of Samoilov.¹⁹ In contrast, for solutions of larger, singly charged ions (even though ion-water complexes were formed), the

D's were increased and τ_0 's decreased relative to water at lower temperatures, corresponding to an increased average reorientational mobility for waters ("negative hydration"). However, for certain salts (*e.g.*, KCl and CsCl), with increasing temperature, the values of the *D*'s and the τ_0 's again closely approached those for water, in correspondence with a decrease in their "negative hydration" behaviors.

In the present investigation emphasis has been placed on determining the dependences of the diffusive kinetics and of the intermolecular frequencies on both concentration and on the influence of specific anions relative to cations. The range of concentrations varied typically between 0.5 *m* (approximately equal to 110 waters per ion pair) and the saturation limit of a given salt. At the lower concentrations, the spectral contributions of the relatively small number of H_2O molecules in primary hydration layers are negligible, and the spectra are primarily characteristic of the "bulk-solvent." The extent to which water structure can persist in dilute solutions and the relative influences of ionic size, charge, and the strength and coordinations in the primary layers in disrupting the distant bulk solvent have been the subject of considerable interest. Frank and Wen²⁰ postulated a region of "disrupted water structure" intermediate to the primary hydration layer and the distant solvent. Samoilov¹⁹ has emphasized that ions hydrate in dilute solutions so that a minimum modification of the solvent structure occurs. In such an "intermediate region," the average number of bonds per H_2O would, in general, be lower than for water, and the reorientational freedom of H_2O molecules increased. However, it has been argued²¹ that strong primary ion-

(6) P. S. Leung, S. Sanborn, and G. J. Safford, *J. Phys. Chem.*, **74**, 3710 (1970).

(7) (a) R. E. Hester, "Raman Spectroscopy Theory and Practice," H. A. Szamanski, Ed., Plenum Publishing Co., New York, N. Y., 1967, p 101; (b) D. E. Irish, *ibid.*, p 224.

(8) G. E. Walrafen, *J. Chem. Phys.*, **44**, 1546 (1966).

(9) J. O. Burgman, J. Sciesinski, and K. Sköld, *Phys. Rev.*, **170**, 808 (1968).

(10) D. A. Draeger and D. Williams, *J. Chem. Phys.*, **48**, 401 (1968).

(11) J. P. Mathieu and M. Lounsbury, *C. R. Acad. Sci. Paris*, **229**, 1315 (1949).

(12) J. H. Hibben, *J. Chem. Phys.*, **5**, 166 (1937).

(13) K. S. Singwi and A. Sjölander, *Phys. Rev.*, **119**, 863 (1960).

(14) L. Endom, H. G. Hertz, B. Thul, and M. D. Zeidler, *Ber. Bunsenges. Phys. Chem.*, **71**, 1008 (1967).

(15) J. H. Wang, *J. Phys. Chem.*, **58**, 686 (1954).

(16) C. M. Davis and T. A. Litovitz, *J. Chem. Phys.*, **42**, 2563 (1965).

(17) B. P. Fabricand, S. S. Goldberg, K. Leifer, and S. G. Ungar, *Mol. Phys.*, **7**, 425 (1964).

(18) D. W. McCall and D. C. Douglass, *J. Phys. Chem.*, **69**, 2001 (1965).

(19) O. Ya. Samoilov, "Structure of Aqueous Electrolyte Solutions and the Hydration of Ions," Consultants Bureau Enterprises, Inc., New York, N. Y., 1965.

(20) H. S. Frank and W. Y. Wen, *Discuss. Faraday Soc.*, **24**, 133 (1957).

(21) V. I. Tikhomirov, *J. Struct. Chem. (USSR)*, **4**, 479 (1963).

water interactions can lead to the polarization of H₂O bonds and to a strengthening of bonds beyond the primary layer, which would tend to decrease the reorientational freedom. The relative influence of the reduction of the number of bonds in the intermediate region and of this cooperative strengthening of bonds by polarization would affect the average diffusive kinetics, and determine the structure-“making” or -“breaking” influence of a salt.

At high concentrations, where the nls spectra are characteristic of ions and their strongly coordinated primary layers, the overall diffusive process may primarily involve motions of ions together with their waters of hydration, as reorientations of individual H₂O molecules may involve long delay times. Indeed, nmr measurements²² have indicated that the exchange rates for H₂O molecules between the hydration sheath and the solvent may exceed 10⁻⁴ sec.

The influence, relative to cations, of different anions on the intermolecular vibrational frequencies and the diffusive dynamics of H₂O molecules has been investigated. For solutions of strongly hydrating La³⁺ and Li⁺ cations, the relative influence of Cl⁻ vs. NO₃⁻ anions, and for Mg²⁺, the relative influence of SO₄²⁻ and of Cl⁻ anions were studied. Also, variations in inelastic and quasi-elastic components with anion were compared for KCl, KBr, KI, and KSCN and for CsF, CsCl, and CsBr. The results have been compared (where possible) with optical and relaxation results and with pertinent hydration theories.

Experimental Section

Instruments. The present measurements were made using a beryllium-filtered incident beam and a neutron time-of-flight spectrometer which has been described previously.²³ The application of this type of spectrometer to studies of liquids is described in the literature.²⁴ The solutions (prepared from analytical grade reagents and deionized water) were contained in grooves (having average thickness of 0.42 mm) in a thin Al plate backed by cadmium. A 2-λ layer of an inert polymer film protected against corrosion, and the cell was appropriately shielded to prevent scattering by the sample holder. As reported in extensive detail previously,² the polymer film and the Al window produced negligible spectral distortions or background contributions and the sample thickness yielded negligible spectral distortions from multiple scattering. For the spectra taken at 1°, the sample was cooled by circulating water from an ice-water bath, shielded to avoid the scattering of neutrons by the coolant.

Analysis of Data. The procedures used for the treatment of the data, for checking its reliability and reproducibility, and for the analysis of the quasi-elastic components have been extensively described in the literature,^{2,25} so that only a summary will be given here.

The spectra were corrected for measured background,

for counter efficiency, and for chopper transmission. Background corrections were made at each scattering angle by a channel-by-channel subtraction of the measured spectra of the empty sample holder. Thus, background was predominantly a flat component upon which was superimposed a weaker, broad distribution centering at about channel 146. The latter component varied with chopper speed, as expected for the “180° burst.” While small and significant variations occurred in the background with both scattering angle and cell geometry, spectra independent of a given cell could be systematically obtained after background corrections. The statistical uncertainties shown for the spectra correspond to ±1 standard deviation, calculated from the total and background counts per channel. The solid curves in the neutron spectra were averaged through the data points with regard to statistics. The reproducibility and reliability of spectral features were further tested by (a) comparisons of spectra remeasured with fresh solutions; (b) comparisons of data collected on the four independent counter banks, electronics, and memory banks of the time-of-flight analyzer; and (c) comparisons with background spectra for the empty cell to show that no spectral artifacts from neutrons scattered by the sample holder or shielding arose.

To obtain the quasi-elastic maxima, the low frequency inelastic contribution was estimated using a gas model of mass 18^{26,27} and then subtracted. A value of Γ (the Lorentz half-width at half-maximum) was then chosen which yielded the optimum agreement in shape after a comparison between the measured incident distribution, broadened by Lorentzian functions of varying half-widths at half-maximum, Γ, and an observed quasi-elastic maximum.

Measurements for most of the spectra were made at 1°, where the delayed-diffusion limit of the general Singwi-Sjölander model¹³ has been shown previously to be a valid approximation. For this model

$$\Gamma = \frac{\hbar}{\tau_0} \left(1 - \frac{e^{-2W}}{1 + K^2 D \tau_0} \right) \quad (1)$$

where

$$K^2 = k_0^2 + k_f^2 - 2k_0 k_f \cos \phi$$

and for $k_0 \approx k_f$

$$K^2 \approx 4k_0^2 \sin^2 \phi/2$$

(22) J. A. Jackson, J. F. Lemons, and H. Taube, *J. Chem. Phys.*, **32**, 553 (1960).

(23) G. J. Safford and A. W. Naumann, *ibid.*, **45**, 3787 (1966).

(24) P. A. Egelstaff, Ed., “Thermal Neutron Scattering,” Academic Press, New York, N. Y., 1965.

(25) G. J. Safford, P. C. Schaffer, P. S. Leung, G. F. Doebbler, G. W. Brady, and E. F. X. Lyden, *J. Chem. Phys.*, **50**, 2140 (1969).

(26) B. N. Brockhouse, *Nuovo Cimento, Suppl.*, **9**, 45 (1958).

(27) A. N. Goland and K. Otnes, *Phys. Rev.*, **153**, 184 (1967).

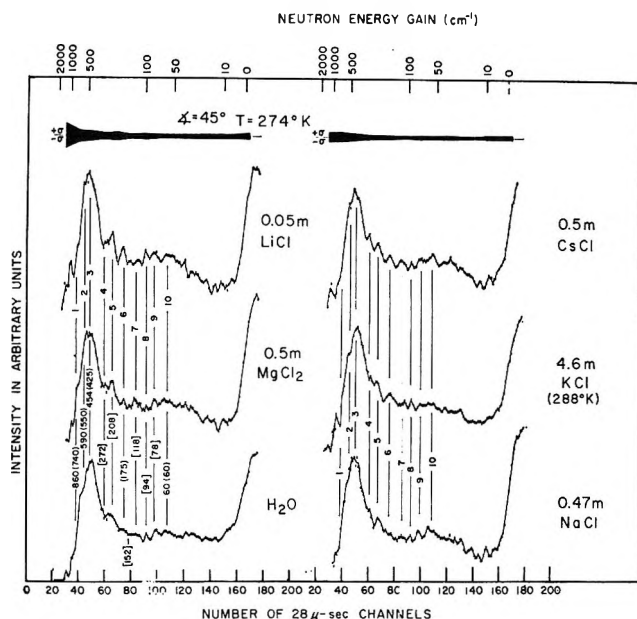


Figure 1. The neutron time-of-flight spectra, measured at 1° and a scattering angle of 45° for dilute solutions of LiCl, MgCl_2 , CsCl, and NaCl and for a 4.6 *m* solution of KCl (at 15°), are compared with the water spectrum at 25° . The vertical lines show the peaks in the water spectrum which occur in solutions at nearly the same frequencies. The frequencies in parentheses are from Raman measurements⁸ and those in brackets are from another measurement.⁹ In this and the following figures, the statistical errors, as calculated from the total and background counts, are represented for comparison with the spectra by the solid strip at the top of the figure. At a given channel, the full width of the strip extends from $+1$ to -1 standard deviation, σ .

and where k_0 = initial neutron momentum vector, k_f = final neutron momentum vector, ϕ = scattering angle, τ_0 = "residence time," D = self-diffusion coefficient, and e^{-2W} = the Debye-Waller factor. Values of D and τ_0 were chosen to yield an optimum fit to a curve of Γ vs. K^2 .

Results and Discussion

The nls spectra reflect the vibrational and diffusive motions of H_2O molecules characteristic of the "bulk-solvent" for dilute solutions and of primary ion-water complexes for concentrated solutions. At low concentrations (typically of 0.5 *m* and below, corresponding to more than 110 waters per ion pair), the torsional components,² as well as the lower frequency modes in the spectra for the CsCl, NaCl, and MgCl_2 solutions, show a pronounced correspondence with those observed for water (Figure 1), which becomes lost in a manner specific to a given salt with increasing concentration (Figures 2 and 3). However, such a correspondence is not observed for dilute LiCl solutions (Figure 2), except at lower concentration (typically below about 0.05 *m*), while in contrast, for KCl solutions (Figure 1), frequencies characteristic of water appear to persist even to concentrations as high as 4.6 *m*. Small frequency

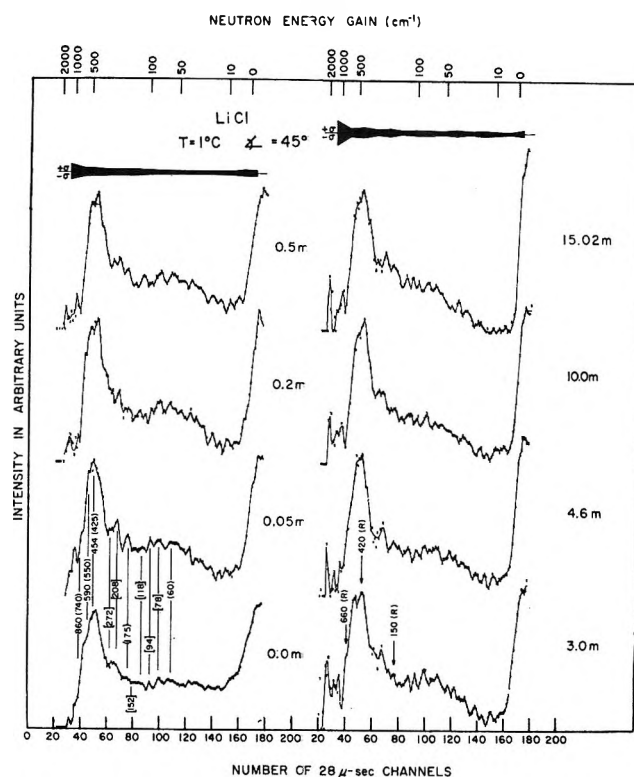


Figure 2. The neutron time-of-flight spectra are shown for LiCl solutions as a function of the concentration. The reported (Raman^{8,12} and IR¹⁰) frequencies are marked with R and IR, respectively.

shifts relative to water and within the experimental resolution cannot be precluded, and variations in intensities of the maxima relative to water do occur.

In correspondence with the similarity to water of the inelastic frequencies, the curves of Γ vs. K^2 for dilute solutions are also nearly within experimental error of that for water (Figure 4). While the individual points are within error of those for water, the points for CsCl lie systematically above that for water, while those for MgCl_2 , NaCl, and LiCl lie below. The near coincidence of these curves implies that the values of D and τ_0 are similar to water and that any changes in the activation energies are small relative to the energy of a hydrogen bond in water (approximately 2.5 kcal/mol). Thus, despite the different hydration powers of magnesium, sodium, and cesium ions, it appears that below about 0.5 *m* these ions do not strongly disrupt the structure of the bulk-solvent relative to water. In contrast to the above salts, LiCl is more effective in disrupting the solvent structure while KCl is less effective.

The ability of such ions to alter the long-range structure of the distant solvent depends on the strength (relative to water) of their primary ion-water interaction, on the polarization of solvent molecules by the primary complexes, and on the degree of structural mismatch between primary hydration complexes and the distant solvent structure.^{21,28-30} Both the relative

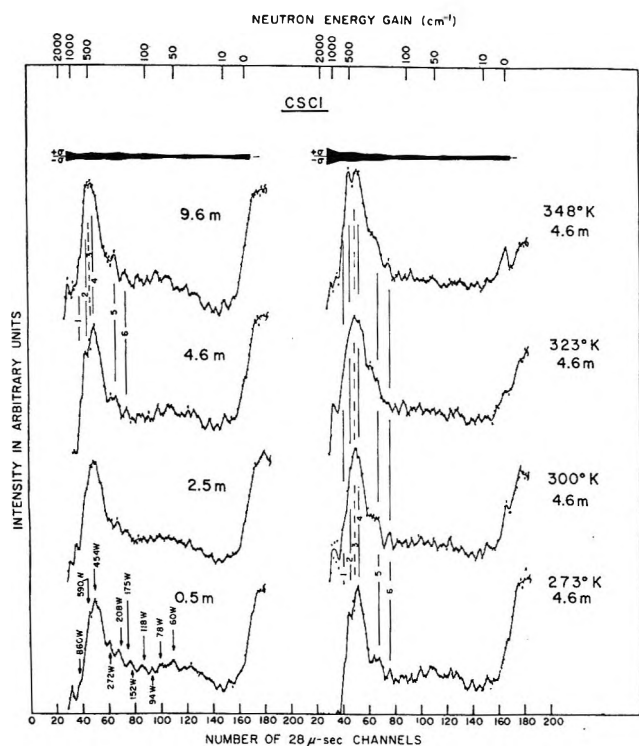


Figure 3. The neutron time-of-flight spectra, measured at 1° and a scattering angle of 45° for CsCl solutions at various concentrations, are shown on the left. They are compared with spectra of a 4.6 m solution as a function of temperature as shown on the right. The frequencies characteristic of pure water are indicated in the spectrum of the 0.5 m solution and are observed to coincide with the frequencies of the inelastic maxima observed at this concentration. The vertical lines 1-6 indicate new frequencies characteristic of cation-water complexes that appear at concentrations above 4.6 m.

number of H_2O molecules and the diffusive freedom in such an intermediate region depend on the transition from the distant region, where the structure and forces are primarily determined by water structure, to the primary hydration complexes, where they are determined by specific ion-water coordinations. The ability of the Li^+ ion to strongly alter the solvent structure at low concentrations could result, in part, from its small number of specifically coordinated primary waters. The small Li^+ ion can polarize water molecules,³¹ as a result of the formation of a strongly coordinated primary hydration layer involving four waters in a tetrahedral coordination,³² and possibly even a second layer.^{33,34} The waters adjacent to hydrated Li^+ ions would undergo large reorientations to bond to the hydrated ions, and a cooperative structural readjustment, involving many molecules, could result. In contrast, larger ions like Na^+ , Mg^{2+} , and Cs^+ accommodate a greater number of primary hydration waters and would not require as large a structural perturbation from the bulk water structure in order for it to couple to the strongly ordered hydration layers about an ion.

With increasing concentration, as shown in Figures 2 and 3, any spectral correspondence to water frequen-

cies characteristic of lower concentrations is rapidly lost, and new frequencies characteristic of librational and metal-oxygen stretching and bending modes in the ion-water complexes appear and intensify (as reported previously²). The observed broadening and damping of the inelastic spectra at intermediate concentration (for example, at 2.5 m CsCl) probably reflects the presence of contributions from both frequencies characteristic of the disrupted solvent and frequencies characteristic of primary ion-water complexes. For small or highly charged ions, such frequencies were attributed to cation-water hydration complexes, where the primary cation-water interaction can involve a degree of covalency.^{7,35} Thus, Nakagawa and Shimanouchi,³⁵ from infrared results, have argued that metal-oxygen bond stretching force constants and the degree of covalency decrease in the progression $\text{Cr}^{3+} > \text{Ni}^{2+} \approx \text{Mn}^{2+} \approx \text{Fe}^{2+} > \text{Cu}^{2+} \approx \text{Zn}^{2+} > \text{Mg}^{2+}$.

In Figure 5 the inelastic spectra of $\text{La}(\text{NO}_3)_3$ and LaCl_3 and of LiCl , LiSCN , and LiNO_3 are intercompared. Both the LaCl_3 and $\text{La}(\text{NO}_3)_3$ spectra show large departures from water, and a strong correspondence is observed between their intermolecular frequencies. A similar, but less pronounced, correspondence is observed between the spectra of the three lithium salts. These results emphasize that the orderings and the coordinations in the primary hydration complexes of small and/or highly charged cations are influenced secondarily by the 1- anions. In correspondence, the observed variations of the associated diffusive kinetics and parameters with 1- anions are smaller relative to those observed with cations (Figures 6 and 7). Thus, the Γ vs. K^2 curve for $\text{La}(\text{NO}_3)_3$ lies close to, but systematically below, that for LaCl_3 . This suggests that the NO_3^- ions (relative to the Cl^- ions) may weaken and perturb the hydration sphere about cations and, hence, the effective negative hydration for nitrate ions is slightly larger than for chloride ions, in keeping with results previously reported in the literature.³⁶⁻⁴⁰

(28) M. Kaminsky, *Discuss. Faraday Soc.*, **24**, 171 (1957).

(29) J. Greyson and H. Snell, *J. Phys. Chem.*, **73**, 3208 (1969).

(30) K. A. Valiyev and M. M. Zripov, *J. Struct. Chem. (USSR)*, **7**, 470 (1966).

(31) O. D. Bonner and G. B. Woolsey, *J. Phys. Chem.*, **72**, 899 (1968).

(32) D. E. Woessner, B. S. Snowden, Jr., and A. G. Ostroff, *J. Chem. Phys.*, **49**, 371 (1968).

(33) J. C. Hindman, *ibid.*, **36**, 1000 (1962).

(34) H. Rüterjans, F. Schreiner, U. Sage, and T. Ackermann, *J. Phys. Chem.*, **73**, 986 (1969), have noted that even at 130° the second hydration layer of the Li^+ ion in LiCl is only partially disrupted.

(35) I. Nakagawa and T. Shimanouchi, *Spectrochim. Acta*, **20**, 429 (1964).

(36) H. S. Frank and M. W. Evans, *J. Chem. Phys.*, **13**, 507 (1945).

(37) T. H. Cannon and R. E. Richards, *Trans. Faraday Soc.*, **62**, 1378 (1966).

(38) R. E. Hester and W. E. L. Grossman, *Spectrochim. Acta*, **23A**, 1945 (1967).

(39) G. A. Andreev, *Proc. Acad. Sci. USSR, Phys. Chem. Sect.*, **145**, 518 (1962).

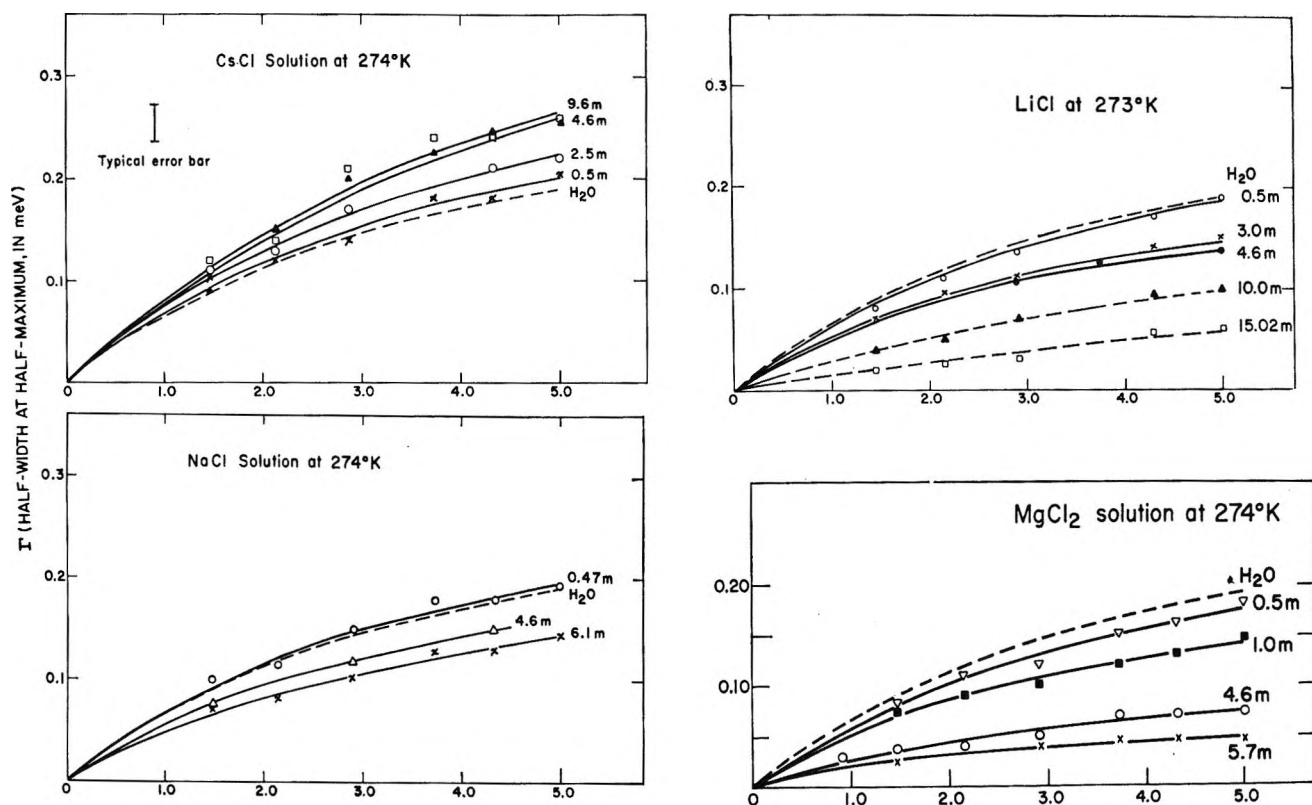


Figure 4. The observed Γ vs. K^2 curves at 1° are shown as a function of concentration for CsCl, NaCl, LiCl, and MgCl₂ solutions. The typical error shown represents the limits to which a value of Γ could be varied without incurring large variations in shape outside of statistical accuracy between an observed quasielastic maximum and the Lorentzian broadened incident energy distribution. The full solid lines through the data points represent fits with the simple delayed-diffusion model (see text) to the data. The dashed lines for the 10.0 and the 15.02 m LiCl solutions were faired through data points, as discussed in the text. At these concentrations, the simple delayed-diffusion model was not adequate to describe the diffusive kinetics.

The effects relative to Cl⁻ and NO₃⁻ of the doubly charged SO₄²⁻ anion on the intermolecular frequencies of cation-water hydration complexes, and on the diffusive kinetics, are shown in Figures 7 and 8. The spectrum for a MgSO₄ solution is compared with the spectra for MgCl₂·6H₂O and MgSO₄·7H₂O. For the magnesium sulfate solution and its corresponding solid hydrate, the frequencies in the region of the librational modes of H₂O molecules coordinated to the cation are closely similar to those observed for a magnesium chloride solution and its corresponding solid salt hydrate, as shown in Table I, indicating a degree of similarity in the primary cation-water coordinations. In this regard, the local orderings obtained from X-ray diffraction for many magnesium salt hydrates^{41,42} and for solutions⁴³ show that the magnesium ion is generally surrounded octahedrally by six water molecules with cation-water distances typically between 2 and 2.2 Å. The similarity in the primary coordination of the magnesium cations in both the sulfate and chloride salts is evidenced in the nls spectra by the similarities of the frequencies characteristic of cation-water coordinations in the solutions and in the solid hydrates. However, for the sulfate, these frequencies (especially the higher frequency modes) and the elastic peak appear more

intense, corresponding to a larger Debye-Waller factor and to a smaller average vibrational amplitude. Thus, the sulfate ion (relative to the chloride ion) appears primarily to have decreased the anharmonicity of the cation-water potential. Further, as shown in Figure 7, Γ vs. K^2 for the 2.3 m solutions of magnesium sulfate lies below that for the more concentrated 4.6 m magnesium chloride solution. Thus, the sulfate ion relative to Cl⁻ further decreases D and increases τ_0 for waters beyond the primary hydration layer.

In contrast to the La³⁺, Mg²⁺, and Li⁺ salts, no significant correspondence in intermolecular frequencies is observed between the four potassium salts shown in Figure 9. Also, the diffusive kinetics show a large anion dependence (Figure 7). Thus, the relative influence of the 1- anions appears to increase with cation radius.

Certain features for observed cesium and potassium

(40) J. P. Mathieu and M. Lounsbury, *Discuss. Faraday Soc.*, 9, 196 (1950).

(41) R. W. G. Wyckoff, Ed., "Crystal Structure," 2nd ed, Vol. 3, Interscience, New York, N. Y., 1965.

(42) W. H. Baur, *Acta Cryst.*, 17, 136 (1964).

(43) A. K. Dorosh and A. F. Skryshevskii, *J. Struct. Chem. (USSR)*, 8, 348 (1967).

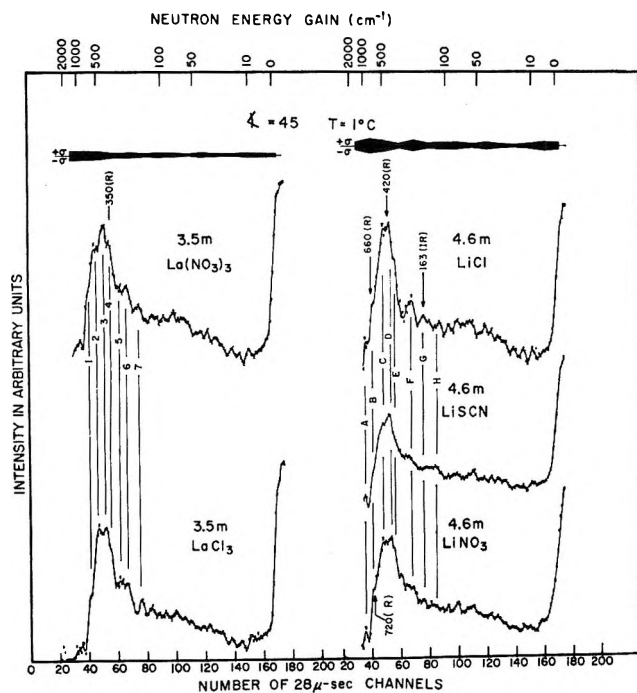


Figure 5. The neutron time-of-flight spectra for $\text{La}(\text{NO}_3)_3$ and LaCl_3 solutions are intercompared as are those for LiCl , LiSCN , and LiNO_3 . The Raman and ir frequencies for LiCl , from Walrafen⁸ and Draeger and Williams,¹⁰ respectively, are shown. The Raman frequency shown for LiNO_3 was from Mathieu and Lounsbury.¹¹ The correspondence of observed nis frequencies is indicated by the vertical lines 1-7 for the lanthanum salts and by the lines A-H for the lithium salts.

salt solutions and their dependence on concentration, on anion, and on temperature will now be considered in more detail. At 1° and concentrations typically above $2.0\ m$, the diffusive kinetics of the bromide and chloride solutions are in accord with a "negative hydration" behavior. The self-diffusion coefficients and the residence times determined from eq 1 relative to water are in the progressions (see Table II) $D_{\text{CsCl}}^* \approx D_{\text{CsBr}}^* \approx D_{\text{KBr}}^* > D_{\text{KCl}}^* > D_{\text{H}_2\text{O}}^* > D_{\text{CsF}}^* > D_{\text{KF}}^*$, and $\tau_{\text{KF}} > \tau_{\text{CsF}} > \tau_{\text{H}_2\text{O}} > \tau_{\text{KCl}} > \tau_{\text{KBr}} > \tau_{\text{CsBr}} \approx \tau_{\text{CsCl}}$. As shown in Figure 8, the inelastic frequencies for a $4.6\ m$ CsF solution correspond well with those observed for the KF solution and for $\text{KF} \cdot 2\text{H}_2\text{O}$ and show no significant similarity to those observed for CsBr and CsCl (Figure 9). Thus, F^- anion in the presence of the larger, singly charged cations K^+ and Cs^+ appears principally to determine the coordinations of the primary water, and the relative influence of the cations appears to be secondary. While the curve of Γ vs. K^2 for CsF (Figure 10) lies well below those for CsBr , CsCl , and water, it lies above that for KF . Hence, Cs^+ does not show as strong a "positive hydration" behavior as KF , possibly due to ion pairing. The larger Cs^+ ion may also weaken solvent-solvent bonds more effectively than the smaller K^+ cation.

For concentrations of CsBr above $2.0\ m$ and of CsCl above $4.6\ m$, the inelastic spectra show maxima that

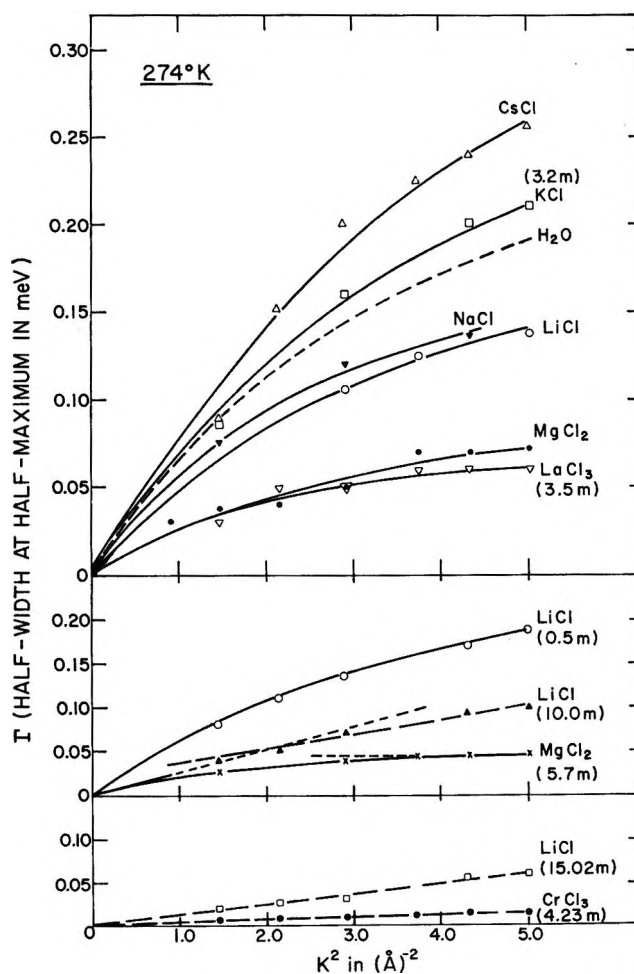


Figure 6. At the top, the observed Γ vs. K^2 curves at 1° are compared to show the dependence on cation for a series of $4.6\ m$ (indicated otherwise) chloride solutions. Curves shown at the middle and at the bottom illustrate various functional forms observed for Γ vs. K^2 (see text). The line extensions on the $10.0\ m$ LiCl and $5.7\ m$ MgCl_2 curves are drawn to emphasize the existence of a linear relationship for Γ vs. K^2 over the portion of the curve indicated.

differ from those of water, and that occur at nearly identical frequencies for both of these salts. The near independence on anion of the inelastic frequencies (Figure 9) and the Γ vs. K^2 curves (Figure 10) for both CsCl and CsBr solutions suggests that the spectra correspond primarily to cation-water complexes. As noted by Hindman,³³ such "structure-breaking" cations may form hydration complexes while yet decreasing the solution viscosity. However, for such large, singly charged cations, the primary coordination layers may not be complete and direct ion pairing may occur.⁴⁴ Relative to these cesium solutions, both the intermolecular frequencies and the curves of Γ vs. K^2 (hence, the diffusive parameters) for the potassium halide solutions show a larger variation with anion. This difference is most probably due to a weaker structure-break-

(44) R. M. Lawrence and R. F. Kruh, *J. Chem. Phys.*, **47**, 4758 (1967).

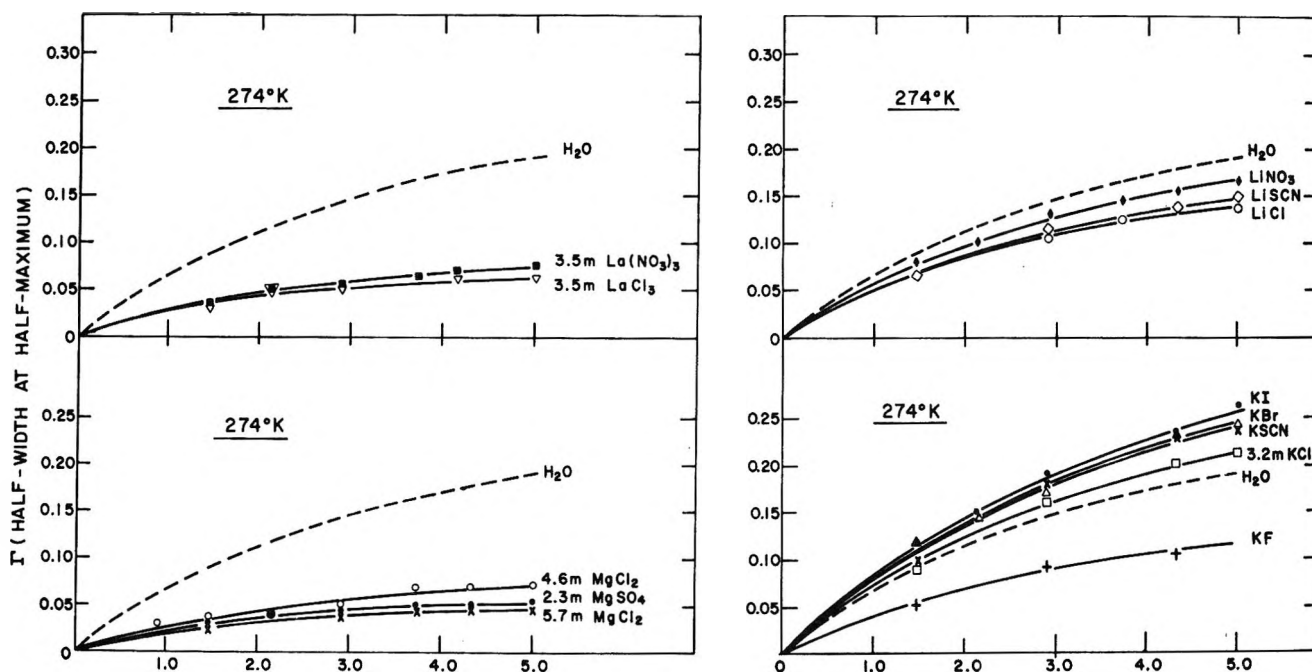


Figure 7. Observed Γ vs. K^2 curves at 1° are compared for a series of lanthanum, magnesium, lithium, and potassium salts to show the dependences on anion. The concentrations of the solutions are 4.6 m , unless otherwise indicated.

Table I: Observed and Calculated Modes of the $\text{Mg}(\text{H}_2\text{O})_6^{2+}$ Octahedral Complex

Observed frequencies, cm^{-1}	Nis ^{a, f}		Calculated	Assignment	
	Raman	Ir			
706	...	719 ^{a, i}	607 ^h	Rocking	} librational modes
575	Twisting	
454 (w) ^p	...	460 ^{b, h}	471 ^h	Wagging	
382	370 ^{d, i}	310 ^{b, h}	320 ^h	ν_1 sym stretch mode of complex	
	360 ^{c, e, f}		
	370 ^{b, k}		
	360 ^{f, l}		
	365 ^{d, l}	...	425 ^l		
	365 ^{c, l}		
	380 ^{b, m}		
337 (w)	205 ^{b, k}	ν_2	
	315 ^{f, l}		
	315 ^{d, l}		
222	258 ^{b, k}	...	251 ^k	ν_3	
	240 ^{c, e, f, l}		
180	134 ^k	ν_4	} ir active
267	269 ^k	ν_5	
...	499 ^k	ν_6	

^a $\text{MgCl}_2 \cdot 6\text{H}_2\text{O}$. ^b $\text{MgSO}_4 \cdot 7\text{H}_2\text{O}$. ^c MgSO_4 solution. ^d $\text{Mg}(\text{NO}_3)_2$ solution. ^e $\text{Mg}(\text{ClO}_4)_2$ solution. ^f MgCl_2 solution. ^g (w) = weak. ^h Reference 35. ⁱ I. Gamo, *Bull. Chem. Soc. Jap.*, **34**, 760 (1961). ^j R. E. Hester and R. A. Plane, *Inorg. Chem.*, **3**, 768 (1964). ^k M. R. Lapont, *C. R. Acad. Sci. Paris*, **244**, 1481 (1957). ^l A. daSilveira, M. M. Marques, and N. M. Marques, *C. R. Acad. Sci. Paris*, **252**, 3983 (1961); *Mol. Phys.*, **9**, 271 (1965). ^m J. P. Mathieu, *C. R. Acad. Sci. Paris*, **231**, 896 (1950).

Table II: Self-Diffusion Coefficients and Average Residence Times for Water Molecules in Ionic Solutions at 1°

		$\tau_0 \times 10^{12}$ sec (from eq 1)	$D \times 10^6$ cm^2/sec (from eq 1)	$D^* \times 10^6$ cm^2/sec (from the slope of Γ vs. K^2 curve near origin)
	H_2O	2.4	0.8	1.2
	MgSO_4 2.3 m	10.2	0.45	0.56
	MgCl_2 0.5 m	2.8	0.6	1.1
	1.0 m	3.5	0.76	1.0
	4.6 m	6.1	0.4	0.5
	5.7 m	11.1	0.37	0.46
	LiCl 0.5 m	2.4	0.75	1.1
	3.0 m	3.3	0.67	1.0
	4.6 m	3.2	0.64	0.9
	NaCl 0.47 m	2.3	0.81	1.25
	4.6 m	2.8	0.75	1.05
	6.1 m	3.1	0.52	0.85
	CsF 4.6 m	2.9	0.53	0.99
	CsCl 0.5 m	2.2	0.77	1.2
	2.5 m	2.0	0.84	1.4
	4.6 m	1.4	0.90	1.4
	9.6 m	1.5	0.90	1.5
	CsBr 2.5 m	2.25	0.71	1.42
	4.0 m	1.75	0.74	1.31
	KBr 4.6 m	1.83	0.83	1.43
	KI 4.6 m	1.7	0.82	1.47
	KSCN 18.0 m	2.3	0.5	0.99
	4.6 m	1.7	1.0	1.44

it has been suggested⁴⁵ that in KCl solutions the anions may primarily disrupt the solvent structure, as the K^+

(45) G. W. Brady and J. T. Krause, *J. Chem. Phys.*, **27**, 304 (1957).

ing effect of the K^+ ion (approximately the size of an H_2O molecule) relative to the larger Cs^+ ion. Indeed,

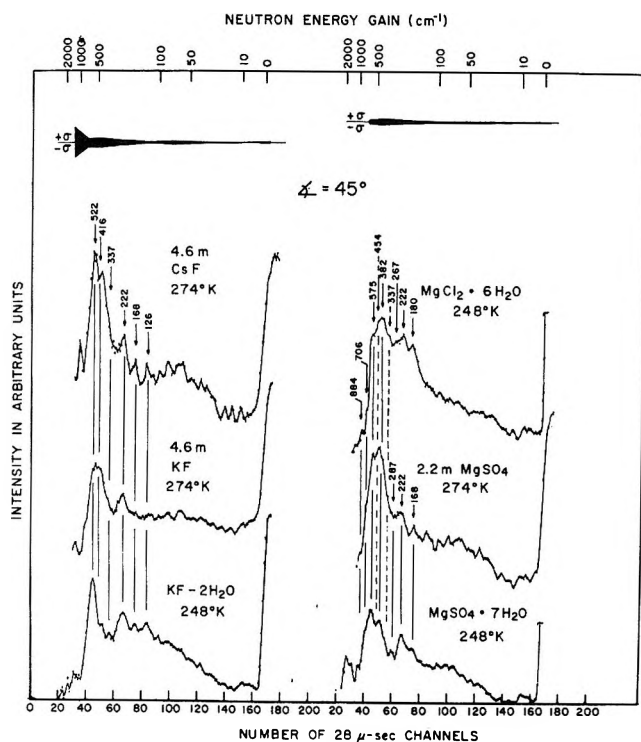


Figure 8. The nis spectrum of a 4.6 *m* CsF solution is compared with the spectra of 4.6 *m* KF and of KF·2H₂O. The spectrum of 2.2 *m* MgSO₄ is also compared with the spectra of 4.6 *m* MgCl₂ and MgSO₄·H₂O. These spectra were measured at 1° for the solutions and at -25° for the solid hydrates.

ion may not have a sufficiently strong field to withdraw molecules from the solvent structure. Relative to CsCl at 1°, KCl is a "weaker structure breaker." This then results in its Γ vs. K^2 lying below that for CsCl and for the persistence, below 25°, of frequencies characteristic of water (Figure 11), which give way to ion-water frequencies with increasing thermal disruption of the solvent, as discussed below.

The most pronounced correspondence in the characteristic inelastic frequencies of the cation-water hydration complexes and in the Γ vs. K^2 is observed by comparing spectra of CsBr at concentration >2.0 *m* to those for more concentrated CsCl solutions (concentrations >4.6 *m*). The concentration dependence could result in part both from an earlier disruption of solvent by the larger Br⁻ anion (relative to Cl⁻), and from the formation of a relatively larger number of cation-water pairs at low concentrations, due to the smaller degree of ion pairing in CsBr than in CsCl. Further, at concentrations above 2.5 *m* for CsBr and above 4.6 *m* for CsCl, both the inelastic frequencies (Figure 3) and the Γ vs. K^2 curves (Figures 4 and 10) show only relatively small changes with an additional increase in concentration. A similar behavior in self-diffusion coefficients has been reported by Endom, *et al.*¹⁴ This "saturation" could result from an increased ion pairing with increasing concentration, to the extent

that, with a further addition of salt, the formation of new hydration complexes would be limited.

With increasing temperature, the spectra for CsCl and KCl indicate a decrease in the "negative hydration" behavior and an increase in the number of primary ion-water pairs, in keeping with that reported by Endom, *et al.*¹⁴ Above 25° the inelastic frequencies characteristic of ion-water complexes in CsCl and in KCl persist and become more prominent as the temperature is increased to 75°. The diffusive kinetics show a corresponding trend (Figure 15 in ref 2). At 1° the Γ vs. K^2 curves for both CsCl and KCl are above that for water, in correspondence to increases in the D 's and reductions in the τ_0 's relative to water. However, by 25° the Γ vs. K^2 curve has decreased and crossed below that for water, while that for CsCl nearly coincides with the water curve. Thus, between 0 and 25°, a trend is observed for both these salts, such that diffusive mobility, initially greater than water, becomes comparable to or more restricted than for water. Further, this trend is accentuated at higher concentrations. The curve for 9.6 *m* CsCl at 1°, which is only slightly above that for 4.6 *m* CsCl, lies significantly below it at 75° (Figure 10), in keeping with a more rapid thermal breakdown of the water-water coordination than of the primary ion-water coordinations. Indeed, it has been argued⁴⁶ that the thermal decomposition of the Cs-H₂O hydration complex is not appreciable until 100°.

Similar, but more pronounced, changes with both concentration and temperature are observed for KSCN solution. At 1° a 4.6 *m* solution of KSCN shows a structure-breaking behavior. The curve of Γ vs. K^2 (Figures 7 and 10) lies above those for water and for KCl, and inelastic frequencies, characteristic of ion-water frequencies, are observed. Thus, at 1° the SCN⁻ appears to have more efficiently disrupted the solvent structure than Cl⁻. However, with increasing concentration (Figure 10), the curve for KSCN decreases and approaches that for water. Simultaneously, the inelastic frequencies become better resolved and defined,² in accord with an increase in the relative number of primary ion-water coordinations with bondings similar in strength to pure water. As the temperature² is increased above 1°, Γ vs. K^2 for KSCN decreases, approaches that for water, and then falls below it. Correspondingly, the ion-water inelastic maxima also sharpen and become better defined with increasing temperature. Again, such behavior reflects an increase in primary hydration with increasing temperature, as discussed above for CsCl.

In Figure 7 it is observed that Γ vs. K^2 for a 4.6 *m* KSCN solution lies well above those for water and KCl, nearly coinciding with that for KBr. In contrast, the Γ vs. K^2 for LiSCN lies only slightly above that for LiCl. Thus, in the presence of the strongly hydrating

(46) M. Eigen and E. Wicke, *Z. Elektrochem.*, 55, 354 (1951).

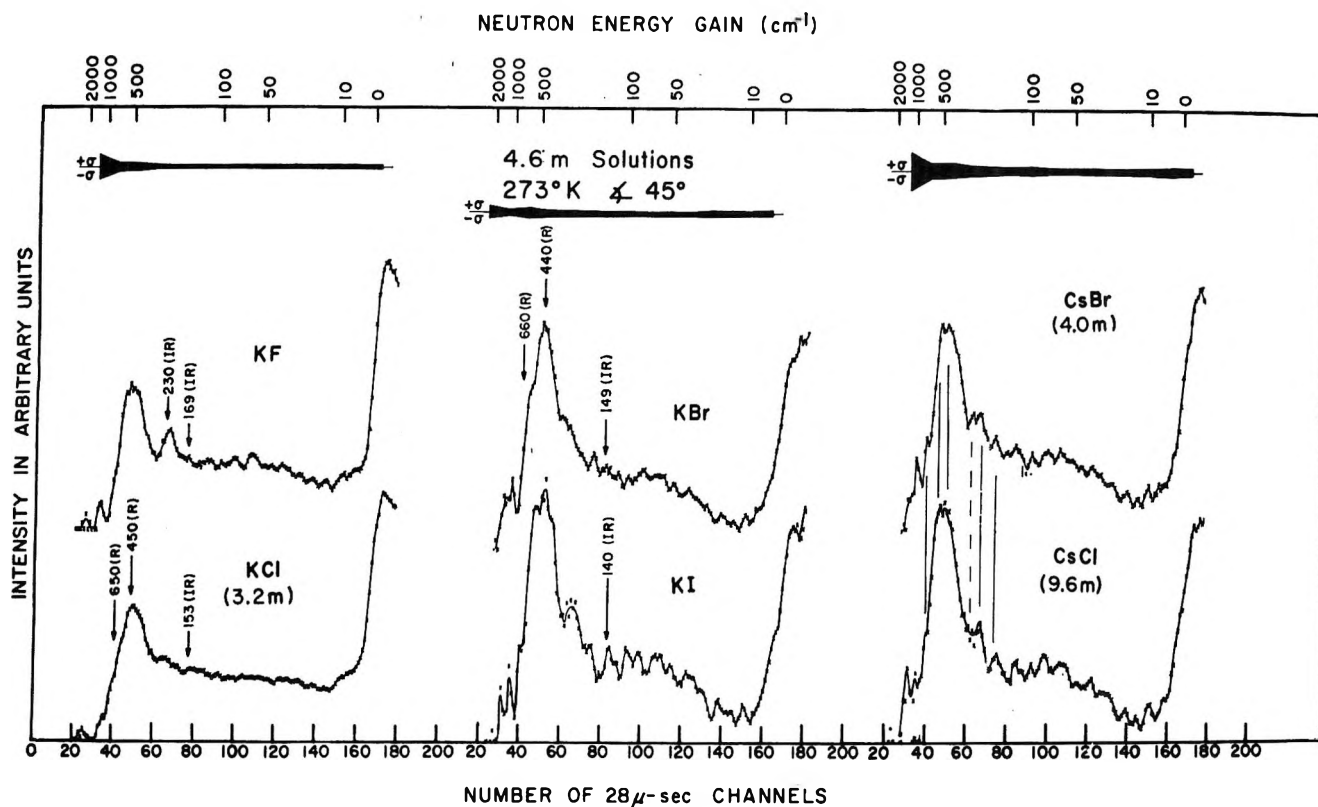


Figure 9. The neutron time-of-flight spectra for potassium halides are compared. The frequencies marked (R) and (IR) are those from reported Raman⁸ and ir,¹⁰ respectively. The spectra of 4.0 m CsBr and 9.6 m CsCl are intercompared. The vertical lines are to indicate a similarity in the observed frequencies between the spectra.

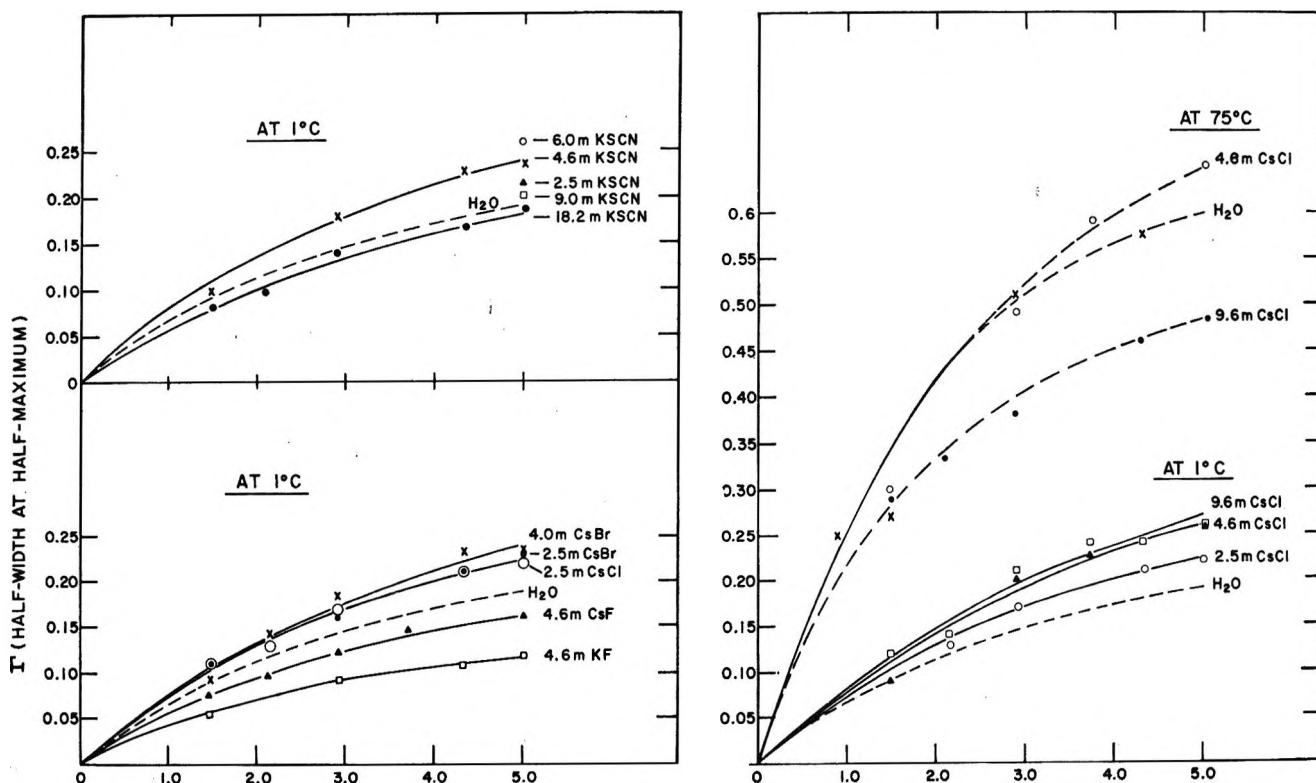


Figure 10. The observed Γ vs. K^2 curves at 1° for KSCN, CsBr, CsCl, and CsF at various concentrations are shown at the left. For 2.5, 6.0, and 9.0 m KSCN solutions only one point (to confirm observed trends) was measured. The temperature and concentration effects on Γ vs. K^2 for CsCl solutions are shown on the right. The dashed lines at 75° were fairings through data points, as the validity of the simple delayed-diffusion model is questionable at higher temperatures (see text).

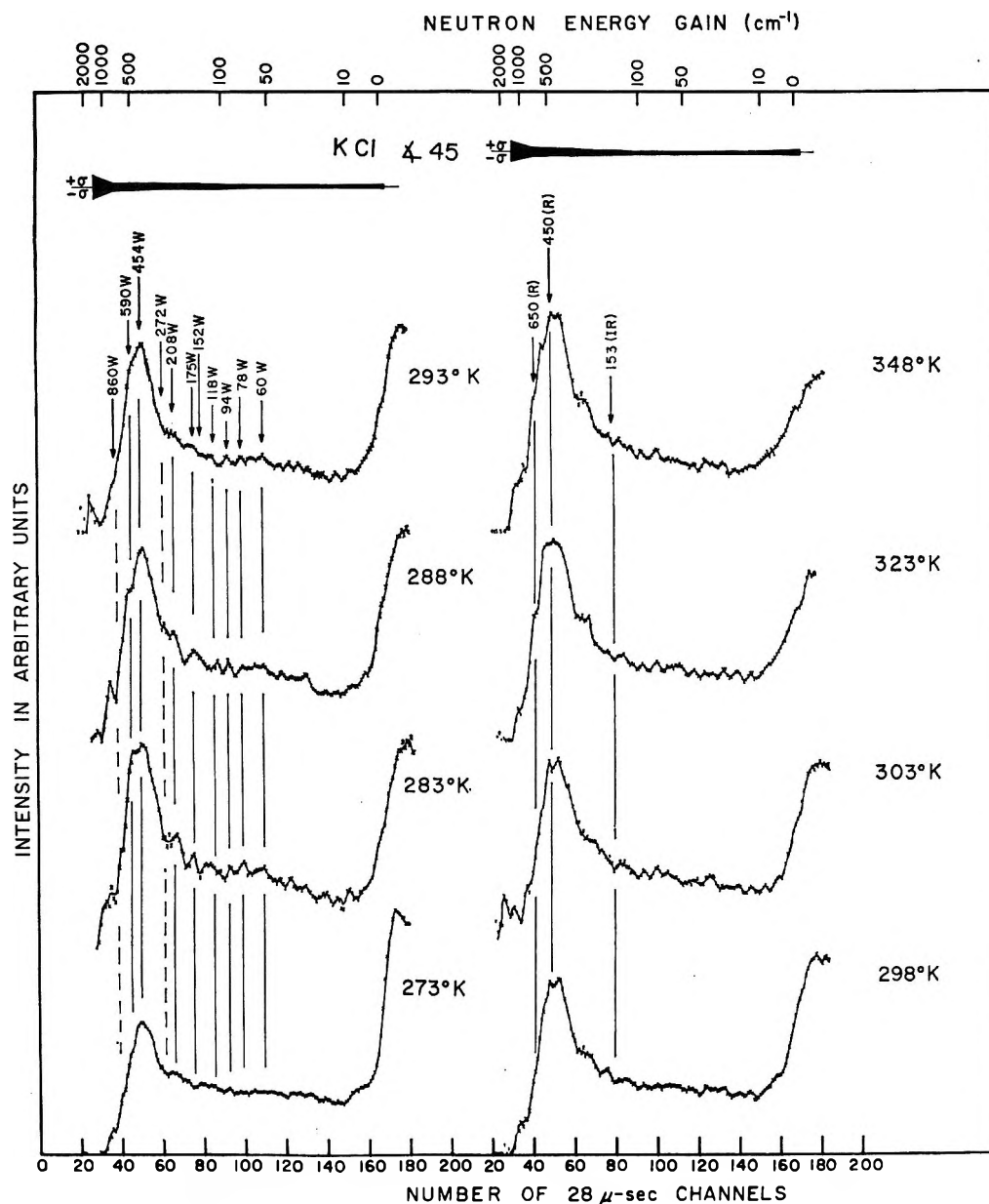


Figure 11. The neutron time-of-flight spectra for 4.6 *m* KCl solution (3.2 *m* at 1°) are shown as a function of temperature. The frequencies marked W correspond to those observed for water.¹ The Raman and ir frequencies, which were reported by Walrafen⁸ and Draeger and Williams,¹⁰ are also indicated.

Li^+ ion, the structure-breaking influence of the SCN^- ion relative to Cl^- ion is smaller than in the presence of the K^+ ion. Indeed, Brady⁴⁵ has suggested that, in KCl solutions, the anion is primarily responsible for disrupting the water structure rather than the smaller K^+ ion, which is about the size of an H_2O molecule. It has been suggested⁴⁷ that the linear SCN^- ion may, to an extent, be able to incorporate into the solvent structure, which could partially decrease the influence of its size. Thus, the structural disruption effect appears to be smaller than for Br^- and I^- . However, the anion-water bonds formed from the anisotropic charge distribution may give rise to structural mismatches between anion-water complexes and the solvent structure. This would, in part, be responsible for

a larger disruption than for Cl^- ion. In contrast, in LiSCN , where waters are strongly coordinated to the Li^+ , SCN^- is only slightly more effective than Cl^- in disrupting the structure.

For KCl solutions, evidence determined from the derivative of the solubility with temperature has been cited⁴⁸ that suggests a second-order transition may occur near 22°. Also X-ray diffraction measurements⁴⁹ indicate that both ion-water coordinations and "water-like" regions may coexist below 22°, but a more homo-

(47) P. S. Bogoyavlenskii and Hsu Kó-min, *J. Struct. Chem. (USSR)*, **1**, 397 (1960).

(48) M. I. Schachparonow, *Zh. Fiz. Khim.*, **27**, 111 (1953).

(49) V. I. Danilow and W. E. Neumark, *Z. Phys. Physik. Z. Sowjet-union*, **10**, 673 (1936).

geneous distribution of the H₂O molecules occurs above 22°. In regard to such evidence, it is noted that the temperature dependence of the observed widths of the quasi-elastic maxima shows a discontinuous change near 29° for a 4.6 *m* KCl solution (Figure 12).

As reported previously,² at lower temperatures, a delayed diffusion model appears to account for the shape and for the dependences of the observed width on *K*² and on temperature. Nevertheless, for most solutions, a temperature is reached above which "free-particle" motions⁵⁰ may also contribute. To examine the temperature behavior, it is convenient to plot the observed dependence of Γ vs. *K*² in terms of the dimensionless parameters^{1,50} $\Gamma/kT = y$ and $\hbar DK^2/kT = x$ for a series of temperatures (Figure 12).

For a KCl solution, at small values of *x*, the values of *y* fall on the *y* = *x* line as expected for the classical diffusion, but fall below this line at larger *x* values. Between 1 and 25°, at larger values of *x*, *y* increases in a regular manner with temperature, in accord with jump diffusion (eq 1), for which

$$y = \frac{\hbar}{\tau_0 kT} \left[1 - \frac{e^{-2W}}{1 + \frac{kT\tau_0}{\hbar} x} \right]$$

At large *x* values, $y \rightarrow \hbar/\tau_0 kT$, and as the residence time decreases exponentially with increasing temperature, *y* would increase. However, near 30°, *y* vs. *x* is observed to decrease abruptly, and curves above 30° are systematically low. Above 30° the *y* vs. *x* curves again begin to increase with temperature. The change in *y* near 30° could be associated with the onset of contributions from a "free particle" diffusive motion with characteristic times, $\tau_g = MD/kT$, which near 30° have become comparable to the neutron interaction time. *M* would correspond to the net mass of a number of molecules moving in a correlated manner and would approximately correspond to about 80 to 100 waters (*i.e.*, five to six ions and their hydration layers). The rise in the *y* vs. *x* curves above 30° with temperature could correspond to a decrease in *M* with increasing temperature, so that τ_g would again become short compared to the interaction time and, hence, a delayed diffusion behavior would again predominate.

Such a decrease in *y* near the transition temperature could also occur if a sudden change in the jump diffusion parameters (*D*, τ_0) occurred due to a change of solution structure. At lower temperatures, the hydrated ions may be "spanned" by regions of the solvent around local orderings similar to water, and diffusion would mainly be due to activated jumps of individual molecules with an average activation energy lower than that for water. Near the transition temperature, the thermal excitation may break the weaker bridging solvent structure, decouple the hydrated ions, and allow correlated motions of groups of hydrated ions to

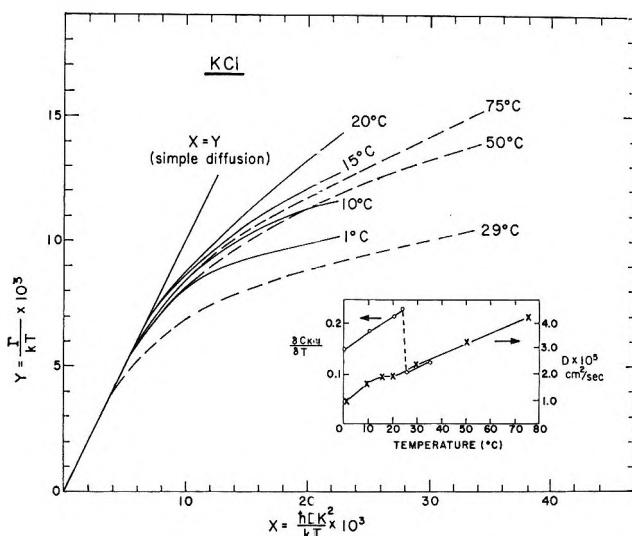


Figure 12. The observed temperature dependences of $\Gamma/k_B T$ vs. $\hbar DK^2/k_B T$ are shown for a 4.6 *m* KCl (3.2 *m* at 1°) solution. In the insert, the values of the self-diffusion coefficients obtained from the initial slopes of the Γ vs. *K*² curves are plotted vs. temperature (×). The reported⁴⁸ temperature derivative of the solubility is also plotted as a function of temperature (O).

occur. With additional increases in temperature, a further reduction in the size of the higher hydration layers and in the correlation range could occur. At present, the above explanations must be considered tentative. However, they can provide a plausible and consistent explanation for the observed changes in the solubility, X-ray, and neutron data.

For certain strongly hydrating ions, at sufficiently high concentrations such that a majority of the waters present are strongly coordinated with the primary hydration layers, the observed diffusive kinetics may not be solely due to the thermally activated jumps of individual H₂O molecules. Indeed, nmr measurements have indicated that the exchange times for H₂O molecules from the primary hydration layers may exceed 10⁻⁴ sec for such cations as Be²⁺, Al³⁺, Ga³⁺, and Cr³⁺.^{21,51,52} The possibility then exists that, within the range of his interaction times that are experimentally observable, the only observable contribution to the diffusive broadenings would arise from ions which diffuse together with their hydration layers, in keeping with the proposal by Olson, *et al.*⁵³ If such motions of the hydrated ions were in accord with classical diffusion,²⁶ then the Lorentzian half-width would be given by

$$\Gamma = \hbar DK^2 \quad (2)$$

(50) P. A. Egelstaff, *Advan. Phys.*, **11**, 203 (1962).

(51) R. E. Connick and R. E. Poulson, *J. Chem. Phys.*, **30**, 759 (1959).

(52) M. Alei, Jr., and J. A. Jackson, *ibid.*, **41**, 3402 (1964).

(53) M. V. Olson, Y. Kanazawa, and H. Taube, *ibid.*, **51**, 289 (1969).

The observed width would be a linear function of K^2 . The values of the D 's and of the slopes of Γ vs. K^2 should be small relative to those for a single H_2O , due to the higher mass.

In Figure 6, a series of Γ vs. K^2 's measured at 1° for different salts and different concentrations illustrates the experimentally observed functional shapes of various diffusive kinetics. The curve for 0.5 m LiCl solution shows a Γ vs. K^2 similar to that for pure water, in keeping with the simple jump diffusion model. In like manner, the Γ vs. K^2 curve for the 5.7 m $MgCl_2$ solution again is in accord with the simple jump diffusion model. However, at this concentration, the magnesium ion has effectively increased the value of τ_0 and decreased the value of D relative to water and the 0.5 m LiCl solution. Thus, at higher K^2 values, Γ is observed to approach the constant value of \hbar/τ_0 expected for the simple jump diffusion. In contrast, for both the 15.02 m LiCl and the 4.3 m $CrCl_3$ solutions, Γ has a dependence on K^2 which is linear over the entire range of observed K^2 values. However, the slopes and, hence, their values of D lie well below those for the more dilute solutions. Further, the curve for $CrCl_3$ lies below that for the 15.02 m solution of LiCl which, as noted above, would be expected in view of the masses if the primary contribution to diffusion involved the classical diffusion of hydrated cations. Indeed, in such a case, the slope, $\hbar D$, would be smaller for the heavy, higher charged ion than for the lighter lithium ion and its hydration layer in accord with the observation. If the concentration is reduced slightly for lithium chloride (from 15.02 to 10 m), the curve of Γ vs. K^2 is no longer linear over the entire range of K^2 , but appears to have two nearly linear regions. Thus, in the 10 m solution of LiCl, the observed diffusive kinetics may involve the motions of hydrated lithium ions, as well as jump reorientations of individual H_2O molecules.

General Discussion

The variations and trends of the intermolecular frequencies and the diffusive kinetics with concentration, with ions, and with temperature, as observed in this investigation, are in agreement with many previously reported theoretical and experimental results. In dilute aqueous ionic solutions, hydrated ions affect the more distant solvent structure in a manner specific to the size and charge of the ion, but "remnants" of water structure can persist.^{54,55} It is not implied that such a "waterlike" solvent structure is in exact correspondence to the pure solvent. Rather, the solvent structure maintains an ordering, a relaxation time, and an activation energy closely similar to water. Thus, Samoilov¹⁹ has argued that hydration in dilute solutions occurs with a minimum modification of the water structure. He suggests that while the heat of hydration contributed from the sum of energy over many molecules may be large, the interaction energy of an

ion with a single water molecule outside its hydration sphere could be small. In agreement, pmr¹⁷ has indicated that the solvent at some distance from a hydrated ion may have a relaxation time similar to that of pure water, and the X-ray maxima⁵⁶ for dilute solutions persisted at the same positions as those of water. Spectroscopic results have also shown spectral features and maxima for solutions similar to those for water.^{54,55}

The degree to which a "remnant" solvent structure beyond the primary hydration layer persists or is disrupted with increasing concentration depends specifically on the ions present. Thus, the results of recent Raman studies of alkali metal-nitrate solutions⁵⁷ have shown that in dilute solutions, the hydrated NO_3^- ion experiences a nonspecific effect of the cation field due to the cation induced polarity of its hydration sheath. However, typically at concentrations of 1.5 m and above, this dependence becomes cation specific and varies as $Li^+ > Na^+ > K^+ \approx Cs^+$. In reasonable agreement with the results of this investigation, Kaminisky²⁸ and, more recently, Greyson and Snell,²⁹ have obtained evidence that strongly hydrating ions like Mg^{2+} and Li^+ can perturb the bulk-solvent, while weakly hydrating ions like K^+ and Cl^- ions compete for water molecules with existing solvent structure. Thus, the hydration complexes formed by strongly hydrating cations appear able to produce significant changes in the distant solvent by long-range interactions.²⁹⁻³¹ Such longer range structural modifications most probably do not result from large dipole-field interactions which, for most $1+$ cations (with the exception of Li^+), are insufficient to reorient H_2O molecules beyond the first layer.³³ However, as pointed out by Hindman,³³ the component of the ionic field in the H bond direction of the primary waters may redistribute the charge on the water protons and give rise to a cooperative polarization that can alter the "structural temperature" of the solvent. This argument is consistent with ir⁵⁸ results, which indicate that the strong and partially covalent cation-water coordinations can lead to a polarization and an increase in the bond strength between the primary hydration layer and the surrounding waters.

Recently an explanation for the effects of ions on the solvent structure has been proposed by Tikhomirov.²¹ He argues that the water molecules in the immediate vicinity of the ions are strongly reoriented and coordinated in a manner specific to the cation. As a result, there is an "intermediate region" of structural misfit between the hydrated ion and the more distant

(54) D. E. Irish, B. McCarroll, and T. F. Young, *J. Chem. Phys.*, **39**, 3436 (1963).

(55) G. E. Walrafen, *ibid.*, **36**, 1035 (1962).

(56) J. Beck, *Physik. Z.*, **40**, 474 (1939).

(57) D. E. Irish and A. R. Davis, *Can. J. Chem.*, **46**, 943 (1968).

(58) G. Zundel and A. Murr, *Z. Phys. Chem. (Frankfurt am Main)*, **54**, 49 (1967).

solvent in which water molecules must reorient to accommodate these two structures. As a result, in this region the average number of bonds per water molecule would, in general, be reduced relative to water (a "negative hydration" trend). However, this reduction in the average number of bonds may be countered by the polarization of the primary water by the ion-field component in the bond direction, which lowers the effective temperature of the solution (a "positive hydration" trend). Thus, the mobility relative to water of molecules in the "intermediate region" will depend on the degree to which the reduction in the number of bonds due to the structural misfit has been compensated by polarization. Tikhomirov²¹ argued that such polarization effects may be transmitted beyond the second and third hydration layers. The more covalent the primary cation-water interaction is, the stronger are the deformations of charge on the H₂O molecules in the primary layers, and further is the "transmission" of such polarization effects. With increasing concentration, the hydrated ions act on a decreasing number of "free-solvent" molecules, and the effects of polarization and of mismatches become more severe. Further, for certain salts, ion pairing may increase with concentration, as discussed above for the CsCl and CsBr solutions.

At lower temperatures, the "boundary-line"⁵⁹ between structure-breaking and -making cations is generally reported to occur between Na⁺ and K⁺, in accord with the observed dependence of the Γ vs. K^2 curves on cation (Figure 6). However, there exists ample evidence^{14,28,59} that the structure-breaking and -making effects vary with both concentration and temperature, in a similar manner to that observed in the present and previous² investigations. Thus, Kaminsky²⁸ has pointed out that the ordering of H₂O molecules about strongly hydrating ions like Be²⁺, Mg²⁺, and Li⁺ becomes increasingly disturbed and diminishes with increasing temperature. Endom, *et al.*,¹⁴ from spin-echo measurements of the self-diffusion coefficients of H₂O molecules in aqueous solutions, reported that certain salts (*i.e.*, KCl, KBr, KI, CsCl, CsBr), at low temperatures (typically 1 and 25°), show a structure-breaking tendency. In contrast, at higher temperatures they show a structure-making tendency, such that the self-diffusion coefficients are less than that for water. Thus, in accord with the present results, as the solvent structure is thermally disrupted, an increase in the solvation occurs. Also, Ionov,⁵⁹ from nuclear quadrupole relaxation measurements, argued that, above 50°, none of the salts, CsCl, KCl, NaCl, and LiCl, produces an increase in the rotational freedom of water molecules

relative to pure water, and at 90°, these salts only decrease the relative rotational freedom. Thus, as the solvent structure is thermally disrupted, an increase in the solvation occurs.

In general, the larger halide and nitrate anions, while able to form ion-water coordinations, act as "negative hydrators." In solutions of small and/or highly charged ions (Li⁺ and La³⁺) which form strong primary cation-water coordinations, the neutron spectra show only minor variances with anions in intermolecular frequencies and the diffusion kinetics relative to those for solutions of larger 1+ cations like K⁺. Hindman³³ has suggested that the high density of negative charge in the H₂O molecule associated with the lone-pair regions might provide a larger interaction energy between the water molecule and a cation than between the water molecule and an anion of equal radius. Similarly, Syrnikov⁶⁰ calculated, by the molecular orbital method, the fraction of the energy of interaction between water molecules and alkali metal cations and halide anions associated with quantum mechanical effects. He found that the energy of delocalization of electrons upon hydration decreases in going from lithium to cesium, and the interaction is smaller for the anions than for the cations. Also, Brady⁶¹ has argued from X-ray diffraction studies of LiCl solutions that the hydration of the Cl⁻ ions may not be "true" in that their ionic fields may not be sufficiently strong to withdraw solvent molecules from the liquid pseudo-lattice and realign them around the anions. The Cl⁻ ions are thus disposed in a fairly regular manner outside the primary hydration layer of the cations in the solutions. This is in keeping with Solovkin's⁶² observation that, in the presence of smaller cations, the surface density of water molecules about the anion depends on the cation. However, as the size of the cation increases, it becomes independent of the cation. These arguments are in agreement with the present results.

Acknowledgments. The authors wish to thank Dr. G. E. Walrafen for many helpful suggestions and his continued interest during the course of this investigation. They also wish to express gratitude to Dr. H. S. Frank, Dr. H. G. Hertz, Dr. C. M. Davis, Jr., and Dr. T. A. Litovitz for valuable discussions. They acknowledge the aid of Mr. W. Fredrickson in taking data.

(59) V. I. Ionov and R. K. Mazitov, *J. Struct. Chem. (USSR)*, **9**, 787 (1968).

(60) Yu. P. Syrnikov, *ibid.*, **7**, 466 (1966).

(61) G. W. Brady, *J. Chem. Phys.*, **28**, 464 (1958).

(62) A. S. Solovkin, *J. Struct. Chem. (USSR)*, **9**, 240 (1968).

A Neutron Inelastic Scattering Investigation of the H₂O Molecules in Aqueous Solutions and Solid Glasses of Lanthanum Nitrate and Chromic Chloride¹

by P. S. Leung, S. M. Sanborn, and G. J. Safford¹

Union Carbide Corporation, Sterling Forest Research Center,

York 10987 (Received March 2, 1970)

The intermolecular frequencies below 900 cm⁻¹ and the diffusive kinetics of H₂O molecules in La(NO₃)₃ and CrCl₃ solutions have been investigated, above and below their glass transitions, using neutron inelastic scattering. The persistence, at all temperatures, of frequencies characteristic of cation-water hydration complexes, which are primarily cation dependent, indicates that the local structures about the cation in the solution and in the glass are similar. For 3.5 *m* LaCl₃ and La(NO₃)₃ solutions at 1°, the reorientations of individual H₂O's primarily contribute to the observed diffusive kinetics, which are also observed to be only slightly anion dependent. For concentrated solutions of the small or highly-charged cations (*i.e.*, Cr³⁺ and Li⁺), the motions of the whole hydration complex contribute primarily to the diffusive kinetics, and the self-diffusion coefficient decreases as the size of the complex increases. At temperatures near the *T_g*'s of the solutions, the relaxation times associated with the diffusive motions of both the individual H₂O's and the hydration complexes are longer than the neutron interaction time, and these motions no longer contribute to the spectra. These results have been compared with reported glass transition temperature measurements. It is suggested that the formation of a solid glass at low temperatures could be primarily associated with the restriction of the diffusive motions involving hydrated cations by "bridging" anions. Thus, higher glass transition temperatures would be associated with anions of higher basicity.

I. Introduction

Upon being supercooled, aqueous solutions of many multivalent ions become increasingly viscous and, below a characteristic temperature (*T_g*), form solid glasses.^{2a} It has been suggested that with decreasing temperature, "liquid-like" diffusive motions become damped as *T_g* is approached, and a behavior akin to a harmonic solid is approached. On the basis of Raman spectra, it has been suggested^{2b} that the formation of strongly coordinated, centrosymmetric cation-water complexes may partially inhibit the formation of crystalline ice and promote glass formation. Recently, Angell and Sare^{2a} have studied the dependence of *T_g* on cation, on anion, and on concentration. For a given concentration and anion, the value of *T_g* increased with cationic charge. However, for a given cation, the variations in *T_g* with anion were also large, and *T_g* increased in the progression: chloride < nitrate < sulfate, *i.e.*, with the basicity of the anion. Solutions containing quasi-spherical, singly-charged anions had lower *T_g*'s, while those containing asymmetric anions had higher *T_g*'s. This dependence was attributed to the bonding of the anions to the H₂O molecules in the cation hydration sheath. It was suggested that the anions thus order their environment, reduce the configurational entropy, and raise *T_g*.

For salts with a common anion and cationic charge, the *T_g*'s decrease linearly with concentration to a point such that they become independent of the cation and

then approach the *T_g* for vitreous ice. Thus, a concentration is reached below which the cations become effectively shielded by their hydration sheaths, which correspond to approximately 6 to 8 H₂O molecules for LiCl, 17 to 20 H₂O molecules for divalent cations, and 24 to 31 H₂O molecules for trivalent cations. Further, Angell and Sare^{2a} argued that chloride solutions at low temperatures tend to separate into "salt-rich" and "solvent-rich" regions. In the former, H₂O molecules and anions may be oriented about cations with local orderings similar to their corresponding solid salt hydrates. Similar conclusions have been reached from observed Raman³ and neutron inelastic scattering⁴ (nis) investigations of concentrated ionic solutions made at temperatures above 1°. In contrast, according to Angell and Sare,^{2a} the observed dependence of the *T_g*'s on concentration for nitrate solutions did not appear to indicate such a phase separation. The tendency to separate may still be present; however, evi-

* To whom correspondence should be addressed.

(1) This work is partly supported by the Office of Saline Water, Department of the Interior.

(2) (a) C. A. Angell and E. J. Sare, *J. Chem. Phys.*, **52**, 1058 (1967); (b) R. E. Hester and W. E. L. Grossman, *Spectrochim. Acta*, **23A**, 1945 (1967).

(3) R. E. Hester and D. E. Irish in "Raman Spectroscopy Theory and Practice," H. A. Szamanski, Ed., Plenum Publishing Co., New York, N. Y., 1967, pp 101, 224.

(4) G. J. Safford, P. S. Leung, A. W. Naumann, and P. C. Schaffer, *J. Chem. Phys.*, **50**, 4444 (1969).

dence for such a separation may not be detected by experiments due to the high T_g 's for nitrates.

In this investigation, the spectra for solutions, glasses, and solid salt hydrates of $\text{La}(\text{NO}_3)_2$ and CrCl_3 have been measured by neutron inelastic scattering to provide information at a molecular level which can complement the measurements on T_g , discussed above. Previously, nis^{4,5} has been used to investigate simultaneously the intermolecular frequencies and the diffusive kinetics of H_2O molecules in ionic solutions, and their dependences on anion, cation, concentration, and temperature. For concentrated solutions of small and/or multivalent ions (*e.g.*, La^{3+} , Mg^{2+} , Li^+ , and F^-), frequencies characteristic of primary ion-water hydration complexes are observed. These frequencies show a strong correspondence to those of the respective solid salt hydrates, suggesting a similarity in the local ordering of the hydration complexes. In contrast, at low concentrations, the nis spectra primarily reflect the bulk solvent, and information has been obtained on the ability of salts to perturb and disrupt the solvent structure relative to water.

The absence of optical selection rules in nis allows, in principle, all motions, including vibrations and diffusive motions, to be observed. Diffusive motions give rise to a broadening of the incident energy distribution (the "quasi-elastic" component). By studying the dependence of the widths and areas on scattering angle, and the dependence upon temperature of the quasi-elastic component, information may be obtained on the functional form of the diffusive kinetics and the numerical values of the associated diffusive parameters. As reported previously,^{4,5} below 25° , for most salt solutions, the diffusive kinetics are in accord with a delayed-diffusion approximation.⁶ Small and/or highly charged ions decrease the self-diffusion coefficient, D , and increase the residence time, τ_0 , relative to water. Ion-water interactions give rise to higher activation energies for the movement of H_2O molecules relative to pure water; thus, these salts act as "positive hydrators."⁷ In contrast, salts of ions of low charge-to-radius ratio increase D and decrease τ_0 relative to water and act as "negative hydrators".⁷

In this investigation the intermolecular frequencies (below 900 cm^{-1}) and changes in the diffusive kinetics from 1° to below T_g have been observed for $\text{La}(\text{NO}_3)_3$ and CrCl_3 solutions. It might be expected that any ordering involving the ion-water complexes would be similar in the glass and in the supercooled liquid, and any effects arising from the coupling of such complexes to a lattice (as for the solid salt hydrates) would be absent. Further, in the supercooled liquid, any relaxational broadening would be reduced relative to temperature above 1° , where most previous measurements on water and ionic solutions have been made. This should further facilitate comparisons between the spectra of the supercooled solutions and the glasses.

II. Experimental Section

A. Instrumental. The measurements were made using the beryllium-filtered incident beam and a time-of-flight spectrometer described in detail previously.⁴ The solutions were prepared from reagent grade materials and deionized water. The solution samples were 0.42 mm in average thickness and were contained in an aluminum sample holder, appropriately shielded so that the neutrons could only be scattered from the liquid. A thin layer of an inert polymer film ($2\ \mu$ in thickness), plated on the cell and the aluminum windows, afforded protection against corrosion without significantly contributing to background. As detailed previously,⁴ measurements have shown that the above sample thickness yielded negligible spectral distortions due to multiple scattering. For spectra measured below 0° , the samples were cooled by flowing liquid nitrogen or liquid nitrogen boil-off gas through a channel in the sample holder and the temperature was controlled to $\pm 2^\circ$. Care was taken to prevent condensation on the scattering surface of the sample. For spectra taken at $+1^\circ$, the sample was cooled by circulating water from an ice bath and was shielded to avoid scattering of neutrons by the coolant. The glass transitions for the solutions were determined using a simple differential thermal analysis technique, identical with that described by Angell and Sare.^{2a} A Honeywell Electronic 19 dual pen recorder was used to follow the differential emf and temperatures. The two trivalent salts measured and their concentrations were chosen as they had high glass transition temperatures, and measurements had shown that when these solutions were held above their glass transitions in the supercooled state for the periods over which the spectra were measured (typically 6 hr), no significant degree of crystallization had occurred. In addition, the high glass transition temperatures allowed the samples to be cooled to the vicinity of the glass transition directly in the sample holder at a sufficiently rapid rate so that crystallization did not occur.

B. Analysis of Data. The spectra were corrected for background, for counter efficiency, and for chopper transmission. The background corrections were made by a channel-by-channel subtraction of the spectra obtained for the empty sample holder, and were found to be predominantly a flat component upon which was superimposed a weaker broad distribution, centering at about channel 146. This latter component, which varied with rotor speed, is ascribed to the 180° burst. Statistical uncertainties were calculated from the total number of background counts and the number of ob-

(5) P. S. Leung and G. J. Safford, *J. Phys. Chem.*, **74**, 3696 (1970).

(6) K. S. Singwi and A. Sjölander, *Phys. Rev.*, **119**, 863 (1960).

(7) O. Ya. Samoilov, "Structure of Aqueous Electrolyte Solutions and the Hydration of Ions," Consultants Bureau Enterprises, Inc., New York, N. Y., 1965.

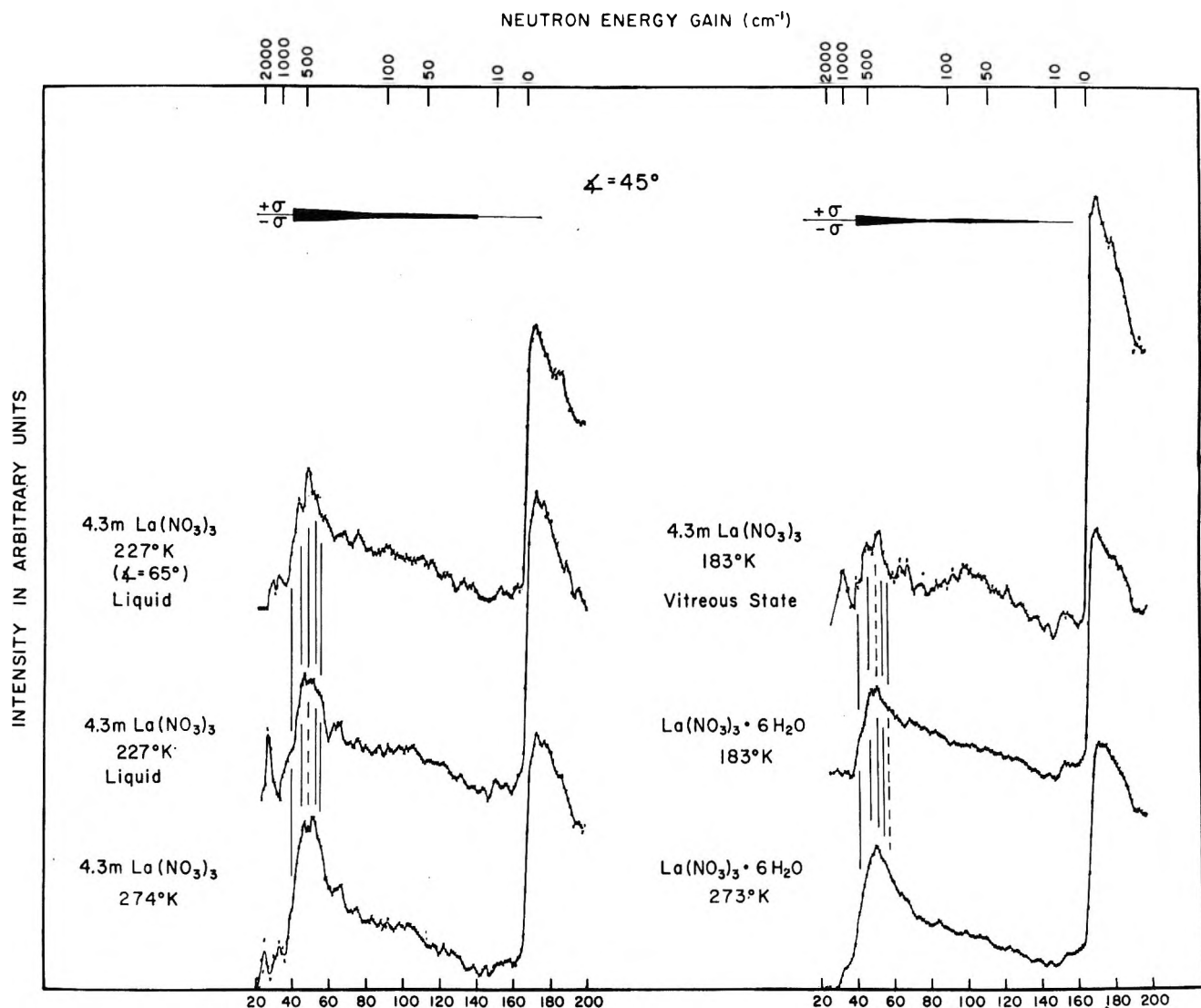


Figure 1. The time-of-flight spectra for a $\text{La}(\text{NO}_3)_3$ solution at temperatures above and below the glass transition are compared with its solid hydrate. The vertical lines indicate the similarity in the frequencies. The corresponding frequency distributions for the glasses and supercooled solutions are shown in Figure 3.

served counts per channel. Further, the reproducibility and reliability of spectral features were checked by comparisons of spectra remeasured at different times with new solutions; comparisons of data collected from four independent counter banks, electronics, and memory banks from the time-of-flight analyzer; and a comparison with background spectra for the empty cell to show that no spectral features or maxima arose from the sample holder or the aluminum window. The solid curves in Figures 1 to 3 were averaged through the data points with regard to statistical uncertainties. The half-width at half-maximum, Γ , for the Lorentzian function associated with a diffusively broadened incident energy distribution was determined in a manner described in detail previously.⁴ Specifically, Γ 's were selected by comparing the observed quasi-elastic component with the measured incident-energy distribution which had been further broadened by a series of

Lorentzian functions of varying half-widths at half-maxima.

III. Results and Discussion

A. Inelastic Spectra. The time-of-flight spectra for neutrons scattered from solutions of CrCl_3 and $\text{La}(\text{NO}_3)_3$, at temperatures above and below their glass transitions, are shown in Figures 1 and 2 and compared with those of the corresponding solid salt hydrates and of hexagonal ice. The corresponding frequency distributions shown in Figure 3 were calculated assuming the cubic one-phonon cross section^{8,9} and a Debye-Waller factor of unity.⁴ The following features and trends were observed. (a) A strong correspondence in spectral features and frequencies (below 900 cm^{-1})

(8) L. S. Kothari and K. S. Singwi, *Solid State Phys.*, **8**, 109 (1959).

(9) L. V. Tarasov, *Soviet Phys.-Solid State*, **3**, 1039 (1961).

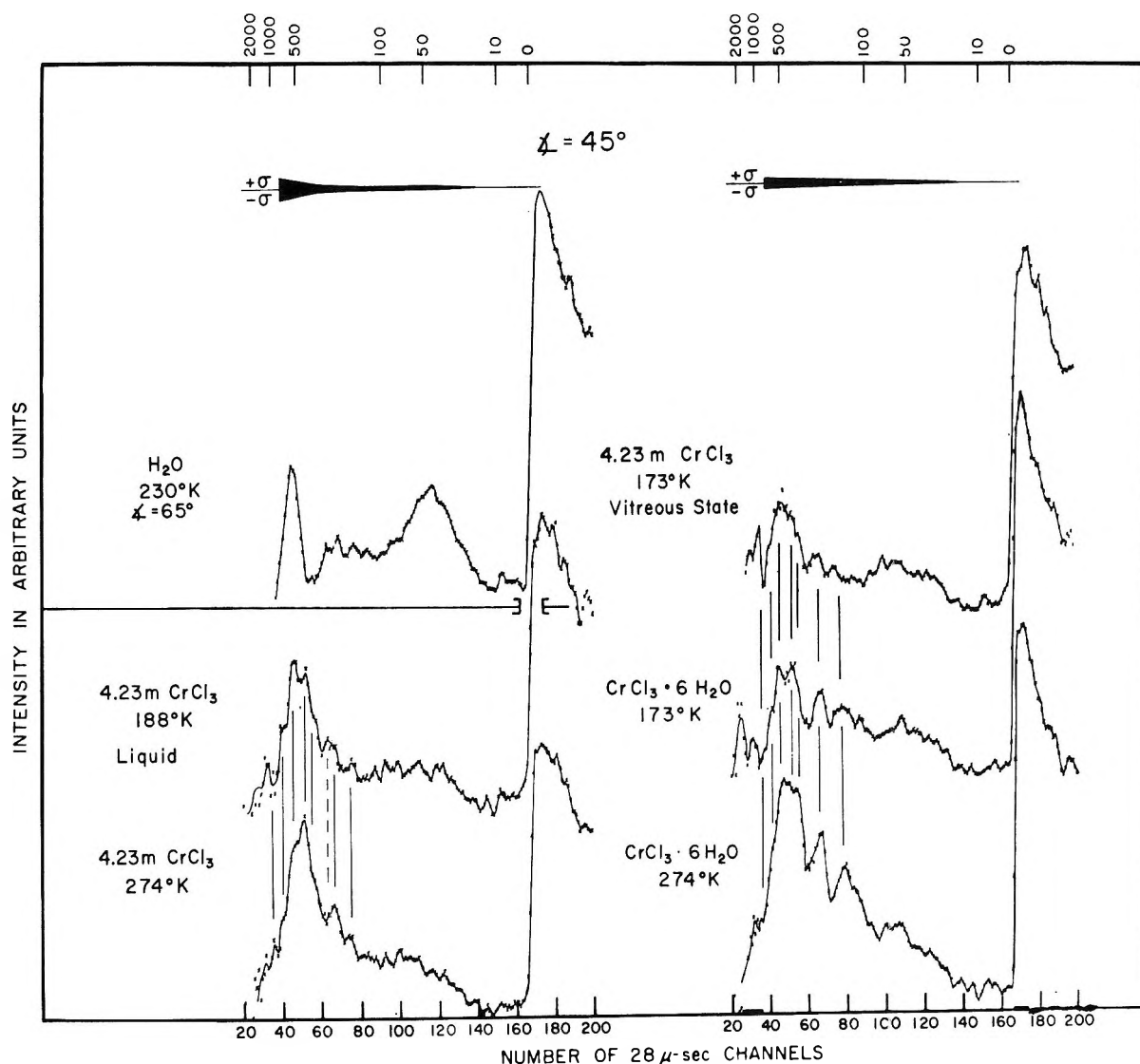


Figure 2. The time-of-flight spectra for a CrCl_3 solution at temperatures above and below the glass transition are compared with its solid hydrate. The vertical lines indicate similar frequencies among the spectra. The correspondence between these frequencies and the reported ir frequencies and the frequency distribution are shown in Figure 3.

exists between the supercooled solutions above T_g and the solid glasses. (b) The observed frequencies (which differ from those of water and ice) are associated with the characteristic modes of cation-water hydration complexes, and good correspondence is observed with reported infrared and Raman frequencies. Thus, for CrCl_3 , certain of these frequencies have been assigned to the librational modes of H_2O molecules and to the metal-oxygen stretching modes characteristic of the $\text{Cr}(\text{H}_2\text{O})_6^{3+}$ complexes. The Cr^{3+} -water coordinations may involve a degree of covalent bonding.¹⁰ Evidence has also been cited for the existence of octahedral ion-water complexes in solutions of rare earth halides.¹¹ In previous investigations,⁴ similar frequencies, characteristic of strongly coordinated, primary cation-water complexes, were observed for solutions containing La^{3+} , Mg^{2+} , and Li^+ cations. Such frequencies (as well as the diffusive kinetics and param-

eters) were found to be only weakly affected by -1 anions and to be primarily determined by the cation-water coordinations. (c) The spectra of the solutions at 1° and of the solid crystalline hydrates also show inelastic maxima at frequencies similar to those observed for the glasses and for the supercooled liquids. However, in the solutions at 1° , these maxima are broadened by the increased diffusional and relaxational rates. The change in intensity could vary due to the population factor. In the spectrum of $\text{CrCl}_3 \cdot 6\text{H}_2\text{O}$, these maxima appear nearly as sharp as in the spectra of the glass and the supercooled liquid. However, for $\text{La}(\text{NO}_3)_3 \cdot 6\text{H}_2\text{O}$, despite the absence of any relaxational broadening, these frequencies appear broader than for

(10) I. Nakagawa and T. Shiranouchi, *Spectrochim. Acta*, **20**, 429 (1964).

(11) A. Pabst, *Amer. J. Sci.*, **222**, 426 (1931).

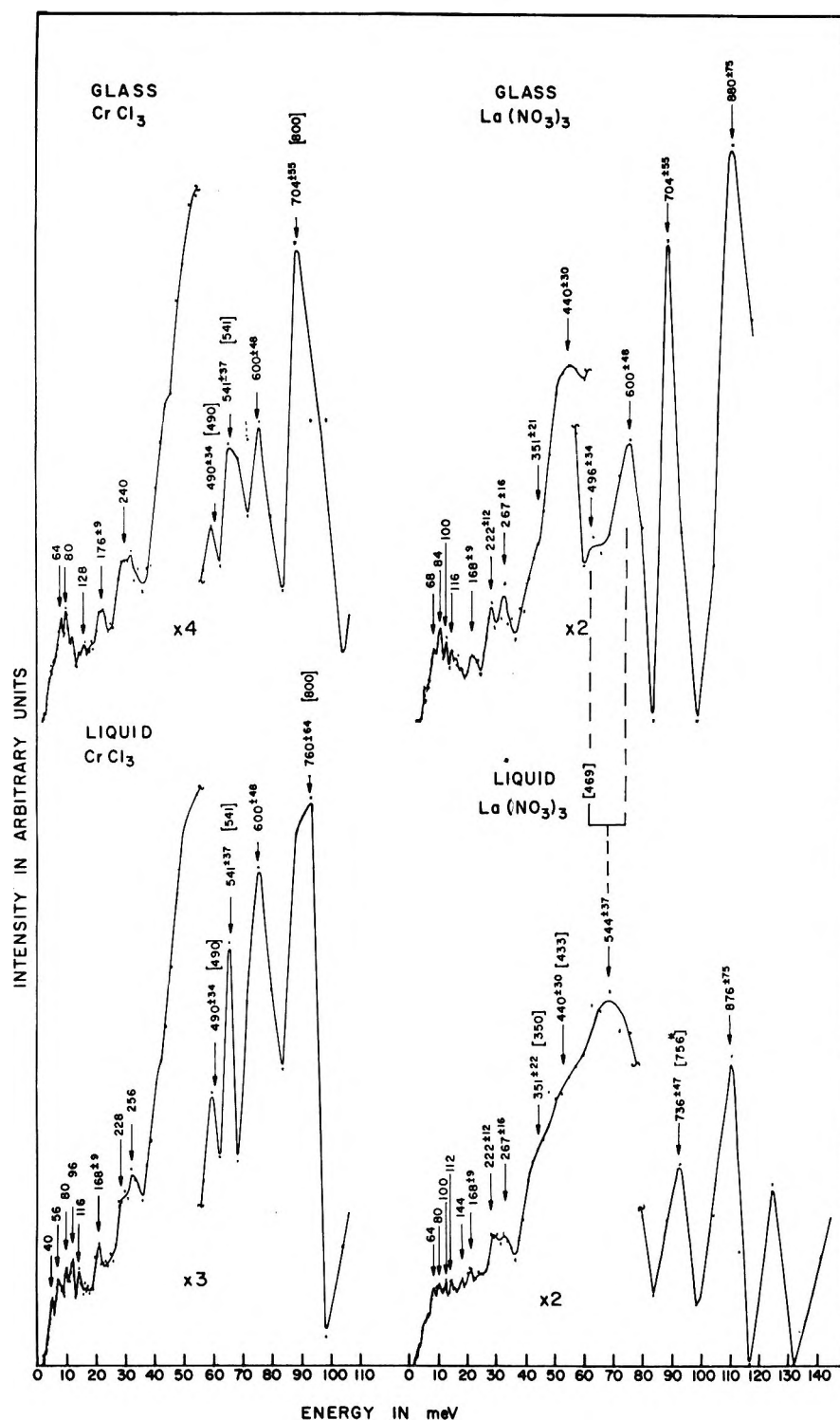


Figure 3. The one-phonon frequency distributions calculated from the time-of-flight spectra of CrCl_3 and $\text{La}(\text{NO}_3)_3$ solutions above and below their glass transitions are compared. The spectra shown for CrCl_3 were measured at 173°K (glass) and 188°K (liquid), and the spectra for $\text{La}(\text{NO}_3)_3$ were measured at 183°K (glass) and 277°K (liquid). In order to reduce the size of the graph, the intensity of the right half of each spectrum has been reduced by the factor indicated on the graph. Frequencies enclosed by brackets are reported in frequencies (see ref 10, 17, 18) of the corresponding hydrates. The frequency with an asterisk was calculated from the reported value of the $\text{La}(\text{OD}_2)$ "rocking" vibration. A noticeable change in intensity is observed for $\text{La}(\text{NO}_3)_3$ in passing from the glass to the liquid in the region around 160 cm^{-1} where anion-water frequencies occur. This change may be due to the broadening of the liquid spectrum as compared to that of the glass. This change is less noticeable for the CrCl_3 however. In general, the spectra of the glasses exhibit better resolution. Note, for example, the splitting of the frequency which occurs at 554 cm^{-1} in liquid $\text{La}(\text{NO}_3)_3$ into two components (440 cm^{-1} and 600 cm^{-1}) in the spectra of the glass. This and other small shifts cannot be excluded because of experimental resolution and the uncertainty in assigning frequencies.

either the glass or the supercooled liquid. It therefore appears possible that, in $\text{La}(\text{NO}_3)_3 \cdot 6\text{H}_2\text{O}$, coupling of the "hydrated ions" to the lattice has split their characteristic frequencies into unresolved components, making them appear broadened. For $\text{CrCl}_3 \cdot 6\text{H}_2\text{O}$, the influences of such coupling of complex vibrations to the lattice would be relatively less pronounced due to the stronger, and partially covalent, primary cation-water coordinations.

These results suggest a degree of similarity in the coordinations and local ordering of hydrated cations between the glasses and the corresponding supercooled, concentrated, viscous liquids. Such cation-water complexes could, in part, be responsible for the ability of supercooling and inhibiting the formation of hexagonal ice,^{2b} and, at lower temperatures and concentrations, for the formation of "salt-rich" and "water-rich" regions of the type postulated by Angell and Sare.^{2a} On the basis of the above results, the strong dependence of T_g on anions cannot be associated with significant alterations in the cation-water coordinations in these complexes by anions. Rather, in keeping with the argument of Angell and Sare,^{2a} anions may bind to the protons of H_2O molecules already strongly oriented about cations, and thus affect the orderings and diffusive motions of hydrated cations.

B. Quasi-Elastic Spectra. In previous investigations,^{4,5} it has been found that, for many ionic solutions, at lower temperatures the observed shape of the temperature and angular dependences of the quasi-elastic maxima were well approximated by a delayed-diffusion model.⁶ Thus, in solutions, the ion-water complexes, in general, are considered as dynamic, and H_2O molecules oscillate for a period τ_0 , and then rapidly reorientate or jump to a new site. For this model, the incident energy distribution becomes broadened by a Lorentzian function with a half-width at half-maximum given by

$$\Gamma = \frac{\hbar}{\tau_0} \left[1 - \frac{e^{-2W}}{1 + K^2 D \tau_0} \right] \quad (1)$$

where

$$|K^2| = k_0^2 + k_f^2 - 2k_0 k_f \cos \phi$$

and k_0 = initial neutron momentum vector, k_f = final neutron momentum vector, ϕ = scattering angle, τ_0 = "residence time," D = self-diffusion coefficient, e^{-2W} = the Debye-Waller factor. For small values of $|K^2|$, Γ approaches $\hbar DK^2$ and, hence, the Γ vs. K^2 rises linearly as expected for classical diffusion.¹² At larger values of K^2 , Γ approaches a constant value of \hbar/τ_0 . D and τ_0 can be obtained by an optimum fit of eq 1 to the observed Γ vs. K^2 dependence.

In Figure 4, the curves of Γ vs. K^2 for 4.3 *m* $\text{La}(\text{NO}_3)_3$, 4.3 *m* LaCl_3 , 4.23 *m* CrCl_3 , and 15.02 *m* LiCl solutions at 1° are compared with that for water. In

addition, quasi-elastic components observed for the supercooled solutions and the glasses of CrCl_3 and $\text{La}(\text{NO}_3)_3$ are shown, and compared both with the incident energy distribution and with this distribution broadened by the Lorentzian functions with different Γ values. The following features and trends should be noted.

(a) The curves of Γ vs. K^2 at 1° for these solutions all lie below that for water, in accord with a "positive hydration behavior."⁴ Thus, the formation of ion-water hydration complexes (whose characteristic frequencies appear in the inelastic region) decreases the self-diffusion coefficients and increases the residence times, relative to water.

(b) At 1° the curves of Γ vs. K^2 for $\text{La}(\text{NO}_3)_3$ and LaCl_3 solutions rise linearly at the origin, and then approach a nearly constant value at the larger values of K^2 , in accord with the delayed-diffusion model. Further, in correspondence to the behavior discussed above, for the observed inelastic frequencies, the Γ vs. K^2 curves for 3.5 *m* lanthanum solutions show only secondary variations when Cl^- anions are replaced by NO_3^- anions. Again, this implies that both the formation of the hydration complexes and the thermally activated reorientations of the H_2O molecules are determined primarily by cations. The weak dependence on anion is contrary to that for the glass transitions, which, for a given cation, are significantly higher for nitrate solutions than for chloride solutions. This suggests that, in solutions of strongly hydrating cations, the strong anion dependences of the glass transitions could result from other than their influence upon the ordering of H_2O molecules about the cations or upon the activated jumps of individual H_2O molecules. Thus, the possibility exists that the anions may mainly restrict motions involving the entire hydrated cations¹³ and influence the ordering of their environment. Such motions could well contribute negligibly to the nls spectra at 1° and at concentrations of typically 15 H_2O 's per ion pair, where activated jumps of individual H_2O molecules predominate.

(c) In contrast to the results for lanthanum salts, at 1°, Γ is observed to depend nearly linearly on K^2 (over the observed range) for the 4.23 *m* CrCl_3 solution and for the very concentrated (15.02 *m*) LiCl solution. Such a linear dependence is more in keeping with a classical diffusion behavior, for which $\Gamma = \hbar DK^2$. However, from the slopes at the origins of the Γ vs. K^2 curves, it is seen that the self-diffusion coefficients, D , decrease in the progression $\text{H}_2\text{O} > 3.5$ *m* $\text{La}(\text{NO}_3)_3 \approx 3.5$ *m* $\text{LaCl}_3 > 15.02$ *m* $\text{LiCl} > 4.23$ *m* CrCl_3 . The nearly linear dependences of the Γ vs. K^2 curve and the low values of the diffusion coefficient for the concentrated LiCl and CrCl_3 solutions may be explained if it

(12) B. N. Brockhouse, *Nuovo Cimento, Suppl.*, **9**, 45 (1958).

(13) Evidence for hydrated cations ($\text{Cd}(\text{H}_2\text{O})_4^{2+}$) being the mobile entities has been reported: C. T. Moynihan and C. A. Angell, *J. Phys. Chem.*, **74**, 736 (1970).

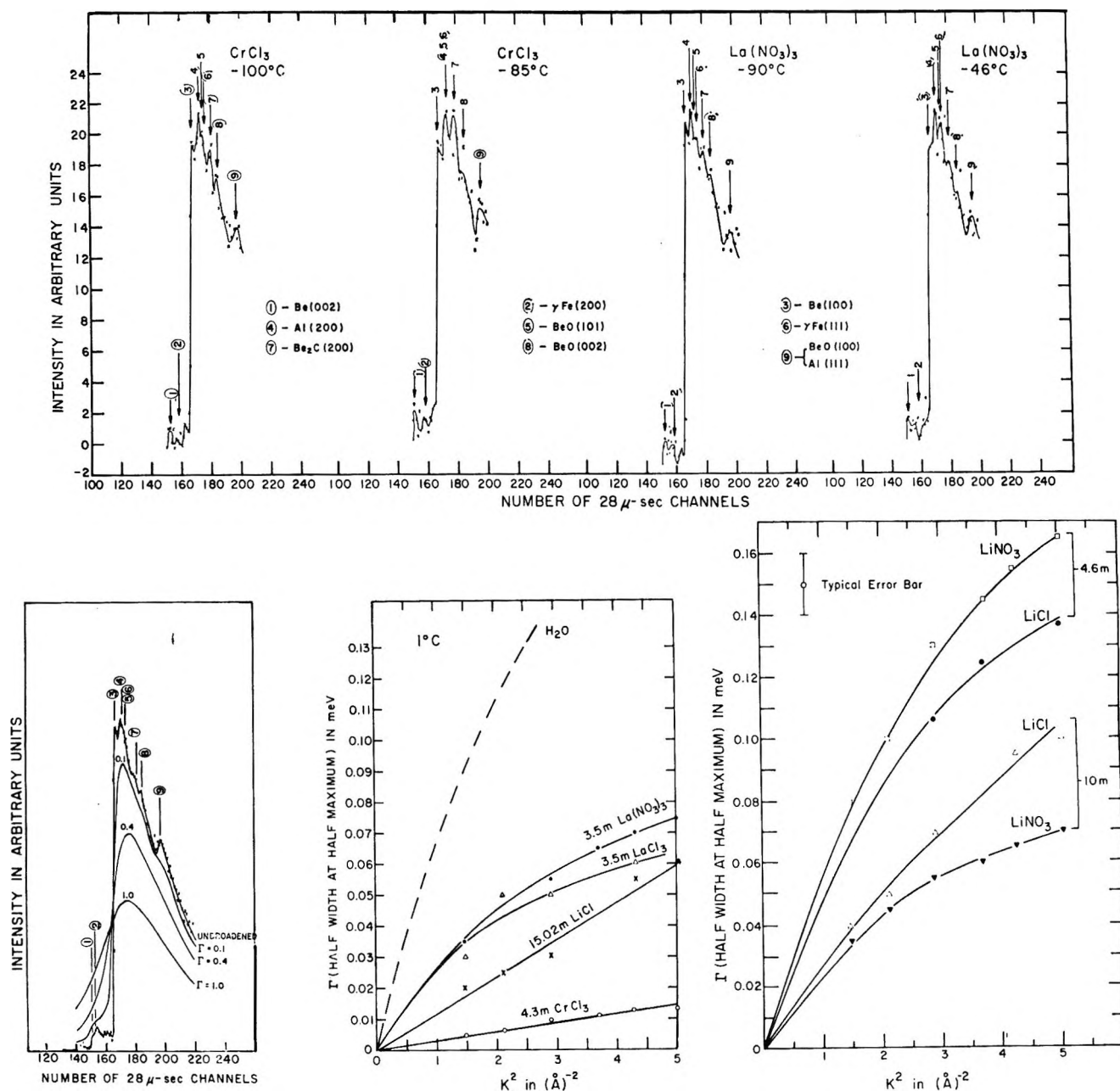


Figure 4. The energy distribution of the incident beam, determined by measuring the distribution of neutrons elastically scattered from vanadium, is shown in the lower left graph. This distribution broadened by Lorentzian functions with various half-widths, Γ , as discussed in the Experimental Section and the main text, is also shown on the same graph.

The quasi-elastic distributions for the supercooled liquid above T_g and for the glass of the 4.23 *m* CrCl₃ and 4.3 *m* La(NO₃)₃ solutions are shown in the upper graph. When compared to the Lorentzian broadened incident distributions, these quasi-elastic distributions have half-width Γ 's below 0.005 MeV, which is close to the resolution limit.

In the lower middle graph, Γ 's are plotted as a function of K^2 for several solutions and H₂O at 1°. The Γ 's for 15.02 *m* LiCl and 4.23 *m* CrCl₃ appear to be linear with K^2 , as expected for classical diffusion. The lower right graph contains the plots of Γ vs. K^2 for 4.6 *m* LiCl and 10 *m* solutions of LiCl and LiNO₃. For 4.6 *m* LiCl and LiNO₃ and for 3.5 *m* La(NO₃)₃ and LaCl₃ solutions, the lines are optimum fits to the delayed-diffusion model (eq 1). The diffusive parameters obtained by the fitting are given in Table I.

Table I

	$D^* \times 10^6$ cm ² /sec (from the slope of Γ vs. K^2 near the origin)	$\tau_0 \times 10^{12}$ sec (from eq 1)
3.5 <i>m</i> La(NO ₃) ₃	0.5	6.3
3.5 <i>m</i> LaCl ₃	0.5	7.9
4.6 <i>m</i> LiNO ₃	1.1	2.8
4.6 <i>m</i> LiCl	0.9	3.2

is assumed that the contribution to the quasi-elastic components primarily arises from diffusive motions which involve motions of the entire cation hydration complex, rather than jump reorientations of individual H_2O molecules. Thus, it has been reported¹⁴ that, for Cr^{2+} and other strongly hydrating cations, the average exchange times for individual H_2O molecules from the hydration sheath can exceed 10^{-4} sec, and, hence, would not contribute significantly to the quasi-elastic component (as discussed above). In addition, at a concentration of 15.02 *m* for LiCl , most of the H_2O molecules should be in the primary layers of the cations. The diffusion coefficient for the strongly hydrated Cr^{3+} cation would then be less than that expected for the lighter lithium ion and smaller primary hydration layer. Also, the results of Angell and Sare^{2a} show that the T_g for a 4.23 *m* CrCl_3 solution lies well above that for a 15.02 *m* LiCl solution, in keeping with a hypothesis that a higher value of T_g could result from a lower degree of mobility for a hydrated cation.

(d) At temperatures below 1° , the "quasi-elastic" components for both the supercooled liquids above T_g and the glasses of CrCl_3 and $\text{La}(\text{NO}_3)_3$ (Figure 4) show no significant broadening within resolution and statistical uncertainties when compared with the incident energy distribution and the Lorentzian broadened distributions. This does not necessarily imply that relaxational motions have ceased. Rather, it implies that any relaxational processes are occurring at such a sufficiently slow rate that their characteristic times exceed the largest neutron interaction time, so that they no longer contribute to the inelastic spectra. As detailed in the literature,^{15,16} a neutron interaction time may be defined by $t_{\text{int}} = 1/kv_0$, where v_0 is the neutron velocity relative to a scattering center. t_{int} may be varied with K (and, hence, with scattering angle). Motions with characteristic times or periods longer than about 10^{-10} sec (longer than t_{int}) would not yield experimentally distinguishable broadenings of the incident energy distribution. Thus, for example, in cooling the 3.5 *m* $\text{La}(\text{NO}_3)_3$ from 1° to just above its glass transition temperature, the relaxational time increases from 6.4×10^{-12} sec to an expected value far in excess of 10^{-10} sec. Correspondingly, as noted above, the inelastic frequencies^{17,18} characteristic of ion-water complexes sharpen, but do not show any major changes in the maxima.

(e) At a concentration of 4.6 *m*, the curve of Γ vs. K^2

for lithium nitrate lies above that for lithium chloride, indicating a stronger "negative hydration effect" for the nitrate ion. In contrast, for the 10 *m* solutions, corresponding to 5.5 water molecules per ion pair, the diffusive kinetics may involve motions of the primary hydration complex. Thus, the curve of Γ vs. K^2 for LiNO_3 is observed to lie below that of LiCl , which may indicate that the nitrate ion, acting as a "bridging" anion, is more effective in restricting diffusive motions involving hydrated cations than the chloride ion.^{2a}

The results of this investigation appear in agreement with the findings of Angell and Sare.^{2a} Multivalent cations form strongly coordinated hydration complexes which could enhance the ability of supercooling and primarily determine the inelastic frequencies and thermally activated reorientations of individual H_2O molecules in the supercooled solutions. Thus, both the relaxation times of individual H_2O molecules and T_g increase with cationic charge. The anions only secondarily influence the cation-water complexes and the diffusive jumps of individual H_2O molecules which predominate at 1° and at concentrations typically of about 15 H_2O 's per ion pair. However, they can strongly affect the diffusive motion of the overall complexes at lower temperatures or higher concentrations, so that T_g would have a major dependence on anion. With decreasing temperature below 0° , the relaxation times for reorientational jumps of individual H_2O molecules increase rapidly, and the binding of anions to protons of H_2O molecules associated with the cation sheath increasingly restricts the diffusive motions of such hydration units. The more basic an anion, the more it could produce a cooperative restriction of the diffusive motions of the hydrated cations, and the higher the T_g would be.

Acknowledgments. The authors wish to thank Drs. C. A. Angell, E. J. Sare, C. T. Moynihan, and H. Friedman for their valuable suggestions and discussions. They acknowledge the aid of Mr. W. Frederickson for his help in taking data.

(14) J. A. Jackson, J. F. Lennox, and H. Taube, *J. Chem. Phys.*, **32**, 553 (1960).

(15) K. E. Larsson, *Inelastic Scattering Neutrons, Proc. Symp.*, **1964**, **2**, 3 (1965).

(16) L. VanHove, *Phys. Rev.*, **95**, 249 (1954).

(17) R. A. Plane, "Saline Water Conversion Report," U. S. Department of the Interior, Washington, D. C., 1967.

(18) C. Postmus and J. R. Ferraro, *J. Chem. Phys.*, **48**, 3605 (1968)

Permittivity and Dielectric and Proton Magnetic Relaxation of Aqueous Solutions of the Alkali Halides

by K. Giese, U. Kaatze, and R. Pottel*

Drittes Physikalisches Institut der Universität Göttingen, Göttingen, Germany (Received March 2, 1970)

From the complex permittivities measured as a function of frequency between 5 and 38 GHz at 25° are derived the static permittivities, principal dielectric relaxation times, and relaxation time distribution parameters of aqueous solutions of all alkali halides (except LiF). The changes of these quantities with the electrolyte concentration are discussed in connection with the changes of the proton magnetic relaxation rates. Assuming simple models for the solutions, the evaluation of these changes yields the following information about the water molecules nearest to the cations and anions: disappearance of the dielectric orientational polarizability especially near the smaller cations but not near the anions; the magnitudes of the residence times near Li⁺, Na⁺, K⁺; arrangements and dynamics near Li⁺ and F⁻ differing from each other.

I. Introduction

A knowledge of the structural and dynamic changes of water induced by the addition of ions is important with respect to many physical and chemical processes in aqueous systems, especially biosystems. The measurements of the complex permittivity of aqueous ionic solutions at various frequencies reported here contribute in providing this type of information.

The essential quantities derivable from the dielectric measurements are the permittivity extrapolated to zero frequency ("static" permittivity), the principal relaxation time of the dielectric orientational polarization of the solvent water, and the width of the relaxation time distribution. The dielectric relaxation time is closely related to the reorientation time of the water molecules, the time after which the correlation between subsequent values of a component of the permanent molecular electric dipole moment vector is lost.

Information about the reorientation time of the water molecules is also available from measurements of the proton magnetic relaxation rate.^{1,2} Proton magnetic and dielectric relaxation measurements complement each other in a useful manner. In some cases, comparable quantities differ considerably for aqueous ionic solutions. A substantial intent of our investigations consists in explaining these differences and in trying to gain additional information from them.

For measurements of ionic influences on water, the alkali halides show the following advantages: they completely dissociate in aqueous solution, an important requirement for dielectric investigations of the solvent; they exhibit a simple and uniform electronic and geometric structure, and within the group of these ions therefore a clear interrelationship of their influence on water can be expected; and for alkali halide solutions, complete proton magnetic relaxation data are available.¹

Several results of dielectric relaxation measurements on aqueous alkali halide solutions were published between 1948 and 1958 by Hasted and O'Konski with coworkers.³ However the number and relative accuracy of these data are not entirely sufficient in order to present a consistent total picture of the influences of the alkali and halide ions on the solvent water.

II. Measurements

The measurements were performed at frequencies between 5 and 38 GHz using wave guides filled with the respective liquids. Within the liquid, a receiving probe was shifted along the direction x of wave propagation. Moving this probe, the wavelength λ and the attenuation exponent $\alpha\lambda$ of a propagating wave $E = \hat{E} \exp[i\omega t - (\alpha + 2\pi i/\lambda)x]$ was immediately determined by adjusting zero interference of the probe signal with a reference signal of fixed phase and calibrated variable amplitude.

From the measured λ and $\alpha\lambda$, the real and imaginary parts ϵ' , ϵ'' of the permittivity $\epsilon = \epsilon' - i\epsilon''$ follow according to

$$\epsilon' = \left(\frac{\lambda_0}{\lambda}\right)^2 - \left(\frac{\alpha\lambda_0}{2\pi}\right)^2 + \left(\frac{\lambda_0}{\lambda_c}\right)^2 \quad \epsilon'' = \left(\frac{\lambda_0}{\lambda}\right)\left(\frac{\alpha\lambda_0}{\pi}\right)$$

with λ_0 = free space wavelength and λ_c = cut-off wavelength of the (empty) line used as measuring cell.

* To whom correspondence should be addressed.

(1) L. Endom, H. G. Hertz, B. Thül, and M. D. Zeidler, *Ber. Bunsenges. Phys. Chem.*, **71**, 1008 (1967).

(2) G. Engel and H. G. Hertz, *ibid.*, **72**, 808 (1968).

(3) J. B. Hasted, D. M. Ritson, and C. H. Collie, *J. Chem. Phys.*, **16**, 1 (1948); G. H. Haggis, J. B. Hasted, and T. J. Buchanan, *ibid.*, **20**, 1452 (1952); J. B. Hasted and S. H. M. El Sabeh, *Trans. Faraday Soc.*, **49**, 1003 (1953); F. A. Harris and C. T. O'Konski, *J. Phys. Chem.*, **61**, 310 (1957); J. B. Hasted and G. W. Roderick, *J. Chem. Phys.*, **29**, 17 (1958).

Further on, only that part of ϵ'' due to polarization processes is of interest here. It is calculated from $\epsilon''(\nu)$ measured at a frequency ν according to

$$\epsilon_p''(\nu) = \epsilon''(\nu) - \frac{2\sigma}{\nu}$$

by subtracting the contribution $2\sigma/\nu$ (σ in sec^{-1}) due to the ion drift. The σ is the electrical (dc) conductivity of the ionic solutions measured at the frequency 5 kHz in the usual manner.

The salts used for preparing the solutions had the purity grades "p.A.," "DABG," or "puriss." The conductivity of the pure water was smaller than $2 \times 10^{-4} \text{ ohm}^{-1} \text{ m}^{-1}$. The measurements were performed on 1 M solutions, and, except RbF, RbBr, CsF, CsBr, also on 0.5 M solutions at the temperature 25°. LiF could not be used because of its low solubility.

III. Determination of Characteristic Quantities from the Results of the Measurements

In plotting the measured values $\epsilon_p''(\nu)$, $\epsilon'(\nu)$ in Cartesian coordinates, one can fit circular arcs to the points $\epsilon_p(\nu)$ of every solution in such a way that the deviations remain within the limits of measuring errors ($\lesssim 1\%$ for ϵ' ; $\lesssim 2\%$ for ϵ_p''). An example is shown in Figure 1. The centers of the circles slightly lie below the ϵ' axis. The position of the center defines the angle $h\pi/2$ explained in Figure 1. The circular arc intersects the ϵ' axis in the points ϵ_1 and ϵ_2 .

Taking from the circular arc the lengths of the chords $\epsilon_2 - \epsilon_p$, $\epsilon_p - \epsilon_1$ for each measuring point $\epsilon_p(\nu)$ (as for example drawn in Figure 1) and plotting the ratio

$$v \equiv \frac{1}{\nu} \frac{|\epsilon_2 - \epsilon_p|}{|\epsilon_p - \epsilon_1|} \quad (1)$$

vs. $\log \nu$ yields a descending straight line for every solution. Figure 2 shows a few examples. Here additionally the curve $1/\nu$ vs. $\log \nu$ was plotted, and at the intersection of this curve with the v vs. $\log \nu$ lines, the relationships $v = v_r \equiv 2\pi\tau_s$ and $\nu = \nu_r \equiv 1/(2\pi\tau_s)$ hold. The intersection point sharply determines the relaxation frequency ν_r (the frequency at the top of the circular arc, Figure 1, where $d\epsilon_p''/d\omega = 0$) and the principal relaxation time τ_s of the respective solution.

Because of the measured points $\epsilon_p(\nu)$ lying on circular arcs (Figure 1), and because of the linearity of the v - $\log \nu$ plots (Figure 2), $\epsilon_p(\omega)$ can be described to very good approximation by the function

$$\epsilon_p(\omega) - \epsilon_1 \approx \frac{\epsilon_2 - \epsilon_1}{1 + (i)^{1-h}(\omega\tau_s)^{1-b}} \quad (2)$$

with $\omega \equiv 2\pi\nu$. The b is related to the slope of the $v(\log \nu)$ lines (Figure 2) by

$$b \approx -\frac{\log e}{2\pi\tau_s} \frac{\Delta v}{\Delta \log \nu} \quad (3)$$

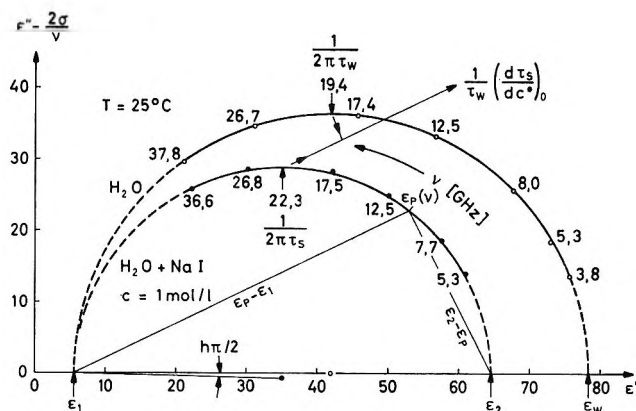


Figure 1. Imaginary part $\epsilon'' - 2\sigma/\nu$ vs. real part ϵ' of the complex permittivity $\epsilon_p = \epsilon' - i(\epsilon'' - 2\sigma/\nu)$, without conductivity contribution $2\sigma/\nu$, from measurements in dependence on the frequency ν performed on pure water and on an aqueous 1 M NaI solution.

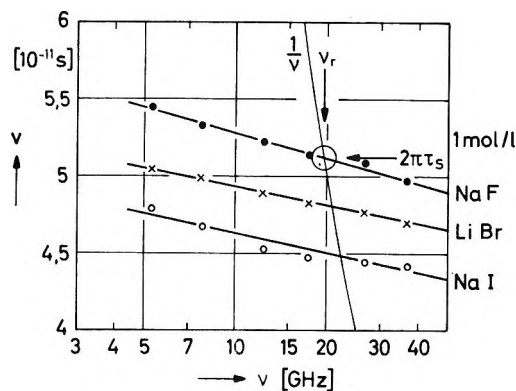


Figure 2. The ratio v , eq 1, of the chord lengths $|\epsilon_2 - \epsilon_p|$, $|\epsilon_p - \epsilon_1|$ (Figure 1) divided by the frequency ν vs. the frequency ν in log scale from measurements on three different salt solutions. The additional curve $1/\nu$ vs. ν (log) serves to determine the relaxation frequency ν_r and the relaxation time τ_s , respectively.

In the description by the function eq 2 with $1 > b > h > 0$, the dielectric relaxation of aqueous ionic solutions characteristically differs from that of pure water and aqueous solutions of nonelectrolytes. The $\epsilon_p(\omega)$ of pure water with $b_w \approx 0.006$, $h \approx 0$ closely approximates the Debye function following from eq 2 with $b = h = 0$, while $\epsilon_p(\omega)$ of aqueous solutions of organic nonelectrolytes⁴ obeys the Cole-Cole function, eq 2 with $1 > b = h > 0$.

The function $\epsilon_p(\omega)$, eq 2, with $1 > b > h > 0$ does not exactly satisfy the generally valid Kramers-Kronig relations⁵ (!) which connect the real and imaginary parts of the permittivity to each other. Therefore, eq 2 on principle only represents an approximate description of $\epsilon_p(\omega)$ which cannot hold more or less beyond the mea-

(4) R. Pottel and U. Kaatz, *Ber. Bunsenges. Phys. Chem.*, **73**, 437 (1969).

(5) H. Fröhlich, "Theory of Dielectrics," Clarendon, Oxford, 1958, p. 8.

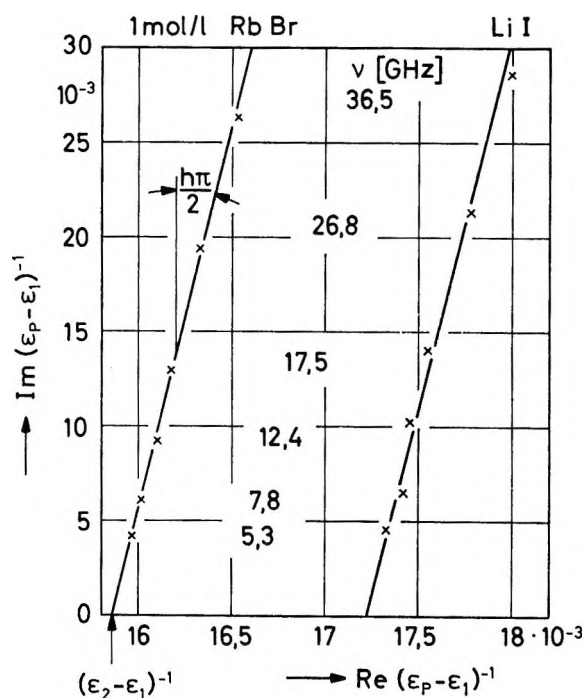


Figure 3. Imaginary part vs. real part of $(\epsilon_p - \epsilon_1)^{-1}$ from measurements of the complex permittivity $\epsilon_p(\nu)$ in dependence on the frequency ν performed on two different salt solutions.

suring frequency interval [about $-0.65 < \log(\omega\tau_s) < 0.3$]. Consequently, the terminal points ϵ_1 , ϵ_2 of the circular arc (Figure 1) do not agree with the correct asymptotic values of the permittivity at infinite frequency, $\epsilon(\infty) \equiv \epsilon_\infty$, and at zero frequency, $\epsilon(0) \equiv \epsilon_s$, respectively. If a symmetrical continuation of the locus diagram (Figure 1) from the measured part toward the correct terminal points ϵ_∞ , ϵ_s is assumed, then

$$\epsilon_\infty \approx \epsilon_1 - \frac{b-h}{2} (\epsilon_2 - \epsilon_1) \quad (4)$$

$$\epsilon_s \approx \epsilon_2 + \frac{b-h}{2} (\epsilon_2 - \epsilon_1) \quad (5)$$

holds.

To the function $\epsilon_p(\omega)$, eq 2, belongs a relaxation time distribution function which when plotted vs. $\ln(\tau/\tau_s)$ is symmetrically bell shaped with respect to the principal relaxation time τ_s . Its width at the points of half-maximum value amounts to

$$\frac{\Delta\tau}{\tau_s} \approx \frac{b+h}{\pi(1-b)} \quad (6)$$

for $h < b \ll 1$.

In order to determine ϵ_2 and h more accurately than is possible from the $\epsilon_p(\nu)$ locus diagrams (Figure 1), we plotted the measured $\epsilon_p(\nu)$ data in the complex $(\epsilon_p - \epsilon_1)^{-1}$ plane (for example Figure 3) using $\epsilon_1 = 5.4 \pm 0.5$. This ϵ_1 value is common to all solutions as was found from the circular arc plots of $\epsilon_p(\nu)$. According to eq 2,

$(\epsilon_p(\nu) - \epsilon_1)^{-1}$ represents a straight line inclined to the imaginary axis by the angle $h\pi/2$ and intersecting the real axis at $(\epsilon_2 - \epsilon_1)^{-1}$. The ϵ_2 values obtained from diagrams like Figure 3 were used for calculating ν , eq 1. Then from the ν - $\log \nu$ plots (Figure 2), τ_s and b (eq 3) were taken.

The characteristic data h , b , ϵ_s , and τ_s derived from the measured $\epsilon_p(\nu)$ values of 1 M solutions are compiled in Table I. A comparison of the τ_s values of 0.5 and 1 M

Table I^a

	F ⁻	Cl ⁻	Br ⁻	I ⁻
Li ⁺	1.3	1.3	1.5	1.6
	3.3	3.3	3.4	3.5
	65.5	65.5	65.0	64.0
	-4.2	-4.2	-7.0	-9.9
Na ⁺	1.3	2.1	2.0	1.8
	4.7	4.5	4.6	4.1
	69.4	67.3	66.7	65.5
	-1.1	-7.3	-9.7	-12.8
K ⁺	1.8	2.7	2.7	1.9
	4.6	5.1	4.4	4.4
	69.9	68.9	68.2	67.8
	-2.6	-7.9	-10.3	-12.2
Rb ⁺	1.4	2.9	1.6	2.5
	5.1	4.9	4.9	4.9
	70.8	69.7	69.5	68.5
	-2.9	-8.0	-10.0	-11.9
Cs ⁺	2.6	2.7	2.7	2.6
	3.1	≈3	≈3	≈3
	71.2	70.7	70.3	69.9
	+0.5	-6.1	-7.3	-9.2

^a Explanation (sequence of the figures in each column): 100 h , 100 b , ϵ_s , $(\tau_s - \tau_w)/(\tau_w c^*)$ [%/mol/kg of H₂O].

solutions indicated that τ_s varies nearly linearly with the molal salt concentration c^* [mol/kg of H₂O]. Instead of τ_s , therefore, in Table I only the relative molal deviations $(\tau_s - \tau_w)/(\tau_w c^*)$ of the principal relaxation times of the solutions from the relaxation time $\tau_w = 0.82 \times 10^{-11}$ sec (at 25°) of pure water are presented, since these quantities will be of primary interest further on. These deviations were determined from the τ_s values of 1 M solutions.

IV. Interpretation of the "Static" Permittivity ϵ_s

In order to get information from the "static" permittivities ϵ_s of the solutions, we assume the following model to be approximately valid.

Each ion together with the surrounding water, as far as it does not contribute to the orientational polarization, is considered to be a sphere consisting of a homogeneous dielectric medium with the permittivity $\epsilon_e \approx 2$. These spheres all together occupy the fraction f of the total volume of the solution. The water between these

spheres is considered to be a homogeneous dielectric medium with the static permittivity $\epsilon_w = 78.3$ of pure water.

Brown⁶ presents a relation between ϵ_s and ϵ_w , ϵ_e , f , valid for this type of mixture of two different dielectrics, from which f can be calculated according to

$$f = \frac{2\epsilon_w + \epsilon_e}{\epsilon_w - \epsilon_e} \frac{\epsilon_w - \epsilon_s}{2\epsilon_w + \epsilon_s} \quad (7)$$

We tested this formula in the case of aqueous tetraalkyl ammonium bromide solutions.⁴ The water molecules around the especially large ions of these salts may be assumed to fully contribute to the orientational polarization. Consequently f in eq 7 can be set equal to the known volume concentrations of the salts. The ϵ_s values calculated from eq 7 with these f values do not deviate by more than 2% from the ϵ_s values derived from measurements.

Inserting the ϵ_s values of the alkali halide solutions from Table I into eq 7, we calculated f values in order to determine from it the quantity of water contained in the spheres with low permittivity ϵ_e , that is the water not contributing to the orientational polarization. With these f values, with the densities ρ of the solutions and the molar weights M_+ , M_- of the ions, with the molar weight $M' = 18$ g/mol and the apparent molar volume $V_M' = 18$ cm³/mol of water, we get the numbers of moles of water, z_f , not contributing to the orientational polarization per mole of electrolyte in a c molar solution according to

$$z_f = \frac{10^3(\rho/c) - (M_+ + M_-)}{M'} - 10^3 \frac{1-f}{cV_M'} \quad (8)$$

The numbers z_f are compiled in Table II. They have the following meaning. The "static" permittivities ϵ_s of the solutions in comparison to ϵ_w of pure water are reduced to a greater extent than that estimated from the decrease in the water concentration. The additional decrement of the "static" permittivity is so large it appears as if z_f moles of water per mole of electrolyte do not contribute to the orientational polarization ("dielectric saturation" in the electric field of the ions).

The z_f values of the Li and Na salt solutions are more reliable than the other values. They are almost independent of the anions (!) so that it is justified to completely attribute them to the cations. Correspondingly, within each line of the remaining data (being less reliable), the average value has been calculated and presented as cation value z_f^+ in the last column.

In some ion crystals, Li⁺ is found to be fourfold and sixfold coordinated by H₂O or O. Thus the number $z_f^+ = 5.5$ of water molecules without orientational polarizability in the hydration shell of Li⁺ seems to be reasonable. Assuming therefore the other z_f^+ values to be significant too and comparing them with the coordination numbers z_+ (Table III) allows the conclusion

Table II^a

	z_f				z_f^+
	F ⁻ (1.16)	Cl ⁻ (1.64)	Br ⁻ (1.80)	I ⁻ (2.05)	
Li ⁺ (0.82)		5.5	5.5	5.4	5.5
Na ⁺ (1.17)	4.3	4.5	4.5	4.5	4.5
K ⁺ (1.49)	3.6	3.1	3.1	2.8	3.2
Rb ⁺ (1.63)	2.7	2.4	2.2	2.0	2.3
Cs ⁺ (1.86)	2.1	1.3	1.4	0.9	1.5

^a () = ionic crystal radii in Å from ref 7.

that differing from Li⁺ the inner hydration shells of the other cations are not completely saturated dielectrically. However, the most remarkable conclusion from Table II ($z_f^+ = z_f$, $z_f^- = 0$) is that the anions (F⁻ included!) do not reduce the orientational polarizability of their hydration water.

V. Interpretation of the Variation of the Dielectric Relaxation Time τ_s in Connection with That of the Proton Magnetic Relaxation Rate $(1/T_1)_s$

To get information from the relative molal changes of the principal dielectric relaxation times τ_s of the solutions with respect to the dielectric relaxation time τ_w of pure water, we first assume the following model to be approximately valid.

Around each cation and anion there are z_+ or z_- water molecules, respectively, having reorientation times τ_+ or τ_- which may be different from the reorientation time τ_w of pure water due to disturbance of the microdynamics of water by the ions. The undisturbed water of molality $c_w^* - (z_+ + z_-)c^*$ in c^* molal solutions has the reorientation time τ_w of pure water (molality $c_w^* = 55.5$ mol of H₂O/kg of H₂O). The orientational motions of water molecules in different solvent regions are independent of each other. The water molecules in all solvent regions contribute the same amount to the static permittivity as in pure water (here we at first ignore the result of section IV).

For this model solution the function

$$\frac{\epsilon_p(\omega) - \epsilon_\infty}{\epsilon_s - \epsilon_\infty} = \frac{1 - (z_+ + z_-)c^*/c_w^*}{1 + i\omega\tau_w} + \frac{z_+c^*/c_w^*}{1 + i\omega\tau_+} + \frac{z_-c^*/c_w^*}{1 + i\omega\tau_-} \quad (9)$$

represents an approximate description of the permittivity ϵ_p as a function of frequency. In the case of $zc^*/c_w^* \ll 1$ this sum of Debye relaxation terms can be

(6) W. F. Brown, "Handbuch der Physik," Vol. 17, S. Flügge, Ed., Springer, Berlin, 1956, p 105.

(7) B. S. Gourary and F. J. Acrian, *Solid State Phys.*, **10**, 144 (1960).

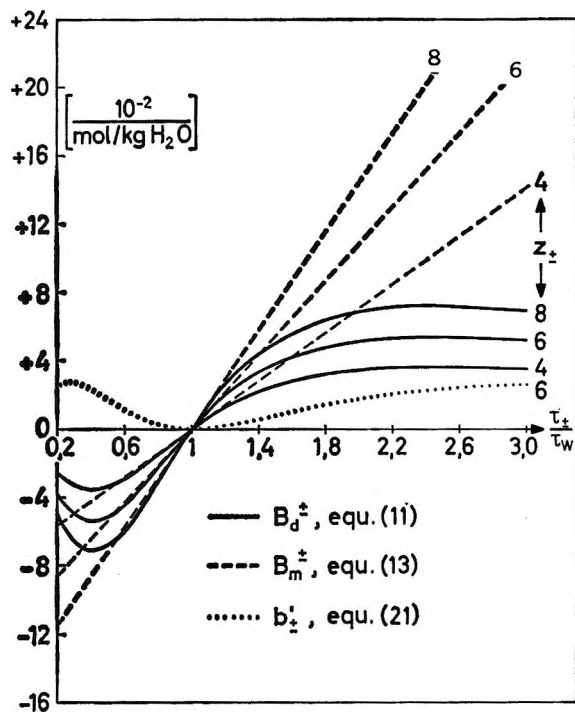


Figure 4. Calculated data of model salt solutions: Relative molal changes B_d^\pm , B_m^\pm of the dielectric relaxation time τ_s and of the proton magnetic relaxation rate $(1/T_1)_s$, respectively, and molal changes b_\pm' of the dielectric relaxation time distribution parameter b due to cations (+) or anions (-) vs. the reorientation time ratio τ_\pm/τ_w of z_\pm disturbed water molecules per ion.

fitted to the measured $\epsilon_p(\nu)$ as well as the function represented by eq 2. Forming from eq 9 the equation $(d\epsilon_p''/d\omega)_{\omega_r} = 0$, which determines the principal relaxation time $\tau_s(c^*) = 1/\omega_r(c^*)$, and differentiating $(d\epsilon_p''/d\omega)_{\omega_r} = 0$ with respect to the solute molality c^* for $c^* \rightarrow 0$, we get the limiting relative molal change of the relaxation time τ_s

$$\frac{1}{\tau_w} \left(\frac{d\tau_s}{dc^*} \right)_{c^* \rightarrow 0} \equiv B_d = B_d^+ + B_d^- \quad (10)$$

with

$$B_d^\pm = 2 \frac{\frac{\tau_\pm - \tau_w}{\tau_w} \frac{z_\pm}{c_w^*}}{\left(\frac{\tau_\pm}{\tau_w} + \frac{\tau_w}{\tau_\pm} \right)^2} \quad (11)$$

According to the observed linearity of $\tau_s(c^*)$ the values of $(\tau_s - \tau_w)/(\tau_w c^*)$ of 1 M solutions compiled in Table I are taken to be equal to B_d .

Referring to the same model of an aqueous ionic solution as described above, Hertz¹ derived a relation between the reorientation times τ_+ , τ_- of disturbed water molecules and the relative molal change of the proton magnetic longitudinal relaxation rate $(1/T_1)_s$ of solutions with respect to the relaxation rate $(1/T_1)_w$ of pure water

$$\frac{1}{(1/T_1)_w} \left(\frac{d(1/T_1)_s}{dc^*} \right)_{c^* \rightarrow 0} \equiv B_m = B_m^+ + B_m^- \quad (12)$$

with

$$B_m^\pm = \frac{\tau_\pm - \tau_w}{\tau_w} \frac{z_\pm}{c_w^*} \quad (13)$$

Graphical representations of B_d^\pm and B_m^\pm as a function of τ_\pm/τ_w are shown in Figure 4.

Now we will compare the information about the disturbed water molecules contained in the B_d and B_m values as determined from dielectric or proton magnetic relaxation measurements, respectively. For this purpose we insert the B_m^+ and B_m^- values from Hertz¹ (recalculated from his Table 6, setting $B_m^{K^+} = B_m^{Cl^-}$) into eq 13 and calculate τ_+/τ_w and τ_-/τ_w taking for z_+ and z_- the number of water molecules in the inner hydration layer (coordination number) of the cation or anion, respectively. These τ_\pm and z_\pm values we put into eq 11 to get B_m^\pm values reduced to "dielectric scale" (Figure 4) which we denote by $(B_m^\pm)_{red}$. The difference values $B_d - (B_m^-)_{red}$ with B_d from Table I and the $(B_m^+)_{red}$ values are compiled in Table III.

Table III^a

	$B_d - (B_m^-)_{red}$				B_d^+	$(B_m^+)_{red}$
	F ⁻ (5.1)	Cl ⁻ (6.1)	Br ⁻ (6.7)	I ⁻ (7.8)		
Li ⁺ (4.9)		-3.2	-3.8	-2.9	-3.3	+4.4
Na ⁺ (6.8)	-5.7	-6.3	-6.5	-5.8	-6.1	+4.3
K ⁺ (7.7)	-7.2	-6.9	-7.1	-5.1	-6.6	-1.0
Rb ⁺ (8.2)	-7.5	-7.0	-6.8	-4.9	-6.6	-3.1
Cs ⁺ (9.3)	-4.1	-5.1	-4.1	-2.2	-3.9	-4.3

^a () = z_+ or z_- , respectively, according to eq 14. All B values in %/mol/kg of H₂O.

The number of water molecules in the inner hydration layer of the ions was calculated from the difference between the total number of water molecules in the solution and the number of water molecules outside of concentric spheres with the radius $r_c^\pm + r_w$ around each cation or anion, respectively ($r_c^\pm =$ crystal radii of the ions, Table II; $r_w = 1.38$ Å, the radius of H₂O). The apparent molar volume of water outside these spheres is assumed to be equal to that in pure water, $V_m' = 18$ cm³/mol. This method yields

$$z_\pm = 2 \frac{1 + r_w/r_c^\pm}{1 + \frac{5r_w}{8r_c^\pm}} \frac{\frac{4\pi}{3} N_L (r_c^\pm + r_w)^3 - V_m^\pm}{V_m'} \quad (14)$$

with $N_L = 6 \times 10^{23} \text{ mol}^{-1}$ and V_M^+ and V_M^- being the apparent partial molar volumes of the ions from ref 8 (except F^-) referred to $V_M^+ = 42.3 \text{ cm}^3/\text{mol}$ from ref 9.

1. *Anionic Effects.* Within the limit of uncertainty of the B_d and B_m^- values, Table III shows the differences $B_d - (B_m^-)_{\text{red}}$ to be essentially independent of the anions. So it is justified to conclude $(B_m^-)_{\text{red}} \approx B_d^-$ which means that the dielectric and proton magnetic relaxation data yield the same information about the influence of the anions on the surrounding water (z_- molecules per ion). This information consists in the increased reorientation time ratio $\tau_-/\tau_w \approx 2.6$ produced by F^- and the decreased ratios $\tau_-/\tau_w \approx 0.9, 0.8,$ and 0.4 produced by $Cl^-, Br^-,$ and I^- , respectively, as already presented¹ and discussed² by Hertz.

The result $B_d^- \approx (B_m^-)_{\text{red}}$ is plausible recalling that all z_- water molecules nearest to an anion fully contribute to the dielectric orientational polarization ($z_f^- = 0$, Table II) so that the dielectric as well as the proton magnetic relaxation responds to the orientational behavior of the hydration water.

2. *Cationic Effects.* As $B_d - (B_m^-)_{\text{red}}$ in Table III is found to be almost completely due to the cations, the average value has been calculated within each line of Table III and is presented as cation value B_d^+ in the next to last column. A comparison of corresponding B_d^+ and $(B_m^+)_{\text{red}}$ values (in the last column of Table III) shows reasonable agreement only for Cs^+ and Rb^+ , while there are drastic differences for Li^+ and Na^+ . This situation can be understood partly by considering that almost all water molecules nearest to Cs^+ and Rb^+ contribute to the dielectric orientational polarization ($z_f^+ \ll z_+$, Tables II, III) while those nearest to Li^+ and Na^+ do not ($z_f^+ \approx z_+$). So with Cs^+ and Rb^+ both the proton magnetic and the dielectric relaxation respond to the decreased reorientation time ratios $\tau_+/\tau_w \approx 0.7$ and 0.8 , respectively,¹ while with Li^+ and Na^+ , only the proton magnetic relaxation can respond to the increased reorientation time ratios $\tau_+/\tau_w \approx 2.5$ and 1.5 , respectively,¹ of the z_+ water molecules nearest to the ions.

However, the preceding consideration does not explain why B_d^+ of $Li^+, Na^+,$ and K^+ is negative. An explanation requires a modification of the solution model. There are at least four effects which produce negative changes of the dielectric relaxation time τ_s but which do not significantly reduce the proton magnetic relaxation rate $(1/T_1)_s$ with increasing electrolyte concentration. A detailed discussion will appear in a later publication.¹⁰ Among them the effect most probably responsible for the negative B_d^+ values of $Li^+, Na^+,$ and K^+ has been proposed by Hertz.¹ After switching off an external electric field, "an additional decay of the electric polarization is caused by the exchange process of the water molecules into and out of the regions of low polarization (without orientational

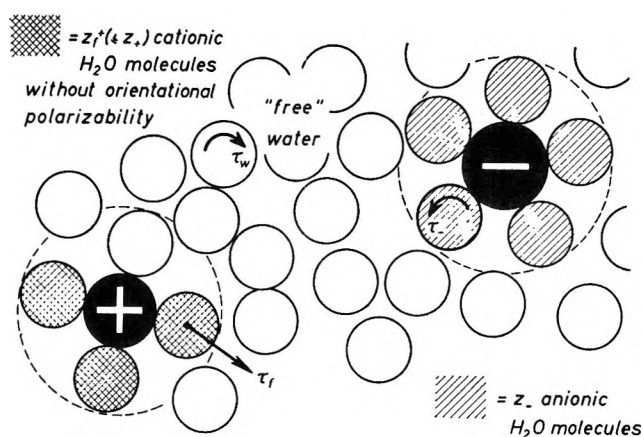


Figure 5. Model of the aqueous ionic solutions introduced in section V2. τ_f , residence time; τ_w, τ_- reorientation times; z_+, z_- coordination numbers.

polarizability) formed by the hydration spheres" of small cations. Regarding this we modify the preceding model of the solution (at the beginning of section V) in ascribing the cationic influence on the water only to the suppression of the orientational polarizability which z_f^+ water molecules experience while they spend the limited time τ_f around a cation (Figure 5).

During a short time interval dt , $z_f^+ c^*(dt/\tau_f)$ moles of water per kg of H_2O of a c^* molal solution are exchanged between the regions without orientational polarizability near the cations and the "free" water of molality $c_w^* - z_f^+ c^* - z_- c^*$ having the reorientation time τ_w of pure water. The water molecules leaving the regions without orientational polarizability after an external electric field was switched off also do not contribute to the orientational polarization $P_w(t)$ of the "free" water. So $P_w(t)$ is changed during dt by

$$dP_w(t) = -P_w(t) \frac{z_f^+ c^*}{c_w^* - z_f^+ c^* - z_- c^*} \frac{dt}{\tau_f} - P_w(t) \frac{dt}{\tau_w} \quad (15)^{11}$$

due to the water molecules leaving the "free" water and entering the regions without orientational polarizability and due to the ordinary dielectric relaxation of the "free" water. By this enlarged decay of the free water polarization with the decay time $\tau_w' (< \tau_w)$ according to

$$\frac{\tau_w}{\tau_w'} = 1 + \frac{z_f^+ c^*}{c_w^* - z_f^+ c^* - z_- c^*} \frac{\tau_w}{\tau_f} \quad (16)$$

(8) H. S. Harned and B. B. Owen, "The Physical Chemistry of Electrolytic Solutions," Reinhold, New York, N. Y., 1950, p 253.

(9) B. E. Conway, *et al.*, *Z. Phys. Chem.*, **230**, 157 (1965).

(10) R. Pottel and coworkers, to be published.

(11) Equation 15 has been derived with the assumption that the correlation time of the fluctuations of the component of the permanent electric dipole moment of the water molecules in the direction of the external electric field is essentially larger than the time between translational jumps.

eq 9 is modified to give

$$\frac{\epsilon_p(\omega) - \epsilon_\infty}{\epsilon_s - \epsilon_\infty} = \frac{1 - \frac{z_- c^*}{c_w^* - z_f^+ c^*}}{1 + i\omega\tau_w'} + \frac{\frac{z_- c^*}{c_w^* - z_f^+ c^*}}{1 + i\omega\tau_-} \quad (17)$$

From this follows B_d as in eq 10 and B_d^- as in eq 11 but B_d^+ according to

$$B_d^+ = -\frac{z_f^+ \tau_w}{c_w^* \tau_f} \quad (18)$$

based on the supposition that B_d^+ is completely due to the exchange process.

With z_f^+ from Table II, B_d^+ from Table III, and $c_w^* = 55.5$ mol/kg of H_2O , eq 18 yields $\tau_f/\tau_w \approx 3.1, 1.3,$ and 0.8 for $Li^+, Na^+,$ and K^+ , respectively. Comparing these data with the reorientation time ratios $\tau_+/ \tau_w \approx 2.5, 1.5,$ and 0.9 , respectively, derived from $B_m^+,$ one arrives at the reasonable conclusion that the time after which a water molecule reorients in contact with the ion is not far from the time after which it leaves the hydration sphere.

VI. Orientational Polarizability and Reorientation of the Hydration Water around Li^+ and F^-

The excess decrement of the static permittivity of Li^+ halide solutions indicates that $z_f^+ \approx z_+$ water molecules per Li^+ ion (Tables II, III) do not contribute to the dielectric orientational polarization (section IV). One may plausibly imagine that these z_f^+ water molecules are in contact with the Li^+ ion and that their permanent electric dipole moments $\bar{\mu}_d$ are so rigidly oriented in the strong radial ionic electric field (Figure 6a) that no electric dipole rotation is possible.

On the other hand the increase of the proton magnetic relaxation rate of Li^+ halide solutions produced by Li^+ indicates that the water molecules nearest to the Li^+ ions must, according to $\tau_+/\tau_w \approx 2.5$ (section V2), execute a restricted proton-around-proton rotation (which is necessary for proton magnetic relaxation to come about). Thus the dielectric and magnetic data are only compatible with a rotation of the hydration water molecules around their electric dipole axes (Figure 6a) which probably is restricted by the repulsion between the protons of neighboring water molecules.

The increase of the proton magnetic relaxation rate of alkali- F^- solutions produced by F^- indicates that the water molecules nearest to the F^- ions also must accomplish a proton-around-proton rotation which, according to $\tau_-/\tau_w \approx 2.6$ (section V1), is just as much slowed down as in the case of Li^+ . But in contrast to Li^+ , the F^- ions produce no excess decrement of the static permittivity (section IV) so that the neighboring water molecules are expected to nearly fully contribute to the dielectric orientational polarization by a rotation of their permanent electric dipole moment, $\bar{\mu}_d$. From the finding of $B_d^- \approx (B_m^-)_{red}$ (section V1) it follows

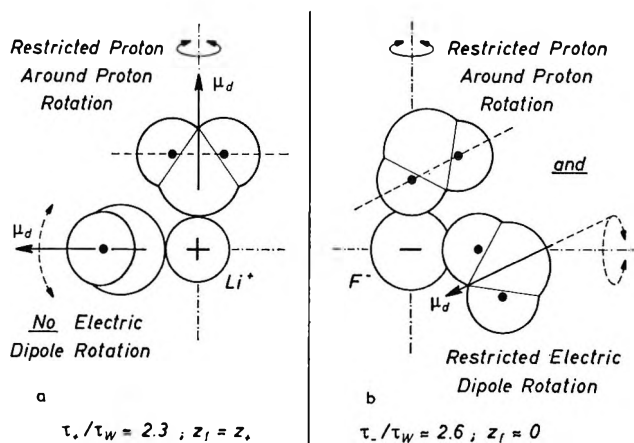


Figure 6. Arrangement and dynamics of the water molecules in the inner hydration layer of Li^+ (a) and F^- (b).

that this rotation is as much restricted as the proton-around-proton rotation. So the dielectric and magnetic data in this case are only compatible with an asymmetrical arrangement of the water molecules in contact with the F^- ion and a restricted rotation of these molecules around an axis not coinciding with the electric dipole axis (Figure 6b). The asymmetrical orientation of the electric dipole of a water molecule in the electric field of a small anion has, for example, been mentioned by Everett and Coulson in 1940¹² and has now found experimental support from the present dielectric and magnetic data.

VII. Interpretation of the Variation of the Relaxation Time Distribution parameter, b

As stated in section III the measured frequency response $\epsilon_p(\omega)$ of the complex permittivity of the aqueous ionic solutions implies a relaxation time distribution characterized by the relaxation time distribution parameters b and h . The parameter b , derived from the measured $\epsilon_p(\omega)$ values according to eq 3, obeys the general relation

$$b = 1 + \left[\frac{1}{\epsilon_p''} \frac{d\epsilon'}{d(\omega\tau_s)} \right]_{\omega\tau_s=1} (\cos(h\pi/2)) \quad (19)$$

For the model of the ionic solutions introduced at the beginning of section V we have taken eq 9 to approximately express $\epsilon_p(\omega)$. With ϵ' and ϵ_p'' from eq 9 inserted into eq 19, b becomes dependent on the electrolyte molality, c^* . Then the relative molal change of b for $c^* \rightarrow 0$ is (regarding $h \ll 1$) given by

$$\left(\frac{db}{dc^*} \right)_{c^* \rightarrow 0} \equiv b' = b_+' + b_-' \quad (20)$$

with

(12) D. H. Everett and C. A. Coulson, *Trans. Faraday Soc.*, **36**, 633 (1940).

$$b_{\pm}' = 2 \frac{\tau_{\pm}}{\tau_w} \left(\frac{1 - \frac{\tau_w}{\tau_{\pm}}}{\frac{\tau_{\pm}}{\tau_w} + \frac{\tau_w}{\tau_{\pm}}} \right)^2 \frac{z_{\pm}}{c_w^*} \quad (21)$$

A comparison of the b values for 0.5 and 1 M solutions indicated that b varies almost linearly with the molal salt concentration, c^* . Accordingly the values of $(b - b_w)/c^*$ of 1 M solutions (b from Table I, $b_w \approx 0.006$, section III) are taken to be equal to b' .

With the quantities B_d (section V), b' , and B_m^+ , B_m^- derived from the dielectric or proton magnetic relaxation measurements, respectively, we have four known quantities which on principle could serve to calculate the four interesting unknown quantities τ_{\pm}/τ_w , z_{\pm} by eq 10, 13⁺, 13⁻, and 20 without any further information. The supposition is that the model of the ionic solutions introduced at the beginning of section V suffices to nearly explain the change of the dielectric relaxation time τ_s induced by the ions. According to sections V1,2 this can only be expected to hold for the Cs halide solutions. Among the b values (Table I) of these solutions only that of the CsF solution is reliable enough for evaluation. So we have used the data of only the CsF solution to examine whether or not the method of calculating τ_{\pm}/τ_w and z_{\pm} in the manner just mentioned is consistent with the method in section V which involves taking z_{\pm} from eq 14 and then calculating τ_{\pm}/τ_w from B_m^{\pm} by eq 13⁺ and 13⁻. The results are compiled in Table IV. Within the limits of

Table IV

		By eq 10, 20, 13 ⁺ , 13 ⁻	By eq 14, 13 ⁺ , 13 ⁻
Cs ⁺	z_+	11.5	9.3
	τ_+/τ_w	0.81	0.76
F ⁻	z_-	5.3	5.1
	τ_-/τ_w	2.58	2.63

accuracy of the primary data, Table IV shows excellent agreement between the results derived from combining dielectric and proton magnetic relaxation data (3rd column) and the results derived solely from the magnetic data and an estimation of the coordination numbers z_{\pm} (4th column). So it is justified to use together, as in

section V, the dielectric and proton magnetic relaxation data in order to get additional information about the more complex dielectric relaxation in solutions of cations smaller than Cs⁺.

VIII. Conclusion

For the interpretation of the static permittivity and the dielectric relaxation time of aqueous ionic solutions we have introduced three models. These models obviously are more or less simplified pictures of the real solutions.

In the first model, concerning the static permittivity (section IV), the solvent water is divided into regions with and without orientational polarizability, the latter regions being the cation solvation shells.

In the second model, concerning the dielectric and proton magnetic relaxation (section V), the solvent is divided into cationic, anionic, and undisturbed water having different reorientation times (τ_+ , τ_- , τ_w) but equal orientational polarizability. Because of the feature of the first model being neglected here, the second model is limited to reproduce the dielectric behavior of solutions with large cations.

The third model (section V2, Figure 5) combines the features of the first and second model, and additionally includes the exchange of water molecules between the regions with and without orientational polarizability. But in this model the water near cations of medium and large size is artificially divided into molecules without orientational polarizability and molecules having the reorientation time (τ_w) and orientational polarizability of pure water. Therefore, the third model is especially appropriate to reproduce the dielectric behavior of solutions with small cations.

In order to adjust the third model to solutions with cations of medium and large size, one should uniformly attribute a reduced (but not vanishing) orientational polarizability and a modified reorientation time (τ_+) to all the water molecules near the cations. Together with the exchange process, such a model would become relatively complicated while not much more substantial information can be gained than by considering the simpler models mentioned above. So we have left out this refinement here. It will be presented in a later publication.¹⁰

Acknowledgment. Financial support by the Deutsche Forschungsgemeinschaft is gratefully acknowledged.

Direct Proton Magnetic Resonance Cation Hydration Study of Uranyl Perchlorate, Nitrate, Chloride, and Bromide in Water-Acetone Mixtures¹

by Anthony Fratiello,* Vicki Kubo, Robert E. Lee, and Ronald E. Schuster

Department of Chemistry, California State College, Los Angeles, Los Angeles, California 90032 (Received March 2, 1970)

A cation hydration number study has been carried out for solutions of $\text{UO}_2(\text{ClO}_4)_2$, $\text{UO}_2(\text{NO}_3)_2$, UO_2Cl_2 , and UO_2Br_2 in water-acetone mixtures by the direct proton magnetic resonance (pmr) method. At temperatures below -85° , proton exchange is slow enough to permit the observation of separate pmr signals for bulk water molecules and water molecules in the UO_2^{2+} solvation shell. In ClO_4^- solutions, UO_2^{2+} is hydrated by a maximum of four water molecules and complex formation is negligible. Bidentate complexing occurs with NO_3^- and the equilibrium quotient for the formation of the mononitrato complex is roughly an order of magnitude greater than that for the dinitrato complex. Complexing is evident in the Cl^- and Br^- solutions but spectral complexities prevented an unambiguous identification of the species.

Introduction

The direct proton magnetic resonance (pmr) method has proved to be particularly well suited for the measurement of cation hydration numbers²⁻⁶ and for the quantitative estimation of competitive solvation^{7,8} and complex formation⁹⁻¹³ in aqueous electrolyte solutions. When proton exchange can be slowed by the addition of an inert solvent such as acetone, and by cooling the sample to low temperatures, usually in the range of -50 to -100° , separate pmr signals frequently can be observed for bulk water and water molecules in the cation solvation shell. Signal area measurements then provide accurate cation hydration numbers. Cations investigated in this manner include diamagnetic Al^{3+} , Ga^{3+} , In^{3+} , Be^{2+} , and Mg^{2+} ,^{2-4,11,12} Sc^{3+} , Y^{3+} , and Th^{4+} ,^{9,10} Sn^{4+} , UO_2^{2+} , and Zn^{2+} ;⁵ paramagnetic Co^{2+} ,⁶ and, in a preliminary manner, Er^{3+} , Fe^{2+} , Fe^{3+} , and Ni^{2+} .⁵

Although the complexing ability of the UO_2^{2+} ion is well known, the hydration number of this cation has been estimated only indirectly from spectroscopic¹⁴ and thermochemical studies.¹⁵ Also, a pmr study of the behavior of this ion in aqueous solvent mixtures and the nature of its complexes with a variety of anions would be a valuable complement to the results of investigations by other methods.¹⁴⁻²⁰ Since preliminary measurements had indicated that UO_2^{2+} fell within the scope of this technique,⁵ a study of the ClO_4^- , NO_3^- , Cl^- , and Br^- solutions of this cation was undertaken.

Experimental Methods

The $\text{UO}_2(\text{ClO}_4)_2$, $\text{UO}_2(\text{NO}_3)_2$, acetone, and acetone- d_6 (99.5%) were reagent grade and they were used as received. The Cl^- , Br^- , and several of the NO_3^- solutions were prepared by the addition of HCl and

HBr (Brinkmann, ultrapure) and reagent grade HNO_3 to solutions of $\text{UO}_2(\text{ClO}_4)_2$. Salt concentrations were determined by the passage of $\text{UO}_2(\text{ClO}_4)_2$ and $\text{UO}_2(\text{NO}_3)_2$ stock solutions through a Dowex 50W-X8 cation-

* To whom correspondence should be addressed.

- (1) Presented in part at the 158th National Meeting of the American Chemical Society, New York, N. Y., Sept 7-12, 1969.
- (2) (a) R. E. Schuster and A. Fratiello, *J. Chem. Phys.*, **47**, 1554 (1967); (b) L. D. Supran and N. Sheppard, *Chem. Commun.*, 832 (1967).
- (3) A. Fratiello, R. E. Lee, V. M. Nishida, and R. E. Schuster, *J. Chem. Phys.*, **48**, 3705 (1968).
- (4) N. A. Matwiyoff and H. Taube, *J. Amer. Chem. Soc.*, **90**, 2796 (1968).
- (5) A. Fratiello, V. Kubo, R. E. Lee, S. Peak, and R. E. Schuster, *J. Inorg. Nucl. Chem.*, in press.
- (6) N. A. Matwiyoff and P. E. Darley, *J. Phys. Chem.*, **72**, 2659 (1968).
- (7) A. Fratiello, R. E. Lee, V. M. Nishida, and R. E. Schuster, *J. Chem. Phys.*, **47**, 4951 (1967).
- (8) A. Fratiello, R. E. Lee, V. M. Nishida, and R. E. Schuster, *Inorg. Chem.*, **8**, 69 (1969).
- (9) A. Fratiello, R. E. Lee, V. M. Nishida, and R. E. Schuster, *J. Chem. Phys.*, **50**, 3624 (1969).
- (10) A. Fratiello, R. E. Lee, and R. E. Schuster, *Inorg. Chem.*, **9**, 391 (1970).
- (11) A. Fratiello, R. E. Lee, and R. E. Schuster, *Mol. Phys.*, **18**, 191 (1970).
- (12) A. Fratiello, R. E. Lee, and R. E. Schuster, *Inorg. Chem.*, **9**, 82 (1970).
- (13) A. Fratiello, D. D. Davis, S. Peak, and R. E. Schuster, *J. Phys. Chem.*, in press.
- (14) V. M. Vdovenko, L. G. Mashirov, and D. N. Suglobov, *Radio-khimiya*, **6**, 299 (1964); **9**, 37 (1967).
- (15) I. I. Lipilina and O. Ya. Samoilov, *Doklady. Akad. Nauk SSSR*, **98**, 99 (1954).
- (16) H. W. Crandall, *J. Chem. Phys.*, **17**, 602 (1949).
- (17) R. H. Betts and R. K. Michels, *J. Chem. Soc.*, S286 (1949).
- (18) S. Ahrlund, *Acta Chem. Scand.*, **5**, 1271 (1951).
- (19) S. Peterson, *J. Inorg. Nucl. Chem.*, **17**, 135 (1961).
- (20) D. Banerjee and K. K. Tripathi, *ibid.*, **18**, 199 (1961).

exchange column, thoroughly washing the resin, and titrating the resultant acid solution with standardized NaOH. The pmr spectra were obtained immediately after the samples were prepared.

All pmr chemical shift and area measurements were made with a Varian A-60 and a Varian HA-100 nmr spectrometer, each equipped with a variable temperature accessory for studies from -150 to $+200^\circ$, and an electronic signal integrator. The samples were cooled in the probe until the spectra revealed separate resonance signals for bulk and cation solvation shell water molecules. At this point, the signals were integrated at least three times. The experimental method has been described in more detail elsewhere.^{3,7}

Experimental Results

The cation hydration numbers for aqueous acetone solutions of $\text{UO}_2(\text{ClO}_4)_2$ and $\text{UO}_2(\text{NO}_3)_2$ are presented in Table I, and the water pmr spectra arising from two

Table I: Cation Hydration Numbers in Aqueous-Acetone Solutions of $\text{UO}_2(\text{ClO}_4)_2$ and $\text{UO}_2(\text{NO}_3)_2$

Salt	Molality	Mole ratios		
		$\text{UO}_2^{2+}:\text{H}_2\text{O}:\text{acetone}$	UO_2^{2+} hy no.	
$\text{UO}_2(\text{ClO}_4)_2$	0.39	1.00:13.3:40.5	4.0	
	0.36	1.00:13.8:43.8	4.0	
	0.29	1.00:17.0:54.6 ^a	4.0	
	0.24	1.00:13.3:66.8	3.9	
	0.21	1.00:13.1:69.1 ^b	3.9	
	0.13	1.00:13.3:131	4.3	
	$\text{UO}_2(\text{NO}_3)_2$	0.39	1.00:18.5:38.1	2.1
		0.66	1.00:7.78:23.6	1.9
0.28		1.00:18.5:56.3	2.0	
0.26		1.00:18.5:55.4 ^b	2.1	
0.23		1.00:22.1:69.6 ^a	2.0	
0.22		1.00:18.5:72.4	1.7	
0.17		1.00:18.5:95.4	1.3	
0.093		1.00:18.5:180	~ 0	

^a Samples contain a 1:1 mole ratio of HClO_4 to UO_2^{2+} .

^b Samples contain acetone- d_6 .

of these solutions are shown in Figures 1 and 2. In Table II, and in Figures 3 and 4, similar results are given for water-acetone mixtures containing regulated mole ratios of anion to UO_2^{2+} ion, the concentrations resulting from the addition of HNO_3 , HCl , or HBr to a $\text{UO}_2(\text{ClO}_4)_2$ solution. The hydration numbers listed in both tables were measured with a 5–10% precision, and they represent the result of several integrations with duplicate samples. The two entries listed as ~ 0 indicate that the solvation shell water signal either was too small to be accurately integrated (NO_3^- solution), or not observable (Cl^- solution). The acetone to water

Table II: Cation Hydration Numbers in Acidified Aqueous-Acetone Solutions of $\text{UO}_2(\text{ClO}_4)_2$

Acid	Salt Molality	Mole ratios		UO_2^{2+} hy no.	
		$\text{UO}_2^{2+}:\text{H}^+:\text{H}_2\text{O}:\text{Acetone}$			
HNO_3	0.45	1.00:0.94:14.7:36.8		2.8	
	0.40	1.00:0.97:13.9:39.4		2.6	
	0.66	1.00:0.00:7.78:23.6 ^a		1.9	
	0.28	1.00:0.00:18.5:56.3 ^a		2.0	
	0.26	1.00:0.00:18.5:55.4 ^{a,b}		2.1	
	0.27	1.00:0.98:19.9:59.7 ^a		1.5	
	HCl	0.32	1.00:1.00:16.4:49.2		3.3
		0.31	1.00:1.00:16.9:50.7		2.8
0.44		1.00:1.02:12.1:35.1		3.1	
0.26		1.00:1.96:20.1:59.7		1.8	
0.27		1.00:1.87:19.6:56.9		1.9	
0.16		1.00:1.96:20.1:100 ^c		1.9	
0.22		1.00:2.94:23.5:70.0		1.0 (± 2.0)	
0.18		1.00:4.61:29.5:87.3		~ 0	
HBr	0.41	1.00:0.95:12.8:38.4		3.0	
	0.41	1.00:1.01:13.1:38.0		3.0	
	0.38	1.00:1.01:13.8:40.6		3.0	
	0.25	1.00:0.95:12.8:64.1 ^c		3.0	
	0.30	1.00:2.05:18.0:52.2		3.0	
	0.28	1.00:2.02:18.7:55.1		3.1	
	0.24	1.00:3.07:22.9:65.2		2.3	
	0.22	1.00:3.01:23.4:70.2		2.4	

^a $\text{UO}_2(\text{NO}_3)_2$ was used instead of $\text{UO}_2(\text{ClO}_4)_2$. ^b Sample contained acetone- d_6 . ^c Sample contained a 5:1 mole ratio of acetone to water.

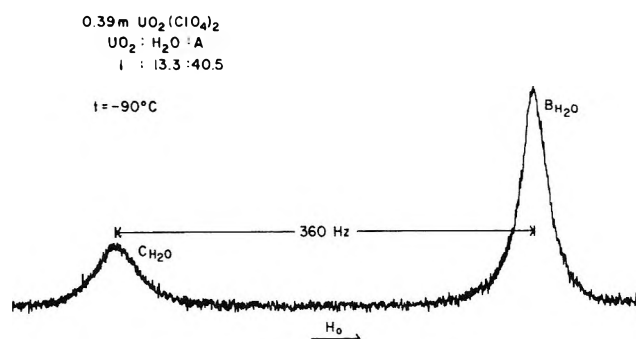


Figure 1. The water pmr spectrum of a $\text{UO}_2(\text{ClO}_4)_2$ solution in a water-acetone mixture, recorded on a Varian A-60 nmr spectrometer. The signals arising from bulk water ($\text{B}_{\text{H}_2\text{O}}$) and water molecules in the UO_2^{2+} ion solvation shell ($\text{C}_{\text{H}_2\text{O}}$) are labeled, and the mole ratios of all species are given in the diagram.

mole ratios were varied from about 3:1 to 10:1 for the systems represented in Table I, whereas, with the exception of the two solutions noted, this solvent mole ratio was maintained at 3:1 for all solutions of Table II. The hydration number measurements were made in the temperature range -85 to -100° , the exact tempera-

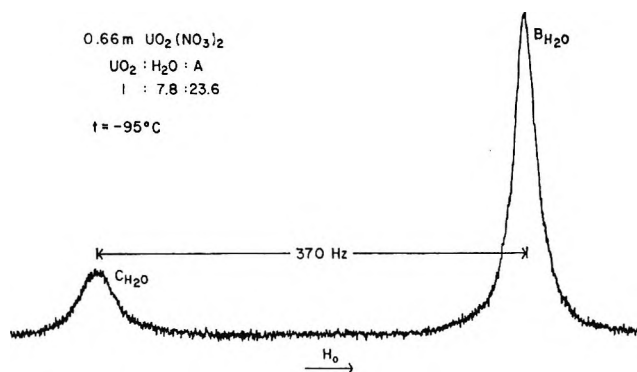


Figure 2. The water pmr spectrum of $\text{UO}_2(\text{NO}_3)_2$ solution in a water-acetone mixture, recorded on a Varian A-60 nmr spectrometer. The signals arising from bulk water ($\text{B}_{\text{H}_2\text{O}}$) and water molecules in the UO_2^{2+} ion solvation shell ($\text{C}_{\text{H}_2\text{O}}$) are labeled, and the mole ratios of all species are given in the diagram.

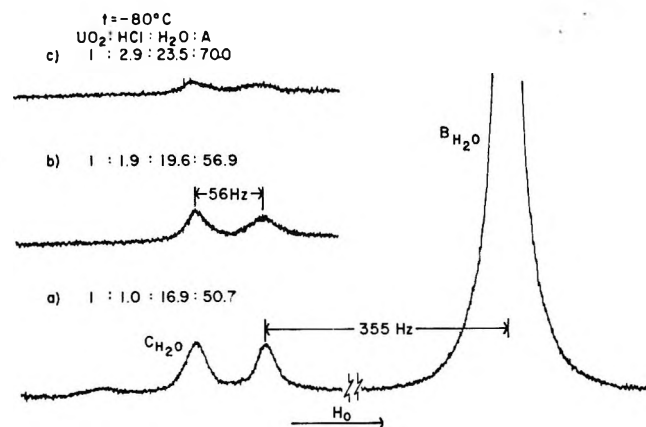


Figure 3. The water pmr spectra of solutions of $\text{UO}_2(\text{ClO}_4)_2$ in water-acetone mixtures containing (a) 1:1, (b) 2:1, and (c) 3:1 mole ratios of HCl to UO_2^{2+} . The spectra were recorded on a Varian HA-100 nmr spectrometer. The signals arising from bulk water ($\text{B}_{\text{H}_2\text{O}}$) and water molecules in the UO_2^{2+} ion solvation shell ($\text{C}_{\text{H}_2\text{O}}$) are labeled, and the mole ratios of all species are given in the diagram.

ture in each case being that at which the bulk water and cation solvation shell water signals were well defined. The coordinated water signal appeared about 9.50 ppm downfield from internal acetone in the ClO_4^- and NO_3^- solutions, and approximately 9.33 ppm in the halide systems, taking the center of the multiplet as the point of measurement.

Discussion

From the separation of the bulk and solvation shell signals in Figures 1 and 2 for acid free solutions of $\text{UO}_2(\text{ClO}_4)_2$ and $\text{UO}_2(\text{NO}_3)_2$, respectively, one can estimate that the lifetime of a proton at a particular site is approximately 0.005 sec.²¹ This is only an order of magnitude calculation since the position of the bulk water signal and, consequently, the signal separation, depends on the acetone and added acid concentration, and temperature. The complexed water signal is essen-

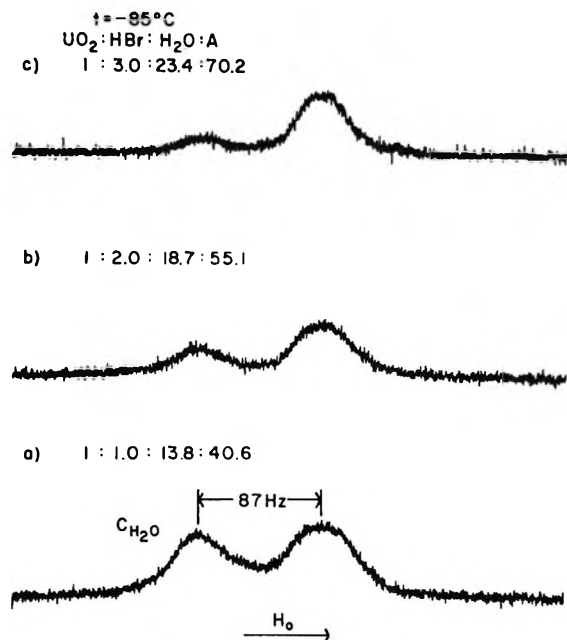


Figure 4. The pmr signals of water molecules in the UO_2^{2+} ion solvation shell in $\text{UO}_2(\text{ClO}_4)_2$ solutions in water-acetone mixtures containing (a) 1:1, (b) 2:1, and (c) 3:1 mole ratios of HBr to cation. The spectra were recorded on a Varian HA-100 nmr spectrometer. The mole ratios of all species are listed in the diagram.

tially independent of concentration, but it does exhibit a temperature dependence which we have observed only in a qualitative manner. The bulk water signal acid dependence was obtained from a comparison of the spectrum of Figure 1 with that corresponding to the $\text{UO}_2(\text{ClO}_4)_2$ solution of Table I designated as containing HClO_4 . In both cases the solvation shell water proton chemical shift was 9.50 ppm (± 0.08 ppm) downfield from internal acetone, whereas the addition of HClO_4 displaced the bulk water signal 1.42 ppm downfield from its position in the acid free solution spectrum. Since protonation of the hydration water molecules is minimized by the presence of the positive charge on the central cation, only anions and neutral bulk water molecules can engage in this process. The low-field displacement of a water signal upon protonation has been treated in detail elsewhere.²²

The data of Table I demonstrate a rapid means of determining whether inner shell, cation-anion complex formation is occurring. The addition of acetone produces a reduction of the dielectric constant of the medium, eventually to that of acetone, about 20 at 25°, at high concentrations of this component.²³ Even though

(21) H. S. Gutowsky and C. H. Holm, *J. Chem. Phys.*, **25**, 1228 (1956).

(22) J. A. Pople, W. G. Schneider, and J. J. Bernstein, "High-resolution Nuclear Magnetic Resonance," McGraw-Hill, New York, N. Y., 1959, Chapters 15, 18.

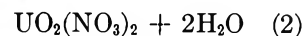
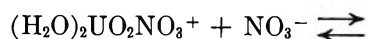
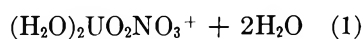
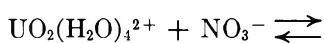
(23) H. S. Harned and B. B. Owen, "The Physical Chemistry of Electrolytic Solutions," 3rd ed, Reinhold, New York, N. Y., 1963, p 161.

these pmr measurements are made at -85 to -100° , the bulk dielectric constant should still be only about 35, a much lower value than that of pure water.²³ Thus, if inner-shell complex formation is induced in solution, a decrease in the cation hydration number should be noted.

From Table I, the UO_2^{2+} ion is hydrated by four water molecules in ClO_4^- solutions over a 3:1 to 10:1 range of acetone to water mole ratio, and this value is not changed by the addition of HClO_4 . This lack of dependence of the hydration number on solvent composition and acid concentration rules out the possibility of complex formation and hydrolysis, and it indicates that 4 is the maximum inner-shell hydration number of this cation. The inability of ClO_4^- to complex UO_2^{2+} ion in the presence of sufficient water to complete the first solvation shell has been demonstrated by ir methods.¹⁴ However, this direct measurement of a hydration number of four contrasts with the value of six derived from thermochemical measurements.¹⁵ This discrepancy may result from the sensitivity of other methods extending beyond the first solvation shell.

In agreement with other spectroscopic and ion-exchange studies,¹⁶⁻²⁰ the hydration numbers of Table I attest to the formation of complexes between UO_2^{2+} and NO_3^- ions. As the mole ratio of acetone to water is increased from 3:1 to 10:1, the UO_2^{2+} ion hydration number decreases from its maximum value of four observed in ClO_4^- solutions, to essentially zero in NO_3^- solutions. Since only one acetone resonance signal is observed in all spectra, and based on the results of other studies which demonstrated the low solvating ability of acetone in aqueous solutions of similar concentrations,^{3,4,7,8} it may be assumed that only water molecules are solvating the UO_2^{2+} ion. Also, hydrolysis does not contribute appreciably to these low values since the presence of acid does not alter the results. Therefore, the hydration number decrease is most reasonably interpreted in terms of a replacement of water molecules by NO_3^- ions. The replacement of four water molecules by two NO_3^- ions in the UO_2^{2+} ion solvation shell means the complexing is bidentate in nature.

To place the complex formation in these systems on a more quantitative basis and to permit the identification of the species present, experiments were carried out in which known amounts of anion were added to UO_2^{2+} ion in water-acetone mixtures of a 1:3 mole ratio. This is the lowest acetone concentration which could be studied at the temperatures required by this pmr method. It was anticipated that equilibrium quotient measurements would be possible for processes such as



Presumably only one water molecule would be displaced in each step in halide solutions, and the study of higher complexes would be possible.

From the UO_2^{2+} ion hydration numbers in the NO_3^- solutions of Table II, it may be concluded that an equilibrium situation prevails at each anion to cation mole ratio, and the processes possibly are represented by eq 1 and 2 above. Assuming eq 1 applies in the 1:1 $\text{NO}_3^-:\text{UO}_2^{2+}$ solutions, the hydration number of 2.7, the average of the two entries of Table II, can be accounted for if 65% of the UO_2^{2+} ion is present as $(\text{H}_2\text{O})_2\text{UO}_2\text{NO}_3^+$ and the remainder as $\text{UO}_2(\text{H}_2\text{O})_4^{2+}$. The constancy of the hydration number with salt concentration in the 2:1 $\text{NO}_3^-:\text{UO}_2^{2+}$ solutions is consistent with the complete formation, within experimental error, of $(\text{H}_2\text{O})_2\text{UO}_2\text{NO}_3^+$. The process of eq 2 would then apply to the 3:1 $\text{NO}_3^-:\text{UO}_2^{2+}$ solutions and the cation hydration number of 1.5 would imply the presence of 25% of the UO_2^{2+} ion as $\text{UO}_2(\text{NO}_3)_2$ and the remainder as $(\text{H}_2\text{O})_2\text{UO}_2\text{NO}_3^+$. These considerations lead to a value of roughly ten for the ratio of K_1 to K_2 .

Although the UO_2^{2+} ion hydration numbers of Table II definitely reflect complex formation in the Cl^- and Br^- solutions, several features of these data and the spectra of Figures 3 and 4 present a hindrance to an unambiguous identification of the species present. For example, the solutions containing a 1:1 mole ratio, Cl^- or Br^- to UO_2^{2+} , exhibit two signals of approximately equal intensity for water molecules in the cation solvation shell. A third, broad signal appears in the same region of the Cl^- solution spectra but its area cannot be accurately determined. A simple complex such as $(\text{H}_2\text{O})_3\text{UO}_2\text{X}^+$ possibly would give rise to two pmr signals, but with an area ratio of 2:1. Next, the relative areas of the two principal hydration water signals in the Cl^- ion solution spectra of Figure 3 apparently are unchanged with concentration, whereas in the Br^- ion solution spectra in Figure 4, one of these signals broadens and appears to decrease in area as the anion concentration is increased. Thus, the signals of Figure 4, and by analogy those in Figure 3, probably are due to different complexes, rather than water molecules in different environments in the same complex. Finally, the cation hydration number decreases by one unit for each mole of Cl^- ion added to solution, while the value is about 3 in the 1:1 and 2:1 Br^- to UO_2^{2+} solutions, and only slightly less in the 3:1 solution.

The hydration numbers of Table II are not consistent with a combination of simple complexes, and most likely species of unusual stoichiometry, possibly even polymer-like complexes are present. However, in the absence of more information, it is not worthwhile to speculate further as to the nature of the species. More extensive application of ir and Raman techniques to

these aqueous-acetone solutions may be fruitful. A clarification also would be provided by oxygen-17 and halide ion nmr, an approach presently planned in these laboratories.

Acknowledgments. This work was supported by Research Grant No. 14-01-0001-2162 from the Office

of Saline Water, by a National Science Foundation instrument grant, GP-8347, for the purchase of the Varian HA-100 spectrometer, and by a National Institutes of Health Research Career Development Award (A. F.), No. 5-K4-GM-42334. The authors are grateful to Dr. W. E. Keder for helpful discussions.

A Hydrogen-1 and Tin-119 Nuclear Magnetic Resonance Cation Hydration Study of Aqueous Acetone Solutions of Stannic Chloride and Stannic Bromide¹

by Anthony Fratiello,* Shirley Peak, Ronald E. Schuster,

Department of Chemistry, California State College, Los Angeles, Los Angeles, California 90032

and Don D. Davis

Bell Telephone Laboratories, Incorporated, Murray Hill, New Jersey 07974 (Received March 2, 1970)

A cation hydration number study of aqueous acetone solutions of SnCl_4 and SnBr_4 has been carried out by means of ^1H and ^{119}Sn nmr spectroscopy. At low temperatures, proton exchange is slow enough to permit the observation of separate pmr signals for bulk water and water molecules in the Sn^{4+} solvation shell. Direct-signal integration yielded an average cation hydration number of about two in both the Cl^- and Br^- systems. This hydration number result, the appearance of only one solvation shell water signal, and the similar resonance position of this signal in all solutions were interpreted in terms of the presence of $\text{Sn}(\text{H}_2\text{O})_6^{4+}$ and SnX_6^{2-} as the dominant species. Only one ^{119}Sn nmr signal was observed for these solutions at $+25^\circ$, but the chemical shift dependence on dielectric constant was consistent with the presence of these two species undergoing rapid intermolecular exchange.

Introduction

Although proton exchange in aqueous electrolyte solutions is rapid at room temperature, recent studies have shown that by cooling the sample this exchange frequently can be slowed sufficiently to permit the observation of separate proton magnetic resonance (pmr) signals for bulk water and water molecules bound in the cation solvation shell.²⁻¹³ Signal area measurements then provide an accurate value of the average hydration number of the cation. This direct pmr method has been used to determine hydration numbers for diamagnetic Al^{3+} , Ga^{3+} , In^{3+} , Be^{2+} , and Mg^{2+} ,²⁻⁴ diamagnetic UO_2^{2+} ,^{5,6} and paramagnetic Co^{2+} ,⁷ and to estimate competitive solvation in aqueous mixtures.^{8,9} Since inner shell, cation-anion complex formation involves the replacement of water molecules of hydration, this method is a valuable tool for evaluating the extent of such processes. Complex formation in aqueous-acetone solutions of $\text{Sc}(\text{NO}_3)_3$, $\text{Y}(\text{NO}_3)_3$, and $\text{Th}(\text{NO}_3)_4$,^{10,11}

GaCl_3 , GaBr_3 , and GaI_3 ,^{12,13} and $\text{UO}_2(\text{NO}_3)_2$, UO_2Cl_2 , and UO_2Br_2 ,^{5,6} has been studied by this nmr technique.

A preliminary cation hydration number study re-

* To whom correspondence should be addressed.

(1) Presented in part at the 158th National Meeting of the American Chemical Society, New York, N. Y., Sept 7-12, 1969.

(2) (a) R. E. Schuster and A. Fratiello, *J. Chem. Phys.*, **47**, 1554 (1967); (b) L. D. Supran and N. Sheppard, *Chem. Commun.*, 832 (1967).

(3) A. Fratiello, R. E. Lee, V. M. Nishida, and R. E. Schuster, *J. Chem. Phys.*, **48**, 3705 (1968).

(4) N. A. Matwiyoff and H. Taube, *J. Amer. Chem. Soc.*, **90**, 2796 (1968).

(5) A. Fratiello, V. Kubo, R. E. Lee, S. Peak, and R. E. Schuster, *J. Inorg. Nucl. Chem.*, in press.

(6) A. Fratiello, V. Kubo, R. E. Lee, and R. E. Schuster, *J. Phys. Chem.*, **74**, 3726 (1970).

(7) N. A. Matwiyoff and P. E. Darley, *ibid.*, **72**, 2659 (1968).

(8) A. Fratiello, R. E. Lee, V. M. Nishida, and R. E. Schuster, *J. Chem. Phys.*, **47**, 4951 (1967).

(9) A. Fratiello, R. E. Lee, V. M. Nishida, and R. E. Schuster, *Inorg. Chem.*, **8**, 69 (1969).

vealed evidence for tin halide complexes in water-acetone mixtures.⁵ This report represents an attempt to place the results on a more quantitative basis, using both ^1H and ^{119}Sn nmr spectroscopy. In these studies, ambiguities concerning the identification of the species can sometimes be minimized by metal-ion nmr spectra.

Experimental Methods

The reagent grade anhydrous stannic halides, acetone, and acetone- d_6 (99.5%, Stohler) were used as received. The anhydrous nature of the salts was verified by the pmr spectra of their acetone solutions. To avoid the decomposition that attends sample heating, the solutions were prepared by mixing the reagents at -100° , and the spectrum was recorded immediately thereafter. No pmr spectral evidence for acetone decomposition was detected for SnCl_4 or SnBr_4 solutions, but the appearance of extraneous signals in SnI_4 solutions precluded the study of this halide.

The pmr chemical shift and area measurements were made with a Varian A-60 spectrometer equipped with a variable temperature device for studies from -150° to $+200^\circ$, and an electronic signal integrator. The samples were cooled in the spectrometer probe until the proton exchange rate had been reduced sufficiently to permit the observation of a resonance signal for water molecules in the Sn^{4+} solvation shell and in bulk medium. The water proton signal areas were integrated several times, and together with solution concentrations the areas permitted hydration number calculations. A more detailed description of the pmr method has been given elsewhere.^{3,8}

Although tin has three magnetically active isotopes, each with spin $1/2$, ^{119}Sn was chosen because of its slightly greater abundance (8.7% compared to 7.7% and 0.4% for ^{117}Sn and ^{115}Sn , respectively). The ^{119}Sn nmr measurements were made at $\pm 25^\circ$ using a Varian DP-60 spectrometer, operating in the wide line mode at 24.3 MHz and 15.3 kG. The field scan was calibrated with a fluxmeter and frequency counter. The measurements were made primarily with SnCl_4 solutions and with only one SnBr_4 solution. The lower solubility and signal intensity of SnBr_4 limited the study to a 1:8 salt to water mole ratio, and at this concentration the resonance peak was barely detectable. The chemical shifts were determined by calibrating the field sweep, making several recordings of the pure SnCl_4 signal, and comparing these with the spectra of a series of aqueous solutions. The pure SnCl_4 spectrum was recorded at the beginning and end of each series in order to establish the stability of the spectrometer.

Experimental Results

The cation hydration numbers and solvation shell water chemical shifts for solutions of SnCl_4 and SnBr_4 in water-acetone mixtures are listed in Table I. A representative water pmr spectrum is shown in Figure 1.

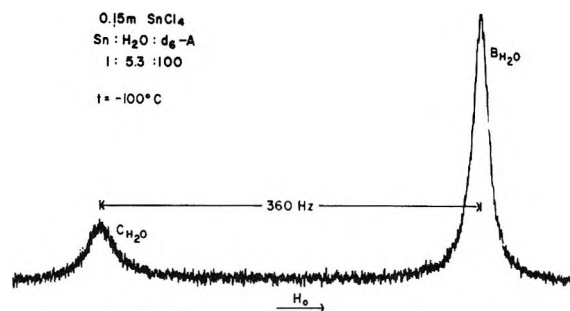


Figure 1. The water pmr spectrum of a SnCl_4 solution in a water-acetone mixture, recorded on a Varian A-60 nmr spectrometer. The signals arising from bulk water ($\text{B}_{\text{H}_2\text{O}}$) and water molecules in the Sn^{4+} solvation shell ($\text{C}_{\text{H}_2\text{O}}$) are labeled, and the mole ratio of all species is given in the diagram.

Most concentrations were prepared in duplicate, and the hydration numbers were measured with a precision of $\pm 10\%$. The chemical shifts listed in the last column indicate the separation, in Hz, between the solvation shell water signal and internal tetramethylsilane refer-

Table I: Cation Hydration Numbers in Aqueous Acetone Solutions of SnCl_4 and SnBr_4 at -100°

Salt	Molality	Mole ratios			Sn^{4+} hy no.	$\delta(\text{CH}_2\text{O})$, Hz
		SnX_4 :	HClO_4 :	H_2O :acetone		
SnCl_4	0.15	1.00:	0.00:	5.32:100 ^a	1.5	677
	0.17	1.00:	0.94:	7.51:100	1.6	662
	0.15	1.00:	1.00:	8.00:100 ^a	1.8	668
	0.14	1.00:	1.00:	8.00:110 ^a	1.7	669
	0.20	1.00:	0.97:	9.87:75 ^a	1.4	672
	0.17	1.00:	1.52:	8.09:101	1.7	656
	0.13	1.00:	1.47:	7.59:125 ^a	1.8	669
	0.17	1.00:	2.02:	7.88:101	1.6	660
	0.17	1.00:	2.01:	8.10:100	1.8	658
	0.15	1.00:	2.09:	8.12:113 ^a	1.4	665
	0.17	1.00:	1.01:	8.29:100 ^b	0.7	608
	SnBr_4	0.22	1.00:	0.70:	6.30:75	2.2
0.22		1.00:	1.03:	9.00:75	2.0	661
0.17		1.00:	1.06:	8.49:100 ^a	1.7	672
0.17		1.00:	1.13:	8.12:100 ^a	1.7	666
0.17		1.00:	1.51:	7.31:100	2.1	648
0.22		1.00:	1.58:	8.76:76	2.1	652
0.17		1.00:	1.53:	12.3:100	1.7	680
0.17		1.00:	1.70:	8.74:100	2.0	655

^a Samples were prepared using acetone- d_6 . ^b Samples were prepared using acetone- d_6 and HCl.

(10) A. Fratiello, R. E. Lee, V. M. Nishida, and R. E. Schuster, *J. Chem. Phys.*, **50**, 3624 (1969).

(11) A. Fratiello, R. E. Lee, and R. E. Schuster, *Inorg. Chem.*, **9**, 391 (1970).

(12) A. Fratiello, R. E. Lee, and R. E. Schuster, *Mol. Phys.*, **18**, 19 (1970).

(13) A. Fratiello, R. E. Lee, and R. E. Schuster, *Inorg. Chem.*, **9**, 82 (1970).

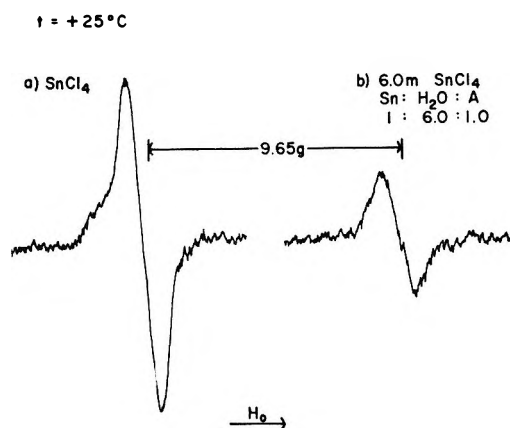


Figure 2. The ^{119}Sn nmr spectra of (a) pure SnCl_4 and (b) a solution of SnCl_4 in a water-acetone mixture, recorded at 25° on a Varian DP-60 nmr spectrometer, operating at 24.3 MHz and 15.3 kG.

ence. The solvation shell peak was broad in most spectra, producing a 1% precision in the shift values. Measurements were possible only over the solvent range indicated in Table I, since the samples either froze at -100° at higher water concentrations, or the water signals were too broad to be treated quantitatively. Although -100° is listed as the temperature of study in Table I, the measurements in some cases were made a few degrees on either side of this value.

The chemical shifts of ^{119}Sn in solutions of SnCl_4 and SnBr_4 in a range of water-acetone mixtures are summarized in Table II, and spectra for pure SnCl_4 and one of these solutions are shown in Figure 2. The addition of water, acetone, or HCl in all cases produced a displacement of the ^{119}Sn signal to higher field than that of pure SnCl_4 . Thus, the δ values listed were calculated from $(H_{\text{soln}} - H_{\text{SnCl}_4})10^6/H_0$, where H_0 is

Table II: ^{119}Sn Chemical Shifts in Aqueous Acetone Solutions of SnCl_4 and SnBr_4 at 25°

Salt	Molality	$\text{SnX}_4:\text{H}_2\text{O}:\text{acetone}$	ϵ at 25°a	δ , ppm ^b
SnCl_4	9.18	1.00:6.06:0.00	80	673
	8.25	1.00:6.70:0.00 ^c	80	732
	5.95	1.00:6.06:1.02	58	631
	5.38	1.00:7.03:1.02	60	666
	4.90	1.00:8.07:1.02	62	686
	4.50	1.00:9.04:1.02	63	686
	4.43	1.00:6.06:2.02	47	800
	3.40	1.00:6.06:3.18	41	830
	2.90	1.00:6.06:4.07	37	915
	2.47	1.00:6.06:5.10	34	(967)
SnBr_4	Pure			640
	6.9	1.00:8.02:0.00		(1210)

^a From ref 16. ^b Shifts are with respect to pure SnCl_4 , measured separately. ^c Sample contained a 2:1 mole ratio of HCl to SnCl_4 .

15.3 kG. The concentrations differ markedly from those used in the pmr studies represented in Table I, because the low natural abundance of ^{119}Sn prevented the use of higher acetone concentrations. However, the water to SnCl_4 mole ratios are essentially the same in both cases.

Discussion

At room temperature, aqueous solutions of the tin tetrahalides exhibit only one water pmr signal, averaged by proton exchange among the positions corresponding to the species present. However, the spectrum of Figure 1 shows that at about -100° , the exchange is slow enough to observe separate peaks for the Sn^{4+} solvation shell and bulk water. From the signal separation of 355 Hz observed in the acid-free solution of Figure 1, and the fact that a temperature increase of only $5\text{--}10^\circ$ causes a coalescence of the two signals, the lifetime of a proton in the solvation shell is approximately 5×10^{-3} sec.¹⁴ This represents only a rough estimation since the signals are not of equal area, and the bulk water signal chemical shift, and, consequently, the signal separation, depends on acetone and acid concentration. In the 1:1 acid to SnCl_4 solutions, the water peak separation was reduced to about 180 Hz, and to 80 Hz in the 2:1 solutions. However, the chemical shift data of Table I indicate that the solvation shell signal varies only slightly over this acid range. Thus, excess acid protons bond primarily to neutral bulk water molecules, rather than water molecules in the shell of a positive ion. The low-field displacement of a water signal in acid solution has been discussed previously.¹⁵ In general, the solvation shell water signal position varies to a significant extent only with temperature, although a quantitative study of this effect has not been made.

Another important feature of the data of Table I is the low cation hydration number, approximately two, observed in each system. This low value must be the result of processes such as hydrolysis or complex formation, since Sn^{4+} could be expected to be hydrated to a greater extent. In the Br^- solutions, hydrolysis can be completely ruled out as a contributing process by the constancy of the hydration number at a value of two over a wide range of acid concentration. The slight increase in the hydration number from about 1.5 to 1.7 as the acid to Sn^{4+} mole ratio was increased from 0 to 2 is an indication that hydrolysis is occurring in the Cl^- solutions, but not to the extent that it is the primary reason for the low values.

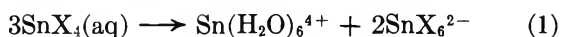
In view of these considerations, the hydration numbers can be attributed most reasonably to Sn^{4+} -halide complex formation. In spite of the low salt molalities

(14) H. S. Gutowsky and C. H. Holm, *J. Chem. Phys.*, **25**, 1228 (1956).

(15) J. A. Pople, W. G. Schneider, and H. J. Bernstein, "High-resolution Nuclear Magnetic Resonance," McGraw-Hill, New York, N. Y., 1959, Chapters 15 and 18.

used in this study, this process would still be favored by the high acetone concentration, and subsequent reduced dielectric constant, and the low temperature of study. The dielectric constant should increase from about 20, that of pure acetone at these solvent compositions, to about 35 at -100° .¹⁶ Even so, the ion-pairing tendency should increase substantially from that in pure water, assuming a simple reciprocal dielectric constant and temperature dependence.¹⁷

The identification of the complexes present can be attempted by a detailed consideration of the hydration numbers, pmr spectral features, ^{119}Sn nmr spectra, and the results of other investigations.¹⁸ First, the average hydration number of 2 could be simply explained by the presence of $(\text{H}_2\text{O})_2\text{SnX}_4$ as the dominant species in solution. However, while this possibility cannot be absolutely precluded, the data mentioned above can be more logically interpreted in terms of a process such as



occurring in both systems. If complex formation is complete, the stoichiometry results in an average Sn^{4+} hydration number of 2. This process is supported by the pmr spectra of these solutions which showed in all cases only one resonance signal for acetone and only one resonance signal for the Sn^{4+} solvation shell water molecules. Numerous studies have demonstrated that acetone can solvate a cation only if there is an insufficient amount of water present to complete the principal solvation shell.^{3,4,8,9} In such cases, a solvation shell acetone signal is readily observed. Thus, the absence of such a peak in these spectra, and the presence of a bulk water peak, are taken as evidence that Sn^{4+} is solvated only by water. Other equilibria which would produce the observed average hydration number of roughly 2 also can be postulated. For example, $(\text{H}_2\text{O})_2\text{SnX}_4$ in equilibrium with $(\text{H}_2\text{O})_3\text{SnX}_3^+$ and $(\text{H}_2\text{O})\text{SnX}_5^-$ is such a process. While such possibilities cannot be disproved, the data of this and other studies are more consistent with the prevalence of the process of eq 1.

The single complexed water signal could result from rapid intramolecular exchange, if different Sn^{4+} -halide complexes were formed in each system. However, such complexes are distinguishable in Al^{3+} and Ga^{3+} solutions, and presumably they should be observable here.^{9,12,13} The postulate of $(\text{H}_2\text{O})_2\text{SnX}_4$ as dominating in each case, while supported by the observation of only one complexed water pmr peak, is discouraged by the chemical shift data of Table I. In the solutions containing HClO_4 , the position of this signal was about 665 ± 5 Hz downfield from TMS for Cl^- solutions, and 662 ± 8 Hz in the Br^- solutions. The size and surface charge density differences between Cl^- and Br^- should produce a greater chemical shift difference than that observed. The presence of $\text{Sn}(\text{H}_2\text{O})_6^{4+}$ as the principal hydrated species in all solutions is consistent with

these average chemical shifts. Furthermore, as seen in Table I, the decrease in hydration number when HCl is added to the SnCl_4 solution confirms the presence of higher chloro complexes such as SnCl_6^{2-} .

The ^{119}Sn nmr chemical shift data of Figure 2 and Table II do not lend themselves to an unambiguous interpretation, yet some features of interest were observed. The detailed ^{119}Sn study of a variety of tin compounds, including the tetrahalides and their mixtures, by Burke and Leuterbur¹⁹ provided the basis for the experimental approach used here. At the low field of 5.3 kG which they used, a ^{119}Sn nmr signal could not be observed for saturated solutions of the tetrahalides. As indicated by the spectrum of Figure 2, the use of a 15.3-kG field makes this observation possible even in solutions diluted with acetone. Only at the concentrations represented by the last SnCl_4 entry of Table II and the one SnBr_4 solution listed were the chemical shift measurements uncertain. The discussion will deal with only the SnCl_4 results, since they were obtained over a reasonable solvent concentration range.

The ^{119}Sn nmr spectra and the SnCl_4 data of Table II can be summarized as follows. Only one signal was observed in all solutions over a range of about 3000 ppm upfield and downfield from pure SnCl_4 . The position of this signal varies only slightly with water concentration from a molality of 9.2 to 4.5, but greater displacements are produced by changes in the acetone concentration. The addition of HCl displaced this signal an additional 50 ppm upfield from that of a comparable acid-free solution. The appearance of only one signal may mean that $(\text{H}_2\text{O})_2\text{SnCl}_4$ is the principal species present, or that eq 1 or a similar process represents the system but intermolecular exchange is rapid at $+25^\circ$. The pmr data previously discussed and the results of other studies to be described minimize, but cannot completely preclude, the presence of a mixture of intermediate complexes undergoing rapid exchange. Of the processes being considered, only those involving an equilibrium would be strongly dependent on dielectric constant, with a decrease in this parameter displacing the equilibrium to the right. Notice that as the water concentration is increased from a 6:1 to 9:1 mole ratio with tin, the dielectric constant changes only slightly and, as mentioned above, the ^{119}Sn chemical shift remains almost unchanged. The addition of acetone produces a much greater decrease in dielectric constant and corresponding shift displacement of almost 300 ppm. This strong dependence of chemical shift on

(16) H. S. Harned and B. B. Owen, "The Physical Chemistry of Electrolytic Solutions," 3rd ed, Reinhold, New York, N. Y., 1963, p 161.

(17) R. A. Robinson and R. H. Stokes, "Electrolyte Solutions," Academic Press, New York, N. Y., 1959.

(18) L. A. Woodward and I. E. Anderson, *J. Chem. Soc.*, 1284 (1957).

(19) J. J. Burke and P. C. Leuterbur, *J. Amer. Chem. Soc.*, 83, 326 (1961).

dielectric constant argues against the presence of solely $(\text{H}_2\text{O})_2\text{SnCl}_4$, and in favor of a mixture of complexes, perhaps $\text{Sn}(\text{H}_2\text{O})_6^{4+}$ and SnCl_6^{2-} .

Finally, the results of other studies support the contention that the products of eq 1 dominate in these solutions. Raman measurements of aqueous solutions of SnBr_4 containing excess Br^- demonstrated the presence of SnBr_6^{2-} , and at high anion concentrations this species dominates.¹⁸ Moreover, in aqueous SnCl_4 solutions the process of eq 1 has been suggested to explain the appearance of SnCl_6^{2-} even in the absence of excess Cl^- .¹⁸ Thus, it is reasonable to assume that in the solutions of Tables I and II, the presence of large amounts of acetone would produce the same result as large anion concentrations, that is the formation of the hexahalo complex. By analogy, similar Raman measurements and an ion-exchange study of concentrated gallium halide solutions demonstrated the presence of $\text{Ga}(\text{H}_2\text{O})_6^{3+}$ and GaX_4^- as the dominant species.²⁰⁻²² Their presence as the sole species in much more dilute solutions in aqueous acetone mixtures was confirmed by

pmr and ^{69}Ga nmr studies.^{12,13} It is apparent that Raman and variable temperature ^{119}Sn and ^{17}O nmr measurements in these aqueous acetone solutions would be decisive in the identification of the species present.

Acknowledgments. A. F. wishes to gratefully acknowledge the support of the National Institutes of Health, Research Career Development Award No. 5-K4-GM-42334. He also wishes to thank the Bell Telephone Laboratories, Inc. for the opportunity to use their facilities during the course of this work. The portion of this work done at California State College, Los Angeles, was supported by Research Grant No. 14-01-0001-2162 from the Office of Saline Water and by National Science Foundation instrument grant. No. GP-8347. The authors are grateful to Dr. Dean C. Douglass for his helpful comments.

(20) L. A. Woodward and A. A. Nord, *J. Chem. Soc.*, 3721 (1956).

(21) T. F. Young, L. F. Maranville, and H. M. Smith, "The Structure of Electrolytic Solutions," W. J. Hamer, Ed., Wiley, New York, N. Y., 1959, Chapter 4.

(22) K. A. Kraus and F. Nelson, see ref 21, Chapter 23.

Molecular Motion and Structure of Aqueous Mixtures with Nonelectrolytes As Studied by Nuclear Magnetic Relaxation Methods

by E. v. Goldammer and H. G. Hertz*

Institut für Physikalische Chemie und Elektrochemie der Universität, Karlsruhe, Germany (Received March 2, 1970)

Appropriate sets of reorientational correlation times τ_c —to be derived from nuclear magnetic relaxation times—and self-diffusion coefficients D are introduced. Between these quantities rules are given which must hold if the mixture has certain structural properties as to be described. After a brief discussion of the pure components of the binary mixtures water and acetonitrile, pyridine, methanol, ethanol, *tert*-butyl alcohol, acetone, and tetrahydrofuran, the structural rules are applied to the experimental results reported. These latter data are τ_c and D of both components of the mixture and of different nuclei as a function of the composition and the corresponding activation energies. Among the various nuclei are the heteronuclei ^{14}N and ^{17}O of some of the organic molecules. The most important result of this investigation is the statement that generally a structural reinforcement appears in the water-rich region and that, however, rigid long-lived hydration spheres do not exist for the organic solutes studied. Furthermore, some evidence for the association of the organic molecules which finally develops to a certain degree of microheterogeneity will be reported.

1. Introduction

It is the purpose of the present paper to contribute to our knowledge of the structure of aqueous solutions of nonelectrolytes. The structure of a liquid may be described in a number of different ways. For instance one may say that the liquid contains numbers n_i of clusters with i particles or that in a solution the solute particles are surrounded by hydration cages of n_h solvent mole-

cules. Partly we shall use this structure description on the following pages. To distinguish this type of description from other possible approaches we will call it in the following the "aggregate approach." The limiting case of this aggregate approach is the simple association of two molecules.

* To whom correspondence should be addressed.

Another more general description which we shall use as well concerns the molecular distribution function approach. In particular, the pair distribution function $f^{(1,1)}(\mathbf{r}_{11}, \Omega_{11}, x_1)$ gives the probability to find a molecule 1 at \mathbf{r}_{11} relative to a given reference molecule 1 and with the orientation Ω_{11} (set of three Eulerian angles). Both \mathbf{r}_{11} and Ω_{11} are taken relative to a coordinate frame fixed in the reference molecule 1. $f^{(1,1)}(\mathbf{r}_{11}, \Omega_{11}, x_1)$ concerns a mixture of molecules 1 and 2 and the argument x_1 indicates that the mole fraction of particle 1 is x_1 . Likewise, in the mixture there may be defined pair distribution functions

$$f^{(1,2)}(\mathbf{r}_{12}, \Omega_{12}, x_1), f^{(2,1)}(\mathbf{r}_{21}, \Omega_{21}, x_1), \text{ and } f^{(2,2)}(\mathbf{r}_{22}, \Omega_{22}, x_1)$$

where the first number of the index indicates the reference molecule. Then the degree of structure in a mixture has to be defined as the deviation of $f^{(1,1)}, f^{(1,2)}, \dots$ from those functions which describe the distribution of molecules which is completely uniform in space and isotropic regarding relative molecular orientation.¹ The complete description of the structure of the liquid has to be carried out not only by the pair distribution function but also by the higher molecular distribution functions which concern more than two molecules. Thus, the statement that there exists a number of clusters of i particles in the liquid is equivalent to the statement that there is a finite probability to find $i - 1$ molecules as seen from a given reference molecule in a certain relative configuration according to the geometry of the cluster.

It is well known that so far there is no experimental method available from which the structural informations just indicated can be derived in a direct way. X-Ray diffraction methods give only averages of $f(\mathbf{r}, \Omega, x_1)$ over all orientational details; thus one obtains $f(r, x_1)$; however, the complications arising in mixtures of polyatomic molecules are well known. We omit here the enumeration of the many methods or attempts to derive structural information—mostly in the aggregate approach—in a more or less indirect way from thermodynamic, spectroscopic, or other experimental data.

The starting point as concerns solution chemistry is the famous problem as to what an extent nonpolar molecules or nonpolar (here hydrocarbon) groups are hydrated in aqueous solution (iceberg formation, hydration of the second kind, or hydrophobic hydration, see, e.g., ref 1), i.e., of what kind is the structure reinforcement, if it at all exists, in these solutions.

The central principle of the present work is the statement that the above-mentioned structural properties of a liquid should in some way be reflected by the nature of the molecular motions in this liquid.

In section 2 the connection between structural properties and the molecular motions will be outlined. A number of rules for these interrelations will be given. In section 4 experimental data regarding the aqueous

mixtures with acetonitrile, pyridine, methanol, ethanol, *tert*-butyl alcohol, acetone, and tetrahydrofuran are reported. The experimental data are rotational correlation times as derived from nuclear magnetic relaxation times, self-diffusion coefficients, and the activation energies for both these quantities. To have a better understanding of the mixtures a brief sketch of the motional behavior of the pure components is given. The application of the above-mentioned rules to the experimental results allows the decision whether certain structural aggregates do exist or not or whether the molecular distribution functions assume sharper or flatter maxima in the mixture as compared with the pure liquids forming the components.

One remark should be added here. It is clear that a huge amount of literature exists regarding the possible structural properties of the aqueous mixtures studied here. We consider our work essentially to be the demonstration of the straightforward application of a number of rules within the conceptual framework underlying the method concerned. Thus we shall refrain from a discussion of each result we obtain in the light of the bulk of other knowledge of this topic accumulated in the literature. The room available in this article would not allow this undertaking. We feel, however, that our results are not in striking contrast to the general view accepted in the literature.

2. Structural Properties and Molecular Motions

A. Introduction of Quantities to Be Used. As has already been mentioned above the central principle of the present work is the statement that the structural properties of a liquid should be in some way reflected by the nature of the molecular motions in the liquid. These motions of a liquid in thermodynamic equilibrium may be characterized by the behavior of a number of appropriately chosen time correlation functions. The experimental data to be presented here are the time integrals of three different time correlation functions²⁻⁵

$$D = \frac{1}{3} \int_0^\infty \overline{\mathbf{v}(0)\mathbf{v}(t)} dt \quad (1)$$

$$\tau_c = \int_0^\infty \overline{Y_{2m}^*(0)Y_{2m}(t)} dt \quad m = 0, \pm 1, \pm 2 \quad (2)^6$$

and

$$\beta = \int_0^\infty \frac{\overline{Y_{2m}^*(0)Y_{2m}(t)}}{(r(0))^3 (r(t))^3} dt \quad m = 0, \pm 1, \pm 2 \quad (3)$$

(1) H. G. Hertz, *Ber. Bunsenges. Phys. Chem.*, **68**, 907 (1964).

(2) F. Reif, "Fundamentals of Statistical and Thermal Physics," McGraw-Hill, New York, N. Y., 1965.

(3) P. A. Egelstaff, "An Introduction to the Liquid State," Academic Press, London, 1967.

(4) R. Zwanzig, *Ann. Rev. Phys. Chem.*, **16**, 67 (1965).

(5) A. Abragam, "The Principles of Nuclear Magnetism," Clarendon Press, Oxford, 1961.

(6) If $\overline{Y_{2m}^*(0)Y_{2m}(t)}$ has the form e^{-t/τ_c} , then its Fourier transform is $2\tau_c/1 + \omega^2\tau_c^2$, and for $\omega = 0$ one obtains eq 2.

1 in the next neighborhood—*i.e.*, the first coordination sphere—of molecule 2. $\tau_{c21}^{(1,2)}$ regards the vector connecting atomic position 2 of molecule 1 (now the solute) with atomic position 1 of molecule 2 (now the solvent) in the solvation sphere of 1 at $x_2 \approx 1$. The extension of the other symbols is obvious (see Figure 1).

We confine our consideration to molecules and aggregates which are essentially of spherical symmetry. The more complicated treatment of markedly non-spherical systems is possible, in principle; in the following pages it will occasionally be necessary to treat the cases of anisotropic motions.

B. Structural Rules. Now we are prepared to present some rules which form a bridge between the structural properties of the liquid and the molecular motions. We first use the aggregate approach.

Rule No. 1. If the probability is essentially 1 to find a crystallike geometric arrangement of solvent molecules around a solute molecule, *i.e.*, that there exists a rigid long-lived solvation cage, then

$$\left. \begin{aligned} D^{(1)+} &= D^{(2)} \text{ for } x_1 \approx 1 \\ D^{(2)+} &= D^{(1)} \text{ for } x_2 \approx 1 \end{aligned} \right\} \quad (4)$$

must hold as a necessary condition.

Furthermore, if the solute molecule is incorporated rigidly, *i.e.*, immovably in the solvation cage in a completely fixed position, then, besides eq 4 the equations

$$\left. \begin{aligned} \tau_{c1}^{(1)+} &= \tau_{c2}^{(1)+} = \dots = \tau_{c1}^{(2)} = \tau_{c2}^{(2)} = \\ &\dots \tau_{c11}^{(2,1)} = \tau_{c12}^{(2,1)} = \dots \text{ for } x_1 \approx 1 \\ \tau_{c1}^{(2)+} &= \tau_{c2}^{(2)+} = \dots = \tau_{c1}^{(1)} = \tau_{c2}^{(1)} = \\ &\dots \tau_{c11}^{(1,2)} = \tau_{c12}^{(1,2)} = \dots \text{ for } x_2 \approx 1 \end{aligned} \right\} \quad (4a)$$

must hold as a necessary condition.

Long-lived means here that the distances between the centers of mass of the cage molecules and that of the central solute molecule are constant for a time τ longer than the time of molecular reorientation $\tau_r \approx 5 \times 10^{-12}$ sec (for H₂O at 25°); *i.e.*, $\tau \gtrsim 10^{-11}$ sec. Rigid means that the well-structured configuration (all intra- and intermolecular distances given) exists a time τ longer than the rotational correlation time of the aggregate, a typical example will be as well $\tau \gtrsim 10^{-11}$ to 10^{-10} sec.

In this paper we shall primarily use the first line of eq 4 and 4a (1 → H₂O); measurements concerning the second line are still somewhat preliminary and of less interest here. The first line of eq 4a has previously been used by one of the present authors (H. G. H.) for the study of the ions F⁻,⁸ Li⁺,⁹ Mg²⁺, and Al³⁺.¹⁰ Here, of course, no intramolecular correlation time for the solute exists, and eq 4a only holds for the times $\tau_c^{(1)}$ and $\tau_c^{(2,1)}$. For the ion BF₄⁻ a full analysis is possible.⁸ [We omit here the case that the hydration sphere is long-lived and rigid; however, the central (solute) particle performs independent rotational motion. No experimental results are so far available to study such behavior. The extension of eq 4a to this case is obvious.]

Rule No. 2. If the probability is essentially 1 to find a geometrical arrangement of solvent molecules around the solute molecule of such a kind that the distance between the center of mass of any solvent molecule in the coordination sphere and the center of mass of the solute molecule has a given constant value, then

$$\left. \begin{aligned} D^{(1)+} &= D^{(2)} \text{ for } x_1 \approx 1 \\ D^{(2)+} &= D^{(1)} \text{ for } x_2 \approx 1 \end{aligned} \right\} \quad (4)$$

must hold as a necessary condition. Now, generally, there does not exist any of the relations eq 4a between the various reorientational correlation times. In this event we have still a long-lived solvation sphere in the sense as defined above, however, only regarding the centers of mass of the molecules. Clearly now the aggregate is no longer rigid.

Rule No. 3. If the probability is essentially 1 to find a long-lived pair association between the solute molecule and one solvent molecule, then

$$\left. \begin{aligned} D^{(1)+} &= D^{(2)} \text{ for } x_2 \lesssim 1/2 \\ D^{(2)+} &= D^{(1)} \text{ for } x_1 \lesssim 1/2 \end{aligned} \right\} \quad (5)$$

must hold as a necessary condition. Now $D^{(1)+}$, $D^{(2)+}$ concerns the one solvent molecule attached to the solute molecule. Furthermore, we must have

$$\left. \begin{aligned} \tau_c^{(1)+} &= \tau_c^{(2)} \text{ for } x_2 \lesssim 1/2 \\ \tau_c^{(2)+} &= \tau_c^{(1)} \text{ for } x_1 \lesssim 1/2 \end{aligned} \right\} \quad (5a)$$

as necessary conditions if the vectors corresponding to the above correlation times have both the direction of the bond between the molecules 1 and 2. If only one of these vectors points in the direction of this bond, then the reorientational correlation time of this latter vector cannot be shorter than that of the other vector not pointing in the direction of the bond, provided both molecules are relatively small. Whereas the reason for the rules 1 and 2 is immediately obvious, the statement of rule 3 concerning the rotational motion arises from the nature of the decay of the respective correlation function under anisotropic or intramolecular rotation.¹¹⁻¹³ Again, here $\tau_c^{(1)+}$ concerns the one solvent molecule attached to the solute molecule.

It is important to note that the fulfillment of eq 4, 4a, 5, 5a is never sufficient to warrant the presence of the corresponding structural situation.

(8) H. G. Hertz, G. Keller, and H. Versmold, *Ber. Bunsenges. Phys. Chem.*, **73**, 549 (1969).

(9) H. G. Hertz and H. Versmold, to be published.

(10) H. G. Hertz and R. Tutsch, to be published.

(11) W. T. Huntress, *J. Chem. Phys.*, **48**, 3524 (1968).

(12) D. W. Woessner, D. S. Snowden, and G. H. Meyer, *ibid.*, **50**, 719 (1969).

(13) H. Versmold, *Z. Naturforsch. A*, **25**, 367 (1970).

Rule No. 4. If $D^{(i)+}$ or $\tau_{c_j}^{(i)+}$ characterizes the motion of a molecule which is a member of a (rigid) long-lived cluster or solvation sphere, then these quantities cannot have any value but must lie within a certain range given by the size of the cluster or solvation sphere. Here, *e.g.*, for the reorientational motion, the Debye relation should be mentioned

$$\tau_c = \frac{4\pi a^3}{3kT} \eta^* \quad (6)$$

where $\eta^* = \eta\zeta$, η = viscosity, ζ = microviscosity factor,¹⁴ and a = radius of the aggregate.

It is well known that this relation is only approximately valid for small molecular aggregates. For translational diffusion the corresponding relation is the Einstein formula

$$D = \frac{kT}{6\pi\eta a\zeta'} \quad (7)$$

where ζ' = microviscosity factor for translational diffusion.¹⁴ If there are aggregates of fluctuating size, then D may be written

$$D = \frac{kT}{6\pi\eta} \sum \frac{p_{a_i}}{a_i\zeta_{a_i}'} \quad (8)$$

where p_{a_i} is the probability that an aggregate of size a_i occurs in the liquid. ζ_{a_i}' is the translational microviscosity factor for the aggregate of size a_i . Likewise

$$\frac{1}{\tau_c} = \frac{3kT}{4\pi\eta} \sum \frac{p_{a_i}}{a_i^3\zeta_{a_i}} \quad (9)$$

where ζ_{a_i} is the rotational microviscosity factor for the aggregate with size a_i . Equation 9 is not the only possible relation between τ_c and the a_i ; another relation will be given below.

Rule No. 5. The rule to be given now does not use the aggregate approach but is written in terms of maximum values of the pair distribution functions. Suppose that $f^{(1,1)}(\mathbf{r}_{11}, \Omega_{11}, x_1)$ at certain sets of coordinates $(\mathbf{r}_{11})_1, (\Omega_{11})_1; (\mathbf{r}_{11})_2, (\Omega_{11})_2; \dots$ assumes relative maximum values $f_1^{(1,1)}, f_2^{(1,1)}, \dots$. Likewise at certain $(\mathbf{r}_{12})_1, (\Omega_{12})_1; (\mathbf{r}_{12})_2, (\Omega_{12})_2; \dots$; $f^{(1,2)}(\mathbf{r}_{12}, \Omega_{12}, x_1)$ has relative maximum values $f_1^{(1,2)}, f_2^{(1,2)}, \dots$. Then the probabilities p_{a_i} occurring in eq 8 and 9 may be expressed in terms of the $f_1^{(1,1)}, \dots, f_1^{(1,2)}$, and it may be shown¹⁶ that the relations

$$1/D^{(1)} = \varphi_{D1}^{(1)}(f_1^{(1,1)}, f_2^{(1,1)}, \dots) + \varphi_{D2}^{(1)}(f_1^{(1,2)}, f_2^{(1,2)}, \dots) \quad (10)$$

$$\tau_c^{(1)} = \varphi_{\tau 1}^{(1)}(f_1^{(1,1)}, f_2^{(1,1)}, \dots) + \varphi_{\tau 2}^{(1)}(f_1^{(1,2)}, f_2^{(1,2)}, \dots) \quad (11)$$

hold.^{16a,b} Here $\varphi_{D_i}^{(1)}$ and $\varphi_{\tau_i}^{(1)}$, $i = 1, 2$, are certain functions which increase monotonously with increasing values of any of the $f_j^{(1,1)}, f_j^{(1,2)}$, $j = 1, 2, \dots$. Since any increase in the degree of structure in the liquid is

manifested by increasing numerical values of $f_j^{(1,1)}, f_j^{(1,2)}$, each structural reinforcement causes $D^{(1)}$, the self-diffusion coefficient of component 1, to decrease and $\tau_c^{(1)}$, the rotational correlation time of the component 1, to increase. Note that eq 10 and 11 are direct consequences of eq 8 and 9. In a previous work one of the authors (H. G. H.) had written a more primitive form

$$\tau_c^{(1)} \sim (f_1^{(1,1)} + f_1^{(1,2)})$$

Clearly, for component 2 one may write in the same way

$$1/D^{(2)} = \varphi_{D1}^{(2)}(f_1^{(2,2)}, f_2^{(2,2)}, \dots) + \varphi_{D2}^{(2)}(f_1^{(2,1)}, f_2^{(2,1)}, \dots) \quad (12)$$

$$\tau_c^{(2)} = \varphi_{\tau 1}^{(2)}(f_1^{(2,2)}, f_2^{(2,2)}, \dots) + \varphi_{\tau 2}^{(2)}(f_1^{(2,1)}, f_2^{(2,1)}, \dots) \quad (13)$$

Rule No. 6. The following rule concerns the solute-solute particle distribution (component 2, 1 at $x_{1,2} \approx 1$). Let us choose component 2 as the solute here. It may be shown that the relation holds (see eq 3 and see below)

$$\mathcal{J}^{(2,2)} = \frac{1}{15\hat{a}_{22}D^{(2)}} \left(1 + \alpha \frac{\langle r^2 \rangle}{\hat{a}_{22}^2} \right) \quad (14)$$

where \hat{a}_{22} is the closest distance of approach between two protons on different solute particles, $\langle r^2 \rangle$ is the mean-square displacement of particle 2 under a translational jump, and $0 \leq \alpha \leq 1$ and depends on the particular mechanism of translational diffusion (for a model proposed by Torrey: $\alpha = 5/12$ ^{7,17}). Generally the expression added to 1 in the parentheses of eq 14 is small. Equation 14 has been calculated for a uniform distribution in space of the particles 2 relative to the reference particle 2. Now our rule 6 reads that if $\mathcal{J}^{(2,2)}D^{(2)}$, as a function of the concentration, deviates significantly from a constant value, and in particular, if starting from $x_2 = 0$ $\mathcal{J}^{(2,2)}D^{(2)}$ decreases with increasing concentration of component 2, then the effective closest distance of approach \hat{a}_{22} increases with concentration which, however, is equivalent to the statement that the solute distribution around a given solute particle is not uniform but that there is a crowding of solute molecules around the reference molecule at low concentrations.

C. Average Values of D and τ_c . Now we must explain the connection between the local quantities D^+ and τ_c^+ and the measured quantities D and τ_c (section

(14) A. Gierer and K. Wirtz, *Z. Naturforsch. A*, **8**, 532 (1953).

(15) H. G. Hertz, *Ber. Bunsenges. Phys. Chem.*, **74**, 666 (1970).

(16) (a) Both component molecules must be essentially of the same size. (b) To simplify the treatment in eq 10 and 11 the same maximum values of the pair distribution function appear. Of course, this is not strictly correct, often for the translational diffusion only the dependence of $f_1^{(1,1)}, \dots, f_1^{(1,2)}, \dots$ on the intermolecular distances will be important.

(17) H. C. Torrey, *Phys. Rev.*, **92**, 692 (1953).

2B). Consider a solution of 2 in 1. In this work 1 will always be H₂O. The molality of 2 is C₂; that of 1 is C₁. Assume that every solute molecule (2) is surrounded by a hydration sphere of n_h water molecules. The self-diffusion coefficient of the water not being a member of the hydration sphere is D^{(1)°}; D⁽¹⁾⁺ is the self-diffusion coefficient of the water in the hydration sphere. Then it may be shown¹⁸ that the relation

$$D^{(1)} = D^{(1)°}(1 - x_2^+) + D^{(1)+}x_2^+ \quad (15)$$

with $x_2^+ = n_h C_2 / 55.5$, $0 < x_2 < 1$ holds. This equation connects the measurable quantity D⁽¹⁾ (and D^{(1)°}) with the "local" quantity D⁽¹⁾⁺. D⁽¹⁾⁺ is to be used in rule 1, eq 4. The relation

$$\begin{aligned} D^{(1)} &= D^{(1)°}(1 - \sum x_i) + \sum x_i D^{(1)i} \\ &\equiv D^{(1)°}(1 - \sum p_i) + \sum p_i D^{(1)i} \end{aligned} \quad (16)$$

is an obvious generalization of eq 14 for many environments; it has not yet been proved rigorously to the authors' knowledge. It forms the basis for eq 8. p_i is the probability that the particle is in the ith environment or configuration.

Now let τ_c⁽¹⁾⁺ and τ_c^{(1)°} be the correlation time in the hydration sphere and free solvent, respectively. Then¹⁸

$$\frac{1}{\tau_c^{(1)}} = \frac{1}{\tau_c^{(1)°}}(1 - x^+) + \frac{1}{\tau_c^{(1)+}}x^+ \quad (17)$$

holds only for configurational change or particle exchange very fast compared with the respective correlation times τ_c⁽¹⁾⁺ and τ_c^{(1)°}. Thus, if τ_h is the lifetime or residence time in a given configuration or environment τ_h ≪ τ_c⁽¹⁾⁺, τ_c^{(1)°} must be fulfilled. For the reverse situation, τ_h ≫ τ_c⁽¹⁾⁺, τ_c^{(1)°} one has¹⁸

$$\tau_c^{(1)} = \tau_c^{(1)°}(1 - x^+) + \tau_c^{(1)+}x^+ \quad (18)$$

The generalization to many configurations or environments is obvious, its validity has been proved.¹⁹

The generalization of eq 17

$$\frac{1}{\tau_c^{(1)}} = \sum \frac{p_i}{\tau_c^{(1)i}} \quad (17a)$$

forms the basis of eq 9. In the most general case the molecule fluctuates fast among a certain number of configurations, say $1 \leq i \leq k$; then after a time τ_{h1} it enters into another environment where again fast fluctuation among other configurations $i < \nu$ occurs. After a time τ_{h2} > τ_{k+1}, . . . τ_ν, it returns to the first class of configurations. Now eq 18 holds where both τ_c⁽¹⁾⁺ and τ_c^{(1)°} are mean correlation times, the mean values formed according to eq 17a with

$$\frac{1}{\tau_c^{(1)°}} = \sum_{i=1}^k \frac{p_i}{\tau_c^{(1)i}}, \quad \frac{1}{\tau_c^{(1)+}} = \sum_{i=k+1}^{\nu} \frac{p_i}{\tau_c^{(1)i}}$$

However, it may happen that we do not know whether we have to apply

$$\frac{1}{\tau_c^{(1)}} = (1 - x^+) \frac{1}{\tau_c^{(1)°}} + x^+ \frac{1}{\tau_c^{(1)+}} \quad (17)$$

or eq 18. Then, as will be shown in the Appendix, for the systems of interest here the error in τ_c⁽¹⁾⁺ as determined from τ_c⁽¹⁾ will be not greater than a factor ~2.

D. *Experimental Determination of D, τ_c, and J.* The self-diffusion coefficient D is directly measurable by tracer methods²⁰ or by (nmr) spin-echo techniques.²¹ All data reported in this paper are obtained by the latter method.

τ_c is to be derived from nuclear magnetic relaxation time measurements. Here only the spin-lattice relaxation time T₁ is of importance. τ_c is related to T₁ in the following way. If the vector considered connects two protons and relaxation is due to magnetic dipole-dipole interaction⁶

$$\tau_c = \frac{2}{3} \frac{b^6}{\gamma^4 \hbar^2} \left(\frac{1}{T_1} \right)_{\text{intra}} \quad (19)$$

$$\frac{1}{T_1} = \left(\frac{1}{T_1} \right)_{\text{intra}} + \left(\frac{1}{T_1} \right)_{\text{inter}} \quad (20)$$

(1/T₁)_{intra} is the intramolecular relaxation rate; it is due to the proton-proton interaction within the molecule. Correspondingly (1/T₁)_{inter} is the intermolecular contribution to the relaxation rate 1/T₁ which is caused by interacting protons on different molecules; γ = gyromagnetic ratio, ħ = Planck's constant/2π, and b = distance between the two protons within the molecule. By special methods it is generally possible to determine (1/T₁)_{inter}. Thus from the measured 1/T₁, (1/T₁)_{intra} is known which according to eq 19 yields τ_c. Equation 19 holds for a molecule with two protons like H₂O. If there are more protons in the molecules, an appropriate averaging over all proton-proton vectors has to be made.²²

Many nuclei have an electric quadrupole moment Q. In this case 1/T₁ = (1/T₁)_{intra} and⁶

$$\tau_c = \frac{40I^2(2I - 1)}{3(2I + 3)} \left(\frac{\hbar}{eQq} \right)^2 \left(\frac{1}{T_1} \right) \quad (21)$$

Now the vector the rotational motion of which is considered is the vector having the direction of the maximum electrical field gradient at the nucleus q, e = elementary charge, I = nuclear spin.

Finally we have^{6,7}

$$J = \frac{1}{6\pi\gamma^4\hbar^2 N_I} \left(\frac{1}{T_1} \right)_{\text{inter}} \quad (22)$$

(18) Second paper of ref 7.

(19) J. R. Zimmerman and W. E. Brittin, *J. Phys. Chem.*, **61**, 1328 (1957).

(20) See, e.g., P. A. Johnson and A. L. Babb, *Chem. Rev.*, **56**, 386 (1956).

(21) H. Y. Carr and E. M. Purcell, *Phys. Rev.*, **94**, 630 (1954).

(22) E. v. Goldammer and M. D. Zeidler, *Ber. Bunsenges. Phys. Chem.*, **73**, 4 (1969).

where N_I is the number of spins per cubic centimeter in the liquid. Equation 22 is valid for magnetic dipole-dipole interaction. $(1/T_1)_{\text{inter}}$ may generally be determined experimentally (see below).

3. Experimental Section²³

All proton and deuteron relaxation times have been measured by the pulse method; the 90°–90° pulse sequence has been applied. The spin-echo equipment used has been described previously,²² and literature cited therein. The resonance frequency was 20 MHz for the protons and 14 MHz for the deuterons. The samples were degassed with the usual freezing–pumping–thawing procedure at the vacuum line. The self-diffusion coefficients were measured by the 90°–180° pulse technique in the usual way.^{21,22} In all cases only the echo decay of the protons has been utilized for the self-diffusion measurements. For the proton and deuteron measurements the temperature was stabilized within $\pm 1^\circ$ by pumping of water or methanol from a Höppler thermostat through the copper probe head.

The proton relaxation times were checked by comparison with our standard value of water at 25°, $T_1 = 3.60$ sec; for the deuteron relaxation the standard comparison value was $T_1 = 0.44$ sec at 25°.^{7,22} Our reference value for the self-diffusion coefficient was 2.50×10^{-5} cm²/sec for water at 25°.²⁴

The relaxation time measurements for ¹⁴N and ¹⁷O were line-width measurements. The apparatus used was the Varian DP 60 spectrometer with the variable frequency unit V-4210 A. The frequency for the ¹⁴N relaxation was 4.34 MHz, that for the ¹⁷O measurements 8.13 MHz. Temperature variation and stabilization for these nuclei was done by the Varian gas-flow device (V-4557-9). The line-width measurements were partly performed by the differential scanning method, partly by the side-band method,²⁵ depending on the line width in the particular case. The line width of ¹⁴N was sufficiently large so that we felt justified to neglect field inhomogeneity broadening. Our ¹⁴N data are in satisfactory agreement with results of other authors (see Table I). For the ¹⁷O line width we reproduced the result $\Delta H = 82 \pm 2.5$ mG for (nonneutral) water at 25° as reported previously.²⁶ All activation energies reported have been derived from measurements at 5, 15, 25, and 35°. Satisfactory straight lines appeared in the plot $\log 1/T_1$ vs. $1/T$; the activation energies are correct to $\pm 20\%$. The accuracy for the T_1 measurements was $\pm 5\%$. The self-diffusion measurements caused the greatest trouble; unfortunately we had to be content when our measurements were reproducible within $\pm 10\%$, the scatter being found sometimes greater than this. The experimental error of the line-width measurements is between 5 and 10%. All materials used were of commercial origin and were used without further purification. The ¹⁷O relaxation measurements were performed with 7% ¹⁷O-enriched methanol and

Table I: Some Nuclear Magnetic Relaxation Rates for Organic Molecules in the Pure Liquid at 25°

Compound	Nucleus	$1/T_1$, sec ⁻¹	$(1/T_1)_{\text{intra}}$, sec ⁻¹	eQq/h , MHz
Acetonitrile } CH ₃ CN	¹⁴ N	246 ^a	246	3.74 ^b
CH ₃ CN				
CH ₃ CN	¹ H	6.2×10^{-2}	4.4×10^{-2}	
CD ₃ CN	² H	0.15	0.15 ^c	
Pyridine } C ₅ H ₅ N	¹⁴ N	675 ^d	675	4.6 ^e
C ₅ H ₅ N				
Methanol } CH ₃ OH	¹⁷ O	440	440	...
CH ₃ OH				
Ethanol } C ₂ H ₅ OH	¹⁷ O	780	780	...
C ₂ H ₅ OH				
CH ₃ CD ₂ OH	² H	0.86	0.86	
CD ₃ CH ₂ OH	² H	1.06	1.06	
Acetone } (CH ₃) ₂ CO	¹⁷ O	163	163	12.4 ^f
(CH ₃) ₂ CO				

^a Woessner, Snowden, and Strom: 228 ± 5 sec⁻¹.³⁸ ^b P. A. Casabella and P. J. Bray, *J. Chem. Phys.*, **29**, 1105 (1958). ^c Woessner, Snowden, and Strom: 0.15 sec⁻¹.³⁶ ^d Kintzinger and Lehn: 671 sec⁻¹ (J. P. Kintzinger and J. M. Lehn, *Mol. Phys.*, **14**, 133 (1968)). ^e E. A. C. Lucken, *Trans. Faraday Soc.*, **57**, 729 (1961). ^f QCC for H₂CO (E. A. C. Lucken, "Nuclear Quadrupole Coupling Constants," Academic Press, New York, N. Y., 1969).

ethanol supplied by Miles-Yeda Ltd., Rehovoth, Israel; the oxygen of acetone exchanges slowly with that of water in nonneutral aqueous solution ($\tau_{1/2} \approx 15$ hr in acidic solution²⁷).

4. Experimental Results and Their Evaluation

A. The Pure Liquids. (i) Water. On the following pages we shall present a number of new experimental results. From these together with some older experimental data we shall draw the relevant conclusions regarding the structure of the mixtures. In this procedure the first step will be the discussion of the structural information which can be obtained from molecular reorientational motion in pure water. Thereafter a brief description of the pure organic components used here will follow.

Suppose water is a mixture of clusters, the clusters containing n_i molecules $i = 0, 1, 2, 3 \dots$; $i = 0$ corresponds to the monomeric water molecule. The reorientational correlation time $\tau_c^{(i)}$ is known for an appreciable temperature range, e.g., at 25° $\tau_c^{(1)} = 2.5 \times 10^{-12}$ sec.^{7,22} Let the correlation time of the i th cluster be $\tau_{ci}^{(i)}$. Then we have

(23) We wish to thank Mrs. I. Siepe for her assistance with some measurements.

(24) N. J. Trappeniers, C. J. Gerritsma, and P. H. Oosting, *Phys. Lett.*, **18**, 256 (1965).

(25) See, e.g., O. Haworth and R. E. Richards, *Progr. Nucl. Magnetic Resonance Spectrosc.*, **1**, 1 (1966).

(26) F. Fister and H. G. Hertz, *Ber. Bunsenges. Phys. Chem.*, **71**, 1032 (1967).

(27) M. Cohn and H. C. Urey, *J. Amer. Chem. Soc.*, **60**, 679 (1938).

$$\frac{1}{\tau_c^{(1)}} = \sum \frac{p_i}{\tau_{ci}^{(1)}} \text{ for } \tau_h \ll \tau_{ci}^{(1)} \quad (23)$$

or

$$\tau_c^{(1)} = \sum p_i \tau_{ci}^{(1)} \text{ for } \tau_h \gg \tau_{ci}^{(1)} \quad (24)$$

where τ_h is a representative lifetime in a given cluster configuration. We know that for the long-lived octahedral hydration sphere of Mn^{2+} $\tau_c \approx 3 \times 10^{-11}$ sec.^{7,28-30} Replacing the central Mn^{2+} ion by a water molecule, we have a cluster of seven molecules. Rounding off the number 7 so as to have 10 in order to take account of the partially bound (short-lived) second hydration sphere we expect $\tau_{c10}^{(1)} \approx 3 \times 10^{-11}$ sec. $\tau_{co}^{(1)}$ is as well known from Hindman and co-workers³¹ measurements of dilute solutions of H_2O in inert organic solvents: $\tau_{co}^{(1)} \approx 5 \times 10^{-13}$ sec. Inserting these numbers into eq 24 with $p_i = 0$ for $i \neq 0, 10$, we find $p_{10} = 0.068$ which is certainly too small. Thus we conclude if there are larger clusters with $i \geq 10$ in water, the lifetime of these clusters must be very much smaller than an average $\tau_{ci}^{(1)}$, that is, $\tau_h \approx 10^{-12}$ to 10^{-11} sec. Putting $1/\tau_{ci}^{(1)} = 0$ for all clusters present, we obtain from eq 23 $p_0 \approx 0.20$ which is a reasonable figure. If this situation really occurs, then the "free" reorientation is the only contribution to the total molecular reorientation in water. One of the authors (H. G. H.) has derived the following formula for $\tau_c^{(1)}$ ⁷

$$\frac{1}{\tau_c^{(1)}} = \frac{1}{\tau_{cc}^{(1)}} + \frac{1 - C_2}{\tau_h}$$

where C_2 is a constant $0 \leq C_2 \leq 1$. $\tau_{cc}^{(1)}$ is the average correlation time for all clusters. In the situation just indicated one has to put $C_2 \rightarrow 0$ (see ref 7); then, with $\tau_{cc}^{(1)} \gg \tau_h$ (τ_h = average residence time in a cluster)

$$\tau_c^{(1)} = \tau_h \quad (25)$$

As shown elsewhere⁷ the interesting consequence of eq 25 is the additional validity of $\tau_c^{(1)} = \tau_r^{(1)}$, where $\tau_r^{(1)}$ is the reorientation time. For an ordinary slow diffusion process we would have $\tau_r^{(1)} = 3\tau_c^{(1)}$. Thus, knowledge of $\tau_r^{(1)}/\tau_c^{(1)}$ would give us the desired information regarding cluster distribution. The dielectric relaxation time τ_d is experimentally well known: 8.2×10^{-12} sec at 25° .³² However, the macroscopic dielectric relaxation time τ_d is connected with the microscopic dielectric relaxation time or reorientation time $\tau_r^{(1)}$ by a factor δ : $\tau_d = \delta \times \tau_r^{(1)}$. δ is not known exactly; $1 < \delta < 2$.^{33,34} With $\delta = 2$ we get $\tau_r^{(1)} = 4 \times 10^{-12}$ sec, thus $\tau_r^{(1)} \neq \tau_c^{(1)}$ and the pure free state rotation or rotational jump model seems not to be correct.

(ii) *Pure Organic Liquids.* As will be seen below the motion of the polar group of the organic molecules is of great interest for our structural investigation in the aqueous mixtures. Therefore, as a starting point, we studied the reorientational motion of the polar group in

the pure organic liquids. We utilized the ^{14}N relaxation in acetonitrile and pyridine and the ^{17}O relaxation in acetone, methanol, and ethanol. Our relaxation rates $1/T_1$ are collected in Table I. For comparison, some data obtained by other authors are also given in this table. The quadrupole coupling constant eQq/h may also be found in Table I for those molecules where experimental data are available in the literature. For acetone only the ^{17}O coupling constant of formaldehyde in the gaseous state has been measured;³⁴ we used this coupling constant for acetone. It will be seen shortly that this approximation is essentially correct. For some of the organic liquids we measured the proton and deuteron relaxation rates, too; the results are included in Table I.

Then, with the data of Table I and with eq 21 we calculated the correlation time of the heteronucleus in the polar group. The results are given in Table II. Furthermore, for methanol and ethanol the correlation time of the hydroxyl group as determined from the deuteron relaxation may be found in Table II. For comparison we added in Table II the correlation times of the hydrocarbon part of the molecules which are of interest in this paper. All these latter data are taken from ref 22.

The correlation time $\tau_c(H-H)$ which is derived from the proton relaxation rate represents an average over the motion of all proton-proton vectors in the molecule.²² $\tau_c(D-C)$ is derived from the deuteron relaxation rate and is the average of all direct CD bond vectors in the molecule. The OD results regard the OD bond vector.

In Table II for the quadrupole coupling constant of the hydrocarbon deuteron a constant mean value of 170 kHz has been assumed.³⁵ The individual coupling constants may deviate from this value by $\pm 10\%$, thus $\tau_c(D-C)$ may be longer or shorter by $\pm 20\%$. The same is true for the OD coupling constant, here the coupling constant of OD in DOD has been used.²² The activation energies for the reorientational motion of the molecules or respective parts of the molecules may also be found in Table II. In all cases the quadrupole coupling constant was assumed to be independent of the temperature which may be only approximately true.

(28) N. Bloembergen and L. O. Morgan, *J. Chem. Phys.*, **34**, 842 (1961).

(29) H. Pfeifer, *Z. Naturforsch. A*, **17**, 279 (1962).

(30) R. Hausser and F. Noack, *Z. Phys.*, **182**, 93 (1964).

(31) J. C. Hindman, A. Svirnickas, and M. Wood, *J. Phys. Chem.*, **72**, 4188 (1968).

(32) See, e.g., R. Pottel and O. Lossen, *Ber. Bunsenges. Phys. Chem.*, **71**, 135 (1967).

(33) R. H. Cole, "Magnetic and Dielectric Resonance and Relaxation," J. Smidt, Ed., North-Holland Publishing Company, Amsterdam, 1963, p 96.

(34) E. Fatuzzo and P. R. Mason, *Proc. Phys. Soc.*, **90**, 729, 741 (1967).

(35) T. T. Bopp, *J. Chem. Phys.*, **47**, 3621 (1967).

Table II: Reorientational Correlation Times and Activation Energies for Some Pure Organic Liquids (25°)

Compound	$\tau_c(^{14}\text{N})$, psec ^a	$\tau_c(^{17}\text{O})$, psec	$\tau_c(\text{DO})$, psec	$\tau_c(\text{H-H})$, psec	$\tau_c(\text{D-C})$, psec	eQq/h for ^2H , kHz ^b	E_a (polar group), ^c kcal/mol	E_a (hydrocarbon part), ^c kcal/mol
CH ₃ CN	1.2			0.4 ^d			1.85 (¹⁴ N)	
CD ₃ CN					0.35	170		1.3 ^e
C ₂ H ₅ N	2.1			1.65			...	
C ₂ D ₅ N					2.2	170		2.4
CH ₃ OH							2.2 (¹⁷ O)	
CH ₃ OD			3.7	0.9		248	2.75 (² H)	
CD ₃ OH					0.45	170		1.7
C ₂ H ₅ OH							2.3 (¹⁷ O)	
C ₂ H ₅ OD			8.0	2.2		248	4.4 (² H)	
C ₂ D ₅ OH					2.5	170		3.4
CD ₃ CH ₂ OH					2.6	170		3.0
CH ₂ CD ₂ OH					2.1	170		3.7
(CH ₃) ₃ COD			47.7	8.0		248		
(CD ₃) ₃ COH					13.5	170		
(CH ₃) ₂ CO		1.1		0.6				
(CD ₃) ₂ CO					0.5	170		1.6
C ₄ H ₈ O (THF)				0.6				
C ₄ D ₈ O (TDP)					0.8	170		2.5

^a psec = 10⁻¹² sec. ^b Assumed average standard values; ²H ≡ D. ^c Definition of E_a : $\tau_c = \tau_c^0 e^{E_a/RT}$. ^d After correction for spin rotation interaction.³⁶ ^e Woessner, Snowden, and Strom: $E_a = 1.37$ kcal/mol.³⁶

We shall now briefly discuss the data collected in Table II and before doing so we state once more—as a standard of comparison—that the rotational correlation time of water at 25° is 2.5×10^{-12} sec.

Acetonitrile. The molecule performs anisotropic rotational motion, the rotation about the symmetry axis of the molecule being very fast. This is seen from the fact that $\tau_c(\text{H-H})$, $\tau_c(\text{D-C}) < \tau_c(^{14}\text{N})$. Woessner and coworkers³⁶ report that the ratio of the rotational diffusion coefficient about the symmetry axis, D_1 , is ca. ten times as great as D_2 , the rotational diffusion coefficient about the axis perpendicular to the former axis.

Pyridine. Our hydrogen and nitrogen reorientation times are rather alike. Thus anisotropic tumbling is not discernible from our measurements although anisotropic motion has been observed for pyridine in a more detailed investigation selecting particular CD vectors in the ring.³⁷

Methanol. The correlation time of both the vectors H-H (methyl) and CD (methyl) is much shorter than that of the vector OD. The relatively long correlation time $\tau_c(\text{DO}) = 3.7 \times 10^{-12}$ sec (longer than τ_c for H₂O) has been confirmed independently as will be described elsewhere.³⁸ The difference between these correlation times is due to the internal rotation of the methyl group.^{22,38}

The ¹⁷O-quadrupole coupling constant in methanol is not known. Use of $eQq/h \approx 8$ MHz which is the coupling constant in H₂¹⁷O gives $\tau_c(^{17}\text{O}) \approx 8 \times 10^{-12}$ sec which, as compared with the $\tau_c(\text{DO})$ values, is too long. We were unable to see any spin-spin coupling

effects of the ¹⁷O resonance; the line shape was Lorentzian. The activation energy of the ¹⁷O relaxation is smaller than the one for $\tau_c(\text{DO})$ (see Table II). Tentatively, we interpret the low activation energy of ¹⁷O as caused by the anisotropic motion of the atomic array C-O-H due to hydrogen bonding and by the modulation of the quadrupole coupling constant due to the internal rotation of the CH₃ group.

Ethanol. Again the correlation time of the alkyl part of the molecule is faster than the OH group. The slow motion of the latter group has been confirmed independently.³⁸ Thus here internal motion in the molecule is present, too. The quadrupole coupling constant of ¹⁷O is again not known ($eQq/h = 8$ MHz would give $\tau_c(^{17}\text{O}) = 14 \times 10^{-12}$ sec which is too long), and as for methanol the activation energy of the ¹⁷O relaxation is remarkably low as compared with E_a of the OD group as found from the deuteron relaxation (Table II). Obviously here as well the ¹⁷O relaxation reflects some internal motion of the nonhydroxylic part of the molecule. Details are unknown as yet.

tert-Butyl Alcohol. Internal rotation about the O-C axis and rotation of the methyl group about the C-C axis causes the difference between the OD and methyl reorientation rate.

Acetone. The result $\tau_c(\text{OC})$ as derived from the ¹⁷O relaxation with the quadrupole coupling constant of

(36) D. E. Woessner, B. S. Snowden, Jr., and E. T. Strom, *Mol. Phys.*, **14**, 265 (1968).

(37) J. P. Kintzinger and J. M. Lehn, private communication.

(38) M. Gruner and H. G. Hertz, to be published.

formaldehyde is confirmed by the dielectric relaxation time at 25° (interpolated): $\tau_d = 2.9 \times 10^{-12}$ sec³⁹ (note $\tau_c \approx 1/3\tau_r$ for microstep rotational diffusion). Since τ_c for the methyl group is much shorter we find internal rotation, according to Woessner's formula⁴⁰ describing the effect of internal rotation on the correlation time, the time constant for the rotation of the methyl groups about the C-C axis is $\tau_i = 0.8 \times 10^{-12}$ sec.

Tetrahydrofuran (THF). The heteronucleus has not been measured as yet. Most likely the molecule performs isotropic reorientational motion, slight anisotropy being possible.

B. The Aqueous Mixtures. (i) Structural Information from Rule 1, First Part. Figure 2 shows the self-diffusion coefficients of H₂O in its mixtures with acetone and ethanol as a function of the concentration (moles of solute/55.5 mol of water, aquamolality) over a limited composition range at 25°. The self-diffusion coefficients of the solute molecules in D₂O are also shown in Figure 2. All diffusion coefficients are given as relative quantities, relative to the self-diffusion coefficient of pure ordinary water = 2.5×10^{-5} cm²/sec.²⁴

Since the D 's of the solute particles have been measured in D₂O for the comparison with the H₂O diffusion coefficients, the experimental values have to be corrected in order to take account of the greater mobility in H₂O as compared with D₂O. Thus the data given in Figure 2 for the solute molecules in the range $x_2 \rightarrow 0$ are multiplied by a factor 1.23 which corresponds to the mobility (and inverse viscosity) ratio in H₂O and D₂O. These corrected diffusion coefficients in the low C_2 range are given as dashed curves in Figure 2. The correction which is necessary for the H₂O diffusion in the ethanol-water mixture because of the exchange of the OH proton has been neglected. Furthermore, one finds vertical dashed lines at $C_2 = C_2^* = 2.4$ and $2.8 \bar{m}$ for acetone and ethanol, respectively, $C_2^* = 55.5/n_h$. The hydration numbers n_h (23 and 20) have been estimated from molar volume considerations. Then, $0 < C_2 < C_2^*$ is the concentration range in which it is meaningful to divide the total solvent water in hydration water and free water where $D^{(1)+}$ and $D^{(1)\circ}$ (see Figure 1) are the respective diffusion coefficients. For $0 < C_2 < C_2^*$ eq 15 holds, whereas for $C_2 > C_2^*$ we directly observe the water of the hydration spheres: $D^{(1)} = D^{(1)+}$, now the word hydration number is no longer meaningful. We call the whole amount of water for $C_2 > C_2^*$ "hydration water." Note that in general $D^{(1)+}$ and $D^{(1)\circ}$ are as well functions of the concentration for $0 < C_2 < C_2^*$.

Now consider rule 1, first part (section 2B). One sees immediately that $D^{(1)+} = D^{(2)}$ (eq 4, $D^{(2)}$ = self-diffusion coefficient of acetone or ethanol) cannot hold for the whole concentration range $0 < C_2 \leq C_2^*$, since at $C_2 = C_2^*$, $D^{(1)} = D^{(1)+} \neq D^{(2)}$. In Table III $D^{(1)}/D^{(2)}$ at $C_2 = C_2^*$ is given. We conclude that long-lived

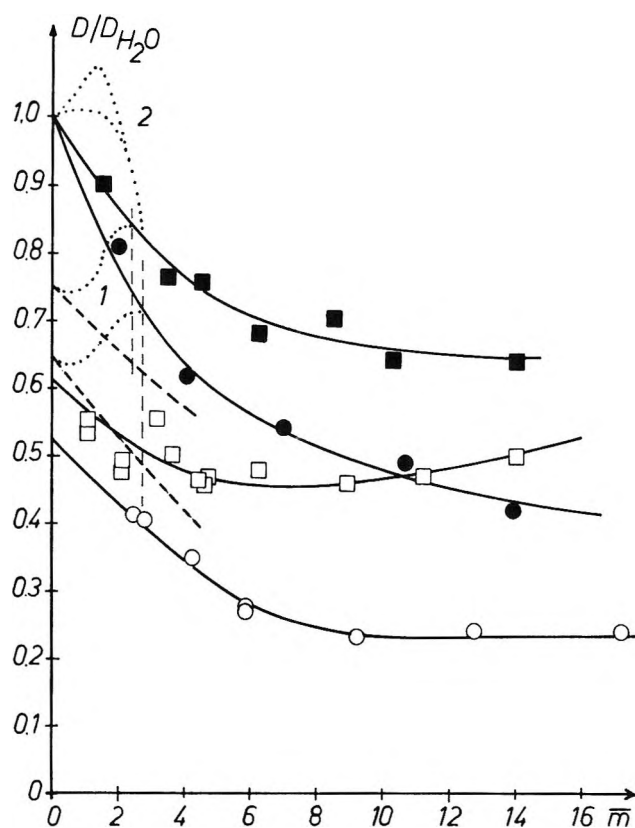


Figure 2. Self-diffusion coefficient of acetone (CH₃)₂CO (□) and ethanol C₂H₅OD (○) in D₂O as a function of the concentration at 25°. ■ and ● give the self-diffusion coefficient of H₂O in the presence of acetone (CD₃)₂CO and ethanol (C₂D₅OH), respectively. All quantities are given relative to $D_{H_2O} = 2.5 \times 10^{-5}$ cm²/sec. The concentration scale is moles of solute/55.5 mol of water. For further details see text.

hydration cages do not exist for acetone and ethanol for the whole concentration range $0 < C_2 \leq C_2^*$. However, $D^{(1)+} = D^{(2)}$ may be valid for a certain concentration range around $C_2 = 0$. Then the two dotted lines 1 give a possible behavior of $D^{(1)+}$ with $D^{(1)+} = D^{(2)}$ at $C_2 \rightarrow 0$ and $D^{(1)+} = D^{(1)}$ at $C_2 = C_2^*$. But eq 15 holds over the total concentration range $0 < C_2 \leq C_2^*$; thus, from eq 15 we have

$$D^{(1)\circ} = \frac{I^{(1)} - \frac{n_h C_2}{55.5} D^{(1)+}}{1 - \frac{n_h C_2}{55.5}} \quad (26)$$

The dotted curves 1 for $D^{(1)+}$ of Figure 2 inserted into eq 26 give the dotted lines 2 for $D^{(1)\circ}$. We see that $D^{(1)\circ} > D^{(1)}(0)$ in a certain concentration range where $D^{(1)}(0)$ is the self-diffusion coefficient of pure water. We do not consider $D^{(1)\circ} > D^{(1)}(0)$ to be a physically realistic situation for these solutions. Without struc-

(39) M. I. Shakparonov and Ya. Yu. Akhadov, *J. Struct. Chem. (USSR)*, **6**, 15 (1965).

(40) D. E. Woessner, *J. Chem. Phys.*, **36**, 1 (1962).

Table III: Hydration Numbers n_h (Estimated from Molar Volume Considerations), Ratio $D^{(1)}/D^{(2)}$ at $C_2^* = 55.5/n_h$, and Hydration Numbers for Possible Long-Lived Hydration Spheres

Solute	n_h	C_2^*, \bar{m}	$\left(\frac{D^{(1)}}{D^{(2)}}\right)_{C_2=C_2^*}$	$n_{h1(0)}$	$n_{h1(0,1)}$	$n_{h1(0,5)}$
Acetone	23	2.4	1.3	16.5		
Ethanol	20	2.8	1.5	19	18	15
Methanol	17	3.3
<i>tert</i> -Butyl alcohol 25 ^o ^a	25	2.2	2.4	19
<i>tert</i> -Butyl alcohol 0 ^o	25	2.2	2.8	23	22	18.5
Acetonitrile	19	2.9	≈1	19.5	18.5	
Pyridine ^b	24	2.3	1.9	12		
THF ^b	24	2.3	1.75	11		
Dioxane ^c	24	2.3	1.75	12		

^a From ref 22 and $D^{(1)}/D^{(1)}(0) = 0.82, 0.65, 0.53, 0.46, 0.42$ for $C_2 = 1, 2, 3, 4, 5$ mol/kg of water, respectively. ^b From ref 22
^c From C. J. Clemett, *J. Chem. Soc. A*, 458 (1969).

ture-breaking effects the self-diffusion coefficient in these solutions cannot increase somewhere while the average $D^{(1)}$ decreases. There is no experimental evidence whatsoever as yet for such a possibility (see also ref 41). At best we can have $D^{(1)0} \leq D^{(1)}(0)$ or $dD^{(1)0}/dC_2 \leq 0$ at small C_2 ; that is, if we introduce $D^{(1)+} = D_2$ for small C_2 , we deduce from eq 26

$$0 \geq \frac{dD^{(1)0}}{dC_2} = \left(\frac{dD^{(1)}}{dC_2}\right)_{C_2 \rightarrow 0} + \frac{n_h}{55.5} \times \left\{ (D^{(1)})_{C_2 \rightarrow 0} - (D^{(2)})_{C_2 \rightarrow 0} - 2 \left(\frac{dD^{(2)}}{dC_2}\right)_{C_2 \rightarrow 0} C_2 \right\} \quad (27)$$

as the condition that $D^{(1)+} = D^{(2)}$ as $C_2 \rightarrow 0$. Still modifying the argument somewhat we can calculate n_{h1} from eq 27 with $(dD^{(1)0}/dC_2)_{C_2 \rightarrow 0} = 0$

$$n_{h1} = \frac{-55.5 \left(\frac{dD^{(1)}}{dC_2}\right)_{C_2 \rightarrow 0}}{(D^{(1)})_{C_2 \rightarrow 0} - (D^{(2)})_{C_2 \rightarrow 0} - 2 \left(\frac{dD^{(2)}}{dC_2}\right)_{C_2 \rightarrow 0} C_2} \quad (28)$$

and formulate rule 1, first part, in the following way. If for a given small C_2 , n_{h1} as calculated from eq 28 is sufficiently large so that a complete hydration sphere surrounding the solute particle can be formed from n_{h1} water molecules, then a long-lived rigid hydration cage may exist up to this small concentration. The corresponding results are given in Table III where the number in parentheses in the headings of columns 5, 6, and 7 indicates the concentration C_2 (\bar{m}) used in eq 28. Figure 3 shows the corresponding data as in Figure 2 for the system *tert*-butyl alcohol-water at 0^o. This system is of particular interest since it has been claimed by Glew and coworkers⁴² that *tert*-butyl alcohol is surrounded by a clathrate cage in liquid aqueous solution (at 0^o). Our results for *tert*-butyl alcohol-water are also presented in Table III. Furthermore results for some other aqueous systems are included in Table III.

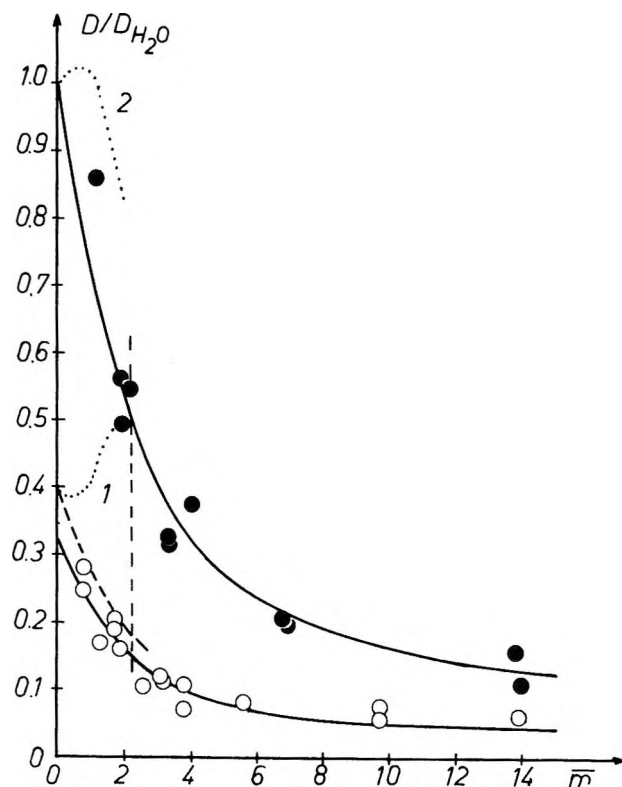


Figure 3. The self-diffusion coefficient of H_2O (●) in the presence of *tert*-butyl alcohol $(CD_3)_3COH$ and the self-diffusion coefficient of $(CH_3)_3COH$ (○) in D_2O as a function of the concentration at 0^o. The data are given relative to $D_{H_2O} = 1.1 \times 10^{-5}$ cm²/sec. The concentration scale is moles of solute/55.5 mol of water. For further details see text.

In all cases the hydration numbers n_h are estimated from molar volume considerations. We see from Table III that, except for acetonitrile, in no case a long-

(41) H. G. Hertz, B. Lindman, and V. Siepe, *Ber. Bunsenges. Phys. Chem.*, **73**, 542 (1969).

(42) D. N. Glew, H. D. Mak, and N. S. Rath, "Hydrogen-Bonded Solvent Systems," A. K. Covington and P. Jones, Ed., Taylor & Francis Ltd., London, 1968, p 195.

Table IV: Rotational Correlation Times in Aqueous Solution in the Limit of Infinite Dilution of the Organic Component (25°)

Compound	n_h	$\frac{\tau_c^{(1)-}}{\tau_c^{(1)}(0)}$	$10^{12}\tau_c^{(1)+}$, sec	$\frac{\{\tau_c^{(2)}(\text{hydrocarbon})\}_{C_2 \rightarrow 0}}{\{\tau_c^{(2)}(\text{hydrocarbon})\}_{\text{pure 2}}}$	$10^{12}\{\tau_c^{(2)}(\text{hydrocarbon})\}_{C_2 \rightarrow 0}$, sec	$\frac{\{\tau_c^{(2)}(\text{polar})\}_{C_2 \rightarrow 0}}{\{\tau_c^{(2)}(\text{polar})\}_{\text{pure 2}}}$	$10^{12}\{\tau_c^{(2)}(\text{polar})\}_{C_2 \rightarrow 0}$, sec
CH ₃ CN	19	1.1	2.7	1.05	0.37 ^a	1.6	1.9
C ₃ H ₅ N	24	1.3	3.2	2.8	5.6 ^b	3.0	6.4
CH ₃ OH	17	1.35	3.4	1.15	{ 1.0 proton 0.5 deuteron	(1.15)	(4.2)
C ₂ H ₅ OH	20	1.5	3.8	0.68	1.5 ^c	(0.68)	(5.5)
(CH ₃) ₃ COH	25	1.65	4.3	0.53	4.3 ^c	(0.53)	(25)
(CH ₃) ₂ CO	23	1.3	3.2	1.3	0.8 ^c	2.2	2.4
THF	24	1.4	3.5	2.4	1.5 ^c

^a Derived from $\tau_c(\text{D-C})$ of Table II. ^b Derived from $\tau_c^{(2)}(\text{hydrocarbon}) = 2 \times 10^{-12}$ sec as rounded off average value of $\tau_c(\text{H-H})$ and $\tau_c(\text{D-C})$ of Table II. ^c Derived from $\tau_c(\text{H-H})$ of Table II.

lived hydration cage can exist at $C_2 \approx C_2^*$ since $D^{(1)}/D^{(2)} \neq 1$, that however, due to the limited experimental accuracy (uncertainty of $\pm 20\%$ for n_h) for ethanol and *tert*-butyl alcohol at 0° a long-lived hydration cage cannot be excluded at $C_2 \leq 1/10 m$. For acetonitrile the "positive" result is due to the fact that $D^{(1)} \approx D^{(2)}$ for $0 < C_2 < C_2^*$ as may be seen from Figure 11, where, however, $D^{(2)}$ is not yet corrected for the higher mobility in H₂O. Clearly, as already mentioned above, rule 1 is never a sufficient condition and thus at this stage really a positive statement concerning a hydration cage for CH₃CN cannot be made. Further information will follow below.

(ii) *Structural Information from Rule 1, Second Part.* We saw in the previous section that from the point of view of rule 1, first part, for certain solutes a long-lived hydration cage cannot be strictly excluded at low concentrations. We ask now whether correlated rotational motion is possible as well at low concentration; that is, we turn to the second part of rule 1.

To examine whether the condition eq 4a is fulfilled we have collected some values for $\tau_c^{(1)+}$, the correlation time of the water molecule in the hydration sphere, in Table IV (25°). The necessary experimental data are partly taken from the literature.²² New results for $\tau_c^{(1)}$ at 25° as a function of the composition may be found in Figures 4, 6, and 7 (see also ref 43). Furthermore, for H₂O-*tert*-butyl alcohol at 25° we measured $B' \equiv \{T_1 d(1/T_1)/dC_2\}_{C_2=0} = 0.30 m^{-1}$ for the water protons. The relation between B' and $\tau_c^{(1)+}/\tau_c^{(1)}(0)$ is eq A5 in the Appendix. $\tau_c^{(1)}(0)$ is the rotational correlation time in pure water. The determination of $\tau_c^{(1)+}/\tau_c^{(1)}(0)$ is based on the slow exchange formula, eq 18. The ratio $\tau_c^{(1)+}/\tau_c^{(1)}(0)$ is so close to unity that the error cannot be great if the exchange is not sufficiently slow (see Appendix).

Furthermore, one finds the relative reorientation times of the solute molecule in the limit $C_2 \rightarrow 0$ in Table IV. The data are understood as relative to the corresponding reorientation times in the pure organic liquids. They are given for the hydrocarbon and the polar part of the organic molecule. The respective

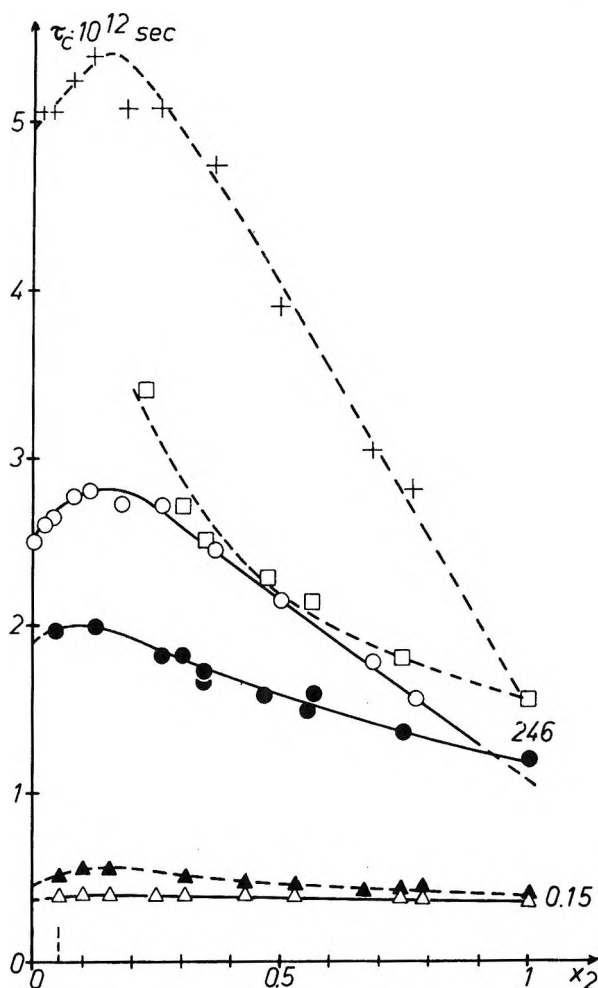


Figure 4. Correlation time $\tau_c^{(2)}(\text{CD}_3)$ (Δ), $\tau_c^{(2)}(^{14}\text{N})$ (\bullet), and $\tau_c^{(1)}(\text{D}_2\text{O})$ (\circ) as a function of the mole fraction $x_2 = x(\text{CH}_3\text{CN})$ in the mixture water-acetonitrile at 25°. The dashed curves give the corresponding data $\tau_c^{(2)}(\text{CD}_3)$ (\blacktriangle), $\tau_c^{(2)}(^{14}\text{N})$ (\square), $\tau_c^{(1)}(\text{D}_2\text{O})$ ($+$) at 5°. The dashed vertical line corresponds to $C_2^* = 55.5/n_h$; for further details see text.

value at $x_2 = 1$ ($x_2 =$ mole fraction of the organic component) is the time given in Table II; the limiting ab-

(43) H. G. Hertz and M. D. Zeidler, *Ber. Bunsenges. Phys. Chem.*, **68**, 821 (1964).

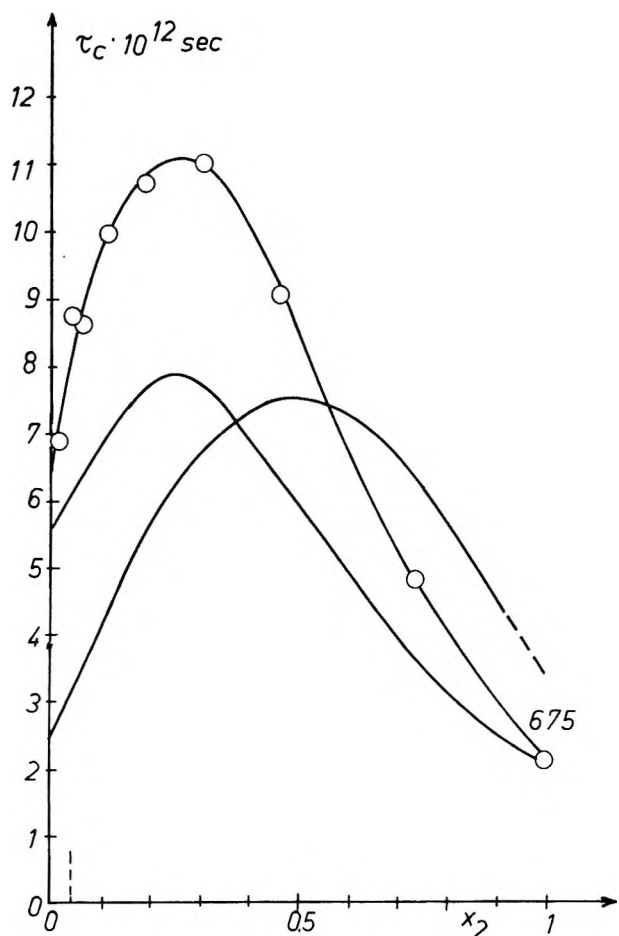


Figure 5. Correlation time $\tau_c^{(2)}(^{14}\text{N})$ (O), $\tau_c^{(2)}(\text{CD})$, and $\tau_c^{(1)}(\text{H}_2\text{O})$ (curve with maximum at $x_2 = 0.5$) as a function of the composition for the mixture water-pyridine at 25° ; $x_2 = x(\text{C}_5\text{H}_5\text{N})$. Vertical dashed line corresponds to $C_2^* = 55.5/n_h$.

solute correlation times for $x_2 \rightarrow 0$ are also introduced in Table IV. The necessary data are partly taken from the literature.²² The new experimental results together with those of ref 22 are presented in Figures 4, 5, 6, 7, and 8. The results of ref 22 are drawn only as solid lines in these figures—if not indicated otherwise—whereas the new experimental results are marked by symbols showing the individual experimental points (and for 25° are connected by other solid curves). The numbers on the right-hand ordinates give the corresponding relaxation rates (in sec^{-1}) for the pure organic liquids; they are identical with the rates quoted in Table I. In all cases the quadrupole coupling constant is assumed to be concentration (and temperature) independent. Thus, since there is always strict proportionality between $(1/T_1)_{\text{intra}}$ and τ_c (see eq 19 and 21), from Figures 4–8 the concentration dependence of the relaxation rates may as well be read off.

Actually, the concentration dependence of the reorientational motion of the alcoholic hydroxyl group is not known for two reasons. (1) The hydroxyl hydrogen exchanges with that of water. (2) The hydroxyl ^{17}O relaxation cannot reflect the motion of the

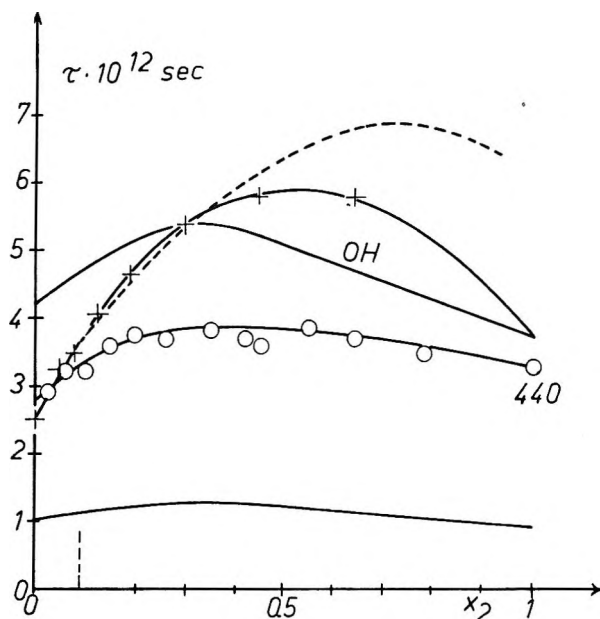


Figure 6. Correlation time $\tau_c^{(2)}(\text{CH}_3)$ (lowest curve), $\tau_c^{(2)}(^{17}\text{O})$ (O), and $\tau_c(\text{H}_2\text{O}-\text{HOR})$ (+) as a function of the composition for the mixture water-methanol at 25° . The absolute value of $\tau_c^{(2)}(^{17}\text{O})$ has been arbitrarily chosen; $x_2 = x(\text{CH}_3\text{OH})$. Vertical dashed line corresponds to $C_2^* = 55.5/n_h$; for further details see text.

OH vector since the activation energy in the pure alcohol is too small. Thus, the only thing we can do for the alcohols is to assume that the OH reorientation time is longer than the alkyl reorientation time by a factor which is independent of the concentration. In Figures 6 and 7 the solid lines marked with OH are obtained in this way. As a consequence, the entries in columns 7 and 8 of Table IV for the alcohols are put in parentheses. The end points at $x_2 = 1$ for the ^{17}O reorientation in Figures 6 and 7 are arbitrarily chosen. The quadrupole coupling constant is not known, and the form of the motion is not clear. Since the activation energy for ^{17}O is smaller than that for ^2H in the OD group, the end points cannot be the same as those of the ^2H reorientation. Likewise the precise vertical position of the two curves for $\text{CD}_3\text{CH}_2\text{OH}$ and $\text{CH}_3\text{CD}_2\text{OH}$ in Figure 7 is not known; contrary to the curves shown one would expect that CD_3 moves faster than CD_2 . The order given in Figure 7 is caused by the constant assumed standard value of the quadrupole coupling constant.

Now we examine the validity of rule 1, second part, and consider first the molecules which have no ring structure. We find the following results. For *tert*-butyl alcohol $\tau_c^{(1)+} = \tau_c^{(2)}(\text{CH}_3)$ cannot be excluded; however, in spite of our poor knowledge of $\tau_c^{(2)}(\text{OH})$ we may safely state $\tau_c^{(1)+} \neq \tau_c^{(2)}(\text{OH})$. For all other molecules of this class the correlation times of the alkyl group and of the polar group which are different at $x_2 = 1$ never converge to the same value as $x_2 \rightarrow 0$; in some cases they even diverge. Also, the hydrocarbon

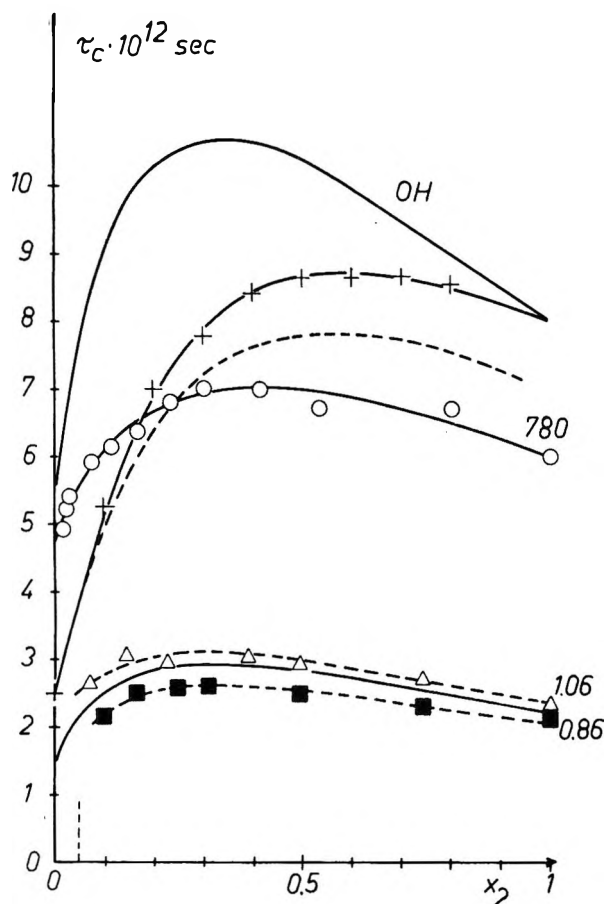


Figure 7. Correlation time $\tau_c^{(2)}(-\text{CH}_2-)$ (■), $\tau_c^{(2)}(\text{C}_2\text{H}_5)$ (lowest solid curve), $\tau_c^{(2)}(\text{CH}_3-)$ (■), $\tau_c^{(2)}(^{17}\text{O})$ (Δ), and $\tau_c^{(1)}(\text{H}_2\text{O}-\text{HOR})$ (+) as a function of the composition for the mixture water-ethanol at 25°. Absolute values of $\tau_c^{(2)}(-\text{CH}_2-)$ and $\tau_c^{(2)}(\text{CH}_3-)$ are only approximately correct; absolute value of $\tau_c(^{17}\text{O})$ is arbitrarily chosen; $x_2 = x(\text{C}_2\text{H}_5\text{OH})$. Vertical dashed line corresponds to $C_2^* = 55.5/n_h$; for further details see text.

correlation times are always shorter than the hydration water correlation time $\tau_c^{(1)+}$ (and even shorter than $\tau_c^{(1)}(0)$). Thus, the nonfulfillment of rule 1, second part (eq 4a), tells us that an overall rigid long-lived complex solute molecule + hydration sphere does not exist for any of the systems of this class.

For THF no information of the ^{17}O relaxation is available; the hydrocarbon vectors move faster than the hydration water (and even faster than pure water). For pyridine there is a slight divergence of the hydrocarbon and ^{14}N relaxation (Figure 5); however $\tau_c^{(1)+} \neq \tau_c^{(2)}$. Consequently, according to rule 1, second part, for the ring molecules as well a long-lived overall rigid complex solute + hydration cage must be excluded.

(iii) *Application of Rule No. 2.* Since we saw in the previous section that the solute-hydration aggregates do not possess overall rigidity, the situation described under rule no. 2 may be appropriate for the two alcohols ethanol and *tert*-butyl alcohol. We arrived at this result as a consequence of our limited experimental

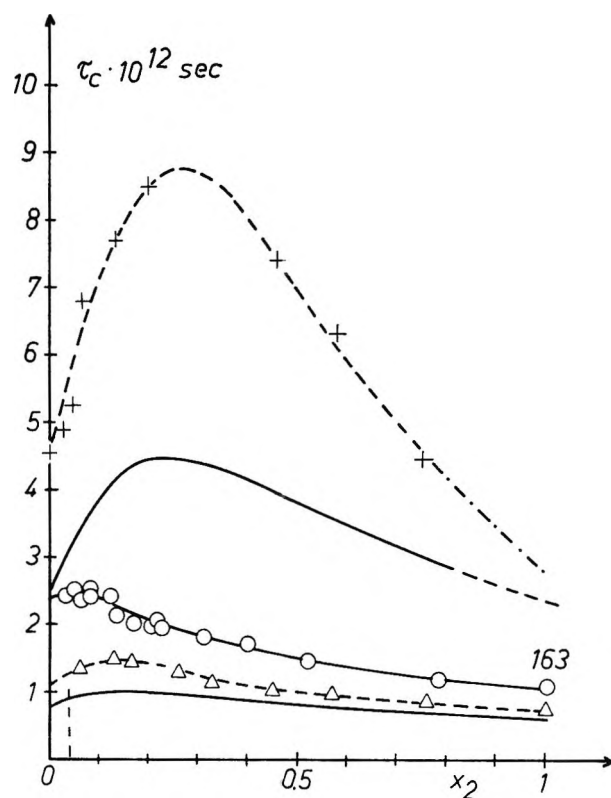


Figure 8. Correlation time $\tau_c^{(2)}(\text{CH}_3)$ (lowest solid line), $\tau_c^{(2)}(^{17}\text{O})$ (O), and $\tau_c^{(1)}(\text{H}_2\text{O})$ (upper solid line) as a function of the composition for the mixture water-acetone at 25°. Further $\tau_c^{(2)}(\text{CH}_3)$ (Δ) and $\tau_c^{(1)}(\text{H}_2\text{O})$ (+) at 5°; $x_2 = x((\text{CH}_3)_2\text{CO})$. Vertical dashed line corresponds to $C_2^* = 55.5/n_h$.

accuracy, that is, the number n_{h1} (eq 28) might be $\approx 20\%$ larger than given in Table III. We recall, however, that the fulfillment of eq 4 is not a sufficient condition for the existence of long-lived aggregates, and we shall indeed find below that as judged from other rules the existence of long-lived hydration spheres is extremely unlikely for all solutes studied here.

(iv) *Structural Information from Rule No. 3.* At the beginning we must make one assumption. For the one or two water molecules per solute molecule which interact with the polar group of the solute molecule $\tau_c^{(1)+} \geq \tau_c^{(1)}(0)$ certainly holds. This means that we exclude the very unrealistic possibility that the re-orientation time of the H_2O molecule attached to the polar group of the solute molecule is shorter than that of ordinary water. Since according to rule no. 3 (second part) for a long-lived pair of two molecules the correlation time of the vector pointing in the direction of the bond must be longer than (or equal to) that of any other vector of the molecular pair, we conclude from Table IV that for pyridine, ethanol, and methanol long-lived solvent-solute pair association *via* the polar group may occur with a probability close to 1. However, for acetonitrile, acetone, and tetrahydrofuran such pair association occurs with lower probability.

For THF no information concerning the $\backslash\text{O}/$ part of the molecule is available. We assumed that $\tau_c^{(2)}$ for $\backslash\text{O}/$ is essentially equal to the $\tau_c^{(2)}$ of the hydrocarbon vectors, since no internal rotation does occur; however, the $\backslash\text{O}/$ correlation time may be slightly longer than 1.5×10^{-12} sec. For $(\text{CH}_3)_3\text{COH}$ polar group– H_2O pair association is possible. It should be mentioned that according to Table IV for methanol and ethanol the ratio of the alkyl (and polar group) reorientation time in the infinitely diluted aqueous solution and that in the pure alcohol is ~ 1 and ~ 0.7 , respectively, whereas the corresponding ratios for the highly diluted alcohols in CCl_4 and pure alcohol are 0.8 and 0.4 for methanol and ethanol, respectively.³⁸ The former change corresponds to a replacement of the alcoholic surroundings by the water surroundings, the hydrogen bonds being kept connected, whereas the latter change corresponds to the switching off of the hydrogen bonds and replacing the alcoholic surroundings by the relatively large CCl_4 molecules.

When we write

$$\frac{1}{\tau_c^{(2)}} = (1 - p_{2a}) \frac{1}{\tau_{co}^{(2)}} + p_{2a} \frac{1}{\tau_{ca}^{(2)}} \quad (29)$$

$$1 - p_{2a} = p_{20}$$

(see eq 17a), we can estimate from eq 29 p_{20} , the fraction of acetone, acetonitrile, or tetrahydrofuran molecules which at $C_2 \rightarrow 0$ are bound to the water molecules. $\tau_{ca}^{(2)}$ is the correlation time in the bound state, $\tau_{ca}^{(2)} \gtrsim \tau_c^{(1)} + (\tau_c^{(1)} + \text{see column 4 of Table IV})$, $\tau_{co}^{(2)}$ is the correlation time in the unbound state, $\tau_{co}^{(2)} \lesssim \tau_c^{(2)}$ (pure) ($\tau_c^{(2)}$ (pure) see column 2 or 3 of Table II). With the results of Table IV, column 8, we find $p_{2a} \approx 0.65$ and $p_{2a} \approx 0.8$ for acetonitrile and acetone, respectively; for THF about the same figure should be expected.⁴⁴

Finally we note that for all solutes investigated here the self-diffusion coefficient is smaller than that of water. Thus the behavior of the translational diffusion is different from that of the rotational motion. Whereas the rotational diffusion of the solute particle in the water cage at $C_2 \rightarrow 0$ may be faster than that of water, the translational motion is always slower as is to be expected from the larger masses of the solute molecule (see *e.g.*, Figure 11). However, it may occur that the self-diffusion of the solute molecule in the water cage is faster than in the pure liquid formed by the solute. This is the case for ethanol and *tert*-butyl alcohol.²²

It is easily seen from Table III that regarding the distance between the solute and the water molecule—not the orientation—long-lived pairs H_2O –solute may be present at $C_2 \rightarrow 0$ in all cases studied here. The first part of rule 3 is always fulfilled.

(v) *Microheterogeneity and Activation Energies.* We now apply the second part of rule 3 (eq 5) to the composition range $x_1 \approx x_2$. As an example consider the

mixture H_2O –acetone at $x_1 = x_2$, *i.e.*, $n_1^\circ = n_2^\circ$ (n_i° , $i = 1, 2$, total number of water and acetone molecules, respectively, in the mixture). Assume for the moment that there are three different molecular species in the liquid: unbound water molecules with correlation time $\tau_{co}^{(1)}$, unbound acetone molecules with $\tau_{co}^{(2)}$ being the correlation time of the vector considered, and bound H_2O –acetone pairs with $\tau_{ca} \equiv \tau_c^{(2,1)}$ for the reorientation of the intermolecular bond vector. The numbers of the three species present are n_1 , n_2 , and n_a , respectively, $p_1^\circ = n_1/n_1^\circ$, $p_2^\circ = n_2/n_2^\circ$, $p_{1a} = n_a/n_1^\circ$, $p_{2a} = n_a/n_2^\circ$. The mean correlation time of water is $\tau_c^{(1)}$

$$\frac{1}{\tau_c^{(1)}} = \frac{p_1^\circ}{\tau_{co}^{(1)}} + \frac{p_{1a}}{\tau_{ca}^{(1)}} = \frac{p_1^\circ}{\tau_{co}^{(1)}} + \frac{p_{1a}}{\tau_{co}^{(1)}} \xi_1 \quad (30a)$$

the mean correlation time of acetone is

$$\frac{1}{\tau_c^{(2)}} = \frac{p_2^\circ}{\tau_{co}^{(2)}} + \frac{p_{2a}}{\tau_{ca}^{(2)}} = \frac{p_2^\circ}{\tau_{co}^{(2)}} + \frac{p_{2a}}{\tau_{co}^{(2)}} \xi_2 \quad (30b)$$

Here $\tau_{ca}^{(1)} = \tau_{co}^{(1)}/\xi_1$; $\tau_{ca}^{(2)} = \tau_{co}^{(2)}/\xi_2$; $k \leq \xi_1 \leq 1$; $k \leq \xi_2 \leq 1$. $\xi_{1,2}$ depends on the angle which the vector considered forms with the intermolecular bond direction and on the rapidity of rotational motion of the vector about the intermolecular bond direction.^{11–13} If there is no such rotation: $\xi_{1,2} = k$; $k < 1$ corresponds to the fact that the pair of two molecules is a “larger” particle^{15,38} than one single molecule. Now for unbound acetone and water we have $\tau_{co}^{(1)} \approx \tau_{co}^{(2)}$, and since the CO vector (the motion of which we observe by the ^{17}O relaxation) has the direction of the $>\text{CO} \dots \text{H}-\text{O}-\text{H}$ bond, $\xi_2 = k$ and we expect from eq 30a and b and rule no. 3 with $p_{1a} = p_{2a}$ ($x_1 = x_2$): $\tau_c^{(1)} \leq \tau_c^{(2)}$ (CO). However, we observe (Figure 8) the contrary, namely $\tau_c^{(1)} > \tau_c^{(2)}$ (CO) at $x_1 = 1/2$. The methyl group of acetone shows internal rotation; thus for these groups $\xi_2 > k$ and $\tau_c^{(2)}$ (CO) $>$ $\tau_c^{(2)}$ (CH_3).

To account for the observed fact $\tau_c^{(1)} > \tau_c^{(2)}$ (CO) one can assume that $p_{1a} > p_{2a}$ at $x_1 = 1/2$. This means that more than one H_2O molecule is attached to the CO of acetone. Such an accumulation of water molecules around a selected acetone molecule would already cause a drastic deviation from the random distribution of H_2O and $(\text{CH}_3)_2\text{CO}$ molecules, and this is a first step toward microheterogeneity.

Let us now consider the temperature dependence of the correlation times. The activation energy, say of $\tau_c^{(2)}$, is partly given by the change of p_{2a} with temperature and partly by the change with temperature of the number of nonhydrogen-bonded acetone–water pairs

(44) It should be mentioned here that Davies and Williams⁴⁵ reported a dielectric relaxation time of acetone and THF in solid H_2O –clathrates of $\tau_d = 1.7 \times 10^{-12}$ sec at 213 and 243°K for acetone and THF, respectively. If one compares this with the entries of Table IV he finds that, due to the uncertainty in the factor connecting τ_d and τ_c , the reorientational motion in the solid is not slower than in the liquid.

(45) M. Davies and K. Williams, *Trans. Faraday Soc.*, **64**, 529 (1968).

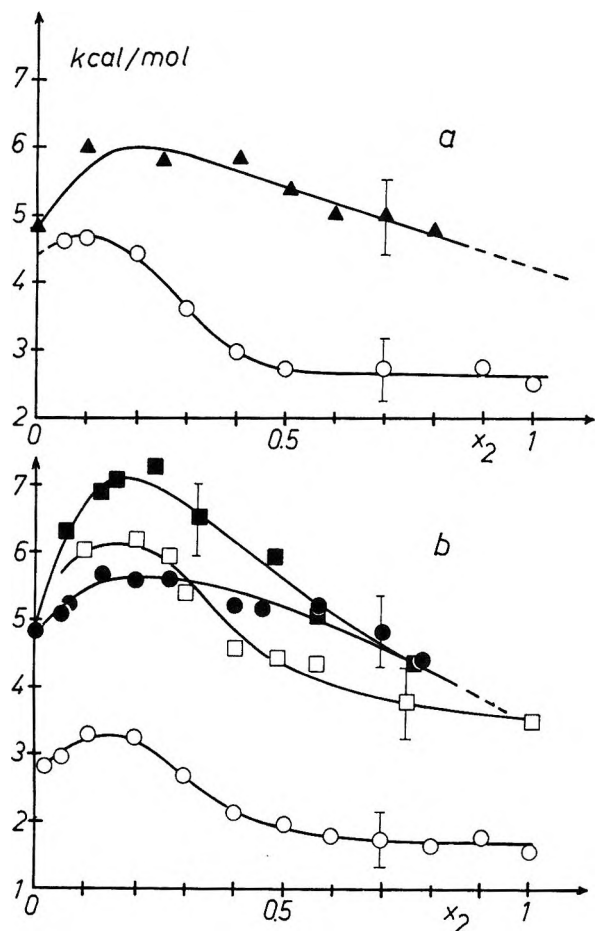


Figure 9. (a) Activation energies for $\tau_c^{(2)}(\text{D}_2\text{O})$ (\blacktriangle) and $\tau_c^{(2)}(\text{CD}_2)$ (\circ) as a function of the composition for the mixture water-tetrahydrofuran. (b) Activation energies for $\tau_c^{(1)}(\text{D}_2\text{O})$ (\bullet) and $\tau_c^{(2)}(\text{DC}_3)$ (\circ) as a function of the composition in the mixture water-acetone. The activation energies for $D^{(2)}$ (\square) and $D^{(1)}$ (\blacksquare) are as well shown; $x_2 = x(\text{organic molecule})$.

and acetone-acetone pairs. The latter contributions correspond to pure acetone and are small. For H_2O the situation is analogous. Thus from eq 30a and b with $p_{1a} = p_{2a}$ one expects about equal activation energies: $E_a(\text{H}_2\text{O}) \lesssim E_a(\text{CO})$. If κ water molecules are attached to the CO group the activation energy for the water reorientation is essentially ΔE , ΔE being the energy for the separation of one water molecule from the acetone. For acetone the activation energy should be $\kappa\Delta E$, because κ water molecules have to be disconnected. On the other hand, $p_{1a} = \kappa p_{2a}$, thus still we expect $E_a(\text{H}_2\text{O}) \lesssim E_a(\text{CO})$. These predictions have to be compared with experimental results which are presented in Figure 9b. We see that the activation energy of water is much larger than that of acetone. This is in clear contradiction with the behavior expected so far. The activation energy of acetone only changes slightly in the range $1 > x_2 > 0.4$. Admittedly, the activation energy shown in Figure 9b is that of the CH_3 group, $E_a(\text{CO})$ has not yet been measured, but the difference between $E_a(\text{H}_2\text{O})$ and $E_a(\text{CH}_3)$ is so great that, con-

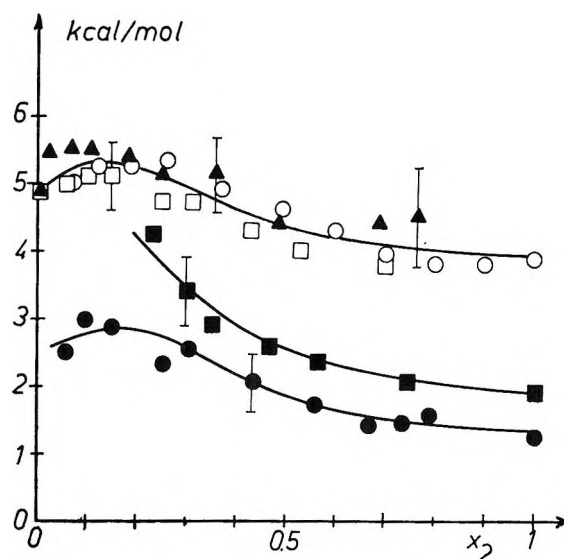


Figure 10. Activation energies for $\tau_c^{(2)}(\text{CD}_3)$ (\bullet), $\tau_c^{(2)}(^{14}\text{N})$ (\blacksquare), $\tau_c^{(1)}(\text{D}_2\text{O})$ (\blacktriangle), $D^{(2)}$ (\circ), and $D^{(1)}$ (\square) as a function of the composition in the mixture water-acetonitrile; $x_2 = x(\text{CH}_3\text{CN})$.

sidering also the similar situation for acetonitrile (Figure 10), we may safely state the result $E_a(\text{H}_2\text{O}) > E_a(\text{CO})$. From this inequality we conclude that the aggregates of κ water molecules are not closely connected with the CO group but that they are more firmly bound among themselves and that the activation energy $E_a(\text{H}_2\text{O})$ corresponds to the disconnection of one water molecule from the other members of the water patch in the mixture. Thus we are again lead to the conclusion that there is a certain degree of microheterogeneity in the mixture.

It is now appropriate to write instead of eq 30a

$$\frac{1}{\tau_c^{(1)}} = \frac{p_1^\circ}{\tau_{co}^{(1)}} + \frac{p_{1c}}{\tau_{cc}^{(1)}} + \frac{p_{1a}}{\tau_{ca}^{(1)}} \quad (30c)$$

where again $p_{1a} = p_{2a}$, p_{1c} is the probability for a water molecule to be a member of a water patch or cluster, and $\tau_{cc}^{(1)}$ is the correlation time in this cluster. The activation energy $E_a(\text{H}_2\text{O})$ then concerns the temperature dependence of the cluster size ($\tau_{cc}^{(1)}$) and that of p_{1c} . Equation 30c passes steadily into eq 23 where now all terms $\sum_{i=1}^{\infty} p_{1i}/\tau_{ci}^{(1)}$ are contracted in the term $p_{1c}/\tau_{cc}^{(1)}$. It might be questionable whether the fast exchange limit eq 17 is still applicable here since from sound absorption measurements it was concluded that the decomposition time of the clusters is relatively long.⁴⁶ When we assume that p_1° , $p_{1a} \approx 0$ at $x_2 = 1/2$, then with $\tau_c^{(1)} = 3.8 \times 10^{-12}$ sec and $\tau_{co}^{(1)} \approx 0.5 \times 10^{-12}$ sec by aid of eq 6 we estimate κ , the number of water molecules in the patch, to be ~ 6 which seems to be reasonable. As C_2 decreases, the water patches

(46) J. M. Davenport, J. F. Dill, V. A. Solov'ev, and K. Fritsch, *Sov. Phys.-Acoust.*, **14**, 236 (1968).

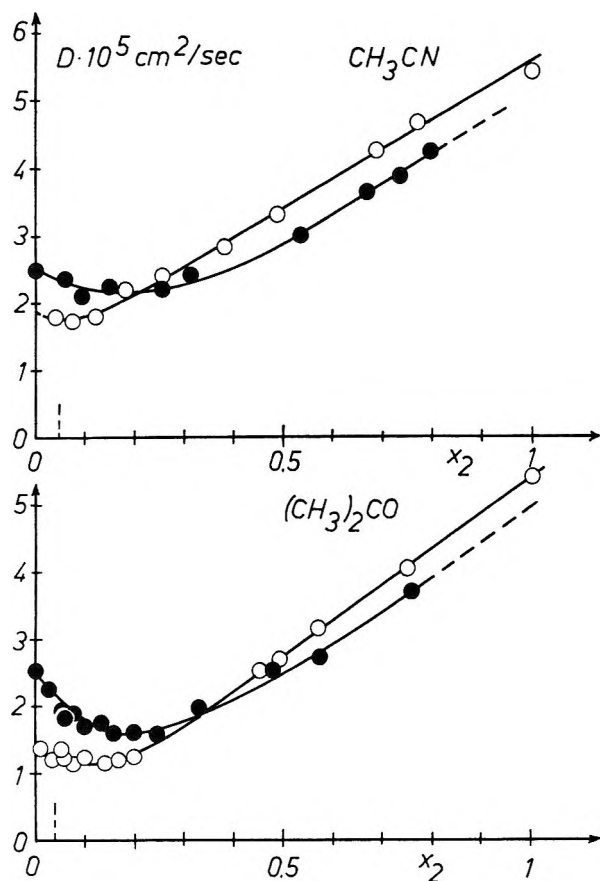


Figure 11. Self-diffusion coefficient of water (●), acetonitrile, and acetone, both (○), as a function of the composition in the mixtures water-acetonitrile and water-acetone at 25°. The vertical dashed lines correspond to $C_2^* = 55.5/n_b$; $x_2 = x(\text{organic component})$.

coalesce more and more; finally they fully surround the (solute) acetone particle and form the hydration of the second kind.

In Figure 9a one finds the activation energy for the reorientational motion of H_2O and THF; the general behavior is similar to that of acetone. In Figure 10 the activation energies for the reorientation for all three vectors, namely that in D_2O , in CN, and in CD_3 , are shown for the mixture $\text{D}_2\text{O}-\text{CD}_3\text{CN}$. Again the concentration dependence corresponds to the general scheme as outlined for acetone + water. The concentration dependence of the self-diffusion coefficients of both components for the systems H_2O -acetone and H_2O -acetonitrile is shown in Figure 11,⁴⁷ and the activation energies of these quantities are included in Figures 9b and 10. It is interesting to note that the translational motions of both the component molecules resemble one another much more than the rotational motions do.

In the mixture water-pyridine at $x_1 = 1/2$ the correlation times of ^{14}N and water are almost equal (Figure 5). The activation energies of the water and pyridine deuterons are shown in Figure 12. Here the inter-

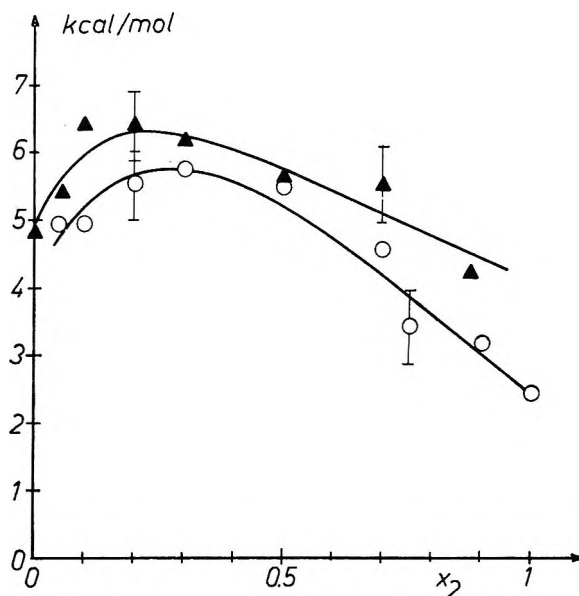
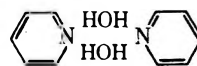
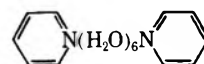


Figure 12. Activation energies of $\tau_c^{(2)}(\text{CD})$ (○) and $\tau_c^{(1)}(\text{D}_2\text{O})$ (▲) as a function of the composition for the mixture water-pyridine; $x_2 = x(\text{C}_5\text{H}_5\text{N})$.

action between the organic molecule and water is much stronger than in the systems described previously and so from the concentration dependences of Figures 5 and 12 we see that the motions of both the component molecules are rather tightly correlated with one another at $x_2 \approx 1/2$. There appears to be a large fraction of water molecules coupled directly to $\text{C}_5\text{H}_5\text{N}$ (approximate equality of τ_c and E_a), and the clustering term $p_{1c}/\tau_{cc}^{(1)}$ (see eq 30c) seems to be small. Thus microheterogeneity is not so evident here. However, a certain degree of geometrical order beyond simple pair formation cannot be excluded. So one must account for the relatively strong increase with decreasing x_2 of the correlation time of pyridine and the slow water reorientation in the composition range $1/2 < x_2 < 1$. This effect could come about by the formation of aggregates



Then, between $1/4 < x_2 < 1/2$ more water is added to this complex, e.g.



Here the maximum in the correlation time of pyridine occurs. With higher dilution the dissociation of the pyridine pair begins which is observed as a decrease in the pyridine correlation time.

(47) The agreement with the results of McCall and Douglas for acetone-water is satisfactory.⁴⁸ Our acetone data are improved as compared with those given in ref 22.

(48) D. W. McCall and D. C. Douglas, *J. Phys. Chem.*, **71**, 987 (1967).

Our information is less complete for the alcoholic systems methanol-water and ethanol-water. As already mentioned one of the reasons for this lack of information is the fact that the alcoholic hydroxyl hydrogen exchanges with the water hydrogen. Thus, for the water reorientation we have information only as a part of the measured average behavior (τ_c) of the alcoholic and water OD or OH and *vice versa*. We have already described in what way the curves for $\tau_c^{(2)}(\text{OH})$, indicated with OH in Figures 6 and 7, are obtained. The measured average τ_c is

$$\tau_c = \frac{2x_1}{2x_1 + x_2} \tau_c^{(1)}(\text{H}_2\text{O}) + \frac{x_2}{2x_1 + x_2} \tau_c^{(2)}(\text{OH})$$

and thus the water correlation time $\tau_c^{(1)}(\text{H}_2\text{O})$ may be determined. The result is seen as the dashed curves in Figures 6 and 7. In particular, in Figure 7 the curve "OH" may be lower; then the dashed H₂O curve would move to higher values.

The activation energies for the systems methanol-water and ethanol-water are shown in Figures 13 and 14, respectively. It is reasonable to assume that over the entire composition range the OH activation energy of methanol and ethanol is larger by roughly a constant factor than that of the methyl and ethyl group. This means that the activation energy of the alcoholic OH and that of the water are very much alike. From Figures 6 and 7 and the accompanying discussion we saw that the correlation times of ROH and H₂O should also not be much different. Thus the motion of the polar ends of both component molecules is similar, and there is no obvious evidence for microheterogeneity. However, with decreasing x_2 at high x_2 , $1/2 < x_2 < 1$, the correlation time of the hydrocarbon (and polar) part and the activation energy for the reorientation of the hydrocarbon (and polar) part of both molecules increase. In this range the H bond between the alcohol molecules is replaced by the H bond alcohol-water. The water molecule is smaller than the alcohol molecule, and still the two properties indicated increase, which must mean that geometrical arrangements exist which are similar to those proposed for the mixture pyridine-water. With decreasing x_2 , $x_2 < 1/2$, more and more water neighbors are added, finally surrounding the hydrocarbon part also, and for very small x_2 , $x_2 < 0.2$, the water molecules added are no more coupled to other solute molecules and thus the correlation time decreases.

The low activation energy of the ¹⁷O relaxation for the alcohols, in particular for ethanol, which extends over an appreciable concentration range, we are unable to explain as yet. At the right-hand ordinate of Figure 12 we have marked the activation energies for the deuteron relaxation of CD₃CH₂OH and CH₃CD₂OH, from which one sees that both these activation energies are larger than that for ¹⁷O and that they show the order to be expected, namely $E_a(\text{CD}_3) < E_a(\text{CD}_2) < E_a(\text{OH})$.

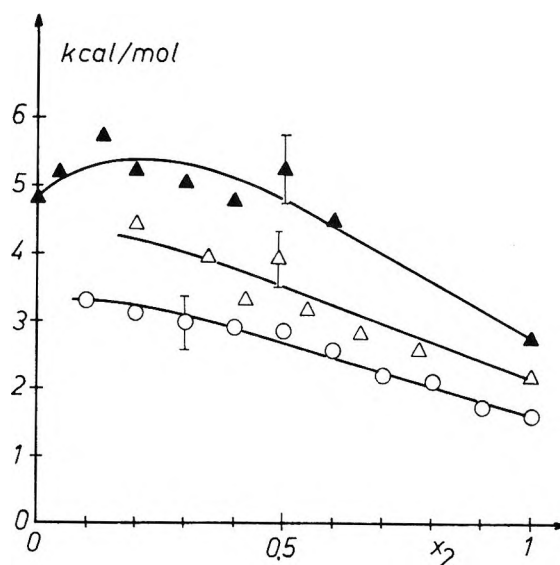


Figure 13. Activation energies for $\tau_c^{(2)}(\text{CD}_3)$ (○), $\tau_c^{(2)}(^{17}\text{O})$ (△), and $\tau_c(\text{D}_2\text{O-DOR})$ (▲) as a function of the composition in the mixture water-methanol; $x_2 = x(\text{CH}_3\text{OH})$.

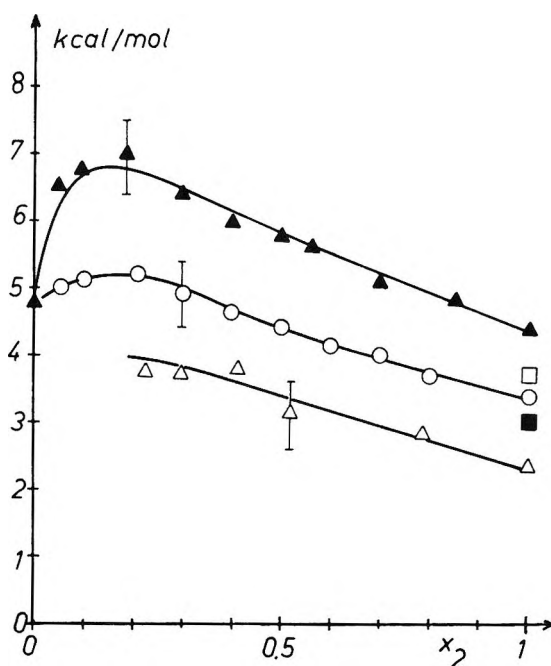


Figure 14. Activation energies for $\tau_c^{(2)}(^{17}\text{O})$ (△), $\tau_c^{(2)}(\text{C}_2\text{D}_5)$ (○), and $\tau_c(\text{D}_2\text{O-DOR})$ (▲) as a function of the composition for the mixture water-ethanol. The activation energies for $\tau_c^{(2)}(\text{CD}_3^-)$ (■), and $\tau_c^{(2)}(-\text{CD}_2^-)$ (□) are only shown for the pure alcohol ($x_2 = 1$).

(vi) *Structural Information from Rule No. 4.* As already mentioned above the reorientational correlation time of a long-lived rigid aggregate of six water molecules + a central particle + a number of about four short-lived associated water molecules is $\sim 3 \times 10^{-11}$ sec. According to Tables III and IV the hydration cages of our solute particles must be much larger aggregates, *i.e.*, we expect $\tau_c^{(1)+} > 3 \times 10^{-11}$ sec. Since,

Table V: Composition of Mixture at Maximum Correlation Time and Minimum Self-Diffusion Coefficient (25°)

Compound	$\left[\frac{D^{(2)}}{D^{(1)}}\right]_{C_2 \rightarrow 0}$	$\left[\frac{n_1}{n_2}\right]_{\tau_c^{(1)} \max}$	$\left[\frac{n_1}{n_2}\right]_{D^{(1)} \min}$	$\left[\frac{n_1}{n_2}\right]_{\tau_c^{(2)}(\text{CH}_3) \max}$
CH ₃ CN	0.9	5.6	4-5	7.5
C ₆ H ₅ N	0.54 ^{a,b}	1.0	1-2	3.0 ^c
CH ₃ OH	~0.6	(2.2-0.5?)	...	2.2
C ₂ H ₅ OH	0.64	(2.3-0.6?)	...	2.3
(CH ₃) ₂ COH 25°	0.4	d
(CH ₃) ₃ COH 0°	0.4	d
(CH ₃) ₂ CO	0.75	3.2	4	6
THF	0.5 ^a	2.7 ^a	5-7	10 ^a
Dioxane			4-5	

^a Reference 22. ^b B. Brun and J. Salvinien, *J. Chim. Phys.*, **64**, 1319 (1967). ^c Here the hydrocarbon part of the ring is concerned.
^d No maximum.

however, for all solutes studied here we find $\tau_c^{(1)} \ll 3 \times 10^{-11}$ sec (see Table IV), we conclude that in no case the cage of water molecules surrounding the solute particle can be a long-lived rigid aggregate.

The self-diffusion coefficient of the ion Mg^{2+} at low concentration is 0.7×10^{-5} cm²/sec, that is $\{D(\text{Mg}^{2+})/D_{\text{H}_2\text{O}}\}_{C_2 \rightarrow 0} = 0.28$ at 25°. This figure is taken from conductivity results.⁴⁹ Such a value of a self-diffusion coefficient corresponds to a long-lived aggregate of more than 6 but less than 20 water molecules. An aggregate of 20-28 water molecules is expected to have $(D/D_{\text{H}_2\text{O}})_{C_2 \rightarrow 0} < 0.28$. As shown in Table V in all cases for the solute particle we have $\{D^{(2)}/D^{(1)}\}_{C_2 \rightarrow 0} > 0.28$. Further, the results given in Table III may be reformulated so as to demonstrate that with the n_h values of column 2 $\{D^{(1+)}/D^{(2)}\} \geq 1$; consequently, $\{D^{(1+)}/D^{(1)}\}_{C_2 \rightarrow 0} = \{D^{(1+)}/D_{\text{H}_2\text{O}}\}_{C_2 \rightarrow 0} > 0.28$. So we again see that long-lived hydration cages must be excluded for the solutes studied in this work. Also for acetonitrile, ethanol, and *tert*-butyl alcohol where according to rule no. 1, first part, or rule no. 2, some evidence for long-lived aggregates appeared, these must now be ruled out.

Thus in the hydration sphere of the solute particles, geometrically well-ordered closed cage configurations occur at best with probabilities < 1 , and we have

$$\frac{1}{\tau_c^{(1)+}} = \sum_{i=1}^{\nu} \frac{p_i^+}{\tau_{c_i}^{(1)+}} \quad (31)$$

$$D^{(1)+} = \sum_{i=1}^{\nu} p_i^+ D_i^{(1)+}; \quad \sum_{i=1}^{\nu} p_i^+ = 1$$

where $i = 1, 2, \dots, \nu - 1$ correspond to truncated cage fragments, and $i = \nu$ correspond to a perfectly closed cage.

(vii) *Structural Information from Rule No. 5.* It may be seen from Figures 4-8 and ref 22 and 43 that for all aqueous mixtures of the type studied here for small x_2 the reorientational correlation time of the water

molecule, $\tau_c^{(1)}$, increases as x_2 increases. Generally, this increase of $\tau_c^{(1)}$ gets slightly stronger as the temperature decreases (Figures 4, 8-10, 12-14). According to rule no. 5, eq 11, this means that one or more of the maximum values of the pair distribution functions increase, and this is an increase of the degree of structure in the solution.

First the question arises: Is this structural reinforcement due to the first ($\text{H}_2\text{O}-\text{H}_2\text{O}$ interaction) or due to the second term (H_2O -solute interaction) in eq 11? For the weakly interacting solutes like acetonitrile, acetone, and THF the structural reinforcement must be ascribed to the first term, that is $f_1^{(1,1)}, f_2^{(1,1)}, \dots$ increase, and the contribution from $f_1^{(1,2)}, f_2^{(1,2)}, \dots$ in the second term on the right-hand side of eq 11 may be neglected. This is a consequence of the fact that for these molecules even the polar end of the molecule (for THF this is to be expected) rotates faster than the water molecules and thus direct solute-water interaction cannot cause the slower motion of the water. For methanol, ethanol, and pyridine the second term containing $f_1^{(1,2)}, f_2^{(1,2)}, \dots$ will probably be more important. Then, in order to give our structural statement a general validity, we must consider the rigid skeleton of rather large molecules—like, *e.g.*, pyridine—also to be a positive contribution to the structure of the liquid, namely an "intramolecular" contribution.¹⁵ However, it can be shown that one or two water molecules bound to the polar group of these solutes with their known reorientation times $\tau_c^{(2)}(\text{polar})$ (see Table IV) cannot cause the whole effect of increasing $\tau_c^{(1)}$. So the $\text{H}_2\text{O}-\text{H}_2\text{O}$ distribution with the maxima $f_1^{(1,1)}, f_2^{(1,1)}, \dots$ will contribute as well to the lengthening of $\tau_c^{(1)}$ significantly in these mixtures. *tert*-Butyl alcohol presents as yet an open question in this regard.

Clearly, at concentration $C_2 < 2.5 m$ the statement of

(49) See, *e.g.*, R. A. Robinson and R. H. Stokes, "Electrolyte Solutions," Butterworths, London, 1965.

a structure reinforcement of the water does not tell more than given by the aggregate approach, but the view is now more general and the model of localized hydration spheres is abandoned. In particular at concentrations $C_2 > C_2^* = 55.5/n_h$ the model of separated, nonoverlapping hydration spheres becomes meaningless, and still the more general distribution function approach allows the statement that the degree of structure is increased as compared with pure H_2O .

It is just remarkable that this increase of structure extends far over the boundary concentration C_2^* and goes up to rather low values of the ratio of the number of water molecules/number of organic molecules. We shall call this ratio at the maximum of the water correlation time $(n_1/n_2)_{\tau_c^{(1)}\max}$. Some results for this quantity are collected in Table V (25°). For the weakly interacting solutes acetonitrile, acetone, and THF beyond the maximum of $\tau_c^{(1)}$ at higher mole fractions of the organic compounds the second term of eq 11 must become more important. Now $f_1^{(1,2)}, f_2^{(1,2)}, \dots$ increasingly determine the correlation time of the water molecule; obviously, the water-organic molecule distribution is orientationally more isotropic, $f_1^{(1,2)}, f_2^{(1,2)}, \dots$ have lower values, and the correlation time decreases. In the mixtures with pyridine, ethanol, and methanol the stronger direct water-solute interaction pulls the maximum of $\tau_c^{(1)}$ more in the direction of lower ratios n_1/n_2 , that is, to higher mole fractions x_2 .

Qualitatively the same information may be obtained from eq 10 regarding the self-diffusion coefficient of the water in the aqueous mixtures. The minima of $D^{(1)}$ occur at about the same composition as the maxima of $\tau_c^{(1)}$ do; some numerical results may be found in Table V.

Now we consider the motion of the solute molecule. Let us begin with the behavior of the hydrocarbon part, the methyl group, say. It is useful to consider two groups of maximum values of the pair distribution function referring to the center of the methyl group: (1) the maxima which occur in the direction of the polar group (at $x_2 \rightarrow 0$ they describe the binding of the polar group with the water, and for larger distances the water-water distribution beyond the polar group enters); (2) the maxima which occur in the other direction as seen from the methyl group, that is, the direction pointing straight into the water at $x_2 \rightarrow 0$. These latter maxima correspond to the weak (c.d. Waals) binding between the methyl group and water and then further out they also reflect the water-water configuration in the second coordination sphere as seen from the methyl group. We recall that all these maximum values contribute to the correlation time of the methyl group. In this case the various maximum values of the pair distribution function are the $f_1^{(2,1)}, f_2^{(2,1)}, \dots$ occurring in the second term of the right-hand side of eq 13. Clearly, at $x_2 \rightarrow 0$ the first term of eq 13 $\rightarrow 0$ since it corresponds to the vanishing 2-2 contribution.

Now we find experimentally (Figures 4, 6-8, and ref 22) that, starting from $x_2 = 0$ in all cases $\tau_c^{(2)}(CH_3)$ increases with increasing x_2 for sufficiently small x_2 . As indicated above in our somewhat simplified scheme this has two sources: The direct effect of the aqueous neighbors of the methyl group and the effect of the polar end transmitted by the molecular skeleton, which, however, is partly decoupled by the internal rotation about C-C, C-O, and other bonds. Regarding the direct coupling methyl-water the increase of $\tau_c^{(2)}(CH_3)$ is due to the second coordination water-water distribution since the next neighbor distributions in the hydration cage should not change very much. Thus the increase of the water structure is also reflected by the motion of the inert methyl protons or deuterons *via* the weak structural bridges extending into the bulk of the aqueous surroundings. In addition, the same "signals" concerning the water structure are also supplied *via* the polar groups.

However, at a certain composition in many cases a maximum of $\tau_c^{(2)}(CH_3)$ occurs (Figures 4, 6-8). This maximum again is developed slightly stronger when the temperature is lower (Figures 4, 8-10, 12-14). Now, the mixture for which the maximum of $\tau_c^{(2)}(CH_3)$ occurs contains more water than the mixture for which the water correlation time $\tau_c^{(1)}$ has its maximum. Some ratios $(n_1/n_2)_{\tau_c^{(2)}(CH_3)\max}$ for which the maximum of $\tau_c^{(2)}(CH_3)$ occurs are also presented in Table V.

Now we saw that the increase of $\tau_c^{(2)}(CH_3)$ at $x_2 \lesssim 0.05$ is determined by the water-water configurations in the second coordination sphere of the solute. The water-water configurations themselves are described by the maxima occurring in the 1-1 distribution, *i.e.*, $f_1^{(1,1)}, f_2^{(1,1)}, \dots$ which determine $\tau_c^{(1)}$. The fact that the distribution functions which determine the water motion still get steeper, whereas those which determine the motion of the organic molecule already become flatter, indicates that the local surroundings of the two kinds of particles must begin to differ. The correlation times of the methyl group become shorter because more and more organic molecules with their more isotropic orientational distribution (of their hydrocarbon part) approach to the direct neighborhood of a given reference organic molecule. This effect depresses the probability to find a water molecule in the neighborhood of the organic molecule; that is, the second term on the right-hand side of eq 13 decreases rapidly and the first term gains more importance. In this way we are again led to the conclusion that microheterogeneity exists in these mixtures. The final value of $\tau_c^{(2)}(CH_3)$ as $x_2 \rightarrow 1$ depends on the nature and structure of the pure organic liquid. For instance, in acetone relatively small maximum values $f_1^{(2,2)}, f_2^{(2,2)}, \dots$ occur in the first and second coordination sphere; the orientational distribution of the molecules relative to one another is almost isotropic, so $\tau_c^{(2)}(CH_3)$ drops to a value lower than in H_2O at $x_2 \rightarrow 0$. In ethanol, however, where

hydrogen bonds exist, the probability to find ordered aggregates is greater and $\tau_c^{(2)}(\text{CH}_3)$ for $x_2 \rightarrow 1$ does not fall to the value it has in the limit $x_2 \rightarrow 0$ in H_2O (see Table IV). It should be noted that in the case of H_2O -*tert*-butyl alcohol at 25° $\tau_c^{(2)}(\text{CH}_3)$ never decreases at all with increasing x_2 .²² This means that the intramolecular structuredness of the *tert*-butyl alcohol and the hydrogen bonds between the *tert*-butyl alcohol molecules cause such a large first term of eq 13 that the correlation time does not decrease as the water contribution in the second term of eq 13 becomes smaller. Thus one can say that water has less structure than the intra- and intermolecular structure together of *tert*-butyl alcohol, it has almost as much structure as the intra- and intermolecular structure together of ethanol, and it has more structure in the same sense than the other organic liquids used here.

The correlation time of the polar group of the solute molecule shows essentially the same behavior and thus yields the same structural information as described for the hydrocarbon part. The experimental uncertainties so far do not allow any more definite statements. Just the same is true for the self-diffusion coefficient of the solute particle.

(viii) *Structural Information from Rule No. 6.* From the Figures 3-9 given in previous work²² of one of the authors (E. v. G.) one sees that the quantity $(1/T_1)_{\text{inter}} D^{(2)}/N_{\text{H}}$ for the organic particle, which is proportional to $\mathfrak{J}^{(2,2)}D^{(2)}$ (see eq 14 and 22), in some cases increases as $C_2 \rightarrow 0$. The same is true—and even with greater regularity—for $(1/T_1)_{\text{inter}}D^{(1)}/N_{\text{H}}$ regarding the water; *i.e.*, $\mathfrak{J}^{(1,1)}D^{(1)}$ increases as $C_1 \rightarrow 0$. Originally, one of the present authors (E. v. G.) together with Zeidler had proposed that the variation of $\mathfrak{J}D$ with composition is due to a change in the mean square displacement $\langle r^2 \rangle$ occurring in eq 14. One can, however, be doubtful whether $\langle r^2 \rangle/\delta^2$ is large enough so as to account for the entire effect observed. Thus we were led to another explanation which is formulated above as rule no. 6. As a consequence we conclude that for some mixtures the organic components as well as the water associate preferentially among themselves in their respective low concentration ranges, $x_2 \approx 0, 1$; $x_1 \approx 0.1$. This again leads us to the statement that there is evidence for microheterogeneity in these mixtures. However, from the data reported in ref 22 one fact is difficult to understand. In some cases the organic component shows a variation of $\mathfrak{J}^{(2,2)}D^{(2)}$ with composition; in other cases it does not.

Analyzing the situation one finds immediately that the precise measurement of $\mathfrak{J}D$ as a function of the composition is a very difficult task, because low concentration measurements are of crucial importance. As a further example we report the data shown in Figure 15. They concern the system *tert*-butyl alcohol-water at 0° . Figure 15a shows the (total) proton relaxation rate as a function of N_{H} , the number of protons/

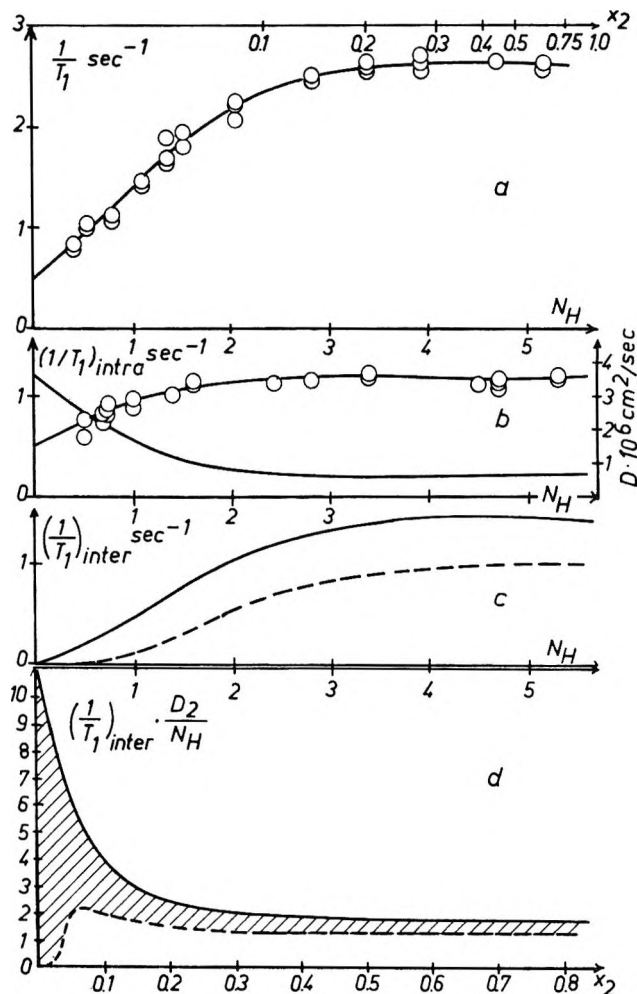


Figure 15. (a) Proton relaxation rate of $(\text{CH}_3)_3\text{COD}$ in D_2O . (b) $(1/T_1)_{\text{intra}}$ for the protons of $(\text{CH}_3)_3\text{COD}$ in D_2O and self-diffusion coefficient $D^{(2)}$ of $(\text{CH}_3)_3\text{COD}$ in D_2O . (c) $(1/T_1)_{\text{inter}}$ for the protons of $(\text{CH}_3)_3\text{COD}$ in D_2O . All data are given as a function of N_{H} , N_{H} in $10^{22}/\text{cm}^3$; temperature 0° . (d) $(1/T_1)_{\text{inter}}D^{(2)}/N_{\text{H}}$ in $10^{-29} \text{ cm}^5 \text{ sec}^{-2}$, as a function of the mole fraction x_2 .

cm^3 , in the system $(\text{CH}_3)_3\text{COD} + \text{D}_2\text{O}$. Figure 15b shows the intramolecular relaxation rate of the methyl protons of *tert*-butyl alcohol. These results are obtained from the deuteron relaxation rate in the mixture $(\text{CD}_3)_3\text{COH} + \text{H}_2\text{O}$. By chance $1/T_1$ of the deuteron is by exactly a factor of 10 larger than $(1/T_1)_{\text{intra}}$ given in Figure 15b. Furthermore, Figure 15b shows the self-diffusion coefficient of $(\text{CH}_3)_3\text{COD}$ in D_2O . The solid curve of Figure 15c gives $(1/T_1)_{\text{inter}}$, the difference of the two relaxation rates presented in Figures 15a and b. Then $((1/T_1)_{\text{inter}}D^{(2)}/N_{\text{H}}) \sim \mathfrak{J}^{(2,2)}D^{(2)}$ is shown in Figure 15d as a function of the mole fraction x_2 . The steep increase of $\mathfrak{J}^{(2,2)}D^{(2)}$ as $x_2 \rightarrow 0$ yields strong evidence for butyl alcohol-butyl alcohol association. However, considering our experimental error, in particular that arising for the extrapolations to $N_{\text{H}} \rightarrow 0$ in Figures 15a and b, the true intermolecular relaxation rate may be as low as shown by the dashed curve in Figure 15d, and the hatched field indicates the uncer-

tainty in $(1/T_1)_{\text{inter}}D^{(2)}/N_H$. One sees that there is evidence for butyl alcohol-butyl alcohol association; however, the definite statement must await better experimental results from improved apparatus for measurements with very weak signals.

5. Summary

We have found essentially three results. (1) Long-lived rigid hydration cages surrounding the solute particles at low concentration are absent. (2) At low concentration of the organic component there is an increase of structure in the solution. (3) There is evidence for solute-solute association in the mixture leading to a certain degree of microheterogeneity.

Acknowledgment. Financial support from the Deutsche Forschungsgemeinschaft is gratefully acknowledged.

Appendix

We wish to calculate the error in the correlation time $\tau_c^{(1)+}$ which arises if one erroneously assumes that the exchange of a nucleus between two different environments is slow whereas actually it is fast. For the slow exchange limit we have (see eq 18)

$$\tau_c^{(1)} = \tau_c^{(1)\circ} + \frac{n_h C_2}{55.5} (\tau_c^{(1)+} - \tau_c^{(1)\circ}) \quad (\text{A1})$$

We divide eq A1 by the correlation time of the pure solvent liquid (here water)

$$\frac{\tau_c^{(1)}}{\tau_c^{(1)}(0)} = \frac{\tau_c^{(1)\circ}}{\tau_c^{(1)}(0)} + \frac{n_h C_2}{55.5} \left(\frac{\tau_c^{(1)+}}{\tau_c^{(1)}(0)} - \frac{\tau_c^{(1)\circ}}{\tau_c^{(1)}(0)} \right) \quad (\text{A2})$$

$\tau_c^{(1)}/\tau_c^{(1)}(0)$ is a function of the concentration; we write the power expansion in C_2

$$\frac{\tau_c^{(1)}}{\tau_c^{(1)}(0)} = 1 + B' C_2 + C' C_2^2 + \dots \quad (\text{A3})$$

where B' , C' are constants. We form $\{d(\tau_c^{(1)}/\tau_c^{(1)}(0))/dC_2\}_{C_2=0}$ and deduce from eq A2 and A3

$$\frac{\tau_c^{(1)+}}{\tau_c^{(1)}(0)} = \frac{55.5}{n_h} \left\{ B' - \frac{1}{\tau_c^{(1)}(0)} \left(\frac{d\tau_c^{(1)\circ}}{dC_2} \right)_{C_2=0} \right\} + 1 \quad (\text{A4})$$

Since according to the same arguments as described

previously before eq 27, we must have $d\tau_c^{(1)\circ}/dC_2 \geq 0$, the maximum value of $\tau_c^{(1)+}/\tau_c^{(1)}(0)$ will be

$$\frac{\tau_c^{(1)+}}{\tau_c^{(1)}(0)} = \frac{55.5}{n_h} B' + 1 \quad (\text{A5})$$

This formula has been used for the entries of Table IV, column 3. In the limit of fast exchange we have (see eq 17)

$$\frac{1}{\tau_c^{(1)}} = \frac{1}{\tau_c^{(1)\circ}} + \frac{n_h C_2}{55.5} \left(\frac{1}{\tau_c^{(1)+}} - \frac{1}{\tau_c^{(1)\circ}} \right)$$

or

$$\frac{\tau_c^{(1)}(0)}{\tau_c^{(1)}} = \frac{\tau_c^{(1)}(0)}{\tau_c^{(1)\circ}} + \frac{n_h C_2}{55.5} \left(\frac{\tau_c^{(1)}(0)}{\tau_c^{(1)+}} - \frac{\tau_c^{(1)}(0)}{\tau_c^{(1)\circ}} \right) \quad (\text{A6})$$

Again we substitute eq A3 on the left-hand side of eq A6 and form $\{d(\tau_c^{(1)}(0)/\tau_c^{(1)})/dC_2\}_{C_2=0}$. The result is

$$\frac{\tau_c^{(1)+}}{\tau_c^{(1)}(0)} = \left[1 - \frac{55.5}{n_h} \left\{ B' - \frac{1}{\tau_c^{(1)}(0)} \left(\frac{d\tau_c^{(1)\circ}}{dC_2} \right)_{C_2=0} \right\} \right]^{-1} \quad (\text{A7})$$

Thus, when we divide eq A7 by eq A4 we obtain the final result

$$\frac{\{\tau_c^{(1)+}/\tau_c^{(1)}(0)\}_{A7}}{\{\tau_c^{(1)+}/\tau_c^{(1)}(0)\}_{A4}} = \left\{ 1 - \left[\frac{55.5}{n_h} \left\{ B' - \frac{1}{\tau_c^{(1)}(0)} \left(\frac{d\tau_c^{(1)\circ}}{dC_2} \right)_{C_2=0} \right\} \right]^2 \right\}^{-1} \quad (\text{A8})$$

We see that with the assumption $\tau_c^{(1)\circ} = \tau_c^{(1)}(0)$, i.e., $d\tau_c^{(1)\circ}/dC_2 = 0$, the error mentioned above is unessential if $55.5B'/n_h \lesssim 0.5$, i.e., $\{\tau_c^{(1)+}/\tau_c^{(1)}(0)\}_{A4} \lesssim 1.5$. Indeed, our results in Table IV are of this order. With $55.5B'/n_h \rightarrow 1$ and $d\tau_c^{(1)\circ}/dC_2 = 0$

$$\frac{\{\tau_c^{(1)+}/\tau_c^{(1)}(0)\}_{A7}}{\{\tau_c^{(1)+}/\tau_c^{(1)}(0)\}_{A4}} \rightarrow \infty$$

For $55.5B'/n_h > 1$ with $\tau_c^{(1)\circ} = \tau_c^{(1)}(0)$ fast exchange cannot be the correct situation, now for fast exchange in any case $d\tau_c^{(1)\circ}/dC_2 > 0$ must be valid.

Finally, the appropriate formulas for an intermediate rate of exchange between the two limits given here may be found in ref 18 and 19.

Theory of Mixed Electrolyte Solutions and Application to a Model for Aqueous Lithium Chloride-Cesium Chloride^{1a}

by Harold L. Friedman* and P. S. Ramanathan^{1b}

Department of Chemistry, State University of New York at Stony Brook, Stony Brook, New York 11790
(Received March 2, 1970)

The general theory of the calculation of the thermodynamic coefficients for electrolyte mixtures from the pair correlation functions for the mixtures is worked out. These correlation functions are computed for several models for aqueous LiCl-CsCl mixtures by means of the hypernetted-chain integral equation, and the theory is applied to them to obtain the free-energy mixing coefficients for these models. Special attention is given to a model having properties close to the experimental ones for this system. The computed results for this model seem to be accurate enough to be useful, judging by three self-consistency tests. The model exhibits three empirically established regularities about as well as experimental systems do. They are Harned's rule, Young's rule that certain mixing coefficients in a common-ion mixture are nearly independent of the common ion, and the rule that the sum of Harned's α coefficients depends linearly on the ionic strength. The model computations also elucidate the role of the mixture limiting law.

1. Introduction

Aside from their importance in connection with the study of all sorts of ionic chemical processes in solution, mixed strong electrolyte solutions are interesting as the framework for several intriguing regularities. The best known is Harned's rule, which states that the logarithm of the activity coefficient of electrolyte A in a mixture with electrolyte B, having a common ion, varies nearly linearly with the concentration of electrolyte B if the ionic strength is held constant.² Another, which may be called Young's rule, states that the heat of forming such a mixture from solutions of pure A and B at the same ionic strength is nearly independent of the common ion.³ A third, Young's cross-square rule, relates the heat of mixing of two electrolytes without a common ion to all the other heats of mixing of two electrolytes which one may generate using the same four ionic species, where all these mixings are at the same fixed ionic strength.³ Another, which does not seem to be associated with a single author, is that the sum of the two Harned coefficients for a particular mixed electrolyte varies linearly with the total ionic strength.^{2,4,5}

The generality with which these rules are stated here may be misleading, since mostly they have been established only for aqueous solutions of electrolytes of at most three charge types, near 25°, and over a limited range of ionic strengths. However, it does seem useful to state them even more generally than we have done, that is, to include in Harned's rule the corresponding behavior of the partial molar enthalpies, to include in Young's rule the corresponding behavior of the excess free energy, etc. The reason is that, from the point of view of the underlying statistical-mechanical theory, each of the rules as originally stated reflects an under-

lying regularity which, if it exists at all, may well be characteristic of the structure of all strong electrolyte solutions.

Using Mayer's cluster theory of ionic solutions⁶ one finds a simple interpretation of Harned's rule in terms of cluster expansions and finds that Harned's rule implies Young's rule.^{7,8} The theory also leads to a form of limiting law for the sum of the Harned coefficients of

* To whom correspondence should be addressed.

(1) (a) Grateful acknowledgment is made of the support of this research by the Office of Saline Water, U. S. Department of the Interior. (b) On leave from Analytical Division, Bhabha Atomic Research Centre, Trombay, Bombay-85, India.

(2) H. S. Harned and B. B. Owen, "The Physical Chemistry of Electrolyte Solutions," 3rd ed, Reinhold, New York, N. Y., 1958.

(3) T. F. Young, Y. C. Wu, and A. A. Krawetz, *Discussions Faraday Soc.*, **24**, 37, 77, 80 (1957). As these discussions show, what is here called Young's rule is not very accurate in cases in which the mixing coefficients (for the enthalpy rather than for the free energy in these discussions) are relatively near to zero. The cross-square rule is a more complicated relation which is more accurate, especially when the mixing coefficients are small. Also, the equivalence of the usual free-energy form of Harned's rule to its corollaries for enthalpies and volumes is stressed here.

(4) E. A. Guggenheim, *Trans. Faraday Soc.*, **62**, 3446 (1966). It is stated here that this relation is not merely empirical but that it can be derived from a single general assumption, his eq 2. This leads to the sum of Harned coefficients being independent of ionic strength; *i.e.*, linear variation with zero slope. However, zero slope is not consistent with many of the data. (Examples: Free-energy data, Figure 14-6-5 of ref 2, where for each mixture a straight line may be passed through all of the experimental points above 0.4 *M* total concentration. Enthalpy data: R. H. Wood and R. W. Smith, *J. Phys. Chem.*, **69**, 2974 (1965), where h_0 is seen to be nearly linear in total concentration in cases in which h_0 is not too small.) It also should be remarked that Guggenheim's eq 2 is not consistent with the mixture limiting law discussed in section 5 of the present paper.

(5) G. Scatchard, *J. Amer. Chem. Soc.*, **83**, 2636 (1961).

(6) J. Mayer, *J. Chem. Phys.*, **18**, 1426 (1950).

(7) H. L. Friedman, *ibid.*, **32**, 1134 (1960).

(8) H. L. Friedman, "Ionic Solution Theory," Interscience, New York, N. Y., 1962.

a mixture. More recently, Wood and Anderson⁹ have shown how to derive Young's cross-square rule from these results. However, two very unsatisfactory features remained. First, no way was found to control the error due to truncation of the cluster expansion after the second or third term, although the three-term results tended to show that two-term results were accurate enough for some purposes.^{7,8} Second, these computations, made for the primitive model, required unreasonably large hard-sphere diameters to give agreement with experiment.

Recent studies aimed at elucidating all these problems by using both a better approximation method and a better model are reported here. The computations of the observable properties of the model by this method yield, at an intermediate stage, the pair correlation functions $g_{ij}(r)$ of the ionic species. These may be defined by the statement that, if c_i is the concentration (ions per unit volume) of species i in the solution, then $c_i g_{ij}(r)$ is the local concentration of i at a distance r from an ion of species j . From the correlation functions one may calculate the osmotic coefficient of the solution by means of the virial equation¹⁰ or, using the compressibility equation, one may calculate the concentration derivatives of the chemical potentials from the zeroth moments of the correlation functions

$$G_{ij} \equiv \int (g_{ij} - 1) dr \quad (1.1)$$

This part of the calculation for mixtures has some aspects having no parallel in the earlier work^{7,10} and is described in the following sections. In the later sections the model used in this study is described, and some results are presented for comparison with experimental data for aqueous LiCl-CsCl solutions.

2. Molecular Theory of Mixing Coefficients in the McMillan-Mayer System

The starting point is the relation of the zeroth moment integrals G_{ab} (eq 1.1) to the generalized compressibility function¹⁰

$$(\partial c_a / \partial \mu_b)_{T, \mu_w} = [c_a \delta_{ab} + c_a G_{ab} c_b] / kT \equiv M_{ab} \quad (2.1)$$

where the derivative, as is appropriate in the McMillan-Mayer system,^{8,11,12} is taken at fixed values of temperature, chemical potential of the solvent, and chemical potential of each solute component except component b . To compute the thermodynamic coefficients of interest we need the matrix elements of the inverse of the matrix M defined by (2.1), namely

$$(M^{-1})_{ab} = (\partial \mu_a / \partial c_b)_{T, \mu_w} \quad (2.2)$$

where the derivative is at fixed concentration of each solute except component b . This procedure has been developed by Kirkwood and Buff¹³ and by Buff and Brout.¹⁴ However in its application to ionic systems a new problem appears, namely, the zeroth moment electroneutrality condition

$$\sum_{s=1}^{m,s} z_s M_{sb} = 0 \quad (2.3)$$

assures that $\det M = 0$ so the coefficients in (2.2) are all infinite. Here z_s is the charge on species s .

These equations are strictly applicable in the thermodynamic limit, *i.e.*, to an infinite system with the specified composition, and the infinite values of $\partial \mu_a / \partial c_b$ may be understood in physical terms as follows. The chemical potential appearing in the above equations is the one usually designated in thermodynamics as the electrochemical potential.¹⁵ It is related to its strictly chemical part, μ_a^{ch} , by the equation

$$\mu_a = \mu_a^{\text{ch}} + z_a \Psi \quad (2.4)$$

where Ψ is the electrical potential of the phase. For a system of finite size, measured by radius r , the variation of electrical potential with concentration of one component is¹⁵

$$d\Psi \simeq r^2 z_b dc_b$$

the strong dependence on r being a consequence of the long range of the Coulomb potential. Thus $d\Psi/dc_b$ is infinite in the $r = \infty$ limit for which eq 2.1 is applicable.

As this analysis implies, the infinities in $\partial \mu_a / \partial c_b$ mutually cancel when these coefficients are combined to obtain expressions for free-energy changes produced by composition changes in which electrical neutrality is maintained, hence for all experimentally accessible composition changes. Therefore the Kirkwood-Buff procedure is directly applicable to ionic solutions, at least as far as *analytical* mathematics is concerned. If the same procedure is followed *computationally*, it is often found to work, apparently because the computed M_{ab} do not exactly obey eq 2.3 so in the computational operations one may not end up by dividing zero by zero. Of course this is not entirely satisfactory because, as the computations get better and eq 2.3 is more accurately satisfied, a point will be reached where, within the round-off error of the computations, one will indeed be dividing zero by zero in following the Kirkwood-Buff procedure. An example has been given in the discussion of this problem for a solution of a single electrolyte.¹⁶

The following procedure for getting expressions for the desired thermodynamic coefficients in terms of the M_{ab} when eq 2.3 is satisfied seems readily applicable to

(9) R. H. Wood and H. L. Anderson, *J. Phys. Chem.*, **70**, 992 (1966).

(10) J. C. Rasaiah and H. L. Friedman, *J. Chem. Phys.*, **48**, 2742 (1968).

(11) W. G. McMillan and J. E. Mayer, *ibid.*, **13**, 276 (1945).

(12) H. L. Friedman, *ibid.*, **32**, 1351 (1960).

(13) J. G. Kirkwood and F. P. Buff, *ibid.*, **19**, 774 (1951).

(14) F. P. Buff and R. Brout, *ibid.*, **23**, 458 (1955).

(15) E. A. Guggenheim, "Thermodynamics," 2nd ed, Interscience, New York, N. Y., 1950.

(16) J. C. Rasaiah and H. L. Friedman, *J. Chem. Phys.*, **50**, 3965 (1969).

arbitrary mixtures of ionic components but here, in the interest of brevity, is set forth for the particular case of a mixture of two electrolytes A and B with a common ion but with arbitrary charge types. A mole of electrolyte A dissolves and dissociates to produce ν_{A1} moles of ions of species 1 and ν_{A3} moles of ions of species 3. A mixture of the two electrolytes is dissolved in a nonionic solvent. We define the particle-number-density ionic strength

$$I \equiv \frac{1}{2} \sum_{s=1}^3 c_s z_s^2 \quad (2.5)$$

and the fraction of I due to electrolyte A

$$y \equiv \frac{1}{2} c_1 (z_1^2 + (\nu_{A3}/\nu_{A1}) z_3^2) / I \quad (2.6)$$

It is convenient to note that, with the definitions

$$l_A \equiv \frac{1}{2} z_1 (z_1 - z_3), \quad l_B \equiv \frac{1}{2} z_2 (z_2 - z_3) \quad (2.7)$$

$$h \equiv (z_1 - z_2) / (2z_3 - z_1 - z_2), \quad Y \equiv 1 - 2y \quad (2.8)$$

we have

$$\begin{aligned} c_1 &= yI/l_A, \quad c_2 = (1 - y)I/l_B \\ c_3 &= -\frac{I}{2z_3} [1 - hY] [z_1/l_A + z_2/l_B] \end{aligned} \quad (2.9)$$

Now the thermodynamic coefficients which are required, and which are, at least in principle, accessible to experimental determination, are

$$\left(\frac{\partial \mu_A}{\partial I} \right)_y \equiv \mu_{AI}, \quad \left(\frac{\partial \mu_A}{\partial y} \right)_I \equiv \mu_{Ay} \quad (2.10)$$

and μ_{BI} and μ_{By} , defined analogously.

These are the matrix elements of the inverse of the L matrix which appears in the equation

$$\begin{pmatrix} dI \\ dy \end{pmatrix} = \begin{pmatrix} L_{IA} & L_{IB} \\ L_{yA} & L_{yB} \end{pmatrix} \cdot \begin{pmatrix} d\mu_A \\ d\mu_B \end{pmatrix} \quad (2.11)$$

Apparently L is a projection of the M matrix.

From eq 2.5-2.8 we find

$$L_{IA} \equiv \left(\frac{\partial I}{\partial \mu_A} \right) = l_A \left(\frac{\partial c_1}{\partial \mu_A} \right) + l_B \left(\frac{\partial c_2}{\partial \mu_A} \right) \quad (2.12)$$

The other elements of L may similarly be expressed as linear combinations of the derivatives

$$K_{ij} \equiv \partial c_i / \partial \mu_j; \quad i = 1, 2; \quad j = A, B \quad (2.13)$$

We next find the relation of these derivatives, which comprise a matrix K , to the elements of M .

For this purpose we define two coordinate systems in which the basis vectors are infinitesimal changes in the chemical potentials of the components. The *general* system has the basis vectors (vector notation is suppressed here) $d\mu_1, d\mu_2, d\mu_3$ while the *ionic* system has the basis vectors $d\mu_A, d\mu_B, d\mu_R$ where

$$\begin{aligned} \mu_A &= \nu_{A1}\mu_1 + \nu_{A3}\mu_3, \quad \mu_B = \nu_{B2}\mu_2 + \nu_{B3}\mu_3 \\ \mu_R &\equiv \nu_{A3}\mu_1 + \nu_{B3}\mu_2 \end{aligned} \quad (2.14)$$

We define the transformation matrix

$$T = \begin{pmatrix} \nu_{A1} & 0 & \nu_{A3} \\ 0 & \nu_{B2} & \nu_{B3} \\ \nu_{A3} & \nu_{B3} & 0 \end{pmatrix} \quad (2.15)$$

and note that

$$\begin{pmatrix} d\mu_A \\ d\mu_B \\ d\mu_R \end{pmatrix} = T \cdot \begin{pmatrix} d\mu_1 \\ d\mu_2 \\ d\mu_3 \end{pmatrix} \quad (2.16)$$

For an arbitrary vector in the general system

$$\mathbf{x} = x_1 d\mu_1 + x_2 d\mu_2 + x_3 d\mu_3 \quad (2.17)$$

and the same vector in the ionic system

$$\mathbf{x} = x_A d\mu_A + x_B d\mu_B + x_R d\mu_R \quad (2.18)$$

the coefficients are related by the equation

$$\begin{pmatrix} x_1 \\ x_2 \\ x_3 \end{pmatrix} = T \cdot \begin{pmatrix} x_A \\ x_B \\ x_R \end{pmatrix} \quad (2.19)$$

Now we observe that the matrix elements of M are the coefficients of the three "vectors"

$$\begin{aligned} d\mathbf{c}_i &= (\partial c_i / \partial \mu_1) d\mu_1 + (\partial c_i / \partial \mu_2) d\mu_2 + (\partial c_i / \partial \mu_3) d\mu_3 \\ i &= 1, 2, 3 \end{aligned} \quad (2.20)$$

in the general system while the desired derivatives (eq 2.13) are coefficients of the same vectors in the ionic system

$$\begin{aligned} d\mathbf{c}_i &= (\partial c_i / \partial \mu_A) d\mu_A + (\partial c_i / \partial \mu_B) d\mu_B + (\partial c_i / \partial \mu_R) d\mu_R \\ i &= 1, 2, 3 \end{aligned} \quad (2.21)$$

In view of (2.19) we have

$$K = T^{-1} \cdot M \quad (2.22)$$

The inverse of T is readily evaluated. We then find in general

$$K = \begin{pmatrix} 1/\nu_{A1} & 0 & 0 \\ 0 & 1/\nu_{B2} & 0 \\ 0 & 0 & 0 \end{pmatrix} \cdot M \quad (2.23)$$

(The matrix multiplying M in (2.23) is not T^{-1} ; this simple form results after evaluating the product in (2.22).) With these results L may be expressed in terms of M . The resulting L matrix is then inverted to obtain the desired coefficients

$$\begin{aligned} \mu_{AI} &= -(\nu_{A1}/ID)(c_2 M_{12} - c_1 M_{22}) \\ \mu_{Ay} &= (I\nu_{A1}/D)(M_{12}/l_B + M_{22}/l_A) \end{aligned} \quad (2.24)$$

$$\begin{aligned} \mu_{BI} &= (\nu_{B1}/ID)(c_2 M_{11} - c_1 M_{21}) \\ \mu_{By} &= -(I\nu_{B2}/D)(M_{11}/l_B + M_{21}/l_A) \end{aligned}$$

where

$$D \equiv M_{11}M_{22} - M_{12}^2 \quad (2.25)$$

To get the corresponding derivatives of $\mu_A^{\text{ex}} = kT(\nu_{A1} + \nu_{A3}) \ln \gamma_{\pm}(A)$ and of $\mu_B^{\text{ex}} = kT(\nu_{B2} + \nu_{B3}) \ln \gamma_{\pm}(B)$, we subtract the corresponding ideal terms from the derivatives given in (2.24). These are obtained directly from the ideal solution condition $M_{ij}^{\text{id}} = c_i \delta_{ij}$ with the result

$$\begin{aligned} \mu_{A_I}^{\text{id}} &= kT(\nu_{A1} + \nu_{A3})/I \\ \mu_{A_y}^{\text{id}} &= kT\nu_{A1}[y^{-1} - 2hz_1/z_3(1 - hY)] \\ \mu_{B_I}^{\text{id}} &= kT(\nu_{B2} + \nu_{B3})/I \end{aligned} \quad (2.26)$$

$$\mu_{B_y}^{\text{id}} = -kT\nu_{B2}[(1 - y)^{-1} + 2hz_2/z_3(1 - hY)]$$

It should be remarked that (2.26) does *not* follow from (2.24) in the limit of infinite dilution.

Of the four coefficients in either (2.24) or (2.26), only three are independent because there is a cross-differentiation relation

$$(\partial\mu_A/\partial c_B)_{c_A} = (\partial\mu_B/\partial c_A)_{c_B} \quad (2.27)$$

which, in terms of y and I as composition variables, reads

$$\nu_{B2}l_B(I\mu_{A_I} - y\mu_{A_y}) = \nu_{A1}l_A(I\mu_{B_I} + (1 - y)\mu_{B_y}) \quad (2.28)$$

Although only written here for the total μ , eq 2.28 also holds for the derivatives of μ^{id} and μ^{ex} .

When the computations are not too accurate, it is often better to neglect eq 2.3, which is then not well satisfied, and express the derivatives μ_{A_I} , etc., in (2.24) directly in terms of the elements of M^{-1} . This procedure is straightforward, but the results are lengthy and are omitted here.

3. Additional Thermodynamic Relations in the McMillan-Mayer System

It is convenient here to introduce a different notation. We define

$$\begin{aligned} g_{A_I} &\equiv \mu_{A_I}^{\text{ex}}/l_A\nu_{A1} & g_{A_y} &\equiv \mu_{A_y}^{\text{ex}}/l_A\nu_{A1} \\ g_{B_I} &\equiv \mu_{B_I}^{\text{ex}}/l_B\nu_{B2} & g_{B_y} &\equiv \mu_{B_y}^{\text{ex}}/l_B\nu_{B2} \end{aligned} \quad (3.1)$$

In general $l_A\nu_{A1} = 1/2(\nu_{A1} + \nu_{A3})|z_1z_3|$ which is unity for a 1-1 electrolyte, so the use of these coefficients simply makes the equations more independent of charge type. For example, the cross-differentiation relation, eq 2.28, becomes

$$I g_{A_I} - y g_{A_y} = I g_{B_I} + (1 - y) g_{B_y} \quad (3.2)$$

For variation in y at fixed I it is customary to expand the mean ionic activity coefficients of each electrolyte component in powers of the concentration of the other, for example

$$\begin{aligned} (\mu_A^{\text{ex}}(y, I) - \mu_A^{\text{ex}}(y, 1))/(\nu_{A1} + \nu_{A3}) \ln 10 = \\ \log \frac{\gamma_{\pm, A}(y)}{\gamma_{\pm, A}(1)} = -kT \sum_{p \geq 1} \alpha_{A,p} I^p (1 - y)^p \end{aligned} \quad (3.3)$$

In terms of these coefficients, the Harned coefficients^{2,8,12} in the McMillan-Mayer system, we have

$$\begin{aligned} g_{A_y} &= +(2kT \ln 10/|z_1z_3|) \sum_{p \geq 1} p \alpha_{A,p} I^p (1 - y)^{p-1} \\ g_{B_y} &= -(2kT \ln 10/|z_2z_3|) \sum_{p \geq 1} p \alpha_{B,p} I^p y^{p-1} \end{aligned} \quad (3.4)$$

For variation of composition at fixed y the electrolyte mixture behaves like a solution of a single electrolyte of varying concentration, a so-called pseudobinary mixture. The mean chemical potential of the electrolyte is

$$\mu_{\pm} = (c_A \mu_A + c_B \mu_B)/(c_A + c_B)$$

and we find

$$\begin{aligned} kT(\partial \ln \gamma_{\pm}/\partial I)_y = (\partial \mu_{\pm}^{\text{ex}}/\partial I)_y = \\ \frac{y g_{A_I} + (1 - y) g_{B_I}}{y/l_A\nu_{A1} + (1 - y)/l_B\nu_{B2}} \end{aligned} \quad (3.5)$$

An appropriate double integration at fixed y of the function in (3.5) gives the osmotic coefficient. This may be compared with the osmotic coefficient obtained by the virial equation to perform a virial-compressibility self-consistency test of the computation for the mixture that is analogous to the one that may be made for the solution of a single electrolyte.¹⁰

For variation of composition at fixed y , the free-energy change may be expressed in terms of the function

$$\begin{aligned} \Delta_m F^{\text{ex}}(y, I) \equiv F^{\text{ex}}(y, I) - \\ y F^{\text{ex}}(1, I) - (1 - y) F^{\text{ex}}(0, I) \end{aligned} \quad (3.6)$$

where F^{ex} is the excess Helmholtz free energy per unit volume. We have

$$dF^{\text{ex}} = \mu_A^{\text{ex}} dc_A + \mu_B^{\text{ex}} dc_B \quad (3.7)$$

the solvent term not appearing in the McMillan-Mayer system. Then we have

$$\partial^2 \Delta_m F^{\text{ex}}/\partial y^2 = \partial^2 F^{\text{ex}}/\partial y^2 = I[g_{A_y} - g_{B_y}] \quad (3.8)$$

Following the usual expansion form for a mixing function^{7,8} we write

$$\begin{aligned} \Delta_m F^{\text{ex}}(y, I) = I^2 kT y(1 - y) \sum_{p \geq 0} f_p(I) Y^p = \\ 1/4 I^2 kT \sum_p f_p(I) [Y^p - Y^{p+2}] \end{aligned} \quad (3.9)$$

By differentiating this with respect to y and comparing it with eq 3.8 we obtain the desired relation

$$\begin{aligned} g_{A_y} - g_{B_y} = -2IkT[f_0 - f_2 + \\ 3Y(f_1 - f_3) + 6Y^2(f_2 - f_4) + \dots] \end{aligned} \quad (3.10)$$

The computed zeroth moment integrals for a mixture of given composition y, I determine the left side of this equation directly as described above. By repeating this determination for several values of y at fixed I

one can determine the Y dependence and the coefficients f_0 , f_1 , and perhaps f_2 . In the computations described below it is found that the Y dependence of the left side is fairly linear so apparently $f_p = 0$ for $p > 1$, which seems to be the experimental situation as well.

Next we find how the coefficients in (3.1) determine the expansion coefficients w_p of the osmotic coefficient ϕ . These expansion coefficients seem best to be defined by the equation¹⁷

$$\Delta_m((1 - \phi) \sum c_s) = -I^2 y(1 - y)(w_0 + w_1 Y + w_2 Y^2 + \dots) \quad (3.11)$$

We also have the thermodynamic relation

$$(1 - \phi)kT \sum c_s = \frac{\partial(F^{\text{ex}}/I)}{\partial(1/I)} \quad (3.12)$$

On combining these equations with (3.9) we find

$$\frac{\partial(f_p I)}{\partial(I)} = w_p \quad p = 0, 1, 2, \dots \quad (3.13)$$

This provides one way to compute w_p . One derives f_p from eq 3.10 from computations at several values of I and performs the required differentiation numerically.

A second way to get the w_p is to fit eq 3.11 to $\phi(y, I)$ computed from the $g_{ij}(r)$ by means of the virial equation.

A third way to get the w_p is to notice that, in view of eq 3.7 and 2.9, we have

$$\frac{\partial(F^{\text{ex}}/I)}{\partial I} = y g_{AI} + (1 - y) g_{BI} \quad (3.14)$$

When this is substituted in (3.12), the Δ_m operator applied, and the result compared with (3.11) we obtain

$$(w_0 + w_1 Y + \dots)kT = \frac{y g_{AI} + (1 - y) g_{BI} - y g_{AI}(1, I) - (1 - y) g_{BI}(0, I)}{y(1 - y)} \quad (3.15)$$

Here $g_{AI}(1, I)$ is the coefficient for a solution of pure A while $g_{BI}(0, I)$ is the coefficient for a solution of pure B. All the other y -dependent functions in the equation pertain to the mixture of composition y, I .

For the important coefficient w_0 there is also a fourth way to relate it to the coefficients in (3.1). We begin by substituting (3.10) in (3.13) to get

$$w_0 - w_2 = -({}^{1/2}kT)(g_{AI} - g_{BI})_{y=1/2} = -({}^{1/2}kT)(g_{AI} - g_{BI})_{y=1/2} \quad (3.16)$$

The second derivatives are abbreviated

$$\partial g_{Ay} / \partial I \equiv g_{AyI}, \text{ etc.} \quad (3.17)$$

Another expression for the difference appearing in the last member may be obtained from eq 3.2

$$w_0 - w_2 = -({}^{1/2}kTI)((\partial/\partial y)(y g_{Ay} + (1 - y) g_{By}))_{y=1/2} = f_0 - f_2 - ({}^{1/2}kTI)(y g_{Ay} - (1 - y) g_{By})_{y=1/2} \quad (3.18)$$

Now when the coefficients appearing here are expressed in terms of Harned coefficients (eq 3.4), we obtain

$$w_0 - w_2 = -\ln 10(\alpha_{A1}/|z_1 z_3| + \alpha_{B1}/|z_2 z_3|) \quad (3.19)$$

In all known cases w_2 is numerically negligible compared to w_0 .

It seems that these four methods to obtain w_0 from the computed correlation functions are independent of each other. Their intercomparison then provides *three* self-consistency tests which are analogous to the virial-compressibility self-consistency tests for simple fluids or solutions of a single electrolyte. However, the virial compressibility test for mixtures, which may be obtained as described following eq 3.5, is not independent of the tests involving w_0 .

4. Change between McMillan-Mayer and Harned-Owen Systems

This problem has been discussed in detail,^{7,8,12} but a few remarks on notation are required to make that discussion easily applicable here. By the Harned-Owen system is meant the solution at total pressure P_0 (1 atm) with quantities of solute measured in moles and quantity of solvent measured in kilograms.² The concentration of solute species i is expressed as molality m_i and is related to c_i , the particle number density in the McMillan-Mayer system, by

$$m_i = c_i V(\mathbf{m}, \pi) / N_a \quad (4.1)$$

where $V(\mathbf{m}, \pi)$ is the volume of the solution per kilogram of solvent when the composition is $\mathbf{m} = m_1, m_2, \dots$ and the pressure on the solution is $P_0 + \pi$ where π is the osmotic pressure when P_0 is the pressure on the pure solvent in osmotic equilibrium with the solution. The ionic strength in the H-O system is then

$$I' = {}^{1/2} \sum m_i z_i^2 = IV(\mathbf{m}, \pi) / N_a \quad (4.2)$$

where I is the ionic strength in the M-M system (eq 2.5).

The relation between y' , the fraction of I' due to electrolyte A, and y (eq 2.6) is more complicated. However what is really needed is the relation of the f_p coefficients of eq 3.9 to the g_p coefficients in the equation

$$\Delta_m G(y', I') = (I')^2 RT y'(1 - y') \times (g_0 + g_1 Y' + g_2 (Y')^2 + \dots) \quad (4.3)$$

This has already been obtained,^{7,8} the result in the present notation is, for the first two coefficients

(17) This definition is preferred to a slightly different one given earlier⁸ because it leads to a simpler relation of w_p to f_p and w_p' to g_p ; see eq 3.13.

$$g_0 = (I/I')f_0 + b_0 + e_0 \quad (4.4)$$

$$g_1 = (I/I')f_1 + b_1 + e_1 +$$

$$(\partial \ln I'/\partial Y')_{I'} \frac{\partial}{\partial I'} \{I' [g_0 - b_0 - e_0]\} \quad (4.5)$$

where b_0 , e_0 , b_1 , e_1 are coefficients of known form^{7,8} depending on the equation of state of the electrolyte solution. For the cases which have been investigated they are small enough to be negligible for most purposes.

Also the factor I/I' can be made nearly unity by the following simple device. For the particle number density c_i and all derived concentration measures in the McMillan-Mayer system we adopt as the unit of volume

$$V(0,0)/N_a$$

where $V(0,0)$ is $V(\mathbf{m}, \pi)$ at $\mathbf{m} = 0, 0, \dots$, the volume per kilogram of pure solvent at the temperature of the solution. Then we have

$$\frac{c_i}{m_i} = \frac{I}{I'} = V(0,0)/V(\mathbf{m}, \pi) \quad (4.6)$$

which is within a few per cent of unity for the systems of interest here. Of course this convention must be used with care in calculations in which temperature variations are considered but it has the advantage that with it

$$g_0 \sim f_0$$

$$g_1 \sim f_1$$

etc. The small errors in these approximations will often be unimportant in view of the fact that the models for which the f_p are computed do not have the same direct potentials as the experimental systems for which the g_p may be measured.

In the H-O system we define the expansion coefficients of the osmotic coefficient by the equation¹⁷

$$\Delta_m((1 - \phi') \sum m_s) = -I'^2 y'(1 - y')(w_0' + w_1'(1 - 2y') + \dots) \quad (4.7)$$

where ϕ' is the osmotic coefficient in the H-O system and m_s is the molality of solute species s in the mixture of composition y', I' . We also have

$$w_p' = \partial(g_p I')/\partial I' \quad (4.8)$$

On comparison with (3.13) and (4.4) we find

$$w_0' = (I/I')w_0 + \partial(I'b_0)/\partial I' + \partial(I'e_0)/\partial I' - (I/I')(\partial \ln V(m, \pi)/\partial \ln I') \quad (4.9)$$

and similarly for w_1' . Then in view of (4.6) and the expected smallness of b_0 , e_0 , and $[V(m, \pi)/V(0,0)] - 1$ we expect

$$w_p \sim w_p'$$

Similarly, in view of (4.6), the Harned coefficients are approximately equal in the M-M and H-O systems.

5. Model and Approximation Method

It has been found that the hypernetted chain (HNC) integral equation, an approximation method for computing equilibrium properties of model systems, gives accurate results for charged-hard-sphere models for aqueous solutions of 1-1 electrolytes at concentrations up to 1 M^{10,16,18} as well as for charged hard-sphere-plus-square-well models for the same systems.^{16,19} The HNC method is found to work equally well for models using more realistic ion-ion potentials which are continuous functions of the interionic distance.²⁰ One such potential function, which has been investigated in some detail in relations to the thermodynamic properties of aqueous solutions of the alkali halides,²⁰ is employed in the present work. In all of these studies the McMillan-Mayer solution theory^{8,11} is exploited so that it is sufficient to specify only the potentials of the interionic forces for ions in the pure solvent. These potentials are assumed to be pairwise additive in the model described here, so it is sufficient to specify the potential for each pair of ionic species.

In the present work the model, which is discussed in greater detail elsewhere,²⁰ is characterized by ion-ion pair potentials of the form

$$u_{ij}(r) = COUL_{ij} + COR_{ij} + CAV_{ij} + GUR_{ij} \quad (5.1)$$

with the following definitions

$$COUL_{ij} = e_i e_j / \epsilon r \quad (5.2)$$

where e_i is the charge on an ion of species i and ϵ is the dielectric constant of the pure solvent.

$$COR_{ij} = B_{ij}/r^9 \quad (5.3)$$

is the core repulsion term. For $+-$ pairs B_{ij} is chosen so this same repulsive potential, together with the electrostatic lattice energy of the $+-$ salt crystal, gives the observed lattice spacing of the crystal.²¹ With this condition in mind B_{ij} may be expressed in terms of the sum of Pauling radii $r_+^* + r_-^*$. The same function is used to express B_{ij} in terms of $r_i^* + r_j^*$ even when i and j have the same sign. With this assumption on the form of B_{ij} the core potential used here passes over to the hard-sphere potential based on the sum of Pauling radii when one allows the exponent of r to increase from 9 to infinity.

$$CAV_{ij} = (1/2\epsilon r^4)[(\epsilon - \epsilon_c)/(2\epsilon + \epsilon_c)] \times (e_i^2 r_j^{*3} + e_j^2 r_i^{*3}) \quad (5.4)$$

(18) P. N. Vorontsov-Veliaminov, A. M. Eliashovich, J. C. Rasaiah, and H. L. Friedman, *J. Chem. Phys.*, **52**, 1013 (1970).

(19) J. C. Rasaiah, *ibid.*, **52**, 704 (1970).

(20) P. S. Ramanathan and H. L. Friedman, in preparation.

(21) L. Pauling, "Nature of the Chemical Bond," Cornell University Press, Ithaca, N. Y., 1960.

is a repulsive term in the potential accounting for the fact that each ion i and j occupies a cavity of dielectric constant $\epsilon_c \sim 2$ and radius r_i^* in the solvent medium.^{8,22}

$$GUR_{ij} = A_{ij} V_w^{-1} V_{mu}(r_i^* + w, r_j^* + w, r) \quad (5.5)$$

is the "Gurney" term, accounting for the contribution of overlapping cospheres to the ion-ion interaction.²³ Here A_{ij} is a coefficient which is treated as an adjustable parameter; the only parameter in the model which is adjusted on the basis of comparison with experimental data for electrolyte solutions. V_w is the mean volume of a solvent molecule; the molar volume divided by Avogadro's number. $V_{mu}(x, y, r)$ is the mutual volume (overlapping volume) of a sphere of radius x with one of radius y when the distance between their centers is r . The "cosphere thickness" w is taken as 2.76 Å, the diameter of a water molecule. If one adopts the simple view that, as two ions get closer together in the region of separation in which their cospheres are intersecting, the cosphere solvent which is displaced in this process returns to the normal state, solvent in cosphere \rightarrow solvent in normal pure state, then A_{ij} is the molar free-energy change in this process.

A model of this kind does not completely neglect the molecular nature of the solvent, which enters not only in the parameter ϵ but also in the parameters w and A_{ij} . However it does neglect effects which make the potential of interaction of three ions different from the sum of the three pair potentials, as well as still higher order terms of this sort.⁸

In the studies of this model for solutions of a single electrolyte²⁰ it is found that one can fit the osmotic coefficient data for all the aqueous alkali halides up to 1 M within 0.005 in ϕ using a single set of Gurney coefficients A_{NaNa} , A_{NaCl} , A_{ClCl} , A_{KCl} , A_{KCl} , etc. Examples are shown in Figure 1 for the two electrolytes of special interest in the present study. While the disagreement of calculated and experimental ϕ is outside the error of the latter, it is felt that it is not worthwhile to seek better agreement by adjusting the parameters of this model because of the limitations of the model.²⁰

The HNC computer program,¹⁰ rewritten to make it applicable to models with continuous pair potential functions,²⁰ is easily extended to apply to solutions with more than two species of ions. The principal modifications are required in the part of the program in which various thermodynamic coefficients are computed from the pair correlation functions, *i.e.*, after the highly optimized part of the program which does the iterative part of the computation. The theory relating the thermodynamic coefficients to the pair correlation functions in mixtures is discussed above in sections 2 and 3, except for aspects which are the same as for solutions of a single electrolyte.¹⁰

It is found that the resulting HNC program for electrolyte mixtures works as well as the ones for single electrolytes although the mixtures require more core

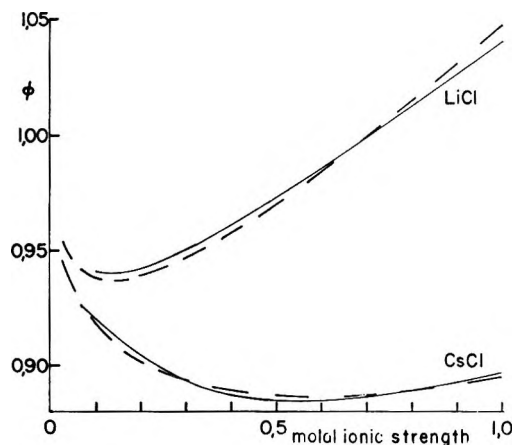


Figure 1. Osmotic coefficients for aqueous solutions at 25°: —, experimental, after R. A. Robinson and R. H. Stokes, "Electrolyte Solutions," Butterworths, London, 1955; ---, computed with Gurney coefficients given in Table I.

space and time of the computer. Typically, a computation for a particular set of parameters at one concentration requires about 2 min on an IBM 360/67 using $N = 512^4$ or 1 min on a CDC 6600 using $N = 1024$.

Applying this program to models for LiCl-CsCl mixtures, it is reasonable to retain the Gurney parameters which give good agreement with experiment for single electrolytes (Figure 1) and to seek agreement with the experimental data for mixtures by adjusting the Gurney parameter A_{LiCs} for the only interaction present in the mixtures which is absent in the unmixed solutions. A satisfactory fit is found for

$$A_{LiCs} = -200 \text{ cal/mol}$$

as shown in Figure 2 for w_0 values derived by eq 3.11.

The corrections needed to convert w_0' into w_0 have not been made, but from the earlier study⁷ of the corrections needed to convert g_0 into f_0 for this system it is found that the agreement of model and experimental results would be improved over that shown in Figure 2 if the appropriate corrections were included.

While it is regrettable that for this mixture the data do not extend below 2 M , this mixture was chosen because it exhibits a larger $|w_0|$ than the other alkali halide mixtures. This is important because it is found that in computations with models with smaller $|w_0|$ there are difficulties stemming from the numerical error in the computed w_0 being a sizable fraction of w_0 itself.

The computed w_0 exhibits the linear dependence on I (for $I > 0.5 M$) that is also shown by the experimental data for various systems. In view of eq 3.19 this is

(22) S. Levine and D. K. Rozenthal in "Chemical Physics of Ionic Solutions," B. E. Conway and R. G. Barradas, Ed., Wiley, New York, N. Y., 1966.

(23) R. W. Gurney, "Ionic Processes in Solution," Dover Publications, New York, N. Y., 1954.

(24) N is the number of points at which each $u_{ij}(r)$ and $g_{ij}(r)$ is sampled.¹⁰

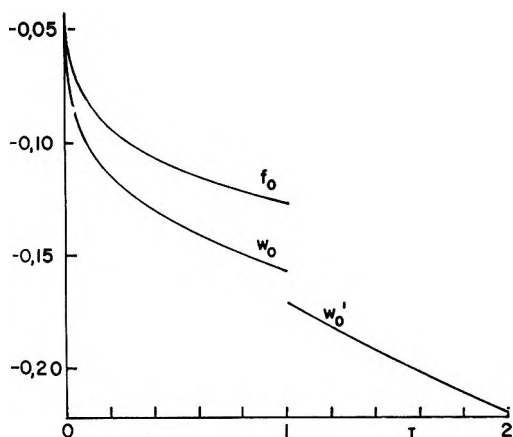


Figure 2. Mixing coefficients for aqueous LiCl-CsCl mixtures at 25°. w_0' , experimental values extrapolated below $I' = 2 M$ (data and extrapolated values tabulated by R. M. Rush, "Parameters for the Calculation of Osmotic and Activity Coefficients and Tables of These Coefficients for Twenty-Two Aqueous Mixtures of Two Electrolytes at 25°," Report ORNL-4402, Oak Ridge National Laboratory, Oak Ridge, Tenn., 1969; data from R. A. Robinson, *Trans. Faraday Soc.*, **49**, 1147 (1953)). f_0 , w_0 , computed with Gurney coefficients given in Table I.

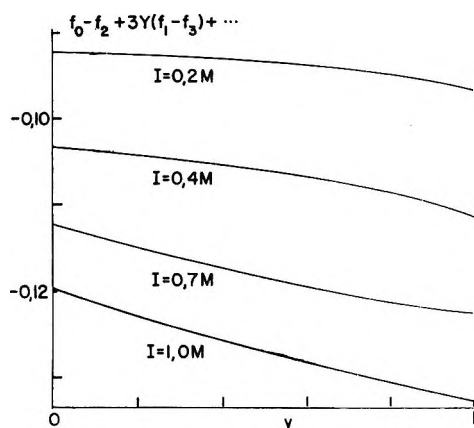


Figure 3. Plot of eq 3.10 for determination of f_p for the LiCl-CsCl model with Gurney coefficients given in Table I.

equivalent to the fourth regularity in the behavior of mixed electrolyte solutions described in the Introduction.

The f_0 values in Figure 2 are derived from eq 3.10. To do this one plots

$$-(g_{Ay} - g_{By})/2IkT$$

as shown in Figure 3 for several values of I . As this figure shows, f_1 is much smaller than f_0 and f_2 is barely significant for this model. For a somewhat similar model, when the computations were made with $N = 1024$ rather than $N = 512$ (see section 6), and carrying 13 significant figures rather than 7, f_0 and f_1 were almost unchanged while plots like those Figure 3 lost almost all curvature.

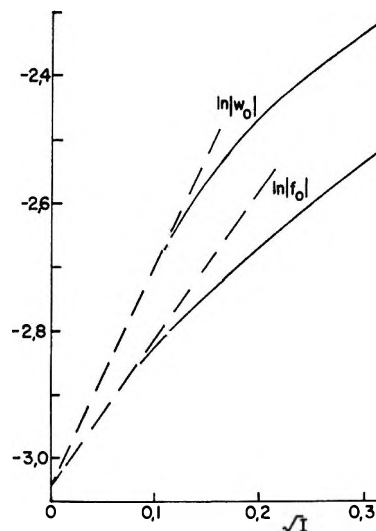


Figure 4. Mixture limiting law for model with coefficients in Table I. The $\ln |f_0|$ limiting law line ---- has slope $(8\pi N_a/V(0,0))^{1/2}(e_3^2/\epsilon kT)^{3/2} = 2.355$ where e_3 is the charge on a chloride ion.^{7,8} The slope of the $\ln |w_0|$ limiting law line is $^{3/2}$ as large, as determined by eq 3.13. The curves — represent the integral-equation results.

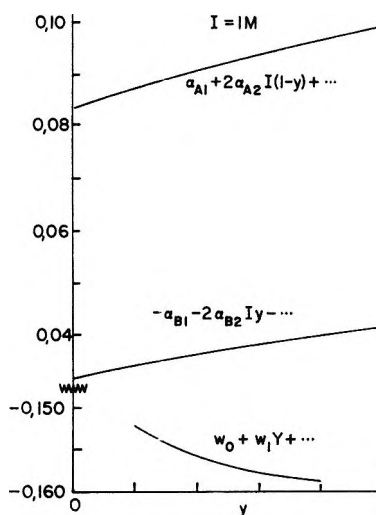


Figure 5. Harned rule plots (eq 3.4) for the determination of the Harned coefficients together with a plot of eq 3.15 for the determination of the w_p , all at $I = 1 M$ for the model in Table I.

At low I both w_0 and f_0 show curvature conforming to a mixture limiting law which has been described earlier.^{7,8} When plotted on a linear concentration scale this limiting law leads to infinite slopes with a common intercept for w_0 and f_0 at $I = 0$, as shown in Figure 2. To display the mixture limiting law one must plot $\ln |f_0|$ and $\ln |w_0|$ as shown in Figure 4. It seems clear from these figures that the approach to the mixture limiting law occurs at concentrations far below those at which the mixing coefficients may be determined by presently known experimental techniques. To some extent the HNC computations reflect the same

Table I: Gurney Coefficients for a Model for Aqueous LiCl–CsCl in Mixtures at 25°

<i>j</i>	A_{ij} , cal/mol		
	Li	Cs	Cl
Li	0	–200	50
Cs		–100	–110
Cl			0

$$\langle \Delta \rangle \equiv \sum c_i |\Delta_i| / \sum c_i \quad (6.1)$$

where Δ_i is the zeroth-moment defect about an ion of species i .¹⁶ For the systems studied in section 5, $\langle \Delta \rangle$ is in each case near 0.01. This is larger than found for similar computations for a single electrolyte, but a mixture model similar to the one discussed in section 5 was studied using a CDC computer (which carries 13 figures compared to 7 for the IBM 360/67) using $N = 1024$ (rather than $N = 512$ in section 5). These more

Table II: Computed Results for LiCl–CsCl Model

	I , molal ionic strength			
	0.2	0.4	0.7	1.0
f_0 , eq 3.10	–0.0938	–0.1065	–0.1185	–0.1270
f_1 , eq 3.10	+0.00064	+0.00117	+0.00175	+0.00217
f_2 , eq 3.10	0.000005	0.0	0.00007	+0.00014
α_{A1} , eq 3.4	0.1044	0.1009	0.0996	0.0993
α_{B1} , eq 3.4	–0.0551	–0.0447	–0.03689	–0.0318
α_{A2} , eq 3.4	–0.0238	–0.01448	–0.0099	–0.0077
α_{B2} , eq 3.4	–0.0179	–0.0104	–0.0067	–0.0049
w_0 , eq 3.11	–0.115	–0.129	–0.145	–0.157
w_0 , eq 3.13	–0.109	–0.127	–0.143	–0.154
w_0 , eq 3.15	–0.118	–0.135	–0.151	–0.162
w_0 , eq 3.19	–0.113	–0.129	–0.144	–0.155

difficulty: for models in which w_0 and f_0 are substantially smaller it is difficult to find whether the computed values are consistent with the limiting laws because the numerical errors become large compared to the effects which are sought!

The Harned coefficients may be obtained *via* eq 3.4 by plotting $g_{Ay}/4.606kTI$ and $g_{By}/4.606kTI$ as shown in Figure 5. These plots are the y derivatives of the plots discussed extensively by Harned and Owen.²⁵ Also shown in Figure 5 is a plot of eq 3.15 for the determination of the w_p . While in this example w_2 appears to be significant, we have neglected it because it is likely to be only numerical noise (*cf.* discussion of f_2 above).

The mixing coefficients for this one model (Table I) at several ionic strengths are shown in Table II.

6. Accuracy of Mixture Computations

As noted in section 3, the comparison of w_0 calculated from the correlation functions in various ways includes the familiar virial-compressibility self-consistency test as well as two others which do not appear for single electrolyte solutions. If one expresses the difference between the largest and smallest w_0 for given I in Table II as an error in ϕ (using eq 3.13), the resulting error in ϕ is 0.0002 at $I = 0.2 M$, 0.0003 at $0.4 M$, 0.0007 at $0.7 M$, and 0.001 at $1 M$. Judging by this test the computations seem quite satisfactory.

Another test is the zeroth moment condition.¹⁶ A suitable measure of this seems to be the quantity

accurate computations, made at many compositions at $I \leq 1 M$, gave $\langle \Delta \rangle = 0.0015 \pm 0.0010$ which is more in the range judged satisfactory for single electrolyte solutions. However the coefficients g_{Ai} , g_{Ay} , etc., were within 1% of those obtained for the same model using the IBM 360/67 with $N = 512$. Therefore it seems that more refined calculations would reduce $\langle \Delta \rangle$ while not significantly changing the results in section 5.

Similar remarks would seem to apply to the second-moment condition,¹⁶ here defined as the vanishing of the quantity

$$\langle \Delta' \rangle \equiv |\sum c_i z_i^2 \Delta_i| / \sum c_i \quad (6.2)$$

where Δ_i' is the second-moment defect about an ion of species i . In the computations reported in section 5 this ranged from 0.03 at $0.2 M$ to 0.16 at $1 M$, while in the better CDC computations it ranged from 0.03 at $0.2 M$ to 0.008 at $1 M$.

Additional information concerning the significance of the Δ and Δ' tests is given in the report on single electrolyte solutions.¹⁶

7. Computations for Other Models

A computation was made for a model for aqueous LiI–CsI mixtures using $A_{LiI} = 45$ cal/mol, $A_{CsI} = -135$ cal/mol, and the other Gurney coefficients the same as those in Table I. These Gurney coefficients give a good fit for the single electrolytes LiI and CsI.²⁰

(25) See, for example, Figure 14-5-1 in ref 2.

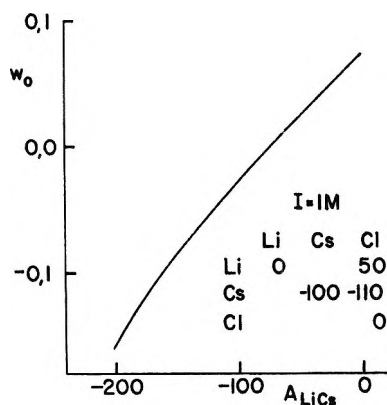


Figure 6. Variation of w_0 with change in Gurney coefficient at $I = 1 M$ for the model in Table I except for the change in the specified Gurney coefficient.

The f_0 computed for this model is the same within 2% from 0.2 to 1 M as that in Table II. Thus these computations reproduce Young's rule. This has been found for other models as well.

Computed results for w_0 for models like that in Table I except for the variation of a single Gurney coefficient are shown in Figures 6 and 7. The nearly linear form of these graphs for A_{ij} not too large seems to be a general feature of models based on eq 5.1. (For single electrolytes the linearity appears in ϕ as a function of one A_{ij} .) This feature makes it quite easy to adjust the Gurney coefficients to improve the agreement of computed and experimental thermodynamic coefficients. However it also implies that the effects produced by the various Gurney coefficients in a model are so similar that it is impossible to find a unique set of Gurney parameters which gives a best fit.

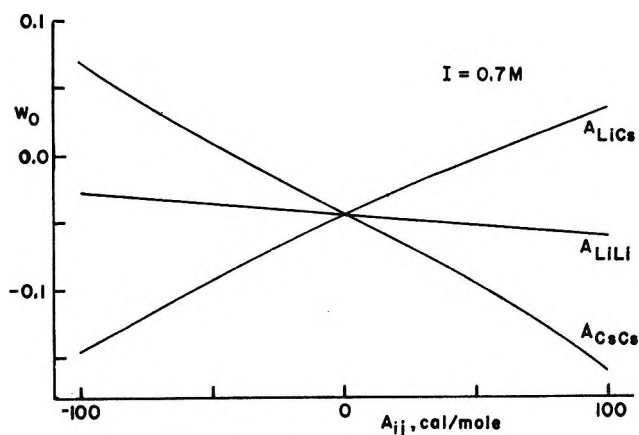


Figure 7. Variation of w_0 with change in specified Gurney coefficient at $I = 0.7 M$ for models in which the unspecified Gurney coefficients are fixed as follows: $A_{LiLi} = A_{LiCs} = A_{CsCs} = A_{ClCl} = 0$; $A_{CsCl} = -135$, and $A_{LiCl} = 50$ cal/mol. The model with these fixed coefficients also fits the data for the single electrolyte solutions.

The small slope of A_{LiLi} relative to the others in Figure 7 is just what is expected on the basis of the relatively small volume of the cosphere of Li^+ and the higher electrostatic repulsion at overlap separations for such small ions.

Acknowledgment. It is a pleasure to express our gratitude to the Computing Center at Los Alamos Scientific Laboratory and to Dr. A. H. Zeltmann of Los Alamos for assistance and use of facilities for the computations done with a CDC 6600 machine. We are also indebted to Mr. M. D. Weiser for invaluable programming assistance at Stony Brook.

Ultrasonic Relaxation in Manganese Sulfate Solutions¹

by LeRoy G. Jackopin² and Ernest Yeager

Department of Chemistry, Case Western Reserve University, Cleveland, Ohio 44106 (Received March 2, 1970)

A two-step, three-state association-dissociation model has been used to interpret the ultrasonic absorption data for manganese sulfate in aqueous solution, combining data obtained in the present work with literature data. The relaxation parameters have been calculated by a weighted nonlinear regression method from the experimental data with the nonrelaxational portion of the absorption treated as an additional parameter to be evaluated rather than assuming the value to be that of pure solvent. This two-step model accounts for the experimental results within the limits of accuracy of the data with no need to invoke a third step. The intermediate state in this two-step model is pictured as consisting of a number of specific configurations all in rapid equilibrium with the barrier heights for conversion from one into the other not much higher than those for the elementary diffusion process for the ions.

Introduction

Renewed interest has been expressed in ultrasonic relaxation in various divalent and trivalent sulfate solutions with the appearance of several papers²⁻⁵ providing additional ultrasonic absorption data, particularly at frequencies in the 10^8 - 10^9 -Hz range. These data have been interpreted in these papers on the basis of a multistep association-dissociation of the cations and anions similar to that proposed by Eigen and Tamm,⁶ but questions still remain concerning the number of relaxational processes and the assignments of the eigenfrequencies and corresponding relaxational absorption magnitudes. A three-step model has been used to explain the ultrasonic data for manganese sulfate and other divalent sulfates by Atkinson and Kor,⁷⁻⁹ Hemmes, Fittipaldi, and Petrucci,⁴ Tamm,³ and Fritsch, *et al.*⁵ All of these groups with the exception of Hemmes, *et al.*, report three relaxation peaks, two of which are quite pronounced and a third much less pronounced at frequencies intermediate to the other two. A relaxation peak at such intermediate frequencies was not observed for manganese sulfate in aqueous solutions by Hemmes, *et al.*,⁴ and Jackopin and Yeager¹⁰ or in a 25 wt % dioxane-water solution by Jackopin and Yeager. In the latter, Atkinson and Kor⁷ obtained data for MnSO_4 showing a discernible, nonrelaxationally shaped absorption peak.

Earlier workers^{7,11,12} reported the low-frequency relaxation to be at 3 MHz in aqueous manganese sulfate solutions. Jackopin and Yeager,¹⁰ however, found a value of 5 MHz, which was later substantiated by Tamm.³ Considerable discrepancy also exists among the values reported^{3,4,9} for the high frequency relaxation with the values generally falling in the range from 150 to 650 MHz for relatively dilute (0.05 to 0.2 M) manganese sulfate solutions and even higher for more concentrated solutions of other divalent sulfates, according to the results of Plass and Kehl.¹³ These workers examined the ultrasonic absorption in various

sulfate solutions at frequencies above 300 MHz by an ultrasonic technique that yielded directly the excess or difference absorption relative to water. They found a relatively broad relaxation peak (relative to water) for such divalent sulfates as CuSO_4 and MnSO_4 . They interpreted the data for CuSO_4 in three ways. (a) The observed high frequency broad peak (relative to water) may correspond to a distribution of relaxation frequencies. An average relaxation frequency was estimated which had an approximate linear concentration dependence. (b) The broad peak (relative to water) may be due to two relaxation curves. (c) The broad peak may correspond simply to a single relaxation process with the nonrelaxational absorption of the solution deviating from the absorption of pure water. For this interpretation Plass and Kehl treated α_{nr}/f^2 as a parameter to be adjusted so as to best fit a single relaxation to their high frequency data. The value of α_{nr}/f^2 so obtained was a few per cent higher than α_w/f^2 . This latter procedure appears the best since it avoids any assumption concerning the nonrelaxational absorption and has been used in the present work.

(1) Portions based on a dissertation by L. G. Jackopin submitted to the Graduate School, Case Western Reserve University, in partial fulfillment of the requirements for the Ph.D. degree, June 1969.

(2) Present address: Chemistry Department, University of Southampton, England.

(3) K. Tamm, "Reports of the 6th International Congress on Acoustics," Paper GP-3-3, Tokyo, 1968.

(4) P. Hemmes, F. Fittipaldi, and S. Petrucci, *Acustica*, **21**, 228 (1969).

(5) K. Fritsch, C. J. Montrose, J. L. Hunter, and J. F. Dill, *J. Chem. Phys.*, in press.

(6) M. Eigen and K. Tamm, *Z. Elektrochem.*, **66**, 93, 107 (1962).

(7) G. Atkinson and S. K. Kor, *J. Phys. Chem.*, **69**, 128 (1965).

(8) G. Atkinson and S. K. Kor, *ibid.*, **70**, 314 (1966).

(9) G. Atkinson and S. K. Kor, *ibid.*, **71**, 673 (1967).

(10) L. G. Jackopin and E. Yeager, *ibid.*, **70**, 313 (1966).

(11) G. Kurtze and K. Tamm, *Acustica*, **3**, 33 (1952).

(12) J. R. Smithson and T. A. Litovitz, *J. Acoust. Soc. Amer.*, **28**, 462 (1956).

(13) K. G. Plass and A. Kehl, *Acustica*, **20**, 360 (1968).

These uncertainties with respect to the ultrasonic relaxation phenomena in divalent sulfates have prompted a reexamination of ultrasonic relaxation in such electrolytes. Manganese sulfate has been chosen as the test system since the low as well as high frequency relaxation for this electrolyte is relatively accessible with conventional ultrasonic techniques. The data obtained in the authors' laboratory^{10,14} together with that reported by Plass and Kehl¹³ have been combined and treated with weighted nonlinear regression data processing techniques.¹⁴

Experimental Section

Ultrasonic absorption measurements¹⁴ have been made at 0.75 to 15 MHz with a Carstensen¹⁵ type apparatus designed to minimize diffraction errors. A conventional send-receive apparatus¹⁴ involving pulse modulated ultrasonic waves with a variable acoustic path has been used from 5 to 95 MHz with application of the diffraction correction of Seki, *et al.*¹⁶ Care was exercised to ensure proper electrical impedance matching, particularly of the calibrated attenuator.

Processing of Data

The absorption coefficients α have been computer calculated from the observed attenuator readings at various distances. The usual least-squares method was used since the standard deviation σ of the attenuation measurement was relatively large in comparison with the standard deviation of the distance measurement. The measured value for α_s/f^2 for water over the frequency range 15–95 MHz (with diffraction corrections) at 25° was 21.16×10^{-17} nep sec²/cm with $2\sigma = 0.11 \times 10^{-17}$ nep sec²/cm for 14 determinations while for 25 wt % dioxane–water the value was 24.43×10^{-17} nep sec²/cm with $2\sigma = 0.14 \times 10^{-17}$ nep sec²/cm for 16 determinations.

The difference or excess relaxational absorption can be calculated¹⁷ with respect to the classical absorption due to shear viscosity and heat conduction. Meixner¹⁸ showed that to a first approximation the individual absorption contributions are additive. For the case of solutions the excess absorption often has been calculated conveniently with respect to the solvent absorption. In the present work the difference absorption was calculated relative to the nonrelaxational absorption as

$$\Delta\alpha = \alpha_t - \alpha_{nr} \quad (1a)$$

$$\Delta\alpha/f^2 = (\alpha_t/f^2) - (\alpha_{nr}/f^2) \quad (1b)$$

$$\mu_r = (\Delta\alpha/f^2)fv = (\Delta\alpha)\lambda \quad (2)$$

where $\Delta\alpha$ is the excess or difference absorption coefficient, μ the absorption per wavelength, f the frequency, v the velocity in the solution, and λ the wavelength of the solution. The subscripts have the following meaning: t, total; r, relaxational; nr, nonrelaxational; s, solvent; and w, water. The nonrelaxational absorp-

tion of a solution can be obtained at frequencies sufficiently high compared to the relaxation frequency. Data have generally been lacking at sufficiently high frequencies in the 2–2 electrolytes. The measurements of Plass and Kehl¹³ at 3 GHz were for relatively concentrated solutions of some divalent sulfates but not manganese sulfate, and these workers were not able to obtain a value for α_{nr}/f from their data without assumptions concerning the nature of the relaxation peaks (as described earlier). Fritsch, *et al.*,⁵ made measurements on more dilute solutions including divalent sulfates but not manganese sulfate at 6 to 7 GHz using Brillouin scattering, but the accuracy is only a few per cent—apparently short of that necessary to establish α_{nr}/f^2 with sufficient precision to resolve the question of whether there are two or three relaxation peaks.

Most workers have approximated α_{nr}/f^2 by using the solvent value (α_s/f^2). The electrolyte, however, modifies the structure of the solvent and the structural relaxation time of the solvent. Even a 1% deviation of α_{nr}/f^2 from α_s/f^2 can seriously disturb the μ_r values and give the illusion of an extra relaxation peak. Tamm³ has attempted to avoid this dilemma by assuming that the 2–2 electrolytes modify the solvent absorption by the same percentage as they modify the shear viscosity. He has attempted to substantiate this assumption by correlating the absorption changes produced by 1–1 electrolytes in water with the corresponding shear viscosity changes. Even so, it is still not clear whether this approach is sufficiently quantitative to avoid misleading conclusions concerning the existence of the intermediate relaxation frequency.

In the present work the α_{nr}/f^2 parameter and the relaxational parameters μ_j (maximum excess absorption per wavelength at the relaxation frequency) and f_j (relaxation frequency) were obtained by means of the equation

$$\mu_r = 2\sum_j [\mu_j f_j / (f^2 + f_j^2)] = \mu_t - (\alpha_{nr}/f^2)(fv) \quad (3)$$

for a double relaxation ($j = 2$). This equation presupposes small velocity dispersion. A weighted nonlinear regression method¹⁹ involving a Taylor expansion has been utilized. Iterative-type computer programs for up to five parameters [two sets of relaxation parameters plus (α_{nr}/f^2)] have been developed. The weighting factor has been taken as inversely propor-

(14) L. G. Jackopin, Ph.D. Thesis, Chemistry, Case Western Reserve University, Cleveland, Ohio, 1969; L. G. Jackopin and E. Yeager, Technical Report 35, Office of Naval Research Contract Nonr 1439(04), Project NR 384-305, Case Western Reserve University, Cleveland, Ohio, June 1969.

(15) E. L. Carstensen, *J. Acoust. Soc. Amer.*, **26**, 858 (1954).

(16) H. Seki, A. Granato, and R. Truell, *ibid.*, **28**, 230 (1956).

(17) K. F. Herzfeld and T. A. Litovitz, "Absorption and Dispersion of Ultrasonic Waves," Academic Press, New York, N. Y., 1959, Chapters 1 and 2.

(18) J. Meixner, *Acustica*, **2**, 1(1) (1952).

(19) A. G. Worthing and J. Jeffner, "Treatment of Experimental Data," Wiley, New York, N. Y., 1950.

tional to the variance.¹⁹ Such a weighting procedure is particularly advantageous when combining data from different sources (*e.g.*, different workers, different apparatus).

Other workers have fitted their data to an equation for either α/f^2 or f/μ_r (the Mikhailov²⁰ technique) and then determined the relaxation parameters μ_j and f_j by the graphical method or by a least-squares method. In general, the use of these different equations gives a different implicit weighting to the data, and care must be exercised to see that such weighting effects do not improperly weight the data. Unfortunately many authors have not taken such into account.

Results

The ultrasonic difference absorption values relative to the solvent, *i.e.*, $(\alpha_t - \alpha_s)\lambda$, at 25° are given in Figure 1 for 0.101 *M* MnSO₄ in water and in Figure 2 for 0.050 *M* MnSO₄ in 25 wt % dioxane-water. The precision varied over the frequency range but fell within the dimensions of the points unless otherwise indicated in these figures.

The weighted nonlinear regression technique was applied to the composite data set of Plass and Kehl¹³ and the present work in aqueous solutions. Unfortunately the data of Plass and Kehl are at 20° while those of the present study are at 25°. The combination of the two sets of data is necessary since neither alone covers a sufficiently wide range of frequencies to permit a reasonably reliable computer calculation of the relaxation parameters for a multistep process. The resulting error in the relaxation parameters is believed to be smaller than introduced by errors in the actual absorption measurements, however, on the basis of the observed temperature dependence for the absorption of MgSO₄ solutions of comparable concentrations at frequencies above 200 MHz, found in other work.²¹

The simplest model—a double relaxation with nonrelaxational absorption different from the solvent—was assumed. The five corresponding parameters were computed, and the results are: nonrelaxational absorption, $(\alpha_{nr}/f^2) = 21.86 \times 10^{-17}$ nep sec²/cm; low relaxation frequency, $f_I = 4.91$ MHz, $\mu_I = 1.36 \times 10^{-3}$ nep; high relaxation frequency, $f_{II} = 266$ MHz, $\mu_{II} = 1.42 \times 10^{-3}$ nep. The excess absorption per wavelength relative to the nonrelaxational value just listed is represented by the solid points in Figure 1. The solid curve has been computed from these five parameters and is to be compared with the solid points. The solid points fall on the curve in all instances within the precision of the experimental data. This includes the 1.5-GHz datum point which falls way off the curve but for which the error limits would still encompass the curve. On this basis one can conclude that two chemical relaxation processes are sufficient to explain the absorption data within the error range and that the postulation of

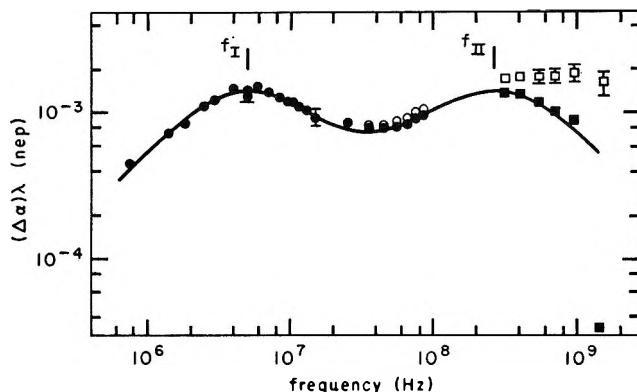


Figure 1. Excess ultrasonic absorption of 0.1 *M* manganese sulfate solution from 0.75 MHz to 1.5 GHz. Open points: excess absorption per wavelength of solution relative to water, $(\alpha_t - \alpha_w)\lambda$; solid points: relative to the nonrelaxational value of solution calculated on the basis of a double relaxational model with a weighted nonlinear regression method, $(\alpha_t - \alpha_{nr})\lambda$. O, ●—present work at 25°; □, ■—Plass and Kehl¹³ at 20°. Error limits are smaller than points unless otherwise indicated.

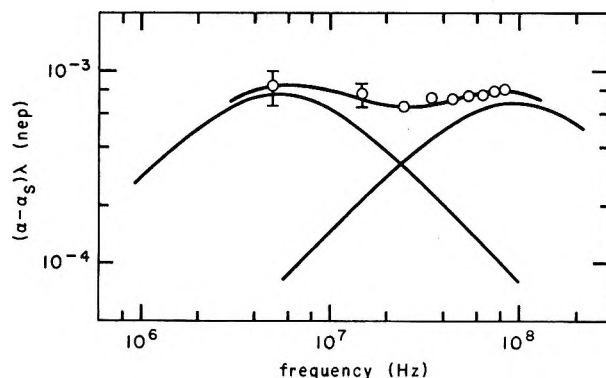


Figure 2. Excess ultrasonic absorption per wavelength for 0.05 *M* manganese sulfate in 25 wt % dioxane-water at 25° relative to the absorption of the solvent. The component relaxation curves were calculated for a double relaxation model by a weighted nonlinear regression method with the absorption of the solvent taken as the nonrelaxational component. Error limits are smaller than points unless otherwise indicated.

a third relaxation apparently is not necessary and is not justified experimentally.

If the nonrelaxational absorption is approximated as that of pure water (*i.e.*, $\alpha_{nr}/f^2 = \alpha_w/f^2$), at least three relaxation components are required to represent the data, corresponding to the open points in Figure 1, as has been found necessary by previous workers in the treatment of their data. The difference between α_{nr}/f^2 from the present treatment and α_w/f^2 is only 3%, and yet this small amount is sufficient to require a third

(20) I. G. Mikhailov, *Dokl. Akad. Nauk SSSR*, **89**, 991 (1953).

(21) L. Goldfarb, Ph.D. Thesis, Chemistry, Case Western Reserve University, Cleveland, Ohio, 1968; L. Goldfarb and E. Yeager, Technical Report 32, Office of Naval Research Contract Nonr 1439-(04), Project NR 384-305, Case Western Reserve University, Cleveland, Ohio, Jan 1968.

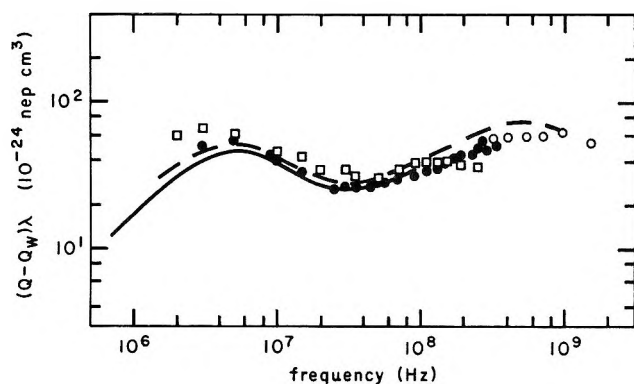


Figure 3. Absorption cross section per wavelength of manganese sulfate solutions relative to that of pure water, as determined by various workers since 1965. \square , Atkinson and Kor,⁹ 0.05 *M*, 25°; \circ , Plass and Kehl,¹³ 0.10 *M*, 20°; \bullet , Hemmes, Fittipaldi, and Petrucci,⁴ 0.20 *M*, 25°; -- Tamm,³ 0.10 *M*, 20° (the curve shown for Tamm's data was obtained by summing the three-component relaxation curves); —, present work, 0.10 *M*, 25°.

relaxation component for interpretation of the data treated in this manner.

The data of various authors for the excess absorption of MnSO_4 solutions relative to water are compared in Figure 3, using the absorption cross section Q defined as

$$Q = 2\alpha/C_oL \quad (4)$$

where C_o is the overall concentration of the electrolyte producing the relaxational absorption and L is the Avogadro number. The recent results of Tamm³ have been included even though they are relative to a non-relaxational value for the solution estimated from shear viscosity measurements and not relative to pure water. At frequencies below 50 MHz, the difference is less than the dimensions of the points. Tamm does not give the data for this manganese sulfate solution in his publication but rather just specifies the three relaxation frequencies and corresponding μ_j values. The summation of these three relaxation components has been plotted in Figure 3. Also shown is the smooth curve for the results obtained in the present work (open data points in Figure 1).

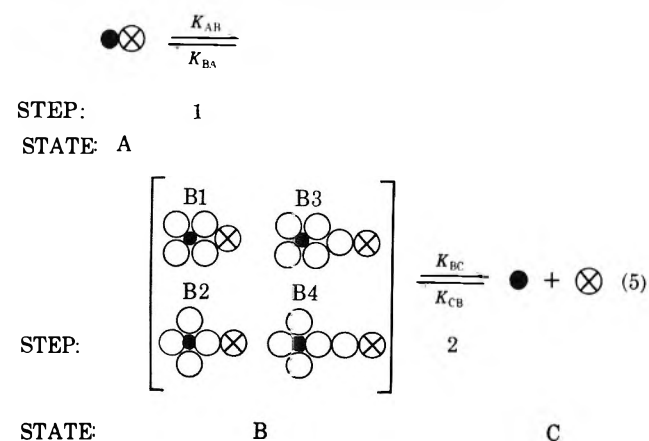
The data of Hemmes, *et al.*,⁴ Tamm,³ and the present study indicate that the low relaxation frequency is at ~ 5 MHz rather than 3 MHz as reported in earlier papers.^{7,11,12} This relaxation frequency should have only a relatively small concentration dependence at the concentrations used for the data in Figure 3, according to the model for the relaxation processes discussed later in this paper. To a first approximation there appears to be agreement among most of the data except in the diffraction region and at the frequency extremes of the different apparatus.

Data for the excess absorption per wavelength relative to solvent for 0.05 *M* MnSO_4 in 25 wt % dioxane-water (Figure 2) are available over a too limited range

to permit the evaluation of four relaxation parameters plus the nonrelaxational absorption. The weighted nonlinear regression method, however, was applied to these results assuming two relaxation frequencies and using the observed solvent absorption as an approximation to the nonrelaxational component. The relaxational components so calculated together with the summation value of the excess absorption per wavelength calculated from them are plotted in Figure 2. At best, these components can only be considered semiquantitative. Nevertheless, no need is evident for the postulation of a third relaxation at frequencies intermediate to the low and high components.

Interpretation of Results

The two ultrasonic relaxation processes are believed to be represented by the following reaction mechanism



where the solid circles represent the Mn^{2+} cation, the open circles the oxygen of the water molecules, and the circles with a cross one of the four oxygen atoms of the sulfate anion. Hydrogen atoms and most of the oxygen atoms of the hydration water molecules are not shown.

State B is a collection of states which are believed to be in rapid equilibrium, some of which are represented in eq 5. The water molecules of a hexahydrated cation can be represented in three dimensions at each face of a cube. Only the four planar water molecules in the inner coordination sphere of the Mn^{2+} cation are shown. In state B1 one sulfate oxygen is in the outer coordination sphere of the Mn^{2+} cation and is situated at the corner of the cube. In state B2 a sulfate oxygen is hydrogen bonded to an inner coordination sphere water molecule of the cation but is not in the outer coordination sphere of the cation. In state B3 an oxygen in the outer coordination sphere of the Mn^{2+} ion is directly hydrogen bonded to an oxygen of a SO_4^{2-} ion. In state B4 the inner hydration sheaths of both the Mn^{2+} and SO_4^{2-} ions are still intact, and none of the water in the outer coordination sphere of the Mn^{2+} is hydrogen bonded directly to an oxygen of the SO_4^{2-} ion. The interconversions of these four states and other less definable states are believed by the authors to be characterized by barrier heights comparable to those involved

in rotation of the hydrated ions and not much higher than those for diffusion. State B1 is probably the closest approach of the two ions before a barrier is reached which is substantially higher than that for diffusion, and consequently states B4 to B2 may be considered as just stages in the diffusional approach together of the two ions. Under such circumstances the treatment of the conversion from state B4 into state B1 as a separate process from the overall diffusional approach of the two ions is very questionable. On these grounds the authors prefer the three-state model represented by eq 5 for the treatment of the relaxational data to the four-state model of Eigen and Tamm,⁶ which treats the two encounter complexes with one water molecule and with two water molecules interspersed between the cation and anion as separate states.

The kinetic and thermodynamic quantities for the two steps corresponding to eq 5 have been calculated from the relaxation parameters as follows. The overall dissociation constant K_d is given by

$$K_d = C_C^2 \gamma_{\pm}^2 / (C_A + C_B) \quad (6)$$

where γ_{\pm} is the mean ionic activity coefficient, C_A and C_B are the concentrations of states A and B, respectively, and C_C is the concentration of state C which is taken as equal to the free cation concentration (C_m). The activity coefficient has been calculated from the semiempirical Davies²² equation (at 25°)

$$\log \gamma_{\pm} = 0.5z_m z_a [I^{1/2} / (1 + I^{1/2}) - 0.3I] \quad (7)$$

where I is the ionic strength and z_m and z_a are the charges of the cation and anion, respectively. The activity coefficients of the uncharged complexes and the water molecules were taken as unity. An iteration technique was used to calculate the C_C , $(C_A + C_B)$, and γ_{\pm} values with the average overall dissociation constant of $6.11 \times 10^{-3} M$ selected from three tabulated values.²³

The equilibrium constant for step 2 has been calculated from the Debye-Fuoss equation²⁴

$$K_{CB} = 4\pi L a^3 \{ \exp[-z_m z_a e^2 / (a\epsilon kT)] \} / 3000 \quad (8)$$

where a is the separation distance between charge centers in the ions, ϵ is the dielectric constant, e is the elementary charge, k is the Boltzmann constant, and T is the temperature. This equation is based on a continuum dielectric model and is not reliable for charge separation distances comparable to the ionic or molecular dimensions. It does not take into account dielectric saturation. Nevertheless most workers have made use of it. The charge separation distances in the four B states, estimated from bond and van der Waals radii, are 5.5 to 9.2×10^{-8} cm. It is relatively difficult to determine the proper distance to use. Consequently, calculations were made for a range of charge encounter separation distances using the dielectric constant of bulk water.

The equilibrium constant K_{AB} was calculated from

$$K_d = K_{AB} K_{BC} / (1 + K_{AB}) \quad (9)$$

and used to calculate C_A and C_B .

The high frequency relaxation is attributed to the diffusion-controlled formation of state B from the free ions (step 2). The equations used for this step take the form¹⁴

$$2\pi f_{II} = 1/\tau_{II} = \gamma_{\pm}^2 k_{CB} C_C^2 F(C_B, C_C) \quad (10)$$

where

$$F(C_B, C_C) = (1/C_B) + (2/C_C) + 2(\partial \ln \gamma_{\pm} / \partial \xi_2) \quad (10a)$$

$$k_{CB} = K_{CB} k_{BC} \quad (10b)$$

$$\mu_{II} = \pi \rho v^2 (\Delta V_{BC})^2 / [2RT F(C_B, C_C)] \quad (11)$$

and ρ is the density and ξ_2 is the reaction variable of de Donder,²⁵ which indicates the instantaneous extent of reaction for step 2. Equations 10, 10a, 10b, and 11 were used to calculate k_{CB} , k_{BC} , and ΔV_{BC} from the experimental data.

The quantities k_{BA} , k_{AB} , and ΔV_{AB} were calculated by means of the additional equations¹⁴

$$2\pi f_I = 1/\tau_I = k_{AB}(1 + K_{AB} k_{CB}' \tau_{II}) \quad (12)$$

$$k_{CB}' = \gamma_{\pm}^2 k_{CB} C_C^2 [(2/C_C) + 2(\partial \ln \gamma_{\pm} / \partial \xi_2)] \quad (12a)$$

$$\mu_I = \pi \rho v^2 (\Delta V_I)^2 k_{AB} C_A \tau_I / (2RT) \quad (13)$$

$$\Delta V_I = \Delta V_{AB} + \Delta V_{BC} k_{BC} \tau_{II} \quad (13a)$$

These equations result from a normalized coordinate treatment²⁶ of a two-step process with the assumption that $\tau_I \gg \tau_{II}$. Only the normalized reaction volume change has been included in eq 11 and 13 since the temperature perturbation associated with the propagation of sound through water and relatively dilute aqueous solutions is relatively small. The signs of the volume change ΔV_{AB} and the normalized reaction volume change ΔV_I were chosen on the basis of electrostriction considerations (*i.e.*, ΔV_{AB} , ΔV_{BC} should be both negative).

If adequate ultrasonic data were available over a range of concentrations, the rate constants could be obtained from the concentration dependence of the relaxation frequencies without the need for the Debye-Fuoss equation. Unfortunately such is not possible with the limited reliable data now available. To obtain such data will require measurements in more con-

(22) C. W. Davies, "Ion Association," Butterworths, London, 1962, Chapter 2.

(23) L. G. Sillén and A. E. Martell, "Stability Constants of Metal-Ion Complexes," 2nd ed, Special Publication 17, The Chemical Society, London, 1964.

(24) R. M. Fuoss, *J. Amer. Chem. Soc.*, **80**, 5059 (1958).

(25) T. de Donder and P. Van Rysselberghe, "Thermodynamic Theory of Affinity," Stanford University Press, Stanford, Calif., 1936.

(26) For details of the generalized treatment of a two-step reaction mechanism and the specific treatment of the mechanism corresponding to eq 5, see ref 14.

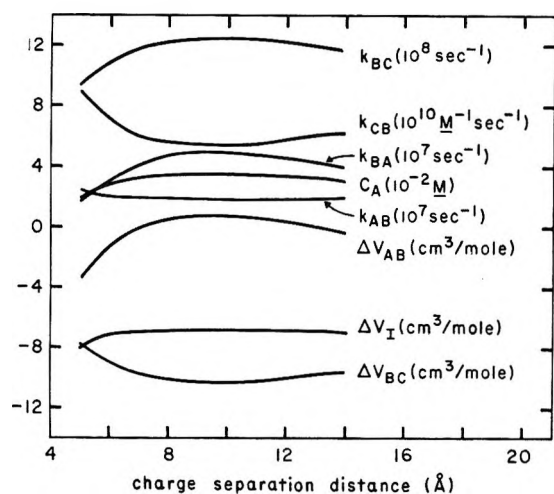


Figure 4. The dependence of the calculated values of the rate constants, reaction volume changes, and concentration of the inner sphere complex as a function of the charge separation distance for state B.

concentrated solutions than used in the present study since the accuracy is too limited in more dilute solutions. Activity corrections of the type represented by the γ_{\pm}^2 term in eq 10, however, are very dubious in relatively concentrated solutions. In principle, it is not correct to develop a relaxational treatment of the second-order diffusion-controlled formation of an encounter complex of two ions while ignoring the perturbation of the ionic atmosphere and the ionic fluxes within the ionic atmosphere, and then to append a correction for ionic atmosphere effects, based on equilibrium considerations. In a sense, the encounter complex corresponds to a limiting distance of approach within the ionic atmosphere concept. A simultaneous treatment of ionic atmosphere relaxation and chemical relaxation is needed and seems possible but remains to be done.

The results of these calculations are given in Figure 4 as a function of the charge separation distance corresponding to state B. The tendency for maxima or minima in these plots arises because the Debye-Fuoss equation for the association constant K_{CB} (eq 8) passes through a minimum with decreasing distance provided dielectric saturation effects are ignored. The calculated rate constants are relatively insensitive to the charge separation distance particularly for values greater than 6 or 7 Å. The values of the rate constants and volume changes are given in Table I for the separation distance of 5.5 Å corresponding to the closest approach for state B (outer coordination sphere). The rate constant (k_{BA}) for the formation of the inner coordination sphere complex, corresponding to state A, compares favorably with the independently obtained nmr value²⁷ of $2.5 \times 10^7 \text{ sec}^{-1}$ at 25° for the removal of a water molecule from the inner coordination sphere. Such is to be expected since the introduction of a ligand such as SO_4^{2-} into the inner coordination sphere of Mn^{2+} proceeds probably through an $\text{S}_{\text{N}}1$ mechanism.

Table I: Rate Constants and Reaction Volume Changes for Aqueous Manganese Sulfate Solution

A. Present study: Two-step model (0.10 M MnSO_4 , 25°)			
A \rightleftharpoons B \rightleftharpoons C			
\bar{k}	$2 \times 10^7 \text{ sec}^{-1}$	$10 \times 10^8 \text{ sec}^{-1}$	
\bar{k}	$2 \times 10^7 \text{ sec}^{-1}$	$8 \times 10^{10} \text{ M}^{-1} \text{ sec}^{-1}$	
$\Delta \bar{V}$	$-2 \text{ cm}^3/\text{mol}$	$-9 \text{ cm}^3/\text{mol}$	
B. Tamm ³ : Three-step model (0.50 M MnSO_4 , 20°)			
MA \rightleftharpoons MwA \rightleftharpoons MwwA \rightleftharpoons M + A			
\bar{k}	$2.2 \times 10^7 \text{ sec}^{-1}$	$3.7 \times 10^8 \text{ sec}^{-1}$	$2 \times 10^9 \text{ sec}^{-1}$
\bar{k}	$2 \times 10^7 \text{ sec}^{-1}$	$2.8 \times 10^9 \text{ sec}^{-1}$	$4 \times 10^{10} \text{ M}^{-1} \text{ sec}^{-1}$
$\Delta \bar{V}$	$-3.5 \text{ cm}^3/\text{mol}$	$+13.3 \text{ cm}^3/\text{mol}$	$-18.3 \text{ cm}^3/\text{mol}$

The signs of the volume changes are not revealed by the experimental data since the square of the volume changes are involved in the equations for μ_{I} and μ_{II} . Both ΔV_{BC} in eq 11 and ΔV_{I} in eq 13 were taken as negative in order to obtain signs for ΔV_{BC} and ΔV_{AB} consistent with what would be expected on the basis of electrostriction effects. The magnitude of the volume change for both steps seems reasonable, although ΔV_{AB} is perhaps somewhat smaller than might be expected for the introduction of a water molecule into the inner coordination sphere of Mn^{2+} .

Also listed in Table I are the values associated with the three-step, four-state model, as evaluated by Tamm³ from his ultrasonic absorption data for MnSO_4 . Tamm used the nmr value for the rate constant for the replacement of water by SO_4^{2-} in the inner coordination sphere of Mn^{2+} . In addition Tamm makes use of the Smoluchowski-Debye-Eigen equation²⁸ for the diffusional controlled rate constant. Tamm's procedure has the disadvantage of preventing any independent comparison of the ultrasonic results with the nmr results. Furthermore the use of the Smoluchowski-Debye-Eigen equation is at least as questionable and perhaps more so than the Debye-Fuoss equation. With Tamm's model and calculations, one of the ΔV terms must be of opposite sign to be consistent with his ultrasonic data and Tamm has taken this to be the ΔV term for the step $\text{MwA} \rightleftharpoons \text{MwwA}$. It is difficult to understand either the sign or large magnitude of this quantity on the basis of electrostriction effects.

Equations 6-13 permit the prediction of the concentration dependence of the ultrasonic relaxation parameters. These predictions are given in Figure 5 for a charge separation distance of 5.5 Å. The rate constants and reaction volume changes were assumed to be concentration independent. Unfortunately neither the present data nor the reliable literature data are sufficient to confirm all of these predictions. Further, it is relatively difficult to compare quantitatively the results

(27) T. J. Swift and R. E. Connick, *J. Chem. Phys.*, **37**, 307 (1962).

(28) M. Eigen, *Z. Phys. Chem. (Frankfurt am Main)*, **1**, 176 (1954).

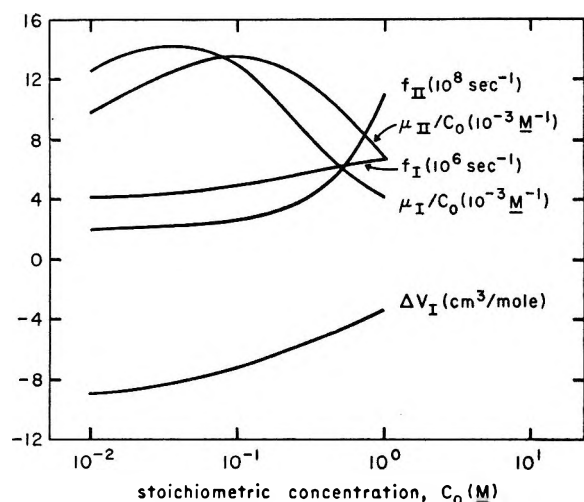


Figure 5. Predicted values for the ultrasonic relaxation parameters of the double relaxation model at various concentrations in aqueous manganese sulfate solutions at 25°.

and predictions of the present model—based on a double relaxation and five parameters—with the experimental results obtained from other models—based on a triple relaxation and six or seven parameters. The predicted concentration behavior of the low frequency relaxation parameters can be compared with the experimental results of Tamm³ since the high frequency effects due to the model and α_{nr}/f^2 are expected to be relatively small. There is relatively good agreement for the concentration dependence of f_I and μ_I in this

case. The relaxation frequency f_I has only a small concentration dependence and increases with increasing concentration. The quantity (μ_I/C_0) exhibits a large concentration dependence and decreases with increasing concentration in both cases. The present model predicts a maximum in this quantity whereas Tamm's experimental results decrease monotonically and somewhat less rapidly. The high frequency relaxation parameters can only be compared with the "peak" values (*i.e.*, the values at the peak of the broadened $(\alpha_t - \alpha_w)\lambda$ curve) of Plass and Kehl¹³ for cobalt sulfate solutions. The relaxation frequency f_{II} and f_{peak} increase linearly with the stoichiometric concentration. Plass and Kehl observed a maximum in $[(\alpha_t - \alpha_w)\lambda]_{peak}/C_0$ with respect to concentration which is in accord with the predicted behavior of the present model.

All things considered, it does not appear necessary to postulate a three-step, four-state model to explain ultrasonic relaxation data for $MnSO_4$ and probably not also for other divalent sulfates.

Acknowledgment. This research has been partially supported by the Office of Naval Research and the Office of Saline Water. The authors also express appreciation to the Harshaw Chemical Company, who provided a graduate fellowship to one of the authors (L. G. J.). The authors acknowledge the use of the computer facilities at Case Western Reserve University, Cleveland State University, and the University of Southampton.

Ionization of Moderately Strong Acids in Aqueous Solution.

I. Trifluoro- and Trichloroacetic Acids

by A. K. Covington, J. G. Freeman, and T. H. Lilley

Department of Physical Chemistry, School of Chemistry, University of Newcastle upon Tyne, England
(Received March 2, 1970)

The extent of ionization of trifluoro- and trichloroacetic acids has been studied by Raman and nmr spectroscopic methods. Acidity constants of between 4 and 9 and between 2 and 5 mol l.⁻¹, respectively, have been estimated. In spite of the uncertainties in such estimations the values are considerably higher than literature values obtained by indicator or conductance methods. This finding can be explained by assuming that the dissociation of an acid takes place in two stages, ionization followed by dissociation of an ion-pair species, and that different experimental methods do not necessarily measure the same aspect of this two-stage process. These conclusions, which are valid for low dielectric constant solutions, are tentative as far as aqueous solutions are concerned and further experimental evidence is required.

In this series of papers, the results will be described of investigations, by those experimental methods which were available and applicable, of the ionization equilibria of a number of acids in aqueous solution. The power of such an approach has recently been demonstrated by Pethybridge and Prue¹ with their studies of iodic acid. The acids chosen are those which are moderately strong (which we arbitrarily define as those with reported pK_a in the range $-2 < pK_a < 2$) in aqueous solution. The object of the investigations has been, besides the use of several experimental techniques, the critical examination of the accuracy of the methods used and of the assumptions, both explicit and implicit, involved in the calculations. Such a critical appraisal of methods is important for it has been suggested² that differences in reported pK_a values can always be attributed to either experimental inaccuracies or the assumptions involved in the treatment of the data. The view held by a few^{3,4} that different experimental methods can, in principle, yield different *apparent* pK values, at least for aqueous solutions, has been dismissed;⁵ however, the possibility is allowed for low dielectric constant solutions.⁶ Acids of moderate strength have been chosen for study because, in their investigation, the classical techniques of conductance, emf, etc., are stretched to their limits, while the newer techniques of Raman and nmr spectroscopy become applicable.

At this stage it may be helpful to comment on the nomenclature to be employed in this series of papers. We shall refer to the constant, conventionally defined as

$$K_a = a_{H^+} a_{A^-} / a_{HA}$$

for the acid HA, as the *acidity constant*, irrespective of the fact that, as we shall seek to show, it may be, depending on the experimental method used, a composite

or overall constant for a two-stage process of ionization and dissociation (*vide infra*, eq 3a). In view of this we are unable to employ the often used terms *ionization constant* or *dissociation constant* which in eq 3a must be distinguished from each other and from K_a which is then only an *apparent acidity constant*. Notwithstanding these considerations, we are forced, because of the lack of a suitable acceptable alternative to refer to the *degree of ionization*, which is to be regarded as synonymous with, but for reasons discussed later is preferred to, the term *degree of dissociation*. The terms ionization and dissociation are hence in this context to be regarded loosely.

In this paper we report studies of trifluoro- and trichloroacetic acids, and in subsequent papers in the series, picric and other acids will be discussed. A pmr study⁷ of methanesulfonic acid is to be regarded as part of this series. Experimental measurements of the proton chemical shifts and of Raman intensities of the two substituted halogeno acetic acids will be reported. Trifluoroacetic acid (TFA) has previously been examined⁸ by pmr chemical shift measurements and was studied simultaneously with the present investigation by the

(1) A. D. Pethybridge and J. E. Prue, *Trans. Faraday Soc.*, **63**, 2019 (1967).

(2) T. F. Young and D. E. Irish, *Ann. Rev. Phys. Chem.*, **13**, 442 (1962).

(3) G. N. Lewis and M. Randall, "Thermodynamics," 2nd ed, K. S. Pitzer and L. Brewer, Ed., McGraw-Hill, New York, N. Y., p 308.

(4) G. Scatchard, *J. Amer. Chem. Soc.*, **83**, 5043 (1961).

(5) E. J. King, "Acid-Base Equilibria," Pergamon, Oxford, 1965, p 55.

(6) Reference 5, p 280.

(7) A. K. Covington and T. H. Lilley, *Trans. Faraday Soc.*, **63**, 1749 (1967).

(8) G. C. Hood, O. Redlich, and C. A. Reilly, *J. Chem. Phys.*, **23**, 2229 (1955).

Raman method in two other laboratories.^{9,10} No nmr study of trichloroacetic acid (TCA) has been reported, and the only quantitative study by Raman spectroscopy was that of Rao,¹¹ who used a photographic plate technique. It was necessary to repeat the pmr measurements⁸ on TFA because they did not extend to sufficiently low concentration to enable the chemical shift contribution of the hydrated proton to be evaluated.

Experimental Section

Chemical shift measurements were made as described in another paper.¹² Bulk diamagnetic susceptibility measurements were made by the Gouy method and corrections were applied.

Raman intensity measurements were obtained with a modified Hilger E612 recording spectrometer as described elsewhere.¹²⁻¹⁴ Assignments have been given^{15,16} for the Raman bands of anion and undissociated acid species in the spectrum of TFA. Quantitative measurements were made on the $\nu_1(A_1)$ anion band at 1438 cm^{-1} . This band, due to the C-O symmetrical stretch vibration,^{11,17} occurs for TCA at 1348 cm^{-1} . Measurements were made on the sodium and ammonium salts of each acid also.

Reagent grade TFA (B.D.H. Ltd.) was twice distilled, and the fraction distilling between 72 and 74° was collected. Titration with standard alkali indicated a purity of 99.91% (average of three weight titrations). Analar grade TCA (B.D.H. Ltd.) was stored over phosphorus pentoxide for several days before use as it is rather hygroscopic. Its purity was found to be 99.99%.

Sodium and ammonium salts of the two acids were prepared by carefully neutralizing the cooled acid with either sodium hydroxide (pellets and 1 M solution) or ammonia (B.D.H. Analar 0.880). The stock solutions thus produced were diluted and after passage through a freshly prepared cation-exchange column (Amberlite IR 120H), analyzed by titration with standard alkali. Titrations were performed using the Radiometer automatic titration equipment. It is very important to prevent the trichloroacetate solutions overheating on neutralization because thermal decomposition occurs readily in presence of alkali. The reported violet coloration¹¹ was never observed.

Results

Pmr measurements. Chemical shift data for TFA are given in Table I. Agreement with the results of Hood, Redlich, and Reilly⁸ at the higher concentrations is good. The method of Hood, Jones, and Reilly¹⁸ was used to obtain the chemical shift of the hydrated proton (11.60 ppm) (Figure 1). This value happens to be almost the same as that assumed by Hood, Redlich, and Reilly⁸ (11.62 ppm) which was the mean of the values for hydrochloric and nitric acids. As has been shown elsewhere,¹² because the effect of anion solvation is important it is essential that the value used should be de-

Table I: Chemical Shifts (δ) and Degrees of Ionization (α) for TFA at 25°

c , mol l. ⁻¹	p	δ_{obsd} , ppm	
	0.004565	0.0509	
	0.007045	0.0717	
	0.009569	0.1047	
	0.01388	0.1542	
	0.01754	0.1889	
	0.02115	0.2235	
0.68	0.02171	0.2315	0.903
1.78	0.04925	0.454	0.748
2.74	0.09051	0.7425	0.641
4.10	0.1532	1.059	0.504
7.25	0.3879	1.717	0.241
8.24	0.5055	0.961	0.183
8.86	0.6061	2.029	0.127
10.12	0.8707	2.376	0.061
13.06	3.000	6.45	

termined from low concentration measurements on the same acid. There is some uncertainty about the value for the chemical shift of the undissociated acid in that, as suggested by Hood, *et al.*,⁸ at high concentrations there may be equilibrium between dimers and monomers. In Table I values of α , termed the degree of ionization, have been calculated from the equation¹²

$$\frac{\delta}{p} = \delta_{\text{H}_2\text{O}} \cdot \alpha + \frac{\delta_{\text{HA}}}{3} (1 - \alpha) \quad (1)$$

where p is related to the mole fraction of the acid x by $p = 3x/(2 - x)$ and $\delta_{\text{HA}} = 6.45$ ppm for the anhydrous liquid acid in contrast to 8.01 ppm the value preferred by Hood, Redlich, and Reilly.⁸ In Figure 2 these values of α are compared with the previous data⁸ and also with Raman results to be described later.

Chemical shift data for TCA are given in Table II. The chemical shift of the hydrated proton was again determined by extrapolating¹⁶ a plot of δ/p to $p = 0$ (Figure 1). The value obtained was 13.45 ppm. The chemical shift of the un-ionized acid is more difficult to evaluate because at room temperature pure TCA is a

(9) M. M. Kreevoy and C. A. Mead, *Discussions Faraday Soc.*, **39**, 166 (1965).

(10) R. E. Weston, private communication.

(11) N. R. Rao, *Indian J. Phys.*, **17**, 332 (1943).

(12) J. W. Akitt, A. K. Covington, J. G. Freeman, and T. H. Lilley, *Trans. Faraday Soc.*, **65**, 2701 (1969).

(13) A. K. Covington, M. J. Tait, and W. F. K. Wynne-Jones, *Proc. Roy. Soc., Ser. A*, **286**, 235 (1965).

(14) A. K. Covington, L. Molyneux, and M. J. Tait, *Spectrochim. Acta*, **21**, 351 (1965).

(15) N. Fuson, K. Josien, E. A. Jones, and J. R. Lawson, *J. Chem. Phys.*, **20**, 1627 (1952).

(16) R. E. Robinson and R. C. Taylor, *Spectrochim. Acta*, **18**, 1093 (1962).

(17) H. Wittek, *Z. Phys. Chem. (Leipzig)*, **B51**, 103 (1942).

(18) G. C. Hood, A. C. Jones, and C. A. Reilly, *J. Phys. Chem.*, **63**, 101 (1959).

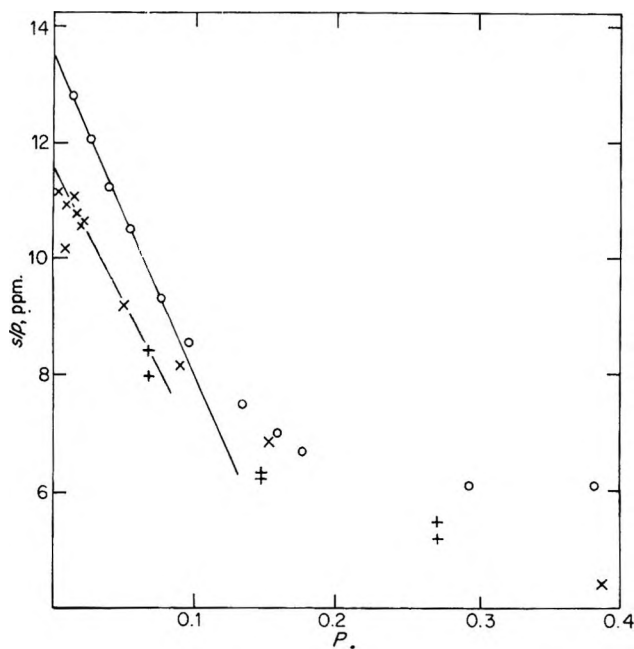


Figure 1. Determination of the chemical shift of the hydrated proton in TFA and TCA solutions: O, TCA, X, TFA (this work); +, TFA (Hood, Redlich, and Reilly⁸).

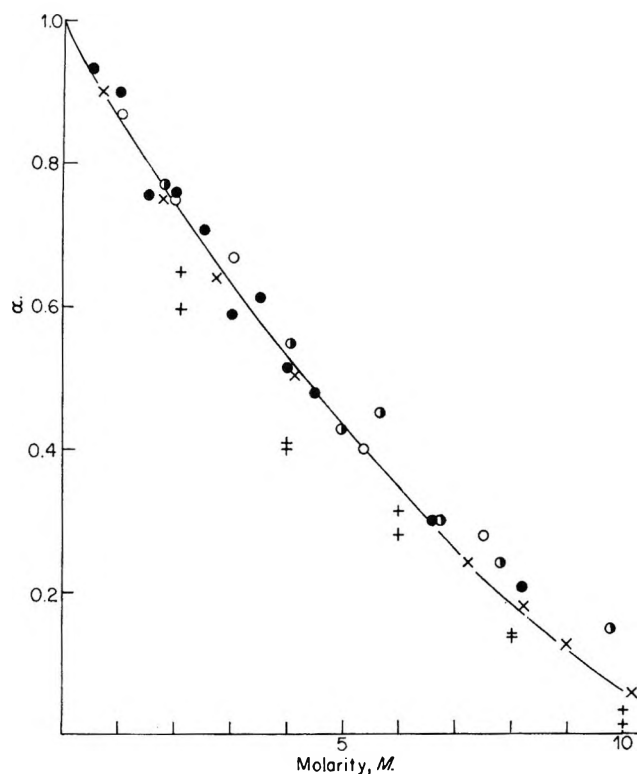


Figure 2. Degrees of ionization for TFA. Raman: O, Kreevoy and Mead⁹; ●, Weston¹⁰; ●, this work. Nmr: +, Hood, Redlich and Reilly⁸; X, this work.

solid. Inspection of Figure 1 shows that s/p for TCA becomes constant as the concentration increases, and this indicates that $\alpha = 0$ when p is large enough. A value of $s_{HA} = 18.24$ ppm was estimated from Figure 1.

Table II: Chemical Shifts (s) and Degrees of Ionization (α) for TCA at 25°

c , mol l. ⁻¹	p	$s_{\text{obsd.}}$, ppm	α values	
			$s_{HA} = 18.24$	$s_{HA} = 16.35$
0.499	0.0140	0.178	0.900	0.909
0.942	0.0276	0.331	0.803	0.819
1.316	0.0398	0.445	0.694	0.718
1.737	0.0546	0.571	0.592	0.625
2.322	0.0774	0.716	0.434	0.479
2.740	0.0952	0.812	0.334	0.386
3.527	0.1335	0.994	0.186	0.250
3.956	0.1573	1.096	0.125	0.189
4.254	0.1754	1.154	0.079	0.151
	0.2923	1.764		
	0.3801	2.292		

Values of α calculated from eq 1 using this value and a lower one (16.35) are given in Table II and compared graphically with Raman derived values in Figure 3.

Raman Measurements. The ν_1 Raman band of the trifluoroacetate anion in the acid and the sodium and ammonium salts solutions was scanned from 1340 to 1580 cm^{-1} . It is a comparatively weak band and in addition lies upon a continuously sloping base line,¹⁶ making base line drawing somewhat subjective. Band areas were obtained using an Allbrit planimeter. Band intensities are estimated to be accurate to 4% because of these limitations. Half-width and frequency of the band maximum were also measured for all solutions. For the intensity measurements compensation for instrumental drift was made in the manner described previously.¹³ A dilute solution of the sodium salt was used as standard for the acid measurements, and concentrated salt solutions for the work on the sodium and ammonium salts. The various standard solutions were intercompared so that the intensity measurements could be brought to a common basis (the 7.753 M sodium TFA solution was chosen).

For both salts studied the Raman intensities, R (Table III), lay on a common straight line within experimental error when plotted against stoichiometric concentration. Half-width and band maxima remained constant with increase in concentration for the ammonium salt but for the sodium salt the band shifted to higher wavelengths and broadened. The changes (4 and 5 cm^{-1} , respectively) were only just outside the likely experimental error.

The problem of the most appropriate salts to use in order to find the specific intensity, and hence the anion concentrations and α values of an acid, has been discussed by Clarke and Woodward,¹⁹ who have given their reasons for preferring the ammonium salt following the arguments of Vollmar.²⁰ For TFA it appears that

(19) J. H. R. Clarke and L. A. Woodward, *Trans. Faraday Soc.*, **62**, 3022 (1966).

(20) P. M. Vollmar, *J. Chem. Phys.*, **39**, 2236 (1963).

Table III: Raman Intensities for TFA and Its Sodium and Ammonium Salts. Values of α and Half-Widths at Half-Height (β) for TFA

NaTFA		NH ₄ TFA		TFA			
Mol l. ⁻¹	R	Mol l. ⁻¹	R ^a	Mol l. ⁻¹	R ^b	α	β , cm ⁻¹
1.784	0.206	1.209	0.135	0.500	0.233	0.934	14.2
2.000	0.259	1.771	0.207	1.000	0.451	0.902	14.6
2.475	0.324	2.418	0.305	1.500	0.567	0.756	14.6
3.567	0.471	3.542	0.475	2.000	0.758	0.758	15.1
4.950	0.571	4.837	0.631	2.500	0.883	0.706	15.6
7.753	1.000	6.055	0.763	3.000	0.873	0.582	15.8
8.459	1.082			3.500	1.075	0.614	16.2
				4.000	1.026	0.513	16.6
				4.524	1.084	0.480	17.2
				6.626	0.983	0.297	20.3
				8.193	0.844	0.206	24.8

^a Relative to 7.753 M NaTFA. ^b Relative to 2.000 M NaTFA.

the sodium and ammonium salts are equally suitable and yield the same values of α which are given in Table III. In Figure 2 they are compared with the Raman results of Kreevoy and Mead⁹ and of Weston;¹⁰ there is good agreement within experimental error.

The ν_1 band of the trichloroacetate ion was scanned from 1220 to 1500 cm⁻¹. It is also situated on a sloping base line, and its intensity is lower than that of the trifluoroacetate ν_1 band. Intensities could be estimated to within 4–5%. Half-widths and band maxima for the salts remained constant within experimental error (± 6 cm⁻¹). Measurement of these parameters was complicated by the presence of a shoulder on the side of the 1348-cm⁻¹ band at about 1370 cm⁻¹. It was present in salt and acid solutions and its position relative to the band maximum was found to be unaffected by the anion concentration or the cation present (Na⁺, NH₄⁺, or Me₄N⁺). Thus the whole band area could be evaluated with the planimeter without incurring error. The relative intensities (Table IV) of the sodium and ammonium salts were linear with concentration and coincident within experimental error. As for TFA it appears that both salts are equally suitable as standards. Values for α are given in Table IV and are compared graphically with the nmr results in Figure 3.

Table IV: Raman Intensities for TCA and Its Sodium and Ammonium Salts. Values of α for TCA

NaTCA		NH ₄ TCA		TCA		
Mol l. ⁻¹	R	Mol l. ⁻¹	R ^a	Mol l. ⁻¹	R ^b	α
1.065	0.277	1.131	0.282	0.61	0.134	0.880
1.916	0.425	1.456	0.338	1.20	0.236	0.785
2.802	0.674	1.867	0.422	1.80	0.281	0.627
3.194	0.721	2.279	0.498	2.40	0.249	0.416
3.852	0.836	2.648	0.620	3.00	0.298	0.396
4.000	0.920			3.60	0.255	0.283
4.258	1.000			4.20	0.168	0.160
				4.80	0.158	0.130

^a Relative to 4.258 M NaTCA. ^b Relative to 4.000 M NaTCA.

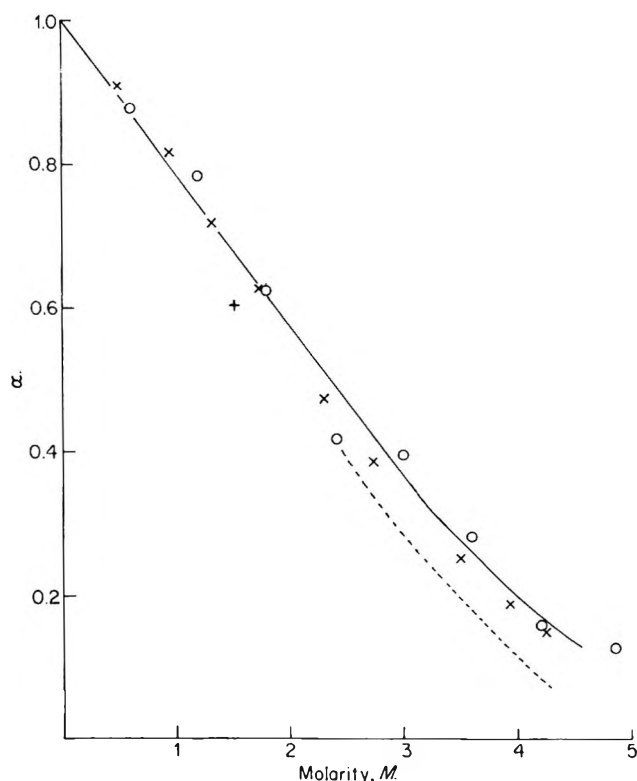


Figure 3. Degrees of ionization for TCA. Raman: +, Rao; O, this work. Nmr: X, this work ($s_{\text{HA}} = 16.35$ ppm); ---, this work ($s_{\text{HA}} = 18.24$ ppm).

Discussion

For TFA the agreement between Raman and nmr results is good (Figure 2) if 6.45 ppm is taken for the chemical shift of the un-ionized acid. Above 6–8 M there is a small divergence between the two methods which is almost within the experimental error but which could arise from a Raman band overlap. The band maximum was observed²¹ to shift from 1438 cm⁻¹ at 0.5 M to 1455 cm⁻¹ at 8 M which suggests that a band

(21) A. K. Covington, *Discussions Faraday Soc.*, 39, 176 (1965).

which appears in the spectrum of the anhydrous acid at about 1455 cm^{-1} is probably contributing to the measured intensity of the ν_1 band at the higher concentrations. Weston²² suggested that the band is due to a dimer and that its intensity was about a tenth of that of the ν_1 band. The origin of the sloping base line, which forms part of a very broad band extending several thousands of wave numbers, is obscure.

If 16.35 ppm is arbitrarily taken for the chemical shift of un-ionized TCA, the agreement between Raman and nmr is good. Figure 3 includes one point estimated by Rao.¹¹ As with TFA, the ν_1 band was observed to broaden and shift to higher wavelengths with concentration, but no quantitative measurements were possible.

Previous values reported for the acidity constant (K_a) of TCA and TFA are summarized in Table V. To

Table V: Values for the Acidity Constants (K_a) of TFA and TCA

	Method	K_a , mol l. ⁻¹	Workers
TFA	Conductance	0.588	Henne and Fox ²⁴
	Acidity function	0.8	Randles and Tedder ²⁶ (data reanalyzed)
	Pmr	1.8	Hood, Redlich, and Reilly ⁸
	Pmr/Raman	4-8	This work
	Refractometry	1.1	Grunwald and Haley ³⁰
TCA	Kinetic	1	Ciapetta and Kilpatrick ³¹
	Indicator (20°)	0.232	von Halban and Brüll ³²
	Pmr/Raman	2-5	This work
	Acidity function	0.5	Lilley ²⁹

derive values for comparison from the α values determined here is difficult, as no activity coefficient data are available at 25° for either acid. Hood, Redlich, and Reilly⁸ used stoichiometric activity coefficient data for TFA derived from freezing point depression measurements.²³ However

$$K_a = \frac{\alpha^2 c}{1 - \alpha} y_{\pm}^2 \quad (2)$$

where y_{\pm} is the mean ionic activity coefficient. To obtain this from knowledge of the stoichiometric activity coefficients requires values of α again. The former are known at 0° and the latter at 25°, so this is not a very satisfactory procedure.

An estimate of K_a can be obtained by extrapolating a plot of $\log \alpha^2 c / (1 - \alpha)$ against c . Although not very satisfactory, the method may be expected to give an upper limit for the acidity constant, since activity coefficients are usually less than unity at 1-1.5 M. A further estimate neglecting activity coefficients can be obtained from

$$K_a = \frac{c}{\lim_{c \rightarrow 0} (1 - \alpha)}$$

Thus the limiting slope of a plot of α against c has a value of $-K_a^{-1}$.

Two values of K_a have been obtained by attempting to estimate values for the activity coefficients. For the first, the activity coefficients for hydrochloric acid were interpolated at the same ionic strength ($I = \alpha c$) as TFA or TCA. The activity coefficients of cesium chloride are among the lowest for 1:1 charge type; thus, if the activity coefficients of the acids are no lower, then interpolation of these values at the same ionic strengths as in the acids will give a probable lower limit for the acidity constants. These alternative activity coefficient values were inserted in eq 2 and $\log \alpha^2 c y_{\pm}^2 / (1 - \alpha)$ was extrapolated to zero concentration (Figures 4 and 5). These various estimates lead to the conclu-

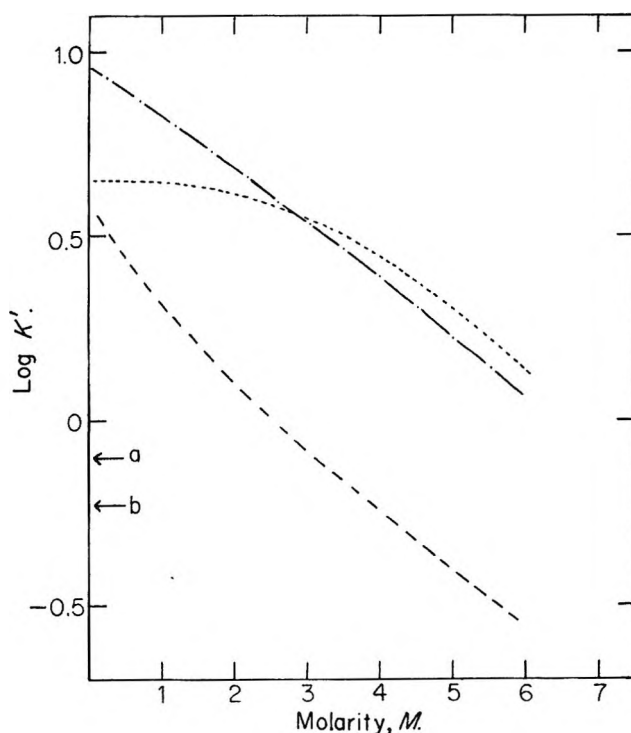


Figure 4. Estimation of the acidity constant for TFA: —, $K' = Q$; ---, $K' = Qy^2_{\text{HCl}}$; - · - ·, $K' = Qy^2_{\text{CsCl}}$, where $Q = c_{\text{H}^+}c_{\text{A}^-}/c_{\text{HA}}$, a = acidity function value,²⁶ b = conductance value.²⁴

sions that the acidity constant of TCA is about 2-5 mol l.⁻¹ and that of TFA about 4-9 mol l.⁻¹. These values are considerably greater than those obtained by other experimental techniques, and these are summarized in Table V. The disagreement is, we believe, too large to be explained simply by the use of incorrect activity coefficient data to obtain K_a from nmr and Raman data.

(22) R. E. Weston, *Discussions Faraday Soc.*, **39**, 178 (1965).

(23) H. H. Cady and G. H. Cady, *J. Amer. Chem. Soc.*, **76**, 915 (1954).

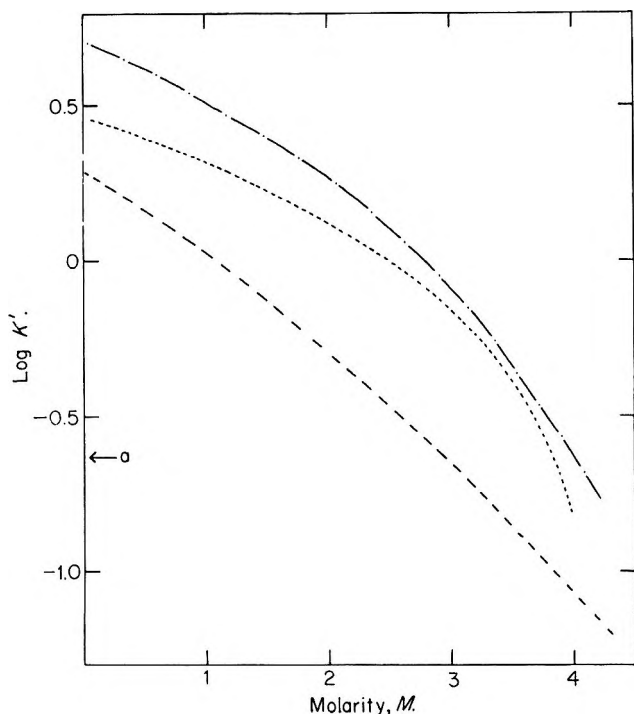


Figure 5. Estimation of acidity constant for TCA: —, $K' = Q$; ---, $K' = Qy^2_{\text{HCl}}$; - · - ·, $K' = Qy^2_{\text{CsCl}}$, $a = \text{indicator value}$.³¹

The assumptions involved in the analysis of the nmr data have been discussed.¹²

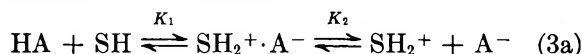
It remains therefore to assess the reliability of the values obtained by other techniques. Henne and Fox's conductance data²⁴ for TFA were of low accuracy and covered only a small concentration range. They were analyzed using the Arrhenius equation ($\alpha = \Lambda/\Lambda_0$). Such a treatment is invalid for an acid of the strength of TFA. This has been pointed out by Redlich and Hood,²⁵ and it is clear that Henne and Fox's data are not worth further consideration. The acidity function data for TFA of Randles and Tedder²⁶ have been reanalyzed by the methods of Bascombe and Bell²⁷ and of Högfeltdt.²⁸ There is some uncertainty about both methods of analysis.²⁹ The acidity constant was estimated from the limiting slope of a plot of α against concentration. Acidity function data for TCA were analyzed similarly.²⁹

Very recently Grunwald and Haley³⁰ have determined an acidity constant for TFA of $K_a = 1.1 \pm 0.3 \text{ mol l.}^{-1}$ by differential refractometry. Detailed comparison with the considerations presented above is difficult because of the nature of the calculation of K_a from the refractive index measurements.

Ciapetta and Kilpatrick,³¹ who studied the hydration of isobutene in the presence of TCA, obtained results of not very high precision, and it is difficult to estimate the accuracy of the value of K_a they gave. Some other imprecise determinations are mentioned by von Halban and Brüll,³² who used a rather refined indicator tech-

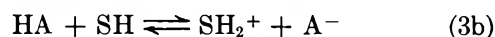
nique in which the concentrations of hydrochloric acid and TCA needed to give the same color intensity in a solution of 2,4-dinitrophenol were compared. The results are of apparently very high precision and have been reanalyzed by King.³³ The difference between this value and the nmr/Raman value (Table V) would therefore appear to be real.

Throughout this paper the preferred term *ionization* has been used. It has not been used synonymously with *dissociation*, although these terms are often so used. The latter term is usually applied to ionophores,³⁴ *i.e.*, species which are ionized in the crystalline state which only "dissociate" when placed in a solvent which decreases the interionic attraction forces. The term ionization is applied to ionogens,³⁴ which only become ionic when reaction occurs between them and the solvent. For acidic equilibria it is plausible that the "dissociation" of an acid should take place in stages. (a) A peripheral solvent molecule assumes the correct orientation and proton transfer occurs from the acid molecule to the solvent molecule. (b) The protonated solvent molecule and the deprotonated acid molecule remain in juxtaposition briefly held by electrostatic (or possibly hydrogen bonding) forces. This entity will for a negatively charged or uncharged acid be essentially an "ion pair." (c) The two species diffuse away. This scheme may be represented by



where SH denotes a solvent molecule. The first step is ionization and the second is dissociation. The same concept was used by Kolthoff and Bruckenstein³⁵ in an investigation of acid strengths in acetic acid, a low dielectric constant solvent.

The intrinsic strength of an acid is a measure of its tendency to transfer a proton to a solvent molecule and hence is measured by K_1 and does not involve the dissociation step. The equilibrium constant for the overall process will be given by $K = K_1K_2$. It does not



follow, however, that this is the constant which is nec-

(24) A. L. Henne and C. J. Fox, *J. Amer. Chem. Soc.*, **73**, 2323 (1951).

(25) O. Redlich and G. C. Hood, *Discussions Faraday Soc.*, **24**, 87 (1957).

(26) J. E. B. Randles and J. M. Tedder, *J. Chem. Soc.*, 1218 (1955).

(27) K. Bascombe and R. P. Bell, *Discussions Faraday Soc.*, **24**, 158 (1957).

(28) E. Högfeltdt, *J. Inorg. Nucl. Chem.*, **17**, 302 (1961).

(29) T. H. Lilley, unpublished.

(30) E. Grunwald and J. F. Haley, *J. Phys. Chem.*, **72**, 1944 (1968).

(31) F. C. Ciapetta and M. Kilpatrick, *J. Amer. Chem. Soc.*, **70**, 639 (1948).

(32) H. von Halban and J. Brüll, *Helv. Chim. Acta*, **27**, 1719 (1944).

(33) Reference 5, p 95.

(34) R. M. Fuoss, *J. Chem. Educ.*, **32**, 527 (1955).

(35) I. M. Kolthoff and S. Bruckenstein, *J. Amer. Chem. Soc.*, **78**, 1, 10 (1956).

essarily given by experimental measurements.⁶ If the concentrations of SH_2^+ and A^- are obtained from conductance measurements and for simplicity ignoring activity coefficients, then

$$K_{(\text{cond})} = \frac{[\text{SH}_2^+][\text{A}^-]}{[\text{HA}] + [\text{SH}_2^+\cdot\text{A}^-]} = \frac{K_1K_2}{1 + K_1} \quad (4)$$

because the ion pair is electrically neutral. The same is true of the indicator method, where essentially a measure of the "hydrogen ion" concentration is obtained and $[\text{SH}_2^+] = [\text{A}^-]$. On the other hand, if it is assumed that the Raman spectra of A^- and $\text{SH}_2^+\cdot\text{A}^-$ are indistinguishable and the proton chemical shift contributions of SH_2^+ and $\text{SH}_2^+\cdot\text{A}^-$ are identical, then

$$K_{(\text{Raman})} = \frac{([\text{SH}_2^+\cdot\text{A}^-] + [\text{A}^-])^2}{[\text{HA}]} \quad (5)$$

$$K_{(\text{pmr})} = \frac{([\text{SH}_2^+] + [\text{SH}_2^+\cdot\text{A}^-])^2}{[\text{HA}]} \quad (6)$$

Since $[\text{SH}_2^+] = [\text{A}^-]$, the Raman and pmr methods should yield the same result and

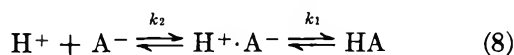
$$K_{(\text{pmr/Raman})} = \frac{K_1K_2 + 2K_1[\text{SH}_2^+] + K_1[\text{SH}_2^+\cdot\text{A}^-]}{K_1K_2 + 2K_1[\text{SH}_2^+] + K_1[\text{SH}_2^+\cdot\text{A}^-]} \quad (7a)$$

If the experimental results are extrapolated to zero concentration, then

$$K_{(\text{pmr/Raman})} = K_1K_2 \quad (7b)$$

Comparing eq 7b with eq 4, suggests that $K_{(\text{pmr/Raman})}$ will be detectably greater than $K_{(\text{ind/cond})}$ if $K_1 > 0.01$. From the ratio of these one can obtain an approximate value for K_1 . For TCA (Table V) using the indicator results of von Halban and Brüll³² eq 4 and 7b give, taking a mean value of $K_{(\text{pmr/Raman})}$, $K_1 = 17$ and hence $K_2 = 0.23 \text{ mol l.}^{-1}$. We assume that extrapolation of $K_{(\text{pmr/Raman})}$ on the basis of eq 2 is not unreasonable in spite of eq 7a, but it is difficult to see how to use the latter for extrapolation as activity coefficients are unknown. For TFA there is no indicator result as reliable but taking 0.8 mol l.^{-1} evaluated from the acidity function data gives $K_1 = 9$ and $K_2 = 0.9 \text{ mol l.}^{-1}$.

The above argument is tentative and further evidence in favor must be sought. The numerical values of K_2 are, however, those to be expected³⁶ with reasonable assumptions about ion size for an ion-pairing constant for a 1:1 electrolyte. Further evidence in support comes from consideration of Raman line broadening in acid solution as being the result of the rate of proton transfer. Kreevoy and Mead^{9,37} have used the same reaction scheme as given in eq 3a but written in reverse



where now H^+ is written as an abbreviation for the solvated proton. If $\text{H}^+\cdot\text{A}^-$ and A^- have essentially the

same spectroscopic properties, then the mean lifetime of all A^- species (A^- and $\text{H}^+\cdot\text{A}^-$) is given by

$$\tau_{\text{A}} = \frac{1}{k_1[\text{H}^+\cdot\text{A}^-]} + \frac{1}{k_2[\text{H}^+][\text{A}^-]}([\text{H}^+\cdot\text{A}^-] + [\text{A}^-])$$

and its reciprocal which will be related to experimental measurements is

$$\frac{1}{\tau_{\text{A}}} = \frac{k_1k_2[\text{H}^+\cdot\text{A}^-][\text{H}^+][\text{A}^-]}{(k_2[\text{H}^+][\text{A}^-] + k_1[\text{H}^+\cdot\text{A}^-])([\text{H}^+\cdot\text{A}^-] + [\text{A}^-])}$$

This is essentially the analysis of Kreevoy and Mead⁹ although not given in detail by them. It is not entirely free of objections.^{10,22} Assuming that $k_2[\text{H}^+][\text{A}^-] > k_1[\text{H}^+\cdot\text{A}^-]$, which corresponds to the assumption⁹ that the conversion of $\text{H}^+\cdot\text{A}^-$ into HA is rate determining, then

$$\frac{1}{\tau_{\text{A}}} = \frac{k_1[\text{H}^+\cdot\text{A}^-]}{([\text{H}^+\cdot\text{A}^-] + [\text{A}^-])}$$

Introducing $1/K_2 = k_2/k_{-2}$ and assuming $[\text{A}^-] \gg [\text{H}^+\cdot\text{A}^-]$ gave⁹

$$\frac{1}{\tau_{\text{A}}} = \frac{k_1}{K_2}[\text{H}^+]$$

If, however, the latter unnecessary assumption is not made, but instead it is noted that the experimental value of α is obtained from

$$\alpha = \frac{[\text{H}^+\cdot\text{A}^-] + [\text{A}^-]}{c_{\text{stoic}}}$$

then

$$\frac{1}{\tau_{\text{A}}} = k_1K_1 \frac{(1 - \alpha)}{\alpha} \quad (9)$$

where

$$K_1 = [\text{H}^+\cdot\text{A}^-]/[\text{HA}]$$

It was shown by Kreevoy and Mead³⁷ that

$$\frac{1}{\tau_{\text{A}}} = 2\pi c(\beta - \beta_1)$$

where in this nomenclature³⁸ β is the half-width at half-height of the broadened Raman band and β_1 the value in absence of exchange, *e.g.*, for the sodium salt. Thus

$$(\beta - \beta_1) = \frac{k_1K_1}{2\pi c} \frac{(1 - \alpha)}{\alpha} \quad (10)$$

(36) N. Bjerrum, *Kgl. Danske Videnskab. Selskab, Mat.-Fys. Medd.*, **7**, No. 9 (1926).

(37) M. M. Kreevoy and C. A. Mead, *J. Amer. Chem. Soc.*, **84**, 4596 (1962).

(38) A. K. Covington, M. J. Tait, and Lord Wynne-Jones, *Discussions Faraday Soc.*, **39**, 172 (1965).

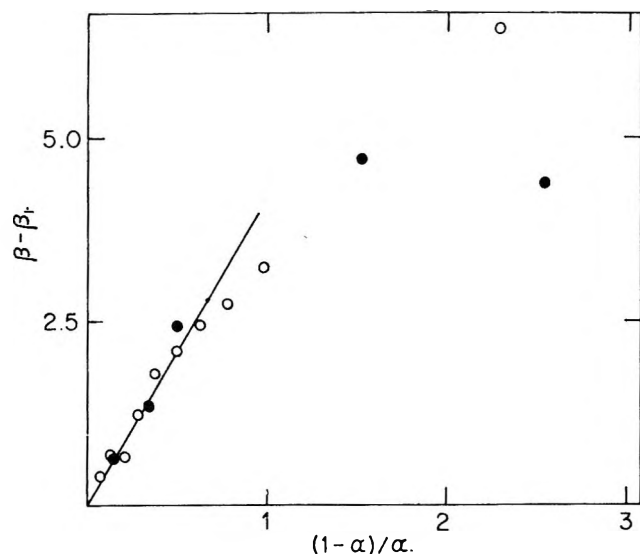


Figure 6. Test of eq 10 for TFA results: ●, Kreevoy and Mead;⁹ ○, this work.

In Figure 6, eq 10 is tested using the experimental data obtained here and compared with that given by Kreevoy and Mead.⁹ Within experimental error both sets of data are in agreement, and the plot is linear up to $\alpha = 0.6$. Deviation from linearity at higher concentration could be accounted for by neglect of activity coefficients becoming important. Whereas the band half-widths obtained in the two investigations differ because of use of different spectrometer slit widths, the broadening is independent of slit width. A similar plot was obtained for Krawetz's data³⁹ on nitric acid which was again linear up to $\alpha = 0.6$. There is some confusion about the use of the term *half-width*, which is used as an abbreviation for *half-width at half-height* and also, with transferred epithet, for *width at half-height*. Such confusion led to the results of Krawetz³⁹ being misabstracted.³⁸ The values given in Table 2 of that paper³⁸ refer to full widths; this affects subsequent columns and values derived therefrom.

Kreevoy and Mead⁹ suggested the two-step dissociation process (8) but did not pursue the analysis. It has also been used by Eigen.⁴⁰ The scheme shown in eq 3a will be a simplification of the true state of affairs which would take into account various solvated⁶ species, including the likely solvated proton species and various solvent-separated ion pairs. If it is assumed that different experimental probes will not make the same distinction between species that are associated and non-associated then the *apparent* acidity constant determined by the usual methods of extrapolation will depend on the method of measurement. A true thermodynamic acidity constant must of course be independent of the method of measurement referring as it does to some defined process such as (3b). The difficulty arises in relating this quantity to the experimental measurements of equilibrium quotients and extrapolating these to zero concentration. A two-stage equilibrium has been nicely demonstrated for triphenylmethyl chloride in liquid sulfur dioxide by Pocker.⁴¹ Further discussion will be deferred until later papers in this series.

Acknowledgment. We acknowledge gratefully, stimulating discussions with Dr. D. E. Irish, Dr. E. J. King, Dr. J. E. Prue, Dr. R. A. Robinson, Dr. R. E. Weston, and Dr. T. F. Young, who nevertheless are not necessarily in complete agreement with us on all points. The presentation of this paper at the T. F. Young Symposium in Chicago and its appearance in this volume is singularly appropriate for it indirectly owes its inspiration to Professor Young through a visit paid to his laboratory by Professor Wynne-Jones in the early 1950's which led to Raman spectroscopy of electrolyte solutions being taken up in Newcastle. Thanks are due also to Dr. R. E. Weston for permission to include some unpublished results and to the Science Research Council for maintenance awards to J. G. F. and T. H. L.

(39) A. Krawetz, Thesis, University of Chicago, 1955.

(40) M. Eigen, *Angew. Chem.*, 3, 1 (1964).

(41) Y. Pocker, *Proc. Chem. Soc.*, 386 (1959).

Young's Mixture Rule and Its Significance

by Yung-Chi Wu

National Bureau of Standards, Washington, D. C. 20234 (Received March 2, 1970)

Young's general mixing rule postulates that in the mixing of two binary solutions of the same ionic strength to produce a ternary solution an excess thermodynamic quantity of the ternary solution may be expressed accurately as the sum of the corresponding excess thermodynamic quantities of the pure binary solutions. Young's corollary to the general rule postulates further that deviations from the rule are a function both of the ionic strength and of the respective solute fractions of the mixture. In terms of Young's two postulates any mixing process at constant ionic strength may be treated as one of four special cases. Young's postulates may also be applied to ternary mixtures of different ionic strength in which the mixing ratio of the constituents is constant.

In the early 1950's, T. F. Young postulated^{1a,b} that "the mixing of the two binary solutions of the same ionic strength produces a ternary solution whose volume is exactly the sum of the binary solutions." This postulate may be expressed as^{1a}

$$\Phi V = y_A \phi_A + y_B \phi_B \quad (1)^{2-5}$$

where ΦV is mean apparent molal volume of the mixture, ϕ_A and ϕ_B are the apparent molal volumes of a binary solution of components A and B, and y_A and y_B are the ionic strength fractions of the respective solutes A and B in the mixture. Young further observed,^{1b} "the usefulness of a mixture rule is measured not only by its ability to represent the facts by itself but also by the nature of deviations from it." With this in mind he made a second postulate to implement the first, namely, that the deviations of experimental data from the rule, Δ_m , are proportional to ionic strength, I , and to the product of the respective solute ionic strength fraction y_A and y_B . The deviation, Δ_m , may be called the "mixing term." It may be expressed as

$$\Delta_m = KI y_A y_B \quad (2)$$

where K is a proportionality factor. The combination of these two postulates yields a mixture rule for volume.

$$\Phi V = y_A \phi_A + y_B \phi_B + K_I y_A y_B \quad (3)$$

Young has used Wirth's density data^{6a,b} for the mixtures of NaCl-KCl and NaCl-KBr^{6c} to illustrate the applicability of eq 1, and the density data for NaCl-HCl^{6a} and NaClO₄-HClO₄^{6b} for eq 3. In fact, this rule may be generalized to include other excess thermodynamic quantities. Thus, McKay⁷ has shown that the excess free energy of mixing $\Delta_m G^E$, takes the same form

$$\Delta_m G^E = -(\alpha_{AB} + \alpha_{BA}) y_A y_B I^2 RT \quad (4)$$

which may be rearranged as

$$\Delta_m G^E / IRT = -(\alpha_{AB} + \alpha_{BA}) y_A y_B I \quad (4a)$$

By comparing eq 2 and 4a the following relationship is obtained

$$K_g = -(\alpha_{AB} + \alpha_{BA}) \quad (5)$$

where the α 's are the Harned coefficients,⁸ R is the gas constant, and T is the Kelvin temperature. Since the ideal heat of mixing is zero, only the mixing term, Δ_m of eq 2 need be considered. Young and his coworkers^{1,9} have verified this rule with a large number of experiments. In the case of the relative apparent molal heat capacity, the system LiCl-KCl-H₂O¹⁰ provides an example illustrating the applicability of this rule. Therefore, eq 3 may be generalized as

$$\Psi_m^E = y_A \Psi_A^E + y_B \Psi_B^E + \Delta_m \Psi^E \quad (6)$$

$$\Psi_m^E = y_A \Psi_A^E + y_B \Psi_B^E + K_\nu y_A y_B I \quad (7)$$

where Ψ^E stands for any excess thermodynamic quantity; the subscripts A and B correspond to the solutes A and B, respectively the subscript m indicates the value of the quantity in the ternary mixture. If the subscript m is not present, the value is of the pure binary solution. K_ν is a proportionality factor.

(1) (a) T. F. Young, *Rec. Chem. Progr.*, **12**, 81 (1951); (b) T. F. Young and M. B. Smith, *J. Phys. Chem.*, **58**, 716 (1954).

(2) This equation first appeared in ref 1a. Its original form was written as

$$\Phi V = f_2 \phi_2 + f_3 \phi_3$$

where ϕ_2 and ϕ_3 are the same as ϕ_A and ϕ_B , respectively. f_2 and f_3 are solute mole fractions instead of ionic strength fractions used here. However, they are identical for 1-1 type of mixtures that the mixture rule was originally based upon. Although Young and his student³ have employed "sation fraction" (same as ionic strength fraction by their definition) for treating their data, the term "ionic strength fraction" was not commonly used for mixtures until 1960's, when Scatchard⁴ and Friedman⁵ published two important papers in the field. The literature cited here either treated 1-1 type of mixtures or used ionic strength fraction notation in the original papers.

(3) M. B. Smith, Ph.D. Thesis, University of Chicago (1942).

(4) G. Scatchard, *J. Amer. Chem. Soc.*, **83**, 2636 (1961).

(5) H. L. Friedman, *J. Chem. Phys.*, **32**, 1351 (1960).

(6) (a) H. E. Wirth, *J. Amer. Chem. Soc.*, **59**, 2549 (1937); **62**, 1128 (1940); (b) H. E. Wirth and F. N. Collier, Jr., *ibid.*, **72**, 5292 (1950).

(7) H. A. C. McKay, *Discussions Faraday Soc.*, **24**, 76 (1957).

(8) H. S. Harned and B. B. Owen, "The Physical Chemistry of Electrolytic Solutions," 3rd ed, Reinhold, New York, N. Y., 1958f.

(9) T. F. Young, Y. C. Wu, and A. A. Krawetz, *Discussions Faraday Soc.*, **24**, 37 (1957).

(10) A. F. Kapustinskii, M. S. Stakhanova, and V. A. Vasilev, *Akad. Nauk Izv.-Otd. Khim. Nauk*, 2082 (1960).

With the addition of the mixing term, the mixture rule has demonstrated^{1,7,9,10} its ability to represent mixture data for such diverse excess thermodynamic quantities as volume, heat, heat capacity, and free energy.

The Mixing Term

The mixing term may be thought of as a measure of the departure from linear additivity and from Young's first postulated mixture rule. The K parameter determines the magnitude of the departure. Therefore, K is a characteristic parameter of the mixing term. In general, K is a function of both y and I such that

$$K_{\psi} = \psi_0 + \psi_1(y_A - y_B) + \psi_2(y_A - y_B)^2 + \text{higher terms} \quad (8)^{11,12}$$

The ψ parameters depend on I only. Because of the limitation in experimental accuracy at the present time, only the first two terms on the right-hand side of eq 8 are necessary. For simplicity, these two independent variables, y and I , may be treated separately.

Constant Ionic Strength (I)

The mixing term at constant ionic strength for most existing data in the literature may be represented by one of the four special cases illustrated in Figure 1.

Curves a, b, c, and d in Figure 1 represent four different cases of mixing. In each the K parameter of eq 3 may be represented by a different function.

Curve a: $K = 0$; $\Delta_m \Psi^E = 0$. A system with such behavior will obey the simple additivity rule as stated by Young's first postulate. Examples have been shown by Young.¹

Curve b: $K = \psi_0$, a Constant; $\Delta_m \Psi^E = \psi_0 y(1 - y)I$. This kind of mixture exhibits a symmetrical departure from additivity rule around $y = 0.5$.¹³⁻¹⁶ Systems which behave in this manner are not too many. This type of behavior is compatible with Harned's rule⁸ for the excess partial molal free energy of mixing provided that the sum of the coefficients of Harned's rule, $\alpha_{12} + \alpha_{21}$, is equal to a constant.^{4,5,7,8,13}

Curve c.

$$K = \psi_0 + \psi_1(1 - 2y) \quad (9)$$

and

$$\Delta_m \Psi^E = y(1 - y)[\psi_0 + \psi_1(1 - 2y)]I \quad (10)$$

Systems which behave in accordance with eq 9 and 10 are common.^{9,13,14,16-18} The expressions (eq 9 and 10) also parallel to the generalized Harned's rule with an additional β term. It appears that for the common ion symmetrical mixtures ψ_0 is much greater than ψ_1 in eq 10, and in many cases, ψ_1 is negligible. However, if the heteroions in a common-ion mixture are of mixed charge type, as in the heat of mixing data reported for NaCl-Na₂SO₄,³ or if the mixture is without a common ion as in those systems reported by Wood, *et al.*,^{17e,f} and Young, *et al.*,⁹ the ψ_1 parameter plays a significant role. As

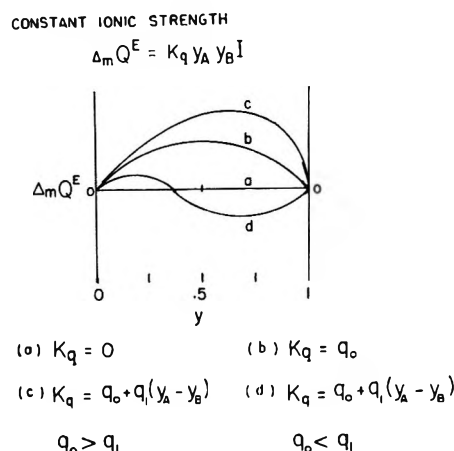


Figure 1. Mixtures at constant ionic strength.

pointed out by Wood,^{17e} ψ_1 may be considered a measure of skewness.

Curve d. K and $\Delta_m \Psi^E$ have the same forms as those shown in eq 10. However, since $\Delta_m \Psi^E$ has both positive and negative values, the following condition must be met: $K = 0$ at $y = 1/2(1 + \psi_0/\psi_1)$. Obviously, ψ_1 must be greater than ψ_0 . Systems which exhibit such behavior are rare. There seems to be only one such system reported in the literature.¹⁹ It concerns $\Delta_m H$ of KCl-Na₂SO₄ at 25°,³ as an illustration the original data have been interpreted and presented in Figure 2.

(11) This expression is empirical. Young has treated mixture data for heat and volume with only the first term in 1951 and 1954,¹ and he used $K = a + by$ in 1957,⁹ which is equivalent to the first two terms of eq 8 (with $a = \psi_0 + \psi_1$ and $b = -2\psi_1$). Scatchard's earlier B coefficient¹² for his free energy of mixing has a similar expression. The present form is perfected by Scatchard⁴ and Friedman.⁸

(12) (a) G. Scatchard and S. S. Prentiss, *J. Amer. Chem. Soc.*, **56**, 2320 (1934); (b) G. Scatchard, *Chem. Rev.*, **19**, 309 (1936); (c) G. Scatchard and R. G. Breckenridge, *J. Phys. Chem.*, **58**, 596 (1954); **59**, 1234 (1955).

(13) (a) E. Glueckauf, H. A. C. McKay, and A. R. Mathieson, *J. Chem. Soc.*, S299 (1949); (b) R. A. Robinson and R. H. Stokes, "Electrolyte Solutions," 2nd ed, revised, Butterworths, London, 1965; (c) H. L. Friedman, "Ionic Solution Theory," Interscience, New York, N. Y., 1962; (d) H. S. Harned and R. A. Robinson, "Multicomponent Electrolyte Solutions," Pergamon Press, Oxford, 1968.

(14) Y. C. Wu, M. B. Smith, and T. F. Young, *J. Phys. Chem.*, **69**, 1868 (1965).

(15) Y. C. Wu, R. M. Rush, and G. Scatchard, *ibid.*, **72**, 4048 (1968); **73**, 2047 (1969).

(16) Volume: (a) ref 1 and 6; (b) H. E. Wirth, R. E. Lindstrom, and J. N. Johnson, *J. Phys. Chem.*, **67**, 2339 (1963); (c) R. M. Rush and G. Scatchard, *ibid.*, **65**, 2240 (1961); (d) W. Y. Wen and K. Nara, *ibid.*, **71**, 3907 (1967).

(17) Heat: (a) ref 1, 9, and 14; (b) J. H. Stern and A. A. Passchier, *J. Phys. Chem.*, **67**, 2420 (1963); (c) J. H. Stern and C. W. Anderson, *ibid.*, **68**, 2528 (1964); (d) J. H. Stern, C. W. Anderson, and A. A. Passchier, *ibid.*, **69**, 207 (1965); (e) R. H. Wood and R. W. Smith, *ibid.*, **69**, 2947 (1965); (f) R. H. Wood and H. L. Anderson, *ibid.*, **71**, 1869, 1871 (1967).

(18) Free energy: (a) ref 4, 5, 7, 8, 13, and 15; (b) R. M. Rush and J. S. Johnson, *J. Phys. Chem.*, **72**, 767 (1968).

(19) This type of behavior is not too uncommon in mixtures of non-electrolytes. See, for example, G. Scatchard, *Chem. Rev.*, **44**, 7 (1949).

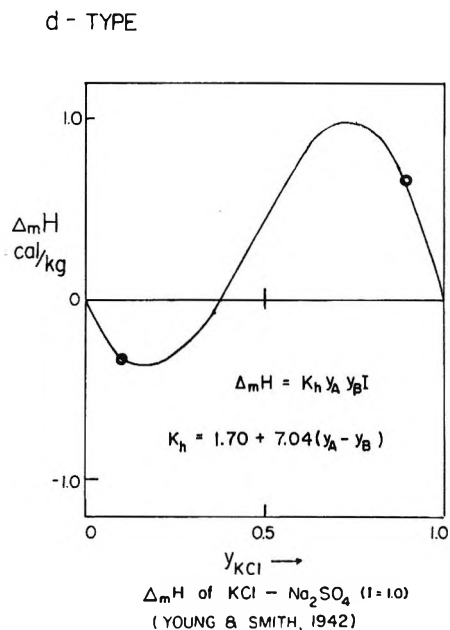


Figure 2. Mixture of type d.

Constant Mixing Ratio

Experimental observation has shown that the K parameter of eq 8 is generally a function of I at constant y . It is well known that Harned's α coefficients are I dependent.^{4,5,8,13} Because of the lack of experimental data, the present discussion in terms of K parameter will be limited to two cases. One is the heat of mixing of LiCl-NaCl^{14,17c,e} and the other is excess free energy of mixing of KCl-MgSO₄.²⁰ It is convenient to consider a constant mixing ratio at the midpoint ($y = 0.5$), for in that case only the first parameter, ψ_0 , need be considered.

Heat of Mixing

For the system LiCl-NaCl, three groups of investigators^{14,17c,e} have performed measurements. Their results which agree well with each other are shown in Figures 3 and 4.

For heat of mixing, eq 7 becomes

$$K_h = h_0 + h_1(1 - 2y)$$

$$\Delta_m H^E = y(1 - y)K_h I$$

From the experimental data the following equations have been derived and plotted as solid curves in Figures 3 and 4.

$$K_h(y=0.5) = 42.6 + 103.2\sqrt{I} - 60.8I \quad (11)$$

and

$$\Delta_m H^E(y=0.5) = (10.6 + 25.8\sqrt{I} - 15.2I)I \quad (12)$$

Clearly, K_h and $\Delta_m H^E$ show a strong dependency on I . It is interesting to note that K_h has a finite value at $I = 0$.

CONSTANT MIXING RATIO $y = 0.5$)

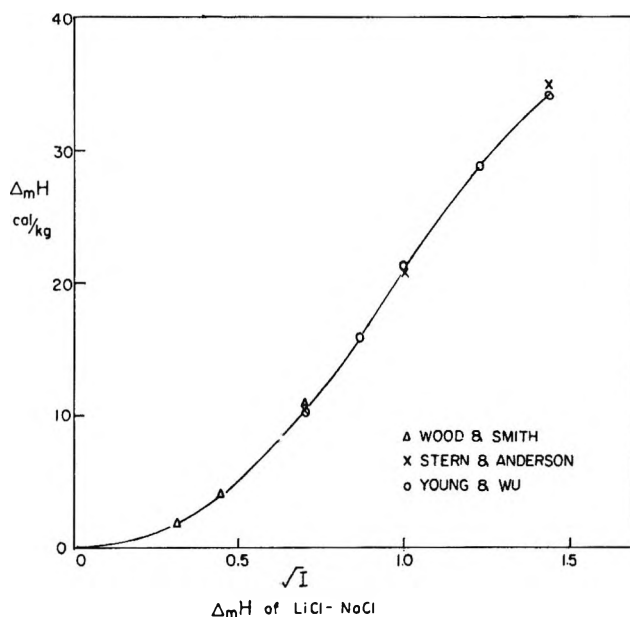
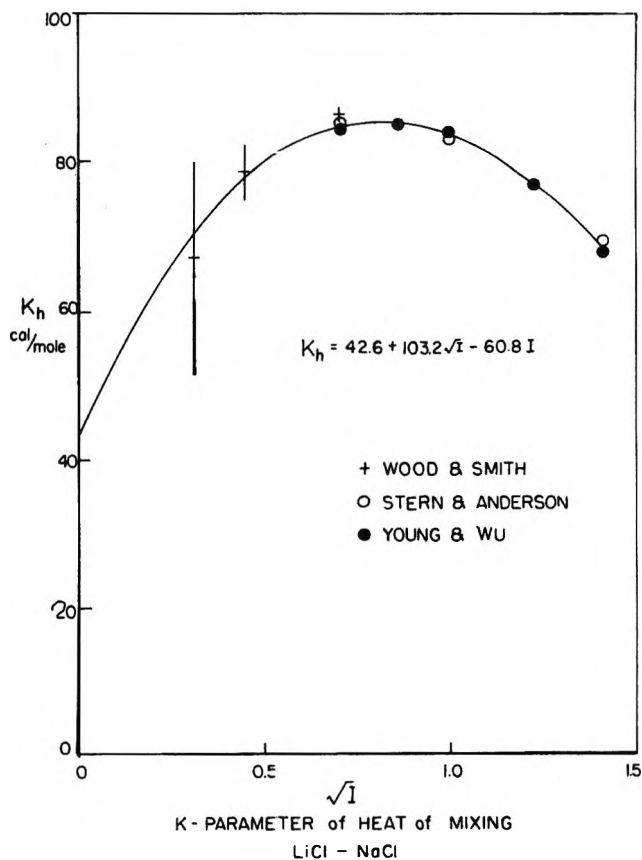


Figure 3. Heat of mixing of system LiCl-NaCl at constant mixing ratio.


 Figure 4. K parameter of heat of mixing of system LiCl-NaCl.

(20) Y. C. Wu, experimental results to be published.

Excess Free Energy of Mixing

The excess free energy of mixing, $\Delta_m G^E$, unlike the volume and the heat of mixing, cannot be measured directly. It must be calculated from the excess partial molal free energies of the components. According to eq 6 we have

$$\Delta_m G^E = G_m^E - yG_A^E - (1 - y)G_B^E \quad (13)$$

and

$$G_m^E = 2RTI[y \ln \gamma_{Am} + (1 - y) \ln \gamma_{Bm} + (1 - \phi_m)] \quad (14)$$

for mixtures of 1-1 charge type. A valence factor must be included for other charge types of mixtures. In eq 13 and 14, the subscript m designates a quantity in the mixture; without it, the quantity is that of the pure binary solution.

If any one of the three coefficients γ_{Am} , γ_{Bm} , and ϕ_m is measured, the other two may be determined through an appropriate thermodynamic relationship and G_m^E may be obtained. McKay⁷ has performed such a calculation to obtain $\Delta_m G^E$ and G_m^E . Also he and his co-workers²¹ have developed the McKay-Perring method and have shown how to obtain the three coefficients from each other *via* cross differentiation and application of the Gibbs-Duhem relation. Scatchard⁴ has derived equations for γ_{Am} , γ_{Bm} , and ϕ_m by the partial differentiation of G_m^E with respect to the concentration of each respective component by setting G_m^E in polynomial form similar to the common expression for $\log \gamma$ and ϕ in binary solution. Recently he also has developed an ionic component method²² to treat unsymmetrical mixtures without a common ion as well as symmetrical mixtures with a common ion. This method offers an advantage for simplifying the treatment by selecting a single ion as a component for systems such as $MgCl_2$ - Na_2SO_4 - H_2O with addition of $NaCl$ solution to it. Guggenheim²³ has developed an expression for G_m^E in accordance with Brønsted's principle of specific ion interaction.²⁴ Finally, there is the formal application of the Gibbs free-energy equation

$$dG_m^E = G_{Am}^E dn_A + G_{Bm}^E dn_B + G_{Wm}^E dn_W \quad (15)$$

If one of the excess partial molal free energies is measured while the other two independent variables are kept constant, eq 15 may be integrated to give

$$\left[\int_{n_j=0}^{n_j} dG_m^E = \int_{n_j=0}^{n_j} G_{Jm}^E dn_J \right]_{P,T,n_i \neq j} \quad (16)$$

Friedman^{5,13c} has elucidated this method in detail.

An application of the last method to the system KCl - $MgSO_4$ has been performed.²⁰ Here G_{Jm}^E of KCl was measured by the emf method with glass- $Ag, AgCl$ electrodes. The details of the experimental procedure and the method of calculation are to be published in the near future. Only the final results are shown in Figures 5

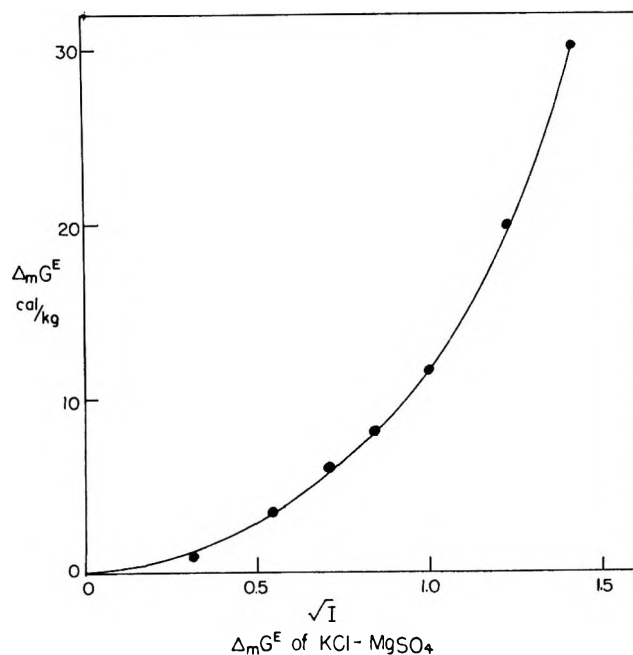


Figure 5. Excess free energy of mixing of system KCl - $MgSO_4$ at constant mixing ratio.

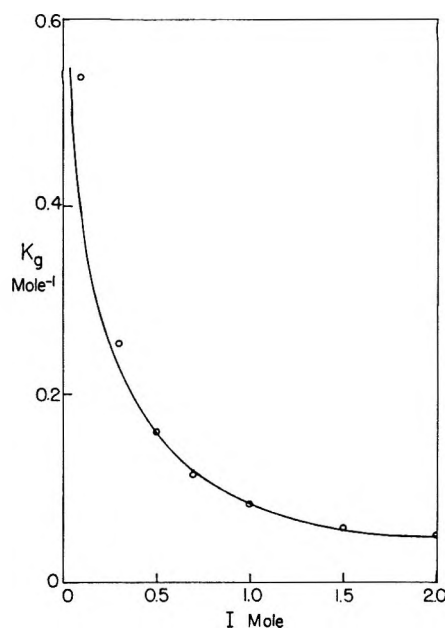


Figure 6. K parameter of excess free energy of mixing of system KCl - $MgSO_4$.

and 6. The following expressions were obtained by a least-squares analysis of the data

$$K_{\rho(y=0.5)} = -0.17 \ln I + 0.084I \quad (17)$$

(21) H. A. C. McKay, *Nature*, **169**, 464 (1952); H. A. C. McKay and J. K. Perring, *Trans. Faraday Soc.*, **49**, 163 (1953).

(22) G. Scatchard, *J. Amer. Chem. Soc.*, **90**, 3124 (1968); **91**, 2410 (1969).

(23) E. A. Guggenheim, *Trans. Faraday Soc.*, **62**, 3446 (1966).

(24) J. N. Brønsted, *J. Amer. Chem. Soc.*, **44**, 877 (1922).

and

$$\Delta_m G^E_{(y=0.5)} = 1/4 RTI^2(-0.17 \ln I + 0.084I) \quad (18)$$

It should be noted that the uncertainty of $\Delta_m G^E$ at lower concentrations is relatively higher, because it is a small difference between two large values of excess free energy of the mixture and of the pure binary solutions. Combining the experimental error and the uncertainties of the literature values of the activity coefficient and the osmotic coefficient, it is estimated that the absolute error is about ± 1 cal/mol (the thermochemical calorie (defined) is equal to 4.1840 J).

Discussion

The formulation of the mixture rule for solutions other than electrolytes has long been known. Among the pioneers, Scatchard²⁵ has treated the subject extensively. Much of the terminology and formalism employed in this paper parallels his usage for nonelectrolytes as well as for electrolytes.

Before the advance of the theory of Debye and Hückel,²⁶ two renowned principles dealing with the mixture of electrolyte solutions were developed. These were the "ionic strength principle" of Lewis²⁷ and the "principle of specific ionic interaction" of Brønsted.²⁴ While the former is merely a limiting law, the latter offers a good approximation in treating a large number of existing experimental data for dilute concentrations. Following the thesis of Brønsted, Scatchard^{4,12,22} and Guggenheim²³ have derived the ionic interaction coefficients. From Mayer's cluster theory²⁸ Friedman^{5,13c} obtained another set of coefficients. Experimentally, Harned⁸ established the so-called "Harned's coefficients" of Harned's rule. In general, they all have dealt with the chemical potential in a mixture. While these coefficients all correspond to each other thermodynamically, they differ microscopically in physical nature. The point in question is whether or not they should vanish at infinite dilution for common, ion symmetrical mixtures. Experimentally, any meaningful observation of lower limit of concentration today is about 0.1 *m*. This concentration seems to be still too high to draw any conclusive answer to this question on the vanishing of the coefficients.

Thermodynamic studies provide an alternative approach to the problem. They distinguish the effect of interaction from ideality and led Young to discover the mixture rule which originally dealt with heat and volume. The significance of the rule was recognized by Owen²⁹ soon after its formulation, and in his discussion of the pressure effect on electrolyte solutions he has shown its usefulness. Subsequently, Rush and Scatchard^{16c} and Wirth⁶ and his coworkers^{16b} have applied the rule successfully to the volume of mixing. Direct confirmation to the rule on the heat of mixing has been extensively demonstrated by Young and his coworkers,^{1b,9,14} Wood, *et al.*,^{17e,f} and Stern, *et al.*^{17b,c,d}

In discussing Young's results of heat of mixing, McKay⁷ showed that the excess free energy of mixing had the same form. The applicability of the mixture rule is clearly established. No exception so far has been found.

Young's first postulate is a simple additivity rule. The significance of the mixture rule rests with his second postulate, *i.e.*, the mixing term, in which the characteristic parameter *K* is a measure of the effect of an additional electrolyte. It is clearly shown in Figure 1. The four cases summarize effects on thermodynamic quantities of a mixture of electrolytes at a constant total ionic strength. If there were no mixing effects at all, a system would obey the simple additivity rule of Young's first postulate as indicated by curve a. The mixture of NaCl-KCl at *I* = 1.0 shows no change of volume of mixing.^{1,6} In the same system, however, there is a symmetrical thermal effect as indicated by the heat of mixing.⁹ Curve b represents this type of behavior. Apparently, the ionic interaction of Na⁺-K⁺ induces no volume change, or, at least the volume effects cancel each other.

The heats of mixing of the systems³ NaCl-Na₂SO₄ and KCl-Na₂SO₄ may be used as examples of type c and type d mixtures, respectively. The thermal effect on the SO₄²⁻ ion is stronger than that of the Cl⁻ ion in a common-ion mixture of the system of NaCl-Na₂SO₄. As shown by Smith,³ the thermal effect increases as the ionic strength fraction of SO₄²⁻ ion increases and reaches a maximum at $y_{SO_4^{2-}} \approx 0.65$. In the case of KCl-Na₂SO₄,³ the thermal effects of ionic interactions are much more complicated. It has been shown³ that the thermal energies of the interaction of Na⁺-K⁺ with common anion Cl⁻, and that of Cl⁻-SO₄²⁻ with common cation Na⁺ are of the same sign (heat liberated), and yet the heat of mixing of KCl-Na₂SO₄ changes sign from negative to positive through the zero line at $y_{KCl} \approx 0.4$ and *I* = 1.0. If Young's cross-square rule^{9,14} holds over the whole composition range for this system then we would expect the system of NaCl-K₂SO₄ will behave the same as KCl-Na₂SO₄. No data are available. It is also interesting to note that the ψ_1 coefficient is generally smaller than ψ_0 coefficient, but in the last case ψ_1 is greater than ψ_0 . It seems to indicate that Ψ_1 is a measure of opposite charge pair interaction; otherwise, there would not be any opposite effect in the last case.

The concentration dependence of parameter *K* is clearly shown in Figures 4 and 6. Friedman has dis-

(25) G. Scatchard, *Chem. Rev.*, **8**, 321 (1931); **44**, 7 (1949).

(26) P. Debye and E. Hückel, *Physik. Z.*, **24**, 185 (1923).

(27) G. N. Lewis and M. Randall, "Thermodynamics," McGraw-Hill, New York, N. Y., 1923.

(28) J. E. Mayer, *J. Chem. Phys.*, **18**, 1426 (1950).

(29) B. B. Owen, "Electrochemical Constants," National Bureau of Standards Circular 524, U. S. Government Printing Office, Washington, D. C., 1953, p 193.

cussed the g_0 coefficient in his "ionic solution theory."^{1a} He has shown that, for common-ion mixtures of symmetrical electrolytes, the limiting law takes the following form

$$d \ln g_0/d\sqrt{I} = 2z_1^2 A/\sqrt{V_w} \quad (19)$$

where V_w is the specific volume (liters/kilogram) of pure solvent, A is the Debye-Hückel limiting law constant, and z_1 is the valence of ion species 1. For heteroion unsymmetrical mixtures, as in the case of KCl-MgSO₄, the limiting law is much more complicated. The cluster theory, even for pairwise interactions, only leads to a cumbersome expansion of the cluster sum. To avoid the mathematical complexity an empirical equation was derived from experimental results

$$K_g = -a \ln I + bI \quad (20)$$

and

$$dK_g/dI = -a/I + b \quad (21)$$

where a and b are empirical constants.

It follows that as $I \rightarrow 0$, $K_g \rightarrow \infty$; and $dK_g/dI \rightarrow -\infty$. The system of KCl-MgSO₄ seems to follow these equations closely. (A theoretical treatment by Friedman³⁰ shows that K_g actually does not diverge as $I \rightarrow 0$, but instead becomes finite, but very large.)

Acknowledgement. The author wishes to thank Professors G. Scatchard and H. L. Friedman for helpful discussions.

(30) H. L. Friedman, private communication.

Osmotic and Activity Coefficients for Binary Mixtures of Sodium Chloride, Sodium Sulfate, Magnesium Sulfate, and Magnesium Chloride in Water at 25°.

III. Treatment with the Ions as Components¹

by G. Scatchard, R. M. Rush,² and J. S. Johnson

*Chemistry Division, Oak Ridge National Laboratory, Oak Ridge, Tennessee 37830, and
Department of Chemistry, Massachusetts Institute of Technology, Cambridge, Massachusetts 02139
(Received March 2, 1970)*

Equations for the excess free energy, osmotic coefficient, and activity coefficients are derived from the ion-component treatment of Scatchard (1968). Applications of these equations to the reciprocal salt system Na-Mg-Cl-SO₄ and to synthetic sea-water solutions are discussed. These are compared with the earlier neutral-electrolyte treatment of Scatchard (1961). The ion-component treatment provides a better estimate of the osmotic and activity coefficients when only data on the two-ion (single-salt) systems are available, provides as good a fit to the three-ion (common-ion) data, and provides a means of calculating values for the four-ion (noncommon-ion) systems using only parameters derived from the three-ion data.

The treatment of electrolyte solutions with the ions as components³ (with the restriction, of course, of electroneutrality) promises to be considerably more powerful than the treatment with neutral electrolytes as solutes⁴ used in papers I and II of this series.^{5,6} The equations of ref 3 are not, however, convenient for computation. In this paper, we develop more tractable expressions with the ion-component approach and illustrate their application to several solutions containing more than one electrolyte solute.

Equations

In ref 3, the excess free energy, G^e , of a solution was divided into a Debye-Hückel contribution, $(G^e)^{DH}$, and

a non-Debye-Hückel part, $(G^e)^n$

$$G^e/RT = (G/RT) - (n_0\bar{G}^{\circ}_0/RT) - \sum_i n_i [(G^{\circ}_i/RT) - 1 + \ln m_i] = (G^e/RT)^{DH} + (G^e/RT)^n \quad (1)$$

G is the total Gibbs free energy of the system; $n_0\bar{G}^{\circ}_0$,

(1) (a) Research jointly sponsored by the Office of Saline Water, U. S. Department of the Interior, and the U. S. Atomic Energy Commission under contract with Union Carbide Corp. and under Contract No. AT(30-1)-905 with the Massachusetts Institute of Technology. (b) Presented in part at the symposium "Structures of Water and Aqueous Solutions," in honor of T. F. Young at the Chemistry Department, University of Chicago, Chicago, Ill., June 18, 1969.

(2) Address inquiries to this author at Oak Ridge National Laboratory.

Table I: Free Energy Equations

$$\begin{aligned}
 \text{(a)} \quad \left(\frac{G^e}{RTW} \right) &= \left(\frac{G^e}{RTW} \right)^{\text{DH}} + \left(\frac{G^e}{RTW} \right)^{\text{nI}} + \left(\frac{G^e}{RTW} \right)^{\text{nII}} \\
 \text{(b)} \quad \left(\frac{G^e}{RTW} \right)^{\text{DH}} &= mS \sum_a^+ \sum_f^- x_a x_f (z_a + z_f) \frac{X_{af}}{a'_{af}} \\
 \text{(c)} \quad X_{af} &= \frac{a'^2_{af} I - 2a'_{af} \sqrt{I} + 2 \ln(1 + a'_{af} \sqrt{I})}{a'^2_{af} I} \\
 \text{(d)} \quad \left(\frac{G^e}{RTW} \right)^{\text{nI}} &= \sum_a^+ \sum_f^- x_a x_f \left(B_{af}^{(1)} m^2 + \frac{1}{2} B_{af}^{(2)} m^3 + \frac{1}{3} B_{af}^{(3)} m^4 + \dots \right) \\
 \text{(e)} \quad \left(\frac{G^e}{RTW} \right)^{\text{nII}} &= \sum_a^+ \sum_b^+ \sum_f^- x_a x_b x_f \left(B_{abf}^{(0,1)} m^2 + \frac{1}{2} B_{abf}^{(0,2)} m^3 + \frac{1}{3} B_{abf}^{(0,3)} m^4 \right) \\
 &+ x_a x_b x_f (x_a - x_b) \left(\frac{1}{2} B_{aab}^{(1,2)} m^3 + \frac{1}{3} B_{aabf}^{(1,3)} m^4 \right) + x_a x_b x_f (x_a - x_b)^2 \frac{1}{3} B_{aaab}^{(2,3)} m^4 \\
 &+ \sum_a^+ \sum_f^- \sum_g^- x_a x_f x_g \left(B_{fag}^{(0,1)} m^2 + \frac{1}{2} B_{fag}^{(0,2)} m^3 + \frac{1}{3} B_{fag}^{(0,3)} m^4 \right) \\
 &+ x_a x_f x_g (x_f - x_g) \left(\frac{1}{2} B_{ffg}^{(1,2)} m^3 + \frac{1}{3} B_{affg}^{(1,3)} m^4 \right) + x_a x_f x_g (x_f - x_g)^2 \frac{1}{3} B_{fffg}^{(2,3)} m^4 \\
 &+ \sum_a^+ \sum_b^+ \sum_f^- \sum_g^- x_a x_b x_f x_g \frac{1}{3} B_{abfg}^{(2,3)} m^4
 \end{aligned}$$

the free energy of the solvent; n_j , the number of moles of solute j ; \bar{G}°_j , the "standard molal free energy" of j ; m_j , the molality of j ($m_j = n_j/W$, where W is the number of kilograms of solvent); R , the gas constant; and T , the absolute temperature.

Since we are interested in equations expressing free energies in terms of ions, we use equivalent concentrations

$$m'_i = m_i z_i = 2I_i/z_i = x_i m' \quad (2)$$

z_i being the absolute value of the charge on ion i (a script z was used for z_i in ref 3), and I_i is the contribution of i to the ionic strength (I) of the solution. Equation 2 also defines the equivalent fraction of i , x_i , the total equivalent concentration of the solution being

$$m' = \sum_i m'_i / 2 \quad (3)$$

It should be noted that $\sum_i x_i = 2$ and that the total equivalent fraction for ions of each charge sign is 1. Lower case subscripts will be used for ions; a, b, c... designate cations, and f, g, h, ..., anions. Equations in this pattern can be developed for solutions having more than one nonelectrolyte component, but we restrict ourselves here to those containing one neutral solvent and one or more electrolyte solutes.

The bulk of the electrostatic contribution (which is the total contribution at infinite dilution) to G^e is probably accounted for in a Debye-Hückel term (Table I,

eq b and c). In these equations S is the Debye-Hückel limiting slope for $\ln \gamma_{\pm}$ of a univalent electrolyte at infinite dilution ($S = -1.17202$ for an aqueous solution at 25° and 1 atm); $a'_{af} \sqrt{I}$ is the Debye κ times the "distance of closest approach" \bar{a} . Unless a' values are the same for all solute components, eq b (Table I) is somewhat different for finite concentrations from the Debye-Hückel expression used in ref 4. In both cases, residual electrostatic effects are lumped into the non-Debye-Hückel terms.

The non-Debye-Hückel contribution to G^e is expressed as a series of interaction terms involving products of m'_i .

$$\begin{aligned}
 (G^e/RTW)^n &= \sum_i \sum_j b_{ij} m'_i m'_j + \\
 &\sum_i \sum_j \sum_k d_{ijk} m'_i m'_j m'_k + \\
 &\sum_i \sum_j \sum_k \sum_l f_{ijkl} m'_i m'_j m'_k m'_l + \\
 &\dots = m'^2 \sum_i \sum_j b_{ij} x_i x_j + \\
 &m'^3 \sum_i \sum_j \sum_k d_{ijk} x_i x_j x_k + \\
 &m'^4 \sum_i \sum_j \sum_k \sum_l f_{ijkl} x_i x_j x_k x_l + \dots \quad (4)
 \end{aligned}$$

(3) G. Scatchard, *J. Amer. Chem. Soc.*, **90**, 3124 (1968); **91**, 2410 (1969). See also G. Scatchard and R. G. Breckenridge, *J. Phys. Chem.*, **58**, 596 (1954); **59**, 1234 (1955).

(4) G. Scatchard, *J. Amer. Chem. Soc.*, **83**, 2636 (1961).

(5) Y. C. Wu, R. M. Rush, and G. Scatchard, *J. Phys. Chem.*, **72**, 4048 (1968); **73**, 4433 (1969).

(6) Y. C. Wu, R. M. Rush, and G. Scatchard, *ibid.*, **73**, 2047, 4434 (1969).

Table II: Definition of B Coefficients

$$B_{af}^{(1)} = b_{aa} + 2 b_{af} + b_{ff}$$

$$B_{af}^{(2)} = 2(d_{aaa} + 3 d_{aaf} + 3 d_{aff} + d_{fff})$$

$$B_{af}^{(3)} = 3(f_{aaaa} + 4 f_{aaaf} + 6 f_{aaff} + 4 f_{afff} + f_{ffff})$$

9 similar terms involving ag, bf, and bg

$$B_{ab}^{(0,1)} = 2 b_{ab} - b_{aa} - b_{bb}$$

$$B_{abf}^{(0,2)} = 2 \left[\frac{3}{2} (d_{aab} + d_{abb} - d_{aaa} - d_{bbb}) + 3(2 d_{abf} - d_{aaf} - d_{bbf}) \right]$$

$$B_{abf}^{(0,3)} = 3 \left[6(f_{aabf} + f_{abbf} - f_{aaaf} - f_{bbbf}) + 3(2 f_{abff} - f_{aaff} - f_{bbff}) \right. \\ \left. + (f_{aaab} + f_{abbb} - f_{aaaa} - f_{bbbb}) + \frac{3}{4} (2 f_{aabb} - f_{aaaa} - f_{bbbb}) \right] \\ + 3[3(2 f_{abff} - f_{aaff} - f_{bbff})]^*$$

$$B_{aab}^{(1,2)} = 2 \left[\frac{1}{2} (3 d_{aab} - 3 d_{abb} - d_{aaa} + d_{bbb}) \right]$$

$$B_{aabf}^{(1,3)} = 3 [2 f_{aabf} - 2 f_{abbb} - f_{aaaa} + f_{bbbb} + 2(3 f_{aabf} - 3 f_{abbf} - f_{aaaf} + f_{bbbf})]$$

$$B_{aaab}^{(2,3)} = 3 \left[f_{aaab} + f_{abbb} - f_{aaaa} - f_{bbbb} - \frac{3}{4} (2 f_{aabb} - f_{aaaa} - f_{bbbb}) \right]$$

6 additional terms involving a common anion by substituting f for a, g for b, and a for f

3 additional terms with common cation by substituting g for f

3 additional terms with common anion by substituting b for a

$$B_{abfg}^{(2,3)} = 3[24 f_{abfg} - 6 f_{abff} - 6 f_{abgg} - 6 f_{aafg} - 6 f_{bbfg}]$$

In expanding eq 4, terms are included for i less than, equal to, and greater than j , and $d_{ijk} = d_{jik} = d_{kij} = d_{kji}$, etc. For example, for a solution containing only ions i and j , $\sum_i \sum_j b_{ij} m'_i m'_j = 2b_{ij} m'_i m'_j + b_{ii} m'^2_i + b_{jj} m'^2_j$. The coefficients b_{ij} , d_{ijk} , and f_{ijkl} are coefficients which, like \bar{G}^0_i , are functions of temperature and pressure and of the nature of the solvent but not of the composition.

These coefficients cannot be determined independently. However, they can be arranged into groups each of which is measurable. Of the grouped coefficients thus obtained, those which probably make the most important contributions to the excess free energy of solutions containing many types of ions can be determined by measurements on simpler systems.

This was illustrated in ref 3 with the products of concentrations of only two ions. Since $\sum_a x_a = \sum_t x_t = 1$, the contribution to $(G^e/RTW)^n$ is

$$m'^2 \left[\sum_a \sum_t x_a x_t (2b_{at} + b_{aa} + b_{tt}) + \sum_a \sum_b x_a x_b (2b_{ab} - b_{aa} - b_{bb}) + \sum_t \sum_g x_t x_g (2b_{tg} - b_{tt} - b_{gg}) \right] = \\ m'^2 \left[\sum_a \sum_t x_a x_t B_{at}^{(1)} + \sum_a \sum_b x_a x_b B_{ab}^{(0,1)} + \sum_t \sum_g x_t x_g B_{tg}^{(0,1)} \right] \quad (5)$$

The first term in brackets can be evaluated from data on two-component solutions of electrolyte af, and the other two can be evaluated from solutions of two electrolytes with a common ion, *e.g.*, af and bf, and af and ag. In eq 5 and the equations in Tables I, III, and IV, for double summations involving the same types of ions only terms for $b > a$ (or $g > f$) are included. For example, in a solution containing cations a, b, and c and anion f the terms which would appear in the first summation of eq e, Table I, are $x_a x_b x_f$, $x_a x_c x_f$, and $x_b x_c x_f$.

Table III: Osmotic Coefficient Equations

$$\begin{aligned}
 \text{(a)} \quad \phi - 1 &= (\phi - 1)^{\text{DH}} + (\phi - 1)^{\text{NI}} + (\phi - 1)^{\text{NII}} \\
 \text{(b)} \quad (\phi - 1)^{\text{DH}} &= \frac{S}{\sum_i x_i/z_i} \sum_a^+ \sum_f^- x_a x_f (z_a + z_f) \frac{Z_{af}}{a'_{af}} \\
 \text{(c)} \quad Z_{af} &= \frac{\partial X_{af}}{\partial \ln I} = \frac{1 + a'_{af} \sqrt{I} - [1/(1 + a'_{af} \sqrt{I})] - 2 \ln(1 + a'_{af} \sqrt{I})}{a'^2_{af} I} \\
 \text{(d)} \quad (\phi - 1)^{\text{NI}} &= \frac{1}{\sum_i x_i/z_i} \sum_a^+ \sum_f^- x_a x_f (B_{af}^{(1)} m' + B_{af}^{(2)} m'^2 + B_{af}^{(3)} m'^3 + \dots) \\
 \text{(e)} \quad (\phi - 1)^{\text{NII}} &= \frac{1}{\sum_i x_i/z_i} \left[\sum_a^+ \sum_b^+ \sum_f^- x_a x_b x_f (B_{ab}^{(0,1)} m' + B_{ab}^{(0,2)} m'^2 + B_{ab}^{(0,3)} m'^3) \right. \\
 &\quad + x_a x_b x_f (x_a - x_b) (B_{aab}^{(1,2)} m'^2 + B_{aabf}^{(1,3)} m'^3) + x_a x_b x_f (x_a - x_b)^2 B_{aaab}^{(2,3)} m'^3 \\
 &\quad + \sum_a^+ \sum_f^- \sum_g^- x_a x_f x_g (B_{fg}^{(0,1)} m' + B_{afg}^{(0,2)} m'^2 + B_{afg}^{(0,3)} m'^3) \\
 &\quad \left. + x_a x_f x_g (x_f - x_g) (B_{ffg}^{(1,2)} m'^2 + B_{affg}^{(1,3)} m'^3) + x_a x_f x_g (x_f - x_g)^2 B_{fffg}^{(2,3)} m'^3 \right]
 \end{aligned}$$

(f) for a solution containing only ions a, b, f, and g:

$$\begin{aligned}
 (\phi - 1)^{\text{NII}} &= \frac{1}{\sum_i x_i/z_i} \left\{ x_a x_b x_f [B_{ab}^{(0,1)} m' + B_{abf}^{(0,2)} m'^2 + B_{abf}^{(0,3)} m'^3] + x_a x_b x_f (x_a - x_b) \right. \\
 &\quad \times [B_{aab}^{(1,2)} m'^2 + B_{aabf}^{(1,3)} m'^3] + x_a x_b x_f (x_a - x_b)^2 B_{aaab}^{(2,3)} m'^3 \\
 &\quad + x_a x_b x_g [B_{ab}^{(0,1)} m' + B_{abg}^{(0,2)} m'^2 + B_{abg}^{(0,3)} m'^3] + x_a x_b x_g (x_a - x_b) [B_{aab}^{(1,2)} m'^2 + B_{aabg}^{(1,3)} m'^3] \\
 &\quad + x_a x_b x_g (x_a - x_b)^2 B_{aaab}^{(2,3)} m'^3 \\
 &\quad + x_a x_f x_g [B_{fg}^{(0,1)} m' + B_{afg}^{(0,2)} m'^2 + B_{afg}^{(0,3)} m'^3] + x_a x_f x_g (x_f - x_g) [B_{ffg}^{(1,2)} m'^2 + B_{affg}^{(1,3)} m'^3] \\
 &\quad + x_a x_f x_g (x_f - x_g)^2 B_{fffg}^{(2,3)} m'^3 \\
 &\quad + x_b x_f x_g [B_{fg}^{(0,1)} m' + B_{bfg}^{(0,2)} m'^2 + B_{bfg}^{(0,3)} m'^3] + x_b x_f x_g (x_f - x_g) [B_{ffg}^{(1,2)} m'^2 + B_{bffg}^{(1,3)} m'^3] \\
 &\quad \left. + x_b x_f x_g (x_f - x_g)^2 B_{fffg}^{(2,3)} m'^3 \right\}
 \end{aligned}$$

Similar resolutions of the higher terms can be made, with the use as necessary of the relations

$$1 = x + (1 - x) =$$

$$x^2 + 2x(1 - x) + (1 - x)^2 \quad (6)$$

Equation 4 can thus be resolved into two components of $(G^e)^n$, $(G^e/RTW)^{\text{NI}}$ (Table I, eq d) which, along with $(G^e/RTW)^{\text{DH}}$ can be evaluated from measurements on two-ion (two-component or single-salt) solutions, and

$(G^e/RTW)^{\text{NII}}$ (Table I, eq e) obtained from three-ion (common-ion) solutions. Table II relates the upper case coefficients of eq d and e of Table I with the lower case ones of eq 4.

The superscripts on the B coefficients indicate the power to which the concentration is raised in the appropriate term in the osmotic coefficient equation (Table III, eq d). In the case of double superscripts, the first superscript indicates the power to which the

Table IV: Activity Coefficient Equations

$$\begin{aligned}
 \text{(a)} \quad (\ln \gamma_{\pm})_{pq} &= (\ln \gamma_{\pm})_{pq}^{\text{DH}} + (\ln \gamma_{\pm})_{pq}^{\text{NI}} + (\ln \gamma_{\pm})_{pq}^{\text{NII}} \\
 \text{(b)} \quad (\ln \gamma_{\pm})_{pq}^{\text{DH}} &= z_p z_q S \left[\sum_a^+ x_a \cdot \frac{(z_a + z_q)}{(z_p + z_q)} \cdot \frac{X_{aq}}{a'_{aq}} + \sum_f^- x_f \cdot \frac{(z_p + z_f)}{(z_p + z_q)} \cdot \frac{X_{pf}}{a'_{pf}} - \sum_a^+ \sum_f^- x_a x_f \cdot \frac{(z_a + z_f)}{(z_p + z_q)} \cdot \frac{X_{af}}{a'_{af}} \right. \\
 &\quad \left. + \frac{1}{\sum_i x_i z_i} \sum_a^+ \sum_f^- x_a x_f (z_a + z_f) \frac{Z_{af}}{a'_{af}} \right] \\
 \text{(c)} \quad (\ln \gamma_{\pm})_{pq}^{\text{NI}} &= \frac{1}{(1/z_p) + (1/z_q)} \left[\sum_a^+ x_a \left(B_{aq}^{(1)} m' + \frac{1}{2} B_{aq}^{(2)} m'^2 + \frac{1}{3} B_{aq}^{(3)} m'^3 \right) + \sum_f^- x_f \left(B_{pf}^{(1)} m' + \frac{1}{2} B_{pf}^{(2)} m'^2 + \frac{1}{3} B_{pf}^{(3)} m'^3 \right) \right. \\
 &\quad \left. + \sum_a^+ \sum_f^- x_a x_f \left(\frac{1}{2} B_{af}^{(2)} m'^2 + \frac{2}{3} B_{af}^{(3)} m'^3 \right) \right] \\
 \text{(d)} \quad (\ln \gamma_{\pm})_{pq}^{\text{NII}} &= \frac{1}{(1/z_p) + (1/z_q)} \left[\sum_a^+ B_{ap}^{(0,1)} m'_a + \frac{1}{2} B_{aap}^{(1,2)} (m_a'^2 - 2 m'_a m'_p) + \frac{1}{3} B_{aaa}^{(2,3)} (m_a'^3 - 4 m_a'^2 m'_p + 3 m'_a m_p'^2) \right. \\
 &\quad + \sum_f^- B_{fq}^{(0,1)} m'_f + \frac{1}{2} B_{ffq}^{(1,2)} (m_f'^2 - 2 m'_f m'_q) + \frac{1}{3} B_{fffq}^{(2,3)} (m_f'^3 - 4 m_f'^2 m'_q + 3 m'_f m_q'^2) \\
 &\quad + \sum_a^+ \sum_f^- \frac{1}{2} B_{apf}^{(0,2)} m'_a m'_f + \frac{1}{3} B_{apf}^{(0,3)} m'_a m'_f m'_p + \frac{1}{3} B_{aapf}^{(1,3)} (m_a'^2 m'_f - 2 m'_a m'_p m'_f) \\
 &\quad + \sum_a^+ \sum_b^+ \frac{1}{2} B_{abb}^{(0,2)} m'_a m'_b + \frac{1}{3} B_{abb}^{(0,3)} m'_a m'_b m'_p + \frac{1}{3} B_{aabb}^{(1,3)} (m_a'^2 m'_b - m'_a m_b'^2) + \sum_a^+ \sum_b^+ \sum_f^- \frac{1}{3} B_{abf}^{(0,3)} m'_a m'_b m'_f \\
 &\quad + \sum_a^+ \sum_f^- \frac{1}{2} B_{afq}^{(0,2)} m'_a m'_f + \frac{1}{3} B_{afq}^{(0,3)} m'_a m'_f m'_q + \frac{1}{3} B_{affq}^{(1,3)} (m_a' m_f'^2 - 2 m'_a m'_f m'_q) \\
 &\quad \left. + \sum_f^- \sum_g^- \frac{1}{2} B_{pfg}^{(0,2)} m'_f m'_g + \frac{1}{3} B_{pfg}^{(0,3)} m'_f m'_g m'_p + \frac{1}{3} B_{pffg}^{(1,3)} (m_f'^2 m'_g - m'_f m_g'^2) + \sum_a^+ \sum_f^- \sum_g^- \frac{1}{3} B_{afg}^{(0,3)} m'_a m'_f m'_g \right]
 \end{aligned}$$

equivalent fraction difference is raised in the appropriate term in the osmotic coefficient equation (except for $B_{abfg}^{(2,3)}$). The second superscript indicates the power of the concentration in the same manner as the single superscript (Table III, eq e).

With some terms there is an approximation involved in using coefficients evaluated from simple systems in computations for more complicated ones. For example, in a three-ion system, a, b, and f, $x_f = 1$, and coefficients multiplied by $x_a x_b$, by $x_a x_b x_f$, and by $x_a x_b x_f^2$ cannot be distinguished. No approximation will be involved in the contribution of the terms including the first two to a solution containing a, b, f, and g. Although terms corresponding to interactions of a and b cannot be distinguished from terms for a, b, and f, the coefficient for a and b will presumably be the same as for an a, b, and g solution, and since $x_f + x_g = 1$, the total contribution to excess free energy will be correctly evaluated. However, with coefficients of $x_a x_b x_f^2$ or $x_a x_b x_g^2$, there is an approximation from the in-

ability to resolve the coefficients, since in the four-ion system, x_f and x_g are not unity. In Table II, in the expression for $B_{abf}^{(0,3)}$, the grouping of lower case coefficients in the bracket indicated by an asterisk should be multiplied by $x_a x_b x_f^2$. Here we shall multiply by $x_a x_b x_f$ and by the analogous products for $B_{abg}^{(0,3)}$, $B_{afg}^{(0,3)}$, and $B_{bfg}^{(0,3)}$.

The coefficient $B_{abfg}^{(2,3)}$ is included in Tables I and II only for completeness of correspondence between eq 4 and the equations with B coefficients. We believe it will usually be too small to make an appreciable contribution to the excess free energy, and we make no attempt to evaluate it.

Experimental data are usually in the form of measurements of solvent activity, in terms of osmotic coefficients, ϕ , or of mean activity coefficients of the solutes, γ_{\pm} . Expressions for these quantities are obtained by differentiation of the equations for excess free energy

$$\left(\frac{\partial(G^e/RTWI)}{\partial \ln W} \right)_K = -2 \sum_i x_i z_i / z_i (\phi - 1) \quad (7)$$

Table V: Activity Coefficient Equations

For component af in a solution containing ions a, b, f, and g:

$$\begin{aligned}
 \text{(a) } (\ln \gamma_{\pm}^{\text{DH}})_{\text{af}} &= z_a z_f S \left\{ (x_a + x_f - x_a x_f) \frac{X_{\text{af}}}{a'_{\text{af}}} + x_b x_g \left[\frac{(z_a + z_g)}{(z_a + z_f)} \cdot \frac{X_{\text{ag}}}{a'_{\text{ag}}} + \frac{(z_b + z_f)}{(z_a + z_f)} \cdot \frac{X_{\text{bf}}}{a'_{\text{bf}}} - \frac{(z_b + z_g)}{(z_a + z_f)} \cdot \frac{X_{\text{bg}}}{a'_{\text{bg}}} \right] \right. \\
 &\quad \left. + \frac{1}{x_a z_a + x_b z_b + x_f z_f + x_g z_g} \left[x_a x_f (z_a + z_f) \frac{Z_{\text{af}}}{a'_{\text{af}}} + x_a x_g (z_a + z_g) \frac{Z_{\text{ag}}}{a'_{\text{ag}}} + x_b x_f (z_b + z_f) \frac{Z_{\text{bf}}}{a'_{\text{bf}}} + x_b x_g (z_b + z_g) \frac{Z_{\text{bg}}}{a'_{\text{bg}}} \right] \right\} \\
 \text{(b) } (\ln \gamma_{\pm}^{\text{NI}})_{\text{af}} &= \frac{1}{(1/z_a) + (1/z_f)} \left[B_{\text{af}}^{(1)} (m'_a + m'_f) + \frac{1}{2} B_{\text{af}}^{(2)} (m'_a m'_f + m'_f m'_a + m'_b m'_f) + \frac{1}{3} B_{\text{af}}^{(3)} (m'_a m'^2 + m'_f m'^2 + 2 m'_a m'_f m) \right. \\
 &\quad + B_{\text{bf}}^{(1)} m'_b + \frac{1}{2} B_{\text{bf}}^{(2)} (m'_b m'_f + m'_b m'_f) + \frac{1}{3} B_{\text{bf}}^{(3)} (m'_b m'^2 + 2 m'_b m'_f m) \\
 &\quad + B_{\text{ag}}^{(1)} m'_g + \frac{1}{2} B_{\text{ag}}^{(2)} (m'_g m'_f + m'_g m'_f) + \frac{1}{3} B_{\text{ag}}^{(3)} (m'_g m'^2 + 2 m'_g m'_f m) \\
 &\quad \left. + \frac{1}{2} B_{\text{bg}}^{(2)} m'_b m'_g + \frac{2}{3} B_{\text{bg}}^{(3)} m'_b m'_g m' \right] \\
 \text{(c) } (\ln \gamma_{\pm}^{\text{NII}})_{\text{af}} &= \frac{1}{(1/z_a) + (1/z_f)} \left[B_{\text{ab}}^{(0,1)} m'_b + \frac{1}{2} B_{\text{abf}}^{(0,2)} (m'_b m'_f + m'_a m'_g) + \frac{1}{3} B_{\text{abf}}^{(0,3)} (m'_b m'_f m' + m'_a m'_b m'_f) + \frac{1}{2} B_{\text{abg}}^{(0,2)} m'_b m'_g \right. \\
 &\quad + \frac{1}{3} B_{\text{abg}}^{(0,3)} (m'_b m'_g m' + m'_a m'_b m'_g) + \frac{1}{2} B_{\text{aab}}^{(1,2)} (2 m'_a m'_b - m_b^2) + \frac{1}{3} B_{\text{aabf}}^{(1,3)} (2 m'_a m'_b m'_f + m_a^2 m_b^2 - m_b^2 m'_f - m'_a m_b^2) \\
 &\quad + \frac{1}{3} B_{\text{aabg}}^{(1,3)} (2 m'_a m'_b m'_g - m_b^2 m'_g) + \frac{1}{3} B_{\text{aaab}}^{(2,3)} (3 m_a^2 m_b^2 - 4 m'_a m_b^2 + m_b^3) \\
 &\quad + B_{\text{afg}}^{(0,1)} m'_g + \frac{1}{2} B_{\text{afg}}^{(0,2)} (m'_f m'_g + m'_a m'_g) + \frac{1}{3} B_{\text{afg}}^{(0,3)} (m'_f m'_g m' + m'_a m'_g m' + m'_a m'_f m'_g) + \frac{1}{2} B_{\text{bfg}}^{(0,2)} m'_b m'_g \\
 &\quad + \frac{1}{3} B_{\text{bfg}}^{(0,3)} (m'_b m'_g m' + m'_b m'_f m'_g) + \frac{1}{2} B_{\text{ffg}}^{(1,2)} (2 m'_f m'_g - m_g^2) + \frac{1}{3} B_{\text{affg}}^{(1,3)} (m'_f m'_g + 2 m'_a m'_f m'_g - m'_f m_g^2 - m'_a m_g^2) \\
 &\quad \left. + \frac{1}{3} B_{\text{bffg}}^{(1,3)} (2 m'_b m'_f m'_g - m'_b m_g^2) + \frac{1}{3} B_{\text{fffg}}^{(2,3)} (3 m_f^2 m_g^2 - 4 m'_f m_g^2 + m_g^3) \right]
 \end{aligned}$$

and

$$\left(\frac{\partial(G^{\circ}/RTW)}{\partial m'_j} \right)_{W, K \neq j} = \left(\frac{1}{z_p} - \frac{1}{z_q} \right) \ln \gamma_{\pm J} \quad (8)$$

J being an electrolyte made up of p and q ions, with $m'_j = m'_{p(j)} = m'_{q(j)}$. Differentiation of equations for G° with respect to temperature and pressure yield expressions for heats and volumes.

We list in Tables III and IV the equations for osmotic coefficient and $\ln \gamma_{\pm}$, including those terms which involve B 's obtainable from two-ion and three-ion solutions. For convenience, we give also in Tables III and V the equations for the systems of particular interest here, these containing only four ions, a, b, f, and g. In eq d, Table IV, in summations involving terms subscripted with p (or q), terms in which a (or f) are replaced by p (or q) are not included; e.g., there are no terms $B_{\text{ppf}}^{(0,2)}$ (or $B_{\text{aaq}}^{(0,2)}$).

The fit for a given set of osmotic coefficient data can be made within the experimental error for both the neutral-electrolyte and the ion-component treatment if enough parameters are used. For this reason the good-

ness of fit obtainable is not a very useful basis for comparison of the two approaches. However, the ability to estimate ϕ and $\ln \gamma_{\pm}$ for three-ion solutions from data on two-ion solutions is a meaningful criterion. For a solution containing four ions, a further test for the ion-component approach is how well osmotic coefficients can be calculated from two-ion and three-ion data; it is not obvious how to do this with the other approach.

Application

The System Na-Mg-Cl-SO₄. In the previous papers in this series,^{5,6} we have presented the results of isopiestic measurements on the six aqueous binary salt mixtures possible using NaCl, Na₂SO₄, MgSO₄, and MgCl₂. In these papers the results for each salt mixture were analyzed by the neutral-electrolyte treatment⁴ in which the components were considered to be the neutral salts and water. The concentration was expressed as the ionic strength, I , and the solute composition as the ionic strength fraction, y .

We have now analyzed these data by the ion-component treatment³ considering the system to be com-

posed of water and Na^+ (a), Mg^{2+} (b), Cl^- (f), and SO_4^{2-} (g). In this procedure the two-ion parameters involving ions of unlike sign ($B_{af}^{(1)}$, $B_{bg}^{(2)}$, etc.) were derived from the a parameters previously used^{5,6} which were, in turn, derived from the compilation of Lietzke and Stoughton.⁷ The values of these parameters are given in Table VI. The three-ion parameters (those

Table VI: B Parameters for the System

Na (a)-Mg (b)-Cl (f)- SO_4 (g)

$\alpha'_{af} = 1.45397$	$B_{ab}^{(0,1)} = 0.0630$
$B_{af}^{(1)} = 0.04472$	$B_{abf}^{(0,2)} = -0.0228$
$B_{af}^{(2)} = 0.018616$	$B_{abf}^{(0,3)} = 0.00221$
$B_{af}^{(3)} = -0.0010724$	$B_{aab} = 0$
$\alpha'_{bg} = 1.24072$	$B_{abf}^{(1,3)} = -0.00068$
$B_{bg}^{(1)} = -0.14805$	$B_{aabf}^{(2,3)} = 0$
$B_{bg}^{(2)} = 0.024513$	$B_{abg}^{(0,2)} = -0.0066$
$B_{bg}^{(3)} = -0.0009847$	$B_{abg}^{(0,3)} = -0.00147$
$\alpha'_{bf} = 1.60067$	$B_{aabg}^{(1,3)} = 0$
$B_{bf}^{(1)} = 0.14924$	$B_{fg}^{(0,1)} = -0.0243$
$B_{bf}^{(2)} = 0.030385$	$B_{aifg}^{(0,2)} = 0.01105$
$B_{bf}^{(3)} = -0.0012884$	$B_{aifg}^{(0,3)} = -0.00079$
$\alpha'_{bg} = 1.37486$	$B_{ffg}^{(1,2)} = -0.00246$
$B_{br}^{(1)} = -0.10848$	$B_{aifg}^{(1,3)} = 0$
$B_{bg}^{(2)} = 0.033704$	$B_{fffg}^{(2,3)} = 0$
$B_{bg}^{(3)} = -0.001520$	$B_{bifg}^{(0,2)} = 0$
	$B_{bifg}^{(0,3)} = 0.00031$
	$B_{bifg}^{(1,3)} = 0$

involving three-ion interactions, $B_{abf}^{(0,2)}$, $B_{aabf}^{(1,3)}$, etc., as well as those involving the interaction of two ions of like sign, $B_{ab}^{(0,1)}$, $B_{fffg}^{(2,3)}$, etc.) were evaluated by a least-squares procedure using eq f of Table III and the osmotic coefficients for the four systems involving a common ion.⁵ The values for these parameters are also given in Table VI. The experimental data for the common-ion mixtures can thus be described by eq f of Table III and the parameters of Table VI. The standard deviation of this fit is 0.0012 in ϕ .

A comparison of the ion-component treatment with the neutral-electrolyte treatment used previously is given in Table VII in terms of the ability to fit the common-ion data. (The standard deviation given in this table differs slightly from the definition previously used; it was chosen so as to avoid ambiguity regarding the number of variable parameters.) The first two columns of figures compare the two treatments when only the two-ion (single-salt) parameters are used. These figures indicate that, given only the two-ion data, the ion-component treatment provides a better approximation for the osmotic coefficient than the neutral-electrolyte treatment.

The third and fourth columns of Table VII compare the two treatments when terms characteristic of the mixtures [cross terms, $(G^e/RTW)^{nII}$] are included. The results indicate that the quality of the fit is about the same for the two treatments. It should be noted, however, that for the neutral-electrolyte treatment each

Table VII: Standard Deviation for Fits to the Data for the System Na-Mg-Cl- SO_4

$$S = \sqrt{\frac{\sum(\phi_{\text{obsd}} - \phi_{\text{calcd}})^2}{\text{no. of observations}}}$$

	Two-ion terms		All terms	
	N.E. ^a	I.C. ^b	N.E. ^a	I.C. ^b
NaCl- Na_2SO_4	0.0219	0.0054	0.0009	0.0009
Na_2SO_4 - MgSO_4	0.0191	0.0121	0.0010	0.0013
MgSO_4 - MgCl_2	0.0339	0.0066	0.0008	0.0012
MgCl_2 -NaCl	0.0145	0.0056	0.0013	0.0009
NaCl- MgSO_4	0.0097	0.0037	0.0012 ^c	0.0016 ^d
Na_2SO_4 - MgCl_2	0.0191	0.0074	0.0021 ^c	0.0042 ^d

^a N.E., neutral-electrolyte treatment. ^b I.C., ion-component treatment. ^c Cross-term parameters from direct fit to experimental osmotic coefficients. ^d Cross-term parameters from fit to three-ion osmotic coefficients.

mixture is treated independently, while for the ion-component treatment the data for all four common-ion mixtures are taken together and some of the parameters are affected by the data from more than one mixture (e.g., the parameter $B_{ab}^{(0,1)}$ must satisfy the data for both the NaCl- MgCl_2 and the Na_2SO_4 - MgSO_4 mixtures).

For the two four-ion (noncommon-ion) mixtures in Table VII the results computed from two-ion data are also much better with the ion-component approach than with the neutral-electrolyte treatment. The results with cross terms included are much the same for the two methods. This is shown in more detail by the deviation plots in Figure 1. Here the fits using only the two-ion data are decidedly better for the ion-component treatment. When the mixture terms are included, the standard deviations in Table VII suggest a better fit by the neutral-electrolyte treatment. It should be noted again, however, that the neutral-electrolyte treatment involves a direct fit to the data for the mixture in question with parameters characteristic of that mixture. With the ion-component treatment the only parameters used are those derived from the three-ion data and do not depend on any measurements on the four-ion mixtures. The deviation plots in Figure 1 indicate that the fit is only slightly worse with the ion-component treatment. In addition, five points for the Na_2SO_4 - MgCl_2 mixtures at $y_{\text{MgCl}_2} = 0.5$ show a consistent deviation. This consistent deviation is more apparent for the ion-component treatment and contributes to the larger standard deviations in Table VII. We suspect that there may have been experimental or computational errors in these measurements; however, we have been unable to identify such errors and have concluded that disregarding these points would not be justified. The deviation of these points from the bulk of the data would not be so apparent with the neutral-electrolyte

(7) M. H. Lietzke and R. W. Stoughton, *J. Phys. Chem.*, **66**, 508 (1962).

Table VIII: Trace $\log \gamma_{\pm}$ (NaCl) in Mixtures with Na_2SO_4 , MgCl_2 , and MgSO_4 ($y_{\text{NaCl}} = 0$)

I	Two-ion terms		All terms		Platford ^c		
	N.E. ^a	I.C. ^b	N.E. ^a	I.C. ^b	McKay-Perrig	N.E., ^a all terms	
NaCl- Na_2SO_4	1	-0.2151	-0.2258	-0.2278	-0.2287	-0.250	-0.229
	3	-0.2432	-0.2765	-0.2803	-0.2816	-0.308	-0.283
	6	-0.2055	-0.2726	-0.2744	-0.2788	-0.314	-0.280
NaCl- MgCl_2	1	-0.1757	-0.1718	-0.1633	-0.1688	-0.176	-0.166
	3	-0.1416	-0.1303	-0.1124	-0.1112	-0.120	-0.113
	6	-0.0098	0.0146	0.0367	0.0481	0.037	0.049
NaCl- MgSO_4	1	-0.2030	-0.2057	-0.2038	-0.2017		
	3	-0.2181	-0.2310	-0.2242	-0.2187		
	6	-0.1687	-0.1977	-0.1865	-0.1788		

^a N.E., neutral-electrolyte treatment. ^b I.C., ion-component treatment. ^c NaCl- Na_2SO_4 , ref 8; NaCl- MgCl_2 , ref 9.

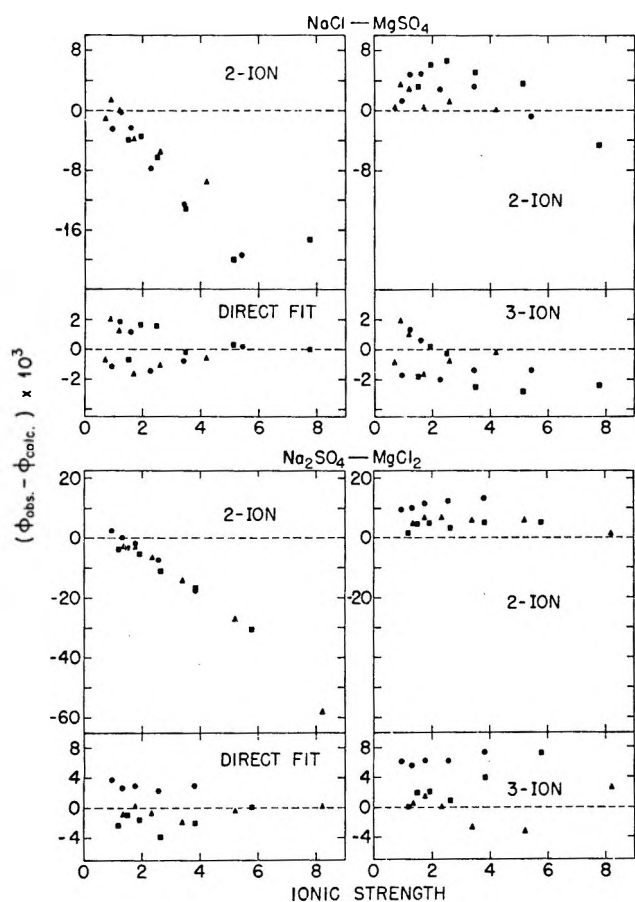


Figure 1. Deviation plots for four-ion data. Neutral-electrolyte treatment (left) and ion-component treatment (right). Ionic strength fractions for second component: \blacktriangle , 0.25, \bullet , 0.5; and \blacksquare , 0.75.

treatment, since the direct fit to the data used in this approach adjusts the parameters to compensate partially for these deviations.

The activity coefficients provide an additional means of comparing the treatments, although there are fewer direct measurements of this quantity for comparison, and the reliability of available data is more questionable, than with osmotic coefficients. Comparison of $\log \gamma_{\pm}$

computed in different ways from osmotic coefficient data are also of interest, both to indicate the uncertainty of activity coefficients obtained in this way and to indicate the extent to which they can be estimated from two-ion data alone, and from two-ion plus three-ion data. Equations for the calculation of $\log \gamma_{\pm}$ for the general case are given in Table IV and for the specific case of component *a* (NaCl) in a mixture of a (Na^+), *b* (Mg^{2+}), *f* (Cl^-), and *g* (SO_4^{2-}) ions in Table V.

A convenient comparison of results obtained by different methods of computing $\log \gamma_{\pm}$ from osmotic coefficients is given by values of "trace" $\log \gamma_{\pm}$, shown in Table VIII. In this case the figures given are for $\log \gamma_{\pm}$ of NaCl in the mixture indicated where the fraction of NaCl is zero. These represent an extrapolated value and can be obtained from the neutral-electrolyte equations with the ionic strength fraction of NaCl equal to zero and from the ion-component equations (Table V) with the appropriate equivalent fractions equal to zero. Again we have compared the neutral-electrolyte and the ion-component treatments with only the two-ion terms and with the cross terms. It should again be noted that the figures in the column "all terms, I.C." were calculated from the parameters derived from all of the three-ion data and in the case of NaCl- MgSO_4 do not involve any direct measurements on this mixture.

The results using only the two-ion terms indicate that, except for the NaCl- MgSO_4 mixtures for which agreement is good for either approach, the ion-component treatment gives values closer to those given by the complete equation than the neutral-electrolyte treatment. When the mixture terms are included the two treatments are in good agreement, the maximum difference being 0.008 in $\log \gamma_{\pm}$.

We have also included in Table VIII values from the isopiestic measurements of Platford on the systems NaCl- Na_2SO_4 ⁸ and NaCl- MgCl_2 .⁹ In these cases Platford calculated activity coefficients by the McKay-

(8) R. F. Platford, *J. Chem. Eng. Data*, **13**, 46 (1968).

(9) R. F. Platford, *J. Phys. Chem.*, **72**, 4053 (1968).

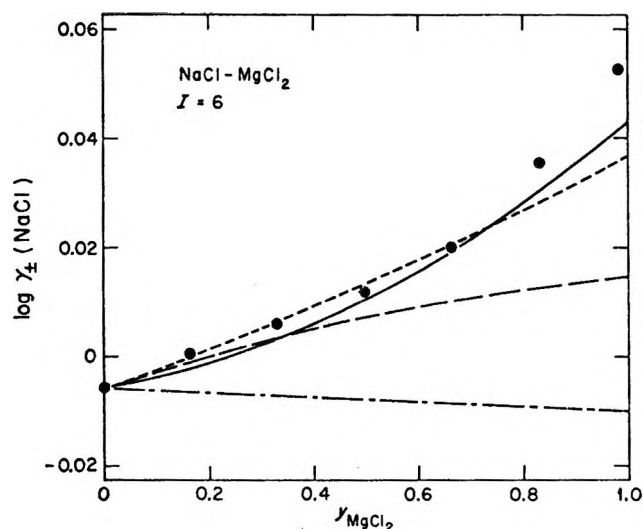


Figure 2. Activity coefficients of NaCl in NaCl-MgCl₂ mixtures: ---, neutral-electrolyte treatment, two-ion parameters; —, ion-component treatment, two-ion parameters; - · -, neutral-electrolyte treatment, direct fit; —, ion-component treatment, three-ion parameters; ●, emf measurements (ref 10).

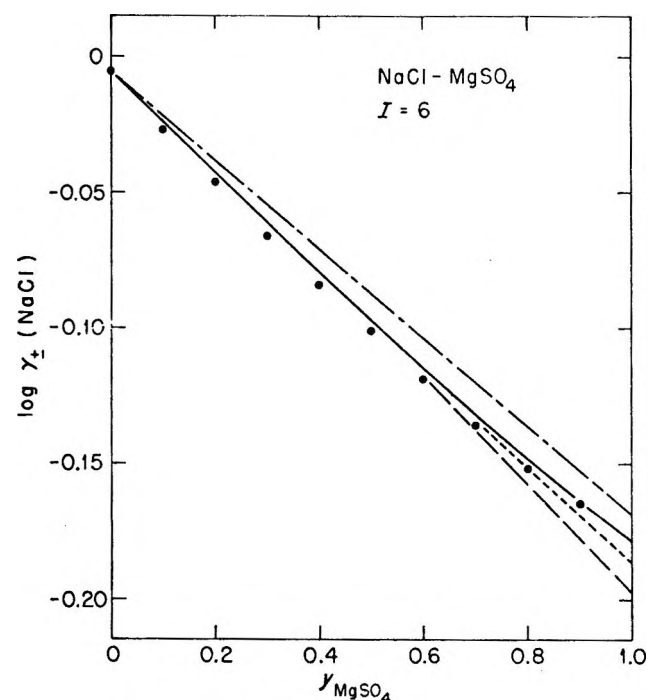


Figure 3. Activity coefficients of NaCl in NaCl-MgSO₄ mixtures: ---, neutral-electrolyte treatment, two-ion parameters; —, ion-component treatment, two-ion parameters; - · -, neutral-electrolyte treatment, direct fit; —, ion-component treatment, three-ion parameters; ●, emf measurements (ref 6).

Perring method, and these results are compared with computations by the neutral-electrolyte method. These results when treated by the neutral-electrolyte method are in good agreement with our results. The differences for the McKay-Perring treatment are prob-

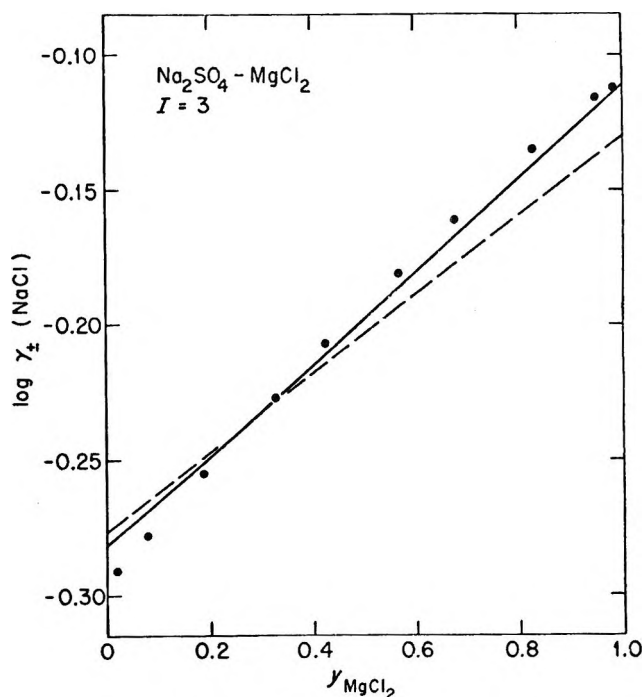


Figure 4. Activity coefficients of NaCl in Na₂SO₄-MgCl₂ mixtures: ---, ion-component treatment, two-ion parameters; —, ion-component treatment, three-ion parameters; ●, emf measurements (ref 6).

ably due in large part to the method of extrapolation to zero concentration used with that method.⁹

A comparison of the various treatments with experimental emf measurements is given in Figures 2-4. The experimental results for the NaCl-MgSO₄ and Na₂SO₄-MgCl₂ mixtures are taken from our previous publications⁶ and those for NaCl-MgCl₂ from the work of Lanier.¹⁰ A discussion of these results relative to the neutral electrolyte treatment has been given in the previous papers in this series.^{5,6} The results for NaCl-MgCl₂ (Figure 2) and NaCl-MgSO₄ (Figure 3) show clearly the increased power of the ion-component treatment when using only two-ion data. In these cases the two treatments give about the same quality of fit to the experimental data when the terms characteristic of the mixtures are included. The ion-component treatment, however, does reproduce more closely the upward curvature of the experimental data at low NaCl fractions. This agreement raises questions concerning our earlier tentative conclusion^{6,10} that the curvature arises from nonideality of the electrodes.

Values of $\log \gamma_{\pm}(\text{NaCl})$ in the system Na₂SO₄-MgCl₂ can be calculated only at the end points and the midpoint by the neutral-electrolyte treatment.⁶ Using the ion-component treatment, values for any point can be calculated and the results at $I = 3$ are shown in Figure 4. Here curves are calculated using only the two-ion parameters and using these plus the three-ion

(10) R. D. Lanier, *J. Phys. Chem.*, **69**, 3992 (1965).

parameters. The agreement is satisfactory at least for the three-ion case. It should be reemphasized that the solid line in Figure 4 was calculated using parameters derived from the three-ion (common-ion) data and does not depend on any direct measurements on the $\text{Na}_2\text{SO}_4\text{-MgCl}_2$ mixtures.

In summary, the following points have been established for the mixtures comprising this system. (1) The ion-component treatment provides a better estimate of the osmotic coefficient or the activity coefficient than the neutral-electrolyte treatment when only data from the two-ion (single-salt) systems are available. (2) For three-ion (common-ion) systems the ion-component treatment provides as good a fit as the neutral-electrolyte treatment. (3) The ion-component treatment provides an entirely adequate means of calculating the osmotic and activity coefficients for the four-ion systems using only the results obtained from the three-ion mixtures.

Synthetic Sea-Water Solutions. We have previously reported¹¹ the osmotic coefficients for synthetic sea-water solutions measured by the isopiestic technique. These solutions were prepared with NaCl, KCl, MgCl_2 , and Na_2SO_4 so as to have the relative composition of sea water. These data when fitted to an equation with a Debye-Hückel term and a power series in ionic strength gave a standard deviation of 0.0003 in ϕ . A comparison of the experimental data with values calculated from an equation derived from data on pure NaCl solutions at the same ionic strength gave a standard deviation of 0.0040.

By combining the KCl with the NaCl, these solutions can be considered as the four-ion system discussed above. Using the parameters of Table VI it is then possible to calculate the osmotic coefficients by the ion-component method. The resulting standard deviations are 0.0048 using only the two-ion terms and 0.0020 using both the two-ion and three-ion terms. The ion-component treatment using only the two-ion terms does not give quite as good a fit as the NaCl equation, but inclusion of the three-ion terms provides a somewhat better fit to the data.

Discussion

Young and coworkers have enunciated a number of empirical rules for changes of excess thermodynamic quantities on the mixing of electrolyte solutions. Usually, these rules have been initially stated and tested for heats and volumes of mixing, but possible applications to excess free energy were clearly in Young's mind,^{12,13} and it is of interest to discuss the connections between the rules and the equations of this paper.

These rules are usually stated for mixings carried out at constant ionic strength, and concentration enters the expressions for $(G^e/RTW)^{\text{DH}}$ as I and $(G^e/RTW)^{\text{NI}}$ as m' . This causes no difficulty if all electrolytes are (1-1)

and have a common ion, as they were in the original applications of the rules, since $m' = I$. However, with electrolyte groups which include ions of different valence, as $\text{Na}^+\text{-Mg}^{2+}\text{-Cl}^-\text{-SO}_4^{2-}$ does, there are differences in the contributions from parameters evaluated from the single-salt solutions between mixed and unmixed solutions; these differences do not drop out as simply as, for example, they did in the discussion of the cross-square rule by the neutral-electrolyte approach.⁶ Since the ion-component method gives at least as good a fit to osmotic coefficient data, mixing rules can be tested for free energies as well by it as by the neutral-electrolyte method. To be able to discuss the rules in terms of coefficients from $(G^e/RTW)^{\text{NI}}$ only, however, we shall limit our attention to 1-1 electrolytes.

For a mixture with a common ion, the first rule is in its simplified form implicit in Brønsted's principle of specific interaction of ions.¹⁴ It states that $(G^e/RTW)^{\text{NI}}$ is very small. Brønsted's reasoning was that electrostatic repulsion prevents two ions of the same sign from approaching closely. An even more powerful reason is illustrated by the terms proportional to the concentration. That in $(\phi - 1)_{\text{af}}^{\text{NI}}$ is $(2b_{\text{af}} + b_{\text{aa}} + b_{\text{ff}})$; that in $(\phi - 1)_{\text{abf}}^{\text{NI}}$ is $(\epsilon b_{\text{ab}} - b_{\text{aa}} - b_{\text{bb}})$. Other upper case coefficients in $(G^e/RTW)^{\text{NI}}$ are likewise seen (Table II) to be differences of an equal number of positive and negative lower-case interaction coefficients which might be expected to be similar in magnitude. Guggenheim¹⁵ extended Brønsted's relation to reciprocal salt pairs. Scatchard and Prentiss¹⁶ applied the relations to the reciprocal salt pair $\text{KNO}_3\text{-LiCl}$. The rule was stated in connection with measurements of volumes and heats of mixing by Young¹² and extended by Young and Smith¹⁷ to mixtures without a common ion. A deviation from the simple rule analogous to the $B^{(0,1)}$ terms in these equations was also given (see also ref 18). If there is no common ion, statement of the rule only in terms $(G^e/RTW)^{\text{NI}}$ is approximate even for 1-1 electrolytes, since there are contributions from $(G^e/RTW)^{\text{DH}}$ and $(G^e/RTW)^{\text{NI}}$ in the mixed solutions not in the equations for the unmixed solutions. For example, if we mix af and bg, the excess free energy for the mixture includes contributions from the single-salt equations for ag and bf.

(11) R. M. Rush and J. S. Johnson, *J. Chem. Eng. Data*, **11**, 590 (1966).

(12) T. F. Young, *Rec. Chem. Progr.*, **12**, 81 (1951).

(13) T. F. Young, Y. C. Wu, and A. A. Krawetz, *Discussions Faraday Soc.*, **24**, 37, 77, 80 (1957).

(14) J. N. Brønsted, *J. Amer. Chem. Soc.*, **44**, 877, 938 (1922); **45**, 2898 (1923).

(15) E. A. Guggenheim, *Beretrn. Skand. Naturforskermoede*, 18th Meeting, Copenhagen, 1929, 298 (1929).

(16) G. Scatchard and S. S. Prentiss, *J. Amer. Chem. Soc.*, **56**, 1486, 2314, 2320 (1934).

(17) T. F. Young and M. B. Smith, *J. Phys. Chem.*, **58**, 716 (1954).

(18) R. M. Rush and G. Scatchard, *ibid.*, **65**, 2240 (1961).

Young's second rule^{13,19} is that the heat of mixing for two electrolytes having a common ion is independent of the common ion. The corresponding rule for free energy would imply that $(\phi - 1)^{nII}$ is independent of the common ion. The rule should hold if only $B_{ab}^{(0,1)}$ ($B_{ig}^{(0,1)}$ if common cation) and other coefficients with only a and b subscripts contribute to $(\phi - 1)^{nII}$, but not necessarily if other terms of higher power in concentration are important.

Young's third rule,¹³ better known as the cross-square rule, states that for a group of electrolytes of the same valence type af, bf, ag, bg, the free energy of mixing 1 mol of af with 1 mol of bg plus that of mixing 1 mol of ag with 1 mol of bf is equal to that of mixing 1 mol of af with 1 mol of bf plus that of mixing 1 mol of ag with 1 mol of bg plus that of mixing 1 mol of bf with 1 mol of bg plus that of mixing 1 mol of ag with 1 mol of af. With our equations, it holds if $B_{abfg}^{(2,3)}$ is zero.

A recent paper²⁰ based on the treatment of Friedman gives terms which appear to be similar to the low-order

concentration terms in the ion-component treatment presented above. In applying these equations²¹ the interaction parameters are determined separately for each ionic strength and vary with ionic strength. Some of the apparent complexities of our treatments arise from the fact that the equations for these treatments include both the variation with the fraction of each solute and with the overall solute concentration.

Since the earlier treatment¹¹ of sea-water compositions as slightly perturbed NaCl solutions was satisfactory at room temperature, the ion-component approach does not result in a great improvement. It is possible, however, that the ion-component treatment will be useful at higher temperatures, for which data now exist.²²

(19) Y. C. Wu, M. B. Smith, and T. F. Young, *J. Phys. Chem.*, **69**, 1868 (1965).

(20) P. J. Reilly and R. H. Wood, *ibid.*, **73**, 4292 (1969).

(21) R. H. Wood, M. Ghamkhar, and J. D. Patton, *ibid.*, **73**, 4298 (1969).

(22) H. F. Gibbard, Jr., personal communication.

Equilibria and Proton Transfer in the Bisulfate–Sulfate System

by D. E. Irish and H. Chen

Department of Chemistry, University of Waterloo, Waterloo, Ontario, Canada (Received March 2, 1970)

Relative integrated Raman intensities have been obtained from NH_4HSO_4 , KHSO_4 , and $(\text{NH}_4)_2\text{SO}_4\text{-HCl}$ aqueous solutions and $\text{KDSO}_4\text{-D}_2\text{O}$ solutions. The apparent concentration quotient, Q_v , and the degree of dissociation, α , have been computed at each concentration. The broadening of the 981-cm^{-1} Raman line of sulfate is directly proportional to the hydronium ion concentration. This dependence is linked to the proton transfer occurring in these systems. An overall second-order rate constant of $5.5 \times 10^{11} \text{ M}^{-1} \text{ sec}^{-1}$ is implied. The spectra and the kinetics are rationalized in terms of the existence of ion pairs.

Introduction

The explanation, in terms of constitution, of properties of sulfuric acid was one of the goals of Professor T. F. Young when, in collaboration with his students L. F. Maranville, H. F. Smith, and L. A. Blatz, he proceeded to design and construct one of the early photoelectric Raman spectrometers. The data obtained in those studies led to significant progress toward attainment of that goal.¹⁻³ At low concentrations the difficulty of obtaining meaningful Raman intensities precluded the possibility of getting an accurate value of K_2 , the second dissociation constant of H_2SO_4 . K_2 has been measured by a variety of other methods, and a value of $0.0102 \text{ mol kg}^{-1}$ at 25° has been obtained essentially independent of the method used.^{4,5} The Raman data were consistent with this value.⁴

The quantitative interpretation of the Raman spectra are complicated by two features. The most intense 981-cm^{-1} line of sulfate ion lies between the 1052- and the 892-cm^{-1} lines of bisulfate ion. At most concentrations these lines overlap, especially in the wings, and some criterion of line shape is required to establish the intensities. The half-widths of Raman lines of acid molecules and their conjugate anions increase with con-

(1) T. F. Young and L. A. Blatz, *Chem. Rev.*, **44**, 93 (1949).

(2) T. F. Young, *Rec. Chem. Progr.*, **12**, 81 (1951).

(3) T. F. Young, L. F. Maranville, and H. M. Smith in "The Structure of Electrolytic Solutions," W. J. Hamer, Ed., Wiley, New York, N. Y., 1959, p 35.

(4) T. F. Young and D. E. Irish, *Ann. Rev. Phys. Chem.*, **13**, 435 (1962).

(5) R. E. Lindstrom and H. E. Wirth, *J. Phys. Chem.*, **73**, 218 (1969).

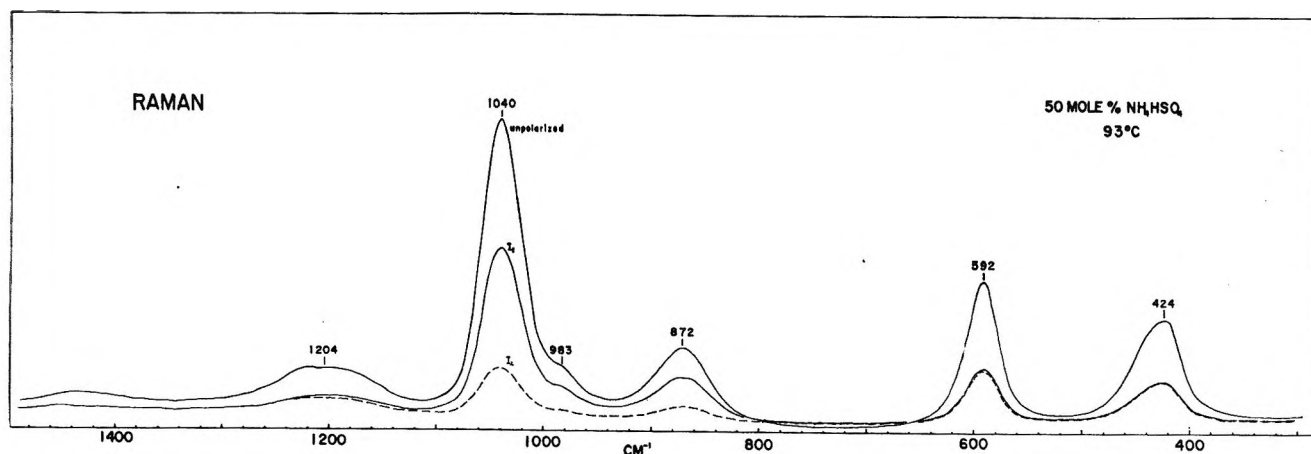


Figure 1. Raman spectra of 50 mol % NH_4HSO_4 at 93° .

centration. This enhances the overlap, compounding the problem. The line broadening has been attributed to rapid proton transfer between acid molecule and anion⁶⁻⁹ and is thus of interest in its own right.

The present vibrational spectral study was initiated with the intent of using the bisulfate-sulfate equilibrium as a probe to determine the effects of background electrolyte on the concentration quotient. The complications necessitated a thorough reexamination of the spectra of bisulfate salts in water, including DSO_4^- in D_2O .

Experimental Section

Materials. Solutions were prepared from NH_4HSO_4 and KHSO_4 (Fisher Certified reagent), NaHSO_4 (fused BDH Analar reagent), H_2SO_4 (95.5% C-I-L CP reagent), and doubly distilled deionized water. Crystalline KD-SO_4 was prepared by adding 59.6 g of D_2SO_4 (99% isotopic purity, Bio Rad Laboratories) to 20 g of K_2SO_4 dissolved in 120 ml of D_2O . This preparation was carried out in a nitrogen atmosphere.

Spectra. Raman spectra excited by the 4358-Å line of mercury were recorded on a Cary 81 Raman spectrophotometer. A saturated NaNO_2 solution or a Kodak 2A Wratten filter was used as optical filter. Filtered solutions were contained in cells equipped with water jackets for temperature control. A Haake constant temperature circulator was used to maintain the temperature at the desired value—usually $25 \pm 0.02^\circ$. Integrated intensities, corrected for cell and instrument settings, were obtained relative to the intensity of the 458- cm^{-1} line of carbon tetrachloride used as an external standard. Line areas were measured with a polar planimeter. Infrared spectra were recorded on a Beckman IR-9 spectrophotometer. Liquid films were contained between AgCl or AgBr plates separated by a 0.0125-mm Teflon spacer.

Curve Analysis. A hybrid analog-digital computer routine was used to resolve band envelopes. Frequency-intensity data are read from spectral charts and punched onto IBM cards. These generate the experi-

mental curve which is displayed on the screen of a storage oscilloscope. A synthetic curve, a sum of invoked component bands each described by a Lorentz-Gaussian product function, is generated. The mean, variance, and area of each component are adjusted until the sum curve and experimental curve superimpose. The difference curve is a measure of the goodness of fit. Differences are minimized.

Results and Discussion

Spectra. The degree of dissociation of bisulfate ion in a 50 mol % ammonium bisulfate solution is small at 93° . Raman spectra recorded with both polarized and unpolarized mercury excitation are shown in Figure 1. The SO_4^{2-} 981- cm^{-1} $\nu_1 A_1$ line appears only as a weak shoulder for 50 mol % NH_4HSO_4 ($\sim 10 M$ at 93°). Other lines of SO_4^{2-} (451, 613, and 1110 cm^{-1}) are not detectable. Therefore all the Raman lines observed except 981 cm^{-1} are due to HSO_4^- ion. The prominent lines, half-widths, and features of HSO_4^- are, respectively, 424 cm^{-1} , 39 cm^{-1} , dp, asymmetric; 592 cm^{-1} , 36 cm^{-1} , dp, asymmetric; 872 cm^{-1} , 59 cm^{-1} , p; 1040 cm^{-1} , 43 cm^{-1} , p; and 1204 cm^{-1} , 115 cm^{-1} , dp. The frequencies depend on concentration. In particular the intense line at 1040 cm^{-1} is found in the region 1052–1055 cm^{-1} in more dilute solutions ($\sim 2 M$). The bisulfate ion is largely surrounded by ammonium cations in the concentrated solution; these are replaced by water molecules on dilution and line frequencies reflect this change in environment. Raman spectra of 2.00 M solutions of NH_4HSO_4 , NaHSO_4 , KHSO_4 , and H_2SO_4 run under identical operating conditions at 25.0° are illustrated in Figure 2. The frequencies are essentially independent of cation. Line overlap is apparent, and the

(6) M. M. Kreevoy and C. A. Mead, *J. Amer. Chem. Soc.*, **84**, 4596 (1962).

(7) M. M. Kreevoy and C. A. Mead, *Discussions Faraday Soc.*, **39**, 166 (1965).

(8) A. K. Covington, M. J. Tait, and W. F. K. Wynne-Jones, *ibid.*, **39**, 1 (1965).

(9) W. J. Albery, *Progr. React. Kinet.*, **4**, 353 (1967).

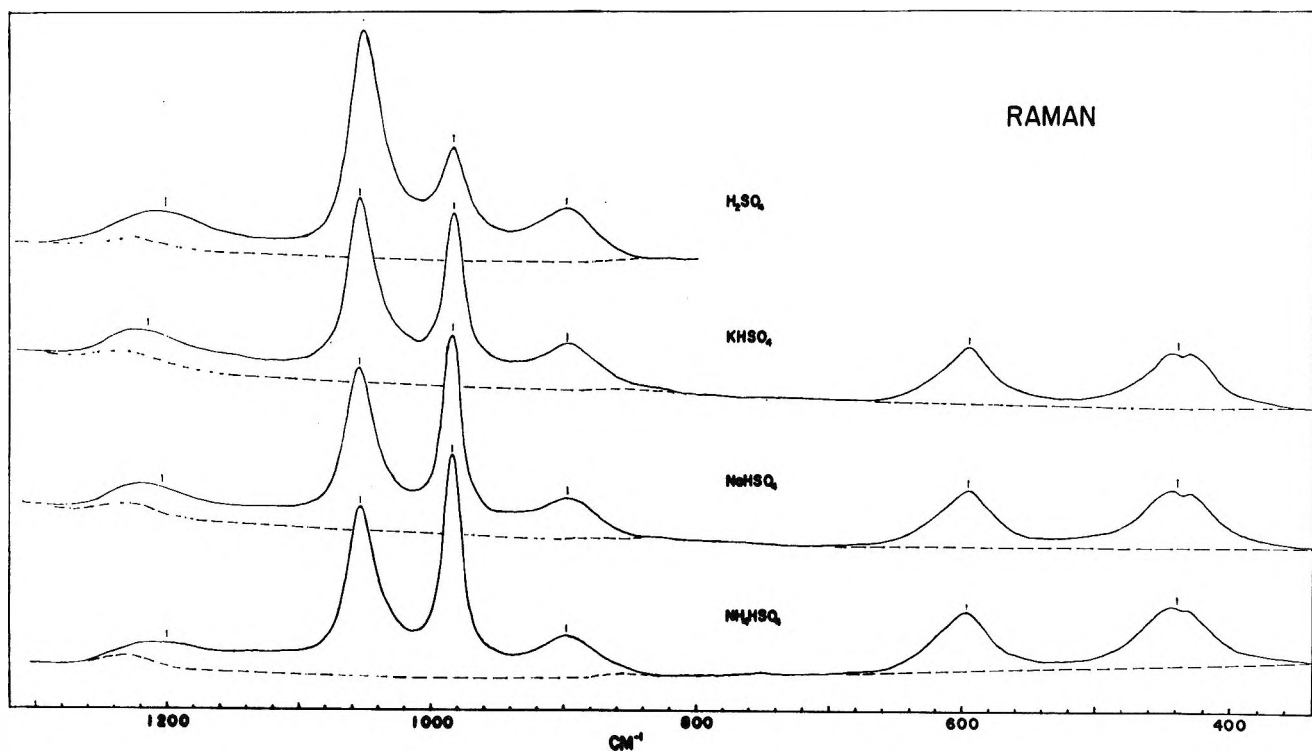


Figure 2. Raman spectra of 2.00 M H_2SO_4 , KHSO_4 , NaHSO_4 , and NH_4HSO_4 solutions.

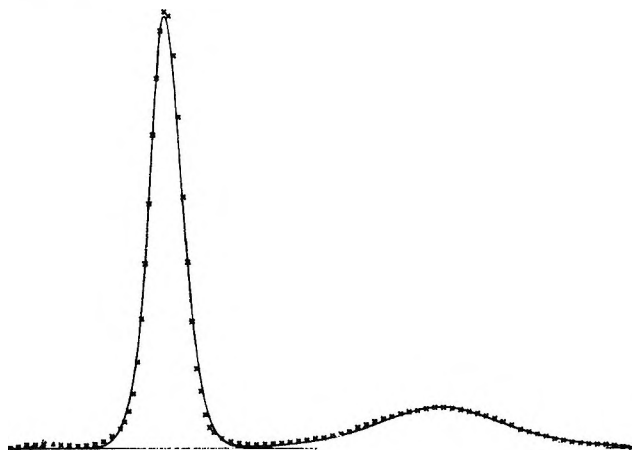


Figure 3. Computer analysis of 0.455 M $(\text{NH}_4)_2\text{SO}_4$ Raman spectrum.

breadths of lines of H_2SO_4 are noteworthy. The intensity ratio of the 981- cm^{-1} line of sulfate and the 1050- cm^{-1} line of HSO_4^- is a qualitative measure of the extent of dissociation. Assuming that molar intensities of both lines are independent of cation, the spectra indicate that the extent of dissociation of HSO_4^- ion is approximately in the order of cations $\text{NH}_4^+ > \text{Na}^+ > \text{K}^+$.

Intensity Study. The spectral region 900–1200 cm^{-1} of SO_4^{2-} can be fitted accurately by computer analysis using a Lorentz–Gaussian product function for line shape. In the plotter portrayal of the computer analysis (Figure 3) the points read from original spectra are designated by X and the sum of two Lorentz–Gaussian functions positioned at 981 and 1110 cm^{-1} is given by the

solid line. Between 0.117 and 1.0 M $(\text{NH}_4)_2\text{SO}_4$ 15 values of the integrated intensity were obtained in triplicate; between 1 and 3.83 M 9 values were obtained in duplicate. Relative integrated intensity is directly proportional to sulfate concentration with very little scatter. Intensities relative to the 458- cm^{-1} line of CCl_4 are

$$I_{981} = 0.281 [\text{SO}_4^{2-}]$$

$$I_{1110} = 0.111 [\text{SO}_4^{2-}]$$

obtained with sensitivity 2 for CCl_4 and 10 for sulfate. The total width at half-peak height (called the half-width in this paper) of the 981- cm^{-1} line was found to be 18.0 cm^{-1} independent of concentration at a slit width setting of 15.0 cm^{-1} .

The computer analysis of the spectral region 800–1400 cm^{-1} of a 0.225 M NH_4HSO_4 solution is illustrated in Figure 4. Analysis of many spectra of many concentrations with line shapes described as Lorentz, Gaussian, and Lorentz–Gaussian indicated that the best fit was obtainable with Lorentz–Gaussian functions. Even so a good fit was not obtainable in the ~ 1020 - and 940 - cm^{-1} regions unless two additional lines were invoked, *viz.* a weak line at 948 ± 4 cm^{-1} and another weak line at 1024 ± 4 cm^{-1} . These lines have not hitherto been reported in Raman spectra of bisulfate solutions. Thus we were concerned lest these be results of the method of curve analysis and not real. The lines were found in solutions of different cation–bisulfate salts— NH_4^+ , H_3O^+ , Na^+ , and K^+ . The asymmetry of the 890- and 1050- cm^{-1} lines is apparent on original traces. In the infrared spectrum where the 981- cm^{-1} line of SO_4^{2-} is

Table I: Data for Aqueous Ammonium Bisulfate Solutions

[NH ₄ HSO ₄]	[H ₂ O]	[SO ₄ ²⁻] ^a	[SO ₄ ²⁻] ^b	[HSO ₄ ⁻] ^c	α ^d	Q_v ^e	I_v ^f	$(w - w_0)$ ^g
8.013	42.6	1.67	1.68	6.33	0.210	0.447	11.4	14 ± 3
6.571	44.0	1.60	1.60	4.97	0.243	0.512	9.76	10 ± 2
5.257	45.3	1.47	1.47	3.79	0.280	0.572	8.20	8.3 ± 0.7
3.942	47.0	1.30	1.28	2.67	0.324	0.612	6.50	7.3
2.957	48.7	0.991	1.02	1.94	0.345	0.537	5.00	4.5
2.007	50.5	0.731	0.705	1.30	0.351	0.381	3.41	4.6
1.045	52.6	0.377	0.365	0.680	0.349	0.195	1.77	2.6
0.963	52.9	0.336	0.337	0.626	0.350	0.181	1.64	2.2
0.911	53.0	0.311	0.319	0.592	0.350	0.172	1.55	2.1
0.828	53.2	0.277	0.290	0.538	0.350	0.156	1.41	1.5
0.682	53.6	0.247	0.240	0.442	0.352	0.130	1.16	2.2
0.641	53.7	0.202	0.226	0.415	0.352	0.122	1.09	1.4
0.470	54.2	0.176	0.168	0.302	0.357	0.093	0.81	1.6
0.427	54.2	0.155	0.153	0.274	0.358	0.085	0.73	1.0
0.225	54.7	0.108	0.082	0.143	0.365	0.047	0.39	0.5

^a Mean values of $I_{981}/J_{981} = I_{981}/0.281$ in moles liter⁻¹. ^b Least-squares fit based on 38 individual measurements. ^c $C - [\text{SO}_4^{2-}]$. ^d $[\text{SO}_4^{2-}]/C$. ^e $Q_v = [\alpha^2/(1 - \alpha)]C$. ^f $I_v = \text{ionic strength} = C(1 + 2\alpha)$. ^g Half-width of 981-cm⁻¹ line (w) - half-width in (NH₄)₂SO₄ solution (w_0).

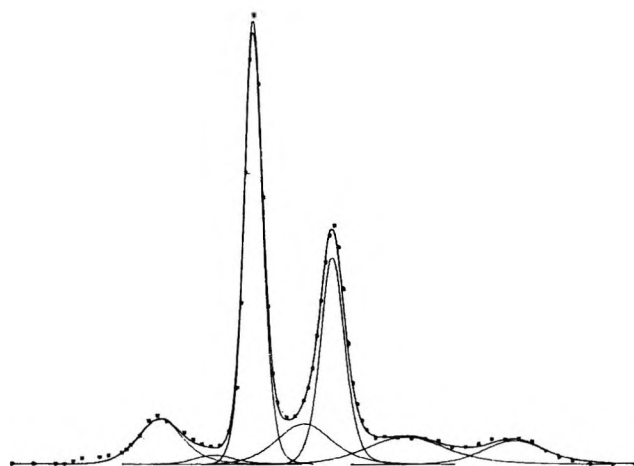


Figure 4. Computer analysis of 0.225 M NH₄HSO₄ Raman spectrum.

very weak (it is forbidden by selection rules but shows up weakly in the solution phase) a distinct shoulder is observable on the low-frequency side of the 1050-cm⁻¹ line of HSO₄⁻. For these reasons we consider these lines real and discuss provisional assignments later. The relative integrated intensities of the 981-cm⁻¹ lines of SO₄²⁻ in the bisulfate solutions were obtained excluding contributions from these two weak components. Division by the molar intensity of SO₄²⁻ ($J_{981} = 0.281$) provides the sulfate ion concentrations. The difference between these and the stoichiometric concentrations of bisulfate salt gives the apparent bisulfate ion concentrations. The apparent concentration quotient and degree of dissociation were obtained in accordance with the definition

$$Q_v = \frac{[\text{SO}_4^{2-}][\text{H}_3\text{O}^+]}{[\text{HSO}_4^-]} = \frac{\alpha^2 C_0}{1 - \alpha}$$

These quantities are given in Table I. As one self-consistency test of the data the intensity of the 1050-cm⁻¹ line of HSO₄⁻ was plotted vs. [HSO₄⁻] obtained by difference, and a straight line was obtained.

The extrapolation of Q_v -concentration data to obtain K_2 cannot be made with high precision because Raman data cannot be obtained at sufficiently low concentrations. A simple extrapolation of a Q_v vs. C plot indicates that K_2 is 0.01 in general agreement with values obtained from methods which provide data in much more dilute solutions.⁴ The extent of dissociation obtained in this work is much less than that reported earlier.³ This is attributed to the difference in the way in which the Raman spectra were resolved. Less intensity has been attributed to the sulfate ion in this work because the 948- and 1024-cm⁻¹ lines are recognized as arising from undissociated species. Similar but fewer data were obtained for KHSO₄ in H₂O, KDSO₄ in D₂O and (NH₄)₂SO₄-HCl mixtures. These are presented in Table II. The degree of dissociation of the deuterated form is less than that of the protonated form as expected.

Proton-Exchange Study. The broadening of the 981-cm⁻¹ line of SO₄²⁻, ($w - w_0$), is directly proportional to the concentration of hydronium ion (Figure 5). All three sets of data—NH₄HSO₄, KHSO₄, and (NH₄)₂SO₄-HCl mixtures—fulfill this proportionality except two points corresponding to 5.70 M HCl and 8.01 M NH₄HSO₄. At these high concentrations the uncertainty in the data is much greater. The 981-cm⁻¹ line of SO₄²⁻ is lower in intensity and the overlap with the 1020- and stronger 1050-cm⁻¹ lines is great. Values of α and Q_v have passed through a maximum. A different situation apparently exists at these high concentrations. We can write $(w - w_0) = A[\text{H}_3\text{O}^+]$, where A is the slope of the line in Figure 5. Explanation in terms of proton-

Table II: Data for KHSO₄, HCl-(NH₄)₂SO₄, and KDSO₄-D₂O

[KHSO ₄]	[SO ₄ ²⁻] ^a	[SO ₄ ²⁻] ^b	[HSO ₄ ⁻] ^c	α ^d	Q _v ^e	I _v ^f	(w - w ₀) ^g
2.999	0.662	0.658	2.341	0.219	0.184	4.31	5.3
2.249	0.562	0.560	1.689	0.249	0.186	3.37	3.6
1.687	0.433	0.457	1.230	0.270	0.168	2.60	2.5
1.265	0.381	0.364	0.901	0.288	0.147	1.99	2.6
0.949	0.277	0.285	0.664	0.300	0.122	1.52	1.6
0.534	0.191	0.169	0.365	0.316	0.078	0.87	2.0
[HCl]	[(NH ₄) ₂ SO ₄]	[SO ₄ ²⁻] ^a	[HSO ₄ ⁻]	[H ₃ O ⁺]	Q _v	(w - w ₀) ^g	
0.50	2.00	1.59	0.41	0.09	0.334	1.5	
1.00	2.00	1.26	0.74	0.26	0.451	1.9	
1.50	2.00	0.94	1.06	0.44	0.389	2.5	
2.00	2.00	0.72	1.28	0.72	0.398	4.2	
3.00	2.00	0.48	1.52	1.48	0.463	9.0	
4.00	2.00	0.35	1.65	2.35	0.502	13.6	
5.70	1.10	0.18	0.92	4.78	0.946	16 ± 6	
[KDSO ₄]	[SO ₄ ²⁻] ^{a,b}	[HSO ₄ ⁻] ^c	α ^d	Q _v ^e	I _v ^f	(w - w ₀) ^g	
2.394	0.368	2.026	0.154	0.0671	3.13	4.1	
1.676	0.254	1.412	0.151	0.0450	2.18	2.6	
1.170	0.174	0.996	0.149	0.0305	1.52	2.1	
0.819	0.150	0.670	0.182	0.0332	1.12	2.2	

^a Mean values of $I_{981}/J_{981} = I_{981}/0.281$ in moles liter⁻¹. ^b Least-squares fit based on individual measurements. ^c $C - [\text{SO}_4^{2-}]$. ^d $[\text{SO}_4^{2-}]/C$. ^e $Q_v = [\alpha^2/(1 - \alpha)]C$. ^f $I_v = \text{ionic strength} = C(1 + 2\alpha)$. ^g Half-width of 981-cm⁻¹ line (w) - half-width in (NH₄)₂-SO₄ solution (w_0).

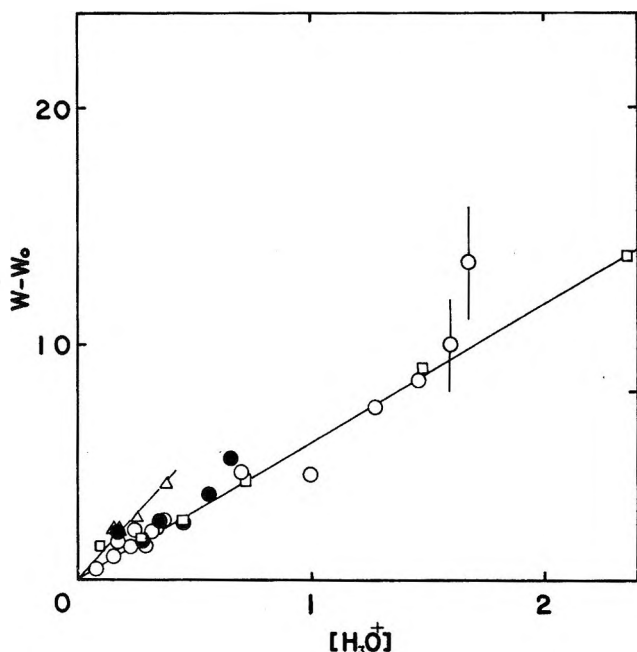


Figure 5. Dependence of line broadening of the 981-cm⁻¹ Raman line of SO₄²⁻ on hydronium ion concentration: O, NH₄HSO₄; ●, KHSO₄; □, (NH₄)₂SO₄-HCl; Δ, KDSO₄-D₂O.

transfer broadening as originally suggested by Kreevoy and Mead^{6,7} and applied by Covington, *et al.*,⁸ is suggested.

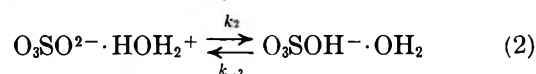
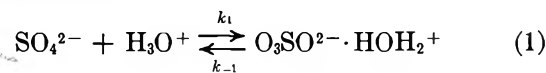
The mean lifetime of the sulfate ion, τ , is given by $(\tau)^{-1} = \pi c (w - w_0)$, where w is the half-width of the Raman line in the acidic solution and w_0 is the half-

width of the same line from a neutral salt solution; c is the velocity of light. Comparison of data for solutions of the same hydronium ion concentration but differing amounts of sulfate ion indicate that within experimental error τ is independent of the concentration of sulfate. The first-order rate law for proton transfer which relates τ and [SO₄²⁻] is rate = $(\tau)^{-1}[\text{SO}_4^{2-}]$. However, the pseudo-first-order rate constant $(\tau)^{-1}$ was shown above to depend on hydronium ion concentration. Thus

$$\text{rate}_f = \pi c A [\text{H}_3\text{O}^+][\text{SO}_4^{2-}]$$

where $\pi c A$ is the second-order rate constant equal to $5.5 \times 10^{11} \text{ M}^{-1} \text{ sec}^{-1}$. This can be compared with the recombination rate of $\sim 1 \times 10^{11} \text{ M}^{-1} \text{ sec}^{-1}$ for the process $\text{H}^+ + \text{SO}_4^{2-} \rightleftharpoons \text{HSO}_4^-$ obtained by Eigen, *et al.*^{10,11} From a similar analysis for KDSO₄-D₂O we obtain a second-order rate constant of $10.4 \times 10^{11} \text{ M}^{-1} \text{ sec}^{-1}$.

Unlike previous studies, the acid molecule in this study, HSO₄⁻, carries a negative charge. Thus direct interaction with SO₄²⁻ is unlikely because of the high coulombic repulsion. The following mechanism finds some support from consideration of the spectra. In the



(10) M. Eigen, G. Kurtze, and K. Tamm, *Z. Elektrochem.*, **57**, 103 (1953).

(11) M. Eigen, W. Kruse, G. Maass, and L. DeMaeyer, *Progr. React. Kinet.*, **2**, 287 (1964).

first step an ion pair is formed between sulfate ion and hydronium ion. Although its concentration is expected to be low, the 948-cm^{-1} line is assigned to it. When nitrate ion forms ion pairs with metal a lower frequency line at about 1020 cm^{-1} is detectable on the low-frequency side of the 1050-cm^{-1} symmetric stretch of free nitrate.^{12,13} The 948-cm^{-1} line of sulfate is analogous. In step 2 the proton is transferred from hydronium to sulfate leaving a hydrated bisulfate ion. All bisulfate in the solutions is considered to be in this form. It has been suggested that hydrates account for most of the variation of activity coefficients of undissociated parts of acids in aqueous solution.¹⁴ Compare also the conclusions of Gillespie and Wasif from apparent molal volume calculations.¹⁵ No way of quantitatively testing the mechanism, or modifications of it, with the half-width data has so far been found. For example, a plot of

$$(w - w_0) \frac{[\text{H}_3\text{O}^+]}{[\text{HSO}_4^-]}$$

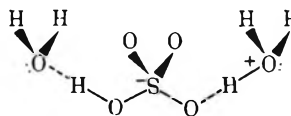
vs. Q_v is linear for systems in which $[\text{H}_3\text{O}^+]$ equals $[\text{SO}_4^{2-}]$ (cf. ref 9). However, the data from the $(\text{NH}_4)_2\text{SO}_4\text{-HCl}$ mixtures cannot be accommodated on this plot. Consideration of the reverse steps is, however, instructive. The overall rate of exchange of protons for the reverse of steps 1 and 2 is given by

$$\text{rate}_r = (\tau_{\text{HSO}_4^-})^{-1} [\text{HSO}_4^- \cdot \text{H}_2\text{O}] = \pi c(w - w_0)_{1050} [\text{HSO}_4^- \cdot \text{H}_2\text{O}]$$

More uncertainty exists in the measurement of w_{1050} because of problems associated with line overlap. No value of w_0 can be directly obtained for the 1050-cm^{-1} line because bisulfate always exists in the presence of sulfate and hydronium ions. However, a small increase in half-width appears to be within experimental uncertainty. Because the system is in equilibrium, $\text{rate}_f = \text{rate}_r$. Thus $5.5 \times 10^{11} [\text{H}_3\text{O}^+][\text{SO}_4^{2-}] = \pi c(w - w_0)_{1050} [\text{HSO}_4^- \cdot \text{H}_2\text{O}]$, and $w_{1050} = w_0 + 5.8Q_v$. Data from all three systems do satisfy this linear relationship with slope of $5.8\text{ cm}^{-1} M^{-1}$. For the 1050-cm^{-1} line of bisulfate w_0 is $26 \pm 1\text{ cm}^{-1}$, by extrapolation. The specific rate constant, $k_r = (\tau_{\text{HSO}_4^-})^{-1}$, is given by $5.5 \times 10^{11} Q_v$. The compatibility of the data, particularly data from systems in which sulfate and hydronium concentrations are equal with data from systems where the concentrations differ, provides strong support for the explanation of line broadening in terms of proton transfer. The detailed mechanism is still uncertain. The high values of the second-order rate constants and the comparison of K_f for the $\text{HSO}_4^- \text{-H}_2\text{O}$ and $\text{DSO}_4^- \text{-D}_2\text{O}$ systems suggest that other steps exist in the mechanism.

The assignment of the 1024-cm^{-1} Raman line is also not definite. Possibly it is a fundamental of $\text{HSO}_4^- \cdot \text{H}_2\text{O}$. Specifically it could arise from an A' stretching

vibration of the SO_2 unit with the other S-O bond contracting. (The 1050-cm^{-1} line is assigned to the SO_3 symmetric stretch.) The species HSO_3^- is reported to have a vibration of 1022 cm^{-1} .¹⁶ To counter this proposal the intensity of the 1050-cm^{-1} line is directly proportional to $\{C - [\text{SO}_4^{2-}]\}$ but the sum ($I_{1050} + I_{1024}$) is not, although there is more uncertainty in I_{1024} . Possibly the 1024-cm^{-1} line is another mode of the ion pair $\text{H}_3\text{O}^+ \cdot \text{SO}_4^{2-}$. The intensity ratio $I_{1024}:I_{948}$ is roughly constant although the departure from a constant may lie outside of the experimental uncertainty. Alternatively another step may exist in the mechanism involving the creation of an ion pair formally written $\text{H}_3\text{O}^+ \cdot (\text{HSO}_4^-) \cdot \text{H}_2\text{O}$. Wyatt¹⁷ successfully calculated a wide variety of properties of concentrated sulfuric acid assuming H_3O^+ is solvated by H_2SO_4 in this concentrated solution. The ion pair suggested here can be thought of as H_3O^+ solvated by HSO_4^- . This would be expected to generate a sulfur-oxygen stretching frequency lower than 1050 cm^{-1} . The structure of such a species could be



Proton exchange would occur through the central sulfate unit as a cooperative event.

Acceptance of the mechanism has implications for the equilibrium data described above. The denominator in the Q_v expression is $(C - [\text{SO}_4^{2-}])$ and is thus the sum $[\text{HSO}_4^- \cdot \text{H}_2\text{O}] + [\text{H}_3\text{O}^+ \cdot \text{SO}_4^{2-}] +$ other sulfate-containing species. α is the fraction of the formal bisulfate concentration present as free sulfate. In the earlier work of Young, *et al.*,³ the measured 981-cm^{-1} Raman line intensity included contributions from the 1024- and 948-cm^{-1} lines. This accounts for the higher values of α which they obtained.

Acknowledgments. This work was supported by the National Research Council of Canada. Deuterium oxide was provided by Atomic Energy of Canada, Ltd., Chalk River. Discussions with Dr. L. J. Brubacher and Dr. E. Grunwald were appreciated. The cooperation and contribution of the Computer Science Division, University of Waterloo, and especially Mr. A. Weerheim to the curve resolving routine is gratefully acknowledged.

- (12) A. R. Davis and D. E. Irish, *Inorg. Chem.*, **7**, 1699 (1968).
- (13) D. L. Nelson, Ph.D. Thesis, University of Waterloo, Waterloo, Ont., 1969.
- (14) E. Högfeltdt, *Acta Chem. Scand.*, **17**, 785 (1963).
- (15) R. J. Gillespie and S. Wasif, *J. Chem. Soc.*, 215 (1953).
- (16) A. W. Herlinger and T. V. Long, II, *Inorg. Chem.*, **8**, 2661 (1969).
- (17) P. A. H. Wyatt, *Trans. Faraday Soc.*, **56**, 490 (1960).

Solvent Structure in Aqueous Mixtures. II. Ionic Mobilities in

tert-Butyl Alcohol–Water Mixtures at 25°

by T. L. Broadwater and Robert L. Kay*

Chemistry Department, Mellon Institute, Carnegie-Mellon University, Pittsburgh, Pennsylvania 15213
(Received March 2, 1970)

Density, viscosity, and dielectric constant data are reported for *tert*-butyl alcohol–water mixtures over the whole composition range at 25°. Cation transference numbers for 0.02 *M* KBr obtained by the moving boundary method and precise conductance measurements on KCl, CsCl, LiBr, NaBr, KBr, Me₄NBr, Bu₄NBr, and Me₄NI are reported for aqueous mixtures containing up to 20 mol % *tert*-butyl alcohol at 25°. The data for Bu₄NBr extend to 70 mol % *tert*-butyl alcohol. The conductance and transference data were extrapolated by the Fuoss–Onsager conductance theory. The resulting limiting ionic conductances were used as a probe to investigate the increased long range order postulated for the water-rich region of aqueous *tert*-butyl alcohol mixtures. As was the case with dioxane–water and ethanol–water mixtures, the hydrophobic hydration of the Bu₄N⁺ ion disappears continuously as *tert*-butyl alcohol is added to water. On the other hand, structure-breaking ions appear to be more efficient in those mixtures by as much as 30% in some cases. However, the order found in structure-breaking power for both cations and anions in these mixtures is almost the reverse of the order found for aqueous solutions, a result that suggests that a second effect, such as an ionic dehydration, contributes to the large excess conductance found in the water-rich region of these mixtures.

Introduction

The nature of the increased long range order encountered in aqueous mixtures of the alcohols has received considerable attention recently. In a review, Franks and Ives¹ have pointed out the extrema found in many properties, primarily in the region containing more than 90 mol % water. They pointed out that the effects are magnified considerably in the case of *tert*-butyl alcohol–water mixtures. Perhaps the most striking example reported in the literature is that of Arnett and McKelvey,² who report a variation in the partial molal heat capacity for sodium tetraphenylborate of 600 cal mol⁻¹ between approximately 5 and 8 mol % *tert*-butyl alcohol in aqueous mixtures at a mean temperature of 15°.

In previous work we have used ions whose properties are known in aqueous solutions as probes to investigate the nature of the structure formed when small amounts of an organic component are added to water. Conductance data have proven to be particularly useful in this respect since they can be readily separated into ionic values with the aid of transference data. The complete range of compositions of the ethanol–water system has been studied extensively.³ The ability of a dipolar organic component to enhance long range order in an aqueous mixture was investigated by conductance measurements on the water-rich region of dioxane–water mixtures.⁴ Here we report measurements on *tert*-butyl alcohol–water mixtures at 25°, a solvent system in which structural effects should be at a maximum.

The literature on *tert*-butyl alcohol–water systems is too extensive for a complete review but three recent publications should be noted.⁵ Besides the review men-

tioned above, Arnett⁶ has measured and discussed the thermodynamic behavior of a number of electrolytes and nonelectrolytes in *tert*-butyl alcohol–water mixtures. Except for a few scattered measurements on long chain electrolytes,⁷ no conductance data could be found for electrolytes in this solvent system.

Experimental Section

An Ubbelohde-type suspended-level viscometer⁸ with a flow time for water at 25° of 500 sec was used for the viscosity measurements. No kinetic energy correction was found necessary. The calibrating liquids were *n*-decane and *n*-hexane, which in turn were based on the water value, η (H₂O, 25°) = 0.008903 poise. A capillary pycnometer with a volume of approximately 20 ml was used for the density measurements.

A method has been developed in this laboratory for the measurement of absolute dielectric constants (no

* To whom correspondence should be addressed.

- (1) F. Franks and D. J. G. Ives, *Quart. Rev. (London)*, **20**, 1 (1966).
- (2) E. M. Arnett and D. R. McKelvey, *J. Amer. Chem. Soc.*, **88**, 5031 (1966).
- (3) R. L. Kay, G. P. Cunningham, and D. F. Evans, "Hydrogen-Bonded Solvent Systems," A. Covington and P. Jones, Ed., Taylor and Francis, London, 1968, p 249.
- (4) R. L. Kay and T. L. Broadwater, *Electrochim. Acta*, submitted.
- (5) (a) M. C. R. Symons and M. J. Blandamer, ref 3, p 211; (b) D. N. Glew, H. D. Mak, and N. S. Rath, ref 3, p 195; (c) E. v. Goldammer and M. D. Zeidler, *Ber. Bunsenges. Phys. Chem.*, **73**, 4 (1969).
- (6) E. M. Arnett, "Physico-Chemical Processes in Aqueous Solvents," F. Franks, Ed., Heinemann, London, 1967, p 105.
- (7) G. L. Brown, P. F. Greiger, and C. A. Krause, *J. Amer. Chem. Soc.*, **71**, 96 (1949).
- (8) Cannon Instrument Company, State College, Pa.

calibrating liquids required) by a bridge method (General Radio Type 1615-A capacitance bridge). It was specifically designed for the relatively high conductances encountered with polar liquids.⁹ The dielectric cell was of the three terminal guarded-type¹⁰ also specifically designed for polar liquids. The cell constant was determined by means of measurements on the cell filled with dry nitrogen using $\epsilon(\text{N}_2) = 1.0005$.

The transference numbers were obtained by the moving boundary method using an improved detector recently described by Kay, Vidulich, and Fratiello.¹¹ In this method boundary movement is detected potentiometrically with platinum microprobes sealed into the moving boundary tube. The power supply and detecting circuits have already been adequately described.¹¹ Two types of cells were used for the measurements reported here—a flowing cell in which the boundary is formed initially between leading and following solutions by means of a pipet. A few runs were carried out using an autogenic-type cell with a cadmium plug as anode. The volumes between microprobe electrodes were determined by calibration runs based on Longworth's value of T^+ (0.02 M aqueous KCl, 25°) = 0.4901.¹² LiCl was used as the following salt for the calibration runs using the flowing cell. The precision obtained in the calibration runs was 0.05% or better.

The conductance measuring apparatus,¹³ the salt cup dispensing device,¹⁴ and the general techniques for preparing solutions¹³ and hygroscopic salts¹⁵ have already been described in detail. The solvent mixtures were prepared by weight and vacuum corrected. All measurements were carried out using a 500-cc conductance cell. In order to avoid atmospheric contaminants, the solvent mixtures and solutions were prepared in a closed system similar to the one used previously.¹³

Reagent grade *tert*-butyl alcohol (J. T. Baker Co.) was refluxed for 12 hr over calcium oxide, fractionally distilled from a 2M Stedman column, and stored under nitrogen for periods as long as a month without any sign of decomposition. It had a specific conductance of $1 \times 10^{-10} \text{ cm}^{-1} \text{ ohm}^{-1}$, and a density of 0.78053 g ml⁻¹ (the density before distillation was 0.78074). Previous values reported for the density of pure *tert*-butyl alcohol at 25° range from 0.7785 to 0.7810.¹⁶ Conductivity water was obtained by passing distilled water through a column of mixed-bed ion-exchange resin.

LiBr was twice recrystallized from acetone, dried in a vacuum oven at 110°, and stored in a desiccator situated in a drybox since it is such a hygroscopic salt. The molecular weight of LiBr was assumed to be 86.86. NaBr and KBr were prepared by the reaction of the appropriate carbonate with HBr. Both salts were twice recrystallized from conductivity water and when partially dry were fused under nitrogen. The KCl was recrystallized from water by the addition of ethanol, dried at a 120°, and fused under nitrogen. Reagent grade CsCl was dried at 110° and used without further

purification. The tetraalkylammonium salts were purified by procedures described previously.¹³

Results

Densities. The density data reported in Table I are in excellent agreement up to 70 mol % *tert*-butyl alcohol with the data of Tommila^{16c} and of Doroshevski,^{16d} whereas those of Irany^{16g} are consistently higher by about 0.08%. Density data for these mixtures containing more than 70% *tert*-butyl alcohol have not been reported previously.

Table I: Viscosity and Density Data for *tert*-BuOH-H₂O Mixtures at 25°

Mol %	$10^3\eta$	ρ	Mol %	$10^3\eta$	ρ
2.00	1.315	0.98509	19.80	4.441	0.89773
3.97	1.850	0.97595	30.27	4.984	0.86552
4.98		0.97083	50.01	4.811	0.82695
6.00	2.379		69.76	4.409	0.80250
7.98	2.818	0.95372	79.31	4.254	0.79530
10.10	3.238		90.88	4.222	0.78672
11.81	3.532		94.22	4.288	0.78349
13.95	3.842		97.34	4.408	0.78135
16.09	4.176		100.00	(4.52)	0.78053

Viscosities. Our viscosity data in centipoises are also summarized in Table I and compared to those of Tommila^{16c} and Irany^{16g} in Figure 1. The three sets of data coincide only below 7 mol % *tert*-butyl alcohol, our data being 5.5% higher than those of Tommila and 3% higher than those of Irany at higher compositions of *tert*-butyl alcohol although the general shape of the curve obtained in all three cases is the same. Our extrapolated value of η for pure *tert*-butyl alcohol is considerably higher than that obtained by the other two workers. The difference cannot be attributed to a higher water content since higher values of η would be obtained for a water impurity in the 45 to 80 mol %

(9) R. L. Kay and K. S. Pribadi, *Rev. Sci. Instrum.*, **40**, 726 (1969).

(10) G. A. Vidulich and R. L. Kay, *ibid.*, **37**, 1662 (1966).

(11) R. L. Kay, G. A. Vidulich, and A. Fratiello, *Chem. Instrum.*, **1**, 361 (1969).

(12) L. G. Longworth, *J. Amer. Chem. Soc.*, **54**, 2741 (1932).

(13) D. F. Evans, C. Zawoyski, and R. L. Kay, *J. Phys. Chem.*, **69**, 3878 (1965).

(14) R. L. Kay, B. J. Hales, and G. P. Cunningham, *ibid.*, **71**, 3925 (1967).

(15) R. L. Kay, C. Zawoyski, and D. F. Evans, *ibid.*, **69**, 4208 (1965).

(16) (a) K. Owen, O. R. Quayle, and E. M. Beavers, *J. Amer. Chem. Soc.*, **61**, 900 (1939), $\rho_0 = 0.7785$; (b) D. R. Simonsen and E. R. Washburn, *ibid.*, **68**, 235 (1946), $\rho_0 = 0.78043$; (c) J. Kentamaa, E. Tommila, and M. Martti, *Ann. Acad. Sci. Fenn., Ser. A*, **2**, 1 (1959), $\rho_0 = 0.78052$; (d) A. G. Doroshevski, *J. Russ. Phys. Chem. Soc.*, **42**, 442 (1910), $\rho_0 = 0.7806$; (e) H. N. Dunning and E. R. Washburn, *J. Phys. Chem.*, **56**, 235 (1952), $\rho_0 = 0.7806$; (f) S. Young and E. C. Fortey, *J. Chem. Soc.*, **81**, 729 (1902), $\rho_0 = 0.78056$; (g) E. P. Irany, *J. Amer. Chem. Soc.*, **65**, 1396 (1944), $\rho_0 = 0.7810$.

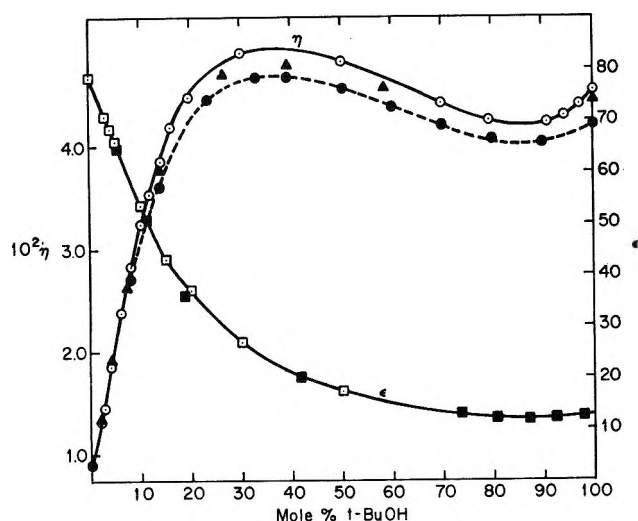


Figure 1. The viscosities and dielectric constants of *tert*-butyl alcohol-water mixtures at 25°: ○, viscosity, this work; ▲, viscosity, ref 16g; ●, viscosity, ref 16c; □, dielectric constant, this work; ■, dielectric constant, ref 18.

region. We believe that our values are higher because we have taken proper care to allow for a surface tension correction that must be applied to most viscometers for measurements on aqueous solvent mixtures. Our commercial viscometers⁸ give a viscometer constant that is 1.2% lower if water rather than hexane, decane, dioxane, ethanol, or methanol is the calibrating liquid.¹⁷ As we have already pointed out, we calibrated our viscometers with pure organic liquids and consequently developed a correction to be applied at mole fractions of water greater than 0.75. If we had used water as our calibrating fluid, the three curves in Figure 1 would be in much better agreement over this whole range of compositions.

Dielectric Constants. The dielectric constant data in Table II were measured as a check on similar data of Brown and Ives,¹⁸ who used a number of calibrating liq-

Table II: Dielectric Constants for *tert*-BuOH-H₂O Mixtures at 25°

Mol %	ε	Mol %	ε
0.00	78.40	15.00	43.09
3.00	70.84	20.06	36.79
4.01	68.43	23.87	32.18
5.00	66.06	30.00	26.76
10.01	53.46	50.00	17.24

uids and a resonance method that can be unreliable unless considerable care is taken with the measurements. As can be seen in Figure 1, our data are in excellent agreement with those of Brown and Ives with the exception of one point.

Transference Numbers. In Table III can be found the experimental details pertinent to the measurements

of the transference numbers for the K⁺ ion in 0.02 M KBr in the aqueous mixtures up to 20 mol % *tert*-butyl alcohol. As noted in the footnote three cells were used: cells β and PV were flowing cells¹¹ and the moving boundary tube had an internal diameter of 5.0 mm in cell β but only 3.5 mm in the other two cells. Although the autogenic cell is the more convenient to use, reproducible results could not be obtained with it for solvent mixtures containing more than 5 mol % *tert*-butyl alcohol. The problem was traced to the cadmium anode although the specific trouble was not determined. When the measurements were switched to the flowing cell which has two Ag, AgCl electrodes well removed from the boundary region, the reproducibility expected was obtained although at higher mole fractions of *tert*-butyl alcohol the precision dropped off somewhat. This can be seen in the second column of Table III where the observed transference numbers are recorded as calculated from the moving boundary equation.¹²

$$T_{\text{obs}}^+ = 10^3 C V F / i t \quad (1)$$

Here the concentration C is in mol l.⁻¹, V is the volume between probe electrodes in liters, F is the Faraday, i is the current in mA, and t the time in seconds. The numbers in parentheses are the average deviations in the last digit of the transference numbers obtained in the repeat runs indicated by N in column three. In those cases where $N = 1$, the number in parentheses is the average deviation in T_{obs}^+ obtained from the various probe combinations. As can be seen, the precision is at least 0.1% with only a few exceptions.

In the fourth column of Table II are the initial concentrations of the following solutions of the salts indicated. Since falling boundaries were used in the flowing cell, the following solution concentrations were slightly below the adjusted Kohlrausch concentration as determined from the ratios of the leading to following solution conductances as given in the fifth column and determined from potential measurements across the probe electrode as outlined in a previous publication.¹¹ The potential gradient across the boundary and consequently the boundary stability is directly proportional to this ratio. In the case of the 20 mol % *tert*-butyl alcohol mixture the runs which used Bu₄NBr as following solution were given greater weight because of the larger conductance ratio of 2.96. The other important factor governing boundary stability is the density gradient across the boundary. Generally a compromise must be made between these two properties in choosing a following solution.

The values of T_{obs}^+ were found to be independent of the current over ranges shown in column six of Table III

(17) For the same reason the recent measurements of the viscosity of water from 8 to 70° [L. Korson, W. Drost-Hansen, and F. J. Millero, *J. Phys. Chem.*, 73, 34 (1969)] are possibly in error and not to be preferred to the earlier values from the Bureau of Standards.

(18) A. C. Brown and D. J. G. Ives, *J. Chem. Soc.*, 1608 (1962).

Table III: Cation Transference Numbers for KBr in *tert*-BuOH-H₂O Mixtures at 25°

Mol % <i>tert</i> -BuOH	T_{obs}^+	N	$10^3 C_F$	Ratio	i (mA)	T_{corr}^+	T_0^+
1.00 ^a	0.4895 (4)	2			0.4-0.6	0.4896	0.4901
2.11 ^b	0.4974 (3)	2	1.42 (NaBr)	1.47	1.0-1.5	0.4975	0.4979
3.62 ^b	0.5031 (4)	2	1.60 (NaBr)	1.45	1.0-1.5	0.5032	0.5031
3.62 ^b	0.5025 (2)	2	0.99-1.3 (LiBr)	2.03	1.5	0.5027	0.5026
5.00 ^a	0.5075 (4)	2			0.6	0.5077	0.5073
6.06 ^b	0.5083 (1)	3	1.45 (NaBr)	1.45	1.0-1.5	0.5085	0.5081
6.17 ^c	0.5086 (3)	1	1.25 (LiBr)	2.04	0.6	0.5088	0.5084
8.03 ^b	0.5083 (5)	2	1.64 (NaBr)	1.42	1.0-1.5	0.5085	0.5081
8.06 ^c	0.5084 (14)	3	1.26 (LiBr)	2.05	0.6-0.8	0.5086	0.5082
10.31 ^c	0.5040 (5)	3	1.24 (LiBr)	2.00	0.4-0.8	0.5041	0.5040
10.31 ^c	0.5038 (5)	1	1.64 (NaBr)	1.41	0.6	0.5039	0.5038
15.05 ^c	0.4920 (6)	4	1.16 (LiBr)	1.90	0.4-0.8	0.4924	0.4928
15.09 ^c	0.4906 (10)	3	1.20 (LiBr)	1.90	0.6-0.8	0.4909	0.4914
20.05 ^c	0.4774 (6)	3	1.21 (LiBr)	1.78	0.4-0.8	0.4778	0.4792
20.07 ^c	0.4786 (3)	2	0.99 (Bu ₄ NBr)	2.96	0.6-0.8	0.4790	0.4803

^a Autogenic cell. ^b Cell β . ^c Cell *PV*.

which amounted to at least a 50% total change. This, of course is an absolutely essential criterion that must be met. The values of T_{corr}^+ for 0.02 *M* KBr given in the next column were obtained from the corresponding T_{obs}^+ values by applying a solvent conductance correction.¹¹

$$T_{\text{corr}}^+ = T_{\text{obs}}^+(1 + \kappa_0/\kappa_s) \quad (2)$$

κ_0 and κ_s are the solvent and solution specific conductances, respectively. A value of $\kappa_0 = 5 \times 10^{-7}$ was used for all the mixtures since this value was consistent with that found by Fratiello for dioxane-water and ethanol-water mixtures.^{11,19} The total correction is very small for a leading solution as concentrated as 0.02 *M*, i.e., less than 0.1%.

Since limiting values for the transference numbers were essential for an analysis of the conductance data, it was necessary to extrapolate the data to infinite dilution. It was for this reason that we decided on a potassium halide for those measurements. Since the transference number is close to 0.5 there is very little change with concentration. The bromide was chosen in place of the traditional KCl because it is most convenient to measure the conductances of the bromides of the tetraalkylammonium salts and consequently transference data for KBr would enable conductances of these salts to be split into ionic values from one difference instead of two. The limiting cation transference numbers for KBr in those mixtures are given in the last column of Table III and were calculated from the equation²⁰

$$T_0^+ = T_{\text{corr}}^+ + [(0.5 - T_{\text{corr}}^+)/\Lambda_0]\beta C^{1/2}/(1 + \kappa d) \quad (3)$$

where²¹ $\beta = 82.43/\eta(\epsilon T)^{1/2}$ and $\kappa = 50.3 C^{1/2}/(\epsilon T)^{1/2}$. It can be seen that this extrapolation should be quite reliable since it amounts to only about 0.3% in the worst case. Also, it should be noted that since the transference number is a ratio of the conductances of the

two ions in the salt, the effects of ionic association cancel and consequently do not affect the extrapolation to infinite dilution.

Molar Conductance. The molar concentrations and conductances are summarized in Table IV along with the specific conductance, κ_0 , of the various solvent mixtures studied. Harned and Owen's equation²² for solution density increments in water along with the solvent densities in Table I were used to calculate the volume concentrations for the alkali halides. For the alkylammonium salts, the data from our previous measurements²³ in water at 25° were used. A few checks on the densities of the most concentrated solutions studied indicated that a negligible error was introduced when these data for solutions in pure water were used for the solvent mixtures. As a check on salt purity each salt was measured in pure water.

The data were extrapolated to infinite dilution by means of the Fuoss-Onsager²¹ conductance equation²⁴ given by

$$\Lambda = \Lambda_0 - SC^{1/2} + EC \log C + JC \quad (4)$$

for nonassociated electrolytes and by

$$\Lambda = \Lambda_0 - S(C\gamma)^{1/2} + EC\gamma \log C\gamma + JC\gamma - K_A\Lambda C\gamma f^2 \quad (5)$$

for associated electrolytes. The viscosity *B* coefficient

(19) A. Fratiello, Ph.D. Thesis, Brown University, 1962.

(20) R. L. Kay and J. L. Dye, *Proc. Natl. Acad. Sci.*, **49**, 5 (1963).

(21) R. M. Fuoss and F. Accascina, "Electrolytic Conductance," Interscience, New York, N. Y., 1959.

(22) H. S. Harned and B. B. Owen, "The Physical Chemistry of Electrolyte Solutions," 3rd ed, Reinhold, New York, N. Y., 1958, p 725.

(23) D. F. Evans and R. L. Kay, *J. Phys. Chem.*, **70**, 366 (1966).

(24) For a spirited discussion and evaluation of other conductance equations see J.-C. Justice, *J. Chim. Phys.*, **65**, 353, 1193 (1969).

Table IV: Equivalent Conductances in *tert*-BuOH-H₂O Mixtures at 25°

KCl				KBr			
10°C	Δ	10°C	Δ	10°C	Δ	10°C	Δ
0.00 Mol %		9.92 Mol %		0.00 Mol %		10.04 Mol %	
$10^7\kappa_0 = 1.35$		$10^7\kappa_0 = 0.016$		$10^7\kappa_0 = 0.97$		$10^7\kappa_0 = 0.67$	
12.847	146.61	6.594	52.84	10.658	148.80	6.612	52.44
22.819	145.54	16.319	52.09	19.606	147.75	16.241	51.75
33.104	144.68	28.029	51.50	29.171	146.87	27.682	51.18
45.149	143.89	40.695	51.00	41.107	146.04	43.654	50.51
61.055	142.99	55.128	50.53	57.279	145.13	62.256	50.01
82.894	141.97	69.589	50.14	73.873	144.32	81.172	49.66
		84.893	49.73			103.579	49.23
1.05 Mol %		15.05 Mol %		2.57 Mol %		15.01 Mol %	
$10^7\kappa_0 = 2.58$		$10^7\kappa_0 = 0.44$		$10^7\kappa_0 = 2.25$		$10^7\kappa_0 = 0.41$	
6.182	125.81	4.319	39.67	9.829	100.67	5.002	40.03
13.783	124.71	9.955	39.12	23.524	99.54	12.228	39.41
27.173	123.51	16.553	38.64	38.048	98.76	21.100	38.89
40.841	122.62	23.862	38.23	53.917	98.09	33.039	38.36
55.204	121.87	31.217	37.88	86.706	96.81	45.015	37.95
72.909	121.10	38.816	37.58	103.342	96.49	62.084	37.48
95.916	120.27	50.871	37.16			80.409	37.06
4.88 Mol %		20.06 Mol %		4.07 Mol %		20.06 Mol %	
$10^7\kappa_0 = 0.72$		$10^7\kappa_0 = 0.21$		$10^7\kappa_0 = 1.93$		$10^7\kappa_0 = 0.21$	
7.299	75.40	7.406	30.97	10.663	82.58	4.583	31.58
15.004	74.71	15.852	30.26	24.572	81.63	9.504	31.04
26.150	74.10	25.444	29.68	39.337	80.96	16.647	30.50
38.151	73.58	38.110	29.07	54.195	80.45	23.901	30.08
51.049	73.12	52.741	28.53	71.298	79.94	34.091	29.60
64.606	72.74	68.485	28.05	88.821	79.50	46.242	29.15
92.222	72.05	92.340	27.46	107.291	79.09	62.258	28.67
CsCl				KBr			
10°C	Δ	10°C	Δ	10°C	Δ	10°C	Δ
0.00 Mol %		14.77 Mol %		5.05 Mol %		50.11 Mol %	
$10^7\kappa_0 = 1.04$		$10^7\kappa_0 = 0.56$		$10^7\kappa_0 = 1.21$		$10^7\kappa_0 = 0.032$	
3.839	151.81	3.591	41.22	14.014	73.82	5.611	12.49
8.653	150.85	8.471	40.65	21.475	73.38	12.210	10.99
14.409	149.97	13.565	40.21	32.876	72.84	18.866	10.10
21.595	149.18	19.406	39.84	47.120	72.33	25.951	9.44
29.514	148.48	26.488	39.43	63.274	71.86	33.379	8.92
38.324	147.77	34.033	39.08	85.272	71.32	41.138	8.50
48.770	147.17	41.715	38.73			53.221	7.99
2.011 Mol %		19.71 Mol %		8.01 Mol %			
$10^7\kappa_0 = 0.94$		$10^7\kappa_0 = 0.21$		$10^7\kappa_0 = 2.16$			
8.348	111.30	3.393	32.34	5.593	59.46		
15.093	110.47	8.314	31.74	14.451	58.74		
22.445	109.83	14.193	31.20	26.058	58.13		
31.442	109.23	22.006	30.63	39.268	57.63		
39.338	108.88	30.523	30.13	52.550	57.23		
48.298	108.39	40.799	29.66	66.838	56.87		
		54.881	29.10	92.275	56.33		
4.32 Mol %		10.06 Mol %					
$10^7\kappa_0 = 1.92$		$10^7\kappa_0 = 1.01$					
3.174	82.94	5.491	53.40				
7.646	82.49	12.268	52.81				
12.465	81.99	20.136	52.28				
17.732	81.63	28.921	51.84				
23.874	81.24	39.690	51.39				
31.131	80.87	52.787	50.92				
41.588	80.39	67.561	50.48				

Table IV (Continued)

Me ₄ NBr				LiBr			
10°C	Δ	10°C	Δ	10°C	Δ	10°C	Δ
0.00 Mol %		6.91 Mol %		1.00 Mol %		15.05 Mol %	
$10^7\kappa_0 = 1.18$		$10^7\kappa_0 = 1.43$		$10^7\kappa_0 = 3.28$		$10^7\kappa_0 = 0.39$	
4.954	120.54	6.316	50.08	11.580	96.30	6.785	30.41
12.055	119.45	12.942	49.57	23.488	95.10	14.727	29.96
21.341	118.40	23.813	49.97	36.124	94.49	24.765	29.55
30.813	117.55	35.697	48.46	49.452	93.86	35.011	29.22
41.504	116.74	50.505	47.89	63.202	93.33	45.322	28.94
56.798	115.76	65.485	47.47	77.910	92.82	56.661	28.68
75.295	114.73	80.654	47.10	93.090	92.35	68.782	28.44
1.05 Mol %		9.89 Mol %					
$10^7\kappa_0 = 3.40$		$10^7\kappa_0 = 0.81$					
4.688	101.22	6.494	41.79				
10.234	100.41	15.599	41.17				
17.823	99.61	28.291	40.56				
27.497	98.82	42.692	40.02				
37.493	98.12	57.073	39.59				
48.857	97.45	71.799	39.20				
		87.455	38.84				
2.00 Mol %		15.06 Mol %					
$10^7\kappa_0 = 0.49$		$10^7\kappa_0 = 0.61$					
8.339	87.01	5.696	32.27				
19.149	85.72	12.059	31.76				
30.025	84.92	19.792	31.25				
41.948	84.24	29.065	30.85				
55.588	83.57	40.953	30.38				
69.639	83.05	53.713	29.96				
85.496	82.36	66.640	29.62				
4.32 Mol %		20.00 Mol %					
$10^7\kappa_0 = 2.03$		$10^7\kappa_0 = 0.27$					
5.655	63.42	7.542	26.07				
12.183	62.84	14.981	25.47				
20.995	62.22	25.858	24.82				
30.953	61.70	38.594	24.21				
43.133	61.18	53.268	23.69				
57.175	60.66	68.100	23.24				
76.161	60.08	84.300	22.85				
				NaBr			
0.00 Mol %		10.02 Mol %					
$10^7\kappa_0 = 2.09$		$10^7\kappa_0 = 0.33$					
8.570	125.87	9.969	44.52				
18.210	124.71	20.512	43.98				
28.511	123.85	31.457	43.56				
38.927	123.14	42.897	43.22				
49.284	122.55	55.608	42.90				
63.159	121.86	70.089	42.59				
81.826	121.09	86.942	42.29				
2.03 Mol %		15.05 Mol %					
$10^7\kappa_0 = 1.43$		$10^7\kappa_0 = 0.39$					
8.918	91.47	5.847	34.66				
19.683	90.69	11.985	34.23				
33.430	89.95	18.652	33.88				
47.693	89.34	25.705	33.56				
63.367	88.80	33.682	33.29				
79.263	88.32	43.883	32.98				
98.863	87.79	55.325	32.68				
5.02 Mol %		20.06 Mol %					
$10^7\kappa_0 = 0.81$		$10^7\kappa_0 = 0.21$					
7.099	63.05	4.620	28.07				
17.075	62.37	12.872	27.37				
27.406	61.89	21.790	26.89				
30.055	61.50	32.014	26.45				
49.658	61.14	43.121	26.08				
65.207	60.74	59.258	25.64				
80.997	60.40	79.999	25.19				
				Bu ₄ NBr			
0.00 Mol %		20.08 Mol %					
$10^7\kappa_0 = 1.37$		$10^7\kappa_0 = 0.21$					
9.958	94.84	5.354	21.52				
16.879	93.97	10.986	21.10				
23.956	93.26	17.180	20.77				
34.076	92.39	23.424	20.50				
45.237	91.56	29.785	20.26				
59.938	90.59	36.300	20.05				
		44.836	19.80				
				LiBr			
0.00 Mol % (Run I)		4.07 Mol %					
$10^7\kappa_0 = 1.63$		$10^7\kappa_0 = 0.70$					
11.756	113.95	8.203	61.36				
24.315	112.74	18.160	60.64				
37.728	111.85	28.877	60.09				
53.058	111.03	38.865	59.71				
69.115	110.30	49.449	59.39				
86.631	109.63	61.597	59.07				
104.007	109.05						
0.00 Mol % (Run II)		8.09 Mol %					
$10^7\kappa_0 = 1.48$		$10^7\kappa_0 = 1.80$					
3.048	115.27	8.961	43.45				
8.339	114.63	18.229	43.02				
14.338	113.65	28.739	42.64				
21.471	113.00	40.284	42.31				
30.498	112.34	50.757	42.05				
42.240	111.64	64.027	41.79				
52.362	111.06						

Table IV (Continued)

Bu ₄ NBr				Me ₄ NI			
10°C	Δ	10°C	Δ	10°C	Δ	10°C	Δ
2.03 Mol %		32.53 Mol %		0.00 Mol %		14.77 Mol %	
10 ⁷ κ ₀ = 1.60		10 ⁷ κ ₀ = 0.088		10 ⁷ κ ₀ = 1.01		10 ⁷ κ ₀ = 0.61	
6.244	67.85	1.977	16.43	5.205	119.32	3.534	32.11
13.004	67.12	4.082	16.07	10.634	118.36	7.796	31.73
19.956	66.54	6.517	15.75	17.940	117.47	14.918	31.26
27.943	65.99	9.343	15.46	27.795	116.50	31.414	30.48
36.439	65.48	13.519	15.12	38.180	115.69	40.740	30.15
44.901	65.04	18.158	14.80	49.604	114.93	50.199	29.83
56.214	64.52	24.437	14.45				
4.95 Mol %		50.11 Mol %		2.02 Mol %		15.06 Mol %	
10 ⁷ κ ₀ = 1.12		10 ⁷ κ ₀ = 0.020		10 ⁷ κ ₀ = 3.28		10 ⁷ κ ₀ = 0.66	
4.567	45.65	1.301	12.97	4.422	85.38	5.860	31.58
12.476	45.01	3.094	12.13	9.526	84.66	12.675	31.00
20.549	44.55	5.253	11.47	17.476	83.83	19.799	30.65
31.419	44.05	7.461	10.98	27.092	83.12	29.835	30.19
46.993	43.84	10.185	10.50	36.905	82.48	41.260	29.76
62.681	42.99	13.072	10.10	47.135	81.96	52.716	29.38
78.475	42.57	18.980	9.48	59.242	81.38	67.055	28.97
8.01 Mol %		70.09 Mol %		5.07 Mol %		19.71 Mol %	
10 ⁷ κ ₀ = 1.00		10 ⁷ κ ₀ = 0.044		10 ⁷ κ ₀ = 1.85		10 ⁷ κ ₀ = 0.21	
7.200	35.80	1.518	8.93	3.343	57.31	3.905	27.12
15.276	35.33	3.738	7.32	8.156	56.76	3.086	26.62
24.475	34.93	6.902	6.18	14.913	56.25	14.624	26.19
33.833	34.59	11.147	5.35	21.026	55.87	21.270	25.75
43.566	34.29	15.826	4.80	28.439	55.49	29.297	25.41
55.344	33.98	20.708	4.41	38.037	55.06	37.835	25.05
		25.870	4.11	49.256	54.62	47.229	24.72
10.04 Mol %				10.06 Mol %			
10 ⁷ κ ₀ = 0.72				10 ⁷ κ ₀ = 1.01			
3.691	32.31			3.855	39.98		
9.316	31.89			7.302	39.63		
15.880	31.53			13.589	39.21		
22.553	31.27			20.078	38.86		
38.481	30.73			27.418	38.52		
48.210	30.34			36.046	38.19		
59.801	30.17			46.252	37.85		

correction to J which was included in our earlier calculations²³ was set equal to zero here. Its inclusion affects the ion size parameter δ but not the value of Λ_0 , the latter being the main interest in this investigation. The parameters Λ_0 , J and K_A were determined by a least squares computer program²⁶ and are summarized in Table V. Since J is an increasing function of δ , the values of the latter replace J in the tables. Also, the standard deviations of the individual points σ_A are included. If no value of K_A is given the parameters were obtained from eq 4.

The first row of Table VI contains the known limiting ionic conductances in pure water at 25° from a compilation by Kay and Evans.²⁶ The second row contains our values of the limiting ionic conductance for pure aqueous solutions. They are based on a value of T_0^+ (aque-

ous KBr, 25°) = 0.4846²⁷ to split the molar conductance for KBr. To within 0.05 Λ unit, our data are in good agreement with the generally accepted values. The limiting ionic conductances in the remaining rows in Table VI refer to rounded solvent composition values and were obtained by difference using the Λ_0 values in Table V and the transference data in Table III. Owing to the extremely large changes in Λ_0 with increasing *tert*-butyl alcohol content, it was necessary to prepare large scale $\Lambda_{0\eta}$ plots in order to interpolate with sufficient precision.

(25) R. L. Kay, *J. Amer. Chem. Soc.*, **82**, 2099 (1960).(26) R. L. Kay and D. F. Evans, *J. Phys. Chem.*, **70**, 2325 (1966).

(27) Reference 22, p 234.

Table V: Conductance Parameters for Salts in *tert*-BuOH-H₂O at 25°

Mol %	Λ_0	d	σ_A	K_A	Mol %	Λ_0	d	σ_A	K_A
KCl					KBr				
0.00	149.97 ± 0.009	3.19 ± 0.02	0.01		10.04	53.54 ± 0.04	2.8 ± 0.1	0.06	
1.05	127.74 ± 0.04	2.8 ± 0.1	0.05			53.68 ± 0.05	9 ± 2	0.04	8 ± 3
4.88	76.78 ± 0.02	3.05 ± 0.09	0.03		15.01	40.99 ± 0.02	2.80 ± 0.06	0.02	
9.92	53.98 ± 0.02	2.33 ± 0.05	0.02			41.05 ± 0.01	4.3 ± 0.3	0.008	4.2 ± 0.7
	54.01 ± 0.03	3 ± 1	0.02	2 ± 1	20.06	32.52 ± 0.03	2.5 ± 0.1	0.04	
15.05	40.61 ± 0.01	2.32 ± 0.07	0.02			32.64 ± 0.02	5.0 ± 0.5	0.01	12 ± 2
	40.66 ± 0.003	4.8 ± 0.1	0.002	6.5 ± 0.3	50.105	14.0 ± 0.2	2.6 ± 0.2	0.24	
20.06	32.22 ± 0.03	2.30 ± 0.07	0.04			15.68 ± 0.08	4.5 ± 0.2	0.03	400 ± 20
	32.35 ± 0.01	3.6 ± 0.1	0.006	8.2 ± 0.6	Me₄NBr				
CsCl					0.00	122.63 ± 0.01	1.38 ± 0.05	0.02	
0.00	153.67 ± 0.03	2.5 ± 0.1	0.04		1.05	102.88 ± 0.004	1.36 ± 0.02	0.005	
2.01	113.31 ± 0.06	2.6 ± 0.4	0.07		2.00	88.62 ± 0.03	1.4 ± 0.1	0.04	
4.32	83.98 ± 0.02	2.5 ± 0.2	0.03		4.32	64.60 ± 0.02	1.42 ± 0.08	0.02	
10.06	54.45 ± 0.02	1.89 ± 0.08	0.03		6.91	51.16 ± 0.02	1.51 ± 0.08	0.03	
	54.52 ± 0.01	5.4 ± 0.6	0.008	5.1 ± 0.8	9.89	42.79 ± 0.01	1.50 ± 0.06	0.02	
14.77	42.07 ± 0.02	1.74 ± 0.07	0.02			42.84 ± 0.006	4.7 ± 0.3	0.004	3.3 ± 0.4
	42.12 ± 0.02	4 ± 1	0.01	7 ± 2	15.06	33.20 ± 0.03	1.7 ± 0.1	0.04	
19.71	33.17 ± 0.03	1.6 ± 0.1	0.05			33.31 ± 0.03	6 ± 1	0.02	11 ± 3
	33.29 ± 0.01	4.4 ± 0.3	0.009	14 ± 1	20.00	27.32 ± 0.03	2.21 ± 0.07	0.04	
LiBr						27.44 ± 0.02	3.8 ± 0.2	0.01	9 ± 1
0.00 (I)	116.88 ± 0.01	3.56 ± 0.04	0.02		Bu₄NBr				
0.00 (II)	116.84 ± 0.03	3.9 ± 0.2	0.04		0.00	97.57 ± 0.003	0.24 ± 0.01	0.004	
1.00	98.65 ± 0.06	3.5 ± 0.2	0.07		2.03	69.40 ± 0.01	0.45 ± 0.04	0.01	
4.07	62.73 ± 0.03	3.0 ± 0.2	0.04		4.95	46.56 ± 0.01	0.98 ± 0.04	0.01	
8.09	44.62 ± 0.01	3.7 ± 0.1	0.02		8.01	36.79 ± 0.003	1.47 ± 0.02	0.004	
15.05	31.43 ± 0.01	3.43 ± 0.04	0.01		10.04	32.98 ± 0.004	1.82 ± 0.03	0.007	
NaBr					20.08	22.43 ± 0.002	2.99 ± 0.01	0.002	
0.00	128.45 ± 0.01	3.45 ± 0.03	0.01		32.53	17.10 ± 0.01	2.94 ± 0.09	0.02	
2.03	93.49 ± 0.04	4.0 ± 0.1	0.05			17.17 ± 0.01	4.7 ± 0.3	0.007	27 ± 4
5.02	64.31 ± 0.002	3.48 ± 0.01	0.003		50.11	13.5 ± 0.1	1.5 ± 0.3	0.19	
10.02	45.800 ± 0.001	3.25 ± 0.004	0.001			14.16 ± 0.03	7.4 ± 0.6	0.02	400 ± 20
15.05	35.674 ± 0.005	3.28 ± 0.03	0.007		70.09	9.2 ± 0.3	2.3 ± 0.5	0.49	
20.06	28.96 ± 0.02	2.91 ± 0.05	0.02			12.41 ± 0.06	7.1 ± 0.3	0.02	3400 ± 67
	29.01 ± 0.01	3.8 ± 0.3	0.01	5 ± 1	Me₄NI				
KBr					0.00	121.45 ± 0.02	1.3 ± 0.1	0.03	
0.00	151.85 ± 0.01	3.42 ± 0.05	0.02		2.02	86.74 ± 0.03	0.9 ± 0.1	0.04	
2.57	102.74 ± 0.05	2.8 ± 0.1	0.06		5.07	58.14 ± 0.01	0.87 ± 0.08	0.02	
4.07	84.38 ± 0.01	3.20 ± 0.04	0.02		10.06	40.73 ± 0.01	1.33 ± 0.08	0.02	
5.05	75.71 ± 0.006	3.19 ± 0.03	0.008		14.77	32.87 ± 0.004	1.97 ± 0.02	0.006	
8.01	60.48 ± 0.02	2.8 ± 0.1	0.04		15.06	32.52 ± 0.02	1.72 ± 0.07	0.03	
	60.56 ± 0.02	8 ± 1	0.02	5 ± 1	19.71	27.90 ± 0.03	2.0 ± 0.1	0.04	
						27.98 ± 0.05	5 ± 2	0.03	12 ± 7

Table VI: Limiting Ionic Conductances in *tert*-BuOH-H₂O Mixtures at 25°

Mol %	10 ³ η	ϵ	Λ_0								
			Li ⁺	Na ⁺	K ⁺	Cs ⁺	Me ₄ N ⁺	Bu ₄ N ⁺	Cl ⁻	Br ⁻	I ⁻
0.00 ^a	0.8903	78.37	38.66	50.20	73.55	77.29	44.42	19.31	76.39	78.22	76.98
0.00	0.8903	78.37	38.62	50.19	73.59	77.29	44.37	19.31	76.38	78.26	77.08
2.50	1.433	72.0	26.4	25.6	52.23	54.8	30.4	12.6	51.6	52.30	50.5
5.00	2.130	65.8	19.0	26.9	38.37	40.3	22.6	8.9	37.3	37.35	35.8
7.50	2.719	59.6	15.4	22.4	31.64	32.9	18.6	7.3	30.9	30.59	29.1
10.00	3.219	53.6	13.2	19.1	26.95	28.0	16.0	6.4	26.6	26.42	24.8
15.00	3.975	43.8	10.6	14.6	20.10	20.9	12.4	5.6	20.5	20.98	19.8
20.00	4.457	36.6		11.9	15.64	16.2	10.3	5.4	16.7	17.09	17.5

^a See ref 26.

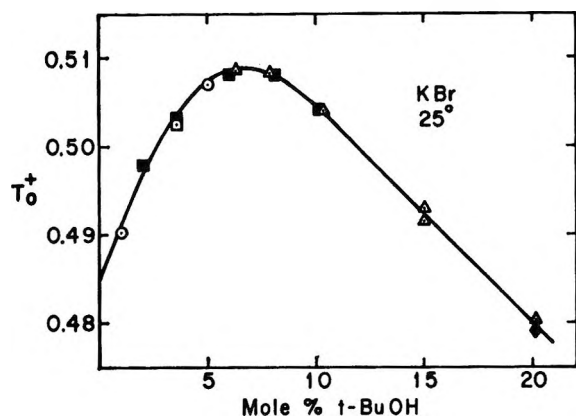


Figure 2. Limiting cation transference numbers for KBr in *tert*-BuOH-H₂O mixtures at 25°: ○, autogenic cell; □, cell β; △, cell PV; open figures LiBr following solution; closed squares LiBr as following solution; ◆ Bu₄NBr, following solution.

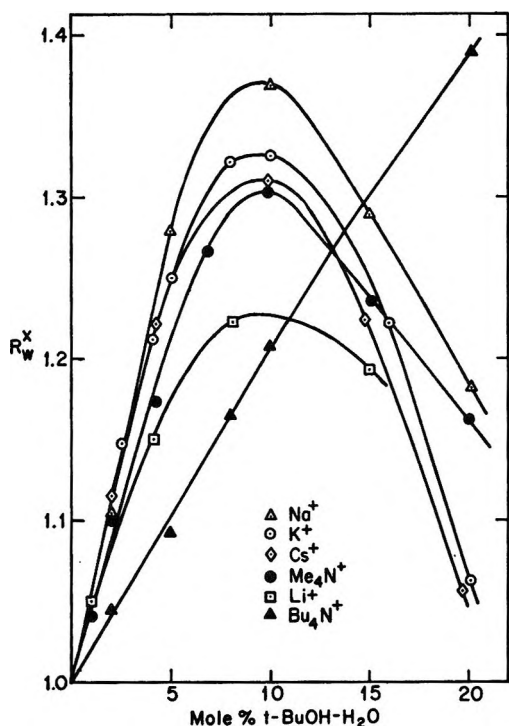


Figure 3. Limiting ionic conductance-viscosity products for cations in *tert*-butyl alcohol-water mixtures at 25° relative to their values for pure water.

Discussion

The limiting cation transference numbers for KBr at 25° in aqueous mixtures containing up to 20 mol % *tert*-butyl alcohol are plotted in Figure 2. The data show a maximum at a mole fraction (6.5% *tert*-butyl alcohol) that is determined by the relative mobilities of the K⁺ and Br⁻ ions in those mixtures. In ethanol-water mixtures the maximum in $T^+(\text{KCl})$ occurs at 11 mol % ethanol.¹⁹ Both maxima occur in the composition region in which alcohol-water mixtures are known to be more structured than pure water.^{1,6} The rather obvious conclusion could be drawn that the K⁺ ion is a more

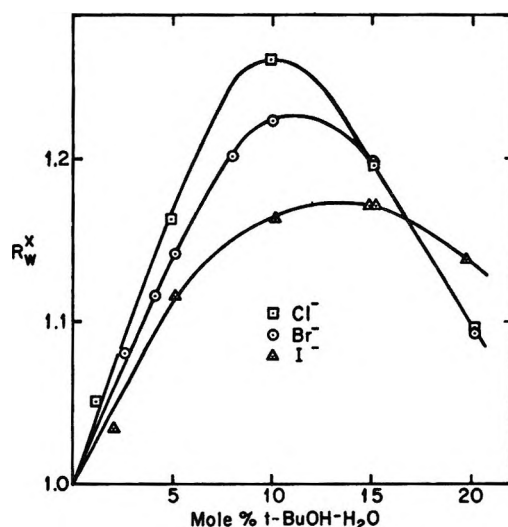


Figure 4. Limiting ionic conductance-viscosity products for anions in *tert*-butyl alcohol-water mixtures at 25° relative to their values for pure water.

efficient structure-breaker than either of the halide ions in alcohol-water mixtures. The same conclusion has been reached from a consideration of the negative temperature²⁸ and pressure²⁹ coefficients reported for T_0^+ (aqueous KCl). At low temperatures and pressures the K⁺ ion appears to have a larger structural excess mobility than the Cl⁻ ion. As the temperature or pressure increases and the amount of structure in water decreases, this structural excess mobility of the K⁺ ion relative to the Cl⁻ ion also decreases. Arnett⁶ has used this argument to explain the excess endothermic heats of solution of ions in aqueous mixtures containing about 10 mol % alcohol. Engel and Hertz³⁰ have shown from nmr relaxation studies that the reorientation time of water molecules undergoes a greater decrease when KI is added to a water-rich mixture of ethanol than when KI is added to pure water. They concluded that KI was a better structure-breaker in these alcohol mixtures than in pure water.

At first glance it would appear that the limiting ionic conductance-viscosity ratios plotted in Figure 3 for cations and in Figure 4 for anions in *tert*-butyl alcohol-water mixtures could also be explained by assuming enhanced structure-breaking properties for the alkali and halide ions in these mixtures. In both figures the $\lambda_{0\eta}$ products for all ions in pure water have been normalized to unity by defining R_W^X by

$$R_W^X \equiv (\lambda_{0\eta})_X / (\lambda_{0\eta})_{\text{H}_2\text{O}} \quad (6)$$

where X is the mole fraction of *tert*-butyl alcohol in the mixture involved.

(28) R. L. Kay and G. A. Vidulich, *J. Phys. Chem.*, **74**, 2718 (1970).

(29) R. L. Kay, K. S. Pribadi, and B. Watson, *ibid.*, **74**, 2724 (1970).

(30) G. Engel and H. G. Hertz, *Ber. Bunsenges. Phys. Chem.*, **72**, 808 (1968).

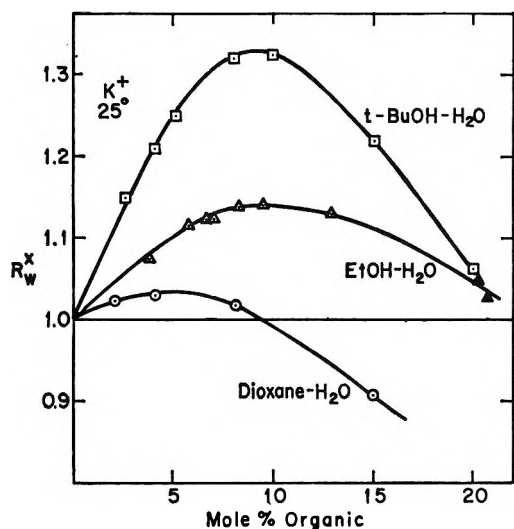


Figure 5. Comparison of the limiting conductance-viscosity product for the K^+ ion in various aqueous mixtures at 25° relative to its value in pure water.

The first point to notice in Figures 3 and 4 is that the maxima in the λ_{07} products occur at approximately 10 mol % *tert*-butyl alcohol with the exception of the Bu_4N^+ and the I^- ions. The Bu_4N^+ ion is a special case because of hydrophobic hydration and will be handled separately. The second point is that the extrema previously found in the λ_{07} products for ethanol-water and dioxane-water mixtures are enhanced considerably in *tert*-butyl alcohol-water mixtures. This can be seen in Figure 5 where the R_w^X values for the K^+ ion are compared for three different aqueous solvent mixtures. The increase in this product for the K^+ ion amounts to 33% in *tert*-butyl alcohol and 14% in ethanol and both occur very close to 10 mol % alcohol. On the other hand, in dioxane-water mixtures the increase in R_w^X for the K^+ ion amounts to less than 4% and occurs at about 5 mol % dioxane. Furthermore, in dioxane the small maxima occur at a different mol % dioxane for different ions or are missing for some ions.⁴

Perhaps the most important point to notice in Figures 3 and 4 is the fact that the height, of the maxima are not in the order expected. If the height is associated with structure-breaking power the order should be $Cs^+ > K^+ > Me_4N^+ > Na^+ > Li^+$ and $I^- > Br^- > Cl^-$ if we use the temperature coefficient of the λ_{07} products as a criterion for structure-breaking power. This is illustrated in Table VII where the fractional change in this product between 10 and 45° is compared to the fractional change in the maximum value of R_w^X for *tert*-butyl alcohol-water mixtures. It can be seen that the order of ions as far as the latter property is concerned is $Na^+ > K^+ > Cs^+ > Me_4N^+ > Li^+$ and $Cl^- > Br^- > I^-$. Thus the order for the anions is just the reverse expected for structure-breaking ions and the same is true for the cations Na^+ , K^+ , and Cs^+ . It would appear that the excess mobilities in a 10 mol % *tert*-butyl

Table VII: Comparison of Structure-Breaking Power

Ion	$[(\lambda_{07})_{100} / (\lambda_{07})_{450}] - 1$	$R_w^X - 1$
Li^+	-0.005	0.230
Na^+	0.036	0.370
K^+	0.122	0.325
Cs^+	0.150	0.310
Me_4N^+	0.043	0.305
Cl^-	0.092	0.260
Br^-	0.111	0.230
I^-	0.115	0.170

alcohol mixture have a contribution from a second source besides structure-breaking. This same order has already been observed in dioxane-water mixtures⁴ and has been attributed to a contribution to the excess mobility resulting from a dehydration of the ions owing to the presence of the second component. The Li^+ , Na^+ , and possibly K^+ ions in that order would be expected to show the greatest increase if dehydration in these alcohol mixtures does take place. Consequently, the maxima in the R_w^X values must be attributed to two effects, structure-breaking and dehydration. Since both of these effects (called negative hydration and loss of positive hydration by Hertz³⁰) would result in a decreased reorientation time of the water molecules, they cannot be separated by a single nmr relaxation study. As a matter of fact, Hertz³⁰ includes both effects under the common name of structure-breaking. However, if nmr relaxation measurements were carried out on a number of salts in *tert*-butyl alcohol mixtures the same order in excess reorientation times should be obtained as is found here. Such measurements are underway in this laboratory at present.

The results obtained here for the Bu_4N^+ in *tert*-butyl alcohol-water are compared to the other cations in Figure 3 and to other solvent mixtures in Figure 6. Up to at least 10 mol % organic component, the Bu_4N^+ ion

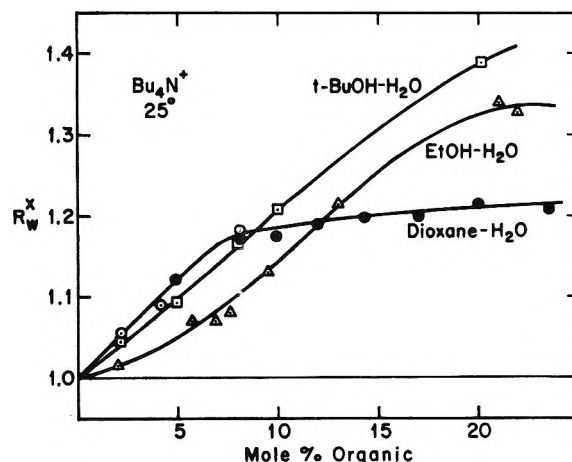


Figure 6. Comparison of the limiting conductance-viscosity product for the Bu_4N^+ ion in various aqueous mixtures at 25° relative to its value in pure water.

has comparable values of R_w^x in dioxane, ethanol, and *tert*-butyl alcohol mixtures with water. It would appear that this ion is completely independent of the degree of structure present in the mixtures and merely undergoes a hydrophobic dehydration as the second component is added to water. The same conclusion was reached by Arnett⁶ from his heat of solution data for aqueous alcohol mixtures.

An inspection of the \bar{a} and K_A values in Table V shows no consistently abnormal effects in the concentration dependence of the conductance of the salts in the *tert*-butyl alcohol-water mixtures. From this it could be concluded that the degree of overlap of ionic cospheres is negligible up to 0.01 *M* in *tert*-butyl alcohol-water mixtures. The ion pair association detected in those mixtures increases generally as ionic interaction with the solvent and the dielectric constant decrease. The abnormally low \bar{a} values for Bu_4NBr in pure water increase to more normal values as the proportion of *tert*-butyl alcohol increases and the dielectric constant decreases. The same effect was found in dioxane-water mixtures⁴ and was discussed in some detail.

The association constants of Bu_4NBr in 50 and 70 mol % *tert*-butyl alcohol were 400 and 340, respectively, which is considerably lower than the values that would be predicted from conductance measurements on this salt on pure alcohols.³¹ Extrapolation of a $\log K_A$ vs. $1/\epsilon$ plot for the normal alcohols predicts values of K_A of 860 and 45×10^3 for Bu_4NBr in the above mixtures, respectively, indicating that stabilization of the bromide ion by hydration is still a very important factor in a 70 mol % *tert*-butyl alcohol-water mixture.

Acknowledgment. The dielectric measurements were carried out by Mr. K. S. Pribadi and Mr. K. R. Srinivasan. Also, we wish to acknowledge the technical assistance of Mr. Donald R. Henning and Mr. T. Vitucio with the conductance and transference measurements, respectively. This work was supported by Contracts No. 14-01-0001-1729 and 14-30-2577 with the Office of Saline Water, U. S. Department of the Interior.

(31) D. F. Evans and P. Gardam, *J. Phys. Chem.*, **73**, 158 (1969).

Transport Processes in Hydrogen-Bonding Solvents. IV. Conductance of Electrolytes in Formamide at 25 and 10°

by John Thomas¹ and D. Fennell Evans²

Department of Chemistry, Case Western Reserve University, Cleveland, Ohio 44106 (Received March 2, 1970)

Precise conductance measurements are reported for NaCl , KCl , KBr , Me_4NI , Et_4NI , Pr_4NBr , Pr_4NI , Bu_4NBr , Bu_4NI , and *i*- Am_3BuNI in formamide at 25 and 10° and for CsCl , NaBPh_4 , Et_4NBr , Et_4NI , and DiBuBr_2 at 25°. The formamide was purified using a mixed bed ion-exchange resin which gave specific conductances of $1-5 \times 10^{-7}$ $\text{ohm}^{-1} \text{cm}^{-1}$. The concentration dependence for these salts in formamide is compared to that observed in the alcohols and water, and many similarities are observed. It is suggested that a multiple step ionic association process is operative in all of these solvents and is a feature common to all hydrogen-bonding solvents.

Introduction

One way of viewing protic solvents is in terms of the structure that hydrogen bonding can impose on the liquid. In addition to the alcohols and water, which have been extensively studied, the amides constitute an important type of solvent within this classification. Each alcohol molecule can form two hydrogen bonds, giving rise to a one-dimensional structure consisting of chains of molecules. Water can form four hydrogen bonds of tetrahedral orientation which results in the for-

mation of three-dimensional structures. Formamide can have a maximum of three hydrogen bonds per molecule, enabling a two-dimensional sheetlike structure to be formed. Formamide, therefore, constitutes a significant link between the most complex and important liquid, water, and the simpler, but well-characterized alcohols.

(1) For further details see John Thomas, Ph.D. Thesis, Case Western Reserve University, Jan 1970.

(2) To whom all correspondence should be directed.

In spite of this importance, relatively few accurate physical measurements on formamide or its electrolyte solutions are available. This scarcity of reliable data reflects the difficulty in obtaining formamide of high purity. As pointed out by Notley and Spiro,³ who obtained precise transference numbers in this amide, unless extreme precautions are taken it is impossible to obtain formamide with a specific conductance of less than 10^{-5} ohm⁻¹ cm⁻¹ and a water content of 0.01 *M*.

The transport and thermodynamic properties of electrolytes in the normal alcohols⁴⁻⁶ and water^{7,8} have been reported. In the alcohols it was found that association constants were larger in magnitude than predicted by theory and showed a dependence upon ion size that was, in some cases, opposite to that predicted by Coulombic theory. This behavior was rationalized in terms of a multiple-step association process in which desolvation of the anion is an important feature. In water, association constants are small, as expected from the high dielectric constant, and consequently cannot be unambiguously determined. The deviation from expected behavior for electrolytes in aqueous solution are similar, although smaller, to those observed in the alcohols.⁹ This suggests that some of the features that have been attributed to the unique three-dimensional structure of water may be a more general feature of hydrogen-bonding solvents. To investigate this possibility, we have determined the conductance of a number of electrolytes in formamide.

Experimental Section

Solvent Purification. Formamide is hygroscopic and unstable by nature and therefore difficult to obtain as a solvent in pure form. The best commercially available grade of formamide (Fisher Scientific Co.) has methanol, water, and other undesirable compounds as impurities. It has a water content of about 0.04 *M*, specific conductance of $1.0-9.0 \times 10^{-4}$ ohm⁻¹ cm⁻¹, and a density of 1.1239.

The purification method of Notley and Spiro¹⁰ which employs molecular sieve 3A for the removal of water and an ion-exchange resin for the removal of ions was used with certain modifications. This method allows formamide to be obtained which is low in water content (0.008 *M*) and has the lowest specific conductance (1×10^{-7} ohm⁻¹ cm⁻¹) ever reported. Other methods of purification such as addition of drying agents (*e.g.*, sodium sulfate), distillation at lower pressure, and fractional crystallization, gave formamide of specific conductance 1×10^{-5} ohm⁻¹ cm⁻¹.¹¹ The lowest water content recorded before was¹⁶ 0.018 *M*, and the lowest specific conductance, on a small sample, was 6×10^{-7} ohm⁻¹ cm⁻¹.

Large quantities of formamide (*e.g.*, 18-20 l.) are required for preparation of 550 g of ion-exchange resin. Since the best commercially available grade is prohibitively expensive and not very pure, we used technical grade formamide (Aldrich Chemical Co.) with the fol-

lowing preliminary purification. Formamide was percolated through a column (5-cm diameter) containing 1 kg of molecular sieve 3A (Union Carbide). The absorption of water and colored impurities was facilitated by heating the column to 60° with electrical tape.

To remove most of the ionic impurities, the dried formamide was distilled *in vacuo* at a pressure of about 0.1 mm and a temperature of 52°. Before heating, the formamide was pumped overnight to remove most of the methanol and other volatile organic impurities. The distillation required about 40 hr to yield 3 l. The distillate was slightly basic, but upon bubbling dry nitrogen through it for about 3 hr, the dissolved ammonia was removed. This gave samples with a specific conductance of 2×10^{-5} ohm⁻¹ cm⁻¹, which is about 30 times lower in specific conductance and 5 times lower in water content than the best commercial grade.

The formamide obtained from this preliminary purification was used to prepare the sodium formamide and sulfuric acid solutions, to wash and dehydrate the resins, and for passing through the mixed resin to obtain pure solvent.¹⁰

Notley and Spiro reported that each preparation of the column yielded about 6 l. of pure formamide. Once the cation and anion resins are mixed the lifetime of the bed depends not only on the amount of formamide treated but also on the idle time. But if the anion and cation resins are stored separately, the degeneration of the resins is slower. We found that by mixing these resins in small batches, larger amounts of pure formamide (up to 10 l.) could be obtained from the 550 g of exchange resin. The individual resins were then well mixed to form the final mixed bed column. The pure formamide obtained from this column had a specific conductance of 1×10^{-7} ohm⁻¹ cm⁻¹, which remained constant over a period of time sufficient to make a conductance run. Earlier workers reported that the specific conductance of their formamide had increased with time. The density of this formamide was found to be 1.1296 g/ml at 25° and 1.1508 g/ml at 10°.

Purification and Crystallization of Salts. The symmetrical tetraalkylammonium halides (Eastman Kodak) were dissolved in either methanol-ether or acetone-ether mixtures, recrystallized, and dried in a vacuum oven at 65° for 12 hr.¹¹

- (3) J. M. Notley and M. Spiro, *J. Phys. Chem.*, **70**, 1502 (1966).
- (4) D. F. Evans and P. Gardam, *ibid.*, **72**, 3281 (1968).
- (5) D. F. Evans and P. Gardam, *ibid.*, **73**, 158 (1968).
- (6) R. L. Kay, C. Zawoyski, and D. F. Evans, *ibid.*, **69**, 4208 (1965).
- (7) D. F. Evans and R. L. Kay, *ibid.*, **70**, 366 (1966); R. L. Kay, D. F. Evans, and G. P. Cunningham, *ibid.*, **73**, 3322 (1969).
- (8) R. L. Kay and D. F. Evans, *ibid.*, **70**, 2325 (1966).
- (9) D. F. Evans and T. L. Broadwater, *ibid.*, **73**, 3985 (1969).
- (10) J. M. Notley and M. Spiro, *J. Chem. Soc. B*, 362 (1966).
- (11) D. F. Evans, C. Zawoyski, and R. L. Kay, *J. Phys. Chem.*, **69**, 3878 (1965).

N,N,N,N',N',N'-Hexabutylamethylenediammonium dibromide (DiBuBr₂) was prepared⁹ by reacting an excess of the corresponding trialkylamine with appropriate alkyl bromide in methanol or ethanol. Recrystallizations were done from methanol by addition of ether. This salt was dried overnight at 60° in a vacuum oven.

Tetramethyl- and tetrabutylammonium perchlorates were prepared by addition of a hot 1 *M* solution of the alkylammonium bromide salt to a hot 0.1 *M* solution of sodium perchlorate.¹² After cooling in ice water, the precipitate was filtered off using a fritted glass funnel and washed with ice-cold water until the effluent was bromide-free. This salt was recrystallized from water and dried *in vacuo* at 60°.

Fisher scientific grade sodium tetraphenylboride was dissolved in a minimum amount of acetone at room temperature.¹³ On addition of reagent grade toluene into the solution, the salt crystallized out. After filtration this was recrystallized three more times and dried *in vacuo* at room temperature.

Sodium and potassium chloride salts (Fisher Certified reagent) were precipitated from a saturated aqueous solution by addition of ethanol.¹⁴ The product was dried first *in vacuo* at 150°, ground in an agate mortar, and then dried again at 150°.

Potassium bromide was prepared by adding Mallinckrodt analyzed reagent potassium carbonate until a pH of 3 was reached.¹⁴ The solution was cooled, and the resulting crystals were twice crystallized from conductivity water. The crystals were dried at 100° at 0.01 mm pressure and then fused under carbon dioxide free nitrogen and ground in an agate mortar, then dried once again in a vacuum oven overnight at 100°.

Cesium chloride (A. D. MacKay optical grade) was ground in an agate mortar, dried at 100° *in vacuo*, and used without further purification.

Conductivity Measurements. The conductance bridge was similar in design and operation to that of Dike's¹⁵ modified version of the Jones-Joseph bridge.¹⁶ The conductance bridge, conductance cells, salt-cup dispensing device, and general techniques were the same as previously described.^{11,14} For the hygroscopic salt, Bu₄NCl, a modified weighing procedure was used.⁶

The weight buret technique was used for LiCl solutions. A concentrated solution was made up, all manipulations being carried out in a drybox. Small increments were added from the weight buret to the cell, and to prevent atmospheric contamination while the cell was open, solvent-saturated nitrogen was passed through the side arm. The run was made in the shortest time possible.

Density measurements were done at 10 and 25° by using calibrated, long, single-necked capillary tube pycnometers. The technique was the same as previously described.¹⁴

Results

The measured equivalent conductances and corresponding electrolyte concentrations in moles per liter are shown in Tables I and II for formamide solutions at 25 and 10°, respectively. Also given is the specific conductance of pure formamide used and *A*, the density increments used to calculate the volume concentrations. The increments were obtained by density measurements on the most concentrated solutions used in the conductance measurements and were assumed to follow the relationship $\bar{d} = d_0 + A\bar{m}$, where \bar{m} represents the moles of salt per kilogram of solution. The values of *A* at 10° were assumed to be the same as those at 25°, an assumption that has been verified in other solvents over short temperature intervals.^{6,7} The data were analyzed with the Fuoss-Onsager equation¹⁷ in the form

$$\Lambda = \Lambda_0 - S\sqrt{c} + Ec \log c + (J - B\Lambda_0)c \quad (1)$$

The value of *B* which corrects for the added electrolyte on the viscosity of the solvent was set equal to zero, since a reliable and complete set of data is not available.³ This correction does not alter the value of Λ_0 , but only changes the values of *J* and consequently of \bar{d} , the ion-size parameter. The solvent properties used in the computations for the data at 25° are dielectric constant $\epsilon = 109.45$ and viscosity $\eta = 0.0331$ P.¹⁸ The corresponding values at 10° were estimated to be $\epsilon = 115.45$ and $\eta = 0.050$ P from plots of these quantities *vs.* temperature.¹⁹ All attempts to analyze the data using the associated form of the Fuoss-Onsager equation gave association constants which were negative or which had standard deviations larger than the value of K_A .

Shown in Tables III and IV are the parameters obtained from eq 1 by a least-squares computer program.²⁰ The values of *J* are given instead of the more customary \bar{d} parameters. The values of \bar{d} obtained were often small, sometimes negative, and obviously bear no relationship to real ion sizes.

The constants α , β , E_1 , and E_2 had the values 0.1391, 13.79, 0.1946, and 2.838 at 25° and 0.1388, 9.126, 0.1936, and 1.867 at 10°, respectively, where in eq 1, $S = (\Lambda_0\alpha + \beta)$ and $E = (E_1\Lambda_0 - E_2)$. These can be

(12) J. F. Coetzee and G. P. Cunningham, *J. Amer. Chem. Soc.*, **79**, 870 (1957).

(13) J. F. Skinner and R. M. Fuoss, *J. Phys. Chem.*, **68**, 1882 (1964).

(14) C. G. Swain and D. F. Evans, *J. Amer. Chem. Soc.*, **88**, 383 (1966).

(15) P. H. Dike, *Rev. Sci. Instrum.*, **2**, 379 (1931).

(16) G. Jones and C. Bradshaw, *J. Amer. Chem. Soc.*, **55**, 1780 (1933).

(17) R. M. Fuoss and F. Accascina, "Electrolytic Conductance," Interscience Publishers, Inc., New York, N. Y., 1959.

(18) L. R. Dawson, E. D. Wilhoit, and P. G. Sears, *J. Amer. Chem. Soc.*, **79**, 5906 (1957).

(19) G. R. Leader, *ibid.*, **73**, 856 (1951); G. F. Smith, *J. Chem. Soc.*, 3257 (1931).

(20) R. L. Kay, *J. Amer. Chem. Soc.*, **82**, 2099 (1960).

Table II: Equivalent Conductances in Formamide at 10°

10°C	Λ	10°C	Λ	10°C	Λ
NaCl		KCl		KBr	
$k = 1.96 \times 10^{-7}$		$k = 1.27 \times 10^{-7}$		$k = 3.79 \times 10^{-7}$	
15.964	16.748	7.152	19.901	6.980	19.892
28.708	16.787	14.772	19.763	12.154	19.797
47.639	16.691	25.672	19.627	18.958	19.696
66.225	16.570	35.015	19.531	28.232	19.591
90.337	16.484	45.945	19.438	39.562	19.486
124.084	16.326	63.079	19.313	53.276	19.374
156.057	16.202	82.347	19.192	70.759	19.261
192.219	16.066	95.036	19.118	102.177	19.086
		113.695	19.019		
Me ₄ NI		Et ₄ NI		Pr ₄ NBr	
$k = 1.31 \times 10^{-7}$		$k = 1.34 \times 10^{-7}$		$k = 2.33 \times 10^{-7}$	
3.542	21.580	2.620	18.511	4.551	16.756
6.754	21.450	6.532	18.361	9.566	16.646
11.543	21.324	11.334	18.254	15.018	16.560
16.153	21.235	17.205	18.154	20.979	16.475
21.855	21.142	22.269	18.081	33.103	16.332
30.274	21.024	28.585	18.004	40.732	16.261
40.920	20.903	37.305	17.911	48.196	16.193
54.404	20.766	46.706	17.817	60.144	16.100
81.342	20.536	70.017	17.625	85.155	15.937
				Bu ₄ NI	
				$k = 1.79 \times 10^{-7}$	
				2.680	15.131
				6.625	14.980
				13.261	14.823
				20.405	14.718
				27.075	14.613
				35.030	14.524
				44.988	14.414
				57.220	14.303
				74.630	14.165
				<i>i</i> -Am ₃ BuNI	
				$k = 2.40 \times 10^{-7}$	
				1.397	15.329
				8.807	15.072
				12.653	14.998
				16.519	14.935
				21.923	14.852
				27.475	14.772
				33.337	14.698
				49.564	14.523
				60.775	14.416

Table III: Conductance Parameters for Formamide Solutions

Salt	25°		
	Λ_0	J	$\sigma\Lambda$
LiCl	26.153 ± 0.011	8.0	0.016
NaCl	27.221 ± 0.007	18.4	0.01
KCl	29.877 ± 0.003	16.5	0.004
KCl	29.85 ± 0.01	17.5	0.002
KBr	29.891 ± 0.001	18.3	0.002
KBr	29.945 ± 0.004	18.2	0.006
CsCl	31.091 ± 0.007	59.2	0.01
NaBPh ₄	16.142 ± 0.008	25.01	0.003
Me ₄ NI	30.11 ± 0.005	0	0.005
Et ₄ NBr	28.191 ± 0.001	9.36	0.001
Et ₄ NI	27.747 ± 0.009	-0.60	0.02
Pr ₄ NBr	25.290 ± 0.005	8.65	0.009
Pr ₄ NI	24.85 ± 0.01	-12.1	0.03
Bu ₄ NCl	23.990 ± 0.008	10.5	0.007
Bu ₄ NBr	24.002 ± 0.006	0	0.01
Bu ₄ NI	23.55 ± 0.01	-19.7	0.002
<i>i</i> -Am ₃ BuNI	23.03 ± 0.006	-28.4	0.008
He ₄ NI	21.622 ± 0.004	-26.5	0.01
DiBuBr ₂	25.867 ± 0.008	135.4	0.010

Table IV: Conductance Parameters for Formamide Solutions

Salt	10°		
	Λ_0	J	$\sigma\Lambda$
NaCl	17.33 ± 0.05	30.0	0.08
KCl	20.217 ± 0.002	10.47	0.003
KBr	20.203 ± 0.001	12.75	0.001
Me ₄ NI	20.29 ± 0.008	-3.6	0.02
Et ₄ NI	18.671 ± 0.008	-5.73	0.01
Pr ₄ NBr	17.003 ± 0.002	2.24	0.004
Pr ₄ NI	16.68 ± 0.01	-20.7	0.02
Bu ₄ NBr	15.697 ± 0.008	8.33	0.015
Bu ₄ NI	15.28 ± 0.01	-15.3	0.02
<i>i</i> -Am ₃ BuNI	15.34 ± 0.007	-24.5	0.01

temperature has been attributed to structural effects arising from the three-dimensional hydrogen-bonded network of water molecules. It is of general interest to ascertain whether the same type of behavior is observed in formamide where a two-dimensional hydrogen-bonded network is possible.

Transference numbers, which allow the unambiguous determination of single ion values, have been measured by Spiro and Notley³ for KCl in formamide at 25°. When combined with the values given in Table III, the value of λ_0 given in Table V results. Transference numbers for KCl in formamide at 25, 30, 40, and 50° have been reported by Gopal and Bhatnagar.²⁴ However, their value at 25° ($t_0^+ = 0.419$), disagrees with the value ($t_0^+ = 0.427$) reported by Spiro and Notley. At least part of this discrepancy can be attributed to the impure formamide used in the temperature studies. As a con-

possible, the results agree with those in Table III within the precision of their measurements.

Discussion

Limiting Ionic Conductances. Potentially, the most interesting aspect of the limiting ionic conductances in formamide is their variation with temperature. In methanol⁶ and acetonitrile,²³ $\lambda_{0\eta}$ at different temperatures is found to show little if any variation. However, in aqueous solution $\lambda_{0\eta}$ changes considerably, some ions having positive temperature coefficients and others with negative temperature coefficients.⁸ This variation with

(23) D. F. Evans and T. L. Broadwater, *J. Phys. Chem.*, **72**, 1037 (1968).

(24) R. Gopal and O. N. Bhatnagar, *ibid.*, **68**, 3892 (1964).

Table V: Limiting Single Ion Conductance in Formamide at 25°

DiBu ²⁺	8.70
He ₄ N ⁺	4.90
<i>i</i> -Am ₃ BuN ⁺	6.34
Bu ₄ N ⁺	6.83
Pr ₄ N ⁺	8.12
Et ₄ N ⁺	11.03
Me ₄ N ⁺	13.41
Li ⁺	9.03
Na ⁺	10.10
K ⁺	12.75
Cs ⁺	13.87
Cl ⁻	17.12
Br ⁻	17.17
I ⁻	16.73
BPh ₄ ⁻	6.04

sequence any attempt to extrapolate the values to 10° would result in uncertainties that would make any structural interpretation in formamide questionable. However, it should be noted that $(\Lambda_{07})_{25}/(\Lambda_{07})_{10}$, Table VI, shows a 6% variation over a 15° temperature range,

Table VI: Temperature Dependence of the Walden Product $(\Lambda_{07})_{25}/(\Lambda_{07})_{10}$ in Formamide

NaCl	1.04	Pr ₄ NBr	0.99
KCl	0.98	Pr ₄ NI	0.99
KBr	0.98	Bu ₄ NBr	1.01
Me ₄ NI	0.98	Bu ₄ NI	1.02
Et ₄ NI	0.98	<i>i</i> -Am ₃ BuNI	0.99

with both negative and positive temperature coefficients being observed. A program to measure transference numbers at 10° is underway. The dependence of λ_{07} upon ionic size in formamide at 25° can be seen in Figure 1. It is obvious that the Stokes law is not obeyed and the Zwanzig equation²⁵ does not provide an adequate description of the system.

Concentration Dependence. The concentration dependence of electrolytes in formamide is most conveniently discussed in terms of the behavior observed in other hydrogen-bonding solvents. The results obtained in the alcohols⁴⁻⁶ and in aqueous solution^{7,9} will be reviewed and compared to those obtained in formamide.

In the alcohols, methanol-pentanol, the quantity of interest is the association constant, K_A , which is a measure of the concentration dependence. In Table VII, the association constants for the tetrabutylammonium halides and perchlorate are summarized, and there are three main points of interest. The first is that K_A increases with increasing anion size. Such behavior is contrary to the predictions of electrostatic theory

$$K_1 = K_1^0 \exp(e^2/\epsilon a_{KK}kT) \quad (2)$$

Table VII: Association Constants for Tetrabutylammonium Salts in Alcohols

Solvent	ϵ	K_A			
		Bu ₄ NCl	Bu ₄ NBr	Bu ₄ NI	Bu ₄ NClO ₄
MeOH	32.60	0	3 ± 1	16 ± 2	33 ± 2
EtOH	24.33	39 ± 5	75 ± 4	123 ± 3	...
PrOH	20.45	149 ± 5	266 ± 6	415 ± 6	769 ± 6
BuOH	17.45	640 ± 5	860 ± 5	1180 ± 10	2200 ± 20
PeOH	15.04	...	2520 ± 3	3220 ± 40	...

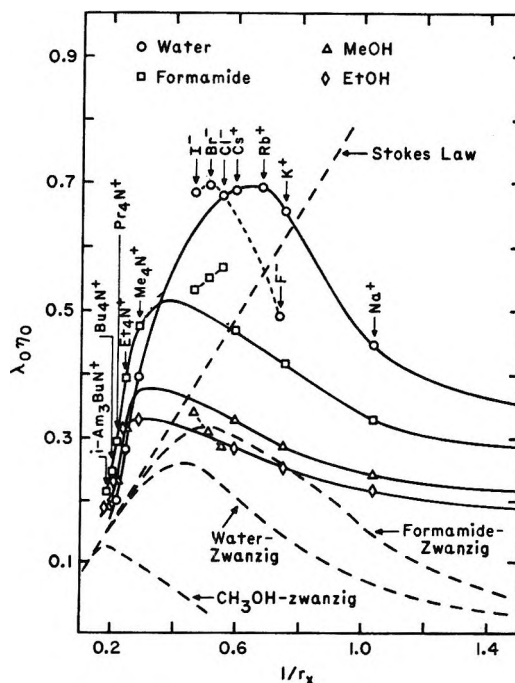


Figure 1. The limiting Walden product for the halide, alkali, and tetraalkylammonium ions as a function of crystallographic size at 25°.

and contrary to the expected and established behavior in solvents such as acetone,^{1,11} acetonitrile,¹¹ nitrobenzene,¹¹ and the halogenated hydrocarbons.²⁶ Secondly eq 2 requires that $\log K_A$ vary linearly with $1/\epsilon$ and to a reasonable approximation such linear behavior is observed.⁵ Finally, the association constants are larger in magnitude than those calculated on the basis of diffusion theory²⁷ from which K_1^0 is given by

$$K_1^0 = (4\pi N/3000)d_K^3 \quad (3)$$

An explanation which accounts for this behavior is one based on a multiple-step association process. A simple mechanism which takes into account these fac-

(25) R. Zwanzig, *J. Chem. Phys.*, **38**, 1603 (1963).

(26) J. T. Denison and J. B. Ramsey, *J. Amer. Chem. Soc.*, **77**, 2615 (1955).

(27) W. R. Gilkerson, *J. Chem. Phys.*, **25**, 1199 (1956); R. Fuoss, *J. Amer. Chem. Soc.*, **80**, 5059 (1958).

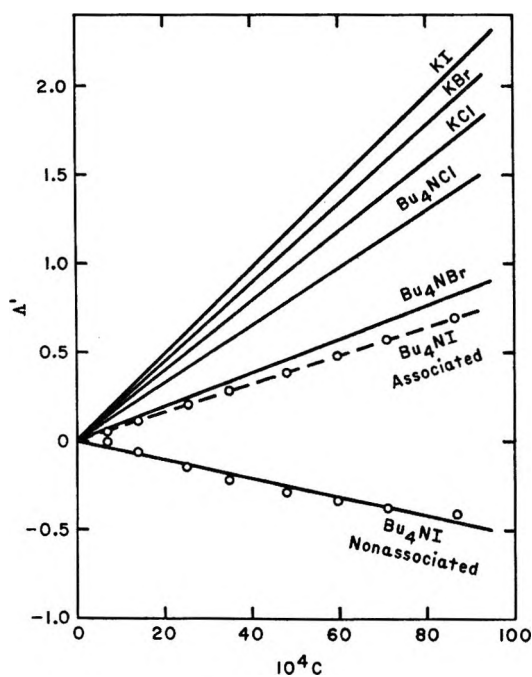


Figure 2. Plot of Λ' showing opposite dependence on anion size for tetrabutylammonium halides compared to potassium halides compared to potassium halides in water at 25°.

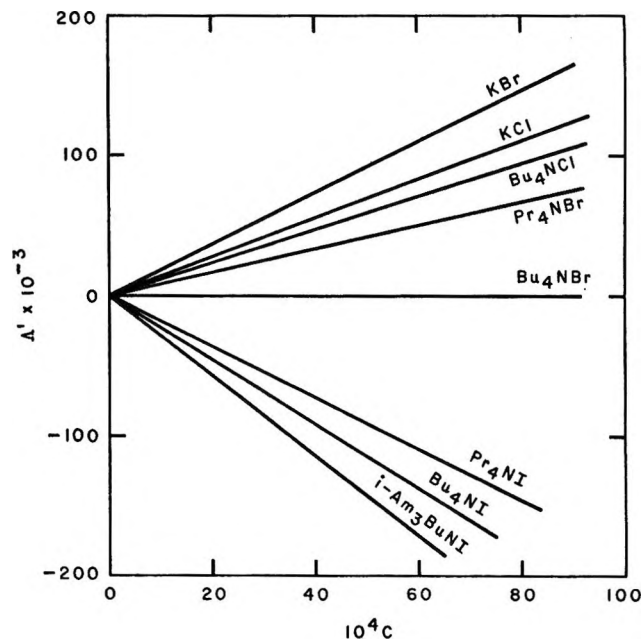
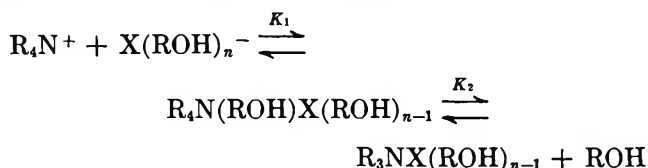


Figure 3. Plot of Λ' vs. c for tetraalkylammonium and potassium halides in formamide at 25°.

tors for the tetraalkylammonium salts is



The value of K_2 should reflect the relative ease of desolvation of the anion, while the value of K_1 is governed by diffusion and is calculable from eq 2 and 3. Since neither of the ion pairs is expected to contribute to the conductance, the association constant K_A is given by

$$K_A = \frac{\sum C(\text{ion pairs})}{(C_{R_4N^+})(C_{X(\text{ROH})_n^-})} = K_1(1 + K_2) \quad (4)$$

In water and formamide, where the dielectric constant is large, association constants are generally small for 1-1 electrolytes and cannot be unambiguously obtained. In this situation, deviations from expected behavior are best analyzed with a rearranged form of eq 1.

$$\Lambda' \equiv \Lambda - \Lambda_0 + S\sqrt{c} - Ec \log c = (J - B\Lambda_0)c \quad (5)$$

A plot of Λ' vs. c should give a straight line of slope $(J - B\Lambda_0)$. Since J is a function of the ion-size parameter, δ , the slope should increase with ionic size. Shown in Figure 2 is a plot of eq 5 for the potassium and tetrabutylammonium halides in water at 25°. In the case of the alkali metal halides, the slope of the line and hence the value of J increases in the order $I > \text{Br} > \text{Cl}$. This is in accord with the prediction of theory. For

the Bu_4N halides the slopes should be even larger than for the potassium salts; however, they are smaller and the dependence upon anion size is reversed.

If the degree of association is large, Λ' will not be linear in c but rather will be curved. The reason for this can be seen from the following argument. For associated electrolytes the equation analogous to (5) is

$$\Lambda'' \equiv \Lambda - \Lambda_0 + S\sqrt{c\gamma} - Ec\gamma \log c\gamma = (J - B\Lambda_0 - K_A f^2 \gamma \Lambda)c \quad (6)$$

where γ is the fraction of free ions and f the activity coefficient. Using the Onsager equation $\Lambda = \Lambda_0 - S\sqrt{c}$, the term $K_A f^2 \gamma \Lambda c$ can be approximated as $K_A f^2 \gamma (\Lambda_0 c - S c^{3/2})$. The $c^{3/2}$ dependence results in curvature of the Λ' plot which increases as K_A becomes larger. However, when K_A is small and γ close to unity, $K_A f^2 \gamma \Lambda c$ becomes essentially linear in c and cannot be separated from J . Comparison of the experimental points and the best straight line through them for aqueous Bu_4NI in Figure 2 shows a small but systematic curvature. This small curvature (0.01%) gives rise to an association constant of 3 to 5. The slightest amount of scatter in the data makes it impossible to determine association constants by analysis with the Fuoss-Onsager equation, because the uncertainty becomes as large or larger than K_A itself.

Shown in Figure 3 is a Λ' plot for the potassium and larger tetraalkylammonium halides in formamide at 25°; for clarity of presentation only the slopes, not the experimental points, are given. Figures 2 and 3 show the same general features, except that the magnitude of the deviation is reduced. This is in accord with the smaller concentration dependence of electrolytes in

formamide, and this concentration dependence is smaller because the values of ϵ and η are larger.

Although K_A cannot be unambiguously determined, it can be estimated by the following approximate calculation. Setting $B = 0$, $\gamma = 1$ and rearranging eq 6 to the form

$$\Lambda''' \equiv \Lambda' - Jc = -K_A f^2 c \quad (7)$$

allows K_A to be estimated from a plot of Λ''' vs. $f^2 c$. Since there is no *a priori* value that can be assigned to δ and hence to J , two values, $\delta = 4$ and 7 have been employed. The resulting values of K_A are given in Table VIII.

Two aspects of Table VIII require comment. When the dielectric constant is large, the cubic dependence of δ in eq 3 predominates over the exponential term in eq 2 and K_A increases with ionic size. This accounts for the fact that Bu_4N salts appear to be more associated than the corresponding Pr_4N salts. However, on this basis alone it is impossible to account for the difference of almost a factor of 2 between the bromides and iodides. The differences in size between these halides is sufficiently small that K_A should show little variation for any given cation.

Table VIII: Estimated Values of Association Constants for R_4NX Salts in Formamide at 25°

Salt	K_A at $\delta = 4$	K^I/K^{Br} ratio	K_A at $\delta = 7$	K^I/K^{Br} ratio
Bu_4NI	2.50	1.95	3.40	1.82
Bu_4NBr	1.29		1.87	
Pr_4NI	1.97	2.2	3.00	1.66
Pr_4NBr	0.88		1.80	

The similarity in anion dependence in the alcohols, water, and formamide taken together with values of K_A which are larger than K_1 suggests a common basis of behavior. The most reasonable explanation is that the multiple-step association process is operative in all the solvents, and hence is a feature common to all hydrogen-bonding solvents.

Acknowledgment. This work was supported by contract No. 14-01-0001-281 with the Office of Saline Water, U. S. Department of the Interior.

Raman Spectra of Silver Nitrate in Water-Acetonitrile Mixtures¹

by B. G. Oliver and G. J. Janz*

Department of Chemistry, Rensselaer Polytechnic Institute, Troy, New York 12181 (Received March 2, 1970)

The Raman spectrum of AgNO_3 in $\text{H}_2\text{O}-\text{CH}_3\text{CN}$ mixtures at 25° has been investigated with He-Ne (6328 Å) and Ar^+ ion (4880 Å) lasers as excitation sources. Particular attention was directed to an investigation of the most intense vibrational modes of the solute and solvent, respectively. In the symmetrical NO_3^- stretching frequency region two frequencies at 1036 and 1041 cm^{-1} are observed. Similarly, two frequencies are found in the $\text{C}\equiv\text{N}$ symmetrical stretching region of CH_3CN when AgNO_3 is added to the mixed solvent. The variations in the relative intensities of these bands with concentration are interpreted relative to ion-pair formation and selective solvation in this mixed solvent system.

Introduction

The system $\text{AgNO}_3-\text{H}_2\text{O}-\text{CH}_3\text{CN}$ is of interest in light of nmr studies of Schneider² and the transport number measurements of Strehlow and Koepf³ which indicate selective solvation and ion-pair formation in these solutions. A Raman spectral investigation of this system was undertaken to evaluate the spectral criteria for ionic interactions and for preferential solvation in mixed solvents.

Experimental Section

AgNO_3 , H_2O , and CH_3CN were purified by the techniques previously used in this laboratory.^{4,5} The solutions were prepared by weight and transferred to Pyrex

* To whom correspondence should be addressed.

(1) Reported, in part, at the Symposium on the Structure of Water and Aqueous Solutions in honor of T. F. Young, Chicago, Ill., June 1969.

(2) H. Schneider, Ph.D. Thesis, Max Planck Institute, 1965.

glass Raman tubes (0.7 mm o.d. and 10 cm long) with optical flats as windows.

The spectra were recorded with a Jarrell-Ash laser-Raman spectrometer (Model 25-300) having both He-Ne (6328 Å) and Ar⁺ ion (4880 Å) lasers (55 and 125 mw, respectively) as excitation sources. All spectra were scanned three or four times to establish consistency of the band shapes and positions. The band contours were examined with a DuPont Curve Analyser, by means of which asymmetric contours were resolved into Lorentzian components. For quantitative work, the integrated intensity of the 2945-cm⁻¹ band of pure CH₃CN was selected as the intensity standard; the integrated intensities in the present work are, thus, all relative to this standard. Correction of the intensity values for variations in refractive index⁶ was considered and found to be within the accuracy of the intensity measurements (about 10%).

Results

(a) *Water Frequencies.* The 2800-3900- and the 1500-1800-cm⁻¹ regions were examined, but no significant changes in the band contours of the solutions relative to pure water were noted.

(b) *CH₃CN Frequencies.* The Raman frequencies observed in pure CH₃CN and in AgNO₃-CH₃CN have been thoroughly studied⁷ so need not be reported here. As water is added to CH₃CN it is sufficient to note that the Raman frequencies of CH₃CN shift, but only slightly, *e.g.*, the bands at 919, 2253, and 2945 cm⁻¹ (pure CH₃CN) gradually change to 925, 2261, and 2949 cm⁻¹, respectively (4.7 mol % CH₃CN-95.3 mol % H₂O); no new frequencies that may not be assigned to CH₃CN and H₂O appear in this mixed solvent system.

Two new bands at 2272 and 929 cm⁻¹ appear when AgNO₃ is added to the solvent. The intensities of these two bands increase with increasing AgNO₃ concentrations, at the expense of the 2253- and 919-cm⁻¹ bands of acetonitrile (*i.e.*, C≡N and C-C stretching frequencies). These two new bands are assigned^{8,9} to C≡N and C-C stretching vibrations of CH₃CN in the primary solvation sphere of the cationic species (*i.e.*, M⁺ ··· N≡C-CH₃; C_{3v} point group symmetry). This is illustrated in Figure 1.

(c) *NO₃⁻ Frequencies.* The doublet in the 750-cm⁻¹ region and the loss of degeneracy in the 1300-cm⁻¹ region for the NO₃⁻, as reported elsewhere^{10,11} for contact ion pairs in aqueous nitrates, were observed in the present studies. Attention, however, was devoted to the 1050-cm⁻¹ region (ν₁(A₁'), NO₃⁻) because of its relatively high intensity.

For solutions of AgNO₃ in anhydrous CH₃CN at very low concentrations (<0.01 M) only one polarized band, 1041 cm⁻¹, is observed. With increasing AgNO₃ concentrations a new line at 1036 cm⁻¹ appears. The 1041-cm⁻¹ band has been assigned¹² as the symmetric stretching mode, ν₁(A₁'), for the "free" or "solvent-

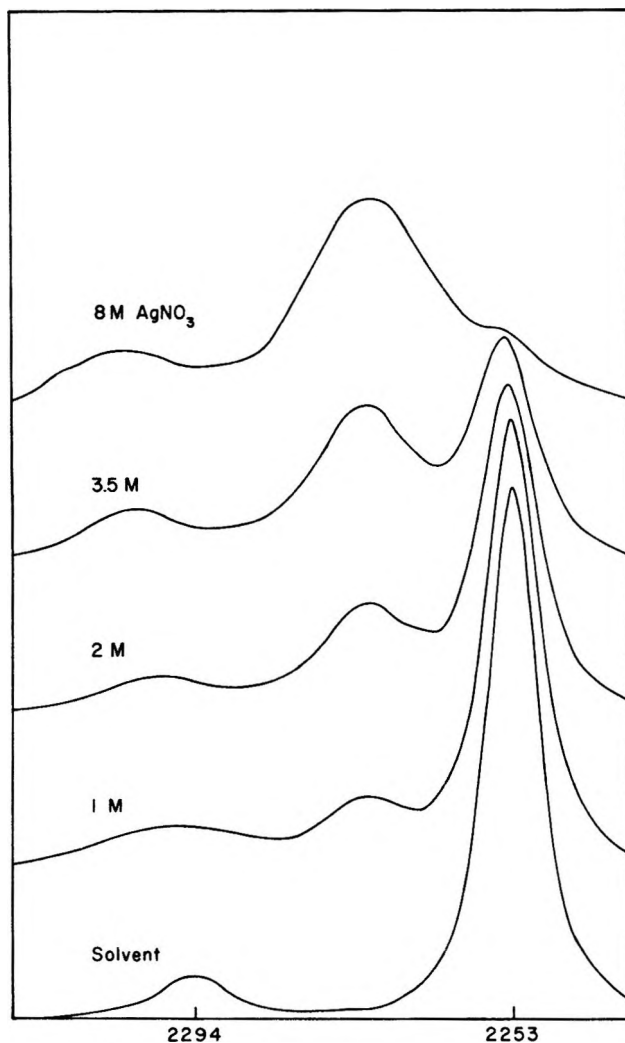


Figure 1. C≡N bands in AgNO₃-11.8 mol % H₂O-88.2 mol % CH₃CN solutions.

separated" NO₃⁻ while the 1036-cm⁻¹ band, as ν₁(A₁') for the NO₃⁻ when it is in the field of the cation, *i.e.*, as an "inner-sphere complex" [Ag⁺NO₃⁻] or, from the viewpoint of electrolytes, as a "contact ion pair."

As H₂O is added a small shift of these two frequencies to higher values occurs, but the band intensities vary markedly. This is illustrated in Figure 2. In

(3) H. Strehlow and H. M. Koepf, *Ber. Bunsenges. Phys. Chem.*, **62**, 373 (1958).

(4) G. J. Janz, M. J. Tait, and C. B. Baddiel, *J. Phys. Chem.*, **69**, 3634 (1965).

(5) R. P. T. Tomkins, E. Andalafit, and G. J. Janz, *Trans. Faraday Soc.*, **65**, 1906 (1969).

(6) D. G. Rea, *J. Opt. Soc. Amer.*, **49**, 90 (1959)

(7) K. Balasubrahmanyam and G. J. Janz, *J. Amer. Chem. Soc.*, **92**, 4189 (1970).

(8) J. C. Evans and G. Y. S. Lo, *Spectrochim. Acta*, **21**, 1033 (1965).

(9) K. F. Purcell and R. S. Drago, *J. Amer. Chem. Soc.*, **88**, 919 (1966).

(10) D. E. Irish and A. R. Davis, *Can. J. Chem.*, **46**, 943 (1968).

(11) D. E. Irish, A. R. Davis, and R. A. Plane, *J. Chem. Phys.*, **50**, 2262 (1969).

(12) G. J. Janz, K. Balasubrahmanyam, and B. G. Oliver, *ibid.*, **51**, 5723 (1969).

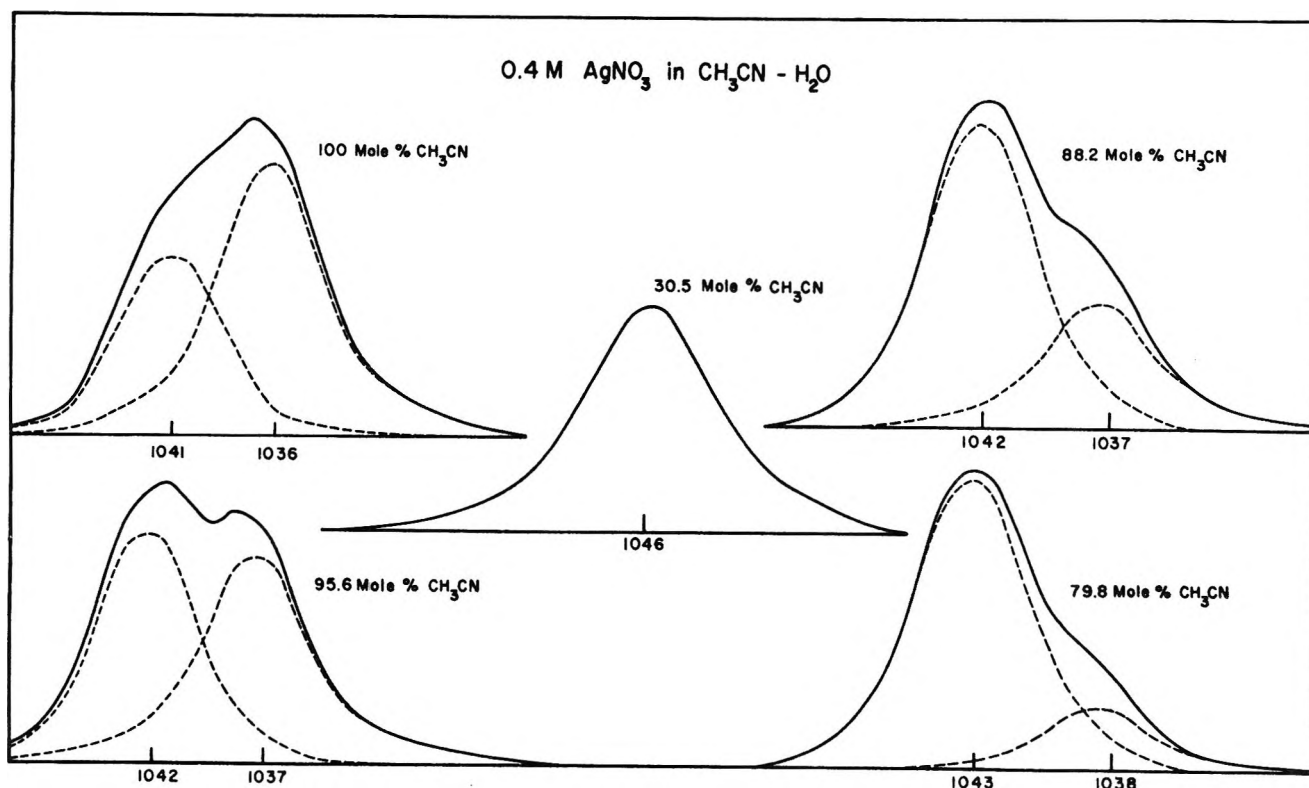


Figure 2. NO_3^- bands in the 1050-cm^{-1} region for 0.4 M AgNO_3 in $\text{H}_2\text{O}-\text{CH}_3\text{CN}$ mixtures.

aqueous solutions the band shape for $\nu_1(\text{A}_1')$ (AgNO_3) is symmetrical for the entire concentration range, to saturation solubility.

As the solute concentration in a mixed solvent of fixed composition (88.2 mol % CH_3CN -11.8 mol % H_2O) was changed, the relative intensity of the 1037-cm^{-1} to the 1042-cm^{-1} band remains almost invariant, about 1:2 for the concentration range $0.4\text{--}3.5\text{ M}$. This contrasts with AgNO_3 in anhydrous CH_3CN , where the relative intensities of these two bands are not invariant for such a concentration interval.

Discussion

It has been shown elsewhere⁷ that Raman intensity measurements can be used to gain values of primary solvation numbers for solutions of AgNO_3 in anhydrous CH_3CN from the expression

$$\frac{I_b}{I_b + I_t} = N \frac{c_{\text{AgNO}_3}}{c_{\text{CH}_3\text{CN}}}$$

where I_b and I_t are the intensities of the 2272-cm^{-1} and 2253-cm^{-1} bands, c_{AgNO_3} and $c_{\text{CH}_3\text{CN}}$ are the concentrations (moles/liter) of AgNO_3 and CH_3CN , and N is the average number of solvent molecules which are coordinated by the solute in the primary layer. It should be noted that various additional factors may contribute to the molar intensity, such as an induced dipole (from ion-dipole force fields) and/or changes in the bulk dielectric constant, and that the direct proportionality between Raman intensities and species concentrations

(above) is an approximation and implies that the specific molar intensity of the ($\text{C}\equiv\text{N}$) stretching mode is numerically the same for the solvated acetonitrile and bulk. Support for this assumption is found in this work from the observation that the intensities 2272 cm^{-1} in the most concentrated AgNO_3 solutions (*ca.* 8 M) and of the 2253 cm^{-1} for the pure solvent were virtually equal. Independent support for the viewpoint that the contribution of the other factors to the molar intensity variations are possibly a second order of magnitude is the observation of Purcell and Drago,⁹ namely the changes in the $\text{C}\equiv\text{N}$ force constant were not more than 3-5% for a series of CH_3CN , metal-ion adducts.

The graph of $I_b/(I_b + I_t)$ vs. $c_{\text{AgNO}_3}/c_{\text{CH}_3\text{CN}}$ for AgNO_3 in CH_3CN and in two compositions of $\text{H}_2\text{O}-\text{CH}_3\text{CN}$ in Figure 3 shows the extension of this approach to AgNO_3 in mixed solvents. The N values, estimated from the slopes of the curves, are found to vary with concentration, being about 4 in the dilute concentration range ($<0.05\text{ M}$), about 2 in the moderate concentration range (~ 0.05 to 5.0 M), and decreasing to about 1 at higher concentrations ($>5.0\text{ M}$). Support for this equation comes from the fact that solvates of composition $\text{AgNO}_3 \cdot 2\text{CH}_3\text{CN}$ and $\text{AgNO}_3 \cdot \text{CH}_3\text{CN}$ have been crystallized¹³ from $\text{AgNO}_3\text{-CH}_3\text{CN}$ in the concentration ranges where N is 2 and 1, respectively.

The close proximity of the curves and their slopes in Figure 3 indicates that the solvation with respect to

(13) G. J. Janz, M. J. Tait, and J. Meier, *J. Phys. Chem.*, **71**, 963 (1967).

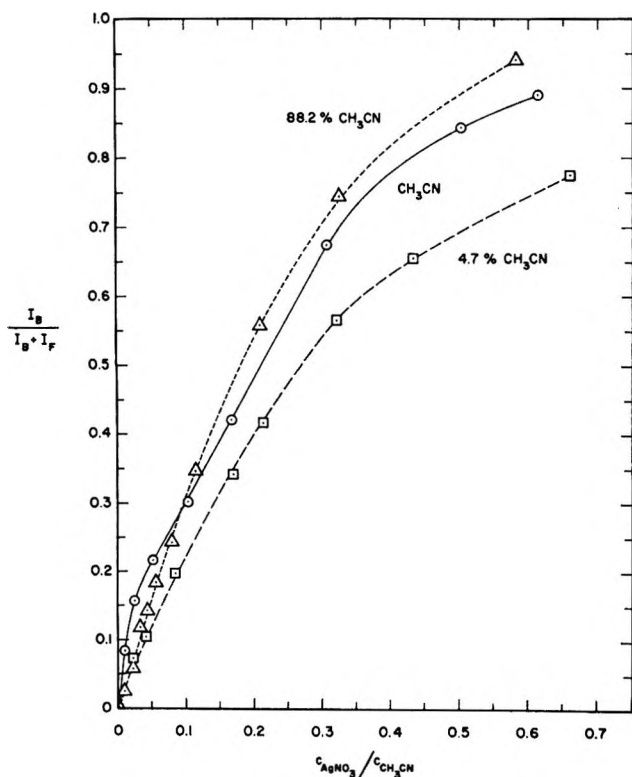


Figure 3. Graph of $I_b / (I_b + I_f)$ vs. $c_{\text{AgNO}_3} / c_{\text{CH}_3\text{CN}}$ for AgNO_3 in CH_3CN , 11.2 mol % H_2O -88.2 mol % CH_3CN , and 95.3 mol % H_2O -4.7 mol % CH_3CN .

CH_3CN is the same in the mixed solvents as it is in pure CH_3CN . Even when the concentration of CH_3CN in the solvent has been reduced to 4.7 mol %, Ag^+ appears to be preferentially solvated by CH_3CN . These findings are in accord with the nmr results of Schneider² and transport number results of Strehlow and Koepf³ which similarly showed Ag^+ to be selectively solvated by CH_3CN in H_2O - CH_3CN mixtures.

The Raman spectrum of 0.4 M AgNO_3 in various mixed solvents (Figure 2) reveals that as the H_2O con-

tent of the solvent is increased the intensity of the 1041- cm^{-1} band increases at the expense of the 1036- cm^{-1} band. As the AgNO_3 concentration is changed in a single mixed solvent (constant H_2O content), the ratio of the intensities of the 1041- to 1036- cm^{-1} bands remained almost invariant over a wide concentration range. Thus, the equilibrium between the contact ion pairs and the free ions is very sensitive to H_2O concentration.

The primary solvation number of Ag^+ with respect to CH_3CN becomes lower with increasing AgNO_3 concentration. With increasing AgNO_3 concentration in anhydrous CH_3CN more and more NO_3^- ions seem to be replacing CH_3CN in the primary coordination sphere of Ag^+ . In the mixed solvents the situation is complicated somewhat by the H_2O which seems to be competing with NO_3^- for positions close to Ag^+ . Thus as the H_2O content of the solvent is increased more and more NO_3^- in the primary layer of the Ag^+ is being replaced by H_2O .

Recent evidence from Raman spectroscopy,^{10,11,14} compressibility,¹⁵ and electrical double layer studies^{16,17} seems to indicate that the NO_3^- ion is hydrated in solution. Such hydration of the NO_3^- by H_2O in the H_2O - CH_3CN solvents would certainly reinforce the above arguments and provide an ample explanation for the experimental results.

Acknowledgments. This investigation was supported by the National Science Foundation, Division of Chemistry, Washington, D. C. It is a pleasure to acknowledge the help and advice given us by Dr. K. Balasubrahmanyam.

(14) A. R. Davis, J. W. Macklin, and R. A. Plane, *J. Chem. Phys.*, **50**, 1478 (1969).

(15) J. Padova, *Bull. Res. Council Israel, Sect. A*, **10**, 63 (1961).

(16) G. J. Hills and R. Payne, *Trans. Faraday Soc.*, **61**, 326 (1965).

(17) R. Payne, *J. Phys. Chem.*, **69**, 4113 (1965).

NOTES

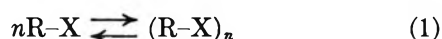
Salt Effects on the Critical Micelle Concentrations of Nonionic Amphiphiles

by John E. Gordon

Department of Chemistry, Kent State University, Kent, Ohio 44240
(Received March 30, 1970)

Added inorganic electrolyte lowers the critical micelle concentration (cmc) of nonionic as well as ionic amphiphiles. The usual account of the latter case, in terms of the shielding of repulsive interactions between charged head groups,¹ cannot be applied to the former. A variety of explanations have been offered for the nonionic case. In 1965 Mukerjee² reviewed these and presented an attractive alternative treatment, based on the McDevit-Long theory,³ in which the Setschenow equation was used to compute the activity coefficients of monomeric and micellar amphiphile, and these were combined according to the mass-law model of micelle formation to predict the dependence of the cmc on salt concentration. The purpose of the present note is to point out that Mukerjee's expression in fact corresponds to no common model of micellization and to present correct derivations for the mass-law and pseudophase models and compare the results with experiment.

The mass-law expression for the association equilibrium 1 is given by eq 2, where R-X is an amphiphile with hydrocarbon and polar moieties R and X, C_{mic} is



$$K = \frac{C_{mic} f_{mic}}{C_{mono}^n f_{mono}^n} \quad (2)$$

the concentration of micelles, C_{mono} is the concentration of monomers, and f_{mic} and f_{mono} are the corresponding activity coefficients. Setting $C_{mono} = cmc$ and neglecting $(\log C_{mic})/n$ gives eq 3.⁴

$$\log cmc = \Delta G/2.303RT - \log f_{mono} + \frac{1}{n} \log f_{mic} \quad (3)$$

To the extent that nonelectrolyte-Nonelectrolyte interactions can be ignored, the activity coefficient, f , of a nonpolar nonelectrolyte in aqueous salt solution is related to that in pure water, f_0 , by eq 4, where C_s is the salt concentration.⁵ The McDevit-Long theory computes k_s on the basis of the work required to make

$$\log (f/f_0) = k_s C_s \quad (4)$$

a hole in the solvent large enough to accommodate the nonelectrolyte. The effect of salt is to alter the cohesive energy density of the medium, and the expression for k_s is eq 5, in which \bar{V}_i is the limiting partial molal volume of the nonelectrolyte (the superscript zero is omitted throughout), $(V_s - \bar{V}_s^0)$ is the electrostriction of the particular salt, and β_0 is the compressibility of water.

$$k_s = \bar{V}_i(V_s - \bar{V}_s^0)/2.303RT\beta_0 \quad (5)$$

Mukerjee² represents $\log f_{mono}$ and $\log f_{mic}$ as sums of parts characteristic of R and of X, e.g., $\log f_{mic} = \log f_{mic}^R + \log f_{mic}^X$. He then sets $\log f_{mic}^R = 0$ on the basis that the nonpolar surface of micellar RX which is exposed to the salt solution is small compared to that in monomeric RX. Equation 3 then takes the functional form (eq 6) which is empirically observed.

$$\log cmc = \Delta G/2.303RT - C_s [(k_s^R)_{mono} + (k_s^X)_{mono} - (k_s^X)_{mic}] \quad (6)$$

The fallacy in this treatment is the neglect of $\log f_{mic}^R = \bar{V}_{mic}^R(V_s - \bar{V}_s^0)/2.303RT\beta_0$. The theoretical expression for k_s , eq 5, involves the volume of the nonelectrolyte, and the fact that its surface area in contact with the water is negligible is irrelevant; \bar{V}_{mic}^R is not negligible. For \bar{V}_{mic}^R and hence $(k_s^R)_{mic}$ to be zero, as in eq 6, micellar R must not be in the same phase as the rest of the system. Mukerjee's calculation is thus for a pseudophase model in which the second phase is the hydrocarbon portion of the micelle.

We believe the following to be the correct application of eqs 4 and 5 to the mass-law model. Since the partial molal volume of RX increases on micelle formation,⁶ one can express \bar{V}_{mic}^{RX} as $(n\bar{V}_{mono}^{RX} + a)$ with a positive. Letting $(V_s - \bar{V}_s^0)/2.303RT\beta_0 = D$ we write

$$(k_s^{RX})_{mono} = D\bar{V}_{mono}^{RX} \quad (7)$$

$$(k_s^{RX})_{mic} = D(n\bar{V}_{mono}^{RX} + a) \quad (8)$$

$$\log (f^{RX}/f_0^{RX})_{mono} = D\bar{V}_{mono}^{RX}C_s \quad (9)$$

$$\log (f^{RX}/f_0^{RX})_{mic} = D(n\bar{V}_{mono}^{RX} + a)C_s \quad (10)$$

Taking $(f_0^{RX})_{mono} = (f_0^{RX})_{mic} = 1$ and substituting in

- (1) See e.g., K. Shinoda, *Bull. Chem. Soc. Jap.*, **28**, 340 (1955).
- (2) P. Mukerjee, *J. Phys. Chem.*, **69**, 4038 (1965).
- (3) W. F. McDevit and F. A. Long, *J. Amer. Chem. Soc.*, **74**, 1773 (1952).
- (4) P. Mukerjee, *Advan. Colloid Interface Sci.*, **1**, 241 (1967).
- (5) F. A. Long and W. F. McDevit, *Chem. Rev.*, **51**, 119 (1952).
- (6) L. Benjamin, *J. Phys. Chem.*, **70**, 3790 (1966).

$$\log \text{cmc} = \Delta G/2.303RT + aDC_s/n \quad (11)$$

eq 3 gives eq 11, which has the correct form but predicts increase in cmc with increasing C_s contrary to experience, since D is positive for the salts in question.

Let us next apply eq 7-10 to the conventional pseudophase model, for which eq 12 applies.⁴ The resulting expression is eq 13. The sign of the coefficient of C_s

$$\log \text{cmc} = \Delta G/2.303RT - \log f_{\text{mono}}^{\text{RX}} \quad (12)$$

is now correct, and its magnitude can be compared with

$$\begin{aligned} \log \text{cmc} &= \Delta G/2.303RT - (k_s^{\text{RX}})_{\text{mono}} C_s \quad (13) \\ &= \Delta G/2.303RT - D\bar{V}_{\text{mono}}^{\text{RX}} C_s \end{aligned}$$

estimates of k_s^{RX} for the same systems used by Mukerjee to test eq 6. These estimates depend upon the additivity of group contributions to k_s .⁷ The first system is octyl glucoside, for which Mukerjee showed $(k_s^{\text{X}})_{\text{mono}}$ to be near zero. Thus $(k_s^{\text{RX}})_{\text{mono}} \approx (k_s^{\text{R}})_{\text{mono}}$ in this case, and Mukerjee's estimate of the log cmc *vs.* C_s slope *via* eq 6 applies also to the present model. This was made² by extrapolating Morrison and Billett's⁸ k_s values for the lower alkanes in sodium chloride solutions (interpolated to 25°) to give $k_s^{\text{C}_8\text{H}_{18}} \approx (k_s^{\text{R}})_{\text{mono}} = 0.36$, *vs.* 0.35 observed. The second system was octylbetaine (observed slope = 0.13). With $k_s^{\text{C}_8\text{H}_{18}} = 0.36$, eq 6 requires $(k_s^{\text{X}})_{\text{mono}} - (k_s^{\text{X}})_{\text{mic}}$ to be -0.23 ($\text{X} = -\text{CH}(\text{N}^+\text{Me}_3)\text{COO}^-$). Mukerjee considered this reasonable in view of the k_s values for glycine = -0.28 in dilute solution and -0.02 at 2 *M* glycine (approximately the concentration in the micelle surface). Equation 13 requires $(k_s^{\text{X}})_{\text{mono}} = -0.23$, equally reasonable in relation to the glycine value. Finally, both equations predict the same average increment per CH_2 group in the log cmc *vs.* C_s slopes for homologous amphiphiles. This was estimated² from ref 8 as 0.032 *vs.* a mean observed value of 0.040.

All of these estimates, however, should be viewed with caution since the values of $(k_s^{\text{R}})_{\text{mono}}$ estimated would be more than twice as large if the k_s values of Schrier and Schrier⁷ for CH_2 and CH_3 were used. A stringent test must await further experience with k_s additivity or direct measurement of $(k_s^{\text{RX}})_{\text{mono}}$ by distribution experiments.

In summary, the pseudophase model of micelle formation, although serious objections to it have been presented,⁴ accounts reasonably well (in conjunction with the McDevit-Long theory) for the effects of salt on the cmc of nonionic amphiphiles while the mass-law model does not.

(7) E. E. Schrier and E. B. Schrier, *J. Phys. Chem.*, **71**, 1851 (1967).

(8) T. J. Morrison and F. Billett, *J. Chem. Soc.*, 3819 (1952).

Salt Effects on the Critical Micelle Concentrations of Nonionic Surfactants

by Pasupati Mukerjee

School of Pharmacy, University of Wisconsin, Madison, Wisconsin 53706 (Received June 4, 1970)

Gordon¹ has criticized the use of the mass-action model of micelle formation in the previous analysis² of the effect of inorganic salts on the critical micelle concentrations (cmc) of nonionic surfactants and has suggested that the two-phase model³ of micelle formation accounts reasonably well for the salt effects. The discussion below is concerned with the nature of the assumptions involved in the application of the mass-action model and the limitations of the two-phase model in describing the salt effects.

Gordon's criticism of the mass-action model is based on a too literal application of the McDevit-Long equation for the salt effect.⁴ If the activity coefficient, f , of a nonelectrolyte solute in a salt solution of molar concentration C_s is represented by the equation $\log f = k_s C_s$, where k_s is the salt effect constant, the McDevit-Long equation states that k_s is proportional to \bar{V}_i , the partial molal volume of the nonelectrolyte. The McDevit-Long equation provides a better explanation of the salt order than the older electrostatic theories.⁴ The equation, however, applies only to nonpolar solutes and even for such solutes it predicts k_s values which are much larger than experimental values. Subsequent research on salt effects has continued to emphasize their complexity.⁵

In our previous work,² although the McDevit-Long equation was cited to provide the rationale for the assumed additivity of the salting-out coefficients of the hydrocarbon chains of the surfactant monomers, the additivity relation actually used was derived as an empirical relation based on the experimental data of Morrison and Billett.⁶ This empirical relation is in no way dependent on the McDevit-Long equation.

The important assumption in the previous work that Gordon focuses attention on is that the salt effect on the micelle is mainly due to the effect on the hydrophilic head groups which are exposed to water; *i.e.*, the effect on the hydrocarbon portion of the micelle is small when compared with the combined effect on the hydrocarbon moiety of the constituent monomers. If the McDevit-

(1) J. E. Gordon, *J. Phys. Chem.*, **74**, 3823 (1970).

(2) P. Mukerjee, *ibid.*, **69**, 4038 (1965).

(3) P. Mukerjee, *Advan. Colloid Interface Sci.*, **1**, 241 (1967).

(4) W. F. McDevit and F. A. Long, *J. Amer. Chem. Soc.*, **74**, 1773 (1952); F. A. Long and W. F. McDevit, *Chem. Rev.*, **51**, 119 (1952).

(5) B. E. Conway, J. E. Desnoyers, and A. C. Smith, *Phil. Trans. Roy. Soc. London*, **256**, 389 (1964); W. L. Masterton and T. P. Lee, *J. Phys. Chem.*, **74**, 1776 (1970).

(6) T. J. Morrison and F. Billett, *J. Chem. Soc.*, 3819 (1952).

Long equation is applied without modification, the salting-out of the micellar hydrocarbon core may actually overcompensate for the salting-out of the hydrocarbon portion of the free monomers.¹ The assumption above thus seems to be incompatible with the McDevit-Long theory.

In defense of the above assumption, as also the McDevit-Long theory, it must be emphasized that the surface of the micelle is essentially hydrophilic or polar⁷ and, therefore, the McDevit-Long equation cannot be applied without modification. Thus, the fact that the polar mannitol, in spite of having a hydrocarbon framework, is actually salted-in very slightly⁸ by sodium chloride cannot be held against the McDevit-Long theory. Theories of salt effects on polar molecules are unsatisfactory. For the micelles, comparisons with proteins should be relevant. The k_s values for proteins⁹ are usually higher than those for small nonpolar solutes such as benzene, but they are very much less than what would be expected from volume ratios by using the McDevit-Long equation. Fibrinogen, for example, with a molecular weight of 330,000,¹⁰ has a k_s value in NaCl solution of 1.07⁹ compared to the value of 0.195 for benzene.⁴ The k_s value of fibrinogen calculated from that of benzene using the volume ratio is about 500. Thus, empirically, to the extent the micellar core with its immediately adjacent protective polar groups can be compared with a compact protein molecule, both containing a distribution of polar and nonpolar groups at the surface, the salt effect on the hydrocarbon part of the micelle with its polar sheath is expected to be small when compared to the combined effect on the hydrocarbon part of the monomers. This, of course, means that the separate accounting of the k_s values for the polar and nonpolar parts of micellized monomers, as also for free monomers, on the basis of an additivity relationship,² can only be approximate.

Even if the McDevit-Long theory is literally applied, assuming that in its interaction with salt solutions the micellar hydrocarbon behaves like the hydrocarbon chains of the monomers, the above assumption still appears to be reasonably justified. McDevit and Long⁴ stated quite clearly that their limiting equation is expected to apply only to very small nonpolar solutes and they ascribed the difference between the high k_s values predicted for benzene and low values observed to the finite size of benzene. For spherical solutes, they suggested that the theoretical k_s value should be reduced by roughly the factor of $a/(a + b)$ when a is an ionic radius and b the radius of the nonpolar solute. As the micelle radius is much larger than the thickness of the monomeric hydrocarbon chains, this factor alone would reduce the k_s value of the micelle very considerably. The $a/(a + b)$ correction factor, or similar factors applicable to nonspherical solutes, suggest that k_s may not be proportional to \bar{V}_i for large solutes. The rough proportionality that is observed experimentally for ordi-

nary nonpolar solutes such as aliphatic and aromatic hydrocarbons^{2,11} may be due in part to the fact that these hydrocarbons have similar thicknesses and, therefore, similar distances of closest approach for ions, and similar values of the effective correction factors. It is thus felt that the assumption of a low k_s value for the hydrocarbon part of the micelle, when compared to the combined k_s values for the constituent monomers in their unmicellized form, is both theoretically and empirically justified.

As regards the two-phase model favored by Gordon,¹ it is certainly curious that the model leads to similar predictions for octyl glucoside and alkyl betaines when compared to the mass-action model. This agreement appears to be fortuitous, however. The two models give very different results for alkyl polyoxyethylene type surfactants. Polyoxyethylenes (polyethylene glycols) are known to exhibit strong salt effects.¹² The difference between the two models can be shown by numerical calculations for a typical system, a branched nonylbenzene (EO)₅₀, where EO stands for an oxyethylene group. For this surfactant, the salt effect constant, k_m , in the equation $\log \text{cmc} = \text{constant} - k_m C_s$,² has been estimated to be 0.34² from the variation of the cmc in NaCl solutions.¹³ The k_s value for nonyl benzene itself, estimated from the value of 0.195 for benzene⁴ and 0.032 for each CH₂ group,² is 0.45. For the oxyethylene groups, the k_s value must include the values for the CH₂ groups as also the ether oxygens. The k_s value estimated from the solubilities of diethyl ether in NaCl solutions¹⁴ is 0.31 at 25°. When compared to the value of 0.22 for butane,⁶ it is clear that the ether oxygen is salted-out with a k_s coefficient of about 0.09, if an additivity relation is employed. For (EO)₅₀, the calculated k_s for the 100 CH₂ groups alone is 3.2, even if the salting-out of the ether oxygen is ignored. The combined k_s value for the monomer should thus exceed 4. The two-phase model thus predicts a k_m -value of more than 4 as compared to the experimental value of 0.34. The mass-action approach, on the other hand, allows for the cancellation of the salting-out of the oxyethylene groups of the monomers and the micelle.² If the cancellation is exact, the predicted k_m value (0.34) should be the same as the k_s value for the nonyl-phenyl

(7) A micelle may be appropriately described as "an oil drop with a polar coat," a description used for compact protein molecules by Eric Rideal and Irving Langmuir according to D. A. Phillips, *Sci. Amer.*, 215, 78 (1966).

(8) E. J. Kelly, R. A. Robinson, and R. H. Stokes, *J. Phys. Chem.*, 65, 1958 (1961).

(9) J. T. Edsall and J. Wyman, "Biophysical Chemistry," Academic Press, New York, N. Y., 1953, Vol. 1, p. 274.

(10) C. Tanford, "Physical Chemistry of Macromolecules," Wiley, New York, N. Y., 1961, p. 381.

(11) N. C. Deno and C. H. Spink, *J. Phys. Chem.*, 67, 1347 (1963).

(12) F. E. Bailey, Jr., and R. W. Callard, *J. Appl. Polym. Sci.*, 1, 56 (1959).

(13) M. J. Schick, *J. Colloid Sci.*, 17, 801 (1962).

(14) P. C. L. Thorne, *J. Chem. Soc.*, 119, 262 (1921).

group, the estimated k_s for nonyl benzene being 0.45. Because of the approximate nature of the additivity relationships employed, and the lack of information on how complete the cancellation of the salt effects on the oxyethylene groups are, exact agreements are not to be expected. The mass-action model, however, is clearly superior to the two-phase model. The experimental fact that k_m values for the polyoxyethylene type surfactants tend to be independent of the EO chain length^{13,15} also argues against the two-phase model and suggests that the cancellation of the EO chain effects in the salt effects on the cmc is a good approximation in the mass-action model.

To summarize, although the two-phase and the mass-action models give similar results for the salt effects on the cmc's of octyl glucoside and alkyl betaines,¹ the salt effects on polyoxyethylene type nonionic surfactants are in poor accord with the two-phase model of micelle formation, various arguments against which have been summarized elsewhere.³ The mass-action model, as used earlier,² appears to be better.

(15) F. Becher, *J. Colloid Sci.*, **17**, 325 (1962).

Evaluation of the Basicity of Methyl Substituted Nitroguanidines by Ultraviolet and Nuclear Magnetic Resonance Spectroscopy

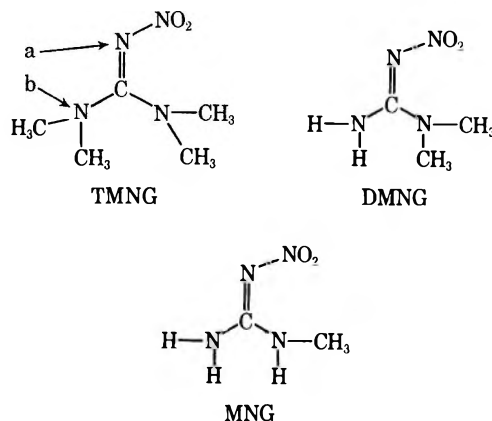
by E. Price, L. S. Person, Y. D. Teklu,

Department of Chemistry, Howard University, Washington, D. C. 20001

and A. S. Tompa

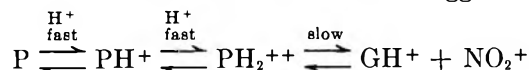
Applied Science Department, U. S. Naval Ordnance Station, Indian Head, Maryland 20640 (Received May 6, 1970)

The position of protonation of 1,1,3,3-tetramethyl-2-nitroguanidine (TMNG) in strong acid has been shown to occur primarily at the dimethylamino site, b.¹ Lockhart,² however, has presented evidence that protonation occurs primarily at the nitrimino site, a, in other



methyl nitroguanidines such as 1-methyl-2-nitroguanidine (MNG) and 1,1-dimethyl-2-nitroguanidine (DMNG). The evidence presented to support protonation at the amino site for TMNG and at the nitrimino site for MNG and DMNG was based on the proton magnetic resonance spectra of these compounds in concentrated nitric, sulfuric, and hydrochloric acids. In very concentrated acid media, it has also been assumed that these compounds are likely to be diprotonated and that denitration occurs under these conditions.

A mechanism for denitration has been suggested.^{3,4}



(G guanidine, P nitroguanidine).⁴ However, the question as to where the first proton adds to the nitroguanidine seems to depend on the type of nitroguanidine and the number of different basic sites in the molecule. For nitroguanidine and symmetrically substituted nitroguanidines, we are limited to only two basic sites excluding the nitro group whereas in unsymmetrically substituted nitroguanidines there are three basic sites. How these basic sites are influenced by methyl substitution and their contributions to the pK_a of MNG and DMNG have been discussed by Bonner and Lockhart.⁵ However, the pK_a and the effect of methyl substitution were not reported for TMNG and 1,3-dimethylnitroguanidine. Now we wish to report the pK_a value of TMNG and to further discuss the effect of methyl substitution on the basicity of nitroguanidines.

The pK_a value of TMNG was determined in concentrated sulfuric acid solutions from ultraviolet absorption data. TMNG in water absorbed at 265 $m\mu$ and followed Beer's law. Upon the addition of TMNG of a definite concentration to sulfuric acid solutions of concentrations ranging from 1 to 29%, the absorption band at 265 $m\mu$ decreased to a minimum value and remained constant upon increasing the sulfuric acid concentration from 30 to 69%. For sulfuric acid concentrations above 69%, the absorption band decreased rapidly.⁶ The absorbance values at 265 $m\mu$ for solutions of TMNG in 15 to 61% sulfuric acid were unchanged after three weeks,⁸ and the wavelength was free of medium effects in the pK_a region. We also wish to point out that

(1) E. Price, R. D. Barefoot, A. S. Tompa, and J. U. Lowe, Jr., *J. Phys. Chem.*, **71**, 1608 (1967).

(2) J. C. Lockhart, *J. Chem. Soc. B*, 1174 (1966).

(3) M. L. Hardy-Klein, *J. Chem. Soc.*, 70 (1957).

(4) R. J. Simkins and G. Williams, *ibid.*, 3086 (1952); 1386 (1953).

(5) T. G. Bonner and J. C. Lockhart, *ibid.*, 3858 (1958).

(6) All spectral measurements were carried out very rapidly on freshly prepared solutions ($10^{-5} M$). These solutions were prepared by mixing a suitable quantity of TMNG in water with 10 to 90% sulfuric acid solutions. The procedures were similar to those described by Arnett and Wu.⁷

(7) E. M. Arnett and C. Y. Wu, *J. Amer. Chem. Soc.*, **82**, 5660 (1960).

(8) It has been reported that nitroguanidines do not begin to appreciably denitrate until the acid concentration is above 70%.³

no absorption band appeared in the region around 225 $m\mu$ on increasing the sulfuric acid concentration. A broad band has been reported to occur at 225 $m\mu$ for other nitroguanidines and has been attributed to protonation at the nitrino site a.⁵

The method of Arnett and Wu⁷ was used to calculate the pK_a value. Since the TMNG molecule contains tertiary nitrogen sites, the H_0''' acidity scale was employed.⁹ The pK_a value was calculated to be -0.82 . A significant feature of the dissociation of $TMNGH^+$ is that the plot of $\log(BH^+)/B$ against H_0''' is a straight line of unit slope. This result is similar to the reported behavior of other nitroguanidines where there are both primary and secondary nitrogen sites in the same molecule.⁴

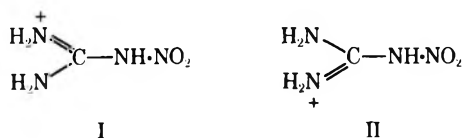
The nmr chemical shift of the $N-CH_3$ resonances of aqueous solutions of methyl derivatives of nitroguanidine was reported to be dependent on the acidity of the medium.¹ A plot of the chemical shift, δ , of the $NC-H_3$ resonance vs. H_0 for TMNG in 0-70% HNO_3 is represented by a sigmoid curve typical of protonation.¹⁰ The " pK_a "¹¹ was determined from the inflection point¹³ and found to be -0.75 . A summary of the results for methyl substituted nitroguanidines are shown in Table I. In light of discussions on the use of H_0 and H_0''' ⁹ and the fact that the solutions must be fairly concentrated with respect to the basic substrate under investigation, we only wish to indicate that the trend in " pK_a " for methyl nitroguanidines (MNG to TMNG) obtained by nmr is similar to the trend in pK_a 's determined from ultraviolet measurements.

Table I: pK_a Values for Nitroguanidinium Ions

	H_2SO_4	HNO_3^c
1,1,3,3,-Tetramethyl-2-nitroguanidinium ion	-0.82^a	-0.75
1-Methyl-2-nitroguanidinium ion	-0.86^b	-1.7
2-Nitroguanidinium ion	-0.93^b	
1,1-Dimethyl-2-nitroguanidinium ion	-1.30^b	-2.1

^a Based on H_0''' scale; ultraviolet method. ^b Reference 5, based on H_0 scale; ultraviolet method. ^c Based on H_0 scale; nmr method.

Bonner and Lockhart⁵ reported from their ultraviolet measurements that protonation occurs at the nitrino site, a, and that the relative basicities of nitroguanidines depend on the resonance stabilization of the ion achieved by contributions from such structures as I and II.



They also stated that the slight increase in basicity (from nitroguanidine to methyl nitroguanidine) pro-

duced by a methyl substitution on the amino nitrogen atom is in agreement with the inductive effect of the group, but the decrease in basicity (from MNG to DMNG) which follows the substitution of a second methyl group on the same nitrogen atom is evidence of the greater strain involved in attaining the planar configurations in the ground state from resonance structures of the type I and II. If this be the case, further methyl substitution on the other amino nitrogen (*e.g.*, as found in TMNG) should lead to even greater strain and nonplanarity in the molecule, and thus produce an even weaker base. However, TMNG in this study was found to have the highest pK_a value (Table I).

We have shown that protonation occurs primarily at the amino nitrogen in TMNG and suggested that protonation also occurs primarily at the amino site in DMNG.¹ We believe that the inductive effect of the methyl groups and steric inhibition to resonance are base strengthening in these compounds. These effects also appear to have a greater influence in TMNG than in DMNG and MNG. The base, TMNG, seems to be unique in that it is symmetrically substituted and has only one type of amino site, whereas MNG and DMNG have two different amino sites, primary and secondary, and primary and tertiary, respectively. In the latter two compounds, we believe that the amino site is protonated first, but the total basicity of the compounds is influenced by the effect of the other amino nitrogen. Thus, the effect of methyl substitution on the base strength in the guanidine series like that observed in the simple aliphatic amines¹⁴ is not easily explained.

The symmetrical 1,3-dimethyl-2-nitroguanidine has not been included in this study because of its low stability in acid media.³ The unusual stability of TMNG in acid media is peculiar. Furthermore, TMNG is highly soluble in most solvents ranging from water to carbon tetrachloride and melts at 84.5° whereas MNG (mp $161-162^\circ$) and DMNG (mp $197-198^\circ$) are not too soluble in most solvents.¹⁵

Acknowledgment. We wish to thank Dr. Preston T. Talbert for helpful discussions. The opinions or assertions made in this paper are those of the authors and are not to be construed as official or reflecting the views of the Department of the Navy or the naval service at large.

(9) E. M. Arnett and G. W. Mach, *J. Amer. Chem. Soc.*, **86**, 2671 (1964).

(10) Unfortunately an H_0''' scale for HNO_3 is unavailable.

(11) " pK_a " represents the value determined from nmr measurements and is not intended to be a thermodynamic value.¹²

(12) Cf. E. M. Arnett in "Progress in Physical Organic Chemistry," Vol. I, 223, Interscience, New York, N. Y., 1963.

(13) R. W. Taft and P. L. Levins, *Anal. Chem.*, **34**, 436 (1962).

(14) H. C. Brown, D. H. McDaniel, and O. Häfiger in E. A. Braude, "Determination of Organic Structures by Physical Methods," 567, Academic Press, New York, N. Y., 1955.

(15) For the preparation of TMNG, DMNG, and MNG see reference 1.

Miscibility of Liquid Metals with Salts.

IX. The Pseudobinary Alkali Metal-Metal

Halide Systems: Cesium Iodide-Sodium,

Cesium Iodide-Lithium, and Lithium

Fluoride-Potassium¹

by A. S. Dworkin and M. A. Bredig

Chemistry Division, Oak Ridge National Laboratory,
Oak Ridge, Tennessee 37830 (Received May 14, 1970)

We have extended our studies of the miscibility of molten salts with metals² to the pseudobinary sections CsI-Na, CsI-Li, and LiF-K of the corresponding ternary systems. Each of the preceding forms the stable pair by more than 10 kcal/mol of a corresponding reciprocal system, $AX + B = BX + A$.

The purified alkali metals contained less than 0.1% impurity. The CsI and LiF were Harshaw optical grade crystals. The results shown in Figure 1 were determined by thermal analysis (cooling curves). The salts and metals (total charge 50 to 200 mmol) were loaded into tantalum capsules (3 in. long, 0.5 in. i.d.) in a drybox under a helium atmosphere where the capsules were then sealed by welding. Temperatures were measured with a Pt-Pt-10% Rh thermocouple placed in a well extending about $\frac{1}{2}$ in. into the capsule from the bottom. Rocking the furnace with the capsules in a horizontal position permitted mixing of the components before each cooling curve was run. The apparatus and experimental procedure are described elsewhere³ in more detail. The decantation technique with which a sample of the liquid metal phase in the LiF-K system was separated has also been described previously.⁴

Figure 1 shows that the temperature vs. concentration phase diagram of the pseudobinary section CsI-Na resembles that of the truly binary system NaI-Na except for a slightly higher consolute temperature (1115 vs. 1036°) and a considerably lower solubility of the salt in the sodium metal ($N_{\text{CsI}}(\text{critical}) = 22$ vs. $N_{\text{NaI}}(\text{crit}) = 41$ mol %). The resemblance is greater when volume fraction, N' , rather than mole fraction is plotted, with molar volumes 100 cm³/mol for CsI, 63 for NaI, and 33 for Na metal: $N'_{\text{CsI}}(\text{crit}) = 46$ and $N'_{\text{NaI}}(\text{crit}) = 56$ vol %.

For the pseudobinary section CsI-Li, a wider miscibility gap is indicated. We were unable to find discrete points on the cooling curves, although we cooled from temperatures as high as 1300°. This implies a very steep rise in the equilibrium temperatures on both sides of a wide miscibility gap and a high consolute temperature. The situation is similar to that in the binary LiI-Li system.⁵

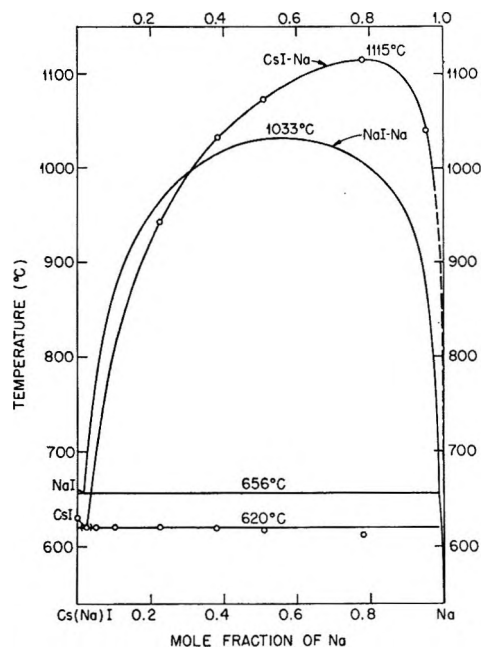


Figure 1. Phase diagram of the pseudobinary system CsI-Na compared with NaI-Na.

Of particular interest is the comparison of the four systems, binary and ternary, NaI-Na and CsI-Na, or LiI-Li and CsI-Li, with the binary CsI-Cs system exhibiting no immiscibility at all. This comparison appears to support Pitzer's notion⁶ that the nature of the metal, or, more specifically, the energy of converting the electronic structure of a real metal into an "ionic" structure, ($"M^+e^-"$), *i.e.* one with localized electrons, is the determining factor in metal-salt miscibility. Conversion energies were given as 19 and 18 kcal/mol for lithium and sodium, as against 9 for cesium.

Significantly, the results for the third ternary system we studied, LiF-K, do not appear to fall in line with this theory. Because of the low conversion energy of potassium metal, 10 kcal/mol,⁶ the theory would predict a high degree of miscibility similar to that in KF-K² where the consolute temperature is only 904° and the solubility of the salt in the metal is very high ($N_{\text{KF}}(\text{crit}) = 80$ mol %). In contrast, thermal analysis, as with CsI-Li, above, gave a very wide miscibility gap in LiF-K, similar to that in LiF-Li,⁵ and we were unable to determine the high consolute temperature. A decantation experiment was run to confirm this finding. A mixture containing 73 mol % K and 27 mol % LiF was

(1) Research sponsored by the U. S. Atomic Energy Commission under contract with Union Carbide Corporation.

(2) M. A. Bredig, "Mixtures of Metals with Molten Salts" in "Molten Salt Chemistry," M. Blander, Ed., Interscience, 1964.

(3) J. W. Johnson and M. A. Bredig, *J. Phys. Chem.*, **62**, 604 (1958).

(4) M. A. Bredig, J. W. Johnson, and W. T. Smith, Jr., *J. Amer. Chem. Soc.*, **77**, 307 (1955).

(5) A. S. Dworkin, H. R. Bronstein, and M. A. Bredig, *J. Phys. Chem.*, **66**, 572 (1962).

(6) K. H. Pitzer, *J. Amer. Chem. Soc.*, **84**, 2025 (1962).

held in the decantation capsule⁴ for several hours at 940°, during which time the liquids were mixed by shaking. The liquid metal phase, of much lower density, was then decanted, and after cooling analyzed for LiF. Only 0.8 mol % LiF was found, confirming the very wide miscibility gap indicated by the thermal analysis experiments.

These observations indicate the need for a more general correlation, beyond the simple theory above, while at the same time retaining the notion of an "ionic" metal structure. Blander and Topol⁷ have derived an approximate relation from conformal ionic solution theory to predict immiscibility gaps in simple reciprocal (ternary) systems of salts containing the monovalent cations A⁺ and B⁺ and anions C⁻ and D⁻.

$$T_c = (\Delta G^\circ/5.5R) + (\lambda_{12} + \lambda_{24} + \lambda_{13} + \lambda_{34})/11R \quad (1)$$

Here T_c is the consolute temperature, ΔG° is the standard molar Gibbs free energy change for the metathetical reaction

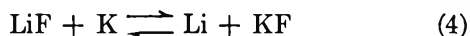


and λ is an energy of mixing parameter depending solely on the properties of the four binary systems. λ is further defined as

$$\lambda_{12} = \Delta G_{12}^E/X_A X_B \quad (3a)$$

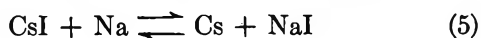
$$\lambda_{13} = \Delta G_{13}^E/X_C X_D, \text{ etc.} \quad (3b)$$

where ΔG_{ij}^E is the excess free energy of mixing in the binary mixture of the salts i and j where AD is salt 1, BD is 2, AC is 3, and BC is 4 and the X 's are Temkin ion fractions. (The same symbols are used here as in ref 7.) In our cases, for instance



we have two binary salt-metal systems, LiF-Li and KF-K, one binary salt system, LiF-KF, and one binary metal system, Li-K. Here, Li is 1, K is 2, LiF is 3, and KF is 4, and the same numbering system is used for eq 5 and 6 below. All the λ values for the binary systems necessary for a quantitative treatment are not available at present. However, we may attempt an explanation of the high T_c found in the ternary LiF-K system from a qualitative consideration of the terms in eq 1 even though this equation was derived for the somewhat different systems of molten salt mixtures.

We find that ΔG° is similar for all three systems, 12 to 13 kcal/mol, the lower value applying to



and



However, the λ terms for the binary systems involved should differ greatly, since λ is more positive the greater the positive deviation from ideality and the tendency to demixing. We know² that miscibility in the LiF-Li

and LiI-Li systems is much smaller than in NaI-Na, and much smaller in KF-K than in the CsI-Cs system in which a miscibility gap does not occur at all. Similarly, miscibility in the binary metal systems Li-K and Li-Cs is smaller than in Na-Cs. Thus both the λ_{12} and λ_{24} terms are larger for eq 6 than for 5 while λ_{12} , λ_{24} , and λ_{13} are larger for eq 4 than for 5. The second term in eq 1 and, therefore, the consolute temperature, T_c , should then be highest for the LiF-K system and lowest for the CsI-Na system, an essential agreement with the experimental results.

It should be noted that the λ terms for the salt-metal systems include the energy of converting the electronic structure of a real metal into an ionic structure. Use of the conformal ionic solution theory is then an extension of our earlier approach in that it considers the energies involved in all four binary systems rather than the conversion energy of just one metal per system.

(7) M. Blander and L. E. Topol, *Inorg. Chem.*, **5**, 1641 (1966).

Reactivity of the Cyclohexane Ion^{1a}

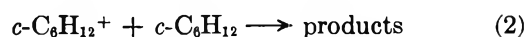
by L. W. Sieck, S. K. Searles,^{1b} R. E. Rebert, and P. Ausloos^{1c}

Radiation Chemistry Section, National Bureau of Standards, Washington, D. C. 20234 (Received May 18, 1970)

In a number of gas phase and liquid phase radiolysis and photoionization studies, the identity and yields of ions which were not known to undergo any fast reactions in the pure parent compound were determined by adding to the system some foreign compound with which the ion in question could undergo reaction to give a distinctive product.² For example, it has been shown³ that the cyclohexane parent ion will react with added *i*-C₄D₈ to form isobutane-*d*₈.



However, in the case of cyclohexane, it has recently been suggested⁴ that reaction between the parent ion and the cyclohexane molecule



which has generally been assumed to be very slow, may effectively compete with fast reactions between the

(1) (a) This research was supported by the Atomic Energy Commission; (b) NRC-NBS Research Associate 1968-1970; (c) to whom correspondence should be addressed.

(2) (a) For a review of radiolysis studies, see "Fundamental Processes in Radiation Chemistry," P. Ausloos, Ed., Interscience Publishers, New York, N. Y., 1968; (b) P. Ausloos, *Progr. React. Kinet.*, **5**, 113 (1970).

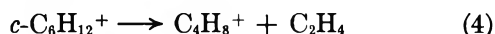
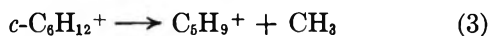
(3) P. Ausloos and S. G. Lias, *J. Chem. Phys.*, **43**, 127 (1965).

(4) S. Wexler and L. G. Pobo, *J. Amer. Chem. Soc.*, **91**, 7233 (1969).

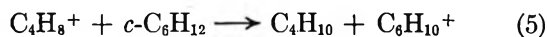
parent ion and added interceptors. In fact, it was suggested that reaction 2 might account for a major portion of the product formation in irradiated cyclohexane. Because no quantitative information was available on the rate of reaction 2 compared to the rates of the other reactions with which it may be competing, we considered it important to determine the rate of reaction 2 to ascertain the extent to which this reaction may contribute to product formation in the radiolysis of cyclohexane. We here report the results of such a determination. As the reader will see below, the work described here is actually an illustration of the difficulties involved in studying very slow ion-molecule reactions.

Two techniques were utilized to determine the rate of reaction 2—or, more correctly, to determine the upper limit of the rate of reaction 2—kinetic mass spectrometry and an analysis of the yields of products formed in reactions of the parent cyclohexane ion with varying amounts of reactive added compounds.

Cyclohexane (I.P. 9.88 eV) was irradiated with 106.7-nm (11.6-eV) photons in the mass spectrometer described previously.⁵ The yields of all observed ions are shown as a function of pressure in Figure 1. At this energy, some fragmentation of the parent ion occurs, yielding mainly $C_6H_9^+$ and $C_4H_8^+$.



The gradual drop in the $C_6H_9^+$ yield with pressure can probably be attributed to the quenching of fragmentation process 3; since no product could be detected which has $C_6H_9^+$ as precursor, it may be assumed that this ion does not react with cyclohexane. The $C_4H_8^+$ ion is known⁶ to react to give $C_6H_{10}^+$ as a product ion.



At pressures below about 80 mTorr, the parent ion yield increases slightly as a function of pressure, due to collisional quenching of the fragmentation processes 3 and 4. Reaction of $C_6H_{12}^+$ to form C_7 – C_{11} ions was detected at higher pressures, resulting in a reduction in the observed yield of $C_6H_{12}^+$ at 0.4 Torr to 45% of its maximum value. Taking into account the increase in residence time with pressure under diffusive flow conditions, a maximum rate constant for disappearance of $C_6H_{12}^+$ of 2×10^{-13} cm³/molecule-sec was derived from these results. This value is necessarily an upper limit for the rate of reaction 2 since a variety of neutral products will be generated during the irradiation of the cyclohexane in the ion source of the mass spectrometer. It would be very difficult to distinguish between a rapid reaction of the $C_6H_{12}^+$ ion with one of these products and a slow reaction of the ion with cyclohexane itself. In fact, the presence in the ion source of 0.02% of a foreign compound with which the cyclohexane ion reacts with a rate constant of 10^{-9} cm³/molecule-sec would

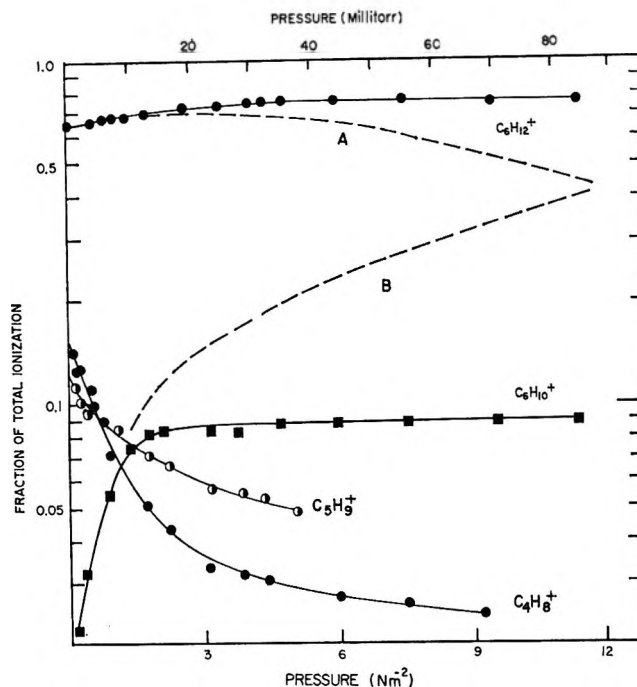


Figure 1. Yields of ions formed in cyclohexane and cyclohexane-isobutene (1:0.00067) mixtures (curves A and B) irradiated at various pressures with 106.7-nm (11.6 eV) photons.

result in an identical reduction in the observed yield of $C_6H_{12}^+$.

Such an effect of a small amount of reactivity impurity on the parent ion yield is shown by curve A (Figure 1), which represents the parent ion yield as a function of pressure when 0.07% isobutene is present. Curve B represents the yield of the $C_6H_{10}^+$ ion formed in reaction 1.

In the closed systems photolysis of cyclohexane-isobutene (1:0.01) mixtures with 10.0 or 11.6–11.8-eV photons, at pressures high enough that fragmentation processes 3 and 4 are completely quenched⁷ (10 Torr), the yield of isobutane formed in reaction 1 is equal to the yield of parent ions. In order to determine the upper limit of reaction 2 as a competing process, experiments were performed in which cyclohexane was irradiated in the presence of very low concentrations of added isobutene. In the γ radiolysis of cyclohexane at a pressure of 50 Torr, the observed yield of isobutane was constant (0.4 molecule of isobutane per positive ion formed in the system) from 3% down to 0.01% added isobutene. At lower concentrations, the yield diminishes as the isobutene concentration is lowered. (At 0.004% isobutene, 0.3 isobutane molecule is formed per positive ion.) Assuming that the reduction in the yield of isobutane at very low isobutene concentration can be traced entirely to the competition from reaction 2, one can estimate that $k_2 \leq 5 \times 10^{-14}$ cm³/molecule-

(5) L. W. Sieck, S. K. Searles, and P. Ausloos, *J. Amer. Chem. Soc.*, **91**, 7627 (1969).

(6) F. Abramson and J. Futrell, *J. Phys. Chem.*, **71**, 3791 (1967).

(7) P. Ausloos, R. E. Rebbert, and S. G. Lias, *ibid.*, **72**, 3904 (1968).

sec. The actual rate constant for reaction 2 is probably lower than this, since at these low concentrations of additive, olefinic products formed in the radiolysis or the impurities in the starting material (impurity level = $0.007\% \pm 0.004\%$) can compete with the additive for reaction with the parent ion.

The results presented here illustrate that irradiation experiments utilizing neutral product analyses are well suited to the determination of upper limits of reaction rates of very slow reactions. This is so because the sample size can be large, and the accumulation of interfering neutral products can be reduced to whatever limit analytical techniques allow by decreasing the irradiation time.

It should be pointed out that the results reported here are not essentially in disagreement with those of the earlier study⁴ in which the disappearance of $C_6H_{12}^+$ via reaction 2 was suggested, even though the mass spectrometric results reported in that investigation show a slightly more drastic reduction of the $C_6H_{12}^+$ ion with increasing pressure than do the results given in Figure 1. This difference can probably be accounted for by the longer reaction path length in the instrument used in that investigation. It is highly unlikely that the proton beam used in that instrument leads to the formation of $C_6H_{12}^+$ ions which are in higher excited states than those formed here by photon absorption, and which, therefore, are more reactive. In the first place, the results indicate that the ions undergo many collisions before reacting, so that an excited ion would, at any rate, be deactivated before undergoing reaction. Secondly, if indeed such excited reactive ions did exist, they would have been detected in the γ -radiolytic experiments reported here.

According to the results presented here, the rate of reaction 2 is at least 10^5 times slower than reactions of cyclohexane ions with lower olefins.⁸ In view of this fact, we can conclude that it is extremely unlikely that reaction 2 makes a significant contribution to product formation in the radiolysis of cyclohexane, either in the presence or absence of additives, since even reaction with small amounts of accumulated products would compete effectively with such a reaction.

(8) L. W. Sieck and S. K. Searles, *J. Amer. Chem. Soc.*, **92**, 2937 (1970).

Mechanism of Ethylene Hydrogenation on Tungsten Trioxide

by S. J. Tauster and J. H. Sinfelt

Corporate Research Laboratories,
Esso Research and Engineering Company,
Linden, New Jersey 07036 (Received June 1, 1970)

An important mechanistic question in the catalytic hydrogenation of ethylene is the form of hydrogen, *i.e.*,

atomic or molecular, which participates in the reaction. We have carried out some experiments using WO_3 as a catalyst which suggest that the reaction may occur without involvement of hydrogen atoms on the surface. In the use of WO_3 as a catalyst, one has a simple indicator for the presence of hydrogen atoms, since the WO_3 undergoes a color change from yellow to blue on contact with hydrogen atoms at temperatures where molecular hydrogen has no effect,¹ *i.e.*, lower than about 400° . The blue form of WO_3 produced on reduction of the oxide may be represented by the general formula H_xWO_3 , which is a hydrogen analog of the tungsten bronzes.² The failure of molecular hydrogen to reduce WO_3 at temperatures lower than about 400° is taken as evidence that hydrogen molecules are not dissociatively chemisorbed to form hydrogen atoms on the surface of the oxide. Since chemisorbed hydrogen atoms are often hypothesized to be intermediates in the catalytic hydrogenation of ethylene, it seemed interesting to determine whether or not WO_3 catalyzed the reaction under conditions where no color change would be expected on contact of the oxide with molecular hydrogen, *i.e.*, where hydrogen atoms would not be expected to form on the surface.

The experiments were conducted in a 3-cm diameter horizontal quartz tube about 50 cm in length. A 30-g charge of WO_3 was employed. It was located in the central part of the tube, consisting of a section about 6 cm long, and was held in place by quartz wool packed on either side of the WO_3 . The entire tube was placed in a horizontal muffle furnace which could be opened at any time to permit visual observation of the WO_3 . An iron-constantan thermocouple positioned in the center of the bed was employed for temperature measurement. Capillary type flowmeters were used for the measurement of hydrogen and ethylene flow rates. Samples of the reactor effluent were periodically analyzed in a chromatographic unit containing a silica gel column. The WO_3 employed in this work was obtained from Sylvania Chemical and Metallurgical Division, Towanda, Pa., and is identified as grade TO-2, Lot No. WO 104B. Purity is claimed to be 99.98% or higher by the supplier. The surface area was $3.0 \text{ m}^2/\text{g}$, as determined by the BET method. After the WC_3 was charged to the reactor, it was heated in flowing helium to reaction temperature over a 2-hr period prior to the catalytic studies.

In a run at 250° and 1 atm total pressure, ethylene and hydrogen flow rates of 5 and 25 l./hr, respectively, were used. Hydrogenation of ethylene to ethane occurred readily at these conditions. The conversion of ethylene to ethane was 25%, a value which was maintained over a period of 22 hr. This corresponds to a reaction rate of approximately 10^{13} molecules/sec cm^2

(1) H. W. Melville and J. C. Robb, *Proc. Roy. Soc. (London) Ser. A*, **196**, 445 (1949).

(2) O. Glemser and C. Nauman, *Z. Anorg. Allg. Chem.*, **265**, 288 (1951).

occurring during this period. During this extended period of substantial ethylene hydrogenation on the WO_3 , there was no evidence of a change in color from the original yellow characteristic of unreduced WO_3 . Similar behavior was observed in several other runs of shorter duration. Some difficulty was experienced in obtaining the same level of catalytic activity on different samples of WO_3 . However, in none of the experiments, conducted at temperatures ranging from 125 to 250°, was a change in color of the WO_3 detected as a result of the ethylene hydrogenation reaction. Data on the dependence of the hydrogenation rate on hydrogen pressure showed the reaction to be first order in hydrogen. Limited data on the dependence of the rate on ethylene pressure indicate that the order in ethylene is between zero and one, which implies an intermediate degree of coverage of the active sites by ethylene. The surface coverage would, of course, be expected to vary with temperature, being lowest at the highest temperatures studied.

It has been demonstrated clearly by Melville and Robb¹ that the "blueing" of WO_3 or MoO_3 is a very sensitive method for detecting hydrogen atoms in a system in which a gas phase reaction between ethylene and hydrogen atoms occurs. This indicates that the "blueing" reaction competes satisfactorily with the addition of hydrogen atoms to ethylene. One might then reasonably expect that the formation of tungsten blue would have been observed in the present work if hydrogen atoms were involved in the reaction. The very rapid formation of tungsten blue from yellow WO_3 has been demonstrated recently by several investigators who employed various forms of platinum to activate molecular hydrogen in experiments with mixtures of platinum and WO_3 .³⁻⁵ In considering the experimental conditions of Melville and Robb, it is to be noted that the ethylene partial pressures were lower by two orders of magnitude than those employed in the present work. However, the Melville and Robb experiments were done at room temperature, which is much lower than the temperatures employed in the current investigation. Consequently, the coverage of the WO_3 surface by ethylene may not have been greatly different in the two investigations, since the effect of temperature should largely compensate for the effect of ethylene pressure on surface coverage.

As a consequence of the present work, it is suggested that the ethylene hydrogenation reaction on WO_3 does not involve adsorbed hydrogen atoms as intermediates, based on the absence of a color change from yellow to blue at the surface of the oxide. It is therefore proposed that the hydrogenation of ethylene on WO_3 involves hydrogen molecules, rather than adsorbed hydrogen atoms. The simplest reaction scheme would appear to be one in which the reaction occurs *via* collision of hydrogen molecules from the gas phase with adsorbed ethylene, involving a direct addition of a hydrogen

molecule to the ethylene double bond. The first-order dependence of the reaction rate on hydrogen pressure is consistent with such a mechanism.

The mechanism of ethylene hydrogenation on WO_3 suggested in the present work is very simple. It is not expected that the proposed mechanism will apply to all types of hydrogenation catalysts. In the case of metal catalysts, for example, adsorbed hydrogen atoms are in all probability involved in the hydrogenation. In any case, the simple mechanism envisioned in the present work would not readily account for all the varied phenomena encountered in ethylene hydrogenation on metals, as exemplified by the many results of experiments with deuterium.^{6,7}

(3) S. Khoobiar, *J. Phys. Chem.*, **68**, 411 (1964).

(4) H. W. Kohn and M. Boudart, *Science*, **145**, 149 (1964).

(5) J. E. Benson, H. W. Kohn, and M. Boudart, *J. Catal.*, **5**, 307 (1966).

(6) J. Turkevich, D. O. Schissler, and P. Irsa, *J. Phys. Colloid Chem.*, **55**, 1078 (1951).

(7) C. Kemball, *J. Chem. Soc. (London)*, 735 (1956).

Time-Dependent Adsorption of Water Vapor on Pristine Vycor Fiber

by Victor R. Deitz and Noel H. Turner

Naval Research Laboratory,
Washington, D. C. 20390 (Received June 15, 1970)

The dehydration and rehydration of many silica powders have been studied and the results have many similarities and some differences.¹⁻³ In all of these cases the samples had been subjected to specified pretreatments entailing liquid water.⁴ This note is concerned with the interaction of water vapor with a pristine fiber drawn from a melt of nonporous Vycor in a tungsten crucible at 2050°. The preparation of the fiber (conducted in an argon atmosphere) is similar to that reported for E-glass.⁵ The rates of water vapor adsorption were determined at surface coverages of less than a monolayer and at contact times up to 4000 min. The term "pristine" is used to define one very important aspect in the pretreatment of the Vycor fiber, namely, that it had never been exposed to an aqueous media.

(1) R. K. Iler, "The Colloid Chemistry of Silica and Silicates," Cornell University Press, Ithaca, N. Y., 1955.

(2) A. V. Kiselev, 10th Colston Soc. Symp., D. H. Everett and F. Stone, Butterworths, London, 1958, p 236.

(3) M. Folman and D. J. C. Yates, *Trans. Faraday Soc.*, **54**, 429 (1958).

(4) J. H. DeBoer and J. M. Vleeskens, *Proc. Kon. Ned. Akad. Wetensch., Ser. B.*, **61**, 2 (1958).

(5) V. R. Deitz, and N. H. Turner, "Symposium of Surface Area Determination," University of Bristol, July 16-18, 1969.

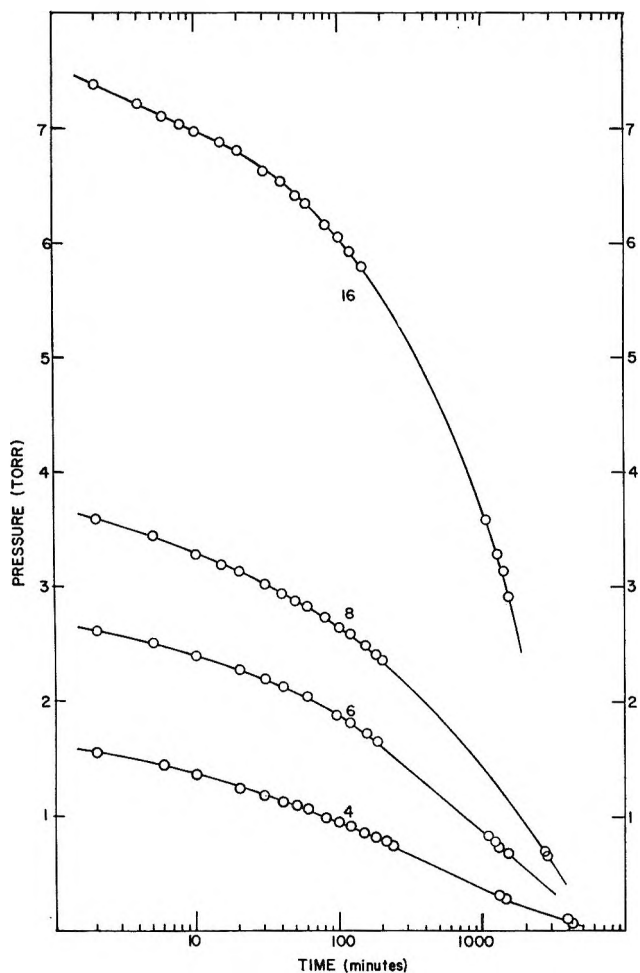


Figure 1. Pressure decrements in the adsorption of water vapor on Vycor fiber at 100° for the indicated number of doses, each being $9.769 \mu\text{mol}$ of H_2O .

The latter is known to modify silica surfaces to varying extents.¹

The sample of Vycor fiber (58.731) had a BET krypton area of 4.3 m^2 per sample (20.4 \AA^2 per adsorbed Kr atom⁵). The geometrical area calculated from the weight, length, and density of the Vycor fiber was 4.2 m^2 . Hence, the Vycor fiber is essentially nonporous and not rough.

After outgassing of the sample at 300° before each experiment for a period of at least 16 hr, the adsorption of water vapor was determined at 60° , 80° , 100° , and 120° . Figure 1 illustrates the pressure decrease for water vapor adsorption at 100° in a fixed volume as a function of time. A cold finger, containing a precisely known quantity of water vapor, was heated rapidly from -196° to room temperature to start the reaction. The four curves in Figure 1 (16, 8, 6, and 4) correspond to the introduction of the indicated number of doses of water vapor, each dose being $9.769 \mu\text{mol}$ of H_2O . Good reproducibility was obtained and there was no dependence of the number of doses; this indicates that the outgassing at 300° before each introduction of water vapor

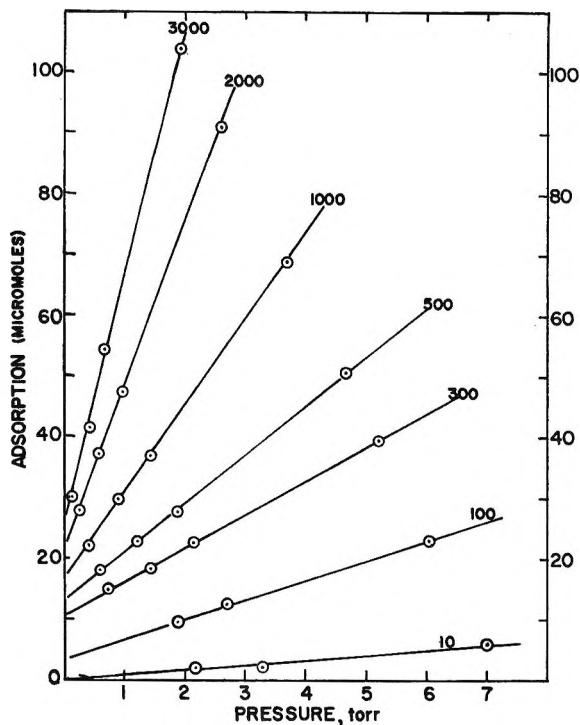


Figure 2. Adsorption of water vapor plotted as isochrones (designations in minutes) using the data of Figure 1.

was adequate for dehydrating the surface of the Vycor fiber. Independent experiments have shown that outgassing at 500° gave the same adsorption data at 120° as the data obtained after a 300° outgassing.

The strong dependence on contact time is the new feature of these observations. Obviously, the reproducibility of water vapor studies among different investigators should depend upon this new parameter. The reaction is indeed a memory process, where time zero is the initial contact of the fiber with the water vapor.

The data of Figure 1 permit the determination of pressure at any specified time interval when a smooth curve is drawn between the observed points. The corresponding adsorption, corrected for wall adsorption, may then be presented by a series of isochrones. Figure 2 gives the isochronal adsorption isotherms (10, 100, 300, 500, 1000, 2000, and 3000 min) of water vapor on the Vycor fiber at 100° . Each isochronal isotherm fol-

$$n_{i,T} = k_{i,T}p + i_{i,T} \quad (1)$$

lows a linear behavior where $n_{i,T}$ is the amount adsorbed, p the pressure, $k_{i,T}$ the slope and $i_{i,T}$ the intercept on the $n_{i,T}$ axis; the subscripts i and T designate the time and temperature, respectively.

The magnitudes of temperature and pressure were selected in order to realize a fractional surface coverage by water molecules. Since the Vycor formulation is mainly silica, it is proposed that the elementary mechanism consists of two consecutive reactions: (I) a chemisorption process to break the Si-O-Si bonds in

the strained surface networks, and to form SiOH groups; (II) the subsequent physical adsorption of water vapor to the reaction products on the surface, mainly the $-\text{Si}-\text{OH}$ groups. The increasing values of $i_{i,T}$ for the isochrones of Figure 2 are ascribed to the chemisorption process. In order to attain 100% geminal formation, $=\text{Si}(\text{OH})_2$, in an octohedral face of β -cristobalite, it is necessary to chemisorb $8.04 \mu\text{mol}$ of water vapor/ m^2 or $34.5 \mu\text{mol}$ per above sample of Vycor fiber. Adsorption above this magnitude is attributed to the monolayer forming on the geminal silanol groups. The limiting value for i has not quite been reached by the 3000-min isochrone at 120° , the most severe condition so far investigated. The linear isochronal adsorption isotherms of Figure 2 suggest that a simplified behavior is valid for the pressure-dependent adsorption that takes place on top of the chemisorbed water.

The summation of the energy requirements to break one $-\text{Si}-\text{O}-$ linkage of the silica network, to break one $\text{H}-\text{O}$ bond in a water molecule, and to form two surface $\text{Si}-\text{OH}$ groups is not large. An estimate, calculated from the enthalpies of formation of definite crystalline hydrated silicas and that of silica and water vapor, is in the range -3.5 to -5.3 kcal per $\text{Si}-\text{OH}$ group. The calculated isosteric isochronal heats of adsorption are of this magnitude.

An indication of time dependency in the water vapor silica reaction can be seen in the work of Hockey and Pethica.⁶ These investigators found different adsorp-

tion after 15 min and after 1 hr; however, these contact times were too short to bring out the new behavior described in this note. The importance of the experimental procedure employed in the dehydration of silica for infrared studies is well established.^{7,8} It is now equally essential to keep a log of the contact time, since the subsequent hydration has now been shown to be a memory process. Previous investigations also have been with dehydrated "silica-gel" type of surface boundaries. A variable amount of surface hydration has been shown to be introduced in the procedure for sample preparation.^{9,10} This complication to an understanding of the silica-water vapor interaction has been brought out by careful heats of immersion measurements. Pristine Vycor fiber, and also pristine E-glass fiber, are not subject to this disturbance. Some processes that add the finish to the glass fiber in reinforced composite materials are concerned with pristine fiber. Thus, the influence of contact time in the adsorption of water vapor may be a critical parameter in the adhesion of polymers in glass reinforced composite materials.

(6) J. A. Hockey and B. A. Pethica, *Trans. Faraday Soc.*, **57**, 2247 (1961).

(7) L. H. Little, "Infrared Spectra of Adsorbed Species," Academic Press, New York, N. Y., 1966.

(8) C. Morterra and M. J. D. Low, *J. Phys. Chem.*, **73**, 321 (1969).

(9) W. H. Wade, R. L. Every, and N. Hackerman, *ibid.*, **64**, 355 (1960).

(10) A. C. Makrides and N. Hackerman, *ibid.*, **63**, 594 (1959).

COMMUNICATIONS TO THE EDITOR

Electron Spin Resonance Spectra of Radicals Formed from Nitrogen Dioxide and Olefins

Sir: Some time ago, Schaafsma and Kommandeur obtained esr spectra from a range of organic compounds, including simple olefins, by reaction with NO_2 , all of which were assigned to charge-transfer complexes.¹

Subsequently, we showed that in the particular case of methylmethacrylate, reaction occurred to give a nitroxide radical,² which was identified by comparing the liquid- and solid-state esr spectra with those of authentic nitroxides. The liquid-phase spectrum taken alone would not have provided a convincing identification, but together with that from the solid, which is a far better "fingerprint" of a nitroxide radical, the identification was thought to be sound.

This was part of a more wide-ranging study of reactions between NO and NO_2 and organic materials³ in which it was shown that both iminoxy radicals and nitroxides could be formed. In many cases, identifications were supported by analysis of detailed hyperfine patterns and by comparison with authentic samples. Solid-state spectra again supported these identifications.

We therefore thought it probable that several of the species detected by Schaafsma and Kommandeur¹ were similar radicals and not charge-transfer complexes, but Bielski and Gebicki nevertheless used the charge-

(1) T. J. Schaafsma and J. Kommandeur, *J. Chem. Phys.*, **42**, 438 (1965).

(2) J. A. McRae and M. C. R. Symons, *Nature (London)*, **210**, 1259 (1966).

(3) W. M. Fox, J. A. McRae, and M. C. R. Symons, *J. Chem. Soc. A*, 1773 (1967).

transfer complex theory¹ to interpret their results for solutions of NO₂ in various unsaturated solvents.^{4,5} We have indicated elsewhere that these spectra were almost certainly all caused by the formation of nitroxide radicals,⁶ but Bielski and Gebicki, accepting that the species studied by Schaafsma and Kommandeur¹ were correctly identified, argued against this⁵ and cast doubt upon our own identifications.³

In order to test these theories, we chose several of their compounds at random and examined the solid state spectra; in all instances the spectra were characteristic of nitroxides, typical parameters being $A_{\text{iso}} = 12.5$ G, $A_{\parallel}({}^{14}\text{N}) = 33$ G, $A_{\perp} = 6$ G, $g_{\parallel} = 2.0025$ and $g_{\perp} = 2.0080$ (for cyclohexene at 77°K). A second test was to see if the spectra were formed reversibly, as required by theory and previously implied.¹ All attempts to remove NO₂ by physical means had no effect on the esr spectral intensities.

Very recently, Jonkman, *et al.*,⁷ have independently drawn the same conclusions. We agree with their more detailed arguments against the charge-transfer complex theory, and there is no need to repeat them here.

Acknowledgment. I thank Messrs. J. G. P. Davies and A. V. Howard and Mrs. P. Spicer for experimental assistance.

(4) B. H. J. Bielski and J. M. Gebicki, "Atlas of esr Spectra," Academic Press, New York, N. Y. 1967.

(5) B. H. J. Bielski and J. M. Gebicki, *J. Phys. Chem.*, **73**, 1402 (1969).

(6) M. C. R. Symons, *Nature (London)*, **217**, 689 (1968).

(7) L. Jonkman, H. Muller, C. Kiers, and J. Kommandeur, *J. Phys. Chem.*, **74**, 1650 (1970).

DEPARTMENT OF CHEMISTRY
THE UNIVERSITY
LEICESTER, LE1 7RH, ENGLAND

M. C. R. SYMONS

RECEIVED JUNE 11, 1970

Kinetic Evidence that G_{OH} in the Radiolysis of Aqueous Sulfuric and Nitric Acid Solutions Is Proportional to Electron Fraction Water¹

Sir: The radiolysis of cerium(IV)–cerium(III)–HCOOH mixtures in air-saturated aqueous 0.4 M sulfuric acid with ⁶⁰Co γ radiation yielded² kinetic evidence for reaction of OH radical with sulfuric acid to form the SO₄⁻ radical. This was confirmed by pulse radiolysis techniques.³ We have extended this kinetic study to include both 4.0 M sulfuric acid and 4.0 M nitric acid solutions.

We obtained⁴ kinetic evidence for primary yields of both OH and SO₄⁻ radicals in the radiolysis of aqueous 4.0 M sulfuric acid. The dependence of $G(\text{Ce}^{\text{III}})$ on

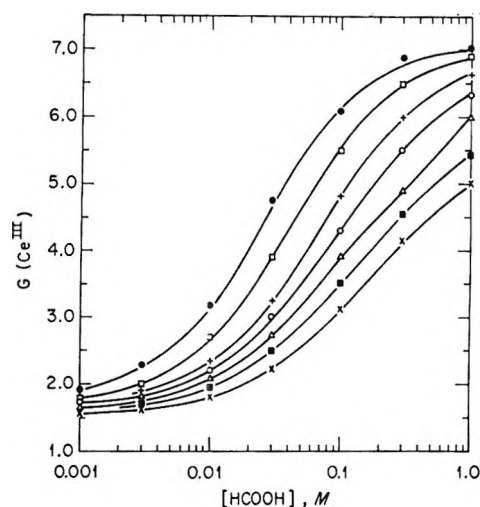


Figure 1. Dependence of $G(\text{Ce}^{\text{III}})$ on $[\text{Ce}^{\text{III}}]$ and $[\text{HCOOH}]$ for reduction of cerium(IV) in air-saturated 4.0 M sulfuric acid induced by ⁶⁰Co γ radiation. Initial $[\text{Ce}^{\text{III}}]$: \times , 3.0×10^{-2} M; \blacksquare , 1.5×10^{-2} M; Δ , 6.0×10^{-3} M; \circ , 3.0×10^{-3} M; $+$, 1.5×10^{-3} M; \square , 6.0×10^{-4} M; \bullet , 3.0×10^{-4} M. Curves are theoretical and represent least-squares fit of the data to eq I.

$[\text{Ce}^{\text{III}}]$ and $[\text{HCOOH}]$, shown in Figure 1, adheres well to eq I

$$G(\text{Ce}^{\text{III}}) = G(\text{Ce}^{\text{III}})^0 + 2(A G_{\text{OH}} + B G_{\text{SO}_4^-})/C \quad (\text{I})$$

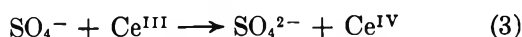
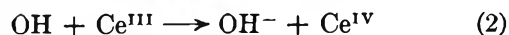
in which

$$A = 1 + (k_3[\text{Ce}^{\text{III}}]/k_6 + k_{-1}[\text{H}_2\text{O}]/k_5 + k_1[\text{HSO}_4^-]/k_4)/[\text{HCOOH}]$$

$$B = 1 + (k_2[\text{Ce}^{\text{III}}]/k_4 + k_{-1}[\text{H}_2\text{O}]/k_5 + k_1[\text{HSO}_4^-]/k_4)/[\text{HCOOH}]$$

$$C = \left(1 + \frac{k_3[\text{Ce}^{\text{III}}] + k_{-1}[\text{H}_2\text{O}]}{k_6[\text{HCOOH}]}\right) \left(1 + \frac{k_2[\text{Ce}^{\text{III}}]}{k_4[\text{HCOOH}]}\right) + \frac{k_1[\text{HSO}_4^-]}{k_4[\text{HCOOH}]} \left(1 + \frac{k_3[\text{Ce}^{\text{III}}]}{k_5[\text{HCOOH}]}\right)$$

and $G(\text{Ce}^{\text{III}})^0$, a function of $[\text{Ce}^{\text{III}}]$, is the value of $G(\text{Ce}^{\text{III}})$ in the absence of HCOOH. Equation I was obtained by the stationary-state hypothesis from the following radical reactions induced by the primary yields of OH and SO₄⁻ radicals.

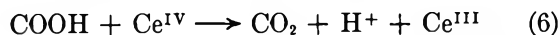
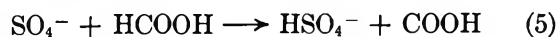


(1) Research sponsored by the U. S. Atomic Energy Commission under contract with Union Carbide Corporation.

(2) T. J. Sworski, *J. Amer. Chem. Soc.*, **78**, 1768 (1956); *Radiat. Res.*, **6**, 645 (1957).

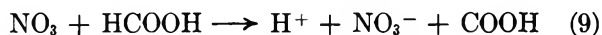
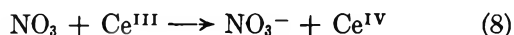
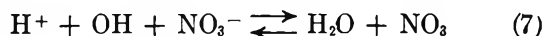
(3) E. Heckel, A. Henglein, and G. Beck, *Ber. Bunsenges. Phys. Chem.*, **70**, 149 (1966).

(4) R. W. Matthews, H. A. Mahlman, and T. J. Sworski, Abstracts of the 17th Annual Meeting of the Radiation Research Society, *Radiat. Res.*, **39**, 534 (1969).



The experimental data were fit to eq I by the method of least squares with the computer program of Lietzke⁵ and yielded $G_{\text{OH}} = 1.78 \pm 0.03$, $G_{\text{SO}_4^-} = 0.94 \pm 0.03$, $k_5/k_3 = 0.0060 \pm 0.0005$, $k_4/(k_1[\text{HSO}_4^-]) = 14.4 \pm 0.5$, $k_2/(k_1[\text{HSO}_4^-]) = 29.6 \pm 2.6$, $k_{-1}[\text{H}_2\text{O}]/k_3 = 0.00017 \pm 0.00005$, and seven values of $G(\text{Ce}^{\text{III}})$ ⁶ for seven different concentrations of cerium(III). These values differ slightly from the preliminary values obtained⁴ with the assumption of negligible hydrolysis of the SO_4^- radical.

Similarly, we obtained⁶ kinetic evidence for primary yields of both OH and NO_3 radicals in the radiolysis of aqueous 4.0 M nitric acid. The dependence of $G(\text{Ce}^{\text{III}})$ on $[\text{Ce}^{\text{III}}]$ and $[\text{HCOOH}]$ again adheres well to eq I in which $G_{\text{SO}_4^-}$, k_1 $[\text{HSO}_4^-]$, k_{-1} , k_3 , and k_5 were replaced by G_{NO_3} , $k_7[\text{H}^+][\text{NO}_3^-]$, k_{-7} , k_8 , and k_9 , respectively.



The best least-squares fit of the experimental data to eq I was obtained by assuming negligible hydrolysis of the NO_3 radical and yielded $G_{\text{OH}} = 2.04 \pm 0.09$, $G_{\text{NO}_3} = 1.56 \pm 0.12$, $k_4/(k_7[\text{H}^+][\text{NO}_3^-]) = 4.8 \pm 0.6$, $k_2/(k_7[\text{H}^+][\text{NO}_3^-]) = 20 \pm 6$, $k_9/k_8 = 0.0070 \pm 0.0005$, and eight values of $G(\text{Ce}^{\text{III}})$ ⁶ for eight different concentrations of cerium(III).

With the approximation that energy partition between water and acid is proportional to the electron fraction of each component, G_{OH} based upon the energy absorbed by water is $1.78/0.70 = 2.54 \pm 0.05$ for 4.0 M sulfuric acid and $2.04/0.79 = 2.58 \pm 0.12$ for 4.0 M

nitric acid. These values of G_{OH} for acidic water are equal within standard errors to the value of $G_{\text{OH}} = 2.59$ for pure water determined in our laboratory.⁷ Therefore, G_{OH} based upon energy absorbed by water is not markedly affected by either sulfuric acid or nitric acid at concentrations as high as 4.0 M. Our previously reported values for G_{OH} in 0.4 M sulfuric acid of 2.92⁸ and 2.96⁹ must be too high for two reasons: (1) we implicitly assumed that $G_{\text{SO}_4^-} = 0$ and (2) we assumed that $G(\text{Fe}^{\text{III}}) = 2G_{\text{H}_2\text{O}_2} + 3G_{\text{H}} + G_{\text{OH}}$ for the ferrous sulfate dosimeter, being unaware of the formation of peroxysulfuric acids.¹⁰

Our results confirm the proposal of Boyle¹⁰ for aqueous sulfuric acid solutions and the evidence of Daniels and Wigg¹¹ for aqueous sodium nitrate solutions that G_{OH} is proportional to electron fraction water. They refute the suggestions that H_2O^+ , precursor of the OH radical, may react with either HSO_4^- to yield the SO_4^- radical¹² or NO_3^- to yield the NO_3 radical.^{13,14}

(5) M. H. Lietzke, ORNL-3259, March 21, 1962.

(6) R. W. Matthews, H. A. Mahlman, and T. J. Sworski, paper presented at the XXII International Congress of Pure and Applied Chemistry, Sydney, Australia, Aug 20-27, 1969.

(7) C. J. Hochenadel and R. Casey, Abstracts of the 13th Annual Meeting of the Radiation Research Society, *Radiat. Res.*, **25**, 198 (1965).

(8) T. J. Sworski, *J. Amer. Chem. Soc.*, **76**, 4687 (1954).

(9) H. A. Mahlman and J. W. Boyle, *ibid.*, **80**, 773 (1958).

(10) J. W. Boyle, *Radiat. Res.*, **17**, 427 (1962).

(11) M. Daniels and E. E. Wigg, *J. Phys. Chem.*, **73**, 3703 (1969).

(12) A. O. Allen, *Radiat. Res.*, **1**, 85 (1954).

(13) W. H. Hamill, *J. Phys. Chem.*, **73**, 1341 (1969).

(14) T. Sawai and W. H. Hamill, *J. Chem. Phys.*, **52**, 3843 (1970).

(15) Guest Scientist from the Australian Atomic Energy Research Establishment, Sydney, Australia.

* To whom correspondence should be addressed.

CHEMISTRY DIVISION
OAK RIDGE NATIONAL LABORATORY
OAK RIDGE, TENNESSEE 37830

R. W. MATTHEWS¹⁶
H. A. MAHLMAN
T. J. SWORSKI*

RECEIVED JUNE 12, 1970